

PLEASE RETURN TO  
MFC BRANCH LIBRARY

INL Technical Library



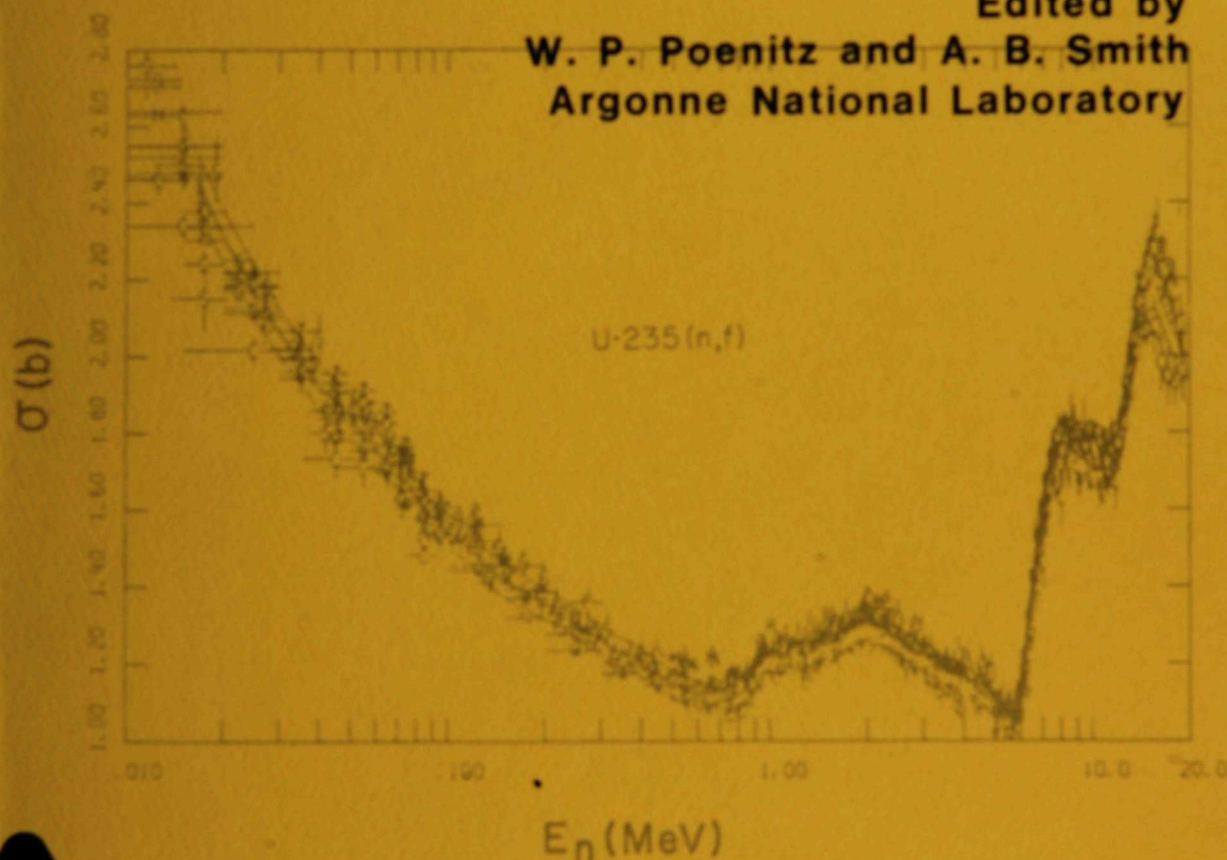
230086

Proce

**NEANDC/NEACRP Specialists Meeting on  
Fast Neutron Fission Cross Sections of  
U-233, U-235, U-238, and Pu-239**

**June 28-30, 1976, at Argonne National Laboratory**

**Edited by  
W. P. Poenitz and A. B. Smith  
Argonne National Laboratory**



BASE TECHNOLOGY



U.S. GOVERNMENT

**ARGONNE NATIONAL LABORATORY, ARGONNE, ILLINOIS**  
**Operated for the U. S. ENERGY RESEARCH**  
**AND DEVELOPMENT ADMINISTRATION**  
**under Contract W-31-109-Eng-38**

The facilities of Argonne National Laboratory are owned by the United States Government. Under the terms of a contract (W-31-109-Eng-38) between the U. S. Energy Research and Development Administration, Argonne Universities Association and The University of Chicago, the University employs the staff and operates the Laboratory in accordance with policies and programs formulated, approved and reviewed by the Association.

#### MEMBERS OF ARGONNE UNIVERSITIES ASSOCIATION

The University of Arizona	Kansas State University	The Ohio State University
Carnegie-Mellon University	The University of Kansas	Ohio University
Case Western Reserve University	Loyola University	The Pennsylvania State University
The University of Chicago	Marquette University	Purdue University
University of Cincinnati	Michigan State University	Saint Louis University
Illinois Institute of Technology	The University of Michigan	Southern Illinois University
University of Illinois	University of Minnesota	The University of Texas at Austin
Indiana University	University of Missouri	Washington University
Iowa State University	Northwestern University	Wayne State University
The University of Iowa	University of Notre Dame	The University of Wisconsin

#### NOTICE

This report was prepared as an account of work sponsored by the United States Government. Neither the United States nor the United States Energy Research and Development Administration, nor any of their employees, nor any of their contractors, subcontractors, or their employees, makes any warranty, express or implied, or assumes any legal liability or responsibility for the accuracy, completeness or usefulness of any information, apparatus, product or process disclosed, or represents that its use would not infringe privately-owned rights. Mention of commercial products, their manufacturers, or their suppliers in this publication does not imply or connote approval or disapproval of the product by Argonne National Laboratory or the U. S. Energy Research and Development Administration.

Printed in the United States of America  
Available from  
National Technical Information Service  
U. S. Department of Commerce  
5285 Port Royal Road  
Springfield, Virginia 22161  
Price: Printed Copy \$12.00; Microfiche \$2.25

---

ANL-76-90  
ERDA-MDC-5/L  
NEANDC(US)-199/L

---

ARGONNE NATIONAL LABORATORY  
9700 South Cass Avenue  
Argonne, Illinois 60439

*Proceedings of the NEANDC/NEACRP Specialists Meeting on*  
**FAST NEUTRON FISSION CROSS SECTIONS OF U-233, U-235, U-238, AND Pu-239**

*June 28-30, 1976, at Argonne National Laboratory*

Cosponsored by Argonne National Laboratory and  
the Organization of Economic Cooperation and Development

*Edited by*

W. P. Poenitz and A. B. Smith  
Argonne National Laboratory

## ORGANIZING COMMITTEE

C. D. Bowman, National Bureau of Standards  
J. C. Browne, Lawrence Livermore Laboratory  
H. E. Jackson, Argonne National Laboratory  
H. T. Motz, Los Alamos Scientific Laboratory  
S. Pearlstein, Brookhaven National Laboratory  
A. B. Smith, Argonne National Laboratory

## MEETING CHAIRMAN

A. B. Smith, Argonne National Laboratory

## SCIENTIFIC SECRETARY

W. P. Poenitz, Argonne National Laboratory

## EDITORS OF PROCEEDINGS

W. P. Poenitz, Argonne National Laboratory  
A. B. Smith, Argonne National Laboratory

## SESSION CHAIRMEN

### *Session I, Ratios*

B. C. Diven, Los Alamos Scientific Laboratory

### *Session II, Absolute*

H. Kuesters, Kernforschungszentrum Karlsruhe

### *Session III, Special Topics*

J. C. Browne, Lawrence Livermore Laboratory

### *Keynote Addresses, Summary Session*

A. B. Smith, Argonne National Laboratory

## WORKING GROUP SESSION CHAIRMEN

### *Group I, Ratios*

C. D. Bowman, National Bureau of Standards

### *Group II, Absolute Values*

R. W. Peelle, Oak Ridge National Laboratory

## ARRANGEMENTS

M. Holden, Argonne National Laboratory

## TABLE OF CONTENTS

### Page

### Welcome

C. E. Till

I

### Introduction

A. B. Smith

II

### Keynote Addresses

1

## THEORY AND APPLICATIONS OF FAST FISSION CROSS SECTIONS

1. Theory of Nuclear Fission : A Review

U. Mosel

3

2. The Importance of Fast Fission Cross Sections in Fast Reactors

E. M. Bohn and R. D. McKnight

31

### Session I

## FAST NEUTRON FISSION CROSS SECTION RATIOS

1. Measurements of Neutron-Induced Fission Cross-Section Ratios Involving Isotopes of Uranium and Plutonium

J. W. Behrens and G. W. Carlson

47

	<u>Page</u>
2. The Fission Cross Sections of Uranium and Plutonium Isotopes Relative to U-235 J. W. Meadows	73
3. Measurements of Neutron Induced Fission Cross Sections Ratios at the Karlsruhe Isochronous Cyclotron S. Cierjacks, B. Leugers, K. Kari, B. Brotz, D. Erbe, D. Groeschel, G. Schmalz, F. Voss	94
4. High Resolution Measurement of the U-238 to U-235 Fission Cross Section Ratio Between 2 MeV and 25 MeV. F. C. Difilippo, R. B. Perez, G. de Saussure, D. Olsen, R. Ingle	114
5. Fission Cross Section Ratio Measurement of U-238 to U-235 for Neutrons with Energies between 4.7 and 8.9 MeV C. Nordborg, H. Conde, L. G. Stroemberg	128
6. Measurements of U-238/U-235 Fission Cross Section Ratios in the Energy Range 2 - 7 MeV M. Cance, G. Grenier	141
7. The U-238/U-235 Fission Cross Section Ratio over the Energy Range 1.2 MeV to 2 MeV P.A.R. Evans, G. B. Huxtable, G. D. James	149
8. Comments on the Evaluation of Fission Cross Section Ratios for U-238 and Pu-239 to U-235 W. P. Poenitz and P. Guenther	154

## Session II

### Page

### ABSOLUTE CROSS SECTION VALUES

1. The Fission Cross Section of U-235 from 1 to 6 MeV  
D. M. Barton, B. C. Diven, G. E. Hansen, G. A. Jarvis,  
P. G. Koontz, and R. K. Smith 173
2. The U-235 Neutron Fission Cross Section Measurement  
at the NBS Linac  
O. A. Wasson 183
3. Measurement of the Neutron Induced Fission Cross  
Sections of Uranium-235 and Plutonium-239 in the  
MeV Energy Range  
I. Szabo and G. P. Marquette 208
4. Absolute Measurements of U-235 and Pu-239 Fission  
Cross Sections with Photoneutron Sources  
M. C. Davis, G. F. Knoll, J. C. Robertson 225
5. Absolute Measurement of 14.6 MeV Neutron Fission  
Cross Sections of U-235 and U-238  
M. Cance and G. Grenier 237
6. The U-235 and U-238 Neutron Induced Fission Cross  
Sections Relative to the H(n,n) Cross Section  
B. Leugers, S. Cierjacks, P. Brots, D. Erbe,  
D. Groeschel, G. Schmels, F. Voos 246
7. The Status of U-235 Fission as a Cross Section  
Standard  
C. W. Carlson and J. B. Czirr 258



	<u>Page</u>
6. The Energy Gap at the Saddle Point Deformation of U-236 F. Kaeppeler and F. Dickmann	391
7. What Happens to the Fission Process above the 2nd- and 3rd- Chance Fission Thresholds? L. Stewart and R. J. Howerton	398
8. An Ionization Chamber with Fast Timing Properties and Good Energy Resolution for Fission Fragment Detection C. Budtz-Jorgensen and H. H. Knitter	415
9. Requirements on Experiment Reporting to Meet Evaluation Needs R. W. Peelle	421
<u>Summary Session</u>	431
1. Report of the Working Group on Cross Section Ratios C. D. Bowman	433
Appendix	442
2. Report of the Working Group on Absolute Fission Measurements R. W. Peelle	450
<u>Concluding Remarks</u>	
A. B. Smith	465

## References

Subject Index	467
Author Index	468
List of Participants	470

## WELCOME

On the behalf of the Argonne National Laboratory and the NEACRP, I would like to welcome all of you to this Specialists Meeting on Fast Fission Cross Sections. Precise knowledge of these cross sections is essential to the development of nuclear power, and particularly to the fast reactor systems that are of primary interest here at Argonne. We hope that this gathering of outstanding specialists will help to more precisely identify the areas of fission cross section uncertainties and that your discussions will in time result in a far more precise knowledge of these vital quantities. The importance of such basic cross section information was brought home to me again at the NEACRP Meeting of the past week where the discussions indicated to me that the Reactor Physics Community is giving more attention to basic differential data than has been the case for many years. We want your stay here to be both productive and pleasant and we will do our best to help you achieve these ends in any way we can.

Dr. C. E. Till

Director, Applied Physics Division, Argonne National Laboratory

U. S. Member of the NEACRP

## INTRODUCTORY REMARKS

This Specialists Meeting was conceived to assess the contemporary status of the fast-neutron-fission cross sections of  $^{233}\text{U}$ ,  $^{235}\text{U}$ ,  $^{238}\text{U}$  and  $^{239}\text{Pu}$ , and associated problems, in both relative and absolute contexts. Somewhat more than a year ago, at the Conference on Nuclear Cross Sections and Technology<sup>a</sup>, it became evident that world-wide fission-cross-section efforts were coming to a focus. It seemed likely that within a year a wealth of new and precise experimental information would be available. That has occurred and the present Specialists Meeting addressed those new, as well as prior results; identifying contemporary accuracies, consistencies and discrepancies; discussing methods, techniques and theoretical capability; and recommending future efforts. The meeting was encouraged and endorsed by both the NEANDC and NEACRP. NEA member states were widely represented by the attendees including those interested in both the microscopic cross sections and their applications.

The promise of this meeting was partly realized before it convened as a large body of new information was made available by attendees prior to their arrival. This material together with previous information now forms a Fast-Neutron-Fission Cross Section Data File of unique coverage and quality. It provided an essential foundation for the discussions at the meeting and will be of continued high value for a wide range of subsequent studies including measurements, evaluations and applied calculations. The meeting consisted of two major sections: 1) review and research papers and 2) two technical-study sessions. The former, with the associated discussions, are a major portion of these proceedings. The results of the technical-study sessions were summarized by the session chairmen respectively addressing the areas of fission-cross-section ratios and of absolute fission cross sections (primarily those

---

a. Proc. of the Conf. on Nuclear Cross Sections and Technology, National Bureau of Standards, NBS-Special Publication 425 (1975).

of  $^{235}\text{U}$ ). The two technical areas are intimately related. This was reflected in the discussions associated with both the research papers and the summaries of the technical-study sessions as recorded in these proceedings. It is the hope of the Organizing Committee and the Chairman that the meeting and the proceedings will provide a comprehensive summary of this essential cross section field that will stimulate and guide both microscopic measurement programs and applied uses of fission cross sections. The proceedings are dedicated to these goals.

The Organizing Committee is very much indebted to Drs. C. Bowman and R. Peelle for their able direction of the technical-study sessions. The Committee is also indebted to the Scientific Secretary, Dr. W. Poenitz, for his comprehensive technical and administrative contributions that were essential to the meeting.

Argonne, July 1976

A. B. Smith, Chairman



*Keynote Addresses*

**Theory and Applications  
of Fast Neutron Fission Cross Sections**



# THEORY OF NUCLEAR FISSION: A REVIEW

U. Mosel

Institut für Theoretische Physik, Universität Giessen,  
63 Giessen, Germany

## ABSTRACT

General properties of nuclear fission are reviewed and related to our present knowledge of fission theory. For this purpose the basic reasons for the shape of the fission barriers are discussed and their consequences compared with experimental results on barrier shapes and structures. Special emphasis is put on the asymmetry of the fission barriers and mass-distributions and its relation to the shells of the nascent fragment shells. Finally the problem of calculating fission cross sections is discussed.

## INTRODUCTION

The process of nuclear fission in which a nucleus splits usually into two parts is the most violent change a nuclear many-body system may undergo. The complexity of this process due to the large number of particles involved has necessitated the use of macroscopic approximation methods in the many-body treatment. These macroscopic methods, mainly the use of the liquid drop model (LDM), have led to a very physical description of the process that can easily be visualized as a split of a charged liquid drop into two halves [1].

The LDM describes fission as the result of a competition between the deforming Coulomb force and the surface energy that favors a spherical shape. Since the work of Bohr and Wheeler [2] and of Swiatecki [2] it is well-known that this model gives a good average description of nuclear fission. However, the elaborate LDM calculations by Nix [3] have also shown the limitations of this model: one of the most dominant features of fission in the actinide region, namely the mass asymmetry, could not be reproduced by the LDM.

Besides this failure several other experimental facts have always pointed to the possible influence of shell effects in nuclear fission, namely the sawtooth-structure of the fragment excitation energies with a minimum at  $A \sim 132$ , the peak of the kinetic energy distributions at the double magic nucleus  $^{132}\text{Sn}$  and the remarkable constancy of the heavy

fragment mass peak at  $A \sim 138$ , with all three properties being independent of the mass of the fissioning nucleus. These results were summarized by H.W. Schmitt in his 1968 Vienna paper [4]. The first two properties can qualitatively be understood on the basis of a simple scission configuration model developed by Terrell, Vandenbosch [5] and Schmitt [4]. Since the doubly magic nucleus  $^{132}\text{Sn}$  is very stiff a mass split involving this nucleus will consist of a nearly spherical Sn-nucleus and a rather elongated second fragment at scission. The excitation energy - believed to be mainly deformation energy - of the Sn nucleus will thus be small and the Coulomb repulsion energy due to the closer distance between the charge centers of the two fragments will be large. Thus the minimum of  $E_x$  and the corresponding maximum of  $E_k$  at  $A \sim 132$  are easily understood in this model that is entirely based on the fragment shell structures. It is, however, also clear that the peak of the mass-distribution at  $A \sim 138 - 140$  does not fit into this simple picture.

It has always been an intriguing question how and when fragment shells form during the fission process and what their relation to the shells of the compound nucleus is. This question became especially interesting when Myers and Swiatecki [6] demonstrated the close relationship between shells, i.e. zones of low single particle level density at the Fermi-surface, and extra nuclear binding and when Strutinsky [7] showed that this connection is a general phenomenon not confined to spherical nuclei. This latter finding demonstrated that strong shells may appear at quite large deformations and may have drastic consequences for the structure of the total energy of a nucleus under deformation like, e.g. causing second minima in the potential energy surface. These shells around the fission barrier might thus help to bridge the large gap in deformation space between the shells of the fissioning nucleus and those of the fragments.

The outline of this article is as follows: In the second part we will briefly review the technicalities of calculating potential energy surfaces, i.e. mainly the shell correction method. It will also contain information on the general connection between deformations and shells. In part III results of calculations for fission barriers are compared with experiment. Special emphasis will be put on the (simplified) question whether the mass-asymmetry of low-energy nuclear fission is dominated by the structure of the fissioning nucleus or by that of the fragments. In part IV finally we will discuss the effects of a double hump in the fission barrier on fission probabilities as well as our present abilities to calculate fission cross sections.

#### SHELL CORRECTION METHOD AND DEFORMED SHELLS

Some of the first calculations of potential-energy surfaces with the purpose of determining nuclear ground state deformations were undertaken by Nilsson who simply summed up single particle energies [8]. The results of these calculations were surprisingly good [8].

It, therefore, came somewhat as a surprise that this same procedure failed when applied to a potential containing also a neck-in degree of freedom [8]. The reasons for this failure have been understood since then:

They are the inadequacy of the volume-conservation constraint and the wrong asymptotic behavior of the Nilsson-model at large deformations which does not allow for a separation of the nucleus into two parts [9]. Whereas the latter restriction can be dropped by use of two-center potentials (see part III) the question of volume conservation, or equivalently self-consistency, does not allow an easy answer.

Since, however, the bulk-properties of nuclei are on the average described rather well by the liquid drop model it is natural to look for a hybrid approach that combines the good description of average properties of nuclei like, e.g., ground state binding energies and fission barriers, with a model that contains the effects of deformed shells, like a deformed shell model. Such a hybrid approach has become known as the "macroscopic-microscopic" or the "shell-correction" method [10].

The first attempts to calculate shell corrections to the LDM were undertaken by Myers and Swiatecki [6] who calculated ground state shell corrections on the basis of a schematically bunched single particle model. The breakthrough, however, came only when Geilikman [11] and Strutinsky [7] realized that the existence of shells, i.e. large gaps in the single particle level schemes, is a general phenomenon not restricted to zero deformation.

The Strutinsky method to calculate the shell corrections is nowadays well understood and has been reviewed by several authors [12]. Furthermore, with the help of self-consistent calculations the accuracy of the method has now been tested [13]. It was found to be of the order of about 0.5-1.0 MeV to be compared with the total shell correction in the range of 0-12 MeV at the ground state and about 2-3 MeV at the saddlepoint.

The shell models used to generate the shell corrections for nuclear fission have to fulfill the basic requirement that they are able to describe the shells of the fissioning nucleus as well as those of the final fragments. Three general types of such models exist: a) the folded Yukawa model in which a Yukawa-force is folded with a uniform, deformed density [14], b) the deformed Woods-Saxon model [15] and c) a modified two center harmonic oscillator model [16] [17]. All three depend on a set of shape-parameters  $\alpha$  that specify a family of nuclear shapes suitable for fission. The total potential energy surface (PES) is then written as:

$$E(\alpha) = E_{\text{LDM}}(\alpha) + \delta U(\alpha) + E_p(\alpha)$$

where  $E_p$  stands for the pairing energy generated in the usual BCS formalism and  $\delta U$  represents the shell correction energy.

One should finally mention that recently self-consistent calculations for fission barriers have been performed by Flocard et al. [18] using the Skyrme force and by Kolb et al. [19] employing a self-consistent K-matrix model. However, as these calculations are still in an exploratory stage and since the results are not nearly as good as those obtained with the Strutinsky-method they will not be discussed any further.

Before going into a detailed comparison of calculated fission barriers with experimental values it is worthwhile to point out some regularities in the appearance of shells along the deformation degree of freedom. It has first been noted by Geilikman [11] that the spectrum of a deformed harmonic oscillator model shows at specific deformations strong degeneracies of the single particle levels. This is the case always when the ratio of the two frequencies of an axially symmetric oscillator is equal to that of two integers. Thus whenever the ratio of axes of an ellipsoidal nucleus becomes a rational number shells do appear (see Fig. 1). Since shells correspond to extra binding relative to the LDM smooth background energy, they are associated with negative values of the shell corrections  $\delta U$ .

These same shells persist in more refined models, like e.g., a deformed Woods-Saxon potential. They thus lead to an oscillatory structure of  $\delta U$  vs.  $\hat{\alpha}$ . If these oscillations occur at a deformation at which the underlying LDM energy is flat the shell corrections can cause second minima and maxima in the fission barriers. In Wong's notation the (1:1) shell is responsible for the existence of spherical nuclei, the ground states of the rare earth and actinide nuclei originate in the (3:4) shell and the (1:2) shell leads to the existence of shape isomeric states [20]. (The numbers give the ratio of minor to major axis in an ellipsoidal shape). It was recently pointed out by Schultheiss et al. that at these same deformations strong cluster structures should be present [21]. It will be interesting to see the general connection between this picture and the geometrical properties as discussed above.

## FISSION BARRIERS, COMPARISON WITH EXPERIMENT

Properties of the Barrier. Experimental information on barrier parameters like the height of the two humps, the relative energy of the second minimum and the widths of the barriers can be obtained from direct reaction studies giving the fission probability as a function of excitation energy combined with measurements of fission isomer excitation functions [22]. In these experiments a direct reaction is used to produce an excited nucleus and the branching ratio for decay by fission either directly or from the isomeric state relative to other decay modes is measured. These branching ratios can then be analyzed by means of a statistical model into which the barrier properties enter through the barrier-penetrability. A comparison of barrier and isomer energies with theoretical values is given in Fig. 2. The theoretical values have been obtained in three independent calculations which differ mainly in the single particle models used. Asymmetric degrees of freedom for the second barrier (see next section) as well as axially asymmetric deformations for the first barrier have been included.

The average discrepancy between theory and experiment is of the order of 1-2 MeV (remember, that the Strutinsky method itself has an inaccuracy of about 1 MeV!). The most serious disagreement appears for Th- and the light U-isotopes. In spite of two somewhat speculative explanations of these discrepancies either in terms of a third minimum or the dynamic barrier [44] the Th-anomaly is still unexplained.

If the picture of a double humped barrier is indeed correct then there should also be a  $\gamma$ -decay from the first isomeric minimum through the first barrier down to the ground state. Indeed in 1973 the existence of such a  $\gamma$ -ray was demonstrated by Russo et al. [23] for the case of  $^{234}\text{U}$ . This measurement has yielded the first direct information on the excitation energy of a shape isomer (2.56 MeV).

The experimental informations described so far depend only on the energies of maxima or minima of the PES but not on their deformation. That the fission isomers were indeed due to shape isomerism was demonstrated by Specht et al. who succeeded in identifying a rotational band built on the shape isomeric ground state [24]. The moment of inertia of this band is about twice of that of the gs-band and represents the largest moment of inertia ever found for nuclei thus confirming - at least in an indirect way - the larger deformation of the fission isomer (see Fig. 3).

Recently Habs, Metag and Specht [55] were also able to measure the lifetime of the rotational states in the second minimum. Since in the rotational model the BE2 value is directly connected with the quadrupole moment the nuclear deformation can directly be obtained in this way. It is found that this quantity as measured by the ratio of axes of an axially symmetric spheroid is 2:1 in agreement with the predictions given earlier on the basis of a schematic single particle model.

Besides this measurement of a rotational band also a spectroscopy of single particle excitations in the second minimum has now begun. The first results on this point were obtained by Vandenbosch and co-workers [25] who derived from measurements of isomer excitation functions and their dependence on angular momentum of the compound nucleus the energy-difference and possible spin assignments for two isomeric states in  $^{237}\text{Pu}$ . Recently also anisotropies in the fragment angular distributions [26] as well as magnetic moments of these states obtained in measurements of the spin precession in an external magnetic field [27] have been obtained in order to determine the quantum numbers of the states in the second minimum.

**Mass Asymmetry.** The predominantly asymmetric mass split in low energy nuclear fission has been known since a long time as well as the fact that lighter nuclei around Pb fission symmetrically [1]. Only rather recently our knowledge on this point has been broadened by mass distribution measurements both on the low A and the high A side of the actinide region. For the former region it was demonstrated by Konecny et al. that the triple-humped mass distribution observed for the Ra-region is indeed genuine and not due to a super-position of first and second chance fission of different compound nuclei at different excitation energies [28].

For the upper end of presently known nuclei mass-distribution measurements have been performed for the heavy Pm-isotopes [29-32]. These measurements that will be discussed in some more detail later on have shown a transition from mass-asymmetry back to a surprisingly sharp mass distribution as obtained in the spontaneous fission of  $^{259}\text{Pm}$  obtained by a (t,p) reaction on a  $^{257}\text{Pm}$  target. Schematically this transition and the different types of mass distributions are shown in Fig. 4 that also illustrates their excitation energy dependence.

As a more quantitative measure of the transition from asymmetry to symmetry in this region may serve the peak to valley ratios of the mass distributions for some representative nuclei shown in Table I.

Turning now to the theoretical description of these phenomena one has to discuss the behavior of the PES under asymmetric deformations.

Müller and Nilsson [33] were the first to demonstrate the instability of the second barrier against  $(Y_3, Y_5)$  type deformations. Since then their finding has been confirmed by several other groups. Fig. 5 shows the calculated energy differences between symmetric and asymmetric saddle points. Fig. 6, comparing the calculated asymmetries at the second saddle point with experiment, shows a rather good semiquantitative description of the absolute magnitude and the A-dependence.

Representative for all these results is the PES for  $^{236}\text{U}$  shown in Fig. 7 as obtained by Mustafa et al. [17]. This PES is a result of a full four dimensional calculation in which the surface has been traced as a function of two symmetric and two asymmetric shape coordinates. For the sake of making an illustration possible the PES has been minimized for a given  $(D, \lambda)$  point with respect to the two other parameters. A priori, however, it is not self-evident that the dynamics of the fission process necessarily follow this lowest energy path (see Section IV). However, the experimentally observed appearance of strong fragment shells in fragment excitation and kinetic energies at least gives a strong indication for the physical significance of the minimization performed.

Fig. 7 shows that an asymmetrically deformed barrier at  $D \sim 5$  fm appears at a mass-division of  $A_H/A_L \sim 146/90$  and that from there on a valley runs down all the way to scission to a slightly smaller asymmetry of  $A_H/A_L \sim 140/96$  in accord with the experimentally observed peak of the mass distribution.

The fact that a continuous valley extends down from the saddle to scission makes it difficult to interpret the origins of this valley in terms of compound or fragment shells alone (one has to remember that at the second saddle point the nucleus is hardly necked-in at all). An analysis of the single particle energies clearly shows that for  $D \sim 2.5$  fm the fragments are well preformed (at symmetry always two states with different parity become nearly degenerate). However, for larger D this point is difficult to decide from the energies alone.

A study by Andersen, however, has shown that the appearance of the shell that is responsible for the asymmetry at the second barrier can be traced back directly to fragment shell properties [33]. In this particular case the shell is due to a repulsion between two single particle states with a low number of nodes in z-direction [35]. These states are most sensitive to the formation of a central barrier between the two nascent fragments in the single particle potential. This finding by Andersen thus continuously links the mass-asymmetry as early as at the second saddle to the shells of the final fragments.

The argument above shows that as soon as the necking-in causes a

central barrier in the s.p. potential a clustering of states will set in. This finding may thus possibly provide the first microscopic evidence for the basic assumption of the cluster model of nuclear fission [36].

Turning now to the two ends of the actinide region one may say that for the mass-distributions in the Ra-region no satisfactory description exists so far [37]. However, the transition back to mass-symmetry in the heavy Pu isotopes found by groups from Argonne, Livermore and Los Alamos can be well described by two-center model calculations (the only ones performed for these nuclei all the way to scission) [17,29].

The comparison of the two results for  $^{251}\text{Pu}(n,f)$  and  $^{251}\text{Pu}(s,f)$  is particularly interesting. As theoretical calculations predict a lowering of the asymmetric saddle by only about 0.1 MeV (compared to 3.3 MeV for Uranium) [38] the excitation energy in the (n,f) reaction should be sufficient to wash out this small difference [39]. That the experimentally found asymmetry, however, still persists in this case points to the influence of the PES between saddle and scission on the mass distribution. In other words: the saddle point shape alone does not determine the mass distribution. Calculations by Mustafa et al., using the modified two center harmonic oscillator model, indeed have predicted the correct behavior in terms of fragment shell influences closer to scission as shown in Fig. 8 [17,40]. A predominance of fragment shells in this particular case of the Pu-isotopes is indeed to be expected as the nucleus  $^{264}\text{Pu}$  can split symmetrically into two doubly magic fragment nuclei  $^{132}\text{Sn}$ . On the basis of these fragment shells it was predicted that the fragment kinetic energies should reach a maximum in the heavy Pu-isotopes and that at the same time the fragment excitation energies go to a minimum [41].

This prediction deviates drastically from all smooth LDM systematics that describe rather well the energetics of the fission of the lighter actinides. It is a typical fragment shell effect in which the special doubly magic structure of the two nascent fragment clusters is felt very early in the descent from saddle to scission. As doubly magic nuclei have a strong preference for spherical shapes, the fragments in the symmetric fission of  $^{264}\text{Pu}$  are expected to be little deformed at scission. This then causes a high Coulomb repulsion leading to large kinetic energies and low fragment excitation energies.

The prediction of a maximum of  $E_k$  and a corresponding minimum of  $E_x$  around  $^{264}\text{Pu}$  has recently been supported by new experiments on the Pu isotopes, 256,257,258 and 259. The data show indeed a significant increase in the kinetic energy and a dip in the excitation energies (see Fig. 9 and 10). [41,42].

Summarizing this section, one can state that overall the theoretical predictions using the Strutinsky shell correction method have been very successful. Major difficulties exist for a correct description of the inner barriers of the Th-isotopes and for an understanding of the excitation-

energy dependence of the mass-distributions in the Ra-region [28]. The mass distributions in the U-region are mainly determined by fragment shell properties as the saddle point shells are strongly influenced by a clustering of s.p. states that go continuously over into the fragment states. For the Fm-isotopes the predominance of the fragment-shell influence is undisputed because of the special fragment structure there. Experimentally this is confirmed by the sudden change of the mass distributions, taken together with an irregular behavior of the fragment kinetic and excitation energies in this region.

### FISSION CROSS SECTIONS

If the process of nuclear fission proceeds through a compound-nucleus the fission cross section is given by (see e.g., Ref. [1]):

$$\sigma_f = \sigma_c \cdot \frac{\Gamma_f}{\Gamma_{\text{tot}}} \quad (5.1)$$

where  $\Gamma_f$  is the fission width,  $\Gamma_{\text{tot}}$  the total decay width and  $\sigma_c$  the compound nucleus formation cross section. The fission width  $\Gamma_f$  is proportional to the number of open channels at the saddle point if the lifetime of the decaying nucleus is so long that the fission channel is randomly populated:

$$\Gamma_f = \frac{1}{2\pi\rho(E)} \cdot \int_0^{E-E_s} \rho_s(E') dE' \quad (5.2)$$

Here  $\rho_s$  is the level-density at the saddle point whose energy is given by  $E_s$ . The quantity  $\rho$  gives the level density at the equilibrium deformation.

If one furthermore assumes that also the neutron decay can be described by the statistical expression [1]:

$$\Gamma_n = \frac{1}{2\pi\rho(E)} \cdot \frac{4\pi}{h^2} \int_0^{E-B_n} \sigma_{\text{inv}} \rho_r(E') dE' \quad (5.3)$$

with  $\rho_r$  being the level-density of the residual nucleus after neutron evaporation,  $B_n$  being the neutron binding energy and  $\sigma_{\text{inv}}$  the cross section for neutron absorption, then the total width and from it the fission probability can be calculated.

Up to about five years ago studies along these lines have used Fermi-gas level-densities in the expressions above. The level-density parameter and the fission barrier height were treated as free parameters and extracted from fits to the data (for a review see Ref. [1]).

By using methods of statistical physics, the level-densities can, however, also be calculated from microscopic single particle energies [45, 46]. Since the preceding sections have shown that the predictions of fission-barrier properties by microscopic models are quite successful it is

tempting to obtain both  $\Gamma$  and  $\rho(E)$  from the same microscopic models thus making a consistent, parameter-free calculation of fission probabilities possible [47]. An example for such a calculation is shown in Fig. 11. It is seen that the model predicts the correct slopes of  $\Gamma_0/\Gamma$ . However, the uncertainties in the fission barrier heights appear in the exponents in the level-density, become thus magnified and can lead to quite drastic deviations in  $\Gamma_0/\Gamma$ . In similar calculations for actinide nuclei only the level-densities have, therefore, been taken from microscopic calculations whereas the barrier-heights have been treated as free parameters to be determined from a fit to direct-reaction data [22,48].

The presence of a double hump in the fission barrier has a marked effect on fission probabilities: resonances in this quantity will appear at excitation energies corresponding to a  $\beta$ -vibrational state (assumed to be the fission degree of freedom) in the second minimum (see Fig. 12). The earliest example for such a resonance is seen in the neutron-induced fission of  $^{238}\text{Th}$  [49]. As seen in Fig. 13 the peak in the fission cross section at a neutron energy of 720 keV rises more than an order of magnitude above the smooth part of the cross section (instrumental resolution  $\sim 5$  keV, peak width  $\sim 14$  keV). Very recently it has been reported by Blons et al. [56] that a fine structure in this resonance could be observed corresponding possibly to a rotational band on top of the  $\beta$ -vibrational resonance.

Similar resonances have also been seen in a number of direct reactions. All these states lie close to the top of the fission barrier near 5 MeV excitation. In order to confirm the character of this resonance as a  $\beta$ -vibration it is desirable a.) to find other resonances close by which correspond to other collective vibrations, e.g. octupole, orthogonal to the fission degree and which are built on the  $\beta$ -vibration and b.) to discover other  $\beta$ -vibrational resonances, i.e. other members of this type of vibration, at lower excitation.

Both aims have been achieved in recent experiments by P. Paul and collaborators in (d,pf) experiments [50,51]. An example is the case of  $^{240}\text{Pu}$  which is illustrated in Fig. 14. One sees that at  $\sim 4.5$  MeV of excitation the otherwise steeply rising cross section levels off corresponding to a 0<sup>+</sup>  $\beta$ -vibrational resonance with other states built on it. The fission probability then steeply rises again until it reaches the next vibrational resonance at 5 MeV which again has several other bands built on it. The great value that lies in such an experiment is that it allows one to determine the energy of a  $\beta$ -vibrational phonon ( $\sim 0.5$  MeV in this case) thus giving more detailed information on the structure of the potential energy surface in the second minimum and simultaneously confirming directly the vibrational character of the resonance.

The existence of rather sharply defined vibrational resonances implies that the coupling to intrinsic single particle states in the second well is small. This is reasonable since e.g. in the case of  $^{239}\text{Pu}$  (d,pf) discussed above the vibrational resonance at 4.5 MeV corresponds to only about 2.0 MeV excitation energy in the second minimum (bottom of second well in  $^{238}\text{U}$  at 2.56 MeV, see Sect. III).

At higher energies, i.e. around the neutron binding energy for example, however, there will be a strong coupling of  $\beta$ -vibrational resonances in the first well and moderate coupling in the second well. This means that the fission probability will spread out over many resonances grouped around the  $\beta$ -vibrational states in the second well and originating in the coupling of the vibrational state to intrinsic states the second well. Each of these intermediate structure resonances will then also show a fine structure due to the coupling to the much denser states in the first well. The most famous example for this situation is the experiment by Migneco and Theobald done at Geel [52,53]. That the many fission resonances indeed can be interpreted in the picture given above was further confirmed by a measurement of the individual spins of the resonances within one group in the case of  $^{237}\text{Np}(n,f)$ . It was shown by Keyworth et al. [54] that all these resonances within an intermediate structure group have indeed the same spin as predicted by the coupling model discussed above. Statistical tests on the  $^{235}\text{U} + n$  fission cross sections have recently shown that also in this system fluctuations in the neutron-cross sections can be explained in terms of fission-probability enhancement due to the presence of states in the second minimum [57].

#### REFERENCES

1. R. VANDENBOSCH and J. R. HUIZENGA, "Nuclear Fission", Academic Press, New York and London, 1973.
2. N. BOHR and J. A. WHEELER, *Phys. Rev.* 56 (1939) 426 S. COHEN and W. J. SWIATECKI, *Ann. Phys. (N.Y.)* 19 (1962) 67.
3. J. R. NIX, *Nucl. Phys.* A130 (1969) 241.
4. H. W. SCHMITT, *Proc. Int. Symp. on Physics and Chemistry of Fission*, Salzburg, Vol. II (IAEA, Vienna 1965), p. 3 R. VANDENBOSCH, *Nucl. Phys.* 46 (1963) 129.
5. J. TERELL, *Proc. Int. Symp. on Physics and Chemistry of Fission*, Salzburg, Vol. II (IAEA, Vienna, 1965), p. 3 R. VANDENBOSCH, *Nucl. Phys.* 46 (1963) 129.
6. W. D. MYERS and W. J. SWIATECKI, *Proc. Int. Symp.*, "Why and How Should We Investigate Nuclides far off the Stability Line", Lysekil, Sweden, 1966, *Ark. Fys.* 36 (1967) 343.
7. V. M. STRUTINSKY, *Nucl. Phys.* A95 (1967) 420; A122 (1968) 1.
8. S. G. NILSSON, *Kgl. Dan. Vidensk. Selsk. Mat. Fys. Medd.* 29 (1955), no. 16.  
C. GUSTAFSON, I. L. LAMM, B. NILSSON and S. G. NILSSON, *Lysekil Symposium*, *Ark. Fys.* 36 (1967) 613.
9. P. HOLZER, U. MOSEL and W. GREINER, *Nucl. Phys.* A138 (1969) 241.
10. M. BOLSTERLI, E. O. FISET, J. R. NIX and J. L. NORTON, *Phys. Rev.* C5 (1972) 1050.  
J. R. NIX, *Ann. Rev. Nucl. Sci.* 22 (1972) 65.
11. B. T. GEILIKMAN, *Proc. Int. Conf. on Nuclear Structure*, Kingston, 1960

(Univ. of Toronto Press, Toronto, 1960), p. 874.

12. W. H. BASSICHIS, A. K. KERMAN, C. F. TSANG, D. R. TUERPE and L. WILETS in: "Magic Without Magic: John Archibald Wheeler", Freeman, San Francisco, 1972.
13. M. BRACK and P. QUENTIN; *Proc. 3rd Symp. on the Physics and Chemistry of Fission*, Rochester 1973 (IAEA, Vienna, 1974), p. 231.  
W. H. BASSICHIS, D. R. TUERPE, C. F. TSANG and L. WILETS, *Phys. Rev. C8* (1973) 480.
14. P. MÖLLER and J. R. NIX, *Rochester Fission Conf. Proc.* [13] p. 103.
15. H. C. PAULI, *Phys. Rep.* 7 (1973) 35.
16. D. SCHARNWEBER, U. MOSEL and W. GREINER, *Nucl. Phys.* A164 (1971) 257;  
M. G. MUSTAFA, U. MOSEL and H. W. SCHMITT, *Phys. Rev. Lett.* 28 (1972) 431;  
B. SLAVOV and A. FAESSLER, *Z. Physik* 271 (1974) 161.
17. M. G. MUSTAFA, U. MOSEL and H. W. SCHMITT, *Phys. Rev.* C7 (1973) 1519.
18. H. FLOCARD, P. QUENTIN, D. VAUTHERIN and A. KERMAN, *Rochester Fission Conf. Proc.* [13], p. 221.
19. D. KOLB, R. Y. CUSSON and H. W. SCHMITT, *Phys. Rev.* C10 (1974) 1529.
20. C. Y. WONG, *Phys. Lett.* 32B (1970) 668 and Private Communication.
21. H. SCHULTHEIS, R. SCHULTHEIS and K. WILDERMUTH, *Phys. Lett.* 53B (1974) 325.
22. B. B. BACK, O. HANSEN, H. C. BRITT and J. D. GARRETT, *Rochester Fission Conf. Proc.* [13], p. 3,25.
23. P. A. RUSSO, J. PEDERSEN and R. VANDENBOSCH, *Rochester Fission Conf. Proc.* [13], p. 271.
24. H. J. SPECHT, J. WEBER, E. KONECNY and D. HEUNEMANN, *Phys. Lett.* 41B (1972) 43.
25. P. A. RUSSO, R. VANDENBOSCH, M. MEHTA, J. R. TESMER and K. L. WOLF, *Phys. Rev.* C3 (1971) 1595.
26. H. J. SPECHT, E. KONECNY, J. WEBER and C. KOZHUHAROV, *Rochester Fission Conf. Proc.* [13], p. 285.
27. R. KALISH, B. HERSKIND, J. PEDERSEN, D. SHAKLETON and L. STRABO, *Phys. Rev. Lett.* 32 (1974) 1009.
28. E. KONECNY, H. J. SPECHT and J. WEBER, *Rochester Fission Conf. Proc.* [13] II, p. 3.

29. R. C. RAIGINI, E. K. HULET, R. W. LOUGHEED and J. WILD, *Phys. Rev.* C9 (1974) 47.
30. J. P. BALAGNA, G. P. FORD, D. C. HOFFMAN and J. D. KNIGHT, *Phys. Rev. Lett.* 26 (1971) 145.
31. J. P. UNIK, J. E. GINDLER, L. E. GLENDENIN, K. F. FLYNN, A. GORSKI and R. K. SJOBLUM, *Rochester Fission Conf. Proc.* [13] II, p. 19.
32. D. C. HOFFMAN, J. WEBER, J. B. WILHELMY, E. K. HULET, J. H. LANDRUM, R. W. LONGHEED and J. F. WILD, LASL Rep. LA-UR 76-1055; D. C. HOFFMAN, LASL Rep. LA-UR-76-1151.
33. P. MÖLLER and S. G. NILSSON, *Phys. Lett.* 31B (1970) 283.
34. B. L. ANDERSEN, *Phys. Lett.* 42B (1972) 307.
35. F. DICKMANN and K. DIETRICH, *Proc. 2nd Int. Symp. on the Physics and Chemistry of Fission*, (IAEA, Vienna, 1969) p. 25.
36. H. FAISSNER and K. WILDERMUTH, *Phys. Lett.* 2 (1962) 212.  
H. FAISSNER and K. WILDERMUTH, *Nucl. Phys.* 58 (1964) 177.
37. H. J. SPECHT, *Lecture Notes, Seventh Polish Summer School on Nuclear Physics*, Mikolajki, 1974.
38. P. MÖLLER, *Nucl. Phys.* A192 (1972) 529.
39. C. F. TSANG and J. B. WILHELMY, *Nucl. Phys.* A184 (1972) 417.
40. M. G. MUSTAFA, *Phys. Rev.* C11 (1975) 1059.
41. H. W. SCHMITT and U. MOSEL, *Nucl. Phys.* A186 (1972) 1.
42. J. P. BALAGNA, J. A. FORELL, G. P. FORD, A. HEMMENDINGER, D. C. HOFFMAN, L. R. VEESER, J. B. WILHELMY, *Rochester Fission Conf. Proc.* [13] II, p. 191.
43. M. BRACK, J. DAMGAARD, H. C. PAULI, A. S. JENSEN, V. M. STRUTINSKY, C. Y. WONG, *Rev. Mod. Phys.* 44 (1972) 320.
44. H. C. PAULI and T. LEDERGERBER, *Rochester Fission Conf. Proc.* [13], p. 463.
45. J. R. HUIZENGA and L. G. MORETTO, *Ann. Rev. Nucl. Sci.* 22 (1972) 427.
46. L. G. MORETTO, *Rochester Fission Conf. Proc.* [13], p. 329.
47. R. VANDENBOSCH and U. MOSEL, *Phys. Rev. Lett.* 28 (1972) 1726.
48. A. GAVRON, H. C. BRITT, E. KONECNY, J. WEBER and J. B. WILHELMY, *Phys. Rev.* C13 (1976) 2374.

49. G. D. JAMES, J. E. LYNN and L. G. EARWAKER, *Nucl. Phys.* A189 (1972) 225.
50. P. D. GOLDSTONE, F. HOPKINS, R. E. MALMIN and P. PAUL, *Phys. Rev. Lett.* 35 (1975) 1141.
51. P. D. GOLDSTONE, F. HOPKINS, R. E. MALMIN, P. VON BRENTANO and P. PAUL, *Phys. Lett. B* (1976) in print.
52. E. MIGNECO and J. P. THEOBALD, *Nucl. Phys.* A112 (1968) 603.
53. H. WEIGMANN, *Z. Physik* 214 (1968) 7.
54. G. A. KEYWORTH, J. R. LEMLEY, C. E. OLSEN, F. T. SEIBEL, J. W. T. DABBS and N. W. HILL, *Rochester Fission Conf. Proc.* [13] I, p. 85.
55. D. HABS, V. METAG and H. J. SPECHT, private communication.
56. J. BLONS, C. MAZUR and D. PAYA, *Phys. Rev. Lett.* 35 (1976) 1749.
57. G. A. KEYWORTH, M. S. MOORE and J. D. MOSES, LASL Rep. LA-UR 76-1318, paper presented at this meeting.
58. J. D. CRAMER and J. R. NIX, *Phys. Rev.* C2 (1970) 1048.

TABLE I

Characteristics of Mass Distributions in High-Z Nuclei.

<u>Nucleus</u>	<u>Reaction</u>	<u>Mass-Distribution</u>	<u>Peak/Valley</u>	<u>Reference</u>
$^{252}\text{Cf}$	sf	Asymm	$\gtrsim 600$	31
$^{254}\text{Fm}$	sf	Asymm	$\gtrsim 60$	31
$^{255}\text{Fm}$	(nf)	Asymm	$\gtrsim 2.5$	29,31
$^{256}\text{Fm}$	(sf)	Asymm	$\gtrsim 12$	31
$^{257}\text{Fm}$	(sf)	Asymm	$\gtrsim 1.5$	30
$^{257}\text{Fm}$	(n,f)	Broadly symm	-	29,30
$^{259}\text{Fm}$	(sf)	Sharply symm	-	32

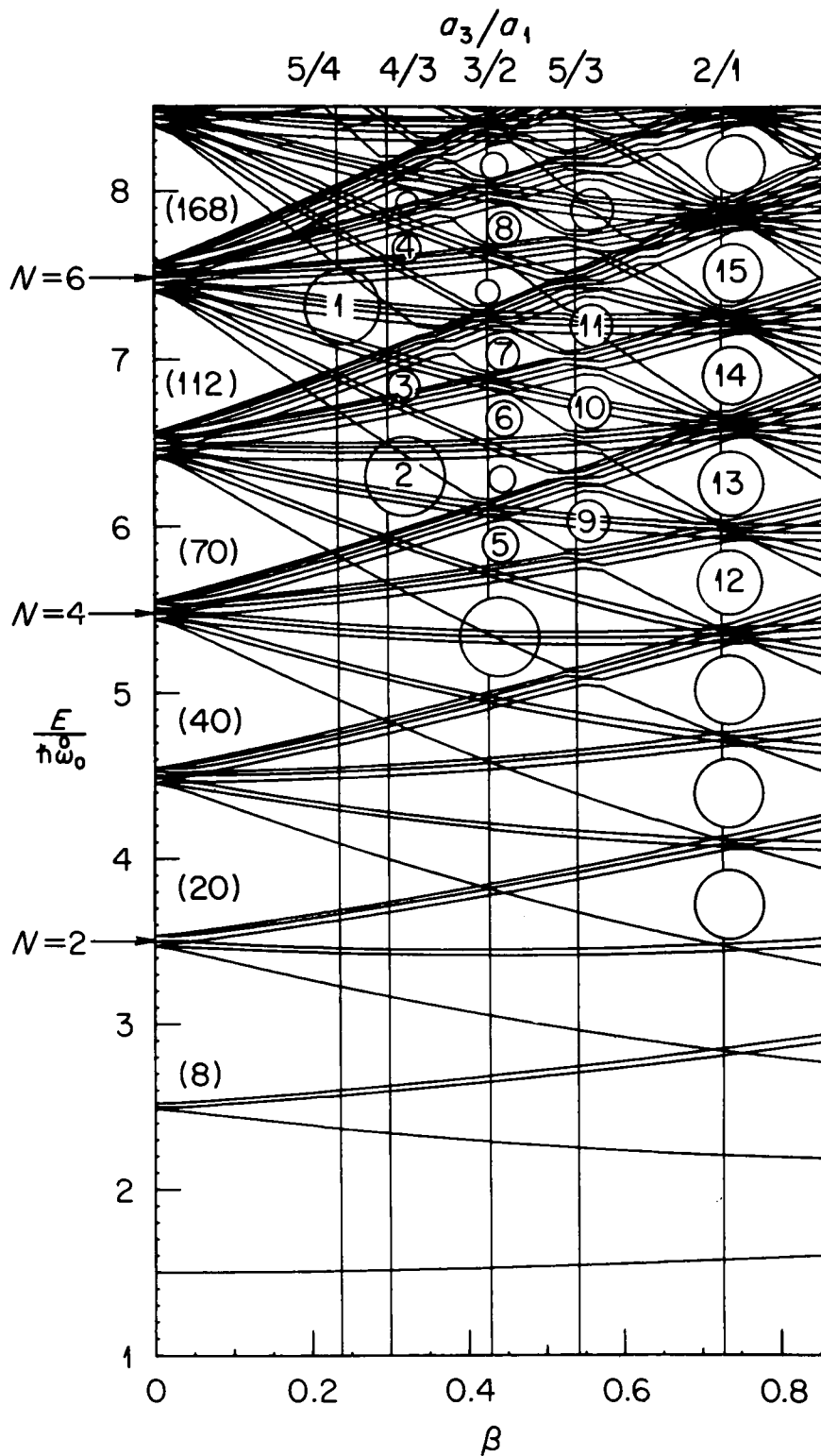


Fig. 1. Single particle states of an axially symmetric harmonic oscillator potential as a function of deformation  $\beta$ . The positions of some of the shells are indicated by circles (from Ref. 20). A weak spin-orbit potential is included.

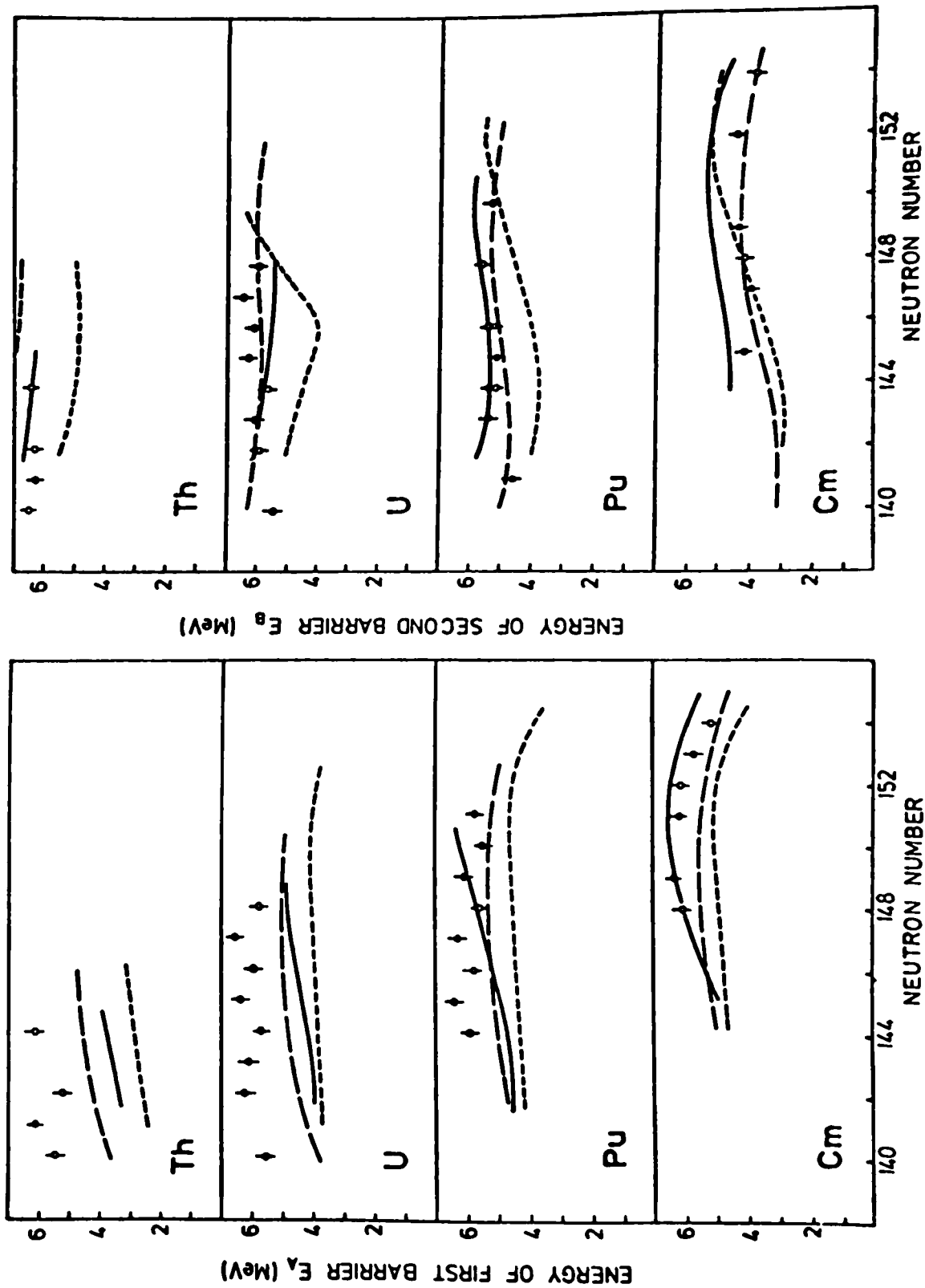


Fig. 2. Measured heights of the first and second barrier in comparison with theoretical predictions based on three different single particle potentials (from Ref. 37 where references to data and theory are given).

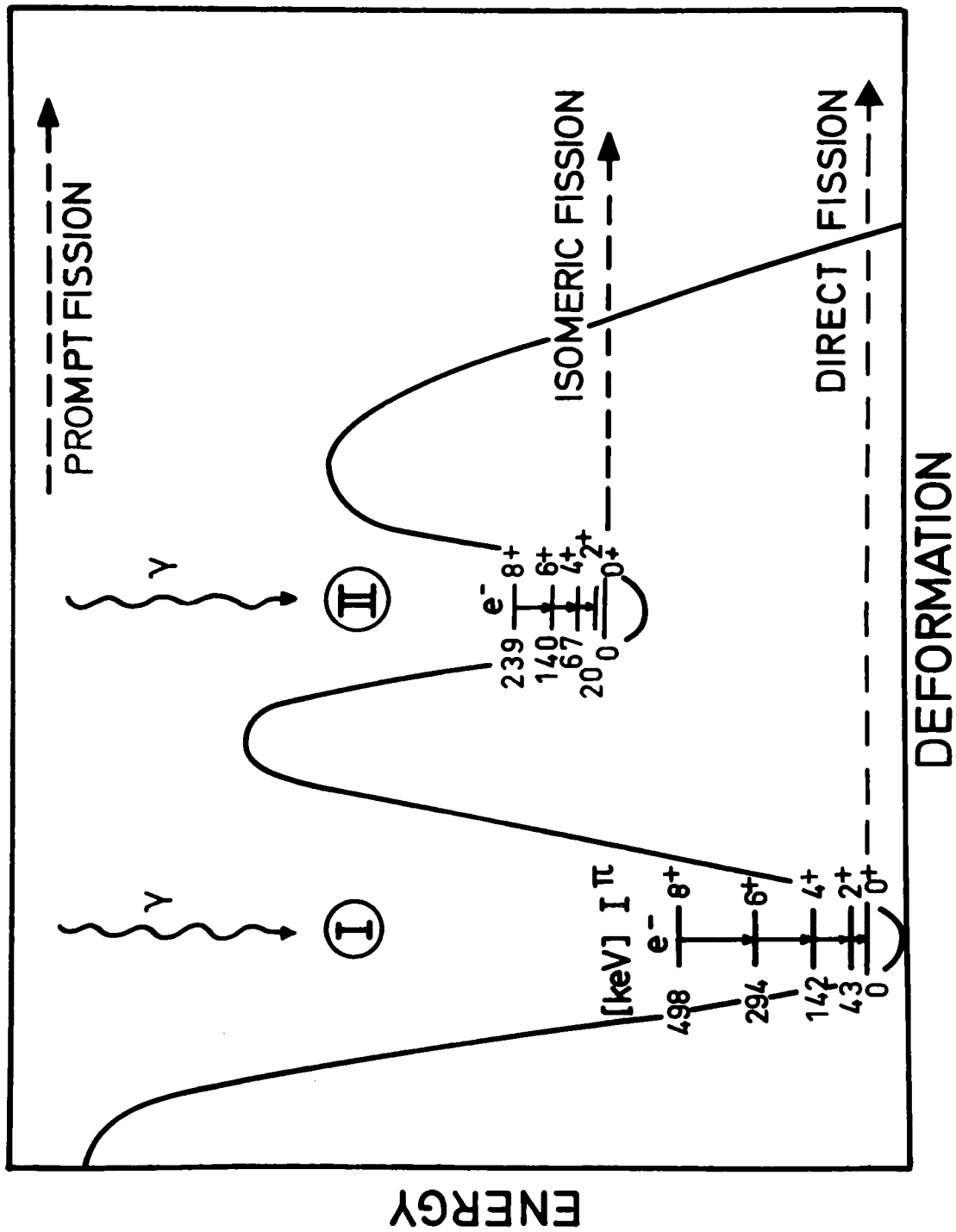


Fig. 3. Experimentally observed transitions within rotational bands in  $^{240}\text{Pu}$  (Ref. 24, from Ref. 37).

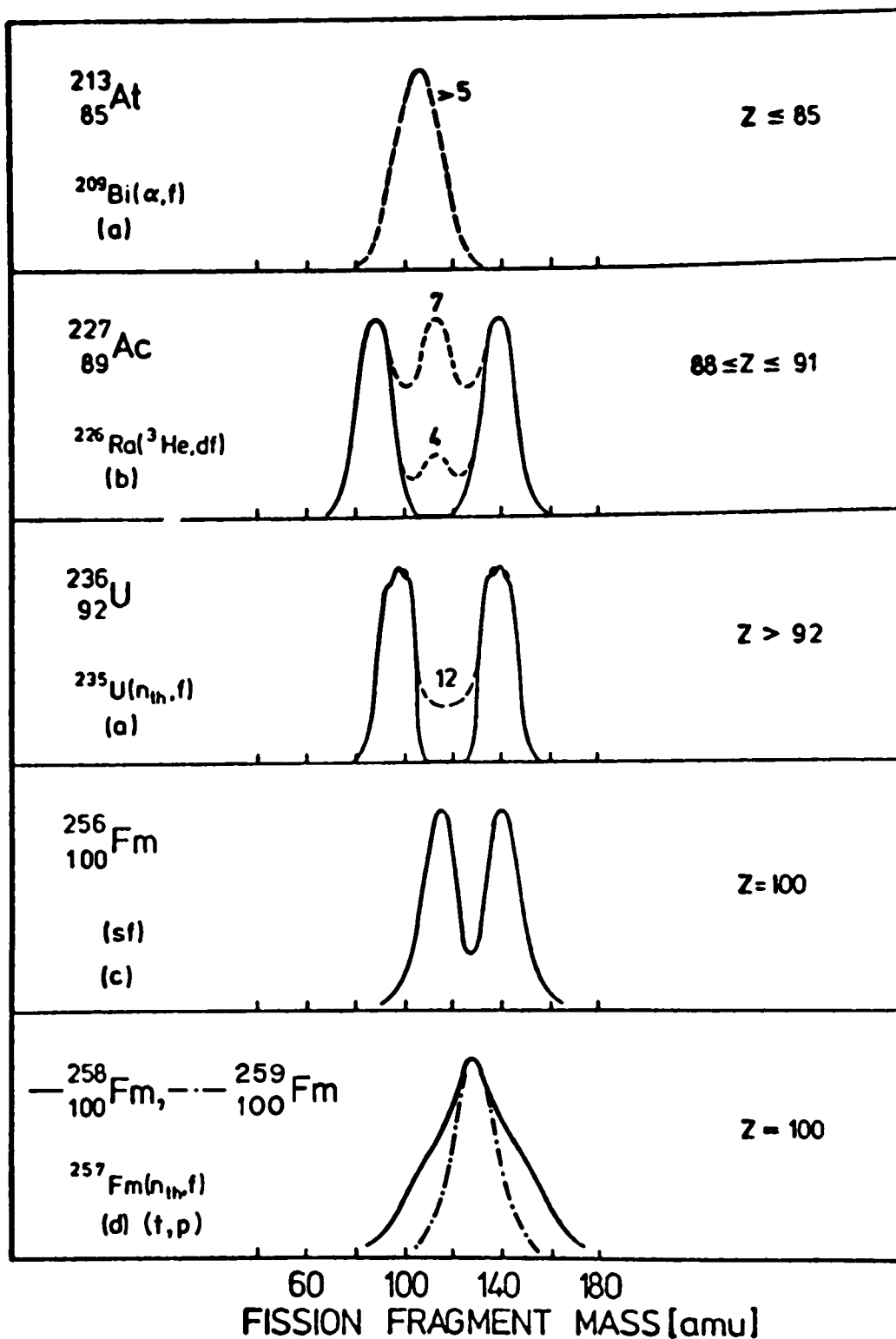


Fig. 4. Schematic fragment mass distributions for different fissioning nuclei. The excitation energy dependence is shown by dashed lines. The numbers give the excitation energy in MeV (based on a figure in Ref. 37).

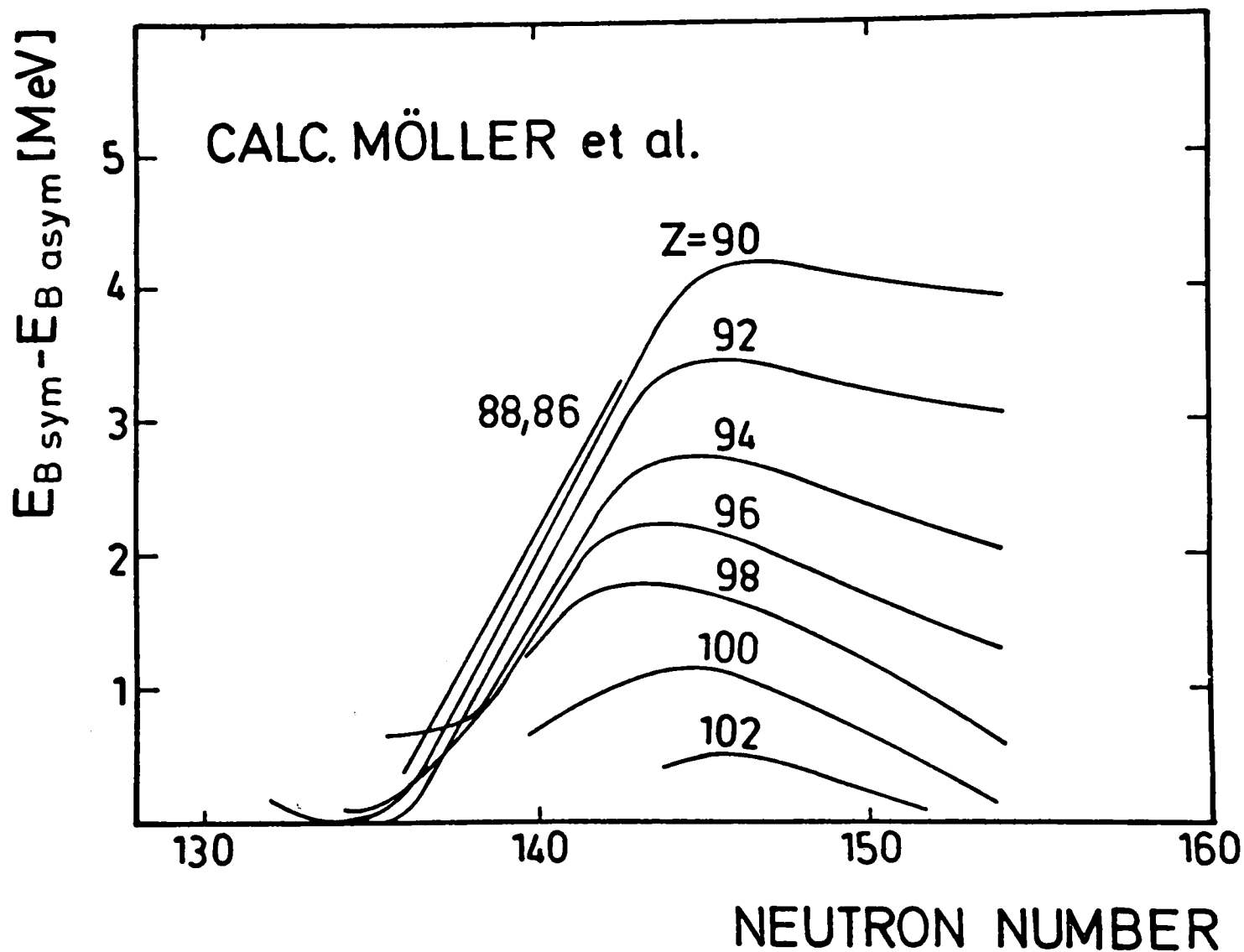


Fig. 5. Calculated energy difference (Ref. 38) between symmetric and asymmetric second barriers. The numbers on the curves give the proton numbers (from Ref. 37).

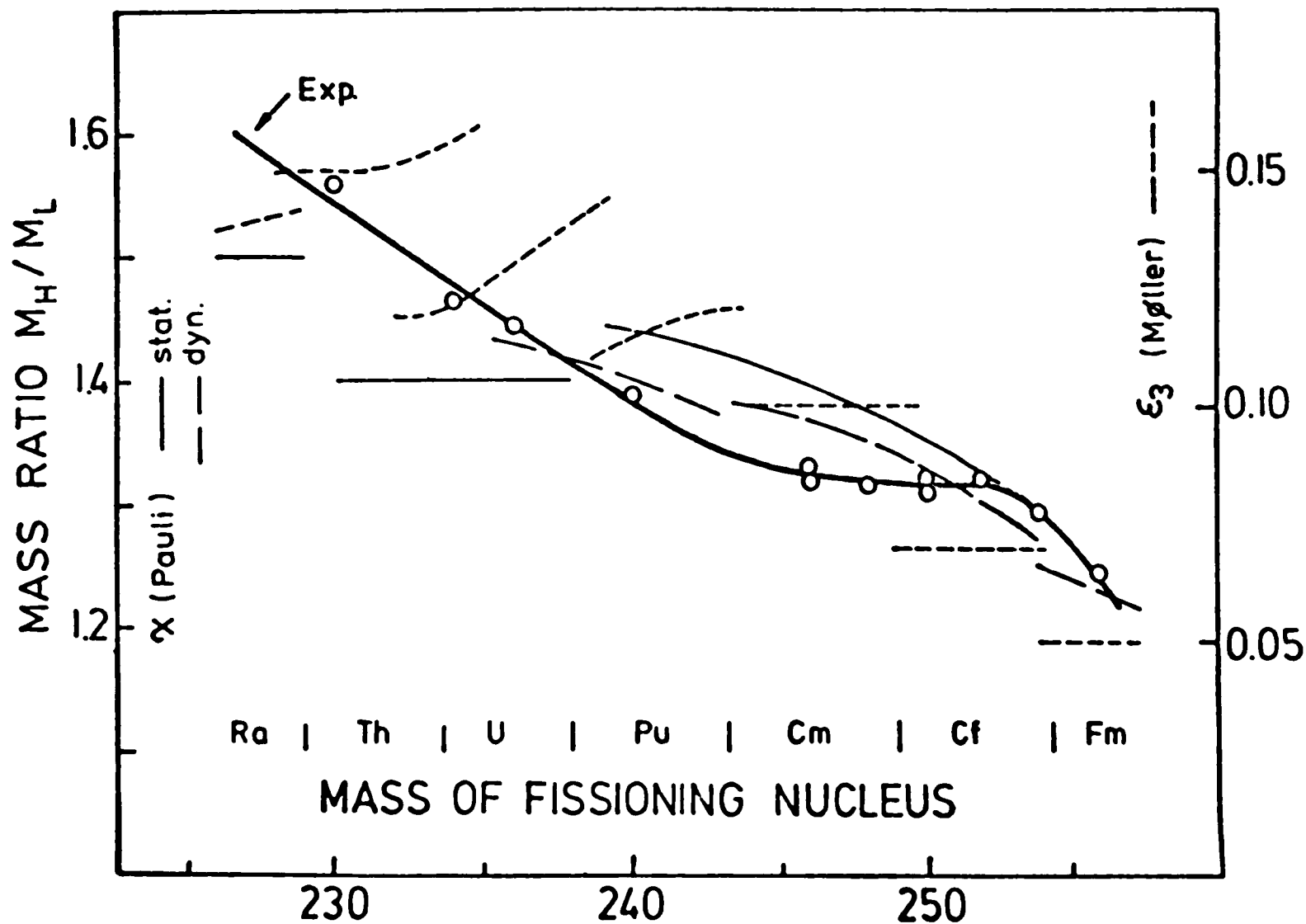


Fig. 6. Comparison of calculated mass asymmetries with experimental data (open circles). The short dashed lines give the octupole deformation of the second barrier (Ref. 38) whereas the thin solid curves show the asymmetry quantity  $\chi$  used by Pauli et al. (Ref. 44). (from Ref. 37).

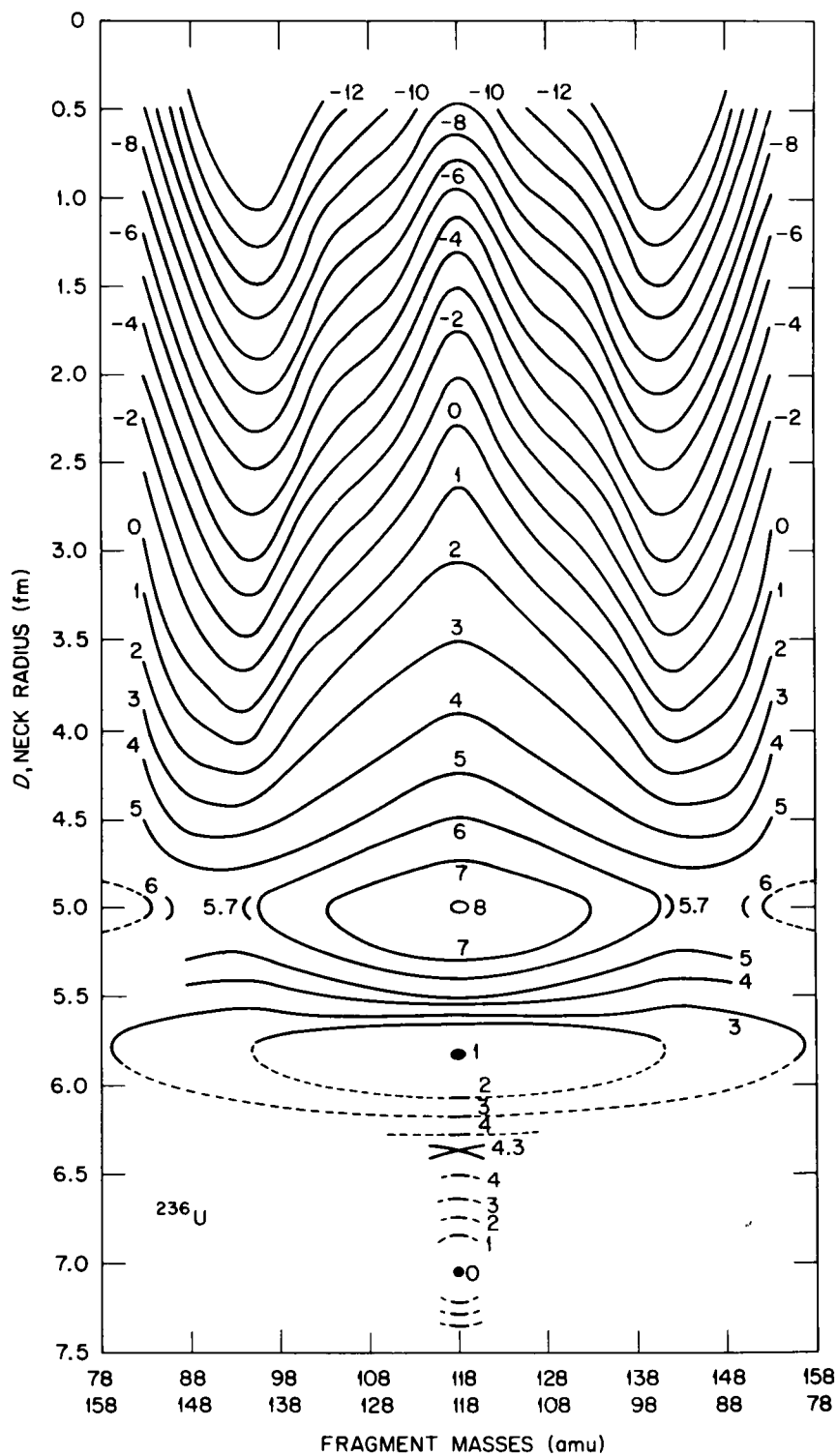


Fig. 7. The two-dimensional potential energy surface  $E(\lambda, D)$  is shown for  $^{236}\text{U}$ ;  $\lambda$  is the volume (mass) ratio and  $D$  the radius of the neck in fermis. The numbers labeling the contour lines give the energy in MeV relative to the ground state (from Ref. 17).

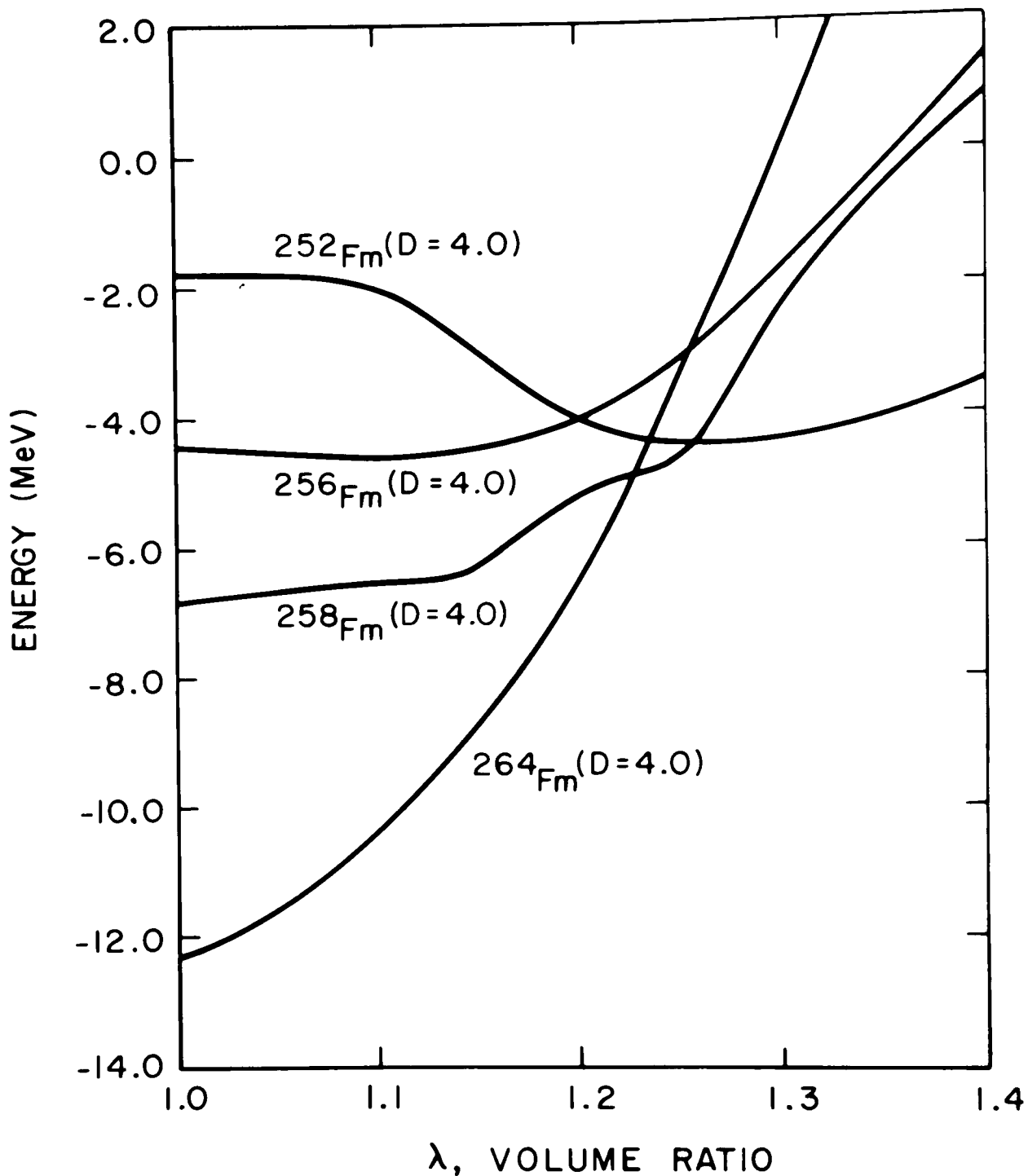


Fig. 8. The potential energies for the indicated nuclei are plotted as a function of  $\lambda$ , the volume (mass) ratio of the portions of the nucleus on either side on the neck plane, for the fixed value of the neck radius  $D=4.0\text{fm}$  (from Ref. 40).

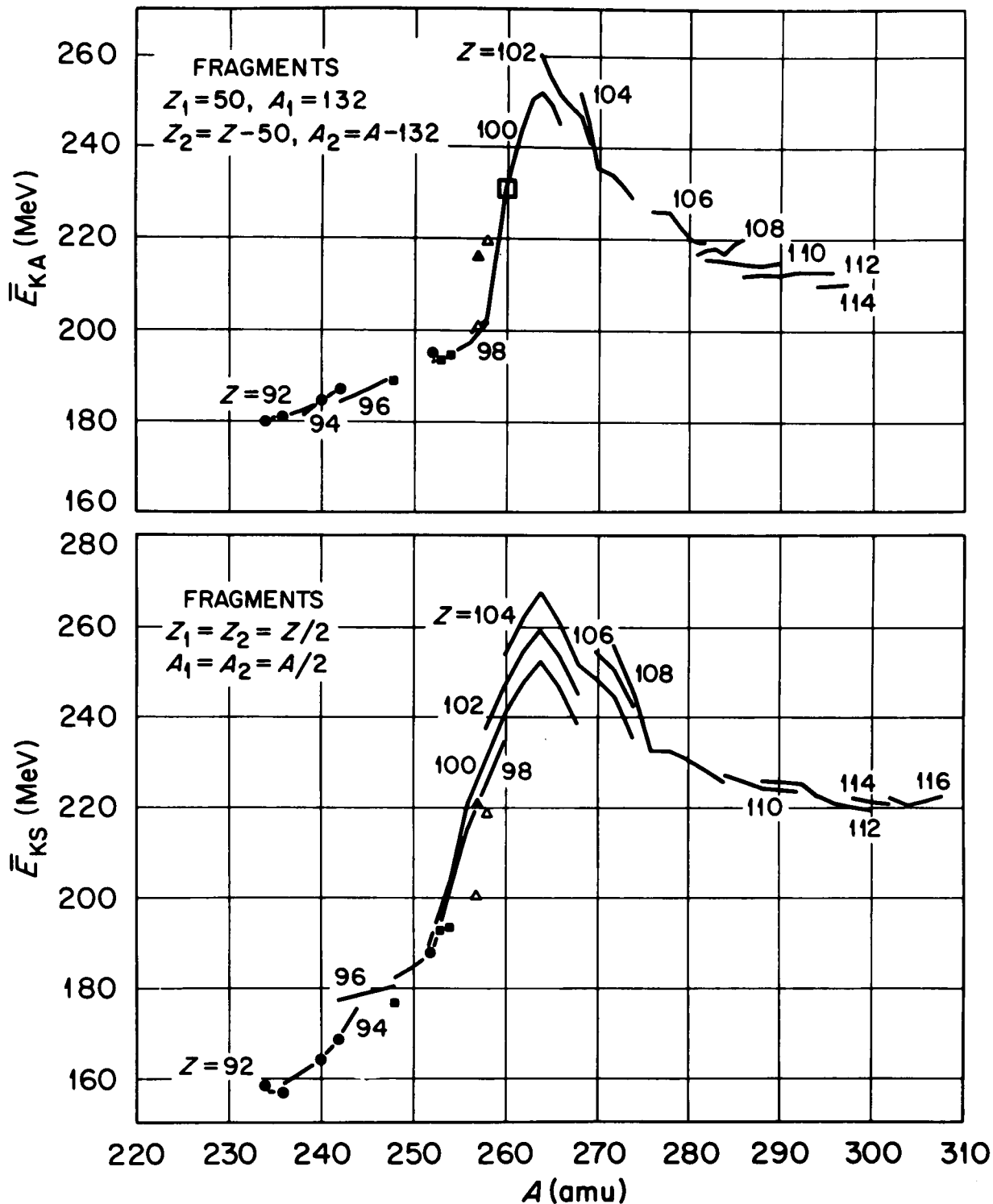


Fig. 9. Total fragment kinetic energy for the symmetric (S) and asymmetric (A) fission of heavy nuclei as function of the compound nucleus mass  $A$  and atomic number  $Z$ . The points show experimental values, the lines are calculated (from Ref. 41 where references to data are given). The  $^{259}\text{Fm}$  point denoted by an open square is taken from Ref. 32.

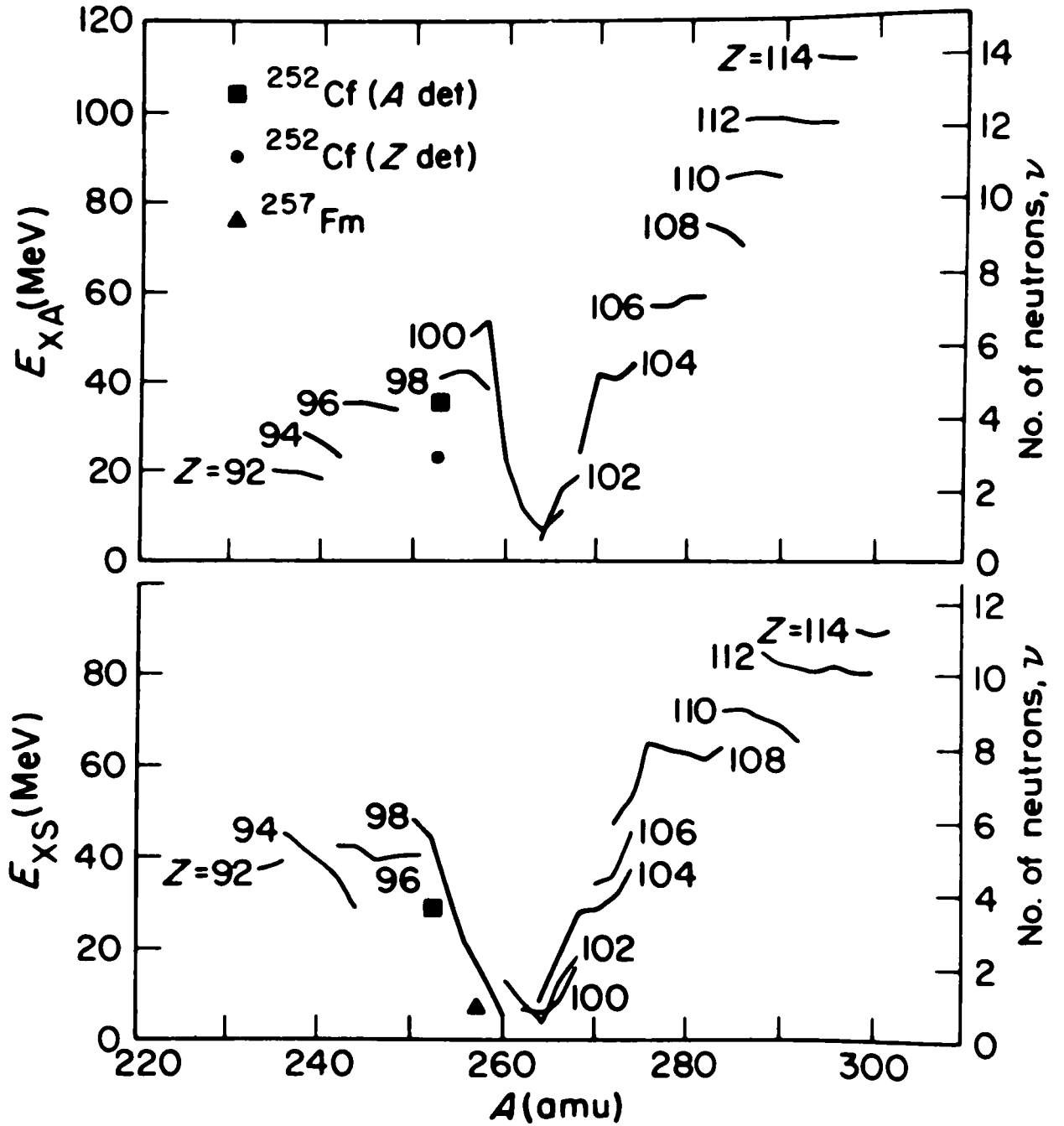


Fig.10. The solid curves represent calculated excitation energies ( $E_x$ ) and neutron multiplicities ( $\nu$ ) for asymmetric (A) and symmetric (S) fission of nuclei from  $Z=92$  to 114. The points correspond to experimental values for the fission of  $^{252}\text{Cf}$  and  $^{257}\text{Fm}$  (from Ref. 42).

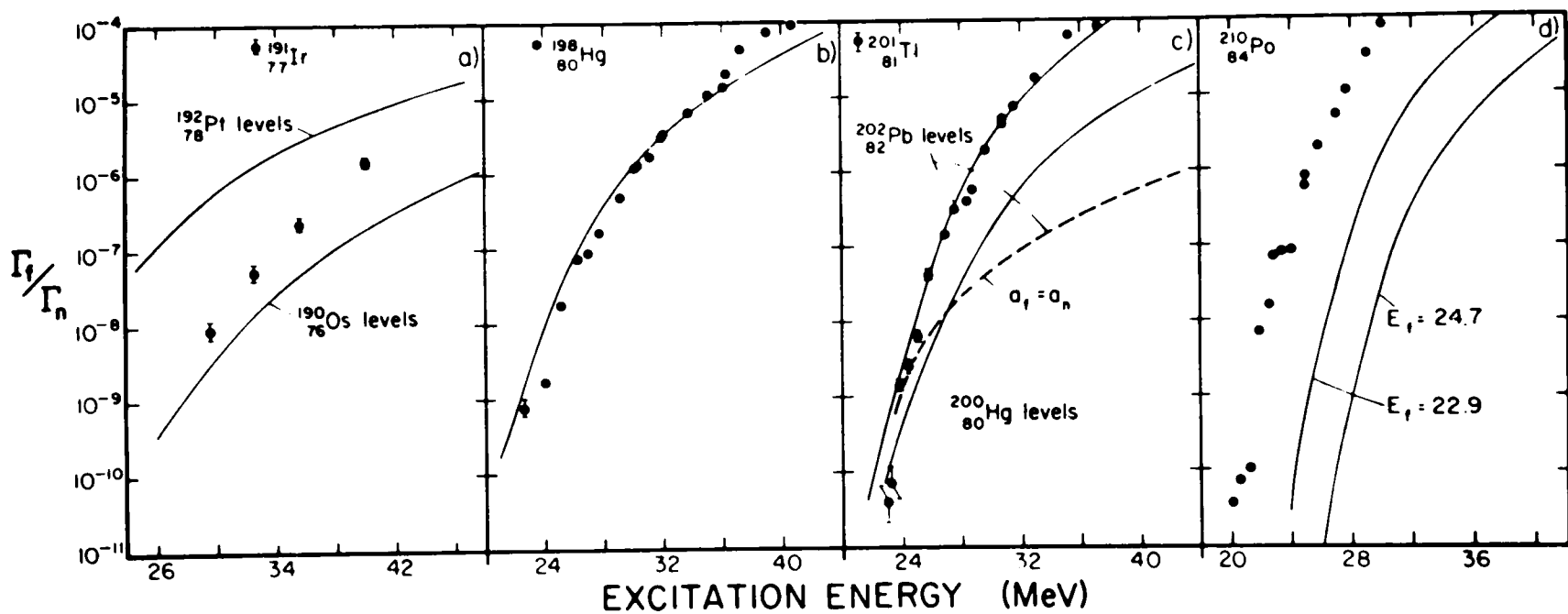


Fig. 11. Comparison between experimental fission probabilities and theoretical results obtained from shell model calculations (from Ref. 47).

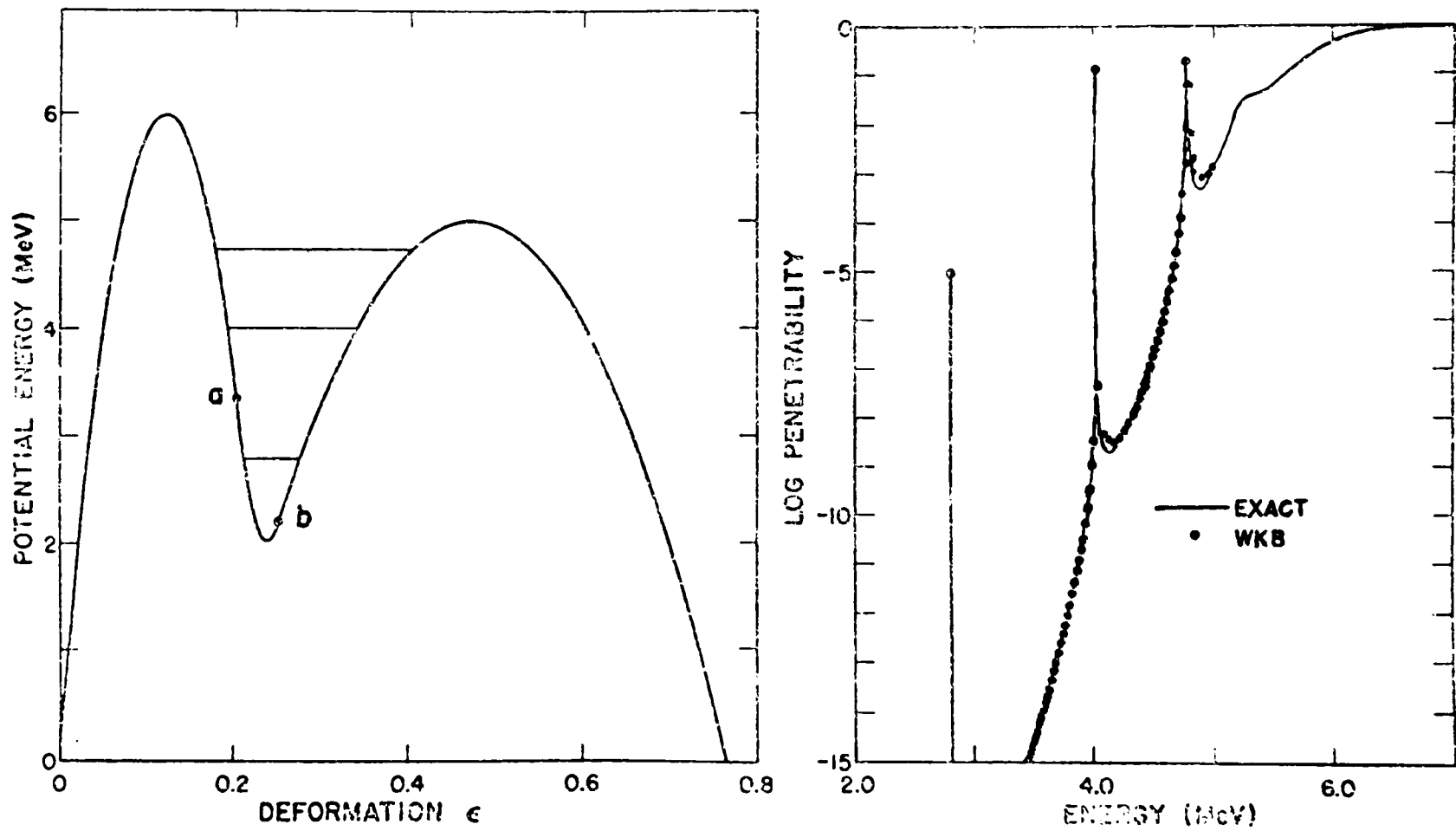


Fig. 12. Connection between quasibound states in the second well and resonances in the fission probability (from Ref. 58).

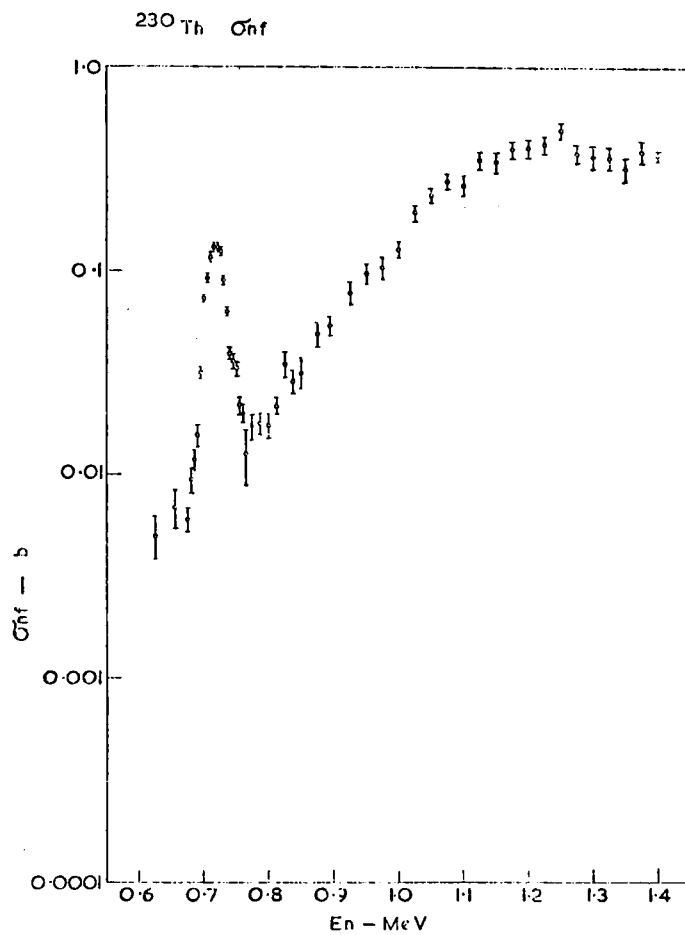


Fig. 13. Fission cross section section of  $^{230}\text{Th}$  as function of neutron energy (from Ref. 49).

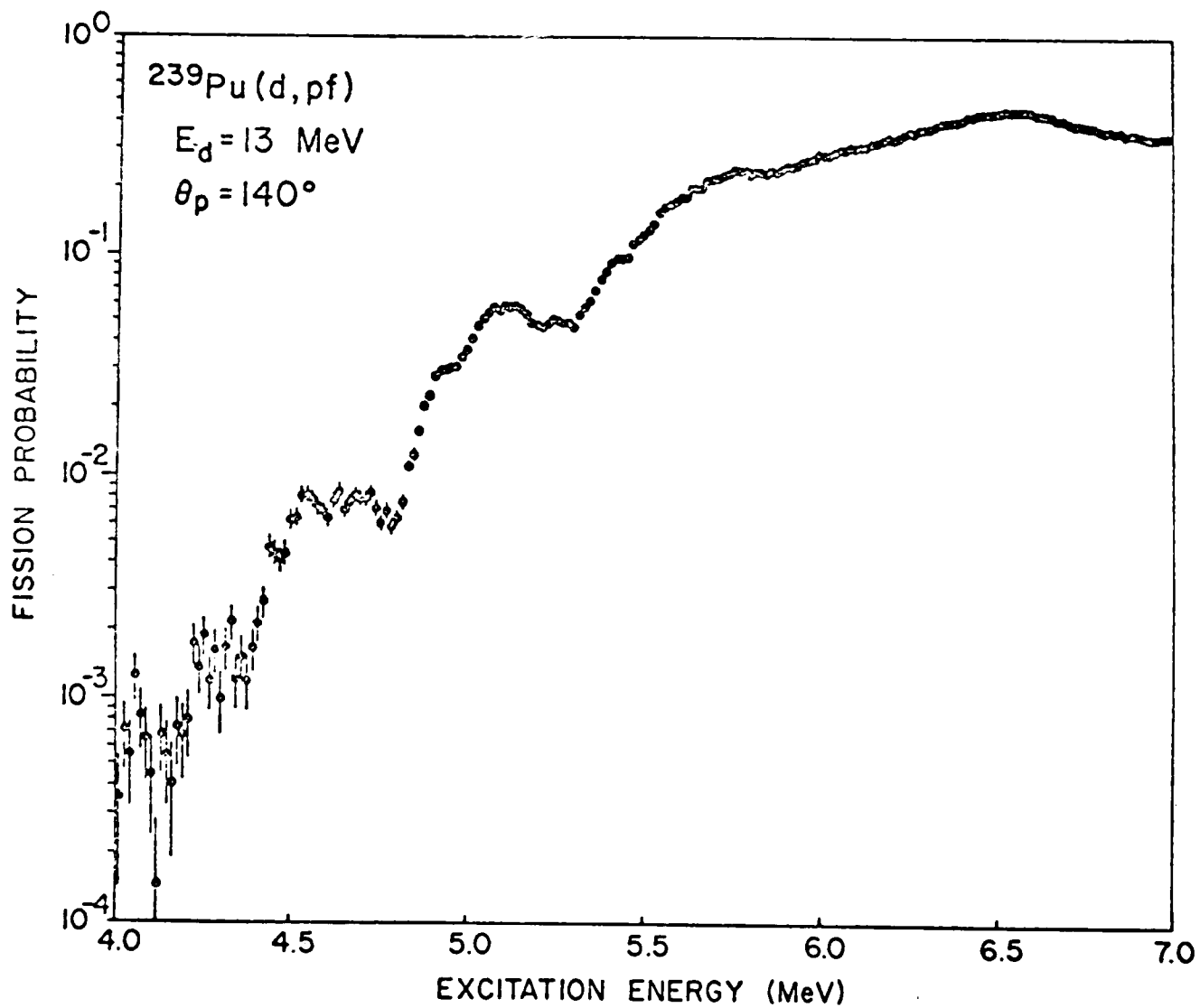


Fig.14. Fission probability of  $^{240}\text{Pu}$  as function of excitation energy (from Ref. 51).

THE IMPORTANCE OF FAST FISSION CROSS SECTIONS IN  
FAST REACTORS

E. M. Bohn and R. D. McKnight

Argonne National Laboratory  
Argonne, Illinois 60439, U.S.A.

ABSTRACT

In most cases requirements on the accuracy of the important fast fission cross sections for fast reactors have not yet been attained. The adequacy of fast fission cross section evaluations are most conveniently tested by computing integral measurements in benchmark fast critical assemblies. Results of sensitivity analyses of the U and Pu fission cross sections for two large benchmark fast critical assemblies (ZPR6-A and ZPR6-7) are presented herein. These sensitivity coefficients emphasize the importance of fast fission cross sections in fast reactor design and, along with the benchmark tests, point out the continued need for improvement in the evaluation of fast fission data.

## I. Nuclear Data Important for Fast Reactors

Commercial breeder reactor designs include the LMFBR and GCFR concepts. Both reactor types employ a mixed plutonium-uranium oxide fuel with a fertile-to-fissile ratio around 5:1. The core composition is comprised of ~35 v/o fuel, ~40 v/o coolant (sodium in the LMFBR, He gas in the GCFR), and ~25 v/o fuel, structural steel. The core composition determines the neutron spectrum characteristic of fast reactors and defines the energy range of importance for fast reactor cross sections. A typical fast reactor spectrum is displayed in Fig. 1; this figure shows both the measured and calculated neutron spectrum at the center of the FTR (Fast Test Reactor) mockup on ZPR-9.<sup>1</sup> The spectrum peaks broadly in the range 60 keV to 800 keV and clearly shows the oxygen resonances at 400 keV and 1 MeV, the iron resonance at 30 keV and the sodium resonance at 3 keV. The spectrum spans four decades on the energy axis and it includes fission from the resonance region for  $^{239}\text{Pu}$  and from the threshold fissioning isotopes,  $^{238}\text{U}$  and  $^{240}\text{Pu}$ . Thus, in the case of fast reactors, a comprehensive knowledge of fast fission cross sections is required.

The current state of nuclear data important for fast reactors is summarized in Table I.<sup>2</sup> The uncertainties listed are nominal uncertainties over the fast reactor spectrum. The desired accuracies listed for each cross section are based on studies<sup>3</sup> of the impact of uncertainties in nuclear data on important fast reactor design parameters. For example, an accuracy of about 1% is required for the  $^{239}\text{Pu}$  (n,f) cross section so that fuel enrichments may be predicted well. As indicated in Table I, the most important cross sections in fast reactors are the heavy metal fission and capture cross sections. The remainder of this paper is devoted to a discussion of the fission cross sections.

## II. Status of Fast Reactor Fission Cross Sections

The fission cross sections that must be known for fast reactors are  $^{239}\text{Pu}$ ,  $^{240}\text{Pu}$ ,  $^{241}\text{Pu}$ ,  $^{235}\text{U}$ , and  $^{238}\text{U}$ . The status of these cross sections is summarized in Table II where nominal uncertainties<sup>3</sup> in each cross section are shown as a function of energy along with the percentage change between ENDF/B Versions III and IV for each cross section. Two features are immediately evident: the uncertainties in the cross sections over the entire energy range are large relative to desired accuracies, and, the changes made in these cross sections going from ENDF/B Version III to Version IV are generally of the same magnitude as the uncertainties. It may be concluded, then, that the measurement and evaluation of fast fission cross sections is very much a dynamic activity.

The relative importance of these fission cross sections in a particular fast reactor design depends upon the contribution of each fissioning isotope to the total fission source in the reactor. For example, in the ZPR6-7 assembly,<sup>4</sup> a benchmark critical assembly typical of (Pu-U) $\text{O}_2$  fueled, sodium cooled fast reactors, the contributions to the fission source in the core are as follows:

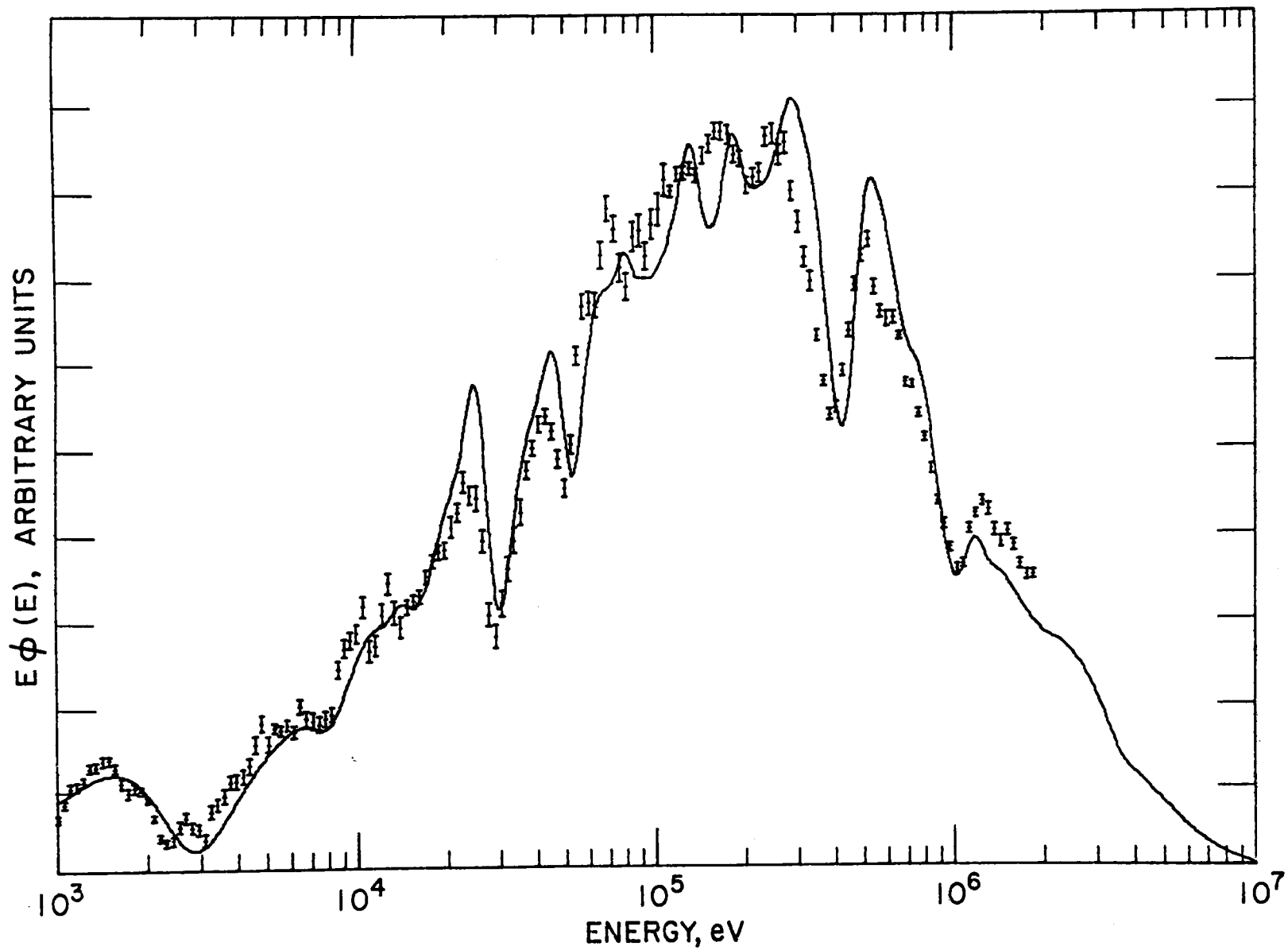


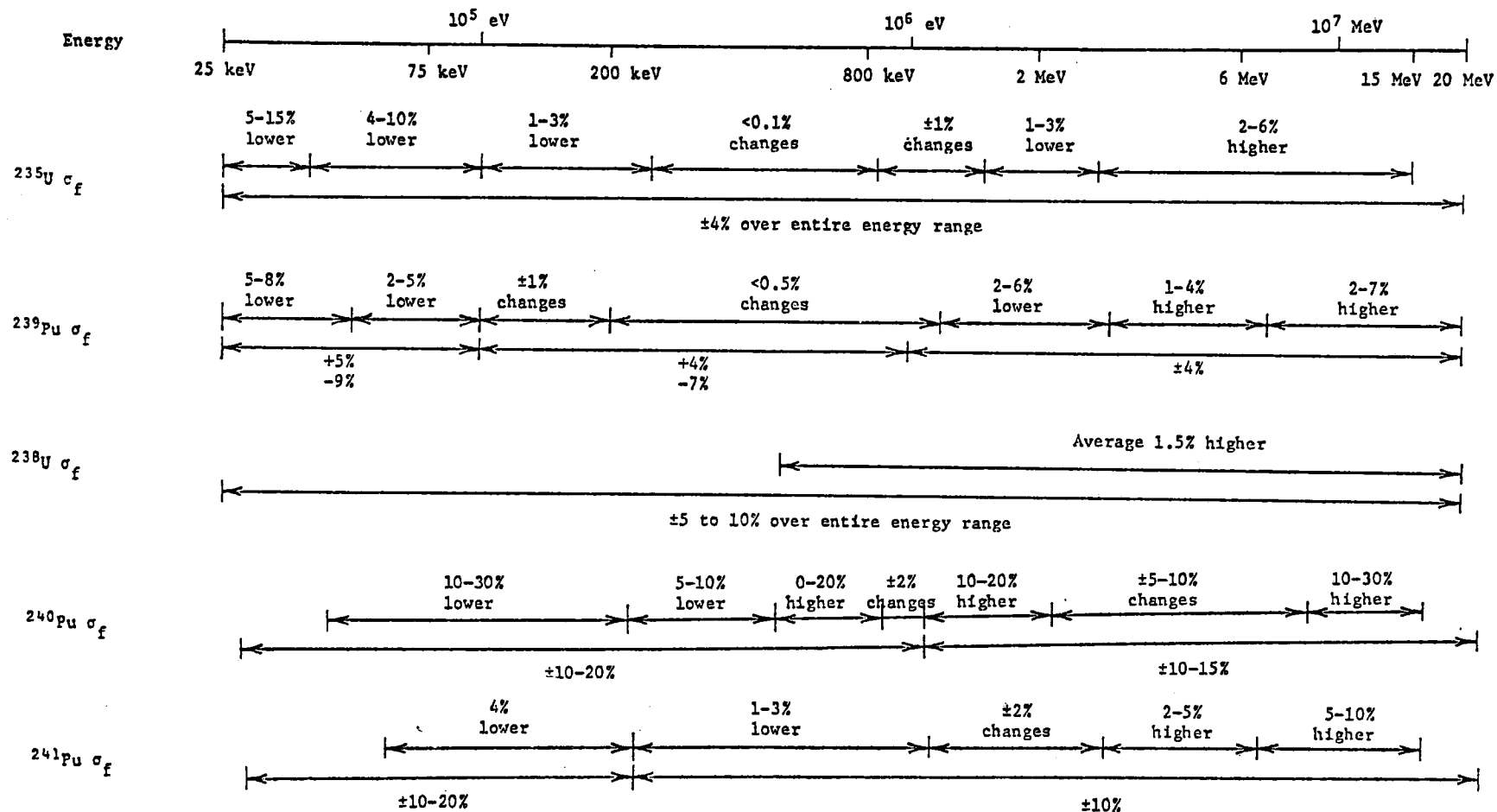
Fig. 1. Neutron Spectrum at the Center of FTR Mockup on ZPR-9. (From Ref. 1).

TABLE I. Nuclear Data Important for Fast Reactors<sup>a</sup>

Nuclear Data	Approximate Uncertainty in Data	Desired Accuracy
$^{239}\text{Pu}(n, f)$	$\sim 5\text{--}10\%$	$\sim 1\%$
$^{239}\text{Pu}(n, \gamma)$	$\sim 10\text{--}15\%$	$< 7\%$
$^{238}\text{U}(n, f)$	$\sim 10\%$	$< 5\%$
$^{238}\text{U}(n, \gamma)$	$\sim 10\text{--}15\%$	$< 2\%$
$^{238}\text{U}(n, n')_{\text{INEL}}$	$\sim 10\text{--}15\%$	$< 8\%$
$^{16}\text{O}(n, n')_{\text{EL}}$	$\sim 5\%$	$< 10\%$
$^{23}\text{Na}(n, n')_{\text{EL}}$	$\sim 5\%$	$< 25\%$
$^{23}\text{Na}(n, \gamma)$	$\sim 20\%$	$< 40\%$
Stainless Steel $(n, \gamma)$	$\sim 30\%$	$< 20\%$
Stainless Steel $(n, n')$	$\sim 10\text{--}20\%$	$< 20\%$
$\nu_{\text{TOT}}; \text{Pu, U}$	$\sim 2\text{--}3\%$	$\sim 1\%$
$\nu_{\text{DELAYED}}; \text{Pu, U}$	$\sim 5\text{--}15\%$	$< 3\%$
$\chi(E); \text{Pu, U}$	$\sim 5\%$ in $\bar{E}$	

<sup>a</sup>From Ref. 2.

TABLE II. Summary of Changes in ENDF/B Nuclear Data - Version 4 Vs. Version 3<sup>a</sup>



Note: The upper scale indicates the cross section modifications incorporated in Version 4 (given as per cent change relative to Version 3). The lower scale indicates the estimated cross section uncertainties.

<sup>a</sup>From R. D. McKnight, ZPR-TM-191, January 1975.

ISOTOPE	Fuel Atom %	Relative Fission Source, $\int \nu \Sigma_f \phi$
$^{239}\text{Pu}$	13%	85%
$^{240}\text{Pu}$	1.7%	2%
$^{241}\text{Pu}$	0.2%	2%
$^{235}\text{U}$	0.1%	1%
$^{238}\text{U}$	85%	10%
	100%	100%

The fission source in the blanket of a fast reactor makes up about 10% of the total reactor source and comes predominately from  $^{238}\text{U}$ . Thus, if the total fission source must be known within a precision of 1% (e.g., to predict fuel enrichment), the fission cross sections of  $^{239}\text{Pu}$  and  $^{238}\text{U}$  must be known with an imprecision of 1% and 5%, respectively.

In the case of a GCFR with its relatively harder spectrum, the fission source in the core contributed by the threshold fissioning isotopes increases to 11% for  $^{238}\text{U}$  and 3% for  $^{240}\text{Pu}$ .

### III. Fast Reactor Benchmark Data Tests

The adequacy of fast fission cross section evaluations for fast reactor design is most conveniently tested by computing integral measurements in benchmark fast reactor critical assemblies. The integral parameters most often computed include criticality or  $k_{\text{eff}}$ , reaction rate ratios and material reactivity worths. The imprecisions in these measurements are 0.5% for  $k_{\text{eff}}$ , ~2% for relative reaction rates and 2-5% for reactivities. A complete set of fast reactor data tests of ENDF/B-IV is given in Ref. 5 and a sampling of some of the important results is given in Table III.

In Table III, ratios of the calculated-to-measured integral parameters are listed for two benchmarks; ZPR6-6A, a U-fueled fast assembly, and ZPR6-7, a plutonium-fueled assembly. These two assemblies are identical in composition with the exception of Pu fuel in ZPR6-7 rather than the  $^{235}\text{U}$  fuel in ZPR6-6A. Thus, comparing results in these two benchmark assemblies offers an opportunity to assess Pu fission cross sections relative to  $^{235}\text{U}$  cross sections. But the relative evaluation of cross sections with integral measurements is not an obvious and straight-forward process. For example, the reaction rate tests in Table III are all consistent with a conclusion that the calculated  $^{239}\text{Pu}$  fission rate is too low relative to  $^{235}\text{U}$  fission or that the  $^{235}\text{U}$  fission rate is too high relative to  $^{239}\text{Pu}$  fission. This observation is also consistent with the relative discrepancies in the material reactivity worths considering that part of the discrepancy could be attributed to a calculation of the total fission rate in the assembly (perturbation denominator). But if  $^{235}\text{U}$  (n,f) were indeed computed high relative to  $^{239}\text{Pu}$  (n,f), the  $k_{\text{eff}}$  of ZPR6-6A would be expected to be higher than  $k_{\text{eff}}$  of ZPR6-7. This is not the case for this set of calculations;  $k_{\text{eff}}$  in both assemblies is computed about 1.5% too low. On the other hand,  $k_{\text{eff}}$  is directly sensitive to an evaluation of  $\nu$ , the number of neutrons released per fission, while the reaction rate ratios are not. Thus, integral tests must be used with care when evaluating cross sections.

TABLE III. Current State of Benchmark Data Testing in Fast Reactors; Ratio of Calculated-to-Measured Integral Parameters<sup>a</sup>

	Critical Assembly ZPR6-6A (U Fueled)	Critical Assembly ZPR6-7 (Pu Fueled)
k	0.9850	0.9844
$^{238}\text{U}(\text{n},\gamma)/^{239}\text{Pu}(\text{n},\text{f})$		1.09
$^{238}\text{U}(\text{n},\gamma)/^{235}\text{U}(\text{n},\text{f})$	1.03	
$^{235}\text{U}(\text{n},\text{f})/^{239}\text{Pu}(\text{n},\text{f})$		1.03
$^{238}\text{U}(\text{n},\text{f})/^{239}\text{Pu}(\text{n},\text{f})$		0.97
$^{238}\text{U}(\text{n},\text{f})/^{235}\text{U}(\text{n},\text{f})$	0.92	
$^{239}\text{Pu} - \rho(\text{Ih/kg})^{\text{b}}$	1.08	1.19
$\text{Na} - \rho(\text{Ih/kg})^{\text{b},\text{c}}$	-5.7	1.43
$^{10}\text{B} - \rho(\text{Ih/kg})^{\text{b}}$	0.93	1.12

<sup>a</sup>References 5, 6; ENDF/B-IV.

<sup>b</sup>Small sample central reactivity worths.

<sup>c</sup>The sodium worth in ZPR6-6A is near zero, and hence the large error is not meaningful.

#### IV. Sensitivity of Data Testing Results to Fission Cross Sections

The most convenient way to demonstrate the importance or impact of cross sections in fast reactors is through the application of sensitivity analysis. Sensitivity coefficients are of the form:

$$\frac{dP}{P} \bigg/ \frac{d\sigma}{\sigma}$$

i.e., the coefficients represent the percent change in an integral parameter per percent change in a cross section. A great deal of work has been done in the area of sensitivity analysis recently and a few representative results are given in Table IV and Figs. 2-5. These results were generated with the VARI-1D code developed at Argonne.<sup>7</sup>

Total integrated sensitivity coefficients for fission cross sections in ZPR6-6A and ZPR6-7 are given in Table IV. These coefficients are energy integrated coefficients, i.e., they represent the percent change in an integral parameter per percent change over the entire energy range in a fission cross section. This type of change may not be realistic from a cross section evaluators point of view except in the case of a re-normalization type change. But these coefficients do present some feel for the relative importance of the fission cross sections in these assemblies. For example, a percent increase in the  $^{239}\text{Pu}$  (n,f) cross section would increase  $k_{\text{eff}}$  in ZPR6-7 by about 0.6% and decrease  $^{238}\text{U}$  (n, $\gamma$ )/ $^{239}\text{Pu}$  (n,f) by 1.06%. Both changes would improve agreement between measurement and calculation. On the other hand,  $^{238}\text{U}$  (n,f)/ $^{239}\text{Pu}$  (n,f) and material reactivities are not improved by an increase in  $^{239}\text{Pu}$  (n,f) alone. Thus, if some of the major discrepancies in fast reactor physics are to be attributed to cross sections, all the nuclear data must be considered, and not just fission cross sections alone.

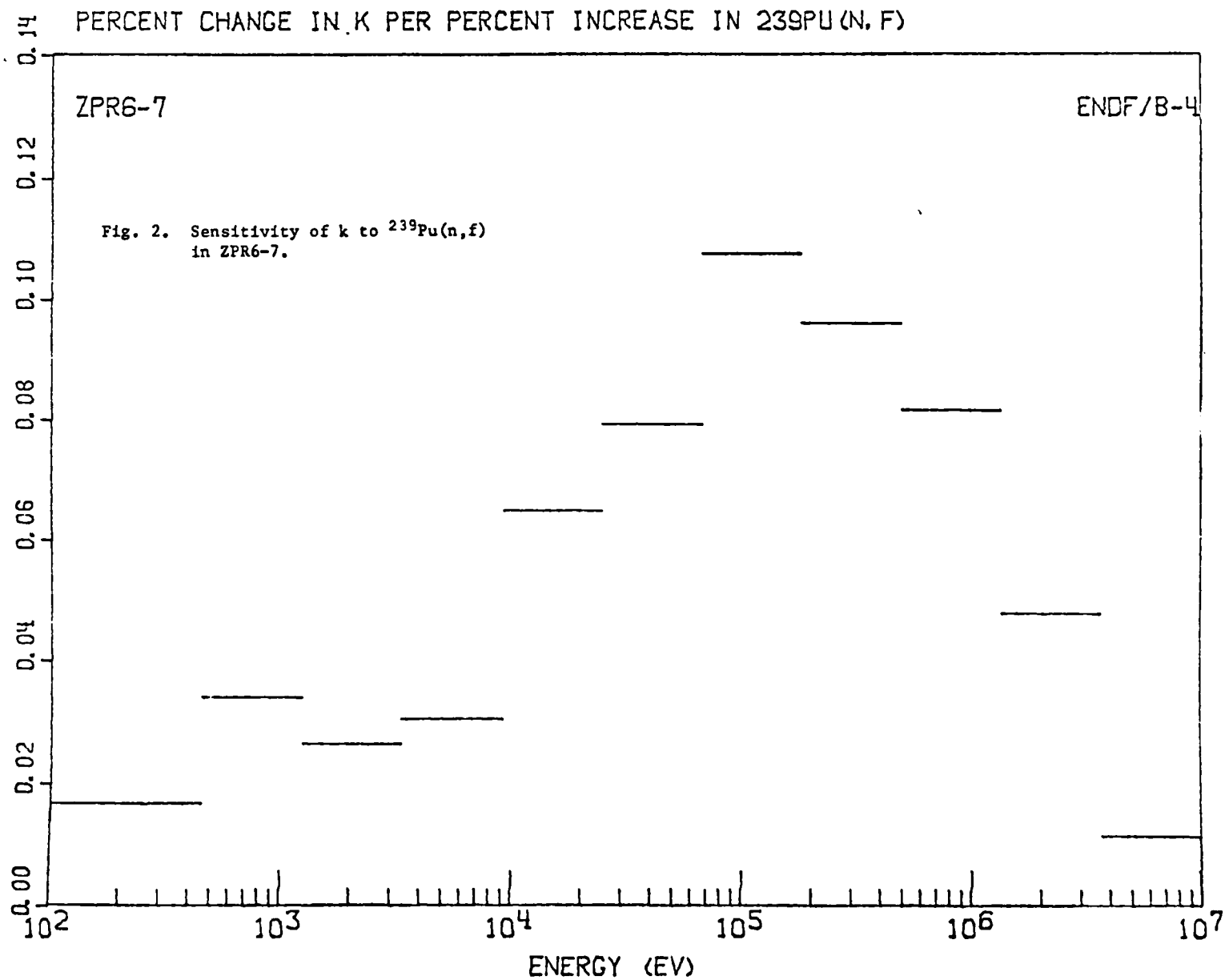
Another feature of note in Table IV is that the  $^{240}\text{Pu}$  (n,f) and  $^{241}\text{Pu}$  (n,f) cross sections have about the same impact on the important integral parameters in ZPR6-7. Thus, a fast reactor designer would like to know both these cross sections with the same degree of certainty; i.e., an equal effort should be spent in the evaluation of each of these cross sections.

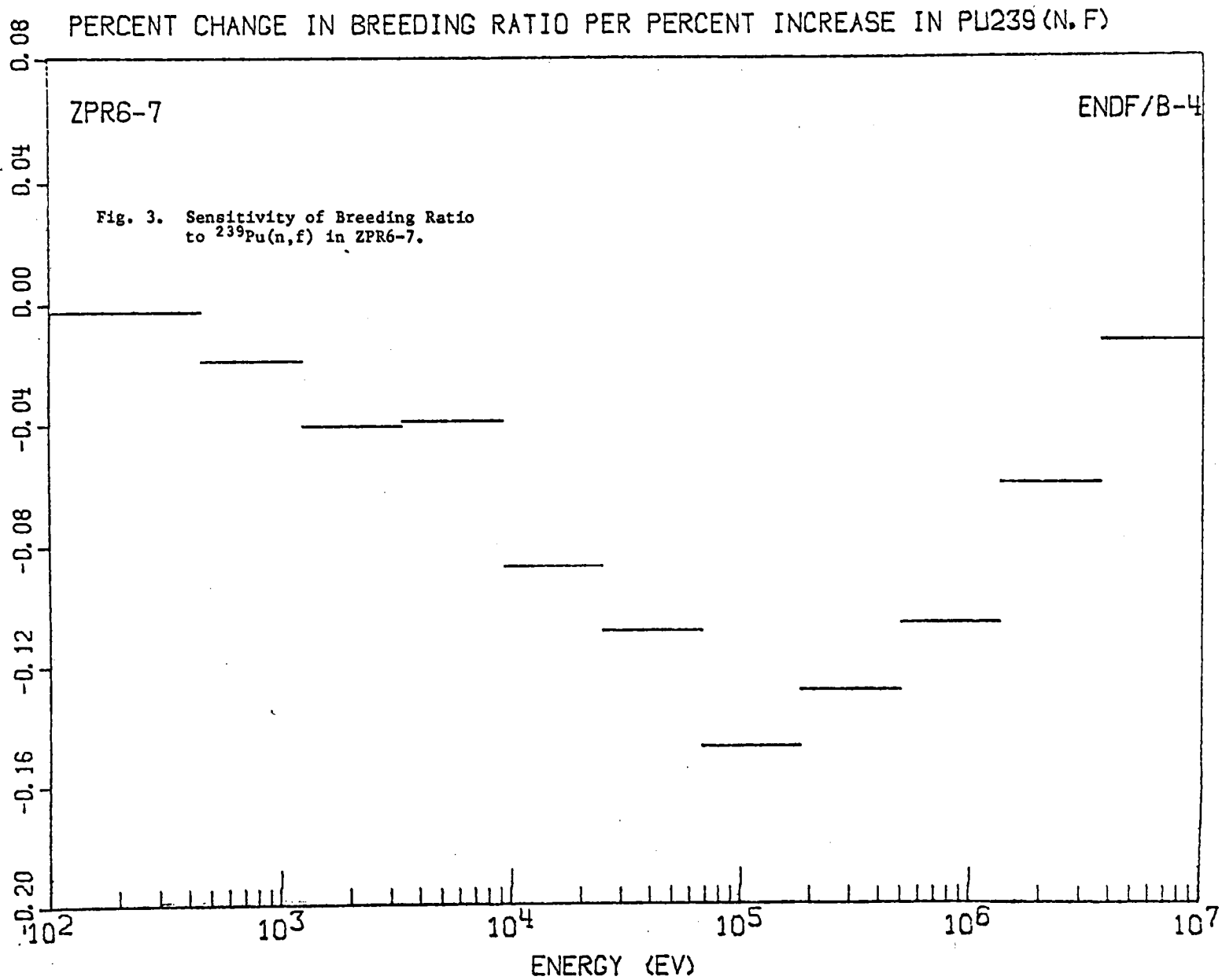
The more interesting set of sensitivity coefficients are displayed in Figs. 2-5. These are energy dependent coefficients computed for 11 broad groups covering the fast reactor spectrum (i.e., the total energy integrated coefficient given in Table IV is the sum of these broad group coefficients). Cross section evaluations often result in a change in the cross section over just a portion of the energy range. For these types of changes interpolation on plots of energy dependent coefficients will yield a quick and sufficiently accurate estimate of the impact of the cross section change. For example, a percent increase in the  $^{239}\text{Pu}$  (n,f) cross section in the range 10 keV to 70 keV would yield  $\sim 0.15\%$  increase in  $k_{\text{eff}}$  in ZPR6-7. Figures 2 and 3 demonstrate that sensitivity of reaction rates<sup>eff</sup> and ratios (e.g.,  $k_{\text{eff}}$ ) can be expected to follow the relative shape of the spectrum weighted reaction rate of the modified cross section ( $^{239}\sigma_f(E)\phi(E)$  in Figs. 2 and 3). But this is not the case for reactivities, as is demonstrated in Figs. 4 and 5. Material reactivities are directly related to the shape of the adjoint spectrum and this spectrum, in turn, is proportional to the fission rate. Thus, sensitivity profiles for scattering materials, e.g., sodium, will display a more complex behavior.

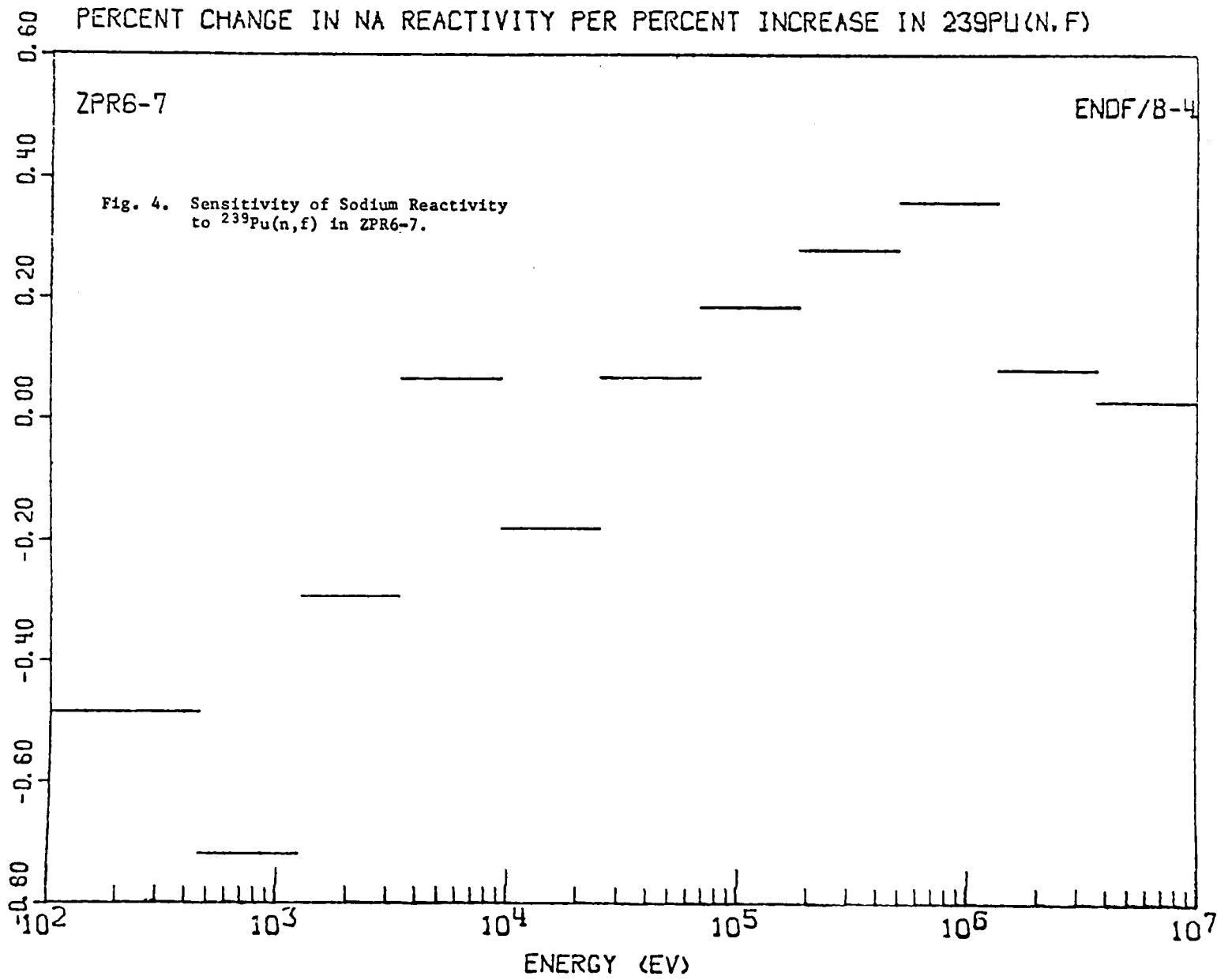
TABLE IV. Sensitivity of Fast Reactor Integral Parameters to  
Fission Cross Sections<sup>a</sup>

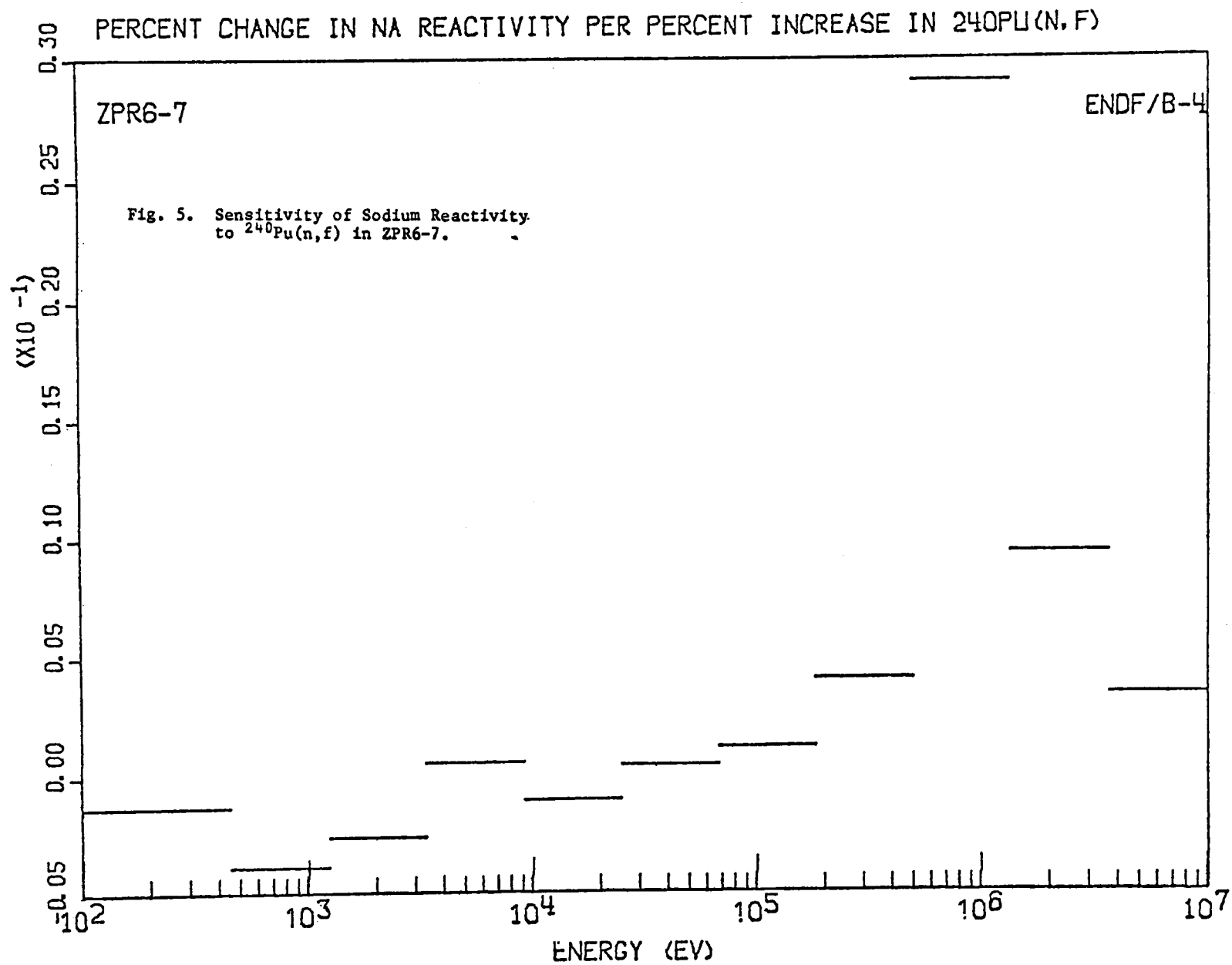
Integral Parameters	$^{235}\text{U}(\text{n},\text{f})$	$^{238}\text{U}(\text{n},\text{f})$	$^{239}\text{Pu}(\text{n},\text{f})$	$^{240}\text{Pu}(\text{n},\text{f})$	$^{241}\text{Pu}(\text{n},\text{f})$
<u>ZPR6-6A:</u>					
k	0.57	0.08			
$^{238}\text{U}(\text{n},\text{f})/^{235}\text{U}(\text{n},\text{f})$	-0.66	0.97			
$^{238}\text{U}(\text{n},\gamma)/^{235}\text{U}(\text{n},\text{f})$	-1.04	-			
$^{239}\text{Pu} - \rho$	-0.82	-0.11			
Na - $\rho$	-0.28	1.51			
$^{10}\text{B} - \rho$	-1.09	-0.22			
<u>ZPR6-7:</u>					
k	0.01	0.08	0.59	0.017	0.013
$^{238}\text{U}(\text{n},\text{f})/^{239}\text{Pu}(\text{n},\text{f})$		0.97	-0.77		0.005
$^{238}\text{U}(\text{n},\gamma)/^{239}\text{Pu}(\text{n},\text{f})$		0.005	-1.06		
Breeding Ratio	-0.012	0.003	-0.078		-0.017
$^{239}\text{Pu} - \rho$	-0.025	-0.13	0.32	-0.016	-0.020
Na - $\rho$	0.08	-0.71	0.04	0.04	-0.04
$^{10}\text{B} - \rho$		-0.23	-0.95	-0.036	-0.017

<sup>a</sup>Total energy integrated coefficients; e.g., a one percent increase in  $^{235}\text{U}(\text{n},\text{f})$  in ZPR6-6A increases k by 0.57% and decreases  $^{238}\text{U}(\text{n},\gamma)/^{235}\text{U}(\text{n},\text{f})$  by 0.66%.









Sensitivity coefficients such as these can be used to obtain an estimate of the effects that changes in a fission cross section evaluation have upon calculated integral parameters. Thus, these coefficients conveniently demonstrate the importance of fast fission cross sections in fast reactor design and can serve as a valuable tool in the continued improvement in the evaluation of fast fission data.

#### REFERENCES

1. T. J. Yule and E. F. Bennett, "Measured Neutron Spectra in a Number of Uranium - and Plutonium-Fueled Reactor Assemblies," *Nucl. Sci. and Eng.* 46 (1971).
2. E. M. Bohn, et al., "Benchmark Experiments for Nuclear Data," *Proc. of Conf. on Nuclear Cross Sections and Technology*, Washington D. C., March 3-7, 1975, NBS-SP 425, Oct., 1975.
3. R. D. McKnight, "The Effects of the Higher Plutonium Isotopes and the Implications of the Uncertainties in their Nuclear Data on Fast Reactor Design," University of Cincinnati Doctoral Dissertation, 1974.
4. C. E. Till, et al., "ZPR-6 Assemblies 6A and 7: Benchmark Specifications for the Two Large Single-Core-Zone Critical Assemblies--<sup>235</sup>U-Fueled Assembly 6A and Plutonium-Fueled Assembly 7--LMFBR Demonstration Reactor Benchmark Program," Applied Physics Division Annual Report, ANL-7910, Argonne National Laboratory (1972).
5. E. M. Bohn, R. Maerker, B. A. Magurno, F. J. McCross and R. E. Schenter, "Benchmark Testing of ENDF/B-IV," ENDF-230 (March, 1976).
6. R. D. McKnight, "Benchmark Testing Using ENDF/B-Versions III and IV," to be published in *Nucl. Sci. and Eng.*, 1976. (See also ANL-ZPR-TM-214, 1975).
7. W. M. Stacey, Jr., and J. R. Regis, "VARI-1D: A One-Dimensional Variational Sensitivity Code," Argonne National Laboratory Report to be issued. (See also ANL reports: FRA-TM-25 and 26, 1972, FRA-TM-57, 1973).

*Session I*

**Fast Neutron Fission Cross Section Ratios**



# MEASUREMENTS OF NEUTRON-INDUCED FISSION CROSS-SECTION RATIOS INVOLVING ISOTOPES OF URANIUM AND PLUTONIUM

J. W. Behrens and G. W. Carlson

Lawrence Livermore Laboratory, University of California  
Livermore, California 94550 USA

## ABSTRACT

A procedure, called the threshold cross-section method, was applied to our experimental data involving four uranium ( $^{233}\text{U}$ ,  $^{234}\text{U}$ ,  $^{236}\text{U}$ , and  $^{238}\text{U}$ ) and five plutonium ( $^{239}\text{Pu}$ ,  $^{240}\text{Pu}$ ,  $^{241}\text{Pu}$ ,  $^{242}\text{Pu}$ , and  $^{244}\text{Pu}$ ) isotopes to determine ratios of fission cross sections relative to  $^{235}\text{U}$ . The data were gathered using ionization fission chambers and the time-of-flight technique at the LLL 100-MeV electron linear accelerator: measurements span the neutron energy range of 0.001 to 30 MeV. Experimental uncertainties common to past measurements were either eliminated or significantly reduced in this study by use of the threshold method, thereby making higher accuracies possible. Our cross-section ratios are absolute in the sense that they do not depend on the work of others. Results from our ratios involving  $^{233}\text{U}$ ,  $^{235}\text{U}$ ,  $^{238}\text{U}$ , and  $^{239}\text{Pu}$  are used to illustrate this method.

## INTRODUCTION

Over the past two decades, many measurements of the neutron-induced fission cross-section ratios involving isotopes of uranium and plutonium have been published. In most cases, these ratios are made with respect to the fission cross section of  $^{235}\text{U}$ , and fall into two categories: ratios in which the measurement includes an *experimental* means for determining the normalization, and ratios that are *arbitrarily* normalized to a value taken from either another experiment or from an evaluation. Ratios belonging to the first category not only give definition to the relative energy dependence of the cross sections but also provide an independent means for obtaining absolute fission cross sections once the cross section of the reference nuclide is known. Fission cross-section ratio measurements involving the relatively long-lived isotopes of uranium ( $^{233}\text{U}$ ,  $^{234}\text{U}$ ,  $^{235}\text{U}$ ,  $^{236}\text{U}$ , and  $^{238}\text{U}$ ) and plutonium ( $^{239}\text{Pu}$ ,  $^{240}\text{Pu}$ ,  $^{241}\text{Pu}$ ,  $^{242}\text{Pu}$ , and  $^{244}\text{Pu}$ ) were recently completed at LLL using our threshold cross-section method.

Our measurements were conducted using ionization fission chambers and the time-of-flight technique at the LLL 100-MeV electron linear accelerator

(linac). The measurements span the neutron energy range of 0.001 to 30 MeV, except where limited by low cross sections in the threshold isotopes. The continuous energy spectrum of the neutron source allowed us to cover the entire energy range of each ratio in one measurement. In this paper our experimental setup and techniques are summarized and references containing more detailed information about our experiment as well as listings of some of our data are given. This work emphasizes the threshold cross-section method as outlined earlier by Behrens [1], and a comparison with the commonly used method illustrates the elimination or significant reduction of experimental uncertainties that is possible with our procedure.

## EXPERIMENTAL PROCEDURE

### Neutron Source and Detectors

Most of the measurements were conducted with fission chambers located at the 34.3-m station of the 250-m time-of-flight tube at the LLL linac. The ratios involving  $^{240}\text{Pu}$ ,  $^{242}\text{Pu}$ , and  $^{244}\text{Pu}$  were measured at 15.8 m to reduce the effect of spontaneous fission backgrounds. The linac was operated at 1440 Hz with an electron pulse width of 10 ns to produce neutrons in a water-cooled tantalum target.

The fission detectors were parallel-plate ionization chambers of modular design, placed back-to-back in a pressure vessel with the foils oriented perpendicular to the incident neutron beam. Both time-of-flight and pulse-height information were processed for each event in our data acquisition system. Table I lists the isotopic compositions and areal densities of our high-purity fissionable materials.

### Timing, Resolution, and Backgrounds

The gamma flash from the tantalum target was used as our main timing reference for most of our measurements. We verified this timing by measuring the positions of the MeV resonances of carbon and our time-to-energy conversion includes the relativistic correction.

The resolution of our experiment was determined by the resolution of the fission detector ( $<9$  ns) and the pulse width of the electron pulses striking the tantalum target ( $\sim 10$  ns). Uncertainty in flight path as well as in finite target and detector thickness resulted in a loss of resolution that was small compared to the magnitude of these two components. Our data have typical energy resolutions of 6% at 20 MeV and 1.5 to 3.0% at 1 MeV.

Out-of-time neutron backgrounds were measured at both time-of-flight stations using the black-resonance absorber technique and were found to contribute negligible error ( $<0.1\%$ ). Time-independent backgrounds resulting from amplifier noise, alpha pileup pulses, and spontaneous fission were subtracted and, in most cases, these corrections also contributed negligible error. A variety of reports further describing our experiment and experimental errors are available [2-7]; several contain listings of our data [4,6,7].

## Comparison of Procedures for Determination of Cross-Section Ratios

A common procedure for fission cross-section ratio determination requires the placement of fission detectors, each containing a high-purity fissionable isotope, such that they are run simultaneously in the same neutron flux. The expected counting rates in these detectors are then

$$r_A(E) = \phi(E)N_A\sigma_A(E) \quad \text{and} \quad r_B(E) = \phi(E)N_B\sigma_B(E),$$

where  $\phi(E)$  is the neutron flux and  $N_A$  and  $N_B$  are the numbers of atoms of isotopes A and B. The ratio of these rates gives

$$\frac{r_A(E)}{r_B(E)} = \frac{N_A\sigma_A(E)}{N_B\sigma_B(E)} \quad \text{or} \quad \frac{\sigma_A(E)}{\sigma_B(E)} = \frac{N_B}{N_A} \frac{r_A(E)}{r_B(E)}.$$

The atom ratio,  $N_B/N_A$ , must be known to determine the fission cross-section ratio,  $\sigma_A(E)/\sigma_B(E)$ . In practice, the fission detectors usually have different fission fragment detection efficiencies that are less than 100% because of fragment losses in the fission foils and other effects. Thus, to account for detector efficiencies, the expression becomes

$$\frac{\sigma_A(E)}{\sigma_B(E)} = \frac{\beta_B N_B}{\beta_A N_A} \frac{r_B(E)}{r_A(E)},$$

where  $\beta_A$  and  $\beta_B$  are the explicit detector efficiencies, and the ratio  $\beta_B N_B / \beta_A N_A$  is the "effective" atom ratio. The measurement must now include either the determination of  $\beta_A$  and  $\beta_B$  or the determination of the effective atom ratio, itself. Efficiencies are usually determined by studying the pulse-height distributions and estimating the fragment losses. The effective atom ratio is usually measured at a neutron energy where the cross-section ratio is assumed to be well-known, e.g., at thermal neutron energy. Experimental uncertainties arising from these added steps can dominate the list of errors and limit the accuracy of the final cross-section ratio. Some investigators indicate that the determination of the effective atom ratio is the critical problem that limits the accuracy of the entire measurement [8,9]. The numbers of atoms,  $N_A$  and  $N_B$ , can be determined by assaying techniques such as alpha counting, isotope-dilution mass spectrometry, and controlled-potential coulometry. The errors associated with these techniques further limit the accuracy of the final result. In recent years this commonly-used procedure has been used in a variety of published fission cross-section ratio measurements with considerable emphasis placed on the discussion of detector efficiencies, fragment losses, and assaying techniques [8-16].

Our data were reduced using a procedure we call the threshold cross-section method. With this method it is possible to obtain results with total uncertainties of less than 1% for each threshold-isotope ratio. Determination of ratios involving two nonthreshold isotopes can be accomplished by using this method more than once, as illustrated in the next section.

The threshold method uses two fission chambers. The first contains a mixture of the two isotopes of interest with an atom ratio,  $\eta$ , of the isotope B to the threshold isotope A. For some range of energies below the threshold

of isotope A, the ratio of fission cross sections,  $\sigma_A(E)/\sigma_B(E)$ , must be negligible when compared with the same ratio above the threshold. The expected counting rate in the mixed chamber is

$$r_m(E) = \phi(E)\beta_m N_A [\sigma_A(E) + \eta\sigma_B(E)] ,$$

where  $\phi(E)$  is the neutron flux,  $N_A$  is the number of atoms of isotope A, and  $\beta_m$  is the efficiency for detecting fission fragments in the mixed chamber. The second fission chamber contains  $N_B$  atoms of pure isotope B and has an efficiency of  $\beta_p$ . The counting rate for this pure chamber is

$$r_p(E) = \phi(E)\beta_p N_B \sigma_B(E) .$$

To measure  $r_m(E)$  and  $r_p(E)$ , the two chambers are exposed simultaneously to the same neutron beam. The ratio of their rates gives

$$R(E) = \frac{r_m(E)}{r_p(E)} = \frac{\beta_m N_A}{\beta_p N_B} \left( \frac{\sigma_A(E)}{\sigma_B(E)} + \eta \right) .$$

Below the threshold of isotope A,  $R(E)$  is a constant,  $Q$ , and the experimental results yield the ratio of the effective numbers of atoms since

$$\frac{\beta_m N_A}{\beta_p N_B} = \frac{Q}{\eta} .$$

Substituting  $Q/\eta$  into the above equation and solving for  $\sigma_A(E)/\sigma_B(E)$ , we obtain the cross-section ratio,

$$\frac{\sigma_A(E)}{\sigma_B(E)} = \eta \left( \frac{R(E)}{Q} - 1 \right) . \quad (1)$$

Only the atom ratio in the mixed chamber,  $\eta$ , is a necessary prerequisite in the determination of the cross-section ratio.

#### RESULTS OBTAINED USING THE THRESHOLD METHOD

Application of the threshold method to the determination of the  $^{238}\text{U}/^{235}\text{U}$  fission cross-section ratio will further illustrate this procedure. In this measurement the mixed chamber, containing a homogeneous mixture of  $^{235}\text{U}$  and  $^{238}\text{U}$ , was prepared from materials of high isotopic purity. The atom ratio,  $\eta$ , of the  $^{235}\text{U}$  isotope to the threshold isotope,  $^{238}\text{U}$ , was determined using mass spectrometry. The pure chamber contained high-purity  $^{235}\text{U}$  and both chambers were exposed simultaneously to the same neutron beam. The ratio,  $R(E)$ , of the counting rates  $r_m(E)$  and  $r_p(E)$ , taken from one of our experimental runs, is shown in Figure 1a. Below the threshold of the  $^{238}\text{U}$ ,  $R(E)$  is a constant,  $Q$ , and is equal to the ratio of effective numbers of atoms multiplied by  $\eta$ . Above the threshold,  $R(E)$  is equal to  $(Q/\eta \times \sigma_{28}/\sigma_{25}) + Q$ . Once  $Q$  is subtracted from  $R(E)$  and these results are multiplied by  $\eta/Q$ , we obtain the ratio of the  $^{238}\text{U}/^{235}\text{U}$  fission cross sections, (Figure 1b). In

the interval from 1.75 to 4.00 MeV an average cross-section ratio of  $0.4422 \pm 0.0039$  was found.

The relative counting uncertainties become large when the fission cross-section ratio becomes small compared to the mixed chamber atom ratio,  $\eta$ . Therefore, the  $^{238}\text{U}/^{235}\text{U}$  ratio was also determined in the same experiment by including separate fission chambers containing high-purity  $^{238}\text{U}$  and high-purity  $^{235}\text{U}$ . These results were normalized to the average value of the threshold method data,  $0.4422 \pm 0.0039$  in the interval of 1.75 to 4.00 MeV (see Figures 1b and 1c). Two separate  $^{235}\text{U}$  fission chambers were used to avoid correlated errors between the two sets of measurements and to provide an experimental determination of the magnitude of the neutron flux change across the four back-to-back fission chambers. Figure 1d shows our ratio over the 0.1 to 1.5 MeV energy range.

It is possible to use the threshold method to determine normalization values for ratios involving two nonthreshold isotopes as illustrated by our  $^{233}\text{U}/^{235}\text{U}$  and  $^{239}\text{Pu}/^{235}\text{U}$  cross-section ratio measurements. For the  $^{233}\text{U}/^{235}\text{U}$  cross-section ratio measurement, we first obtained the  $^{238}\text{U}/^{233}\text{U}$  ratio (Figure 2a). The average of this ratio was  $0.3007 \pm 0.0026$  in the interval from 1.75 to 4.00 MeV. This value, together with our value for  $^{238}\text{U}/^{235}\text{U}$  cross-section ratio gave a normalization for the  $^{233}\text{U}/^{235}\text{U}$  ratio (Figure 2b). For the  $^{239}\text{Pu}/^{235}\text{U}$  cross-section ratio measurement, an auxiliary measurement of the ratio  $^{238}\text{U}/^{239}\text{Pu}$  was made using the threshold method. This data, shown in Figure 3a, yielded an average value of  $0.2895 \pm 0.0042$  in the normalization interval and was used with the  $^{238}\text{U}/^{235}\text{U}$  cross-section ratio to normalize our  $^{239}\text{Pu}/^{235}\text{U}$  ratio (Figure 3b).

Fission cross-section ratio measurements involving  $^{234}\text{U}$ ,  $^{236}\text{U}$ ,  $^{240}\text{Pu}$ ,  $^{241}\text{Pu}$ ,  $^{242}\text{Pu}$ , and  $^{244}\text{Pu}$  were also conducted at the linac. All of our normalization values were determined from the threshold-method cross-section ratios and are given in Table II, along with the values of  $\eta$  as determined by groups at LLL and the Los Alamos Scientific Laboratory. Figures 4 through 6 show our fission cross-section ratios for  $^{234}\text{U}$ ,  $^{236}\text{U}$ ,  $^{240}\text{Pu}$ ,  $^{241}\text{Pu}$ ,  $^{242}\text{Pu}$ , and  $^{244}\text{Pu}$  relative to  $^{235}\text{U}$ .

#### UNCERTAINTIES ASSOCIATED WITH THE THRESHOLD METHOD

The average cross-section ratio,  $A$ , in an energy interval is related to measured quantities by  $A = 2(\bar{R}/Q - 1)$ , where  $\bar{R}$  is the average of  $R(E)$  in the interval (refer to equation 1). The uncertainty in  $A$  can be conveniently written in terms of fractional errors:

$$\frac{\delta A}{A} = \left[ \left( \frac{\delta \eta}{\eta} \right)^2 + \left( \frac{A + \eta}{A} \right)^2 \left( \left( \frac{\delta R}{R} \right)^2 + \left( \frac{\delta Q}{Q} \right)^2 \right) \right]^{1/2}.$$

This error formula shows how the errors from the three measured quantities,  $\eta$ ,  $\bar{R}$ , and  $Q$ , combine to give the total error in the average normalized ratio,  $A$ . The fractional errors from  $\bar{R}$  and  $Q$  are each multiplied by the term  $(A + \eta)/A$  and this factor may be considerably larger than 1 if  $\eta$  is greater than  $A$ .

For our measurements, the energy interval from 1.75 to 4.00 MeV was chosen to compute average threshold method cross-section ratios because, in this energy range, the fission ratios were generally smooth and flat. For each ratio, the energy range chosen for Q varied because the high-energy end of the interval was limited by the onset of a significant fission cross section from the threshold isotope in the mixed chamber. The low-energy end of the Q interval was generally limited by the presence of significant no-beam backgrounds.

Application of the threshold method to our data required that certain corrections be made. In the Q interval, we accounted for the subthreshold fission cross sections of the threshold isotopes. This was accomplished within the measurements by using those ratios involving the high purity fission chambers. For these measurements, the uncertainty in Q from corrections resulting from alpha-particle pileup and spontaneous fission backgrounds was negligible for all the threshold ratios, except for the  $^{244}\text{Pu}/^{239}\text{Pu}$  ratio where the error is estimated to be 0.5%. In all our ratios, the backgrounds were small fractions of the neutron-induced counts in the 1.75 to 4.00 MeV interval where  $\bar{R}$  was computed and the background uncertainty in  $\bar{R}$  was negligible. Out-of-time neutron backgrounds were measured using the black-resonance absorber technique and were found to contribute negligible error within the Q intervals. No correction was made for these backgrounds and it was assumed that these errors were also negligible at higher neutron energies. The neutron beam from the linac was collimated to avoid all but the thin parts of the fission chamber. We corrected the relative count rates of the mixed and pure fission chambers for neutron scattering in the aluminum foils and other chamber parts. The scattering correction was less than 0.5% in magnitude, except at the large aluminum resonances, and the uncertainty from scattering in the corrected ratio  $R(E)/Q$  was negligible.

Our measurements contain the assumption that the efficiencies for detecting fission fragments in the fission chambers are independent of neutron energy. The degree to which this assumption is realized is an especially important question in the mixed chambers. In our mixed chambers, the fissions determining Q were from the nonthreshold isotope, while the majority of the fissions determining  $R(E)$  came from the threshold isotope. We measured the energy dependence of all of our fission chamber efficiencies and our results for the uranium isotopes are available [3]. Fission-chamber pulse-height distributions were obtained simultaneously for a number of wide neutron energy bands by processing both time-of-flight and pulse-height information for each event. Comparison of these distributions at different neutron energies showed that there were energy-dependent effects that increase as the efficiency for detecting fission fragments decreases. Since our fission chambers were designed to permit good separation of fission and alpha-pileup pulses, we were able to choose the bias levels for our data so that the energy variations of the efficiencies were acceptably small (<0.5%).

An accurate determination of  $\eta$ , the atom ratio of the nonthreshold to threshold nuclide in the mixed chamber, was essential for the successful application of the threshold cross-section method. For mixtures involving two isotopes of the same element, mass spectrometry was used to determine the atom ratio. Determining the ratios involving two isotopes of different elements was more difficult, and therefore we used isotope-dilution mass spectrometry

and controlled-potential coulometry. Measurements of  $\eta$ , as determined by groups at LLL and the Los Alamos Scientific Laboratory are reported in Table II, along with their total uncertainties, expressed as standard deviations.

When preparing mixtures of different elements for the foils for the mixed chambers, special care must be taken to ensure that the mixture remains homogeneous. In some instances, the chemistry of plutonium is quite different from that of uranium, e.g., polymerization. Steps should also be taken to insure an accurate determination of  $\eta$ . In our experiment, samples were sent to various laboratories and only two of these labs were able to give atom-ratio determinations that were consistent with the quoted errors.

#### COMPARISON WITH FISSION RATIOS AT THERMAL NEUTRON ENERGY

We made a comparison for the ratios of the fissile isotopes  $^{233}\text{U}$ ,  $^{239}\text{Pu}$ , and  $^{241}\text{Pu}$  to  $^{235}\text{U}$  between our threshold method results and evaluations of thermal energy fission cross-section ratios. This was accomplished by conducting additional fission-ratios measurements at the LLL linac in the energy range from 0.01 eV to 30 keV. The low-energy results were tied to our high-energy ratios in the energy range 0.65 to 30 keV. These thermal measurements provide a cross-check on our high-energy normalization and are not an attempt to improve the thermal values. In Table III, we compare our preliminary results for fission cross-section ratios at thermal neutron energy to recent evaluations of these ratios [17,18] and our uncertainties include estimates of all identified experimental errors. The  $^{233}\text{U}/^{235}\text{U}$  ratio has a discrepancy with the evaluations which we are unable to explain at this time.

#### FURTHER COMPARISONS

Several of our fission cross-section ratios are compared over the neutron energy range including the 1.75 to 4.00 MeV normalization interval in Figure 7. The  $^{238}\text{U}/^{235}\text{U}$ ,  $^{233}\text{U}/^{235}\text{U}$ , and  $^{239}\text{Pu}/^{235}\text{U}$  ratios are discussed below.

##### The $^{238}\text{U}/^{235}\text{U}$ Fission Cross-Section Ratio

In Figure 7a, our data for the  $^{238}\text{U}/^{235}\text{U}$  fission cross-section ratio are compared to others over the neutron energy range of 1.75 to 5.5 MeV. Good agreement is found between our data and that of Jarvis [19], White and Warner [16], Meadows [11], and Poenitz [9]. The data of Stein, Smith, and Smith [15] have the same general shape as our results but their data are approximately 3.5% lower than ours.

##### The $^{233}\text{U}/^{235}\text{U}$ Fission Cross-Section Ratio

Figure 7b presents our data for the  $^{233}\text{U}/^{235}\text{U}$  fission cross-section ratio as compared to others over the energy range of 0.8 to 4.0 MeV. Our results are in good agreement with data of White and Warner [16] and of Pflertschinger and Kaeppler [14]. The data of Meadows [8] agree in shape with our results but are about 5% higher in value.

## The $^{239}\text{Pu}/^{235}\text{U}$ Fission Cross-Section Ratio

Our  $^{239}\text{Pu}/^{235}\text{U}$  fission cross-section ratio is compared in Figure 7c with the results of White and Warner [16] and of Poenitz [12]. Good agreement is found over the energy range of 0.8 to 5.5 MeV.

Table IV contains a detailed comparison of our results with the data of White and Warner [16] at their four neutron energies; 1.0, 2.25, 5.4, and 14.1 MeV. Good agreement is found for the  $^{233}\text{U}/^{235}\text{U}$ ,  $^{238}\text{U}/^{235}\text{U}$ , and  $^{239}\text{Pu}/^{235}\text{U}$  ratios. Several of the remaining ratios do not agree well; however, it should be mentioned that the White and Warner results depend on alpha-decay half-lives because alpha-counting was their main assaying technique. Substituting currently accepted half-life values for those used by White and Warner brings their results into closer agreement with our data.

## CONCLUSIONS

The threshold cross-section method was successfully used to determine fission cross-section ratios of four uranium and five plutonium isotopes relative to  $^{235}\text{U}$ . We found that certain experimental errors common to past normalization methods can be eliminated or significantly reduced by use of this method. However, high-efficiency fission detectors are needed to prevent a significant energy dependence in the efficiency. This is especially true for the detector containing the isotope mixture required for the threshold method. Although the data reduction is slightly more complicated in the threshold method, one gains the advantage that the ratio of effective numbers of atoms may be determined simply and accurately.

We consider the threshold method to be a logical extension of the existing techniques and procedures, and advances in the design of neutron-producing facilities permit these methods to be more fully utilized. The threshold method is not limited to facilities producing white-neutron spectra but the simultaneous sampling of all neutron energies eliminates the effects of any slow variation in detector efficiency over the time period of the measurement.

Work on measuring fission cross-section ratios continues at LLL. Measurements of  $^{237}\text{Np}$  and  $^{241}\text{Am}$  relative to  $^{235}\text{U}$  are presently being made and in the near future,  $^{230}\text{Th}$ ,  $^{232}\text{Th}$ , and  $^{243}\text{Am}$  will also be studied. All ratios will be determined using the threshold method.

## ACKNOWLEDGMENTS

We thank R. W. Bauer, J. D. Anderson, R. L. Wagner, and F. S. Eby for their support and encouragement expressed throughout the course of this investigation. We express special thanks to R. S. Newbury and J. W. Magana for their invaluable contributions. We also thank our electronic and mechanical engineering groups for their efforts in the design and construction of our experimental apparatus as well as the linac operators and staff for their cooperation.

This work was performed under the auspices of the U.S. Energy Research & Development Administration, under contract No. W-7405-Eng-48.

## REFERENCES

1. J. W. Behrens, "Determination of Absolute Fission Cross Section Ratios Using the Method of Threshold Cross Sections," Rept. UCRL-51478, Lawrence Livermore Laboratory (1973).
2. J. W. Behrens and G. W. Carlson, "High-Energy Measurements of the Neutron-Induced Fission Cross Section Ratios Involving  $^{233}\text{U}$ ,  $^{235}\text{U}$ ,  $^{238}\text{U}$ , and  $^{239}\text{Pu}$  Using the Method of Threshold Cross Sections," Rept. UCID-16548, Lawrence Livermore Laboratory (1974).
3. G. W. Carlson, M. O. Larson, and J. W. Behrens, "Measurements of the Energy Dependence of the Efficiency of Fission Chambers," Rept. UCRL-51727, Lawrence Livermore Laboratory (1974).
4. J. W. Behrens and G. W. Carlson, "Measurement of the Neutron-Induced Fission Cross Section of  $^{241}\text{Pu}$  Relative to  $^{235}\text{U}$  from 0.001 to 30 MeV," Rept. UCRL-51925, Lawrence Livermore Laboratory (1975).
5. J. W. Behrens, G. W. Carlson, and R. W. Bauer, "Neutron-Induced Fission Cross Sections of  $^{233}\text{U}$ ,  $^{234}\text{U}$ ,  $^{236}\text{U}$ , and  $^{238}\text{U}$  With Respect to  $^{235}\text{U}$ ," in *Proc. Conf. Nuclear Cross Sections and Technology*, Washington, D.C., (1975), p. 591.
6. G. W. Carlson and J. W. Behrens, "Fission Cross Section Ratio of  $^{239}\text{Pu}$  to  $^{235}\text{U}$  from 0.1 to 30 MeV," Rept. UCID-16981, Lawrence Livermore Laboratory (1975).
7. J. W. Behrens, J. C. Browne, and G. W. Carlson, "Measurements of the Neutron-Induced Fission Cross Sections of  $^{240}\text{Pu}$  and  $^{242}\text{Pu}$  Relative to  $^{235}\text{U}$ ," Rept. UCID-17047, Lawrence Livermore Laboratory (1976).
8. J. W. Meadows, "The Ratio of the Uranium-233 to Uranium-235 Fission Cross Section," *Nucl. Sci. Eng.* 54, 317 (1974).
9. W. P. Poenitz and R. J. Armani, "Measurements of the Fission Cross Section Ratio of  $^{238}\text{U}$  to  $^{235}\text{U}$  from 2-3 MeV," *J. Nucl. Energy* 26, 483 (1972).
10. F. Kaeppler and E. Pfletschinger, "A Measurement of the Fission Cross Section of Plutonium-241 Relative to Uranium-235," *Nucl. Sci. Eng.* 51, 124 (1973).
11. J. W. Meadows, "The Ratio of the Uranium-238 to Uranium-235 Fission Cross Sections from 1 to 5 MeV," *Nucl. Sci. Eng.* 49, 310 (1972).
12. W. P. Poenitz, "Additional Measurements of the Ratio of the Fission Cross Sections of Plutonium-239 and Uranium-235," *Nucl. Sci. Eng.* 47, 228 (1972).
13. W. P. Poenitz, "Measurement of the Ratios of Capture and Fission Neutron Cross Sections of  $^{235}\text{U}$ ,  $^{238}\text{U}$ , and  $^{239}\text{Pu}$  at 130 to 1400 keV," *Nucl. Sci. Eng.* 40, 383 (1970).

14. E. Pfletschinger and F. Kaeppeler, "A Measurement of the Fission Cross Sections of  $^{239}\text{Pu}$  and  $^{233}\text{U}$  Relative to  $^{235}\text{U}$ ," *Nucl. Sci. Eng.* 40, 375 (1970).
15. W. E. Stein, R. K. Smith, and H. L. Smith, "Relative Fission Cross Sections of  $^{236}\text{U}$ ,  $^{238}\text{U}$ ,  $^{237}\text{Np}$ , and  $^{235}\text{U}$ ," in *Proc. Conf. Neutron Cross Sections and Technology*, Rept. CONF-680307, Washington, D.C., (1968), p. 627.
16. P. H. White and G. P. Warner, "The Fission Cross Sections of  $^{233}\text{U}$ ,  $^{234}\text{U}$ ,  $^{236}\text{U}$ ,  $^{238}\text{U}$ ,  $^{237}\text{Np}$ ,  $^{239}\text{Pu}$ ,  $^{240}\text{Pu}$ , and  $^{241}\text{Pu}$  Relative to that of  $^{235}\text{U}$  for Neutrons in the Energy Range 1-14 MeV," *J. Nucl. Energy* 21, 671 (1967).
17. H. D. Lemmel, "The Third IAEA Evaluation of the 2200 m/s and 20°C Maxwellian Neutron Data for U-233, U-235, Pu-239, and Pu-241," *Proc. Conf. Nuclear Cross Sections and Technology*, Washington, D.C., (1975), p. 286.
18. J. R. Stehn, "Thermal Data for Fissile Nuclei in ENDF/B-IV," *Trans. Amer. Nucl. Soc.*, 18, 351 (1974).
19. G. A. Jarvis, "Fission Comparison of  $^{238}\text{U}$  and  $^{235}\text{U}$  for 2.5 MeV Neutrons," Rept. LA-1571, Los Alamos Scientific Laboratory (1953).

TABLE I

Isotopic Analyses of High-Purity Isotopes Using Mass Spectrometry.

Isotope	Isotopic Composition (Mass Number)										Areal Density (g/m <sup>2</sup> )
	233	234	235	236	238	239	240	241	242	244	
<sup>233</sup> U	99.99+			0.001							2.7
<sup>234</sup> U	0.005	99.84	0.10	0.05	0.01						3.0
<sup>235</sup> U		0.03	99.91	0.02	0.04						3.0
<sup>236</sup> U			0.0025	99.99+							1.9
<sup>238</sup> U			0.0006		99.99+						3.1
<sup>239</sup> Pu						99.978	0.020				2.0
<sup>240</sup> Pu						0.800	98.482	0.545	0.173		0.6
<sup>241</sup> Pu					<0.0004	1.372	0.234	98.30	0.088	<0.0004	1.9
<sup>242</sup> Pu					0.011	0.092	0.013	0.012	99.872		1.1
<sup>244</sup> Pu						0.004	0.306	0.074	1.038	98.578	1.1

TABLE II

Threshold Method Normalization Values and Measurements of  $\eta$  for Various Fission Cross-Section Ratios.

Fission Cross-Section Ratio	Threshold Method Normalization Value <sup>a</sup>	Determination of $\eta \pm \delta\eta$				
		Mass Spectrometry		Isotope-Dilution Mass Spectrometry	Controlled-Potential Coulometry	
		LLL <sup>b</sup>	LASL <sup>c</sup>	LLL <sup>b,f</sup>	LASL <sup>d</sup>	LLL <sup>e,f</sup>
<sup>234</sup> U/ <sup>235</sup> U	1.220 ± 0.012	0.6602 ±0.0016	0.6621 ±0.0016			
<sup>236</sup> U/ <sup>235</sup> U	0.7216 ± 0.0099	0.4378 ±0.0011	0.4384 ±0.0011			
<sup>238</sup> U/ <sup>235</sup> U	0.4422 ± 0.0039	0.3397 ±0.0008	0.3391 ±0.0008			
<sup>238</sup> U/ <sup>233</sup> U	0.3007 ± 0.0026	0.1456 ±0.0004	0.1451 ±0.0004			
<sup>238</sup> U/ <sup>239</sup> Pu	0.2895 ± 0.0042			0.1696 ±0.0008	0.1686 ±0.0004	0.1679 ±0.0015
<sup>238</sup> U/ <sup>240</sup> Pu	0.3233 ± 0.0065			0.1743 ±0.0008	0.1716 ±0.0004	0.1719 ±0.0015
<sup>238</sup> U/ <sup>241</sup> Pu	0.3484 ± 0.0055			0.2882 ±0.0013	0.2904 ±0.0006	0.2790 ±0.0024
<sup>242</sup> Pu/ <sup>239</sup> Pu	0.7342 ± 0.0095	0.3361 ±0.0008				0.3353 ±0.0034
<sup>244</sup> Pu/ <sup>239</sup> Pu	0.6406 ± 0.0101	0.4293 ±0.0011				0.4270 ±0.0043

<sup>a</sup>Over the normalization energy interval 1.75-4.00 MeV. Errors indicate total uncertainties expressed as standard deviations.

<sup>b</sup>Analyzed by R. S. Newbury, Lawrence Livermore Laboratory.

<sup>c</sup>As determined by J. H. Capps, Los Alamos Scientific Laboratory.

<sup>d</sup>Determined by J. E. Rein and G. R. Waterbury, Los Alamos Scientific Laboratory.

<sup>e</sup>Determined by J. W. Magana and J. E. Harrar, Lawrence Livermore Laboratory. Direct weighing was used on the  $^{242}\text{Pu}$  and  $^{244}\text{Pu}$  samples.

<sup>f</sup>Assays performed at intermediate steps in the fission foil preparation. These assays indicate that gross errors were not present in the preparation technique.

TABLE III

Comparison to Thermal Fission Cross-Section Ratios Relative to  $^{235}\text{U}$ .

Fission Cross- Section Ratio	Present Work		Lemmel <sup>a</sup>		Difference $\Delta^{a,c}$ (%)	Stehn <sup>b</sup> Thermal Ratio	Difference $\Delta^{b,c}$ (%)
	Thermal Ratio	Percent Error (%)	Thermal Ratio	Percent Error (%)			
$^{233}\text{U}/^{235}\text{U}$	0.879	$\pm 1.6$	0.908	$\pm 0.3$	+3.2	0.911	+3.5
$^{239}\text{Pu}/^{235}\text{U}$	1.279	$\pm 2.4$	1.275	$\pm 0.3$	-0.3	1.267	-0.9
$^{241}\text{Pu}/^{235}\text{U}$	1.772	$\pm 2.5$	1.740	$\pm 0.7$	-1.8	1.722	-2.9

<sup>a</sup>H. D. Lemmel (1975). See Reference 17.<sup>b</sup>J. R. Stehn (1974). See Reference 18.<sup>c</sup> $\Delta \equiv \frac{\text{Evaluated Value} - \text{Present Work}}{\text{Evaluated Value}} \times 100\%$ .

TABLE IV

Comparison of Present Work With White and Warner.<sup>a</sup>

Fission Cross- Section Ratio	Neutron Energy (MeV)											
	1.0			2.25			5.4			14.1		
	Present Work <sup>c</sup>	W/W <sup>a,c</sup>	$\Delta^b$ (%)	Present Work <sup>c</sup>	W/W <sup>a,c</sup>	$\Delta^b$ (%)	Present Work <sup>c</sup>	W/W <sup>a,c</sup>	$\Delta^b$ (%)	Present Work <sup>c</sup>	W/W <sup>a,c</sup>	$\Delta^b$ (%)
<sup>233</sup> U/ <sup>235</sup> U	1.514 ±0.022	1.504 ±0.030	+0.7	1.483 ±0.021	1.454 ±0.029	+2.0	1.410 ±0.026	1.362 ±0.027	+3.4	1.076 ±0.025	1.079 ±0.022	-0.3
<sup>234</sup> U/ <sup>235</sup> U	0.910 ±0.018	0.953 ±0.019	-4.7	1.181 ±0.021	1.127 ±0.023	+4.6	1.213 ±0.025	1.206 ±0.024	+0.6	0.972 ±0.034	0.956 ±0.019	+1.6
<sup>236</sup> U/ <sup>235</sup> U	0.306 ±0.008	0.278 ±0.006	+9.2	0.706 ±0.015	0.655 ±0.013	+7.2	0.800 ±0.018	0.765 ±0.015	+4.4	0.775 ±0.025	0.738 ±0.015	+4.8
<sup>238</sup> U/ <sup>235</sup> U	0.0141 ±0.0006	N.M. <sup>d</sup>		0.426 ±0.006	0.427 ±0.009	-0.2	0.535 ±0.008	0.528 ±0.011	+1.3	0.557 ±0.010	0.549 ±0.011	+1.4
<sup>239</sup> Pu/ <sup>235</sup> U	1.438 ±0.026	1.435 ±0.029	+0.2	1.525 ±0.028	1.520 ±0.030	+0.3	1.592 ±0.033	1.575 ±0.032	+1.1	1.149 ±0.029	1.163 ±0.023	-1.2
<sup>240</sup> Pu/ <sup>235</sup> U	1.245 ±0.028	1.154 ±0.023	+7.3	1.340 ±0.032	1.261 ±0.025	+5.9	1.409 ±0.035	1.409 ±0.028	0.0	1.093 ±0.033	1.047 ±0.021	+4.2
<sup>241</sup> Pu/ <sup>235</sup> U	1.291 ±0.027	1.356 ±0.027	-5.0	1.262 ±0.027	1.325 ±0.026	-5.0	1.273 ±0.035	1.290 ±0.026	-1.3	1.070 ±0.038	1.119 ±0.022	-4.6

<sup>a</sup>P. H. White and G. P. Warner (1967). See Reference 16.<sup>b</sup> $\Delta \equiv \frac{(\text{Present Work}) - (\text{Ref. 16})}{(\text{Present Work})} \times 100\%$ .<sup>c</sup>Errors are one standard deviation total uncertainties.<sup>d</sup>Not Measured.

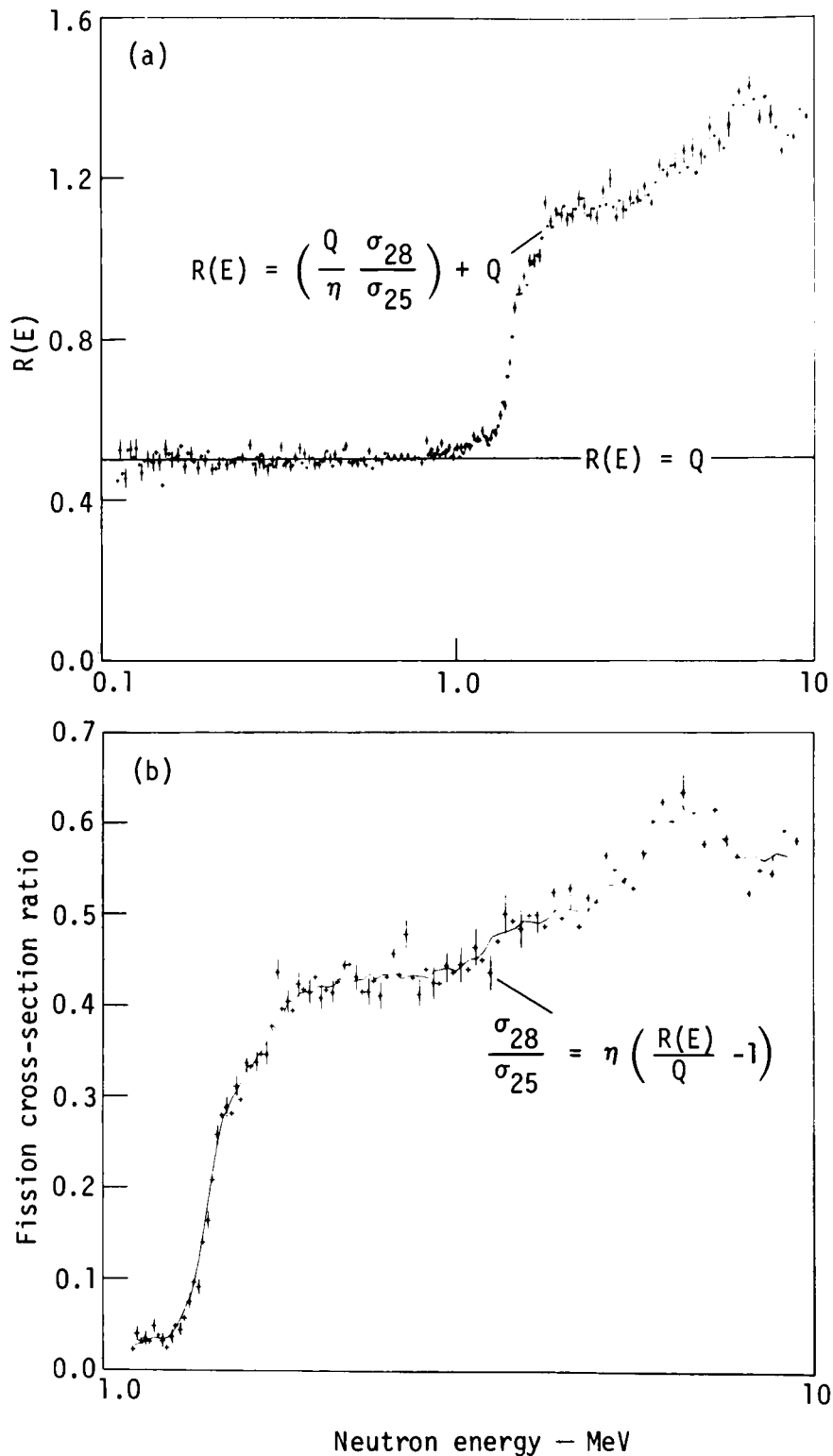


Figure 1. Fission cross-section ratio of  $^{238}\text{U}$  to  $^{235}\text{U}$ : statistical error bars are shown. (a) Threshold method ratio of the mixed chamber to the pure chamber rate file. (b) Threshold method ratio (+) compared to the ratio obtained from the high-purity isotope chambers (continuous line).

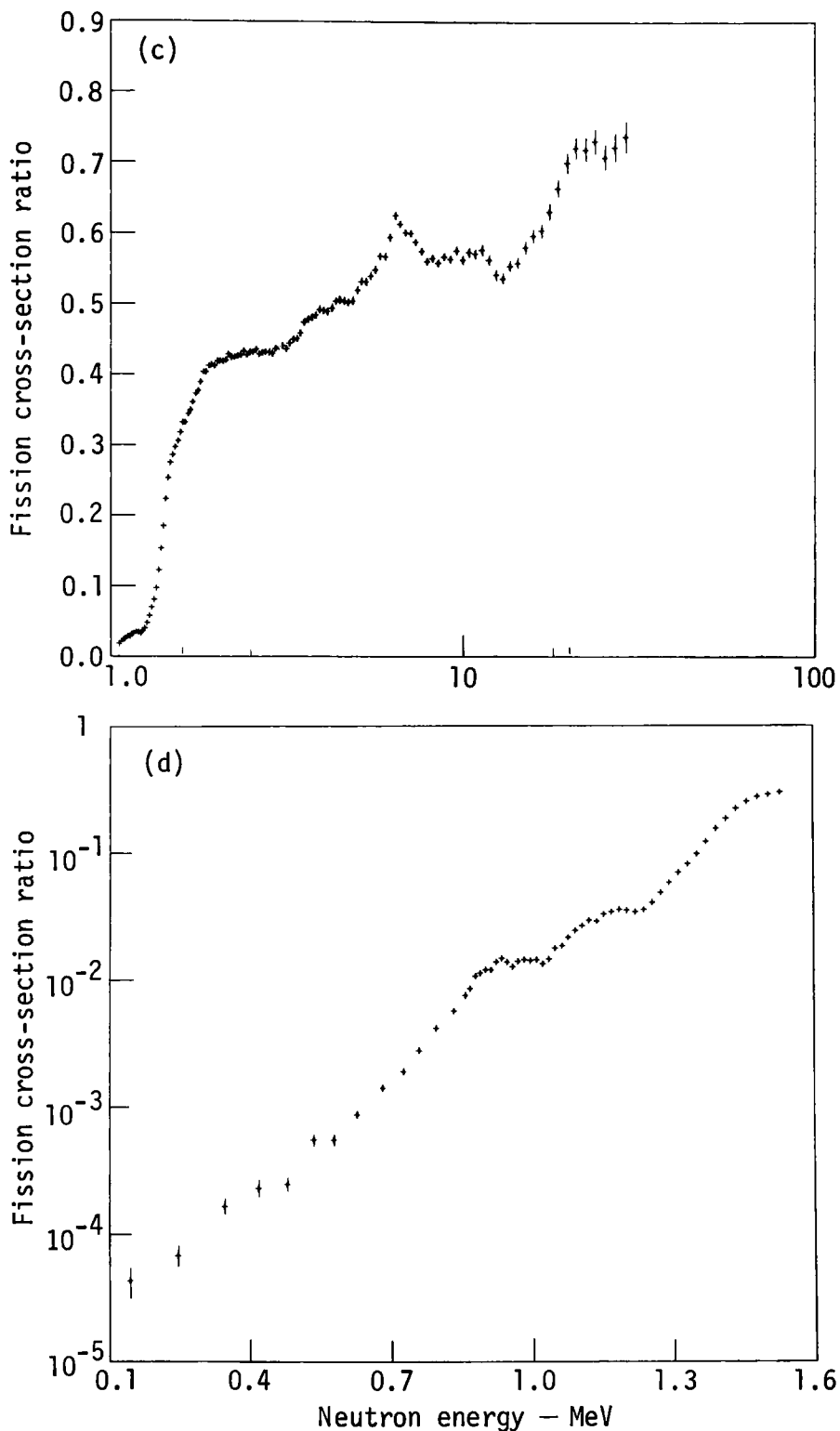


Figure 1. Fission cross-section ratio of  $^{238}\text{U}$  to  $^{235}\text{U}$ : (c) Ratio obtained from the high-purity chambers, normalized to  $0.4422 \pm 0.0039$  from 1.75 to 4.00 MeV. (d) Ratio from the high-purity chambers from 0.1 to 1.5 MeV.

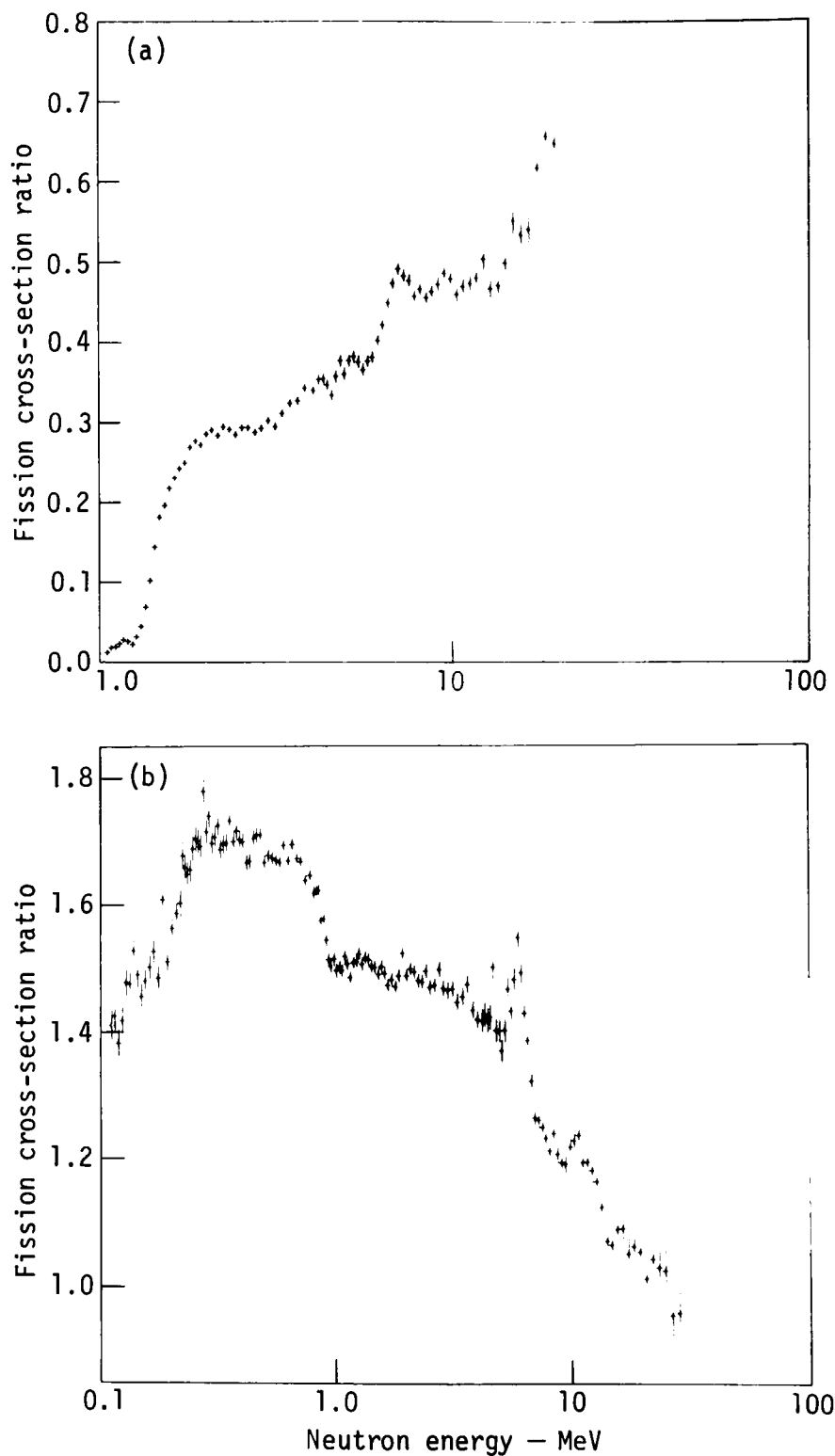


Figure 2. Fission cross-section ratios: statistical error bars are shown for each point. (a) Threshold method ratio of  $^{238}\text{U}$  to  $^{233}\text{U}$ . (b) Ratio of  $^{233}\text{U}$  to  $^{235}\text{U}$ , normalized to  $1.471 \pm 0.018$  from 1.75 to 4.00 MeV.

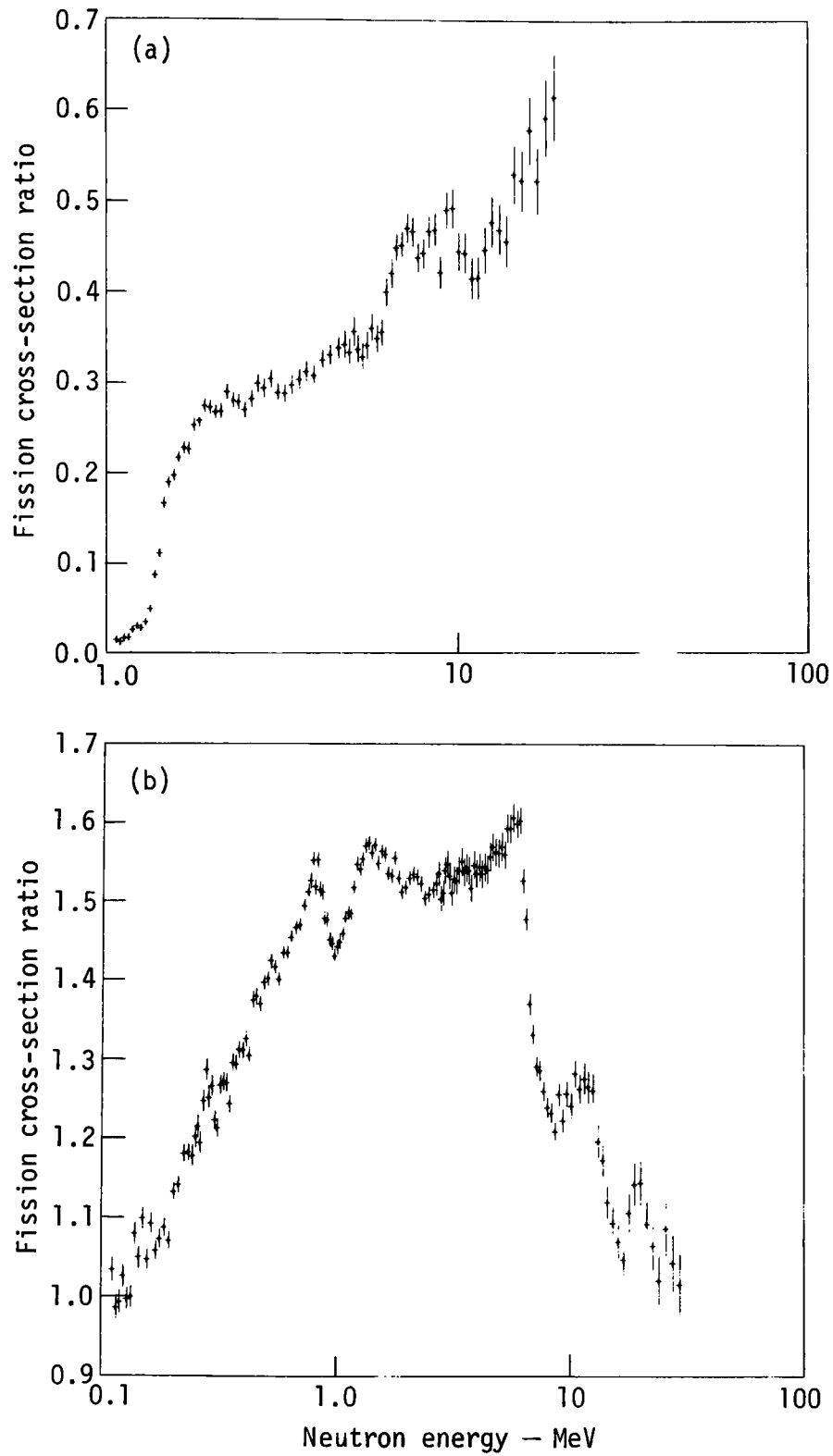


Figure 3. Fission cross-section ratios: statistical error bars are shown for each point. (a) Threshold method ratio of  $^{238}\text{U}$  to  $^{239}\text{Pu}$ . (b) Ratio of  $^{239}\text{Pu}$  to  $^{235}\text{U}$ , normalized to  $1.527 \pm 0.026$  from 1.75 to 4.00 MeV.

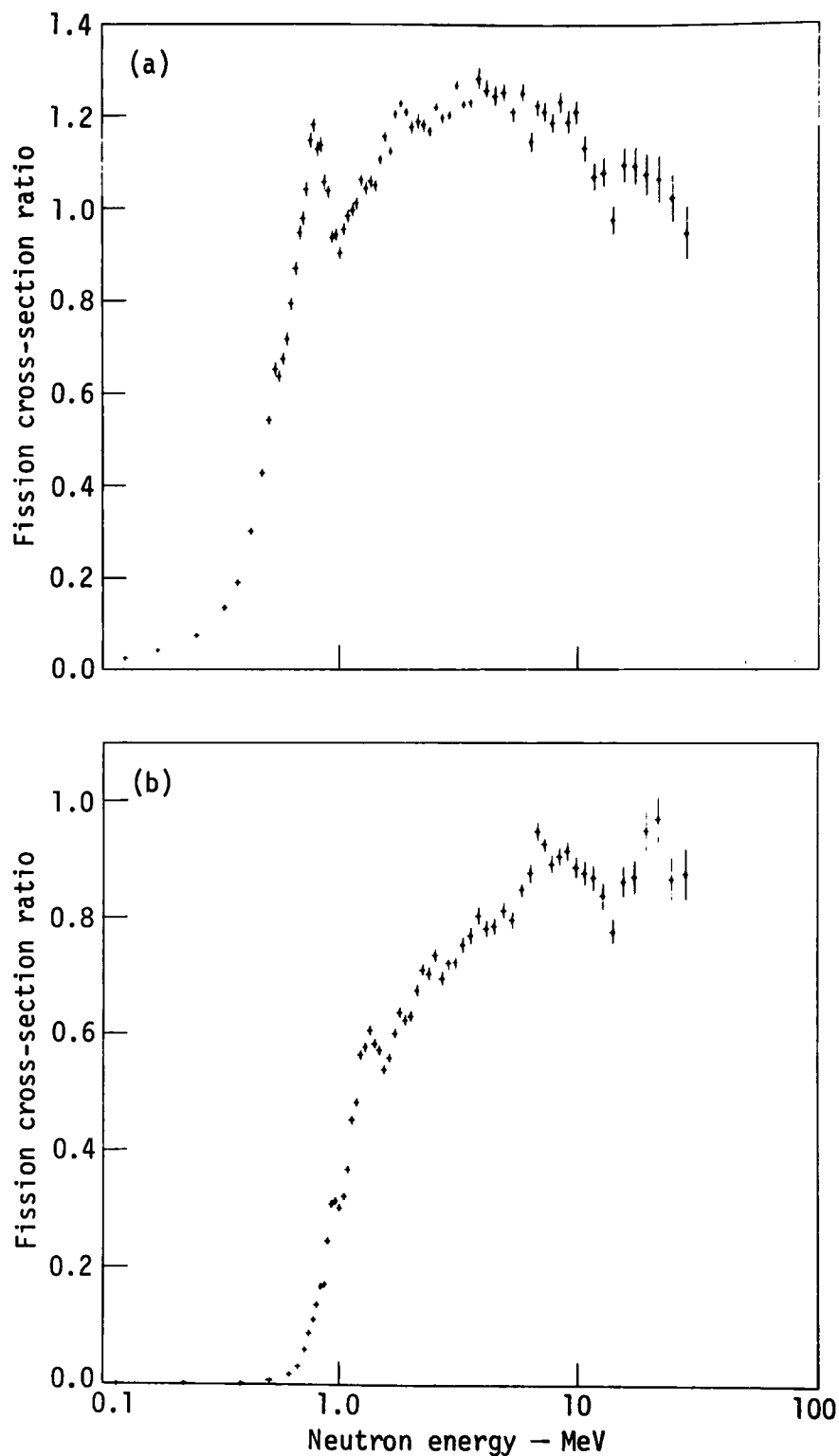


Figure 4. Fission cross-section ratios: statistical error bars are shown for each point. (a) Ratio of  $^{234}\text{U}$  to  $^{235}\text{U}$ , normalized to  $1.220 \pm 0.012$ . (b) Ratio of  $^{236}\text{U}$  to  $^{235}\text{U}$ , normalized to  $0.7216 \pm 0.0099$ .

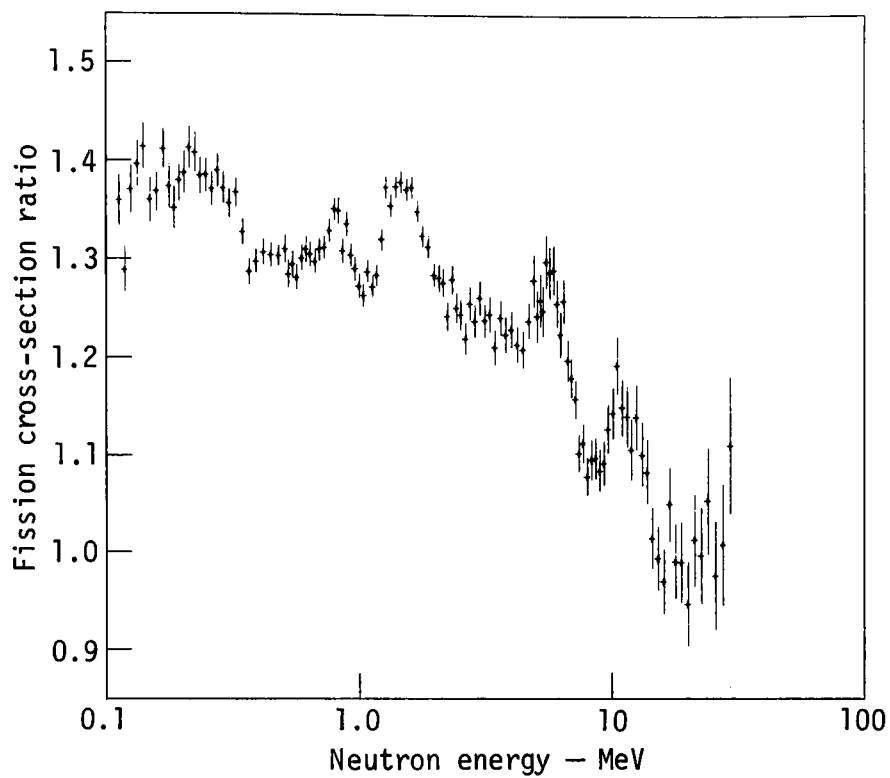


Figure 5. Fission cross-section ratio of  $^{241}\text{Pu}$  to  $^{235}\text{U}$ , normalized to  $1.269 \pm 0.023$  from 1.75 to 4.00 MeV. Statistical error bars are shown for each point.

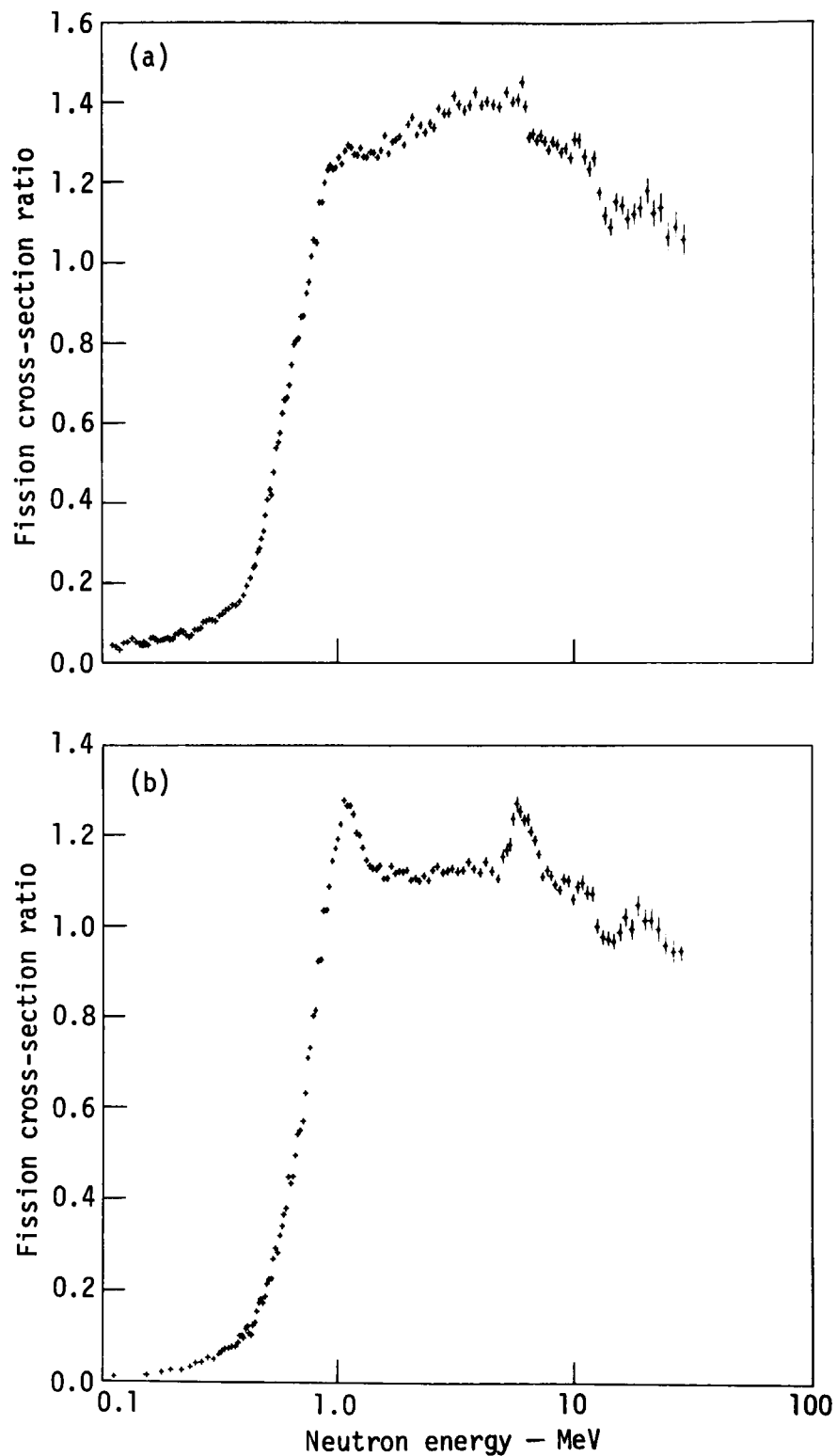


Figure 6. Fission cross-section ratios: statistical error bars are shown for each point. (a) Ratio of  $^{240}\text{Pu}$  to  $^{235}\text{U}$ , normalized to  $1.367 \pm 0.030$ . (b) Ratio of  $^{242}\text{Pu}$  to  $^{235}\text{U}$ , normalized to  $1.121 \pm 0.024$ .

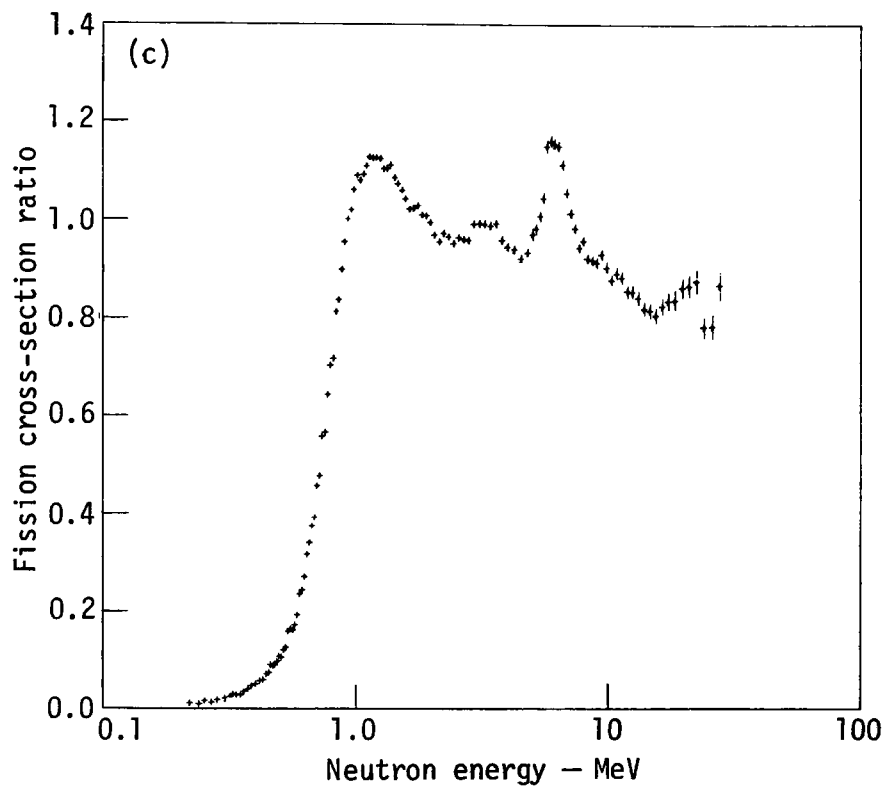


Figure 6. Fission cross-section ratios: (c) Ratio of  $^{244}\text{Pu}$  to  $^{235}\text{U}$ , normalized to  $0.9782 \pm 0.023$ .

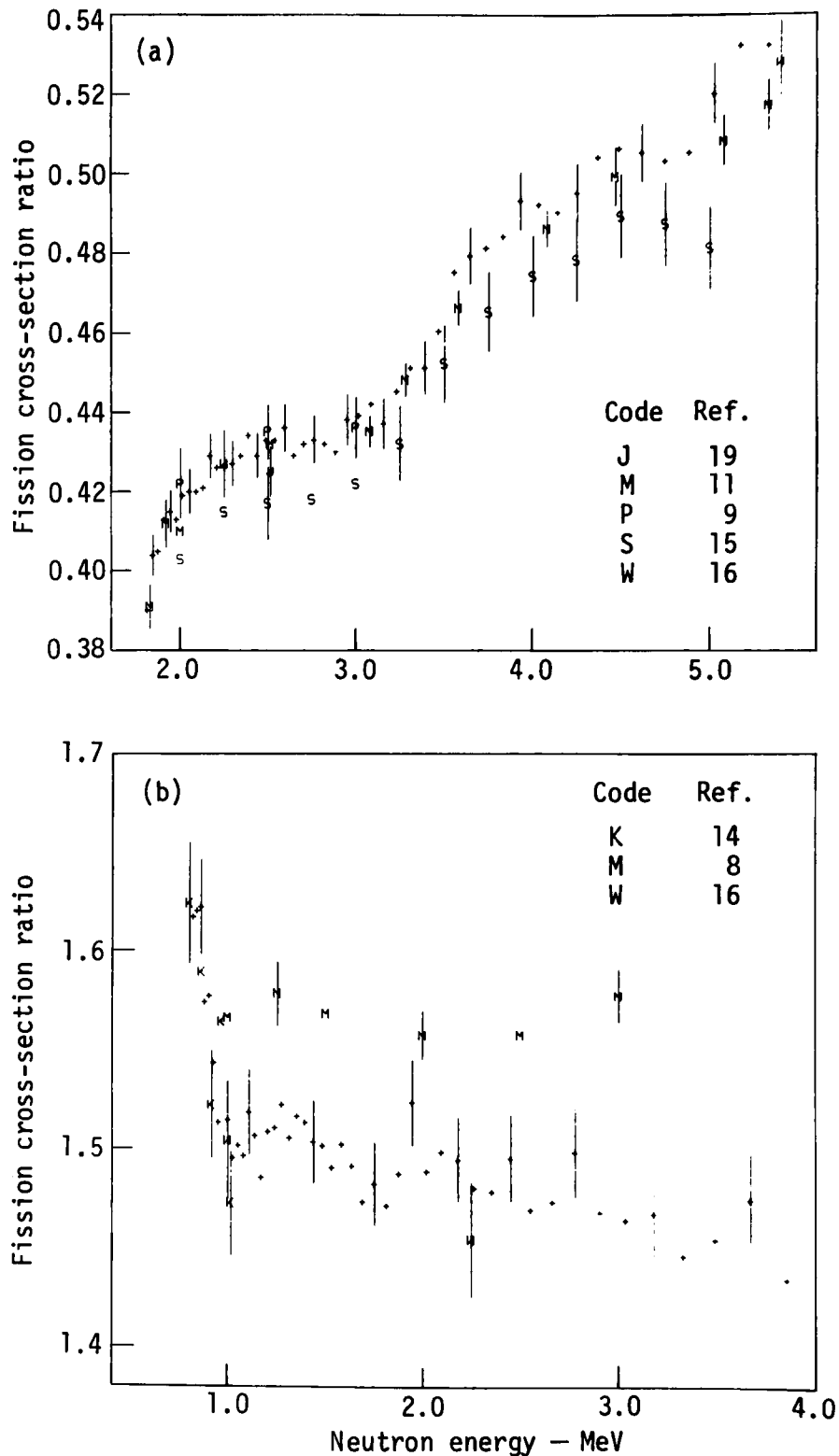


Figure 7. Fission cross-section ratios. Present work is represented by (+) and letter codes indicate the work of other investigators. Error bars represent the *total* uncertainties, expressed as standard deviations. (a) Ratio of  $^{238}\text{U}$  to  $^{235}\text{U}$  from 1.8 to 4.0 MeV. (b) Ratio of  $^{233}\text{U}$  to  $^{235}\text{U}$  from 0.8 to 4.0 MeV.

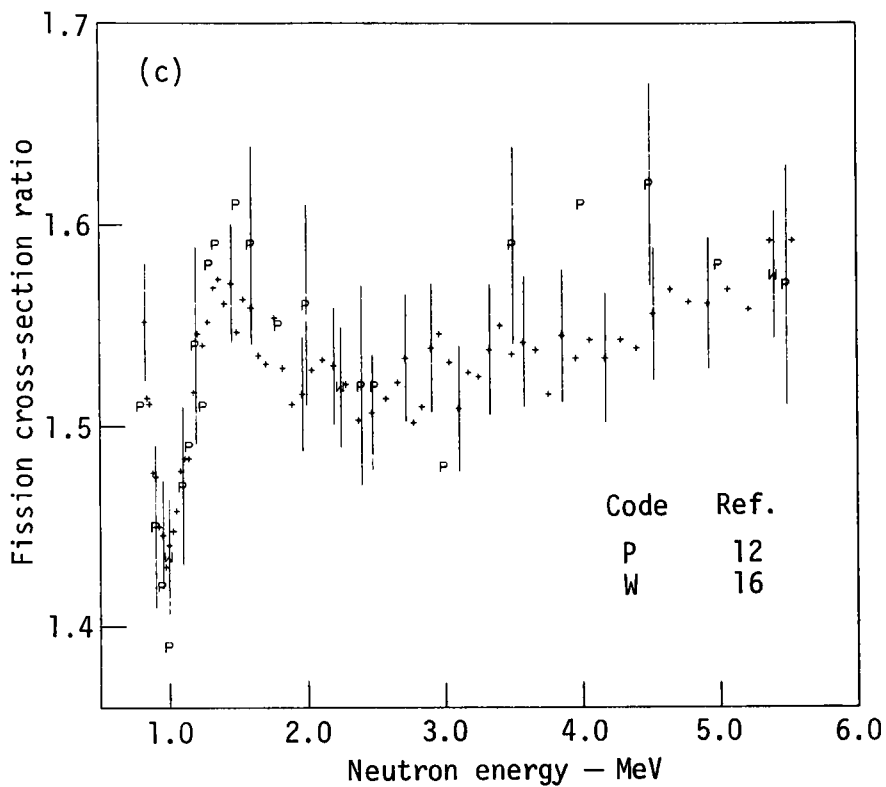


Figure 7. Fission cross-section ratios: Present work is presented by (+) and letter codes indicate the work of other investigators.  
 (c) Ratio of  $^{239}\text{Pu}$  to  $^{235}\text{U}$  from 0.8 to 5.5 MeV.

## DISCUSSIONS

S. Cierjacks Have you tried to compare the threshold method with the usually used technique of determining the efficiencies and the sample masses? What is the agreement between results obtained with the two methods?

J. Behrens We have destroyed the fission chamber to have the foils analyzed, but we kept everything. So far we have not gone into the complicated procedure of determining efficiencies and masses. The method we use eliminates many of these problems. Keep in mind, what is actually required is the atomic ratio in the mixed chamber. If you have a uranium isotope, you go to mass spectroscopy and you get a very good number, say far better than 0.5%. In case of a ratio between a uranium isotope and a plutonium isotope you have the added problem of a quite different chemistry, but still you have the isotopic dilution technique by means of which you get the atomic ratio. We feel that this method is very important and have concentrated our full effort to compare our data with that which other people obtain. We find that we have good agreement with some who quote 1 or even 0.5%.

G. Carlson To answer Dr. Cierjacks question: we cannot do the normalization with the conventional technique because not all material was in the beam. The experiment was not designed for this. We can, however, go down to thermal and compare the result at thermal with our high energy technique. We find good agreement except for U-233 where we have a 3% difference.

W. Poenitz Recently, I read again the paper by Jarvis from LASL, which in my opinion was one of the first good ratio measurements. He used several techniques for mass assignment, one of which utilized a comparison of a natural uranium sample with an U-235 sample. I wonder whether this is not the same or very similar to the technique you used, only that thermal neutrons were involved. I think also J. Meadows has used this technique for quite some time.

J. Behrens Well, it is very clear that what we have done here is merely an extension of existing techniques. We have the opportunity to cover a very wide energy range, all the way up to 30 MeV. We feel that this method which

is not new in any sense, is a good one.

W. Poenitz My second question concerns the Pu-239/U-235 ratio. You show considerable structure in this ratio. Do you have any comments on this?

J. Behrens I believe you are referring to what appears to be a peak in our ratio at about 300 keV. My only comment to that is that we have measured the Pu-239/U-235 ratio with three different fission chambers, each containing various amounts of plutonium, so that we can get very high efficiency. It appears that as far as our measurements are concerned there is reproducibility and thus, yes, there is structure.

G. F. Knoll Do you have a figure on the degree to which your efficiency for fragment counting is less than 100% and is there any chance that this changes with the various isotopes?

J. Behrens As a matter of fact we measured it. We record in a computer the pulse-height spectra as a function of energy. If you look at these pulse-height spectra distributions you find that there are effects which come in if you operate your detector at a 50% fragment detection efficiency or less, or 80% or less, you can see problems. You are in trouble if you have only 50%. Part of our effort went into designing chambers which would have a very high efficiency, greater than 90%.

M. Moore It does not matter because it cancels out with the normalization as long as it is the same for your mixed and the straight detector.

J. Behrens If you bring in the angular distribution you will find a much greater effect from the U-238 than the others. One has to be really careful, it is a major concern. You can get systematic errors which may really hurt you.

R. Peelle My question concerns the energy calibration. Did you have the opportunity to use carbon filters in the beam so you would see the depressions from the carbon resonances.

J. Behrens We use a lot of things to determine our energy scale. As you know there is this discrepancy between our data and the results from Harwell. We have gone back to our U-238/U-235 measurements. We had already measured carbon resonances at 2.079 MeV, the 6.295 MeV. We also looked at several other resonances which may not be as good as carbon. We do depend heavily

on the gamma flash. We find that we have a large number of pulses which appear to be fission due to the gamma fission process. We compare this gamma-flash technique with the carbon resonances results and find good agreement. Since the '75 Washington Conference we have repeated these measurements, and again we are very close.

R. Peelle Like what?

G. Carlson Like 26 keV at 10 MeV.

S. Cierjacks I might comment on this. We have measured at Karlsruhe, for example, the U-238/U-235 ratio at a completely different facility and come up with the same energy scale as that at Livermore. I have a letter from Coates which points out that they have now used the gamma-flash and flight-path technique instead of the carbon resonances (which may be a problem due to the short flight-path length) and obtain the same energy scale as we do. That means all these data sets now agree well in energy scale.

THE FISSION CROSS SECTIONS OF URANIUM  
AND PLUTONIUM ISOTOPES RELATIVE TO U-235

J. W. Meadows

Argonne National Laboratory  
Argonne, Illinois 60439, U.S.A.

ABSTRACT

The cross sections of U-233, U-234, U-238, Pu-239 and Pu-242 have been measured relative to U-235 using the ANL FNG facility. All measurements were within the energy range 0.1-10 MeV. Sample mass ratios were based on the alpha decay ratio, the thermal fission ratio, and the mass analysis of specially prepared isotopes mixtures.

INTRODUCTION

Several years ago a survey of the fission cross section ratio data showed that, although a large amount of work had been done, there were gaps and regions of inconsistency. At about that time the Argonne Fast Neutron Generator became operational with the capability of covering the neutron energy range from below 0.1 to above 10 MeV so I began a series of measurements that were intended to include U-233, 234, 236, and 238 and Pu-239, 240, 241, and 242. This paper reports on the current state of these measurements. The U-233 and some of the U-238 results have been reported elsewhere,[1-3] but they are included for completeness and for comparison with some recent measurements by others. Of the remaining isotopes, only Pu-239 is of direct interest to this meeting but U-234 and 236 and Pu-242 are included because they have some bearing on the reliability of the other results.

Any new data sets presented here must be considered preliminary. They are near their final values but there will be additional measurements to confirm the normalization and, in some cases, additional data will be taken to improve the statistical accuracy. In all cases there will be some extension of the energy range.

EXPERIMENTAL METHOD

A. General

The ideal experimental method involves placing two samples of known

mass ratio, preferably 1.0, in the same monoenergetic neutron flux and measuring their fission rate at the same time. In practice the two samples were mounted on light backing plates and placed back-to-back in a double ionization chamber which was placed near and perpendicular to a neutron source produced by a charged particle reaction. A second measurement was made with the chamber reversed and an average of the two was used. This eliminated differences in the relative fission rates due to sample geometry, to attenuation in the sample support plates and to changes in detector efficiency due to momentum effects.

Neutrons with energies less than  $\sim 5$  MeV were produced by the  $\text{Li-7(p,n)Be-7}$  reaction in a thin layer of natural lithium evaporated on a tantalum backing. Higher energy neutrons were produced by the  $\text{D(d,n)He-3}$  reaction using a gas target. Where necessary, corrections were made for lower energy neutrons from the  $\text{Li-7(p,n)Be}^*-7$ ,  $\text{Li-7(p,n He-3)He-4}$  and  $\text{D(d,pn)D}$  reactions as well as for neutrons produced by  $(d,n)$  reactions with the gas target assembly. Measurements were made to establish the yield and energy spectra from these reactions so corrections could be calculated [4,5]. A pulsed and bunched beam was used and fast timing techniques selected those fissions that were suitably correlated with the beam pulse. The timing requirements were generally not very strict. In most cases a  $\sim 40$  nanosec window was used. A second window about 200 nanosec before the beam pulse measured the epithermal neutron background.

The fission detector, a parallel plate, double ionization chamber, has been described earlier [1]. It was lightly constructed in order to minimize scattering. The detector efficiency was always  $> 90\%$  and was usually  $\sim 98\%$ .

## B. Samples

Samples were prepared by electroplating uranium or plutonium onto polished molybdenum or stainless steel plates. The deposit diameter was 2.54 cm and the area density ranged from 0.025 to  $\sim 0.5$   $\text{mg/cm}^2$ . Most samples were between 0.05-0.15  $\text{mg/cm}^2$ .

The energy dependence of the cross section ratios was measured using pure ( $> 98\%$ ) isotopes but the normalization was usually made with mixtures containing  $> 90\%$  of the principal isotope. These mixtures were designed to have convenient alpha decay and thermal fission rates and the mass ratio were based on these measurements plus the mass analyses. In general this required a knowledge of the half lives and thermal fission cross sections but for the uranium isotopes the result was usually independent of these quantities. For example, in the U-234:U-235 measurement the U-235 sample contained  $\sim 1\%$  U-234 while the U-234 sample contained  $\sim 10\%$  U-235. The alpha decay rates were almost entirely due to U-234 while the thermal fission rates were almost entirely due to U-235. The mass ratio depended only on the relative rates and the consistency of the two sets of measurements provided a check on the mass analysis. (See for example ref. 39).

The same basic technique was used with the plutonium isotopes by adding Pu-239 to the non-fissile ones, but now the results are always dependent on the relative thermal cross sections and alpha decay rates. Table I shows

the half lives and cross sections used [6-13]. The critical ones are indicated.

The alpha count rates were measured in a low geometry counter with a factor  $> 1000$ . The thermal fission rates were measured in the graphite column of the Argonne Thermal Source Reactor at a point where the cadmium ratio for gold was 500. Fortunately, the temperature of the reactor cell during these measurements was 20 deg. C so the cross sections in Table I were directly applicable. Measurements were also made at the FNG by surrounding the detector with hydrogenous moderator. This had the advantage of using the same electronics that were used for the ratio measurements in the MeV range. The cadmium ratios for these measurements were usually 70-100. When the thermal fissions in the two samples were due to different isotopes, corrections were made for the non-Maxwellian spectral shape according to the method described by Westcott [14].

### C. Energy Calibration and Resolution

The neutron energy was a function of the energy of the incident particle. That was controlled by a 90 deg. analysing magnet which was calibrated by three threshold reactions. Those were Li-7(p,n)Be-7 at  $1880.60 \pm .04$  keV, [15] B-11(p,n)C-11 at  $3016.4 \pm 1.6$  keV, [16] and Al-27(p,n)Si-27 at  $5796.9 \pm 3.8$  keV [15]. Higher values were obtained by extrapolation. The extrapolation was a lengthy one (the maximum required field of 7700 gauss corresponds to 16 MeV proton energy). Nevertheless, I estimate the uncertainty in the deuteron energy at this field strength to be less than 250 keV. This corresponds to 11 MeV neutron energy. At 8 MeV the uncertainty declined to  $< 50$  keV. For neutron energies below 2 MeV the uncertainty due to the magnet calibration was 2 keV.

The energy resolution was determined by the energy loss in the target and by the angle subtended by the detector. The latter was a function of the kinematics of the source reaction and was readily calculated. The thickness of the lithium targets were measured if they were less than 100 keV at the Li-7(p,n) threshold. Otherwise the thickness was estimated from the weight of lithium evaporated. Only thin targets of measured thickness were used in regions where the cross section ratios were changing rapidly. In addition the buncher added 2-3 keV to the energy spread but this was comparatively negligible. The uncertainty of the energy resolution was estimated to be  $\sim 10\%$  of the total spread. This is the major contributor to the energy uncertainty.

## TREATMENT OF DATA

A number of corrections were required but most were quite small.

### 1. Room Background

This was a time independent background that affected only the fissile samples. It was caused by thermal and epi-thermal neutrons and was measured concurrently with the fission ratio as described in Section II.A.

It usually amounted to 0.1-0.2%.

## 2. Source Background

This was caused by the (d,n) reactions with the gas target structure. Measurements were made with an empty cell before and after each measurement with the cell filled. It was about 1% near 5 MeV neutron energy and increased to about 15% near 8 MeV.

## 3. Corrections to Detector Efficiency

The only corrections regularly made were for the number of fissions under the alpha peak and for fissions lost due to the finite sample thickness. The former was estimated by a linear extrapolation of the pulse height distribution to zero bias. The latter was based on measurements of specific thermal fission rates for a series of U-235 samples ranging from 0.05 to 0.4 mg/cm<sup>2</sup>. Usually no corrections were made for momentum and angular distribution effects. The first was taken care of by making a second set of measurements with the sample positions reversed. For the second, the effect was small for 0.1 mg/cm<sup>2</sup> samples (<0.2%). However for the thickest samples the maximum correction was 0.7%, and was applied.

## 4. Scattering Corrections

These were calculated using a Monte Carlo procedure and ENDF/B-IV cross sections. Only single scattering was considered and inelastically scattered neutrons were assumed to have an evaporation spectrum. The number of fissions due to scattered neutrons was typically ~ 5%. Very few of these came from distant objects. Most came from objects very near the samples or the neutron source such as the sample support plates (~ 50%) and the lithium target support plate (~ 25%). The correction was largest when one of the samples was a non-fissile isotope but still ranged from 2 - 0.2%. When both samples were fissile isotopes the corrections were quite small.

## 5. Isotopic Impurities and Neutron Energy Spectrum

All samples contained at least a small amount of other isotopes and some of them contained several percent. In addition lower energy neutrons were often produced by secondary source reactions. After making the corrections listed above the measured fission ratio was written as

$$R = \frac{N_1 \sum_g G_g \sum_i P_{1i} \sigma_i(E_g) / \sigma_{25}(E_o)}{N_2 \sum_g G_g \sum_i P_{2i} \sigma_i(E_g) / \sigma_{25}(E_o)}$$

The subscripts 1 and 2 refer to the two samples. N is the number of atoms in the sample, P<sub>i</sub> refers to the isotopic fraction of isotope i, G<sub>g</sub> is the fraction of neutrons in group g with energy E<sub>g</sub>, σ<sub>i</sub>(E<sub>g</sub>) is the fission cross of isotope i at energy E<sub>g</sub>, σ<sub>25</sub>(E<sub>o</sub>) is the fission cross section of U-235 at the energy of the principal neutron group, E<sub>o</sub>. The equation was readily solved for the appropriate fission cross section ratio.

## RESULTS

U-233:U-235

The U-233 results have been published elsewhere [1]. They are shown in Fig. 1 and compared with some other data sets [17-21]. Normalization for this ratio is based chiefly on the relative alpha count rates for the U-233 samples and for the U-235 samples spiked with U-233. The results were confirmed by measuring the thermal fission ratio. Compared to much of the other data these results are high. The shape is very similar to the recent measurements of Behrens et al. [21] but there is a fairly constant difference of  $\sim 5\%$ .

U-238:U-235

Early last year three new measurements of this ratio became available [21-23]. When normalization differences were eliminated it was clear that there were large energy differences in the threshold region. Consequently a new set of measurements were carried out at the FNG with the results shown in Fig. 2. These are  $\sim 20$  keV higher than Behrens et al. [21], lower than Coates [22] by a similar amount and  $\sim 40$  keV higher than Cierjacks [23]. New data submitted for the Work Group of this conference [24,25] appears to remove some of the disagreement in the time-of-flight measurements.

Fig. 3 compares these results with the time-of-flight data at higher energies. The information shown was taken from the CSISRS file and was not renormalized. There is very good agreement with Behrens et al. [21] below 6.5 MeV but above that energy there is a 4% difference. The recent measurements of Difilippo et al. [26] shows a similar difference. If the results of Coates [22] and Cierjacks [23] are normalized in the 2-3 MeV region the agreement is fairly good. Some recent measurements by Nordborg et al. [27] in the 5-9 MeV range show a small normalization difference and agree fairly well as to shape.

U-234:U-235

The data for U-234 (Figs. 4 and 5) are in good agreement with Lamphere [28] as far as shape is concerned but differs as to normalization. The agreement with Behrens et al. [21] is much better but there are small differences in shape and in normalization and there is a 20 keV energy shift similar to the one observed for U-238. The comparison above 6 MeV is particularly interesting as the relative shapes are not at all like those observed for U-238.

U-236:U-235

These results are shown in Figs. 6 and 7. The agreement with the results of Lamphere [17] is fairly good. The results of Stein, Smith and Smith [29] and White and Warner [20] falls somewhat lower. The agreement

with Behrens et al. [21] below 4 MeV is exceptionally good. In the 2 - 4 MeV region the average normalization differs by  $\sim 2\%$ . However in the threshold region there is still an energy difference of about 20 keV. There is substantial disagreement above 6 MeV but the difference is not similar to that observed for U-238 or U-234.

#### Pu-239:U-235

These results are compared with others [18-20,30-37] in Fig. 8. The sample mass ratios were based on alpha counting using the Pu-239 and U-234 half lives in Table I, on relative thermal rates in a well thermalized spectrum at 20 deg. C, and on thermal fission ratio measurements at the FNG with the detector surrounded by a hydrogenous moderator. The estimated error in the final value is 0.7%. The results are in good agreement with Pfletschinger and Kaeppler [18], and in fair agreement with Allen and Ferguson [30], Poenitz [32,33], Nesterov and Smirenkin [19]. The agreement with Carlson and Behrens [37] is quite good in the 2-4 MeV range where the average difference in normalization is about 1%.

#### Pu-242:U-235

The normalization measurements were made using a Pu-242 sample spiked with Pu-239 and a U-235 sample spiked with U-234. The results are shown in Fig. 9. The agreement with Behrens et al. [38] is very good above 1.5 MeV. The average normalization difference is only 0.7%. The threshold region again shows the usual energy shift.

### ACKNOWLEDGEMENTS

The author is indebted to R. J. Armani and K. T. Kucera for preparation of the electroplated samples.

This work was performed under the auspices of the U.S. Energy Research and Development Administration.

### REFERENCES

1. J. W. MEADOWS, *Nucl. Sci. Eng.*, 54, 312 (1974).
2. J. W. MEADOWS, *Nucl. Sci. Eng.*, 49, 310 (1972).
3. J. W. MEADOWS, *Nucl. Sci. Eng.*, 58, 255 (1975).
4. D. L. SMITH and J. W. MEADOWS, Argonne National Laboratory Report, ANL-7938 (1972).
5. D. L. SMITH and J. W. MEADOWS, Argonne National Laboratory Report, ANL/NDM-9 (1974).
6. A. N. JAFFEY, K. F. FLYNN, W. C. BENTLEY, J. D. KARTTUMEN, *Phys. Rev.*,

C9, 1991 (1974).

7. P. De BIEVRE, K. F. LAUER, Y. Le DUIGON, H. MORET, G. MÜSSHENBORN, J. SPAEPEN, A. SPERNOL, R. VANENBROUKX, V. VERDINGH, EANDC (E)-133-AL.
8. A. H. JAFFEY, K. F. FLYNN, L. E. GLENDENIN, W. C. BENTLEY, A. M. ESSLING, *Phys. Rev.*, C4, 1889 (1971).
9. K. F. FLYNN, A. H. JAFFEY, W. C. BENTLEY, A. M. ESSLING, J. INORG. *Nucl. Chem.*, 34, 1121 (1972).
10. A. H. JAFFEY. Private Communication.
11. Nuclear Level Schemes, Academic Press Inc. New York and London, (1973).
12. P. K. ZIEGHER, Y. FERRIS, J. INORG. *Nucl. Chem.*, 35, 3417 (1973).
13. H. D. LEMMEL, Third IAEA Evaluation of the 2200 n/sec and 20° Maxwellian Neutron Data for U-233, U-235, Pu-239 and Pu-241.
14. C. N. WESTCOTT, CRRP-787, Aug. 1958.
15. J. B. MARION, *Rev. Mod. Phys.*, 38, 660 (1966).
16. E. N. BECKNER, R. L. BRAMBLETT, G. C. PHILLIPS and T. A. EASTWOOD, *Phys. Rev.*, 123 2100 (1961).
17. R. W. LAMPHERE, *Phys. Rev.*, 104, 1654 (1956).
18. E. PFLETSCHINGER and F. KAEPELER, *Nucl. Sci. Eng.*, 40, 375 (1970).
19. V. G. NESTEROV and G. N. SMIRENKIN, *Atom. Energ.*, 24, 185 (1967).
20. P. H. WHITE and G. P. WARNER, *J. Nucl. Energy*, 21, 671 (1967).
21. J. W. BEHRENS, G. W. CARLSON and R. W. BAUER, UCRL-76219 (1975).
22. M. S. COATES, D. B. GAYTHER and N. J. PATTENDEN, *Proc. Conf. Neutron Cross Sections and Technology*, Washington, D. C., March 3-7, 1975.
23. S. CIERJACKS, B. BROTZ, D. GRÖSCHEL, I. SCHOUKY, C. M. NEWSTEAD, G. SCHMALZ, R. TOPKI, F. VOSS, EANDC(E)-157.
24. S. CIERJACKS, B. LEUGERS, K. KARI, B. BROTZ, D. ERBE, D. GRÖSCHEL, G. SCHMALZ and F. VOSS, this conference.
25. D. JAMES, this conference.
26. F. C. DIFILIPPO, R. B. PEREY, G. De SAUSSURE, D. OLSEN and R. INGLE. This conference.
27. C. NORDBORG, H. CONDE and L. B. STRÖMBERG, this conference.

28. R. W. LAMPHERE, ORNL-3306, *Nucl. Phys.*, 38, 561 (1962).
29. W. C. STEIN, R. K. SMITH and H. L. SMITH, *Proc. Conf. in Neutron Cross Sections and Technology*, Washington, D. C., March 4-7, 1968. NBS Special Publication 299.
30. W. D. ALLEN and A. T. G. FERGUSON, *Proc. Phys. Soc.*, A70, 573 (1957).
31. M. V. SAVIN, JU. S. ZAMFATNIN, JU. A. KHOKLOV, and I. N. PARAMONOVA, "Fission Cross Sections Ratios of U-235, Pu-239 and Pu-240 for Fast Neutrons", International Nuclear Data Committee, INDC(CCP)-8/U, 16 (1970).
32. W. P. POENITZ, *Nucl. Sci. Eng.*, 40, 383 (1970).
33. W. P. POENITZ, *Nucl. Sci. Eng.*, 47, 228 (1972).
34. F. NETTER, CEA-1913, (1961).
35. M. SOLEILHAC, J. FREHAUT, J. GAURIAN and G. MOSINSKI, *Proc. 2nd. International Conf. on Neutron Data for Reactors*, p.145 Vol. II, IAEA, 1970.
36. D. B. GAYTHER, *Proc. Conf. on Neutron Cross Sections and Technology*, Washington, D. C., March 3-7, 1975. NBS Special Publication 425.
37. G. W. CARLSON and J. W. BEHRENS, Fission Cross Section Ratio of  $^{239}\text{Pu}$  to  $^{235}\text{U}$  from 0.1 to 30 MeV, UCID-16981 (1975).
38. J. W. BEHRENS, G. W. CARLSON, J. C. BROWNE and R. W. BAUER, 1976 ICINN Conference, University of Lowell, Lowell, Mass.
39. G. A. JARVIS, A. P. KUTARNIA, R. A. NOBLES, LA-1571 (1953).

TABLE I

Half Lives and Thermal Fission Cross Sections Used to Establish Sample Mass Ratios. The Critical Ones are Indicated by an \*

Isotope	$t_{1/2}$ , Years	Ref.	$\sigma_F(\text{Maxwellian})$ T = 20° C	Ref.
U-233	*(1.5911 $\pm$ .0015) $\times 10^5$	6	528.1 $\pm$ 1.2	13
U-234	*(2.444 $\pm$ .017) $\times 10^5$	7		
U-235	(7.038 $\pm$ .0048) $\times 10^8$	8	569.4 $\pm$ 1.2	13
U-236	*(2.3415 $\pm$ .0014) $\times 10^7$	9		
U-238	(4.4683 $\pm$ .0034) $\times 10^9$	8		
Pu-239	*24143 $\pm$ 10	10	785.3 $\pm$ 2.2	13
Pu-240	6357	11		
Pu-241	14.89 $\pm$ .11	12	1015 $\pm$ 7	13
Pu-242	3.87 $\times 10^5$	11		

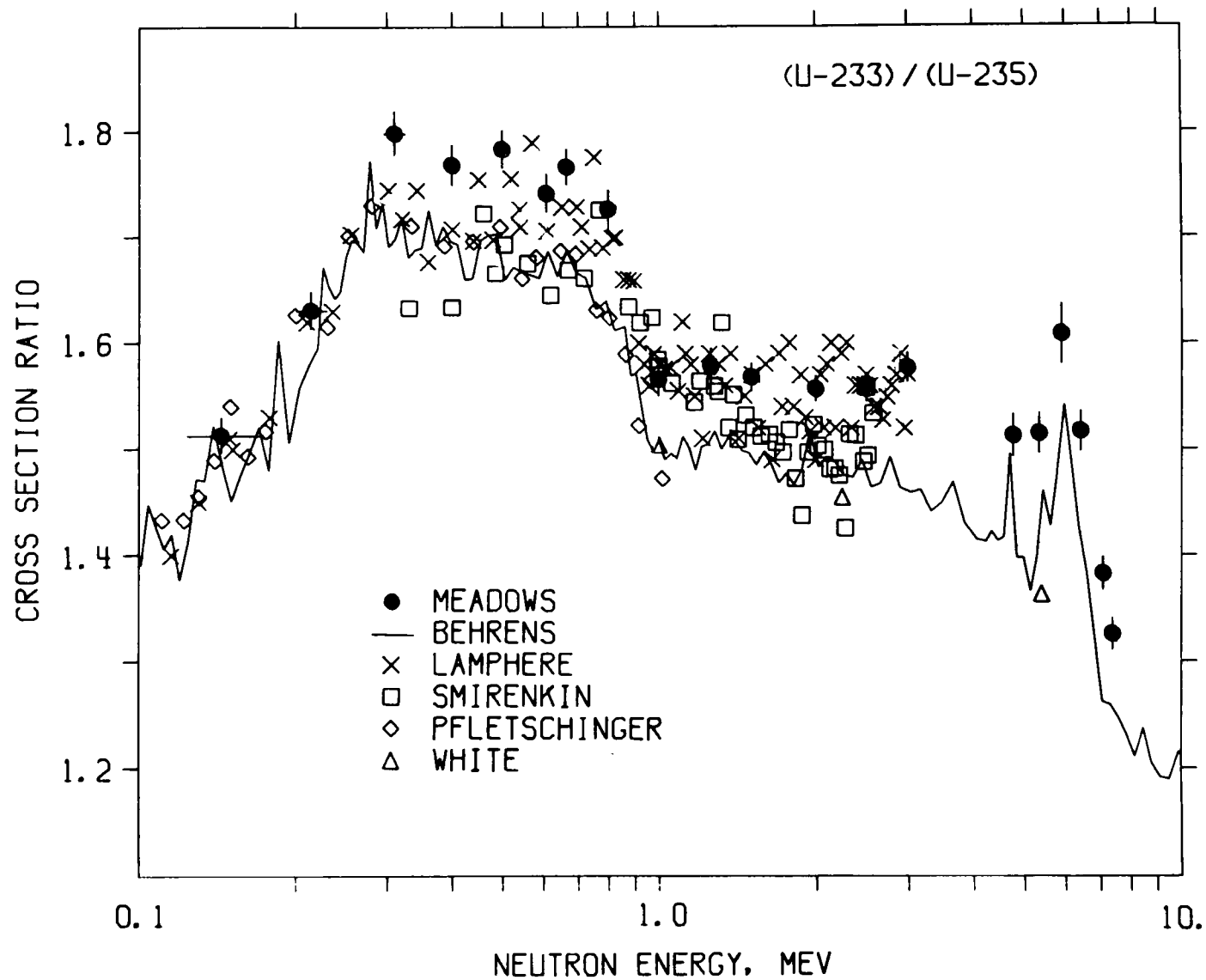


Figure 1. The U-233:U-235 fission cross section ratio.

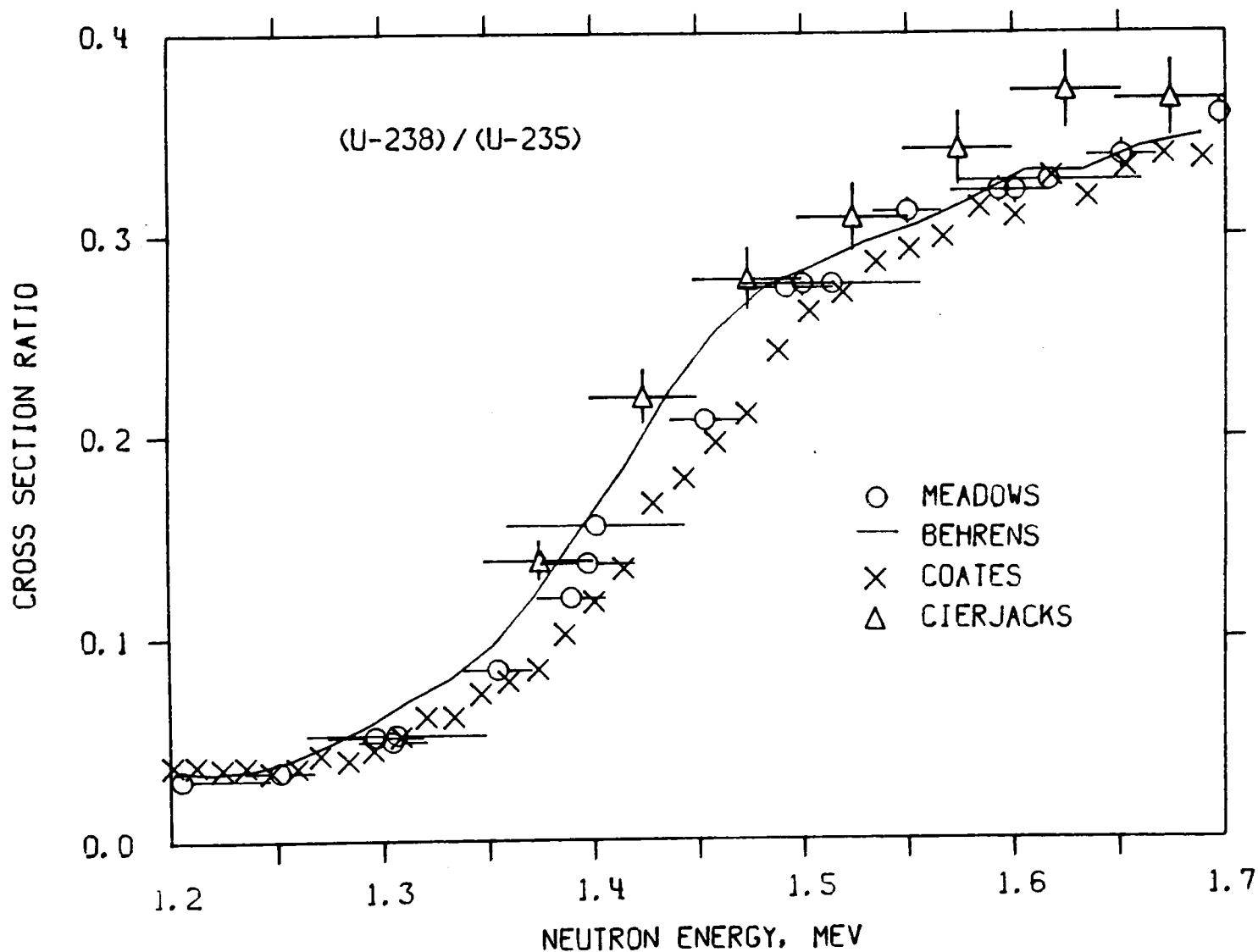


Figure 2. The U-238:U-235 fission cross section ratio near threshold. All data sets have been normalized in the 2-3 MeV energy range.

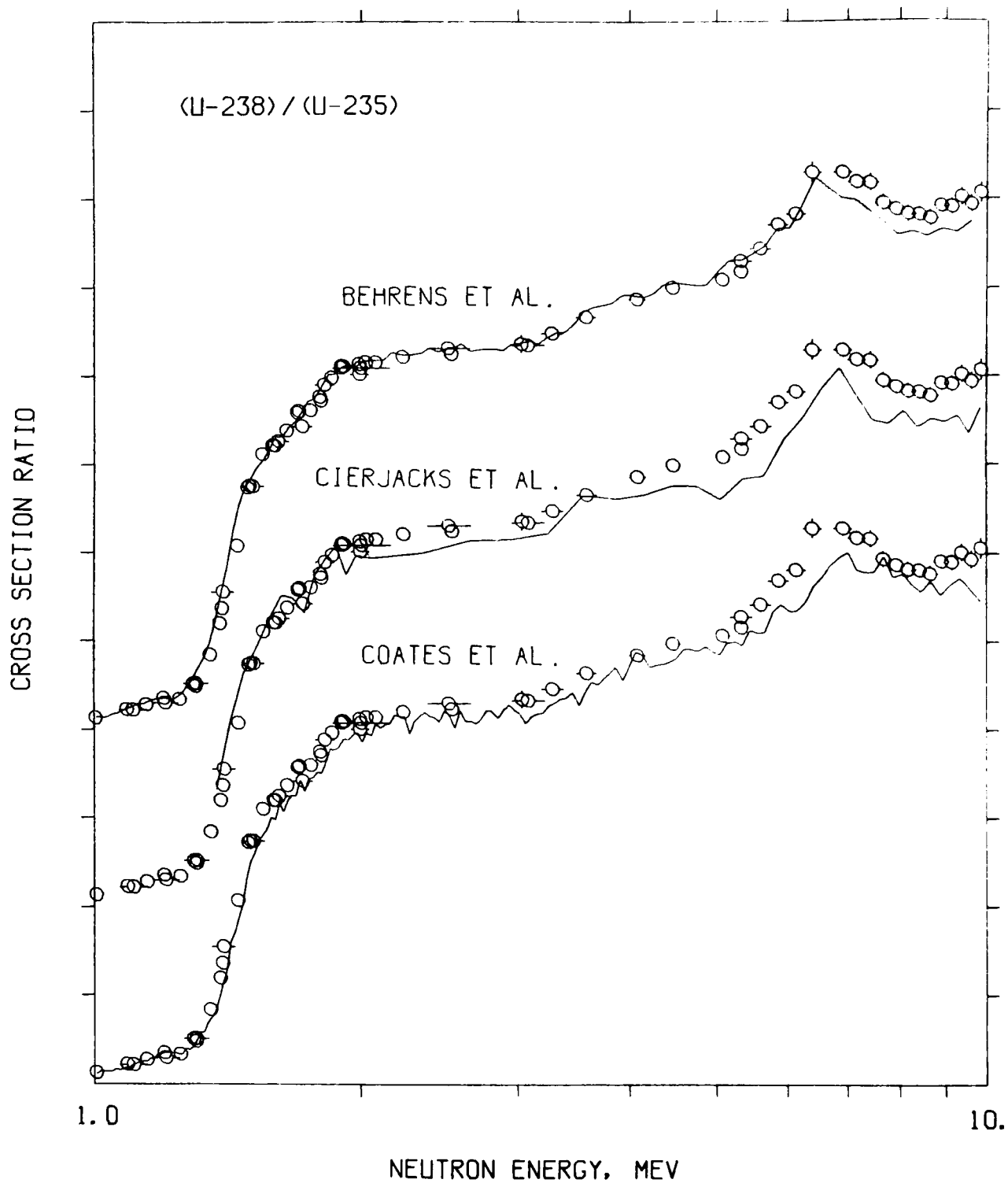


Figure 3. The U-238:U-235 fission cross section from 1 to 10 MeV.

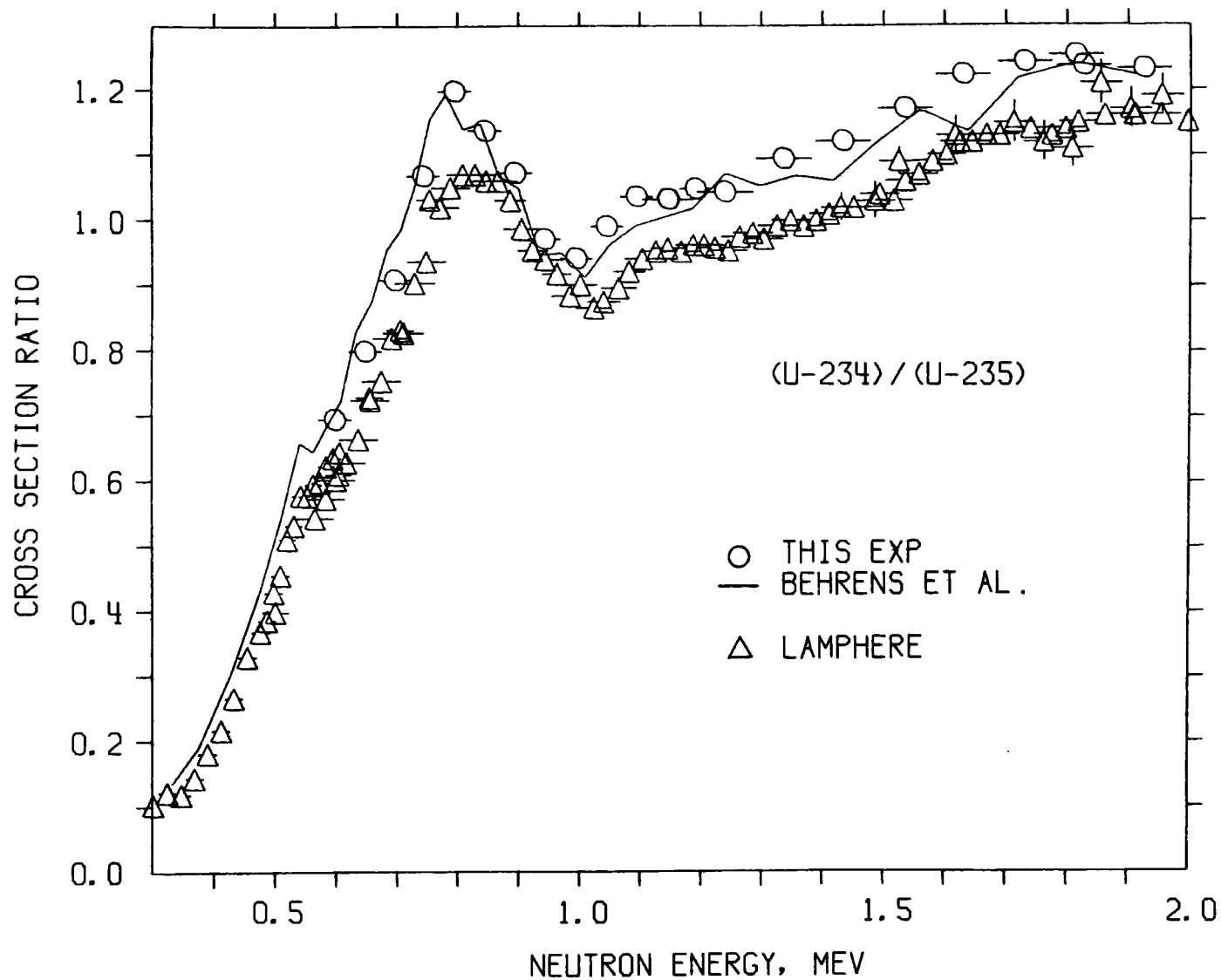


Figure 4. The U-234:U-235 fission cross section ratio below 2 MeV. The error bars show the statistical error and energy resolution.

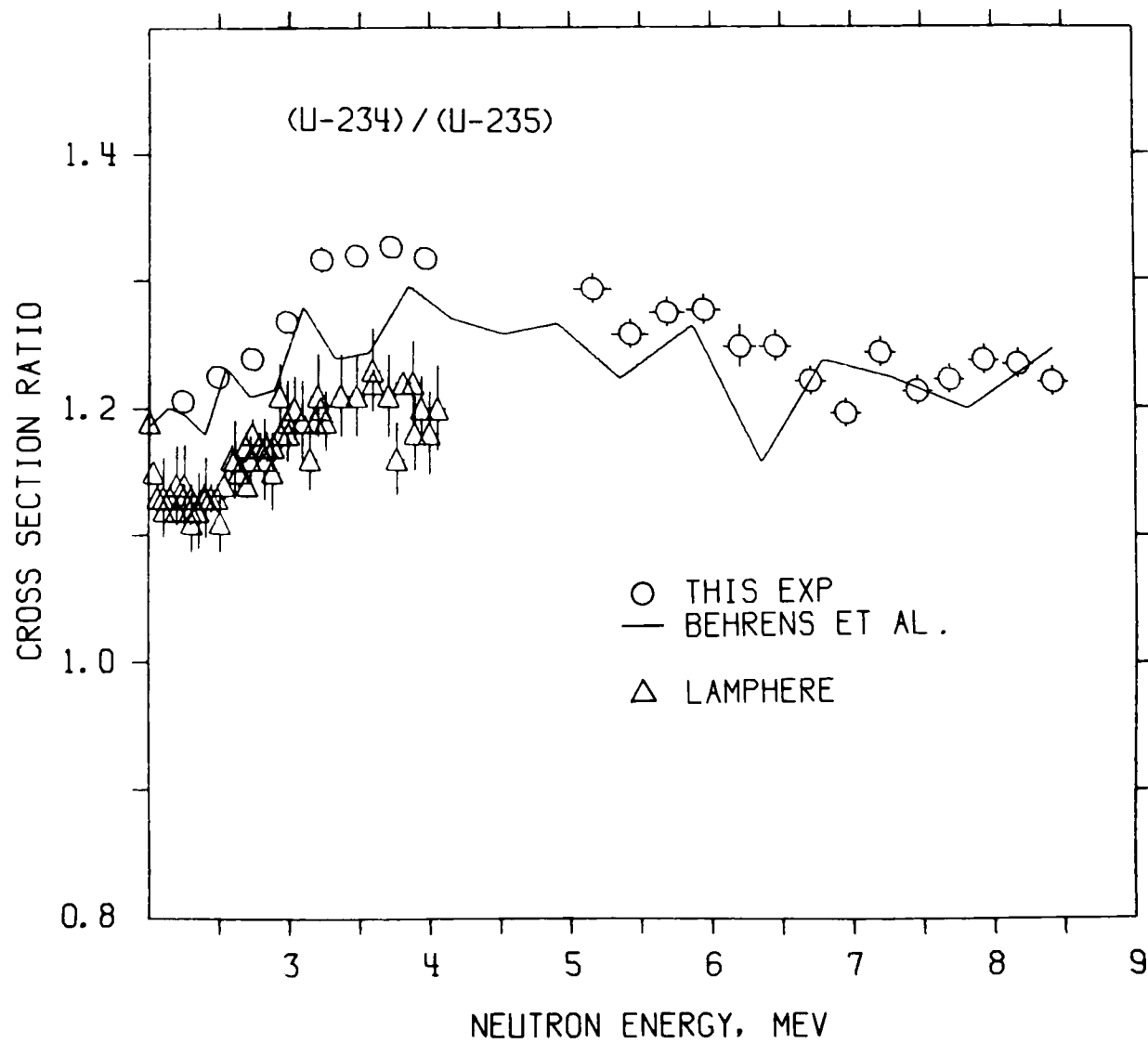


Figure 5. The U-234:U-235 fission cross section ratio above 2 MeV. The error bars show the statistical error and energy resolution.

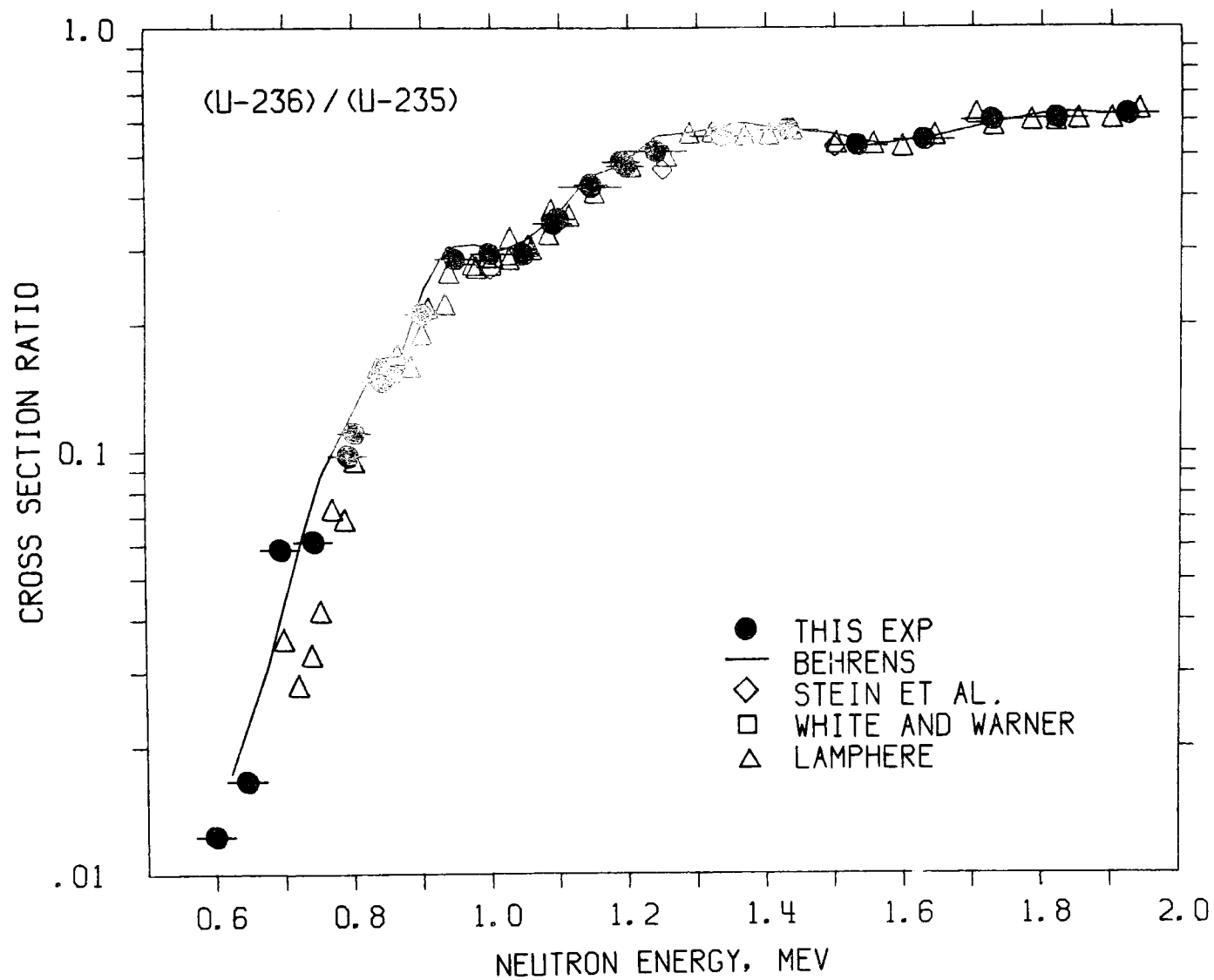


Figure 6. The U-236:U-235 fission cross section ratio below 2 MeV. The error bars show the statistical error and energy resolution.

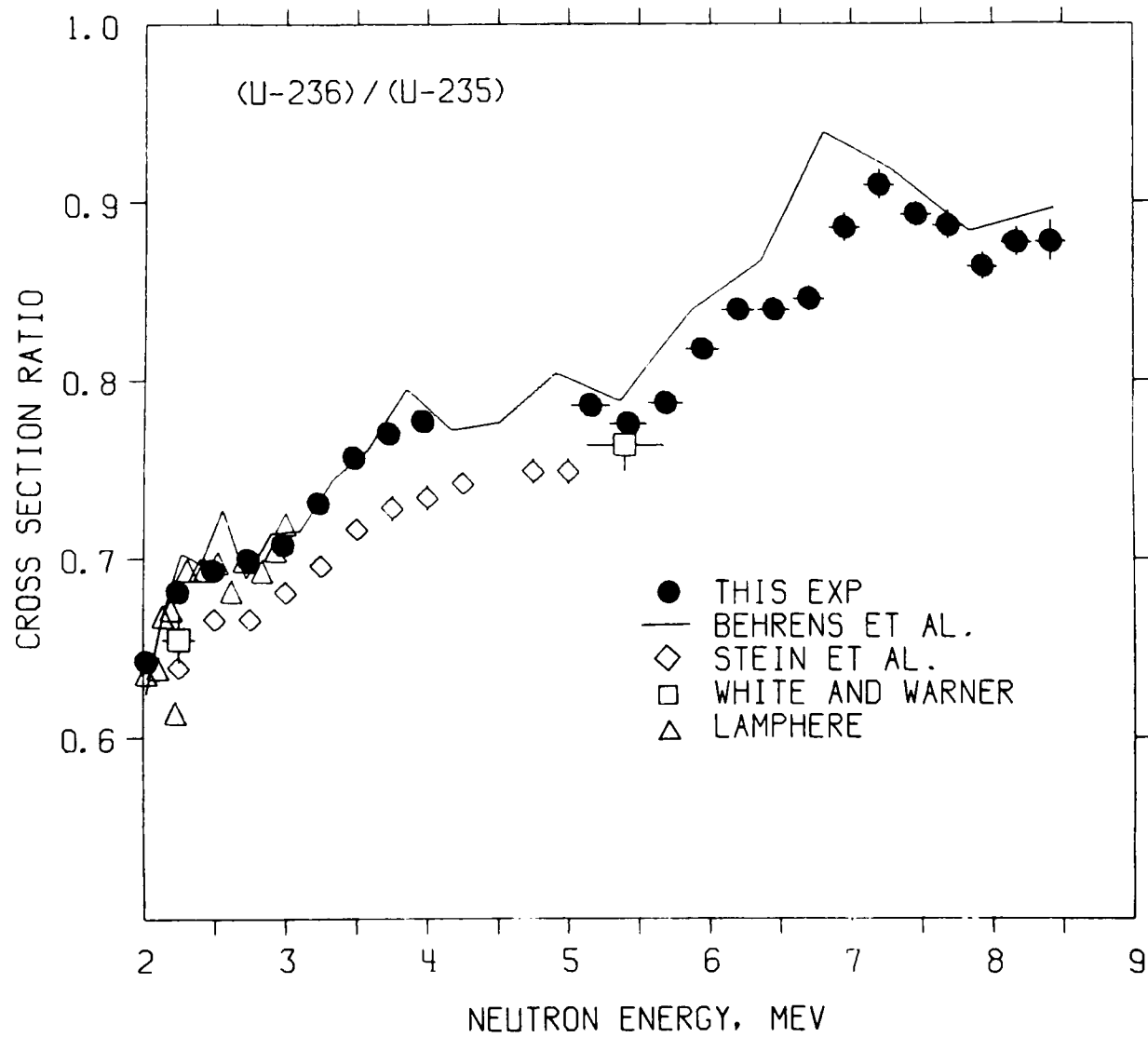


Figure 7. The U-236:U-235 fission cross section ratio above 2 MeV. The error bars show the statistical error and energy resolution.

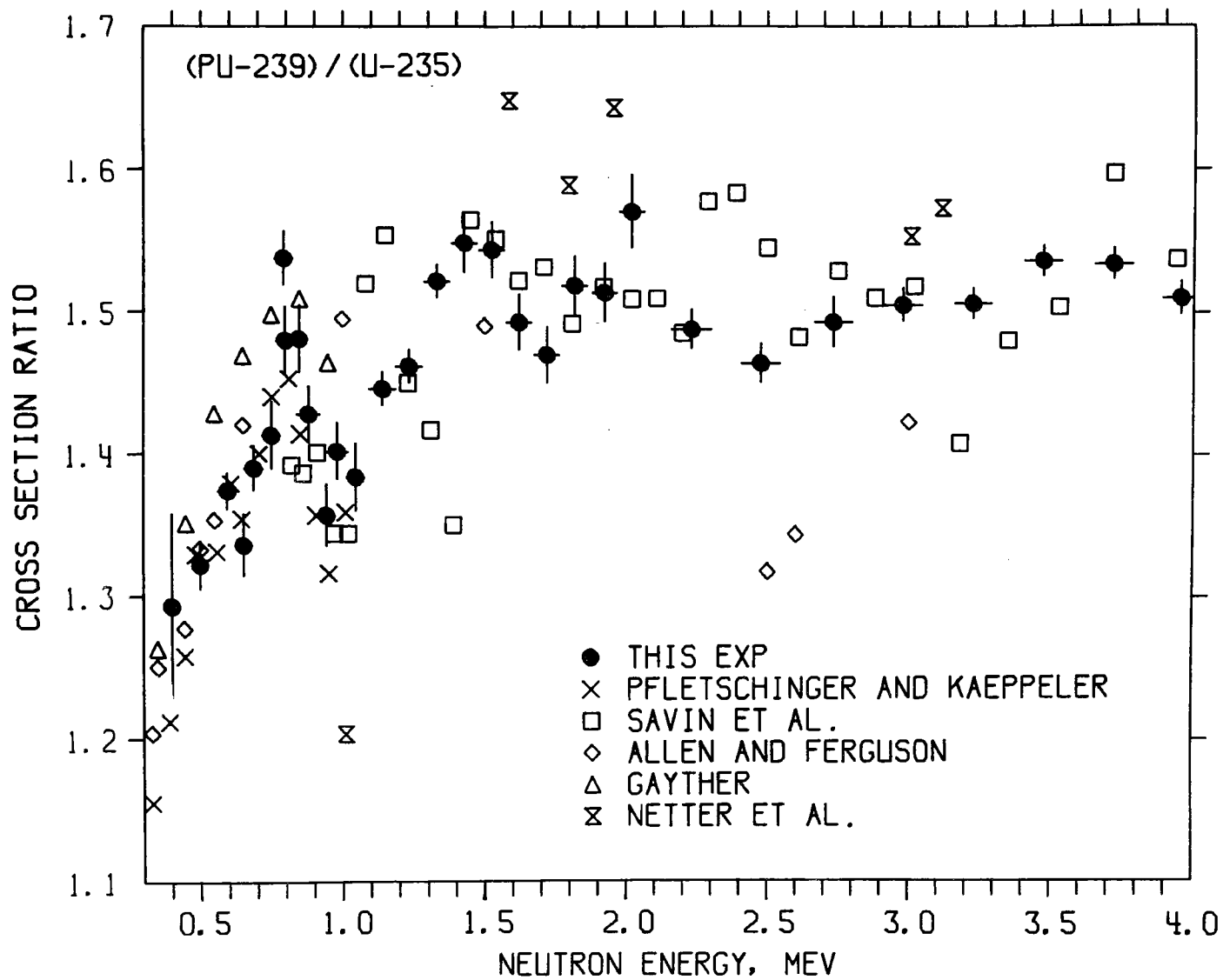


Figure 8a. The Pu-239:U-235 fission cross section ratio. The error bars show the statistical error and energy resolution.

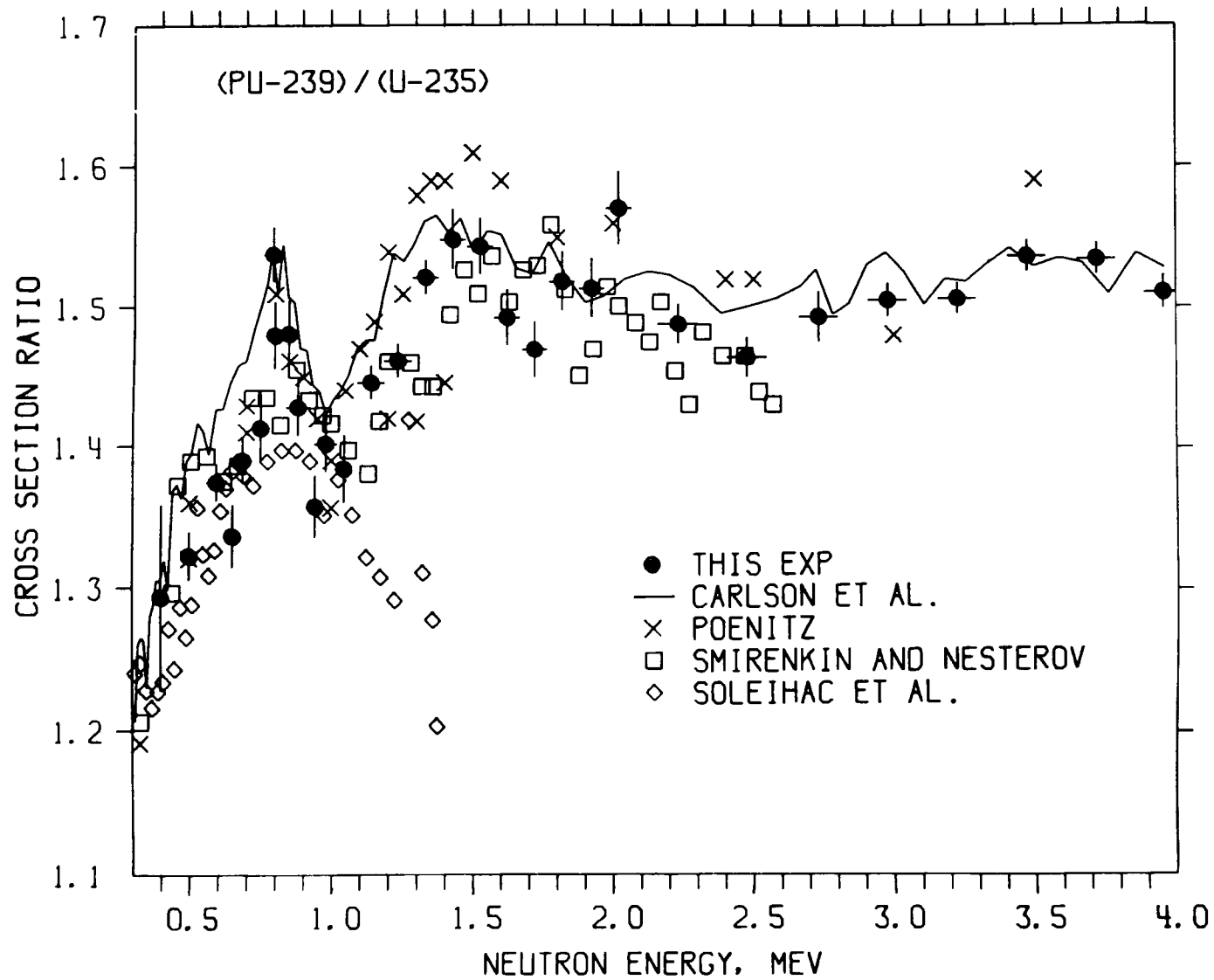


Figure 8b. The Pu-239:U-235 fission cross section ratio. The error bars show the statistical error and energy resolution.

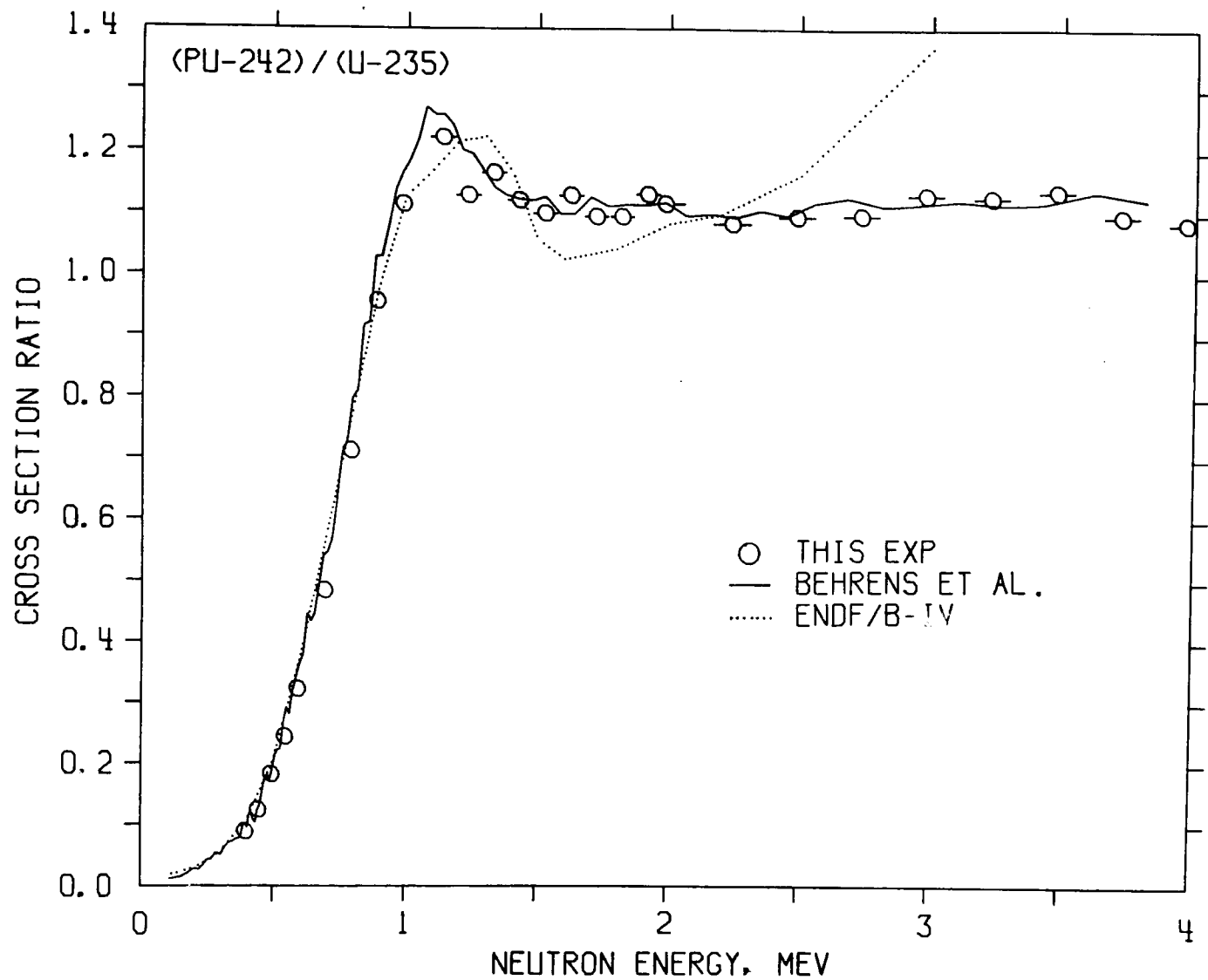


Figure 9. The Pu-242:U-235 fission cross section ratio. The error bars show the statistical error and energy resolution.

## DISCUSSIONS

J. Behrens Would you comment on your detector efficiency? At Livermore we attempted to get our efficiency greater than 90%, realizing that problems may arise for efficiencies lower than that. Would you comment particularly on Pu-239?

J. Meadows I do not know exactly what the efficiency is, I can only comment on the known losses. We know that for the average sample thickness we lose about 1% in the sample. There is another typical 1-2% loss due to the bias. That puts our detection efficiency in the range of 97%. In the thickest sample, which was a  $400 \mu\text{g}/\text{cm}^2$  U-238 sample the efficiency was in the 92% range, based on these estimated losses.

R. Peelle Is it possible to check your energy scale with TOF techniques?

J. Meadows I would say it is rather impractical.

R. Peelle Did you insert a carbon sample in order to check the energy?

J. Meadows No I did not. The distance from the source to the detector is only 6 cm.

S. Cierjacks What is the accuracy of your energy scale?

J. Meadows The accuracy of the charged particle beam energy is presumably quite good, something like 1 or 2 keV.

S. Cierjacks You know there is some discrepancy in other kinds of work, comparing TOF measurements and threshold techniques. At that time your laboratory stated that an uncertainty of 6-10 keV existed.

J. Meadows This uncertainty of 6-10 keV would also include a very thick target. If we had a total energy spread of 60-100 keV, then it would be uncertain by 6-10 keV, based on target thickness and acceptance angle. In the U-238/U-235 measurements the spread was 30-35 keV and I would place the uncertainty at 3-4 keV.

H. Conde Have you considered contributions from the low energy neutrons of the D(d,n) reaction?

J. Meadows Yes. These have all been corrected for. Both the source structure and the  $D(d,n)$  break-up source reaction. In case of the  $Li(p,n)$  reaction we corrected for the second neutron group.

G. Carlson You must have a very long running time with this arrangement.

J. Meadows The typical running time is about 2 hours per point.

R. Peelle Could you summarize your feelings about the energy calibration by saying whether in the threshold region your difference with Behrens is explained by the existing uncertainty or not.

J. Meadows No, I think the uncertainty is less than half the difference.

A. B. Smith I would like to make a general comment as long as we are discussing this energy scale problem. If the monoenergetic machines did not have this kind of accuracy the whole mass-defect table is confused. The charged-particle people do these things with very high precision. So you have to be careful if you throw out the monoenergetic machines. The whole mass sequence would be in trouble.

W. Poenitz It even goes the other way. We are using these mass tables to define the threshold energies and thus our energy scales.

C. Bowman If the energy difference is due to the TOF measurements then this is energy dependent, however for the monoenergetic sources this can be a near constant shift.

A. Smith No, it is usually the calibration of a magnet which gives a similar thing.

W. Poenitz I will discuss in my contribution the problem of energy scales. We analyzed all structural features in the U-238/U-235 ratio and could show that one of the TOF scales must be in error.

A. Carlson I should point out that one set of carbon resonance energies was measured with a monoenergetic source and there is a good agreement with TOF results.

MEASUREMENTS OF NEUTRON INDUCED FISSION CROSS SECTION RATIOS  
AT THE KARLSRUHE ISOCHRONOUS CYCLOTRON

S. Cierjacks, B. Leugers, K. Kari, B. Brotz,  
D. Erbe, D. Gröschel, G. Schmalz, F. Voß

Institut für Angewandte Kernphysik  
Kernforschungszentrum Karlsruhe, F.R. Germany

ABSTRACT

Ratios of the fission cross sections of  $^{238}\text{U}$  and  $^{239}\text{Pu}$  relative to  $^{235}\text{U}$  were measured with the fast neutron time-of-flight facility at the Karlsruhe isochronous cyclotron. With the continuous energy neutron source the entire range from 0.5 - 30 MeV was covered in one experiment. In the experiments gas scintillation counting of the fission fragments and coincidence techniques were employed. Typical energy resolutions range between 0.7 % at 0.5 MeV and 3 % at 30 MeV. For the  $^{238}\text{U}/^{235}\text{U}$  ratio most of the data have counting statistics smaller than 3 %, for the  $^{239}\text{Pu}/^{235}\text{U}$  counting statistics does not exceed 2 %.

INTRODUCTION

A better knowledge of fission cross sections for  $^{235}\text{U}$ ,  $^{238}\text{U}$  and  $^{239}\text{Pu}$  throughout the keV and the MeV-range is essential for the design and the economics of fast breeder reactors. The importance of these cross sections has brought a large number of requests from various countries. Despite the large effort devoted in the past to the determination of these data there are still gaps in the MeV energy range for all three isotopes. In addition several discrepancies appeared in different measurements of these cross sections, even in the determinations of their ratios relative to the  $^{235}\text{U}$  fission cross section.

In this contribution new measurements of the fission cross section ratios  $^{238}\text{U}/^{235}\text{U}$  and  $^{239}\text{Pu}/^{235}\text{U}$  are described which were carried out with the fast neutron time-of-flight facility at the Karlsruhe isochronous cyclotron. The measurements extended from 1-30 MeV for the  $^{238}\text{U}/^{235}\text{U}$  ratio and from 0.5 - 30 MeV for  $^{239}\text{Pu}/^{235}\text{U}$  ratio. The detectors were of unique design which allowed measurements of fission events with high efficiency via detection of coincidences between both fission fragments. The shape measurements for both, the  $^{238}\text{U}$  and  $^{239}\text{Pu}$  ratio relative to U-235 are normalized at 14 MeV. For the  $^{239}\text{Pu}/^{235}\text{U}$  ratio the absolute value will be deduced after accurate mass determinations are finalized.

## EXPERIMENTAL METHOD

### The Time-of-Flight Arrangement

The arrangement of the experimental set up is shown schematically in Fig. 1. Neutron pulses of 1.5 nsec duration and a repetition rate of 100 kHz are produced by the internal beam of the cyclotron. A continuous energy spectrum of neutrons allowing measurements in the range from 0.5-30 MeV originates from a bombardment of thick natural uranium targets with 50 MeV deuterons. The spectrum of neutrons which is extracted at  $0^\circ$  to the incident deuteron beam represents essentially a superposition of an evaporation spectrum with a deuteron break-up spectrum, the latter providing a broad distribution peaking at about half of the incoming deuteron energy. The neutron beam passes through a thin polyethylene window out of the vacuum tank of the cyclotron. An iron end collimator is used to define a narrow neutron beam of 8 cm and 5 cm in the detector positions for the  $^{238}\text{U}/^{235}\text{U}$  and the  $^{239}\text{Pu}/^{235}\text{U}$  measurements, respectively. The measurements of the  $^{238}\text{U}/^{235}\text{U}$  ratio were carried with the 57 m flight path. For the determination of the fission cross section ratio of  $^{239}\text{Pu}/^{235}\text{U}$  the newly installed short flight path could be employed, allowing a measurement at a distance of 11,927 m from the source.

### The Fission Detectors

The basic design of the fission chambers used in our experiments is shown in Fig. 2. For the detection of fission fragments an arrangement of nine gas scintillation chambers in series was used. The scintillation chambers were made of stainless steel. Silver was plated to the inner walls as the reflector material. Each scintillation chamber was separated from its next neighbours by the fission foils. Optical decoupling is provided by the metallized vynes backing of the fission foils. A mixture of 85 % argon and 15 % nitrogen gas flowing continuously through the counter at slightly above atmospheric pressure served as the scintillator. Each chamber is viewed by one Valvo DUVP 56 photo multiplier tube. A fast timing signal is provided from the anode of each photo multiplier.

### Timing and Resolution

For exact timing of the experiment it was necessary to define the time-zero-point of the absolute time scale. This was provided by the prompt  $\gamma$ -rays from the uranium target. The narrow time peaks occurring in the single's spectra of each chamber occurred mainly because of the small, but non-zero efficiency of the gas scintillators for  $\gamma$ -rays. The peaks obtained also in the coincidence spectra at the same position but with very low probability are mainly due to photo-fission events in the fissionable material. Finally our timing was verified by measuring the narrow MeV-resonances of carbon, which confirmed the above assumptions.

The resolution in our experiment is given by the resolution of the fission detectors and the neutron pulse width of the cyclotron, which is about 1.5 ns. The overall time resolution of the detectors was measured from coincidences of fission fragments and  $\gamma$ -rays emitted in the prompt fission of a

$^{252}\text{Cf}$  source. For detection of  $\gamma$ -rays a NE 102 A plastic scintillator was employed. This gave typical time resolutions for our fission counters of 4 ns. Taken in quadrature, the both contributions mentioned above results in a resolution of  $\sim 4.5$  nsec.

### Data Acquisition

A simplified block diagram of the data acquisition system is shown in Fig. 3. For each fission foil of the detector both fission products with fragment energies higher than 15 MeV were detected in the adjacent chambers. A 15 nsec coincidence was required to identify fission events. For time-of-flight determinations the cyclotron provides a start pulse for timing purposes which is synchronized with the neutron burst to better than  $\pm 0.2$  nsec. This pulse and the stop pulse from the detectors are fed to a digital time analyser set to a range of 4096 time channels with 2 nsec channel width. The corresponding eight time spectra are fed via a special interface-unit to a CDC 3100 on-line computer and recorded simultaneously, but accumulated separately on a magnetic disc and sequentially stored on magnetic tape.

### The Samples

Fission samples were provided by the Sample Preparation Group of the CBNM Euratom Laboratory in Geel, Belgium. The fissile material was deposited by electro spraying of the corresponding oxides on 170 (uranium) and 100  $\mu\text{g}/\text{cm}^2$  (plutonium) vycor foils, metallized by 20  $\mu\text{g}/\text{cm}^2$  as described by Verdingh and Lauer<sup>1</sup>). This laboratory will also perform the final mass determination, which unfortunately is not yet finalized. So far only tentative mass values have been given, which were derived from  $\alpha$ -counting. Thus the fission cross section ratios are shape determinations normalized at the well known 14 MeV values.

## CORRECTIONS AND UNCERTAINTIES

For the fission cross section ratio of  $^{238}\text{U}/^{235}\text{U}$ , for which some channel grouping of the original time-of-flight data was made, most of the data have a statistical accuracy of better than 3 %. The corresponding statistical counting errors for the  $^{239}\text{Pu}/^{235}\text{U}$  ratio measurement are typically a few permil and do not exceed 3 % in the whole energy range. In addition to the effect of counting statistics a number of other effects contribute systematic errors to our experimental results. The major effects are listed in Table I.

### Background

A typical time of flight spectrum is shown in Fig. 4. It can be seen, that the time independent background is about 1-2 % in most of the time channels except at the lower and upper end of the spectrum, where the background does not exceed 5 % of the fission events. This situation is even better for the fission spectra of both uranium isotopes  $^{238}\text{U}$  and  $^{235}\text{U}$ . The resulting uncertainty for the fission cross section ratio is included in the statistical error and does not exceed 1 % except for the  $^{238}\text{U}/^{235}\text{U}$  ratio below 2 MeV and above  $\sim 20$  MeV. The time-correlated background measured by comparison of

resonance transmission shapes from carbon, showed that the time-independent background was negligible in our measurements. The possibility of a  $\pm 2\%$  systematic error due to such background could not be excluded.

### Energy Dependent Detector Efficiency

For measurements in the MeV range the incident neutron momentum causes a varying forward peaking of fission fragments. This results in an increased detector efficiency for the fission chamber at that side of the foil which is remote from the neutron source. These effects have been calculated with a program following mainly the treatment of Rossi and Staub<sup>2</sup>). The input data for the calculations are the thicknesses of the various layers of the samples, (uranium or plutonium oxide, vynes and aluminum) and the range and energy loss of fission fragments in these materials<sup>3</sup>). Such results have to be averaged over light and heavy fragments and showed that 7,5 % of the  $^{238}\text{U}$  and 8,0 % of the  $^{235}\text{U}$  fragments were absorbed in the  $^{238}\text{U}/^{235}\text{U}$  ratio measurement. It turned out from such calculations that the differences in the change of the efficiencies for  $^{238}\text{U}$  and  $^{235}\text{U}$  for the ratio measurements of  $^{238}\text{U}$  and  $^{235}\text{U}$  were less than 0,5 %, so that no correction was applied in this case. In the  $^{239}\text{Pu}/^{238}\text{U}$  ratio measurement, in which largely different samples thicknesses were used for Pu and U-foils, the calculations showed a significant energy dependence of the efficiency ratio. The obtained change was 5 % at 20 MeV.

The effect of the anisotropy of fragment emission with respect to the incident neutron beam can also cause differences in the detection efficiencies of both isotopes in a fission cross section ratio measurement. For the two uranium isotopes  $^{238}\text{U}$  and  $^{235}\text{U}$  the effect of anisotropy is significantly different, but this effect is only important, when the fragments are absorbed in thick foils. The energy dependence in the efficiency has been estimated on the basis of the measured anisotropies<sup>4</sup>) and under the assumption, that all loss in efficiency is due to losses of fragments in the foils. These calculations showed a very small effect of less than 0.8 %.

### Electronic Threshold and Dead Time-Corrections

The electronic threshold correction was determined by extrapolating the pulse height distributions from both sides of the samples to the zero pulse heights. Electronic dead time effects were controlled throughout the experiments with test pulses from luminescence diodes applied to each fission chamber. It was confirmed that no pulses were lost or uncorrectly routed. The measurements were conducted in a number of independent runs, in order to ensure that there was no systematic drift in the electronic and the data acquisition system. The experiments were performed at a counting rate  $\sim 600$ – $1200$  events/sec requiring a time-independent dead time correction of  $\sim 1\%$  for the  $^{238}\text{U}/^{235}\text{U}$  ratio and of  $2\%$  for the Pu-239 ratio.

### Sample Mass and Isotopic Composition

The preliminary mass values and the exact isotopic compositions of the samples are listed in Table II. Due to the complex calculation of the masses from the  $\alpha$ -activity, the isotopic composition and the half-lives of the constituent isotopes the determinations have not yet been finished. Thus the uncertainties are  $\sim \pm 15\%$  for  $^{239}\text{Pu}$  and  $\sim 2\%$  for the uranium isotopes. The final determinations which are in progress are expected to give accuracies

of better than 1 %.

With the exception of  $^{238}\text{U}$  for which highly enriched material was available, there was a not negligible isotopic impurity in the samples of  $^{235}\text{U}$  and  $^{239}\text{Pu}$  requiring explicit corrections of the data. In particular corrections were applied for the U-238 content in the  $^{235}\text{U}$  foils (5.4 %) and for the  $^{240}\text{Pu}$  content in the  $^{239}\text{Pu}$  foils (3.9 %). While for the correction of the  $^{238}\text{U}$ -impurity in  $^{235}\text{U}$  the counting rates of  $^{238}\text{U}$  from our own measurement were used the evaluated Los Alamos fission cross sections of  $^{239}\text{Pu}$  and  $^{240}\text{Pu}$  were adopted<sup>5)</sup>.

## RESULTS AND DISCUSSIONS

### $^{238}\text{U}/^{235}\text{U}$ Ratio

The measured fission cross section ratio  $^{238}\text{U}/^{235}\text{U}$  in the range from 1-30 MeV is shown in Fig. 5. No complete comparison with all existing data sets is given here, since a detailed comparison is part of the service provided by the organizers of this Specialists Meeting. Included are only the results of some recent measurements with continuous energy neutron sources<sup>6,7)</sup>.

Our Karlsruhe measurements are normalized at 14 MeV to the value of  $0.55^8)$ . At this energy evaluations assign a comparatively low standard deviation error of 2 % to their ratio value, because of the numerous existing measurements at this point. The numerical values from our measurement are given in Table III. Only the statistical errors are from here which are in time-dependent background which was assumed to be less than  $\pm 2$  %. It can be seen that the overall agreement in shape is good, apart from a disagreement in the peak range from 6 to 7 MeV and the range above  $\sim 20$  MeV. The partial results in the threshold region from 1-2 MeV is shown in Fig. 6 to demonstrate a peculiarity which might deserve a discussion at this meeting. There appears to be a significant shift in the energy scales between the Karlsruhe and Livermore data on the one side and the Harwell results on the other side. If there also exists differences in the energy scales of  $^{235}\text{U}$  measurements as was noted recently then this might call for a revision of quoted data because of the energy dependence at the reference  $\text{H}(\text{n},\text{p})$  cross section. Below  $\sim 1.6$  MeV our cross section ratio became increasingly inaccurate due to the counting statistics which reached 9% at 1.2 MeV thus no ratio values are given below that value.

### $^{239}\text{Pu}/^{235}\text{U}$ Ratio

Our results of the fission cross section ratio are shown in comparison with the preliminary results of Behrens and Carlson<sup>9)</sup> in Fig. 7. Our shape measurement was normalized at 14 MeV to the cross section ratio value of  $1.15^{10)}$ . It can be seen that the overall agreement between the two data sets is good apart from the different rise above about 15 MeV. Numerical values of our data are summarized in Table IV.

## ACKNOWLEDGEMENTS

The authors wish to thank Drs. Lauer, Verdingh and Pauwels for the careful preparation of the fission samples and the preliminary mass determinations. The help of the cyclotron crew headed by Dr. Schweickert and Mr. F. Schulz is gratefully acknowledged.

## REFERENCES

1. V. VERDINGH, K.F. LAUER, *Nucl. Instr. Meth.* 21 (1963) 161.
2. B.B. ROSSI, H.H. STAUB, *Ionization Chambers and Counters*, Mac Graw Hill, New York (1949) p. 227 ff.
3. L.C. NORTHCLIFF, R.F. SCHILLING, *Nuclear Data Tables* A7 (1970) 233.
4. J.E. SIMMONS, R.L. HENKEL, *Phys. Rev.* 120 (1960) 198.
5. R.E. HUNTER, L. STEWARD, T.J. HIROUS, Los Alamos Scientific Laboratory Report, LA-5172, 1973.
6. J.W. BEHRENS, G.W. CARLSON, R.W. BAUER, *Proc. of a Conf. on Nuclear Cross Sections and Technology*, Washington, D.C., March 1975, p. 591-596.
7. M.S. COATES, D.B. GAYTHER, N.J. PATTENDEN, *Proc. of a Conf. on Nuclear Cross Sections and Technology*, Wash. D.C., March 1975, p. 568-571.
8. W.P. POENITZ, private communication, (1976).
9. J.W. BEHRENS, G.W. CARLSON, preliminary data, not published, (1975).
10. C.A. UTTLEY, J.A. PHILLIPS, UKAEA Report No. AERE NP/R 1996 (1956).

TABLE I

## Corrections and Uncertainties in the Ratio Measurements

Effect	Size of the Effect	Resulting Uncertainty	Correction Applied
Time-independent background	max. 5 % < 2 % typical	0.5 % max. < 0.2 % typical	Yes
Time-dependent background	< 2 %	< 0.5 %	No
Energy dependent detector efficiency	max. 5 % for thick U samples < 2 % typical	< 0.2 %	Yes
Electronic threshold	max. 20 % of the total fission spectrum was cut off	< 0.5 %	Yes
Dead time losses	max. 2 % > 1 % typical	negligible	Yes
Isotopic impurities	5.4 % max. for U-235	almost everywhere negligible	Yes
Neutron scattering in Ta- and fission foils	< 1 % typical	< 0.5 % maximal	No

TABLE II  
Isotopic Composition and Areal Density of Fission Foils

<u><math>^{238}\text{U}/^{235}\text{U}</math> Ratio</u>							
Isotopic Composition, Mass Number (at. %)							
Isotope	Foil No.	234	235	236	238	235/238	Areal Density (U $\mu\text{gr}/\text{cm}^2$ )
$^{238}\text{U}$	1						$460 \pm 1 \%$
	2						$444 \pm 1 \%$
	3					0.0001755	$413 \pm 1 \%$
	4						$434 \pm 1 \%$
$^{235}\text{U}$	1						$412 \pm 1 \%$
	2						$430 \pm 1 \%$
	3	1.080	93.331	0.202	5.387		$440 \pm 1 \%$
	4						$319 \pm 1 \%$

$^{239}\text{Pu}/^{235}\text{U}$  Ratio

Isotopic Composition, Mass Number (at. %)											Areal Dens.
Isotope	Foil No	234	235	236	238(U)	238(Pu)	239	240	241	242	(U,Pu-μ gr/cm <sup>2</sup> )
<sup>239</sup> Pu	1										180 ± 15 %
	2										180 ± 15 %
	3					0.008	96.023	3.858	0.103	0.008	180 ± 15 %
	4										180 ± 15 %
<sup>235</sup> U	1										730 ± 1 %
	2										802 ± 1 %
	3	1.080	93.337	0.202	5.387						784 ± 1 %
	4										

TABLE III  
Fission Cross Section Ratio  $\sigma_f^{238}\text{U}/\sigma_f^{235}\text{U}$

$E_n$ (MeV)	$\frac{\sigma_f^{238}\text{U}}{\sigma_f^{235}\text{U}}$	Statistic. Error (%)	$E_n$ (MeV)	$\frac{\sigma_f^{238}\text{U}}{\sigma_f^{235}\text{U}}$	Statistical Error (%)
1.374	0.132	7.2	11.957	0.576	2.5
1.424	0.209	6.3	12.161	0.573	3.0
1.474	0.265	5.7	12.371	0.547	3.0
1.524	0.294	5.5	12.586	0.531	2.9
1.574	0.326	5.4	12.807	0.515	2.8
1.625	0.353	5.3	13.033	0.533	2.7
1.674	0.349	5.3	13.266	0.534	2.6
1.726	0.332	5.4	13.505	0.550	2.6
1.775	0.377	5.4	13.750	0.528	2.5
1.824	0.395	5.2	14.003	0.550	2.4
1.872	0.409	5.2	14.262	0.552	2.4
1.923	0.376	5.3	14.529	0.543	2.4
1.973	0.398	5.4	14.803	0.567	2.3
2.039	0.395	2.2	15.086	0.584	2.2
2.342	0.401	2.3	15.376	0.595	2.2
2.642	0.415	2.5	15.675	0.601	2.2
2.945	0.416	2.7	15.983	0.610	2.1
3.245	0.423	3.0	16.301	0.636	2.1
3.541	0.465	3.1	16.627	0.623	2.2
3.843	0.461	3.3	16.964	0.603	2.2
4.144	0.466	3.5	17.311	0.632	2.2
4.446	0.476	3.7	17.670	0.621	2.2
4.742	0.475	3.8	18.039	0.621	2.2
5.046	0.460	4.1	18.420	0.643	2.2
5.344	0.484	4.1	18.814	0.665	2.3
5.644	0.487	4.2	19.221	0.675	2.3
5.942	0.529	4.0	19.641	0.698	2.3
6.248	0.554	3.9	20.075	0.712	2.4
6.547	0.586	3.5	20.524	0.744	2.4
6.849	0.609	3.3	20.988	0.744	2.5
7.137	0.577	3.3	21.468	0.763	2.6
7.443	0.549	3.2	21.965	0.736	2.7
7.748	0.545	3.0	22.480	0.744	2.7
8.050	0.560	3.1	23.014	0.760	2.8
8.346	0.541	2.9	23.566	0.763	3.0
8.635	0.551	2.9	24.140	0.771	3.2
8.939	0.547	2.8	24.735	0.784	3.4
9.259	0.555	2.8	25.352	0.755	3.7
9.539	0.534	2.8	25.993	0.775	4.0
9.833	0.563	2.7	26.659	0.738	4.3
10.140	0.559	2.6	27.351	0.778	4.5
10.462	0.575	2.7	28.071	0.772	4.8
10.731	0.560	2.8	28.820	0.776	5.1
10.046	0.563	2.6	29.601	0.812	5.3
11.337	0.582	2.6	30.413	0.778	5.7
11.641	0.565	2.6			

TABLE IV\*  
Fission Cross Section Ratio  $\sigma_f^{239\text{Pu}}/\sigma_f^{235\text{U}}$

$E_n$ (MeV)	$\frac{\sigma_f^{239\text{Pu}}}{\sigma_f^{235\text{U}}}$	Stat. Unc. (%)	$E_n$ (MeV)	$\frac{\sigma_f^{239\text{Pu}}}{\sigma_f^{235\text{U}}}$	Stat. Unc. (%)	$E_n$ (MeV)	$\frac{\sigma_f^{239\text{Pu}}}{\sigma_f^{235\text{U}}}$	Stat. Unc. (%)
20.891	1.211	0.5	9.371	1.290	0.6	4.207	1.587	0.7
20.448	1.211	0.4	9.238	1.279	0.6	4.089	1.600	0.7
20.019	1.211	0.4	9.108	1.274	0.6	3.976	1.600	0.7
19.603	1.214	0.4	8.981	1.271	0.6	3.868	1.599	0.7
19.201	1.230	0.4	8.857	1.270	0.6	3.764	1.591	0.7
18.810	1.219	0.4	8.735	1.262	0.6	3.664	1.584	0.7
18.432	1.225	0.4	8.615	1.265	0.7	3.568	1.608	0.7
18.065	1.209	0.4	8.498	1.256	0.7	3.476	1.585	0.7
17.709	1.200	0.4	8.384	1.261	0.7	3.387	1.587	0.7
17.364	1.190	0.4	8.272	1.274	0.7	3.302	1.587	0.7
17.029	1.183	0.4	8.162	1.272	0.7	3.220	1.590	0.7
16.703	1.173	0.4	8.054	1.266	0.7	3.140	1.576	0.7
16.387	1.166	0.4	7.948	1.277	0.7	3.064	1.578	0.7
16.079	1.161	0.4	7.845	1.258	0.7	2.991	1.580	0.7
15.781	1.153	0.4	7.743	1.263	0.7	2.920	1.568	0.7
15.490	1.148	0.4	7.643	1.268	0.8	2.852	1.572	0.7
15.208	1.151	0.4	7.546	1.272	0.8	2.786	1.578	0.7
14.933	1.138	0.4	7.450	1.282	0.8	2.722	1.555	0.7
14.666	1.129	0.4	7.356	1.293	0.8	2.660	1.543	0.7
14.406	1.128	0.4	7.264	1.289	0.8	2.601	1.555	0.7
14.153	1.129	0.4	7.173	1.277	0.8	2.543	1.571	0.7
13.906	1.139	0.4	7.085	1.284	0.8	2.488	1.578	0.7
13.666	1.138	0.4	6.997	1.309	0.9	2.434	1.569	0.7
13.432	1.141	0.4	6.912	1.316	0.9	2.382	1.563	0.7
13.204	1.177	0.4	6.828	1.340	0.9	2.331	1.582	0.7
12.982	1.179	0.4	6.745	1.351	0.9	2.282	1.575	0.7
12.766	1.190	0.4	6.664	1.359	0.9	2.235	1.564	0.7
12.555	1.211	0.4	6.585	1.360	0.9	2.189	1.552	0.7
12.349	1.232	0.4	6.507	1.390	1.0	2.145	1.561	0.7
12.148	1.250	0.4	6.430	1.404	1.0	2.102	1.573	0.7
11.952	1.259	0.4	6.355	1.429	1.0	2.060	1.563	0.7
11.761	1.271	0.5	6.281	1.462	1.0	2.019	1.566	0.7
11.574	1.280	0.5	6.208	1.471	1.0	1.980	1.564	0.7
11.392	1.295	0.5	6.136	1.503	1.1	1.942	1.546	0.7
11.214	1.297	0.5	6.066	1.527	1.1	1.904	1.555	0.7
11.041	1.300	0.5	5.929	1.561	0.6	1.868	1.569	0.8
10.871	1.295	0.5	5.732	1.631	0.7	1.833	1.583	0.8
10.705	1.298	0.5	5.545	1.631	0.7	1.799	1.589	0.8
10.543	1.302	0.5	5.367	1.641	0.7	1.766	1.561	0.8
10.385	1.306	0.5	5.198	1.622	0.7	1.734	1.581	0.8
10.230	1.304	0.5	5.036	1.615	0.7	1.702	1.593	0.8
10.079	1.289	0.5	4.882	1.609	0.7	1.672	1.586	0.8
9.931	1.288	0.6	4.734	1.619	0.7	1.642	1.563	0.8
9.786	1.292	0.6	4.594	1.601	0.7	1.613	1.566	0.8
9.645	1.301	0.6	4.459	1.604	0.7	1.585	1.548	0.8
9.506	1.293	0.6	4.330	1.580	0.7	1.557	1.573	0.8

TABLE IV (cont.) \*

$E_n$ (MeV)	$\frac{\sigma_f^{239}\text{Pu}}{\sigma_f^{235}\text{U}}$	Stat. Unc. (%)	$E_n$ (MeV)	$\frac{\sigma_f^{239}\text{Pu}}{\sigma_f^{235}\text{U}}$	Stat. Unc. (%)
1.531	1.583	0.8	0.763	1.564	1.0
1.505	1.590	0.8	0.748	1.529	1.1
1.479	1.595	0.8	0.733	1.517	1.1
1.455	1.573	0.9	0.719	1.474	1.1
1.430	1.592	0.9	0.705	1.485	1.1
1.407	1.599	0.9	0.691	1.526	1.1
1.384	1.609	0.9	0.678	1.477	1.1
1.361	1.624	0.9	0.665	1.437	1.1
1.340	1.582	0.9	0.653	1.445	1.2
1.318	1.578	0.9	0.641	1.476	1.2
1.297	1.566	0.9	0.629	1.479	1.2
1.277	1.594	0.9	0.618	1.461	1.2
1.257	1.580	0.9	0.606	1.477	1.2
1.238	1.563	0.9	0.596	1.466	1.2
1.219	1.562	1.0	0.585	1.416	1.2
1.200	1.528	1.0	0.575	1.381	1.2
1.182	1.515	1.0	0.565	1.395	1.3
1.164	1.520	1.0	0.555	1.424	1.3
1.147	1.537	1.0	0.546	1.379	1.3
1.130	1.497	1.0	0.536	1.395	1.3
1.114	1.453	1.0	0.527	1.407	1.4
1.098	1.483	1.0	0.519	1.433	1.4
1.082	1.508	1.1	0.510	1.441	1.4
1.066	1.514	1.1	0.502	1.416	1.4
1.051	1.495	1.1	0.494	1.408	1.5
1.036	1.456	1.1	0.486	1.388	1.5
1.022	1.444	1.1	0.478**	1.409	1.5
1.007	1.432	1.1	0.470	1.391	1.6
0.989	1.433	0.9	0.463	1.368	1.6
0.966	1.465	0.9	0.456	1.412	1.6
0.945	1.472	0.9	0.449	1.372	1.7
0.924	1.469	0.9	0.442	1.384	1.7
0.904	1.503	0.9	0.435	1.262	1.8
0.884	1.519	0.9	0.428	1.232	1.9
0.865	1.503	0.9	0.422	1.362	1.8
0.847	1.508	1.0	0.416	1.416	1.8
0.829	1.536	1.0	0.410	1.378	1.8
0.812	1.530	1.0	0.404	1.314	1.8
0.795	1.582	1.0	0.398	1.372	1.8
0.779	1.525	1.0	0.392	1.371	1.8

\* This table contains corrected data supplied by the authors after the end of the meeting. (Note added by the Editors.)

\*\* The low-energy limit for the validity of these data is unclear. Please contact the authors. (Note added by the Editors).

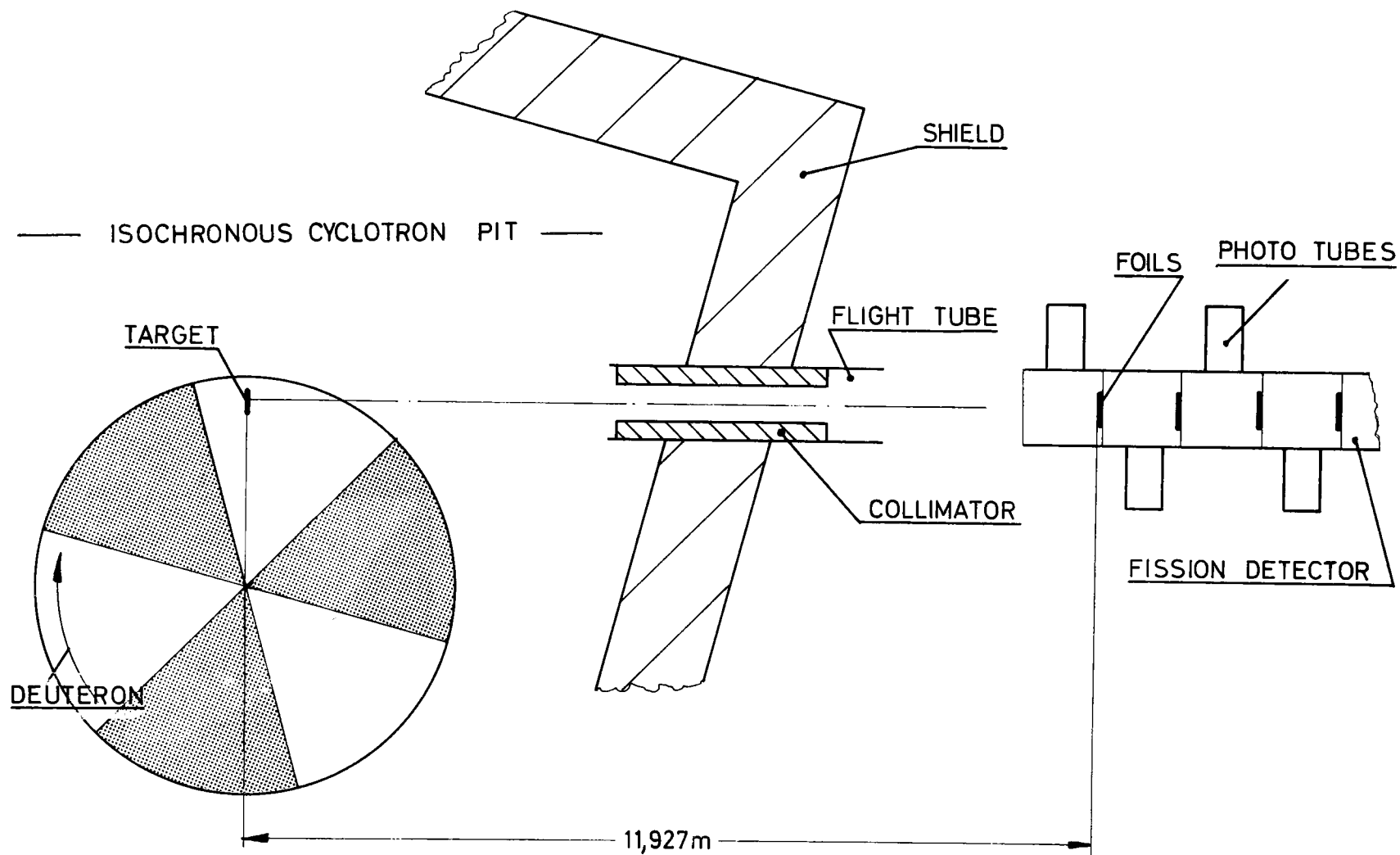


FIG. 1: GEOMETRIC ARRANGEMENT OF THE FISSION EXPERIMENT AT THE KARLSRUHE FAST NEUTRON TIME-OF-FLIGHT FACILITY

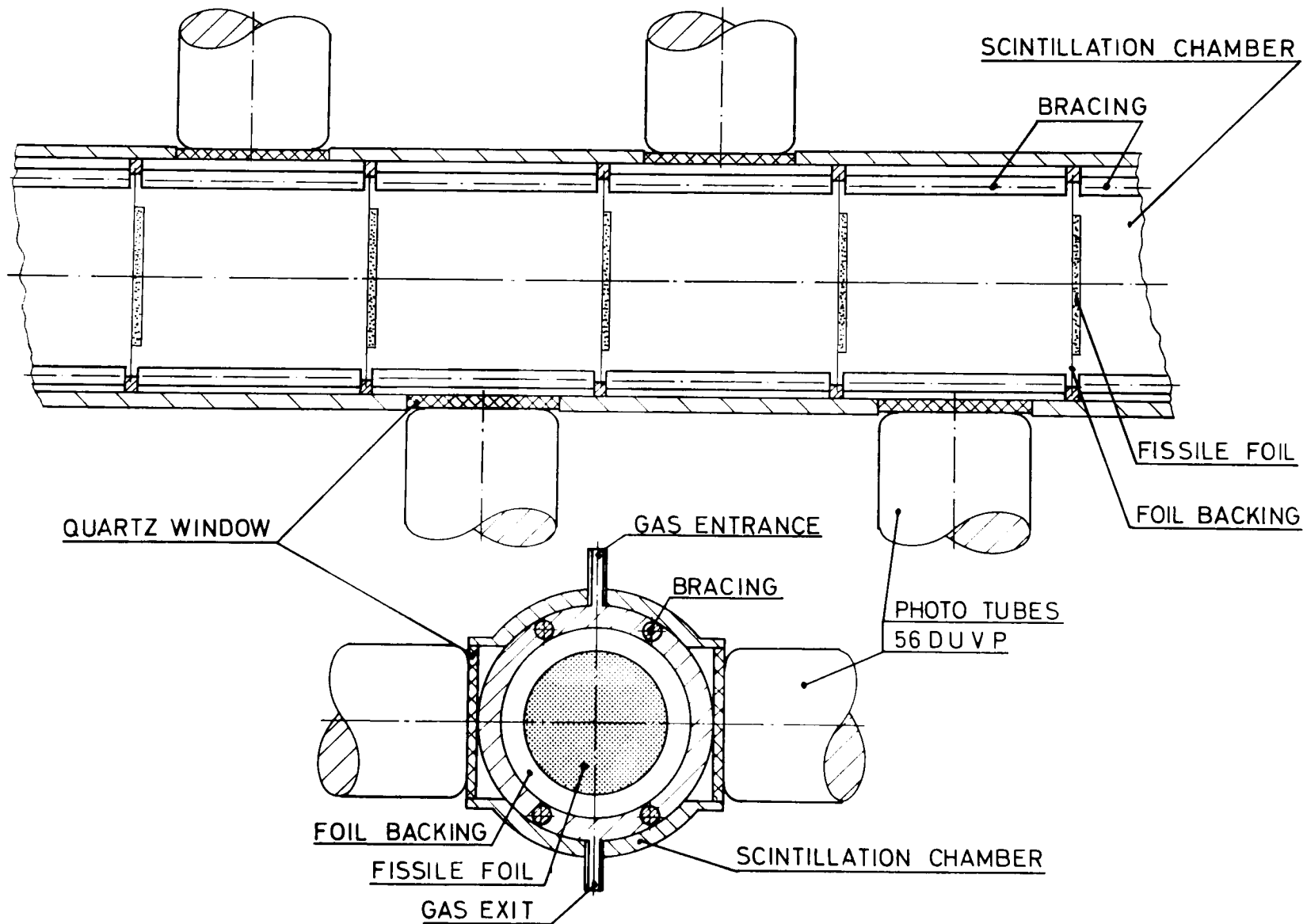
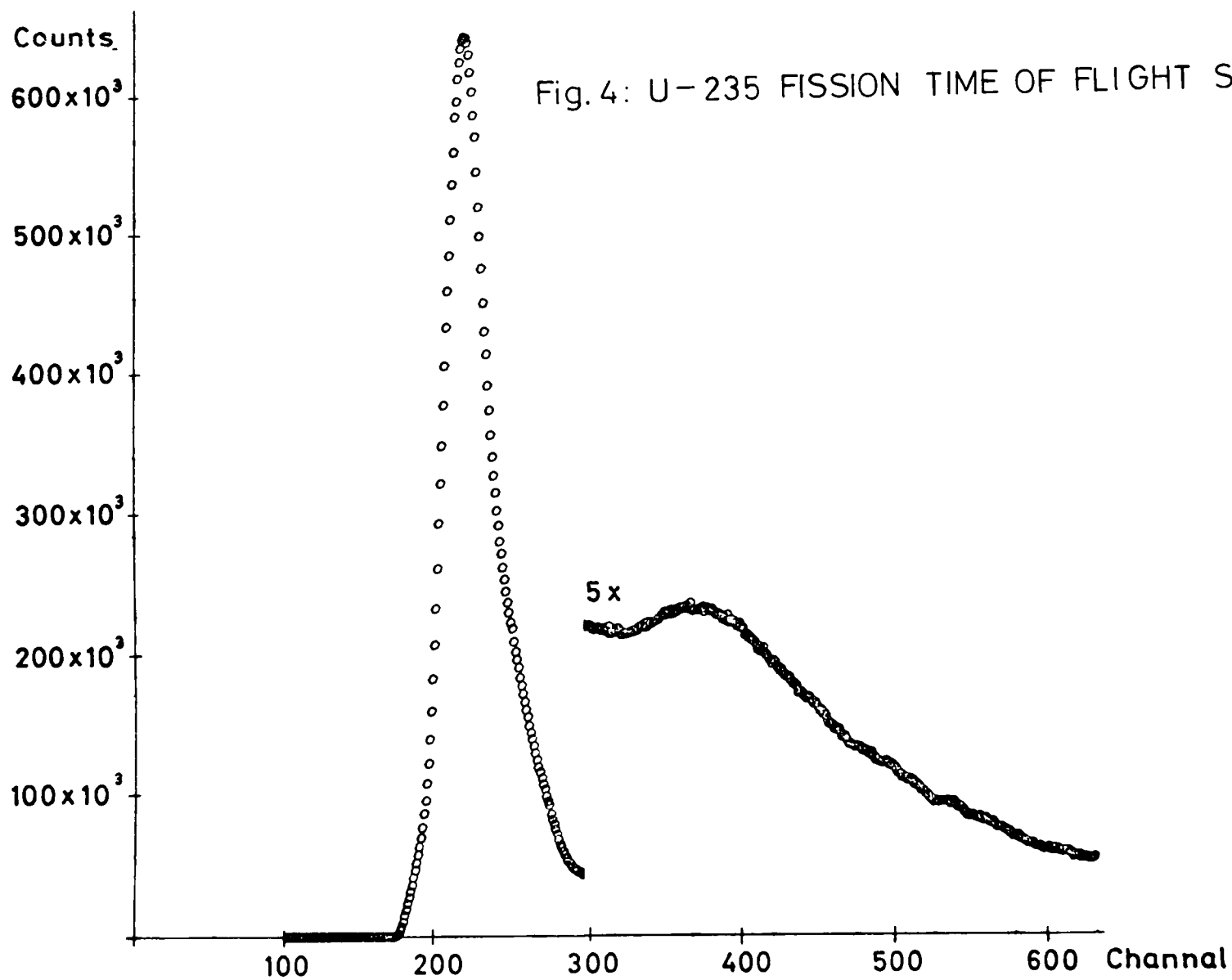


FIG. 2: SCHEMATIC DRAWING OF THE PRINCIPLE FISSION DETECTOR DESIGN





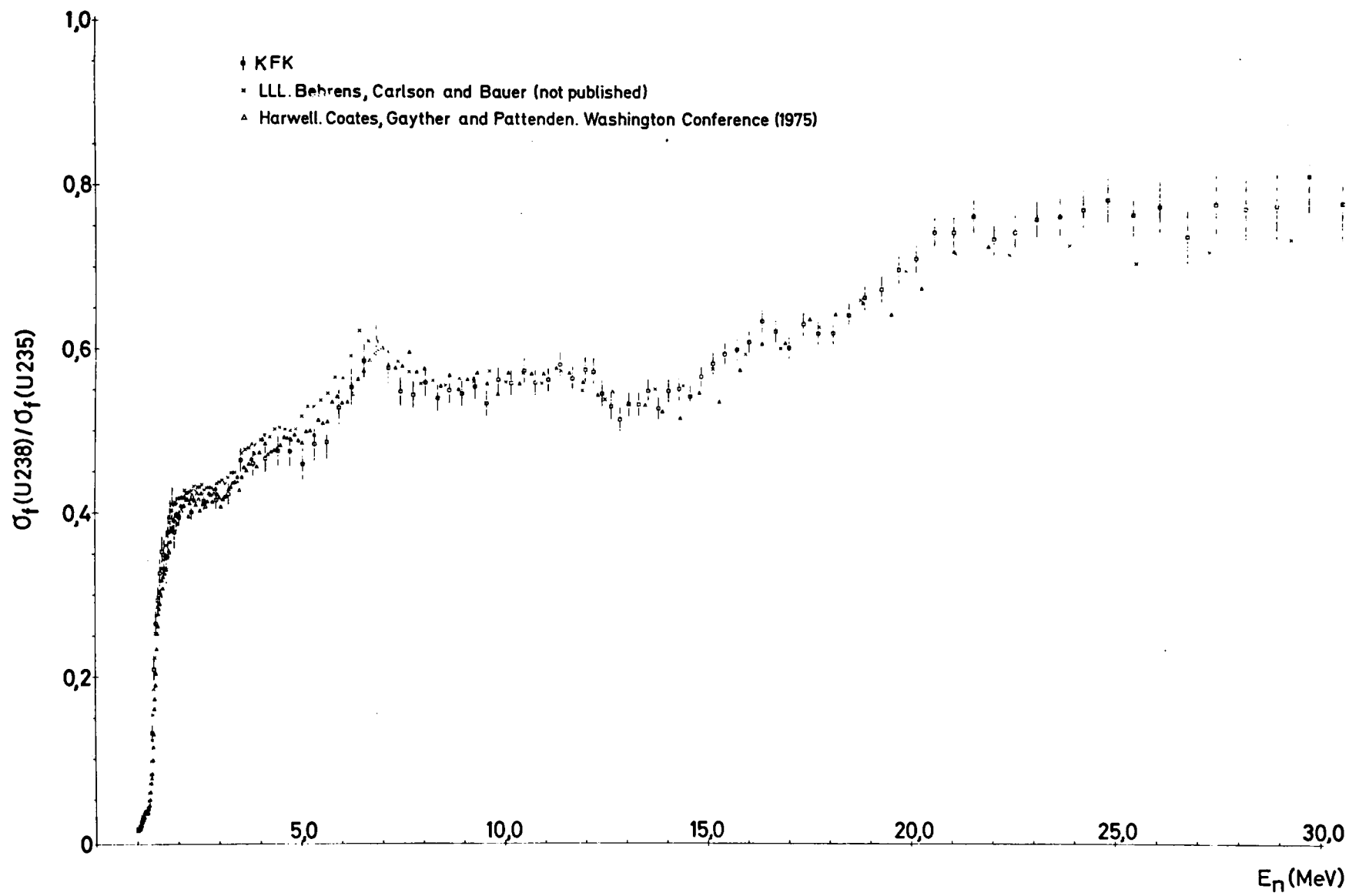


FIG. 5: FISSION CROSS SECTION RATIO  $^{238}\text{U} / ^{235}\text{U}$

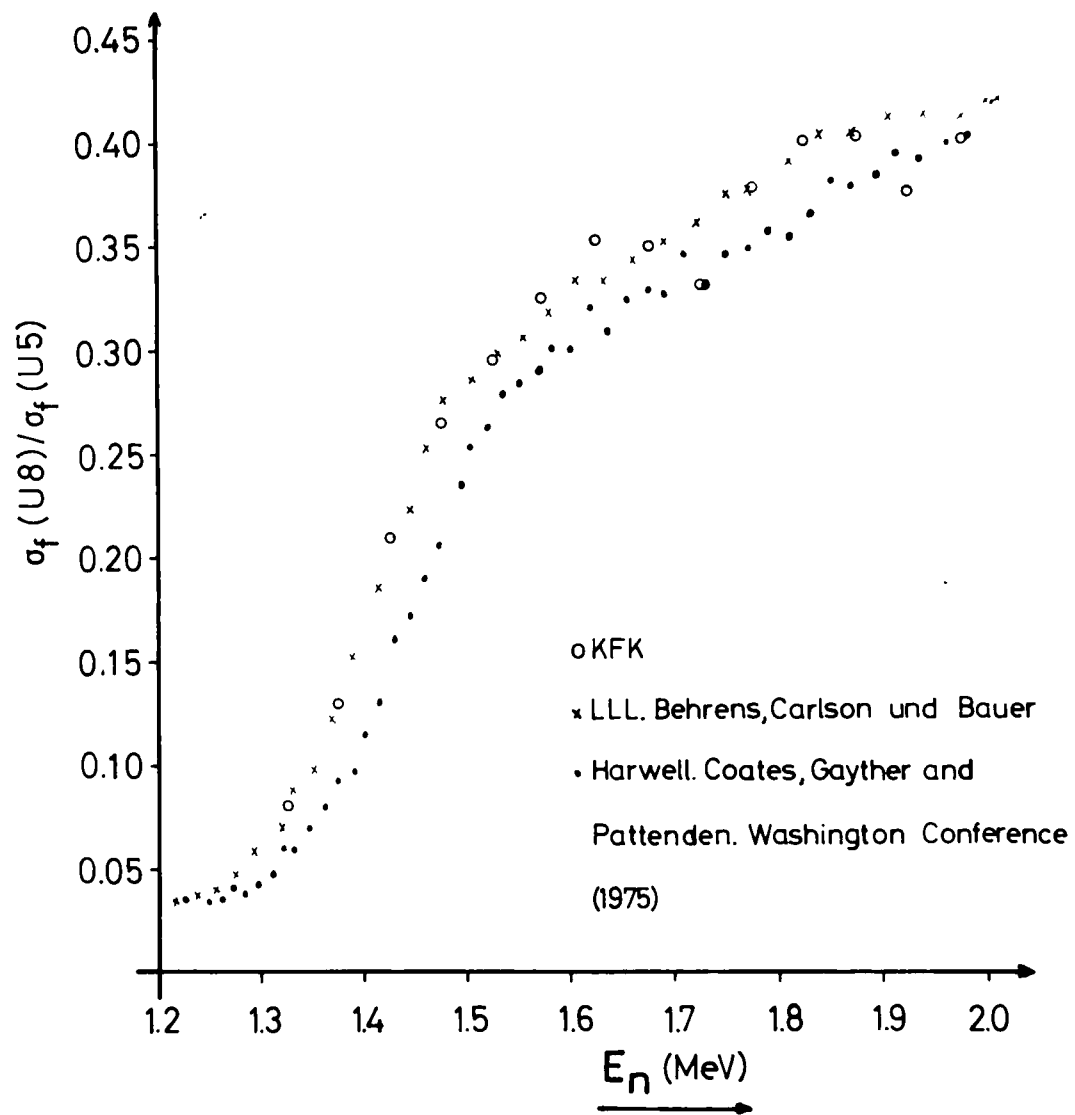


FIG. 6: Partial Results of Fission Cross Section Ratio  $^{238}\text{U} / ^{235}\text{U}$

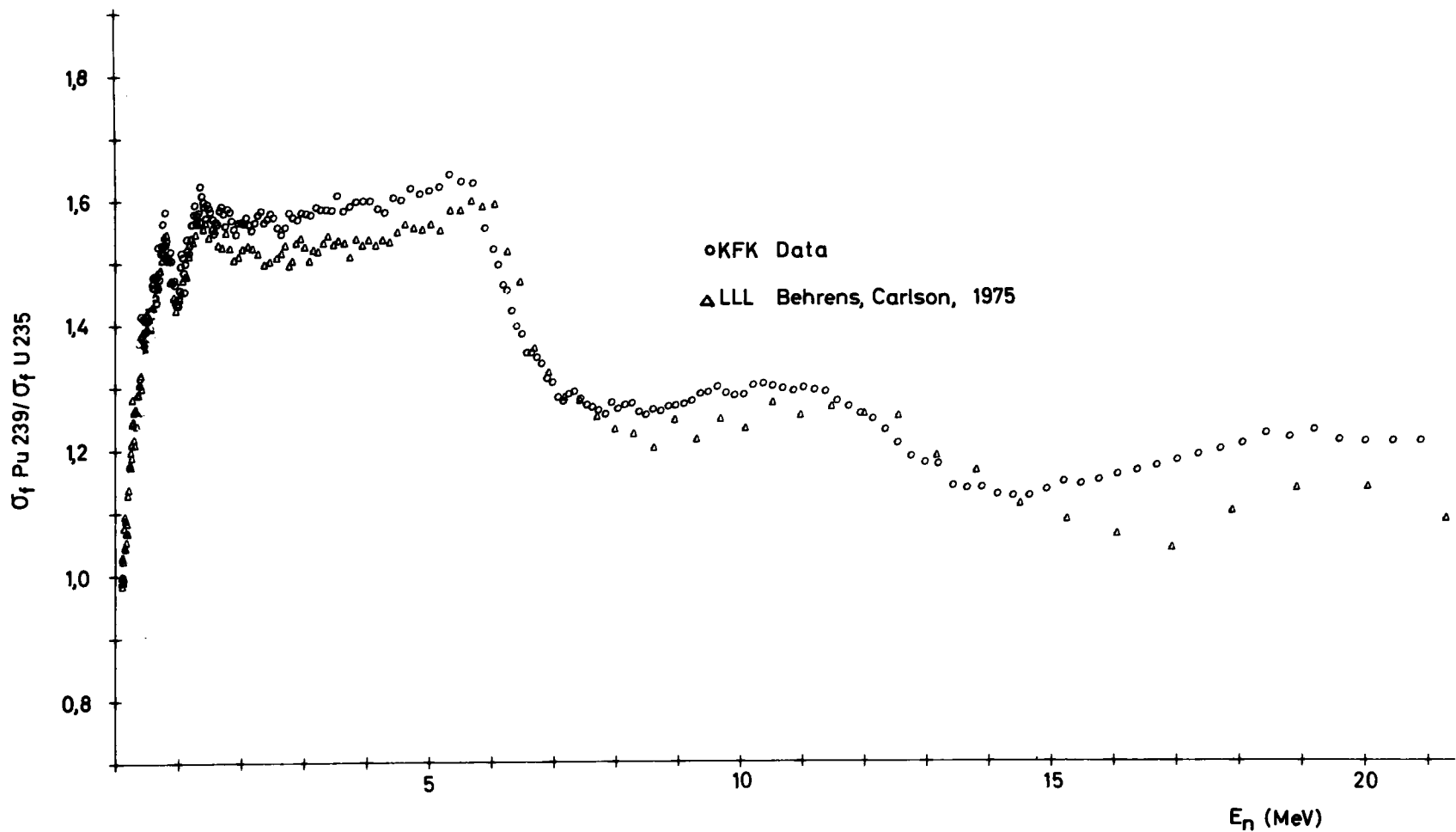


Fig. 7: FISSION CROSS SECTION RATIO  $^{239}\text{Pu} / ^{235}\text{U}$

## DISCUSSIONS

J. Behrens I would like comment on your comparison with the Livermore data. The figure you showed contains data from our UCID report.

S. Cierjacks That's right.

J. Behrens Data were not provided in this report in a table but only in a figure. This was one of our lower efficiency runs. We figured that our efficiency was only around 70%. Since then we completely redesigned our experiment and measured with three different detectors and it will be interesting to make comparisons with these later results.

S. Cierjacks I have just done this. The general trend is not disappearing. The disagreement in shape above 10 MeV is still present.

J. Behrens How high in energy do you go?

S. Cierjacks We stopped at present at 20 MeV.

G. Carlson Have you made a correction for the anisotropy--I did not see it in your table--would you care to give a number?

S. Cierjacks Yes. This is right, in the table I have included this correction in the energy-dependent factor which is inclusive of momentum transfer and anisotropy. The anisotropy correction is not very large for the ratio but more important for the fission cross section measurements themselves.

M. Moore Is there a possibility of pulse overlap?

S. Cierjacks No, not in our case. We have introduced Cd-filters between source and detectors. We cut off the low energy neutrons with that.

M. Moore What was the repetition rate?

S. Cierjacks 20 KHZ with a flight-path of 11m.

M. Moore Well, that won't cut off the overlap.

S. Cierjacks Yes. Nevertheless the overlap neutrons in the critical range are so few. Moderated neutrons would give a constant background--we would see this in the range of the time-independent background which is

very low. In case of U-238 the counts below the threshold would indicate overlap-problems--we see nothing.

A. Carlson I missed the basis for the less than 2% ambient background.

S. Cierjacks We measure with different sample thicknesses the resonances at higher energy. From this we can determine the background. The highest resonance was at  $\sim 8$  MeV.

# HIGH RESOLUTION MEASUREMENT OF THE $^{238}\text{U}$ TO $^{235}\text{U}$ FISSION CROSS SECTION RATIO BETWEEN 2 MeV AND 25 MeV\*

F. C. Difilippo,† R. B. Perez,  
G. de Saussure, D. Olsen, R. Ingle

Oak Ridge National Laboratory  
Oak Ridge, Tennessee 37830, U.S.A.

## INTRODUCTION

There are persistent discrepancies among recent measurements of the  $^{238}\text{U}$  fission cross section in the region from threshold to about 30 MeV.<sup>1-5</sup> Some of those discrepancies may be due to errors in the energy calibration of the measurements.

This paper describes a measurement of the  $^{238}\text{U}/^{235}\text{U}$  fission cross section ratio. Particular attention was paid to the energy calibration of the data. The results of the measurement are provisionally normalized to an evaluated value at 2.5 MeV,<sup>6</sup> but further experiments are in progress to obtain an independent absolute normalization.

## EXPERIMENTAL SET UP

A high purity  $^{238}\text{U}$  fission chamber was placed at a 40 m flight path at ORELA. The important parameters of the chamber are listed in Table I. The ORELA Linac was operated at a repetition rate of 800 pps and the electron bursts were 5 nsec wide. The channel structure for the acquisition of the time of flight data is given in Table II. In Table III we indicate the overall resolution at some typical neutron energies.

In determining the fission cross-section ratio the count rates of two adjacent sections of the chambers were used, one containing  $^{238}\text{U}$  and the other containing  $^{235}\text{U}$ . Data from the other sections of the chamber were not used for this measurement.

---

\* Research sponsored by the Energy Research and Development Administration under contract with the Union Carbide Corporation.

† An IAEA fellow, on assignment from Comision Nacional de Energia Atomica, Argentina.

## ENERGY CALIBRATION

The flight path  $L$  and the initial delay time  $t_0$  were obtained by fitting the positions  $E_i^R$  of well known resonances to the relativistic formula

$$E_i^R = 939.49 [(1 - .00212882 E_i^{NR})^{-1/2} - 1]$$

where

$$E_i^{NR} = .0052273 L^2 / (t_i - t_0)^2$$

where the energies are in MeV, the flight path in m, and the times in  $\mu\text{sec}$ .

The energies of the resonances utilized are listed in Table IV. For the energy calibration of the  $^{235}\text{U}$  section of the chamber, the  $^{235}\text{U}$ , Al, and C resonances were used; for the  $^{238}\text{U}$  section the five C levels were used, as well as the known relative positions of the  $^{238}\text{U}$  and  $^{235}\text{U}$  plates. In addition the 721 eV fission subthreshold level provided a consistency check on the energy calibration.

DETERMINATION OF THE  $^{238}\text{U}/^{235}\text{U}$  FISSION CROSS SECTION RATIO

The following corrections were applied to the data in the process of reduction to fission cross section ratios:

- a) Dead-time correction: An 8  $\mu\text{sec}$  dead-time, longer than the dead-time of any of the components of the equipment, was artificially imposed on the electronics. The dead-time correction amounted to a maximum of 7.6% at 6.8 MeV in the  $^{238}\text{U}$  sections and of 11.3% at 1.2 MeV in the  $^{235}\text{U}$  section.
- b) Background correction: For the  $^{238}\text{U}$  section the background was obtained from the counting rate between clusters of subthreshold resonances. A Wald Walfowitz non-parametric correlation test was applied to verify that the fluctuations in the data between clusters were purely statistical. For the  $^{235}\text{U}$  section the background was estimated from the count rate in the Al resonances at 5.903 and 34.7 keV and in the  $\text{Li}^7$  resonance at 257 keV. The background was essentially negligible for the  $^{238}\text{U}$  sections and amounted to a 0.1% correction for the  $^{235}\text{U}$  section.
- c) Scattering correction: The effect of the neutrons scattered from the 1.57 mm thick magnesium entrance wall of the chamber was neglected because of the large distance (15 cm) between this wall and the  $^{235}\text{U}$  section, or the adjacent  $^{238}\text{U}$  section. Approximately 2% of the neutron beam incident on the  $^{235}\text{U}$  section and the adjacent  $^{238}\text{U}$  section arises from interactions in the aluminum plates. In roughly half those interactions the neutron suffers an inelastic collision with large energy loss. This effect introduced a correction of approximately 1% in the energy region above the Al inelastic scattering threshold.
- d) Normalization: After application of the corrections first discussed the fission ratio was obtained from the count rates of adjacent  $^{238}\text{U}$  and  $^{235}\text{U}$  sections at each congruent energy point. The ratio was then normalized to the value 0.432 at 2.5 MeV.<sup>6</sup>

## RESULTS AND DISCUSSION

The results of our measurement are given in Table V. The energy mesh is the same as that of Behrens *et al.*<sup>2</sup> The errors shown are only the statistical error. The systematic errors due to the scattering corrections and to the normalization are estimated to be about 1.5%.

Comparisons with the data of LLL,<sup>2</sup> Harwell,<sup>4</sup> Karlsruhe,<sup>5</sup> and ANL<sup>3</sup> are shown in Fig. 1 and 2. In Fig. 3 we show a comparison between our data and those of Behrens *et al.*<sup>2</sup> in the neutron energy region from 2 to 13 MeV.

Up to 7 MeV our data and those of LLL<sup>2</sup> and ANL<sup>3</sup> are consistent, but higher than those of Harwell and those of Karlsruhe. Above 12 MeV our data and those of LLL, Harwell and Karlsruhe are all consistent. If the various data sets are renormalized to a common value at 2.5 MeV, the agreement below 7 MeV is improved, but the agreement at high energies is destroyed, as must be accepted on account of the differences in shape between the various sets.

A small systematic difference between our data and those of LLL,<sup>2</sup> illustrated in Fig. 3, may be interpreted as a difference in the energy scale of the two measurements; but it may just as well be interpreted as an inconsistency in shape. The possible difference in energy scale should be further investigated by a direct comparison of the data showing the transmission through the carbon filters. Plots for such a study are being prepared.

## CONCLUSIONS

Below 7 MeV our data agree well with those of LLL<sup>2</sup> and of ANL.<sup>3</sup> Above 7 MeV it is in between those two data sets.

Our data are presently normalized at 2.5 MeV but will shortly be put on an absolute basis.

A very careful energy calibration was performed through the five carbon resonances which allow an accurate determination of the initial delay of the time-of-flight scale. The measurement extends over a wide energy range; in particular the identification of the subthreshold resonance at 721 eV allows a precise check of the flight path length.

## ACKNOWLEDGEMENT

The authors are very indebted to F. Gillespie for providing the Fission Chamber and to J. Behrens for many helpful discussions and for his providing his data as well as data from other sources.

## REFERENCES

1. F. C. DIFILIPPO, "SUR, A Program to Generate Error Covariance Files," ORNL-TM-5223 (1976). (The document contains a complete list of references on the measurements of the  $^{238}\text{U}$  fission cross section.)

2. J. W. BEHRENS, G. W. CARLSON, and R. W. BAUER, "Neutron Induced Fission Cross Sections of  $^{233}\text{U}$ ,  $^{234}\text{U}$ ,  $^{238}\text{U}$ , and  $^{235}\text{U}$  with Respect to  $^{235}\text{U}$ ," Nuclear Cross Sections and Technology, Proceeding of a Conference, Washington, D. C., March 3-7, 1975. NBS Special Publication 425(1975) Vol II p. 591. Also UCRL-76219 (1975) and private communication.
3. J. W. MEADOWS, Nucl. Sci. and Eng. 49, 310 (1972) and Nucl Sci. and Eng. 58, 255 (1975).
4. M. S. COATES, D. B. GAYTHER, and N. J. PATTENDEN. NBS Special Publication 425 (op cit in Ref. 2) Vol II p. 568 (1975).
5. We are indebted to J. W. Behrens for KFK data obtained by private communication from S. Cierjacks (1976).
6. W. P. POENITZ, letter to the participants of the CSEWG Task Force Meeting (March 16, 1976).

TABLE I

## Parameters of the Fission Chamber

	$^{238}\text{U}$ Section	$^{235}\text{U}$ Section
Mass (grams)	4.713 <sup>a</sup>	.650
Number of Plates	30 <sup>b</sup>	5 <sup>c</sup>
Plate Diameter (cm)	10.16	10.16
Plate Thickness (mm)	.33	.127
Coating (mg/cm <sup>2</sup> )	1.0	1.0
Gas Pressure (at) <sup>d,e</sup>	2.0	2.0
Distance Between Plates (mm)	3.175	3.175

<sup>a</sup> Isotopic purity: Less than 2 ppm in isotopes U other than  $^{238}\text{U}$ .

<sup>b</sup> 28 of the aluminum plates have coatings on both sides.

<sup>c</sup> 3 of the aluminum plates have coatings on both sides.

<sup>d</sup> The gas is a mixture of 90% A and 10%  $\text{CO}_2$ .

<sup>e</sup> There are two "blank" aluminum plates between the  $^{238}\text{U}$  and  $^{235}\text{U}$  sections. The magnesium metal chamber walls are 1.575 mm thick.

TABLE II

## Experimental Parameter

Power = 10 Kw    Repetition Rate = 800 pps    Pulse Width = 5 nsec  
 Overlap Filter<sup>a</sup> 83 g of B<sup>10</sup> ( $\sim 0.41$  g/au<sup>2</sup>)

## Channel Structure for the Time-of-Flight Measurements

Number of Channels	Channel Width (nsec)	Energy Range (keV)
4573	2	$\infty$ - 100.20
13615	8	100.20 - .588
3173	128	.588 - .030

<sup>a</sup> This filter has a transmission of 0.25% at E = 5.3 eV.

TABLE III

Resolution for This Experiment

E MeV	Res MeV	Res/E %
2	.0047	.23
3	.0083	.28
4	.0127	.32
5	.0176	.35
6	.0231	.38
7	.0296	.42
8	.0347	.43
9	.0420	.47
10	.0491	.49
20	.136	.68

TABLE IV

Resonances Used in the Determination of the  
Measurement's Energy Scale

---

1.	C	
	7.758 MeV	
	6.293 MeV	Values obtained from ENDF/B-IV
	5.366 MeV	and private communication from
	4.260 MeV	F. G. Perey (1976).
	2.077 MeV	
2.	Al	
	5.903 keV	ENDF/B-IV
3.	$^{235}\text{U}$	
	56.5 eV	ENDF/B-IV
	35.2 eV	ENDF/B-IV
4.	$^{238}\text{U}$	
	721 eV	ENDF/B-IV

---

TABLE V

 $^{238}\text{U}$  to  $^{235}\text{U}$  Fission Cross Section Ratio

LOW ENERGY (MEV)	CENTER ENERGY (MEV)	RATIO	ERROR %
2.30640 01	2.38290 01	7.34970-01	1.38930 00
2.16740 01	2.23690 01	7.45860-01	1.32600 00
2.04070 01	2.10410 01	7.23580-01	1.20090 00
1.92490 01	1.98280 01	6.91510-01	1.23460 00
1.81880 01	1.87190 01	6.52740-01	1.18440 00
1.72130 01	1.77010 01	6.16250-01	1.12280 00
1.63150 01	1.67640 01	6.09490-01	1.01120 00
1.54860 01	1.59010 01	5.95860-01	1.01790 00
1.47190 01	1.51030 01	5.73740-01	9.86550-01
1.40080 01	1.43640 01	5.50650-01	9.64010-01
1.33480 01	1.36780 01	5.33040-01	9.51730-01
1.27340 01	1.30410 01	5.30800-01	8.97220-01
1.21610 01	1.24480 01	5.39810-01	9.27970-01
1.16260 01	1.18940 01	5.59740-01	9.00340-01
1.11260 01	1.13760 01	5.85020-01	8.60280-01
1.06580 01	1.08920 01	5.78080-01	7.78470-01
1.02190 01	1.04390 01	5.72230-01	7.78970-01
9.80670 00	1.00130 01	5.69690-01	7.42510-01
9.41880 00	9.61270 00	5.73900-01	7.07550-01
9.05370 00	9.23620 00	5.76050-01	6.34760-01
8.70950 00	8.88160 00	5.70800-01	6.35660-01
8.38460 00	8.54700 00	5.63870-01	6.12010-01
8.07760 00	8.23110 00	5.71640-01	5.89280-01
7.78730 00	7.93250 00	5.68750-01	5.36980-01
7.51240 00	7.64990 00	5.72820-01	5.53670-01
7.25180 00	7.38210 00	5.97130-01	5.50810-01
7.00470 00	7.12830 00	6.06480-01	5.48350-01
6.77000 00	6.88740 00	6.19370-01	5.50230-01
6.54690 00	6.65850 00	6.26980-01	5.38440-01
6.33470 00	6.44080 00	6.09690-01	5.97100-01
6.13270 00	6.23370 00	5.90280-01	6.26540-01
5.94020 00	6.03650 00	5.62520-01	6.58680-01
5.75670 00	5.84850 00	5.55450-01	6.52690-01
5.58160 00	5.66920 00	5.29120-01	7.06640-01
5.41440 00	5.49800 00	5.28390-01	7.15050-01
5.25460 00	5.33450 00	5.18720-01	7.21060-01
5.10180 00	5.17820 00	5.16860-01	6.85090-01
4.95560 00	5.02870 00	5.10910-01	7.21160-01
4.81560 00	4.88560 00	5.10180-01	7.18040-01
4.68140 00	4.74850 00	5.01880-01	7.17970-01
4.55280 00	4.61710 00	4.99150-01	6.87950-01
4.42950 00	4.49120 00	5.00480-01	7.20870-01
4.31100 00	4.37030 00	4.97300-01	7.28430-01
4.19730 00	4.25420 00	4.88910-01	7.16140-01
4.08810 00	4.14270 00	4.86820-01	7.16150-01
3.98300 00	4.03560 00	4.90340-01	6.80460-01
3.88200 00	3.93250 00	4.86110-01	7.16160-01
3.78480 00	3.83340 00	4.76520-01	7.10700-01
3.69120 00	3.73800 00	4.73200-01	7.16220-01
3.60100 00	3.64610 00	4.74290-01	6.73050-01
3.51410 00	3.55760 00	4.66850-01	7.06020-01
3.43030 00	3.47220 00	4.59930-01	7.00570-01
3.34950 00	3.38990 00	4.49870-01	6.99800-01
3.27150 00	3.31050 00	4.45600-01	6.63040-01
3.19620 00	3.23350 00	4.38340-01	6.90640-01
3.12340 00	3.15980 00	4.30610-01	6.77390-01

TABLE V (Contd.)

 $^{238}\text{U}$  to  $^{235}\text{U}$  Fission Cross Section Ratio

LOW ENERGY (MEV)	CENTER ENERGY (MEV)	RATIO	ERROR %
3.05320 00	3.08830 00	4.36290-01	6.73950-01
2.98520 00	3.01920 00	4.27710-01	6.39450-01
<del>2.91960 00</del>	<del>2.95240 00</del>	<del>4.22780-01</del>	<del>6.76630-01</del>
2.85600 00	2.88780 00	4.29750-01	6.64510-01
2.79460 00	2.82530 00	4.29610-01	6.48230-01
<del>2.73510 00</del>	<del>2.76490 00</del>	<del>4.30670-01</del>	<del>6.50640-01</del>
2.67740 00	2.70630 00	4.33140-01	5.96460-01
2.62160 00	2.64950 00	4.32420-01	6.18940-01
2.56750 00	2.59460 00	4.33580-01	6.04990-01
<del>2.51510 00</del>	<del>2.54130 00</del>	<del>4.31230-01</del>	<del>5.94980-01</del>
2.46430 00	2.48970 00	4.33280-01	5.60110-01
2.41490 00	2.43960 00	4.31970-01	5.72540-01
2.36710 00	2.39100 00	4.29890-01	5.72460-01
<del>2.32070 00</del>	<del>2.34390 00</del>	<del>4.29710-01</del>	<del>5.62620-01</del>
2.27560 00	2.29820 00	4.30950-01	5.33060-01
2.23180 00	2.25370 00	4.34820-01	5.51770-01
2.18930 00	2.21060 00	4.33090-01	5.39890-01
2.14800 00	2.16870 00	4.32430-01	5.38270-01
2.10780 00	2.12790 00	4.30880-01	5.32490-01
2.06880 00	2.08830 00	4.27820-01	5.04980-01
2.03080 00	2.04980 00	4.16710-01	5.35380-01

ORNL-DWG 76-10370

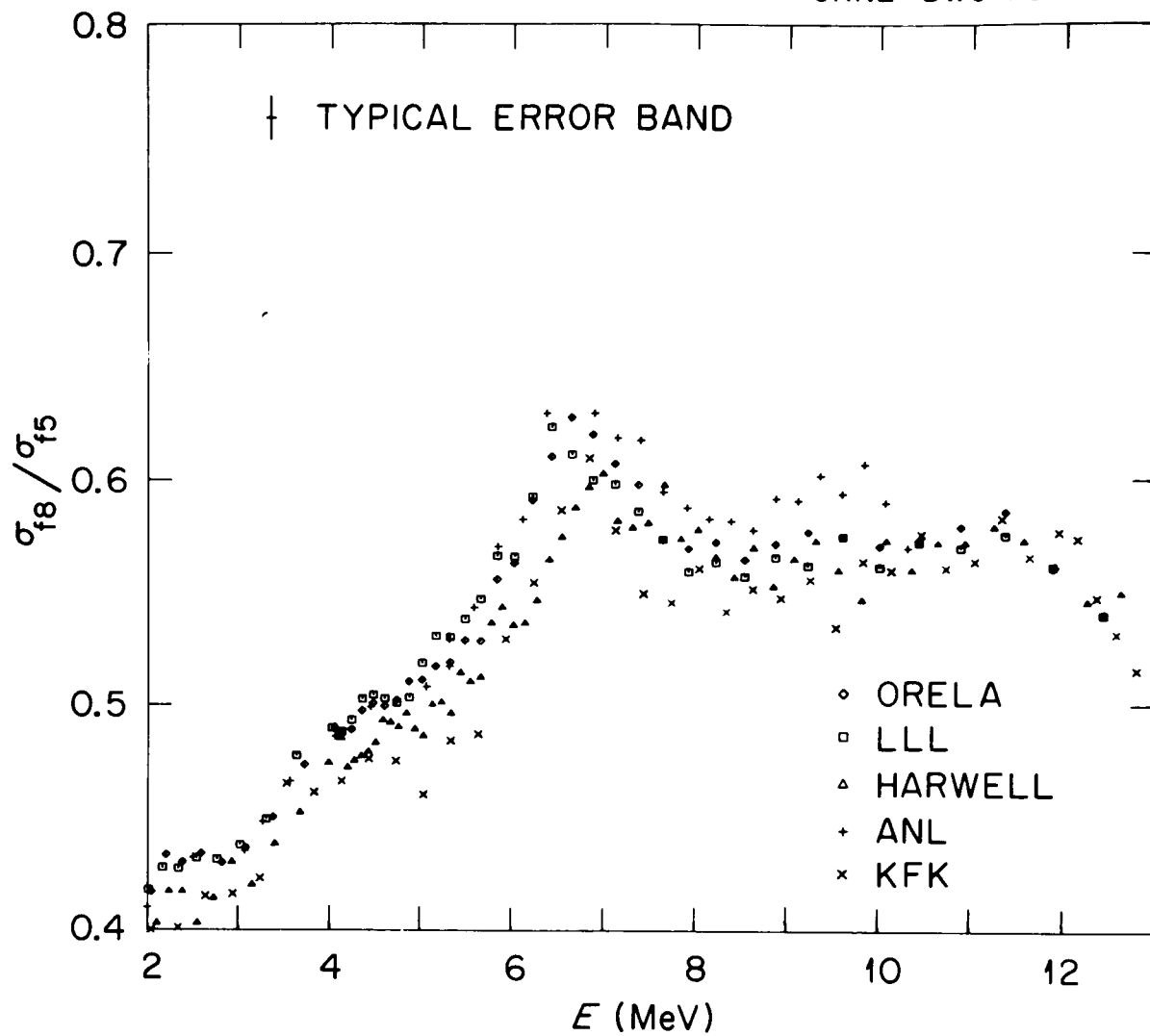


Fig. 1. The Fission Cross Section Ratio of  $^{238}\text{U}$  to  $^{235}\text{U}$  from 2 to 13 MeV.

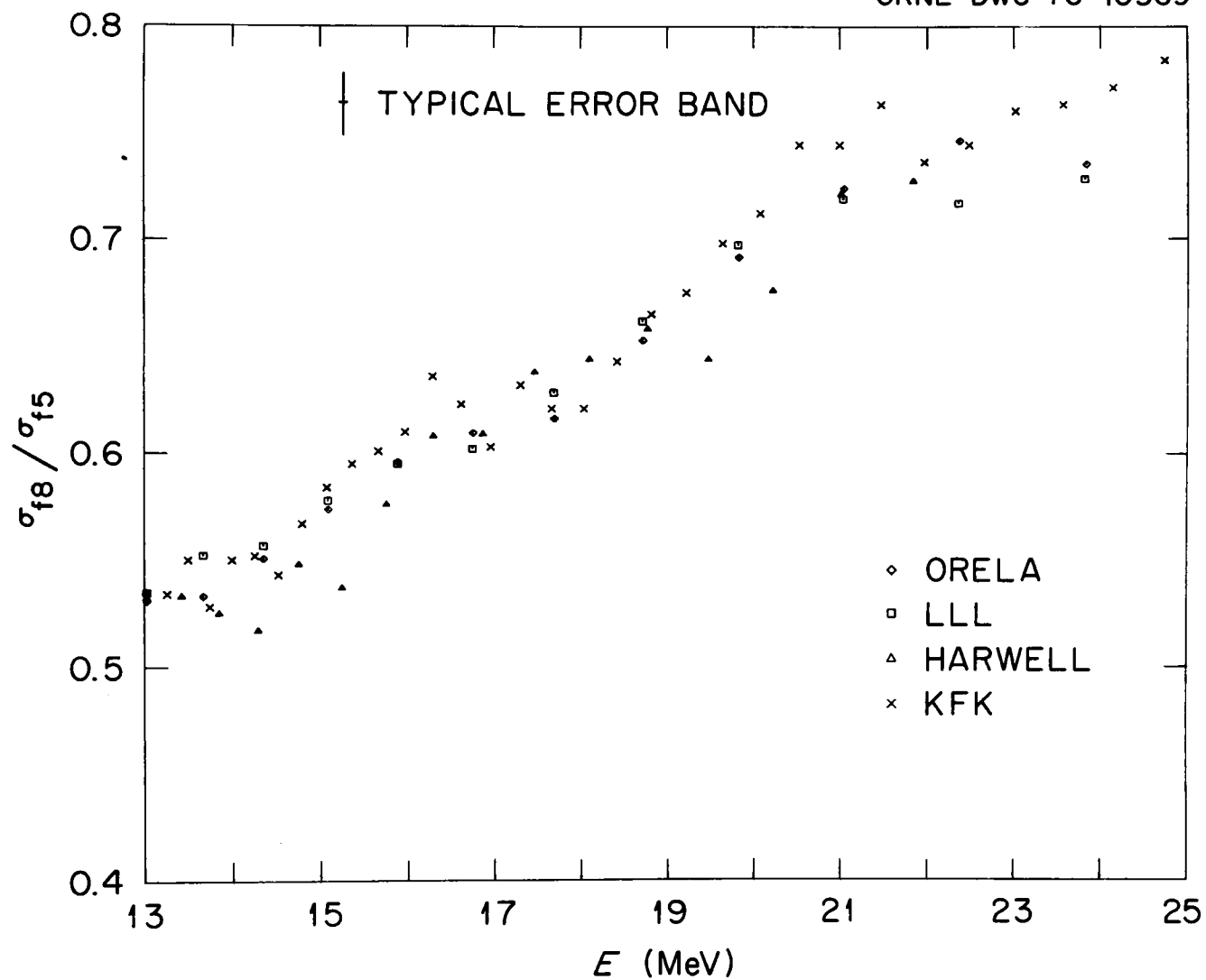


Fig. 2. The Fission Cross Section Ratio of  $^{238}\text{U}$  to  $^{235}\text{U}$  from 13 to 25 MeV.

ORNL-DWG 76-10368

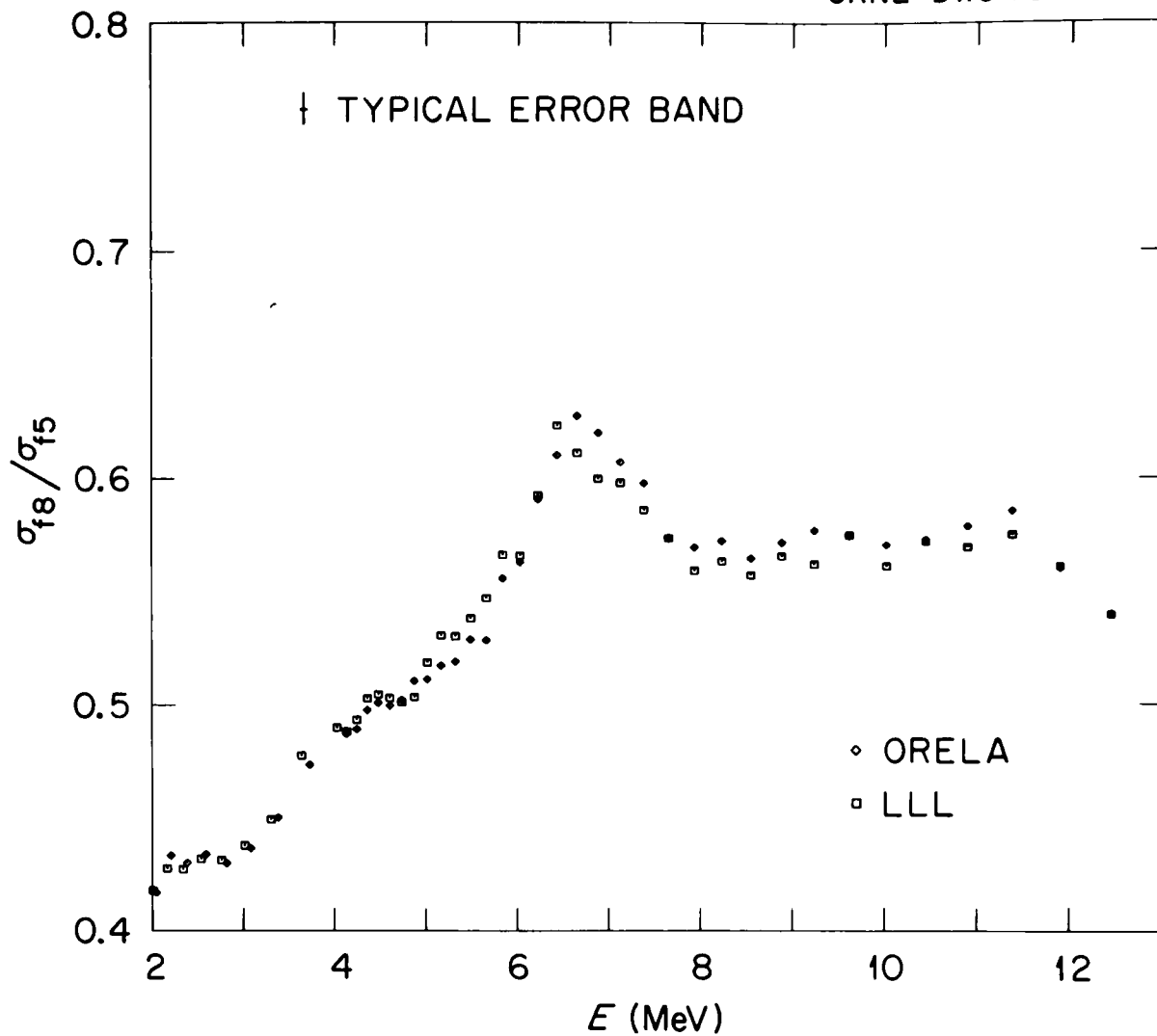


Fig. 3. Comparison of Present Results with Measurements by Behrens et al. (Ref. 2)

## DISCUSSIONS

M. Moore Did you say which energy scale you agree with?

R. Peelle I did not. Unfortunately the data here goes only down to 2 MeV. I do not know at present why values at lower energy were not included--they exist.

W. Poenitz This may have been a misunderstanding insofar as subthreshold fission was excluded from the meeting. Still, 2 MeV is too high for a cut-off.

# FISSION CROSS SECTION RATIO MEASUREMENT OF $^{238}\text{U}$ TO $^{235}\text{U}$ FOR NEUTRONS WITH ENERGIES BETWEEN 4.7 AND 8.9 MEV

C. Nordborg

Tandem Accelerator Laboratory  
S-751 21 Uppsala, Sweden

H. Condé and L.G. Strömberg  
National Defense Research Institute  
S-104 50 Stockholm, Sweden

## ABSTRACT

The ratio between the fission cross section for  $^{238}\text{U}$  and  $^{235}\text{U}$  has been measured with a back-to-back fission chamber for incident neutrons between 4.7 and 8.9 MeV. The obtained data is in fair agreement with those of other recent experiments although the overall spread of data points from these experiments is very large.

## EXPERIMENTAL DETAILS

The experiment was performed at the Uppsala High Voltage EN-type tandem accelerator which is equipped with a pulsed duoplasmatron ion source. The klystron bunching was operated to give pulses with a width of around 3 ns. As a neutron source was used the  $^3\text{H}(p,n)^3\text{He}$  reaction, and the tritium gas was contained in a cell, 26 mm long, diam. 10 mm, at a pressure of about 1.5 atm. The gas cell is manufactured of brass lined with gold with an entrance foil and a beam stop consisting of highly enriched  $^{58}\text{Ni}$  to reduce the background. The fission chamber used was of the back-to-back type with three pairs of fission foils arranged according to Fig. 1, to make possible the use of more fissile material to reduce the time needed to acquire sufficient statistics. The chamber housing was made of aluminum (10 cm in length, diam. 5 cm) and filled with methane gas to a pressure of 1 atm. To avoid the influence of  $\alpha$ -background and thermal neutrons the detector was operated in a time-of-flight mode with a time resolution of the order of 5-7 ns (Fig. 2).

The detector was situated at  $+20^\circ$  relative to the incoming beam at a distance of 20-30 cm from the target. A plastic scintillator detector was used at  $-20^\circ$  to monitor the neutron spectrum incident on the fission chamber by time-of-flight. The monitor was well collimated to accept only neutrons emerging from the neutron target. With the  $^3\text{H}(p,n)$  source one gets a very clean monoenergetic spectrum of neutrons (Fig. 3),

although the gamma background is fairly intensive partly because of the Ni beam stop. The energy spread for the neutrons incident on the fission chamber is of the order of 50 keV when account is taken for contributions from the gas cell as well as the angle acceptance of the fission detector.

The fissile material was deposited on 0.1 mm Al-foils, for  $^{238}\text{U}$  in the form of natural uranium oxide [1] and for  $^{235}\text{U}$  in the form of  $^{235}\text{UF}_4$  [2]. For both isotopes the deposited area and thickness was 30 mm and 1 mg/cm<sup>2</sup>, respectively. The total amount of material and the isotopic purity was very well documented in the case of the  $^{235}\text{U}$  foils whereas some inconsistencies were obtained in the case of  $^{238}\text{U}$  when comparing the information by the supplier with a measurement of the  $\alpha$ -activity from the foils. Therefore, a relative determination of the  $^{235}\text{U}$  content of the  $^{238}\text{U}$ - and the  $^{235}\text{U}$ -foils was made by using the thermal column at the R20 reactor at Studsvik. Measurements were performed both with and without a fission detector shielding of 2.5 mm Cd, thus obtaining the influence of the potential fast neutron component in the reactor beam, which could give rise to fissions in  $^{238}\text{U}$ . By using the known isotopic composition of the  $^{238}\text{U}$  foils, the relative amount of  $^{238}\text{U}$  to  $^{235}\text{U}$  in the two sets of foils could be determined with an accuracy of better than 1.5 %.

#### DATA HANDLING AND CORRECTIONS

Although the experiment in itself is very straightforward great care has to be maintained in applying the necessary corrections to the obtained data.

##### Low Energy Neutrons

Even though the spectrum of neutrons emitted from the target is very clean a small contribution of low energy neutrons, 1.5-4 MeV, is visible. The exact origin of these is not clearly identified, most probably reactions and scattering in the target assembly. By dividing the monitor neutron spectrum into several energy intervals, thus obtaining the relative contribution for each interval and using earlier published cross section ratios an overall correction factor was obtained, slightly varying with incident neutron energy, of between 1 and 1.5 %.

##### Bias Setting

Using a bias in the linear spectrum (Fig. 4) to cut off the  $\alpha$ -background causes a small loss of fission events which has to be estimated. By extrapolation to zero pulse height this part was calculated to be of the order of 1 % for the  $^{235}\text{U}$  spectrum and 2-3 % for the  $^{238}\text{U}$  spectrum. The same type of correction has also to be applied in the mass determination performed at thermal energies and in the final formula of corrections these two terms tend to cancel each other giving a resulting correction which is estimated to be of negligible importance (< 0.1 %).

### Fragment Angular Distributions and Detector Efficiency

Since the fissile layers used in this experiment are fairly thick ( $\sim 1 \text{ mg/cm}^2$ ) as compared to what is used in other experiments, absorption of fission fragments in the layer and a consequent loss of efficiency of the fission detector might be expected. Furthermore the arrangement of the fission foils is not symmetrical. In a separate experiment [3] angular distributions for the fission fragments were determined for both  $^{235}\text{U}$  and  $^{238}\text{U}$  at four neutron energies within the present region, viz. 5.65, 6.75, 7.75 and 8.75 MeV. These are presented in Figs. 5 and 6. Using the approach by Carlson [4] an estimate of the inefficiency of the detector for  $^{235}\text{U}$  and  $^{238}\text{U}$  fission fragments was determined. As could be expected the correction term is largest where the difference in anisotropy for the angular distributions of fragments from the two nuclei is largest, that is at 6.75 MeV being 0.987. To give typical values of the influence of this correction it could be observed that at 5.65 MeV it amounts to 0.992 and at 8.75 MeV it is 0.991.

### Material Deposited vs Solid Angle

The dimensions of the fission detector are fairly extended in length thus resulting in different solid angles for the three pairs of foils and different incident neutron flux. Furthermore the amount of material deposited on the three foils are not equal and a calculation of their relative contribution has to be performed. This correction is however rather small amounting to about 0.7 %.

### Isotopic Composition

The isotopic purity given for the  $^{235}\text{UF}_4$  foils was 97 %  $^{235}\text{U}$  and that stated for the  $^{238}\text{U}$  foils was 0.7 %  $^{235}\text{U}$ . Corrections for fission events resulting from "impurities" in the foils turned out to be small, between 0.1 and 0.6 %.

### In-Scattering from Chamber Housing

The fission chamber housing consists of Al and due to its relatively large size it might give a contribution to the neutron flux incident on the fission foils by scattering, elastic and inelastic. An estimation of this correction has been made giving a result of about 0.5 %. A more exact calculation using the programme MORSE is in progress.

### Total Correction and Estimated Errors

Taking all the separate corrections into account the total correction to be applied to the obtained data was 3 %. The error in the data originates mainly from statistics and the uncertainty in the amount of deposited masses of fissile material. The statistical error for the data points are 2-3 % and the contribution to the absolute error from mass determination and low energy neutron flux calculation is 1.3 and 1 % respectively.

## RESULTS

The corrected data are shown in Fig. 7 (in numerical form in Table I) together with the results of other recent measurements [5, 6, 7, 8]. As can be seen the spread in the data points is far more than the individual errors assigned, getting worse with higher neutron energy. Of these measurements two were made using van de Graaff accelerators, the present experiment and that of Meadows [5], while two have used linacs [6, 7] and one a synchrocyclotron [8] for the neutron production indicating a difference in energy spread of the incoming neutrons. Below 6.5 MeV there is no systematic trend in the data while at higher energies the ones obtained with van de Graaffs tend to be higher. Since the data in the region between 5 and 6.5 MeV is very sensitive to the energy determination an investigation of the calibration of the analysing magnet was performed in the present experiment resulting in a correction of the energies with between 50 keV at 5 MeV neutron energy and 100 keV at 9 MeV.

In all the measurements there seems to be a slight indication of structure between 5.9 and 6 MeV. From the present data no definite conclusion can be drawn, however. The energy region between 5 and 7 MeV will be subject to a more detailed study with improved energy and time resolution and new set of  $^{238}\text{U}$  foils.

## REFERENCES

1. Supplied by the Atomic Energy Company, Studsvik, Sweden.
2. Supplied by BCMN, Geel, Belgium.
3. C. NORDBORG, H. CONDE and L.G. STRÖMBERG, To be published.
4. G.W. CARLSON, "The Effect of Fragment Anisotropy on Fission Chamber Efficiency," Nucl. Instrum. Methods, 119, 97 (1974).
5. J.W. MEADOWS, Argonne National Laboratory, Private Communication (1975).
6. J.W. BEHRENS, G.W. CARLSON and R.W. BAUER, "Neutron-Induced Fission Cross-Sections of  $^{233}\text{U}$ ,  $^{234}\text{U}$ ,  $^{236}\text{U}$  and  $^{238}\text{U}$  with Respect to  $^{235}\text{U}$ ," Proc. 4<sup>th</sup> Conf. on Nucl. Cross-Sections and Technology, Washington (1975), p. 591.
7. S. CIERJACKS, Kernforschungszentrum, Karlsruhe, Private Communication (1976).
8. M.S. COATES, D.B. GAYTHER and N.J. PATTENDEN, "A Measurement of the  $^{238}\text{U}/^{235}\text{U}$  Fission Cross-Section Ratio," Proc. 4<sup>th</sup> Conf. on Nucl. Cross-Sections and Technology, Washington (1975), p. 568.

TABLE I

 $^{238}\text{U}/^{235}\text{U}$  Fission Cross Section Ratios

Neutron Energy (MeV)	Ratio	Statistical Error
4.67	0.503	$\pm 0.014$
4.96	0.510	0.014
5.26	0.499	0.013
5.55	0.528	0.014
5.73	0.548	0.010
5.85	0.575	0.015
6.02	0.561	0.015
6.14	0.590	0.017
6.31	0.597	0.015
6.43	0.600	0.017
6.60	0.621	0.017
6.73	0.632	0.016
6.89	0.611	0.016
7.02	0.606	0.015
7.18	0.597	0.014
7.31	0.598	0.015
7.60	0.581	0.015
7.76	0.571	0.015
7.89	0.575	0.016
8.04	0.570	0.014
8.33	0.577	0.014
8.37	0.579	0.015
8.85	0.587	0.014

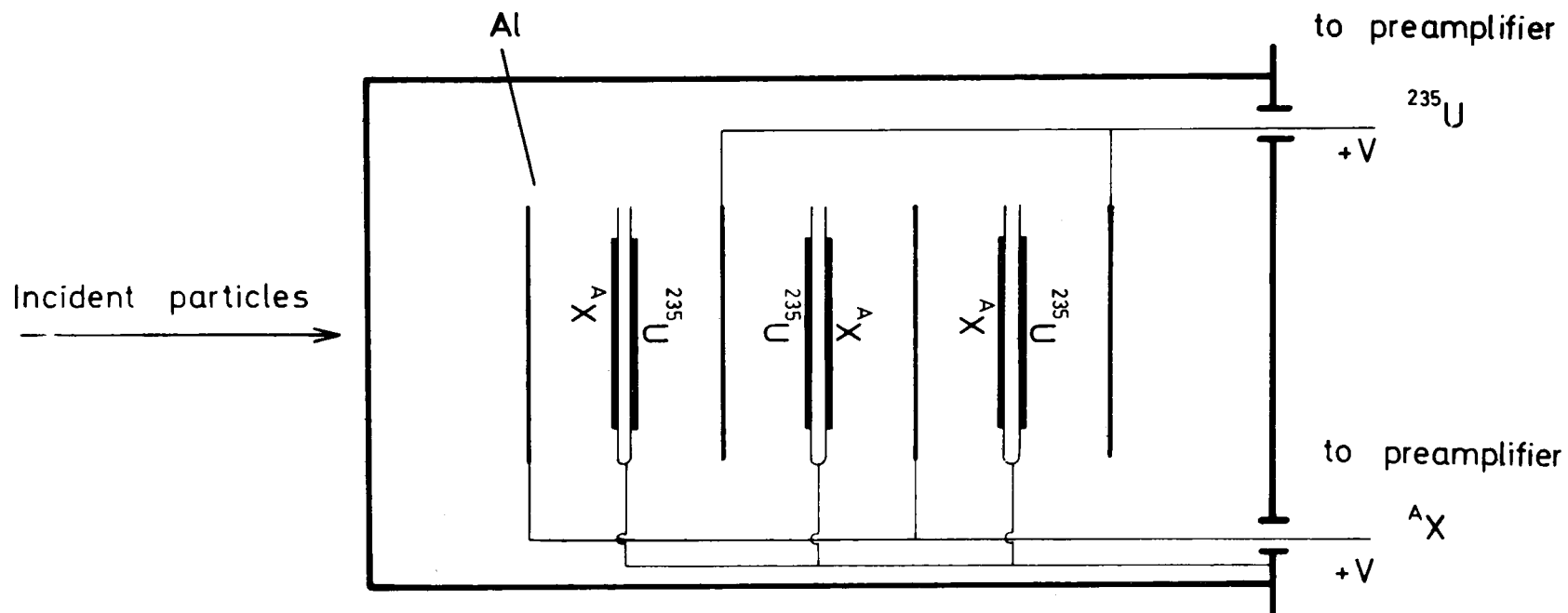


Figure 1. Schematic figure of fission chamber arrangement.

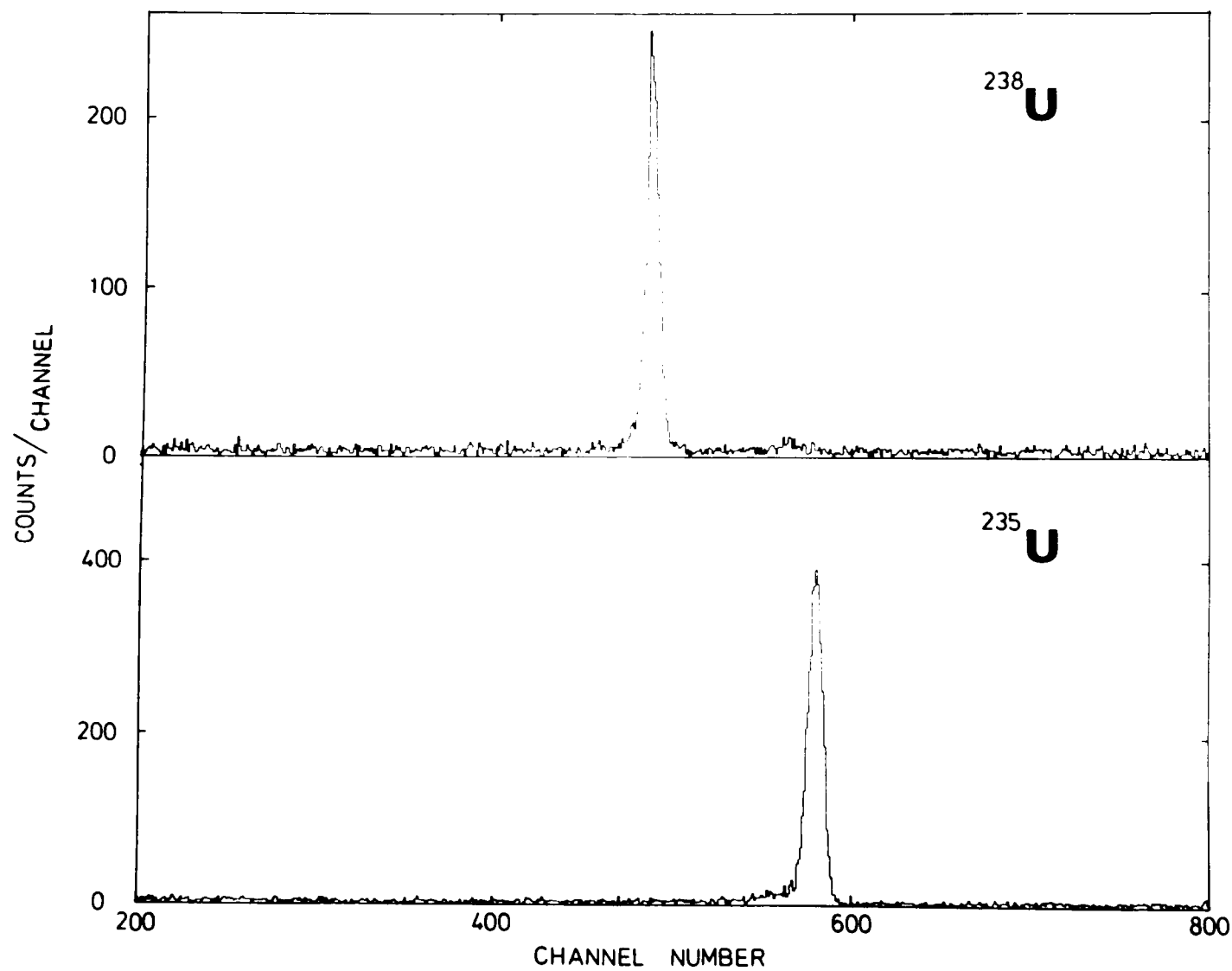


Figure 2. Time spectrum from fission chamber for  $^{238}\text{U}$  and  $^{235}\text{U}$ .

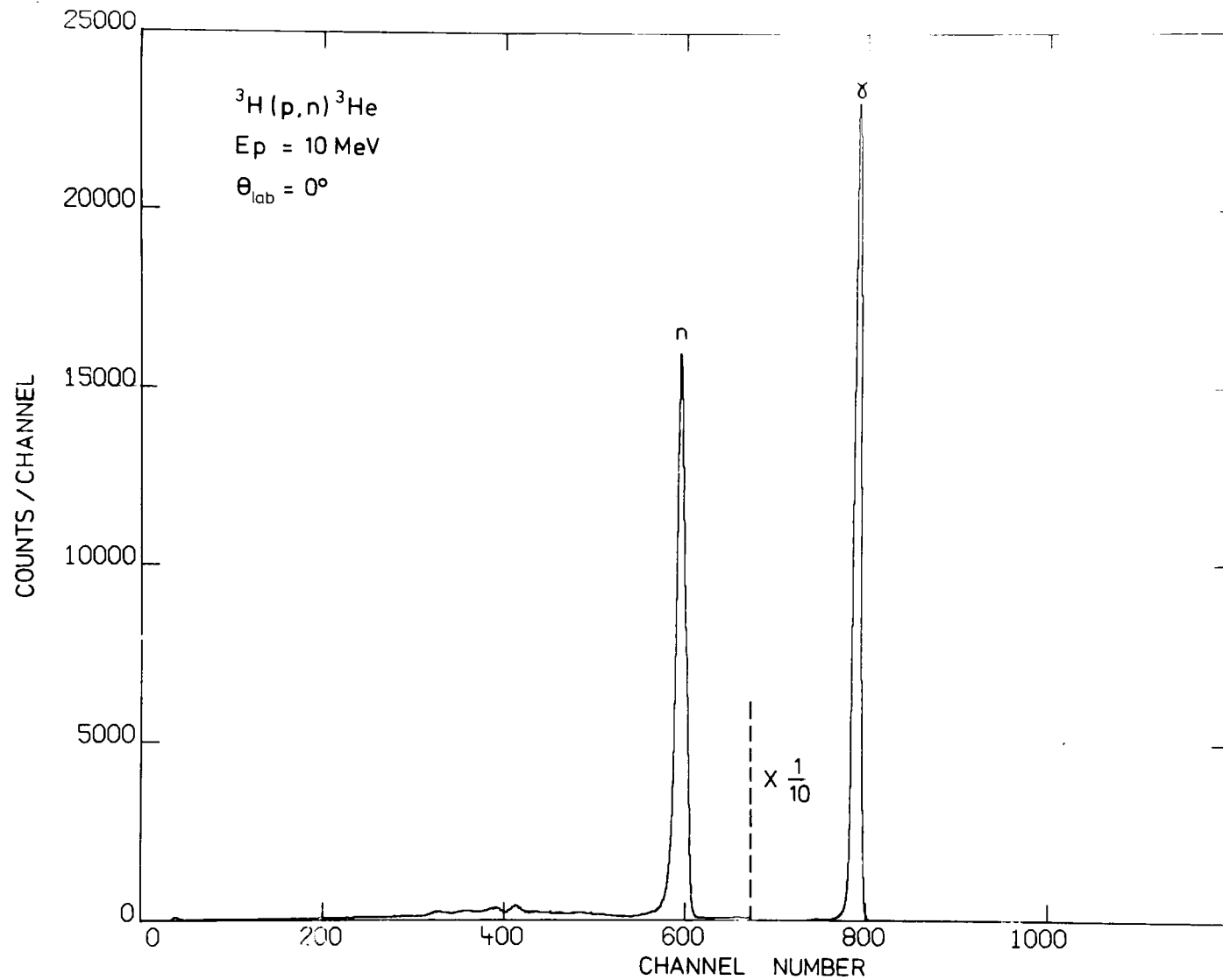


Figure 3. Time-of-flight spectrum of target neutrons obtained with plastic scintillator monitor.

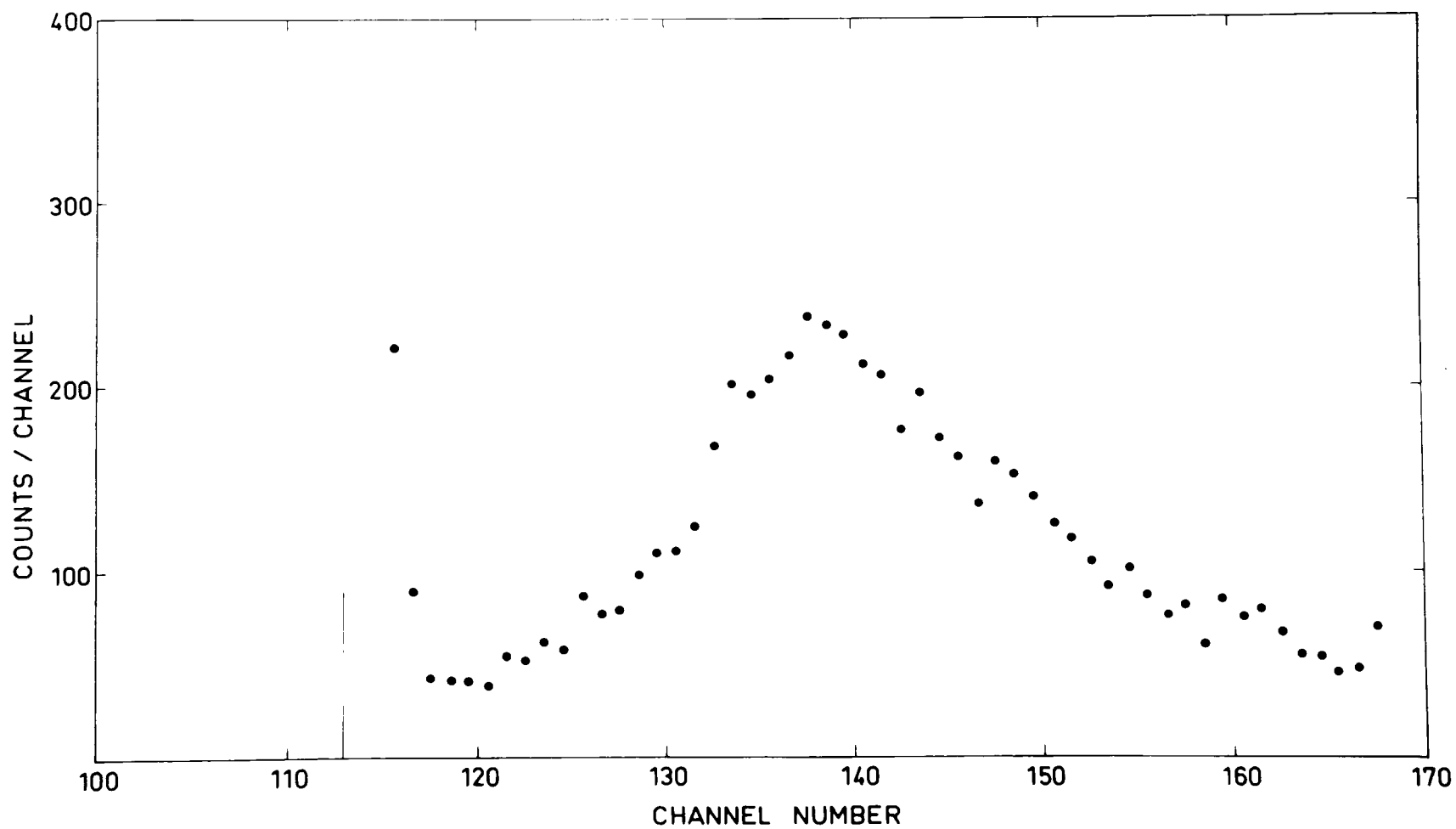


Figure 4. Linear spectrum obtained from fission chamber for  $^{235}\text{U}$ . Vertical line indicates discriminator level.

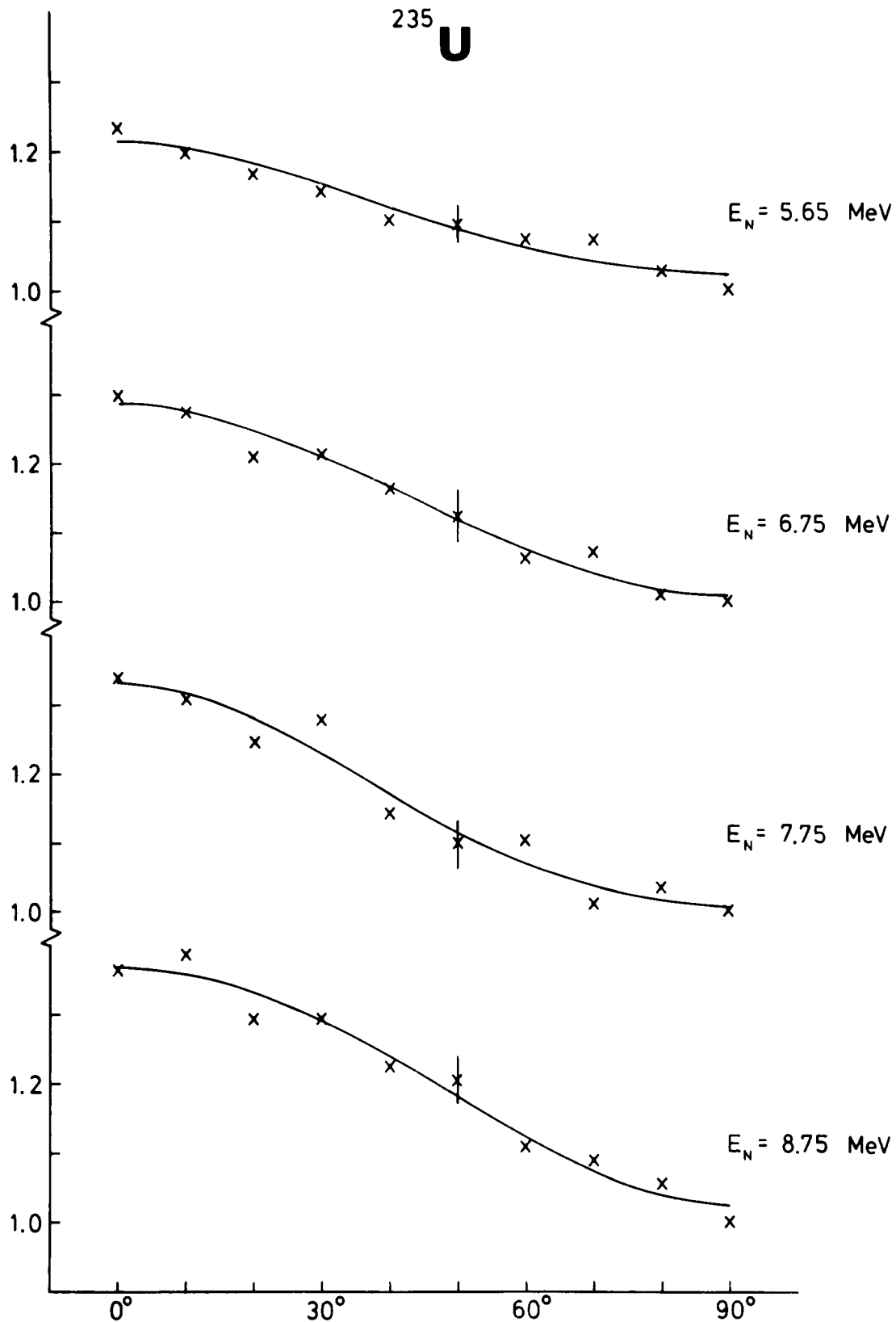
<sup>235</sup>**U**

Figure 5. Angular distributions of fission fragments from <sup>235</sup>U.

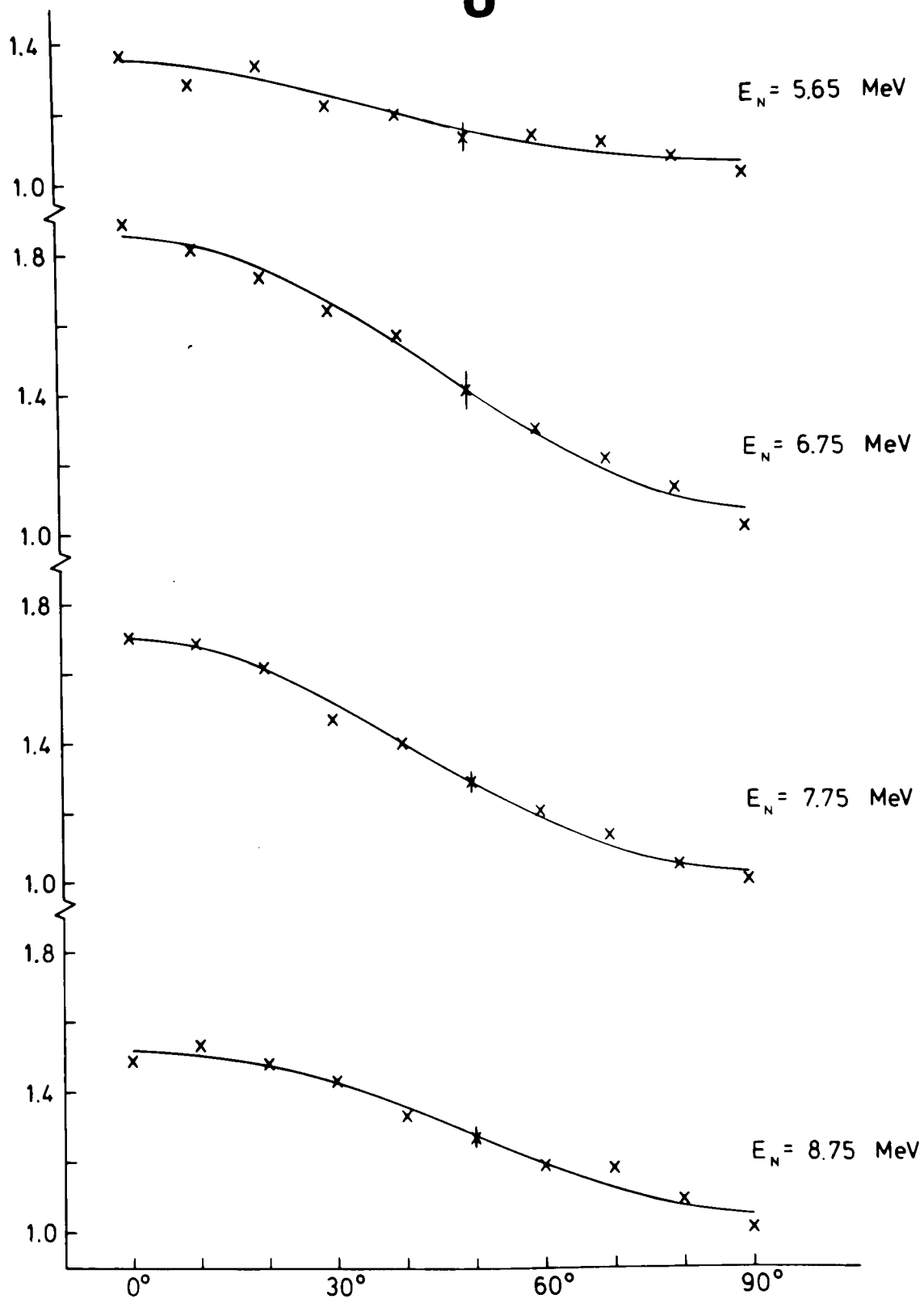
$^{238}\text{U}$ 

Figure 6. Angular distributions of fission fragments from  $^{238}\text{U}$ .

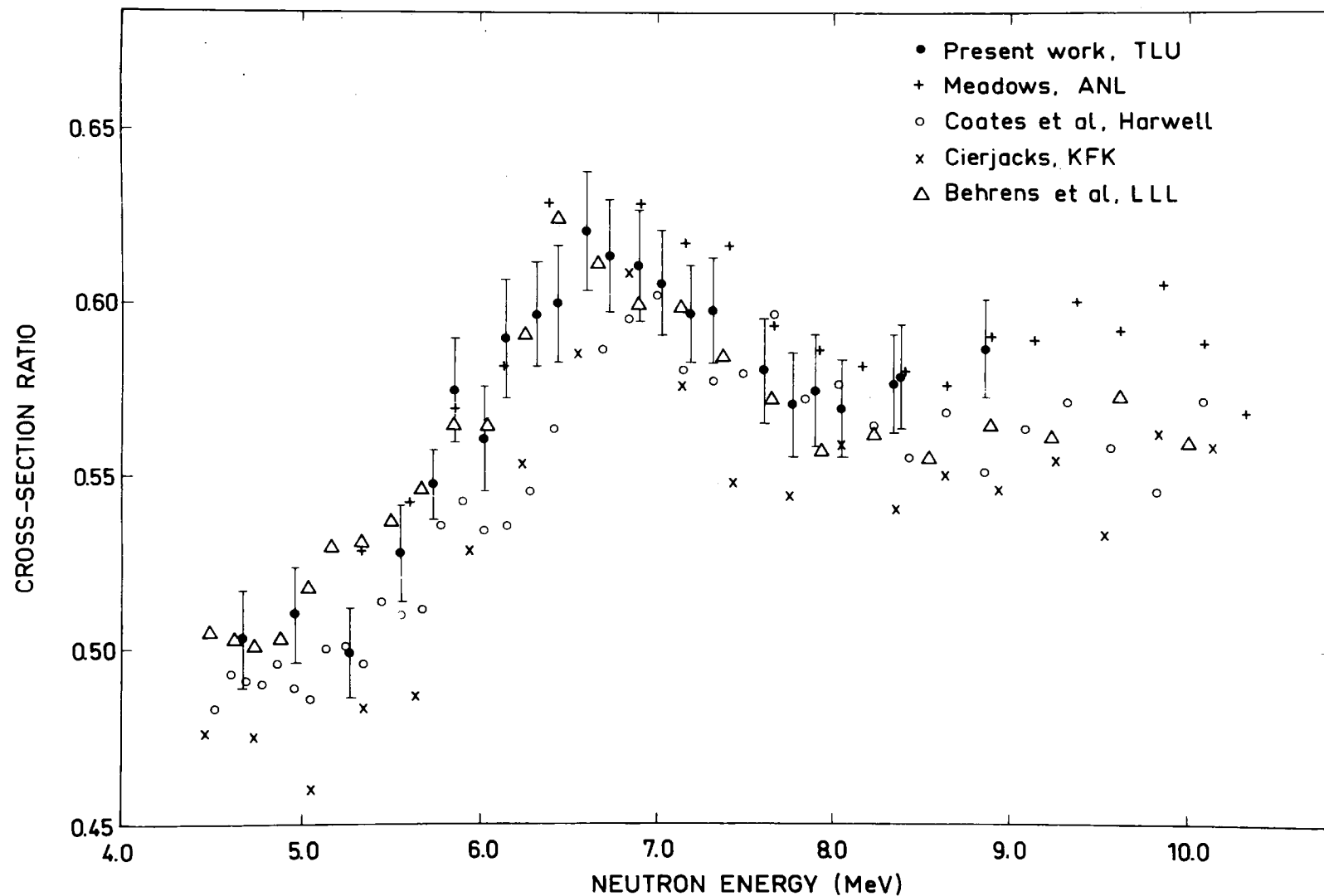


Figure 7. Results of fission cross section ratio measurement in present experiment compared to the results of other recent experiments.

## DISCUSSIONS

C. Bowman It appears the errors were much larger than you should have had in the experiment. Do they include systematic errors?

H. Conde No these were only statistical errors.

S. Cierjacks Did you mention the energy resolution?

H. Conde Yes, it is about 50 keV.

A. Smith If you would neglect your angular anisotropy correction, what would the data look like?

H. Conde There is a figure for this correction in the paper. 1.3% is the largest. It is energy dependent.

A. Smith What would it do at 8 MeV? Would it bring it up or down?

W. Poenitz I will show the energy dependence of this correction later.

H. Conde The correction is largest at the peak (6.4 MeV) and then decreases.

H. Knitter What is the size of the geometrical correction (for different fluxes)?

H. Conde About 0.5%.

S. Cierjacks What is the distance of each foil from the source? You have 6 foils and you are close to the source--so there should be a larger effect.

H. Conde The distance from the source is 30 cm. Between sample packages it is 1 cm. In each package is a pair.

L. Stewart Are your ratios relative or are they absolute?

H. Conde They are absolute.

PART. I      MEASUREMENTS OF  $^{238}\text{U}/^{235}\text{U}$  FISSION CROSS SECTION  
RATIOS IN THE ENERGY RANGE 2 - 7 MeV

M. CANCE, G. GRENIER

*Service de Physique Nucléaire  
Centre d'Etudes de Bruyères-le-Châtel  
B.P. n° 61, 92120 Montrouge, France*

ABSTRACT

Measurements of  $^{238}\text{U}/^{235}\text{U}$  fission cross section ratios have been made with a double  $4\pi$  ionization chamber in the energy range 2 - 7 MeV. A pulsed 4 MeV Van de Graaff accelerator was used with  $\text{T}(\text{p},\text{n})^3\text{He}$  and  $\text{D}(\text{d},\text{n})^3\text{He}$  reactions as neutron sources.

The final values of  $^{238}\text{U}/^{235}\text{U}$  fission cross section ratios are given with 3 % uncertainty.

INTRODUCTION

The large discrepancies between some of the recent experimental data in the energy range 2 - 20 MeV underscore the need for further measurements.

In particular the results of Meadows [1] obtained with a pulsed mono-energetic neutron source differ very much from other data obtained with a continuous neutron spectrum as source. Thus, it was of interest to do new measurements with the first technique.

EXPERIMENTAL TECHNIQUE

1°) Fission Detector

A double  $4\pi$  ionization chamber containing a deposit of  $^{235}\text{U}$  and one of  $^{238}\text{U}$  on vycor foils was used.

This fission detector will be described in part II in session II.

2°) Neutron source

Neutrons in the energy range 2 - 7 MeV were produced by the  $\text{T}(\text{p},\text{n})^3\text{He}$  and  $\text{D}(\text{d},\text{n})^3\text{He}$  reactions using a 4 MeV Van de Graaff accelerator.

Target thicknesses of about 500  $\mu\text{g}/\text{cm}^2$  tritium - titanium on gold backing

were used with the  $T(p,n)^3\text{He}$  reaction.

A deuterium gas target 1 cm long and filled to 2 atm., with a 2  $\mu$  foil of Havar as window, was used in the case of the  $D(d,n)^3\text{He}$  reaction.

The proton or deuteron beam was pulsed to 10 ns width. The repetition rate was 1 MHz.

### 3°) Samples

$\text{UF}_4$  samples fabricated by the B.C.M.N. and described in part II of this paper were used.

### 4°) Experimental Method and Data Acquisition

The time of flight method was used to determine the background due to the alpha activity of the deposit and to fissions induced by low energy neutrons. An accurate background correction was obtained using a biparametric acquisition of pulse height and time pulses.

Background independent of  $T(p,n)^3\text{He}$  neutron source was determined with a titanium target without tritium and found to be negligible.

Deuteron reactions with the materials constituting the gas target and aperture, carbon buildup on the aperture and window, and deuteron implantation in the end of the cell produced lower energy neutrons. Corrections were made by measuring spectra with an empty gas target after each measurement with the target filled.

### 5°) Number of Atoms

The  $^{238}\text{U}/^{235}\text{U}$  fission cross section ratios were based on total number of atoms measured by B.C.M.N. and our Laboratory with  $4\pi$  or low geometry  $\alpha$  counting.

The half lives of isotopes recommended by VANINBROUKX [2] were used.

## CORRECTIONS AND UNCERTAINTIES

- The range of the correction for the time dependent background was 0 - 9 % with an 10 % estimated uncertainty.

- The fission detector was close to the neutron source (about 10 cm) and a correction was made for the angular distribution of the neutron source. Although this correction is small for the  $T(p,n)^3\text{He}$  reaction it increased to about 8 % with the  $D(d,n)^3\text{He}$  reaction at 4 MeV. A 10 % uncertainty was assumed for this correction.

- The correction for fission events due to neutrons scattered elastically and inelastically in the detector structure was evaluated by taking into account the cross sections of the materials used, the angular distribution of

the source reaction and of the scattering cross section, and the effective thickness of the scattering material. A Monte Carlo technique was used in these calculations.

The range of this correction, taking into account the neutrons absorption in the front face of detector, was 0.0 to 0.4 %. The error in the ratios caused by this correction was negligible.

- The error in the ratio of the total number of atoms was obtained from an uncertainty of 1.2 and 2.1 % respectively for  $^{235}\text{U}$  and  $^{238}\text{U}$  deposits.

- The uncertainty on the correction for fission events due to other isotopes of uranium was assumed to be 10 %.

- The errors in the ratios caused by the time independent background and the efficiency detector correction were negligible.

The main uncertainties are listed in Table I with the total uncertainties which are the root - mean - square of all the errors listed.

## RESULTS AND DISCUSSION

The final values of  $^{238}\text{U}/^{235}\text{U}$  fission cross section ratios are given in Table II with 3 % uncertainty.

Our results are compared to data from recent experiments [3,4,5] and to the values of ENDF/B IV in Figs. 1 and 2.

Our values are about 4.5 % lower than that of BEHRENS et al. [3] and the ENDF/B IV values. They are in good agreement with the COATES et al. [4] and CIERJACKS et al. [5] measurements.

## REFERENCES

1. J.W. MEADOWS, "The ratio of the Uranium 238 to Uranium 235 Fission Cross sections from 5.3 to 10.3 MeV". *Nucl. Sc. Eng.*, 58, 255 (1975).
2. R. VANINBROUKX, "The half lives of some long lived actinides A compilation" EUR 5194e C.B.M.N. (1974).
3. J.W. BEHRENS, G.W. CARLSON and R.W. BAUER " $^{238}\text{U}$ :  $^{235}\text{U}$  Fission Cross Section Ratio", UCRL - 76219, Lawrence Livermore Laboratory (1975).
4. M.S. COATES, D.B. GAYTHER and N.J. PATTENDEN "A Measurement of the  $^{238}\text{U}/^{235}\text{U}$  Fission Cross Sections Ratio", Conf. Nuclear Cross Sections and Technology, Washington, DC Mar. 3-7 (1975).
5. S. CIERJACKS, Karlsruhe, Private Communication (1976).

TABLE I

UNCERTAINTIES (%)

EFFECT	$\bar{E}_n \pm \Delta E$ (MeV)								
	7.01	6.50	5.99	5.46	4.90	4.30	3.60	3.15	2.65
	$\pm$ 0.08	$\pm$ 0.07	$\pm$ 0.07	$\pm$ 0.07	$\pm$ 0.08	$\pm$ 0.09	$\pm$ 0.14	$\pm$ 0.05	$\pm$ 0.01
Statistical	0.78	0.78	0.92	0.92	0.78	1	1.08	0.86	0.72
Angular Distribution of Neutron Source	0.8	0.7	0.7	0.5	0.4	0.3	0.2	negligible	
Geometry	0.7	0.7	0.7	0.7	0.7	0.7	0.7	0.7	0.7
Time Independent background	0.6	0.9	0.65	0.1	-	negligible			
Total Number of Atoms	2.4	2.4	2.4	2.4	2.4	2.4	2.4	2.4	2.4
Fissions in other Isotopes	0.25	0.25	0.25	0.25	0.25	0.25	0.25	0.25	0.25
Total Uncertainty of Results	2.8	2.9	2.8	2.7	2.6	2.7	2.7	2.6	2.6

TABLE II

$^{238}\text{U}/^{235}\text{U}$  Fission Cross Section Ratios  
in the Energy Range 2 - 7 MeV

$E_n \pm \Delta E$ (MeV)	7.01 $\pm$ 0.08	6.50 $\pm$ 0.07	5.99 $\pm$ 0.07	5.46 $\pm$ 0.07	4.90 $\pm$ 0.08	4.30 $\pm$ 0.09	3.60 $\pm$ 0.14	3.15 $\pm$ 0.05	2.65 $\pm$ 0.05
$^{238}\text{U}/^{235}\text{U}$	0.589 $\pm$ 0.018	0.592 $\pm$ 0.018	0.548 $\pm$ 0.016	0.510 $\pm$ 0.015	0.487 $\pm$ 0.014	0.482 $\pm$ 0.014	0.443 $\pm$ 0.013	0.416 $\pm$ 0.012	0.410 $\pm$ 0.012

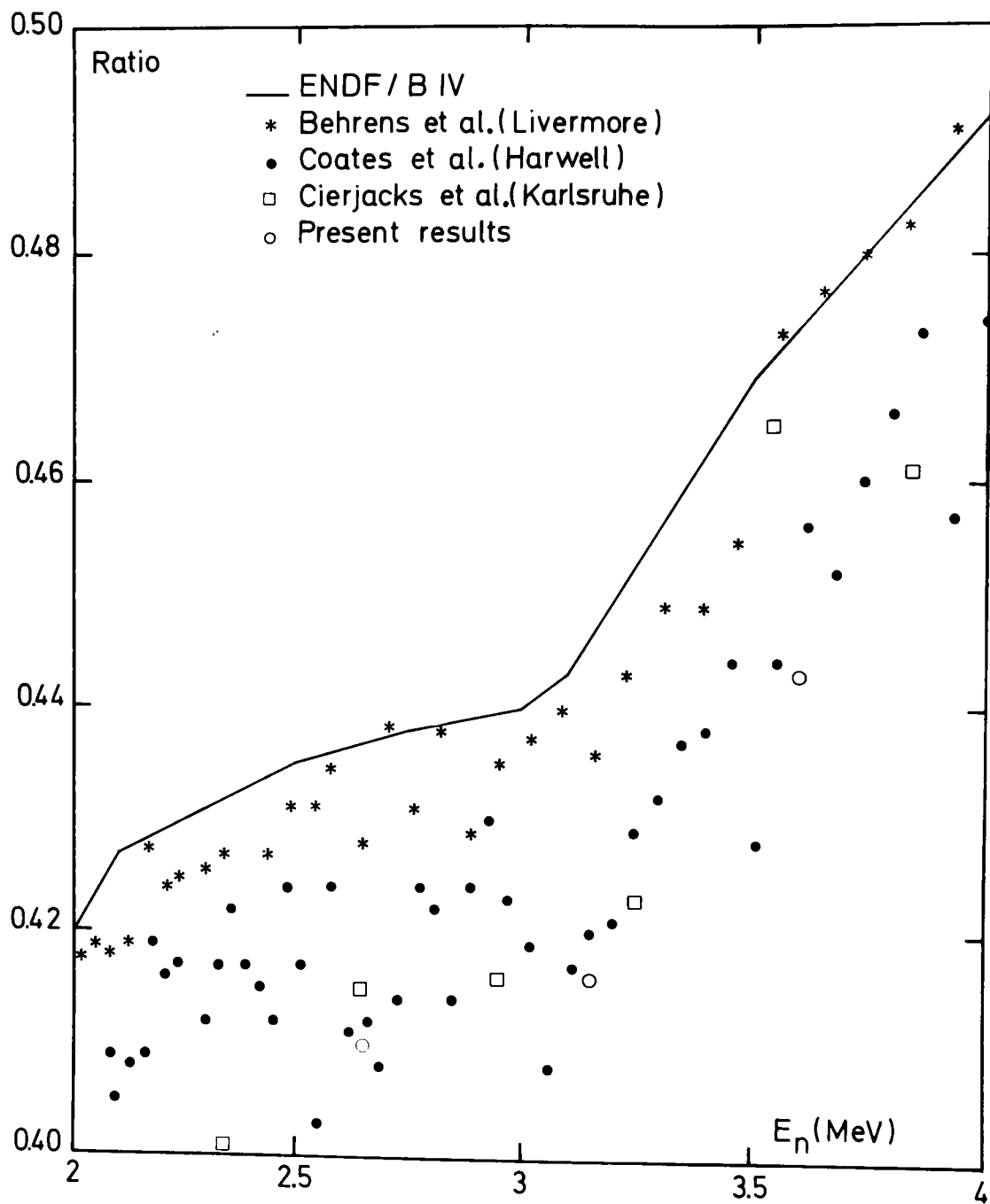


Figure 1. Comparison of recent measurements of  $^{238}\text{U}/^{235}\text{U}$  fission cross section ratio from 2 to 4 MeV.

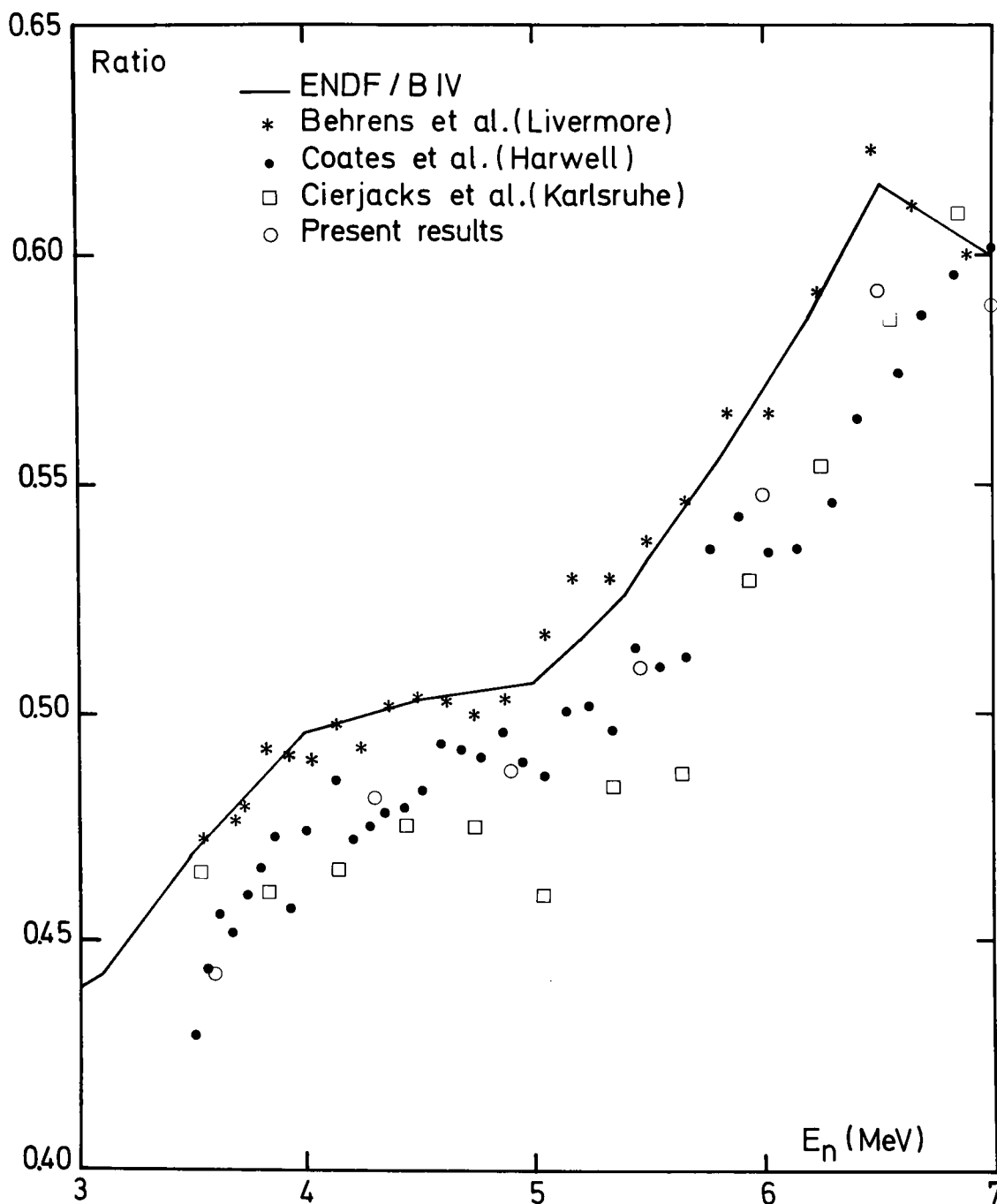


Figure 2. Comparison of recent measurements of  $^{238}\text{U}/^{235}\text{U}$  fission cross section ratio from 3 to 7 MeV.

*DISCUSSIONS*

A. Smith Did you carefully consider the TOF spectrum--did you have a tail on the TOF peak; or has the peak a Gaussian shape?

G. Grenier We observed only a peak.

# THE $^{238}\text{U}/^{235}\text{U}$ FISSION CROSS SECTION RATIO OVER THE ENERGY RANGE 1.2 MeV to 2 MeV

P.A.R. Evans, G.B. Huxtable and G.D. James

UKAEA, Atomic Energy Research Establishment, Harwell, England

## ABSTRACT

The  $^{238}\text{U}/^{235}\text{U}$  fission cross section ratio over the energy range 1.2 MeV to 2 MeV has been determined mainly to establish an accurate energy for the  $^{238}\text{U}$  fission cross section threshold.

## INTRODUCTION

A measurement of the  $^{238}\text{U}/^{235}\text{U}$  fission cross section ratio over the energy range 1.2 MeV to 2 MeV has been made mainly to help resolve an energy discrepancy between the measurement of Coates et al. [1] and the measurements of Behrens et al. [2] and Cierjacks et al. [3]. Recently, Coates et al. [4] have reassessed their method of establishing their energy scale. Their revised results are in better agreement with the curve established by Behrens et al. [3].

The present measurement was carried out on the neutron time-of-flight system of the Harwell synchrocyclotron. Although the experiment was, in a sense, a repeat of that carried out by Coates et al., none of the experimental details is the same except that the same foils and gas scintillation chamber were used. In particular, all factors concerning the determination of neutron energy were different in that a different flight path length and a different time digitizer [5] were used. Also, in the time between the two experiments, the energy scale of the time-of-flight system was carefully assessed [6]. This brief report gives experimental details in sect. 2 and a short account of the way in which the data were treated in sect. 3. The results obtained are presented in sect. 4 and compared with recent measurements.

## EXPERIMENTAL METHOD

In the Harwell synchrocyclotron neutron time-of-flight system, pulses of 140 MeV protons, with 4  $\mu\text{A}$  mean current, 800 Hz repetition rate and 10 ns pulse width (FWHH), strike a tungsten target. Neutrons emerging at  $180^\circ$  to the direction of the proton beam travel along a collimated flight to reach the gas scintillation fission fragment detector placed at 25m from the neutron source. For this experiment there was no water moderator in the neutron beam and the neutron flight path was evacuated over a distance of 14m. To reach the detector the neutrons traverse three mylar windows each 0.013cm thick.

The fission detector was a gas scintillation fission fragment detector through which pure argon flowed continuously. Both fissile materials were deposited to a thickness of  $0.5 \text{ mg cm}^{-2}$  on thin Al backings over a circular area of 7.6 cm diam. The foils were placed back to back at the centre of the chamber and perpendicular to the neutron beam. The chamber was divided optically in the plane of the foils and each half was viewed through quartz windows by two EMI 9816QKB photomultipliers. Pulses from the two tubes viewing the same half of the chamber were added, amplified by an LRS612 amplifier and passed through an LRS623 discriminator to form pulses which were coded by a multi-channel pulse encoder and used to stop the time digitizer [5]. The time digitizer measures the time between a start pulse derived from the synchrocyclotron R.F. modulation and the stop pulse in units of 2.5 ns, the basic channel width. The timing information is then transmitted through CAMAC units for storage on disk by a Honeywell DDP-516 computer. Fission yield spectra for  $^{238}\text{U}$  and  $^{235}\text{U}$  are recorded simultaneously and both spectra show a ' $\gamma$ -flash' peak, caused by the photofission reaction, which, combined with an accurately measured flight path length ( $25.547 \pm 0.005\text{m}$ ), enables the neutron energy at each timing channel to be calculated. A short experimental run with some carbon in the beam was carried out to check the energy determination. The data presented represent an average of two runs in one of which the  $^{235}\text{U}$  foil faced the neutron source and in the other the  $^{238}\text{U}$  foil faced the neutron source. The detector bias was set at about 40 MeV as judged by the single  $\alpha$  pulse height. This level was too low to exclude the observation of (n, $\alpha$ ) reactions from the thin Al windows of the chamber and from the Al foil backing. Consequently the results quoted are confined to below 2 MeV.

#### TREATMENT OF DATA

In the time available to carry out this experiment it was not possible to measure the backgrounds involved. However, an energy dependent background designed to make the  $^{238}\text{U}$  yield equal to zero at 0.2 MeV and 0.4 MeV was subtracted from the data.

No correction was made for the  $^{235}\text{U}$  content of the  $^{238}\text{U}$  foil (0.036%) or for the  $^{238}\text{U}$  content of the  $^{235}\text{U}$  foil (6.06%).

#### RESULTS

The results obtained are shown in fig. 1 by the open triangles. The solid line shown for comparison is derived from the data of Behrens et al. [2]. The circles in this figure show the renormalised data of Coates et al. [4] which have been normalised to .523 at 14 MeV. It will be seen that the energy scale of these three measurements is now in good agreement. The measurement taken with carbon in the beam was of poor statistical quality but was analysed by least squares fits to give curves representing the  $\gamma$ -flash peak and the resonance at 2 MeV. This analysis gives the carbon resonance energy as  $2074 \pm 3 \text{ keV}$ .

#### REFERENCES

1. M.S. COATES, D.B. GAYTHER and N.J. PATTENDEN. Proc. 4th Conf. on Neutron Cross Sections and Technology, Schrack and Bowman (Eds.). NBS Spec. Pub. 425 II 568 (1976).

2. J.W. BEHRENS, G.W. CARLSON and R.W. BAUER. Proc. 4th Conf. on Neutron Cross Sections and Technology. Schrack and Bowman (Eds.). NBS Spec. Pub. 425 II 591 (1976).
3. S. CIERJACKS et al. Unpublished.
4. M.S. COATES - private communication.
5. J.P. ARGYLE, P.E. DOLLEY and G. HUXTABLE. Proc. 2nd ISPRA Nuclear Electronics Symposium. (Euratom, Luxembourg, 1975), EUR 5370e, p.421.
6. G.D. JAMES, D.B. SYME, P.H. BOWEN, P.E. DOLLEY, I.L. WATKINS and M. KING. Report AERE - R7919. (UKAEA, Harwell, 1975).

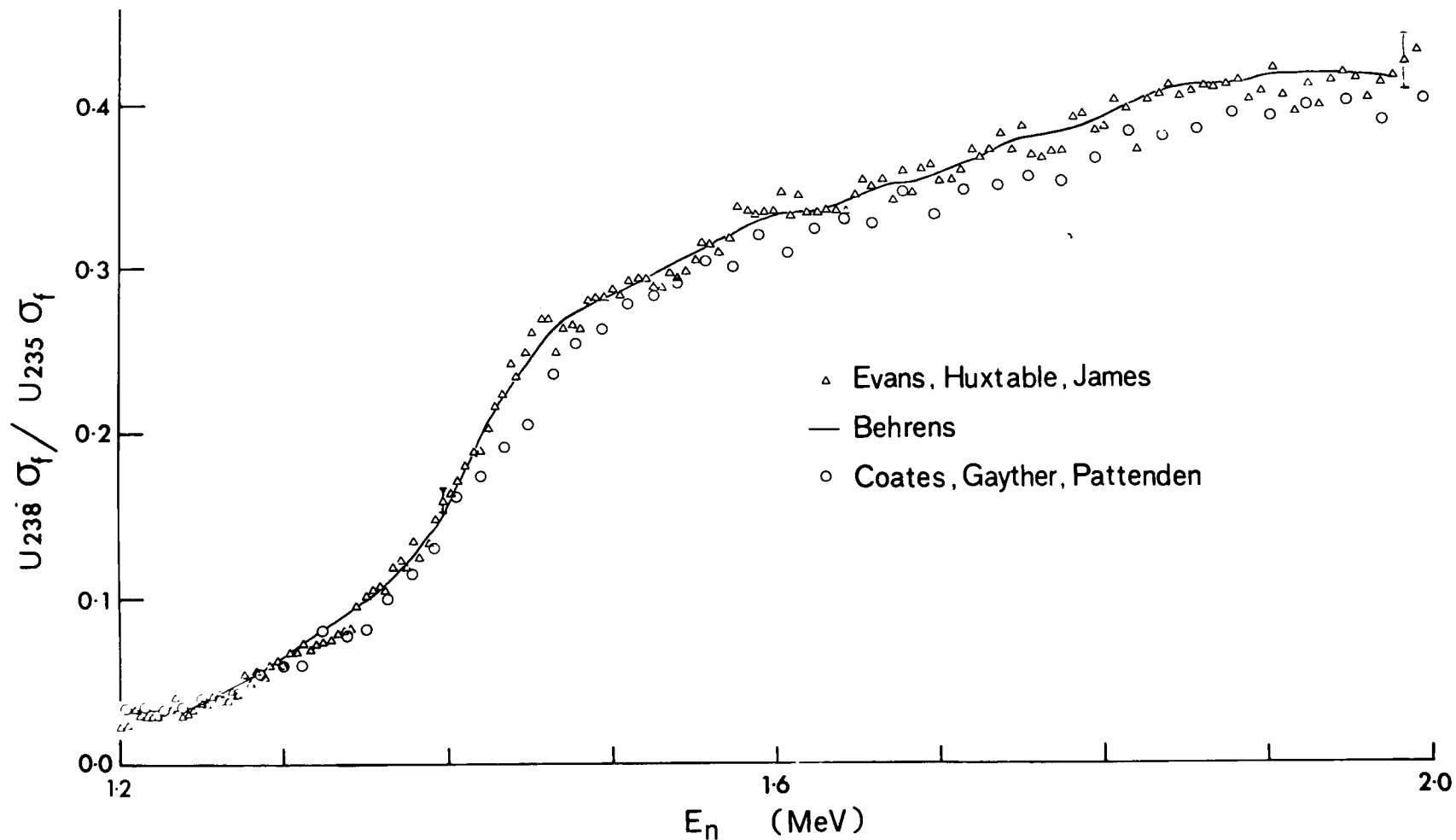


Figure 1. The ratio of the  $^{238}\text{U}$  to  $^{235}\text{U}$  fission cross sections over the energy range 1.2 MeV to 2 MeV. The results of the present experiment ( $\Delta$ ) and compared with the solid line derived from the data of Behrens et al [3] and with the renormalised data of Coates et al [4] ( $\circ$ ).

## DISCUSSIONS

J. Behrens Dr. Coates mentioned that his efficiency was 70% or less. At Livermore we recently ran the U-238 with a purposely low efficiency. We obtained results which look very close to those of Coates. My concern is that the efficiency may possibly be the culprit.

G. James There could still be some effect. The original difference was 25 keV, there is still some difference left ( $\sim 6$  keV). Perhaps the efficiency could account for that.

J. Behrens It goes in that direction. Though we have completely different chambers, we observed that if we go from low-efficiency to high-efficiency data we go from data similar to Harwell to that similar to the Livermore data.

G. James There is a point I should make: the foils we used in our experiment were the same as M. Coates used. However, we had a bias at 40 MeV whereas M. Coates' bias was much higher.

J. Behrens Yes, he mentioned the problems with the  $Al(n,\alpha)$  reaction.

G. James Yes, that is right. I have this problem too, but I got around it by not showing you the data.

L. Stewart Does this mean that one should not use M. Coates' data until we get the revised data set.

G. James That is correct. He has now written this up in a report. The data are here on cards.

W. Poenitz Plots of the corrected data will be available at the Working Session.

COMMENTS ON THE EVALUATION OF FISSION CROSS SECTION RATIOS  
FOR U-238 AND PU-239 TO U-235<sup>\*</sup>

W. P. Poenitz and P. Guenther

Argonne National Laboratory  
Argonne, Illinois 60439, U.S.A.

ABSTRACT

First approximation evaluated fission cross section ratios for U-238/U-235 and Pu-239/U-235 were obtained. The absolute normalization of the U-238/U-235 ratio appears to be established with a 1% uncertainty at the 99% confidence level. Available data for the Pu-239/U-235 ratio are insufficient to obtain a similar low uncertainty level.

INTRODUCTION

An evaluation of a consistent data set of cross sections of major importance for fast reactors (U-238(n, $\gamma$ ), U-235(n,f), U-238(n,f), and Pu-239(n,f) and several standard cross sections (H(n,n), Li-6(n, $\alpha$ ), B-10(n, $\alpha$ ), B-10(n, $\alpha\gamma$ ), and Au-197(n, $\gamma$ )) is presently under way at Argonne National Laboratory. Consistent data set evaluations are commonly applied in the nuclear data field for the evaluation of thermal neutron cross sections and parameters for fissile nuclei (see for example Westcott et al. [1], Lemmel [2]). Attempts to apply these techniques in the fast energy range were made in 1970 by Sowerby et al. [3] and Poenitz [4].

The major phases of the consistent data set evaluation are:

1. Analysis of the existing data (classification, correction and error analysis).
2. Evaluation of the shape of each quantity (for both absolute cross sections and cross section ratios).
3. Evaluation of the normalization factor for each quantity.
4. Removal of the overdetermination by a consistency fit.
5. Reanalysis of the data and determination of unknown errors by comparison with the first run "best value".
6. Repetition of steps 2 - 4.

## 7. "Fine-tuning" of the result.....

Two of the many requirements of such evaluation are that:

1. Only the originally measured quantities are used.
2. Only independent data are used.

However, if one evaluates singular quantities (for example the ratios of the cross sections of U-238(n,f) and Pu-239(n,f) to U-235(n,f)), and does not apply the consistency fit with evaluated absolute cross sections (above step 4), additional ratio values may be derived from absolute values which originated in the same experimental procedure by the same experimenter. Such evaluation (restricted to above listed steps 1,2,3 and 5) was carried out for U-238(n,f)/U-235(n,f) and Pu-239(n,f)/U-235(n,f). All available data were included, imposing restrictions on the analysis of the experimental data (e.g., for some preliminary data sets descriptions of the experiment were not yet available). Thus, the results are of a preliminary nature and only a first approximation data set.

## ANALYSIS OF THE EXPERIMENTAL DATA

Because of the above stated reasons few changes were made and the evaluation result is at present close to a weighted average of the reported data. However, an analysis of the energy scales is part of this step of the evaluation and was considered inevitable in the case of the U-238(n,f)/U-235(n,f) ratio (the  $d\sigma/\sigma/dE$  value around 800 keV is 1 percent per 1 keV).

Several structural features of the U-238(n,f)/U-235(n,f) ratio permit a rough determination of energy scales. Table 1 lists the energies picked for positions labeled A through H. Though any conclusion at any individual point could be argued with respect to compatibility with statistical errors, the purpose of the table was to establish the possible existence of trends. Of specific interest are the four time-of-flight white-source measurements labeled with a star in Table 1.

Table 2 indicates time-zero shifts required to bring any one experiment into agreement with another. Only the data of Coates et al. [5] demonstrated a clear trend. Furthermore, the magnitude of the shift in this case compared with that for other experiments suggests that Coates' energy scale is more likely in error. An examination of required flight path corrections proved excessively large (i.e., > 10 cm).

Though energy scale differences appear to be obvious at the 6.4 MeV peak, no consistent trend could be established between the remaining sets. Still, time zero was adjusted as indicated in Table 2 based on the available information for the parameters given in the same Table.

The monoenergetic data were shifted to meet the resulting energy scale from the TOF measurements (Meadows [6] by 10 keV, Fursov et al. [7] by half the target thickness used in his experiment, and Lamphere [8] by 25 keV).

## SHAPE EVALUATION

A detailed description of the present evaluation procedures will be given elsewhere [9], thus, only a brief account of the techniques used follows here.

Eye-guide curves were drawn through the experimental data and values on this curve were picked at a predetermined energy grid. A unique set of all possible ratios between any two such values forms a matrix with the elements  $S_{ik} = R_i/R_k$ . The weighted averages of the  $S_{ik}$  from all contributing experiments were found. The weighted sums of the columns of this matrix define a system of  $n-1$  equations for  $n$  unknowns. Because only the shape is of interest, the  $n$ -th equation is obtained by defining  $R_n = 1$ . The "roll-back" procedure yields  $R_{n-1}, R_{n-2}, \dots, R_1$ , and thus the shape which is normalized arbitrarily to  $R_n = 1$ .

## NORMALIZATION FACTOR

The normalization factor for the evaluated shape obtained from one experiment  $i$  is given by

$$F_i = \frac{\sum_{k=1}^n \frac{R_{ik}}{R_s} W_k}{\sum_{k=1}^n W_k},$$

where  $R_{ik}$  is one of the  $k=1, \dots, n$  measured values which has the weight  $W_k$ . The normalization factor for the evaluated shape curve is then obtained as the weighted average of all contributing  $F_i$ . The U-238(n,f)/U-235(n,f) ratio shows a strong energy dependence below 2 MeV. This requires a proper accounting of the energy uncertainty in calculating the weight  $W_k$  by replacing the relative fractional error  $\Delta R/R$  with

$$\sqrt{\left(\frac{\Delta R}{R}\right)^2 + \left(\frac{dR}{dE} \frac{\Delta E}{R}\right)^2}.$$

However, for most experiments  $\Delta E$  is not reported or is underestimated as the above considerations of energy-scales indicate. Therefore, the  $E < 2$  MeV range was excluded in determining the normalization factor for U-238(n,f)/U-235(n,f). The first column of Table 3 gives the normalization factors for all available data on U-238(n,f)/U-235(n,f). The factors in this table are based on a provisional normalization of the shape to 0.432 at 2.5 MeV. The second column gives the factors restricted to the 2-3 MeV range where the ratio forms a "plateau" and therefore is insensitive to energy-uncertainties in the experiment. Some of the oldest experiments were not included in this interval. The last column gives the normalization factors restricted to the 14-15 MeV range. A comparison of the weighted averages from the different energy ranges shows a maximum spread of less than 1 percent. This is encouraging and suggests that the normalization for

$U-238(n,f)/U-235(n,f)$  is established with an uncertainty of 1 percent at the 99 percent confidence limit.

## RESULTS AND CONCLUSIONS

The result for the evaluated ratio  $U-238(n,f)/U-235(n,f)$  is shown in Fig. 1. The structure around 17 MeV is not the result of the computerized shape evaluation but was superimposed as a result of considerations of the much better resolution obtained in monoenergetic beam measurements at these energies than obtained in time-of-flight measurements. Fig. 2 shows the difference of the experimental time-of-flight data sets relative to the evaluation result. Three of the sets were shape data only (Coates et al. [5], Cierjacks et al. [32], and Difilippo et al. [33]) and were normalized at 2.5 MeV. Therefore, the figure shows shape differences up to 15 percent with a probability of less than 1 percent (2.5 standard deviations) to be correct. It was suggested that the shape difference of the data by Cierjacks et al. [32] could be caused by a sensitivity to fission fragment angular distributions [34]. However, there is no unique correlation of the differences of the various data sets with  $[W(0^\circ)/W(90^\circ)]_{U^{235}}/[W(0^\circ)/W(90^\circ)]_{U^{238}}$ , which is shown in the same figure. The difference of the data by Coates et al. [5] with the evaluated result is also not correlated with the  $Al(n,\alpha)$  cross section which influenced the threshold setting in this experiment. Fig. 3 shows the difference of monoenergetic data relative to the evaluation result. In this case the differences are due to shape and normalization differences because all values shown in Fig. 3 are absolute ratio data. Differences in Figures 2 and 3 below 2 MeV reflect energy scale problems and are of lesser concern. The evaluation agrees best with the data by Jarvis [22], White et al. [14], Poenitz and Armani [10], Meadows [6] below 6 MeV, Fursov et al. [7] below 5 MeV, Behrens et al. [11], and Difilippo et al. [33]. The status of the ratio  $U-238(n,f)/U-235(n,f)$  could be considered satisfactory and well described by the evaluation result. Unfortunately, several data sets suggest similar trends in shape and normalization which contradict the evaluation result. These are shown in Fig. 1. Above 6.4 MeV the data by Meadows [6], Coates et al. [5], Cierjacks et al. [32], Nordborg et al. [15] show relatively higher values compared with the evaluation result which is very similar to the shapes obtained by Difilippo et al. [33] and by Behrens et al. [11]. The major contradiction of the shape by Cierjacks et al. [32] shown in Fig. 1 is for the ratio of the value at 14 MeV to that at 2.5 MeV. High confidence in this ratio is suggested by the 1% agreement between the normalization factors quoted in the second and third column of Table III.

A rather unsatisfactory result is obtained as a first approximation for the evaluation of  $Pu-239(n,f)/U-235(n,f)$ . The data by Carlson et al. [35] outweigh others in the evaluation of the shape but are contributing only modestly to the determination of the normalization factor. This causes an evaluation result which is above 1 MeV lower than the majority of the data. The situation is demonstrated with Figure 4 where the difference between some newer data sets and the evaluation result is shown. It appears that a major discrepancy exists between the shape of the data by Carlson et al. [35] and most other data sets (references 36 through 43.). More measurements of the  $Pu-239(n,f)/U-235(n,f)$  ratio are desirable.

## REFERENCES

1. C. H. WESTCOTT, K. EKBERG, C. G. HANNA, N. S. PATTENDEN, S. SANATANI, and P. M. ATREE, *Atomic Energy Review* 3 (1965) 3.
2. H. D. LEMMEL, *Proc. of a Conference on Nuclear Cross Sections and Technology*, NBS Special Publication 425, Vol. I, p.286 (1975).
3. M. G. SOWERBY and B. H. PATRICK, *Proc. of the Second International Conference on Nuclear Data for Reactors*, IAEA, Vol. II, p.703 (1970).
4. W. P. POENITZ, *Proc. of a Symposium on Neutron Standards and Flux Normalization*, AEC Symposium Series 23, p.331, (1970).
5. M. S. COATES, D. B. GAYTHER, N. J. PATTENDEN, *Proc. of a Conference on Nuclear Cross Sections and Technology*, NBS Special Publication 425, Vol. II, p.568 (1975).
6. J. W. MEADOWS, *Nucl. Sci. Engineering* 49, 310 (1972), also NSE 58, 255 (1975), also Private Communication, also see second paper in this session.
7. B. I. FURSOV, V. M. KUPIJANOV, B. K. MASLENNIKOV, G. N. SMIRENKIN, and V. M. SURIN, *Proc. of Conference on Neutron Physics*, Kiev 1973, Vol. 4, p.3 (1973).
8. R. W. LAMPHERE, *Physics Rev.* 104, 1654 (1956).
9. W. P. POENITZ, *Proc. of a Symposium on Neutron Standards and Flux Normalization*, AEC Symposium Series 23, p.331 (1970).
10. W. P. POENITZ and R. J. ARMANI, *J. Nucl. Energy* 26, 483 (1972).
11. J. W. BEHRENS and G. W. CARLSON, UCRL-78268, see first paper this session and previous work cited therein.
12. M. CANCE and G. GRENIER, see 6th paper in this session.
13. W. E. STEIN, R. K. SMITH, and H. L. SMITH, *Proc. of Conference on Neutron Cross Sections and Technology*, Washington 1968, Vol. I, p.627 (1968).
14. P. H. WHITE and G. P. WARNER, *J. Nuclear Energy* 21, 671 (1967).
15. C. NORDBORG, H. CONDE, and L. G. STROEMBERG, see 5th paper in this session.
16. W. D. ALLEN and A. T. G. FERGUSON, *Proc. Phys. Soc.* LXX, 8-A, p.573 (1957).

17. I. M. KUKS, L. A. RAZUMOVSKIY, JA. A. SELITSKIY, A. V. FORMICHEV, V. B. FUNSHTEYN, V. I. SHPAKOV, *Conf. on Neutron Physics*, Kiev 1973, Vol. 4, p.18 (1973), and *Atomnaya Energiya* 30, 55 (1971).
18. C. A. UTTLEY and J. A. PHILLIPS, Report AERE-NP/R-1996 (1956).
19. W. NETTER, Report CEA-1913 (1961).
20. G. N. SMIRENKIN, B. G. NESTEROV, and I. I. BANDARENKO, *Atomnaya Energiya* 13, 366 (1962).
21. A. MOAT, see *J. Nuclear Energy* 14, 85 (1961).
22. G. A. JARVIS, R. P. KUTARNIA, R. A. NOBLES, Report LA-1571 (1953).
23. R. H. IYER and R. SAMPATHKUMAR, *Proc. of Symp. on Nuclear Physics and Solid State Physics*, Roorkee 1969, Vol. II, p.289 (1969).
24. A. A. BEREZIN, G. A. STOLIAREV, YU. V. NIKOLSKII, and I. E. CHELNIKOV, *Atomnaya Energiya* 5, 659 (1958).
25. T. A. HALL, P. G. KOONTZ, B. ROSSI, Report LA-128.
26. BRETCHER, cited in Ref. 25.
27. Z-Group, cited in Ref. 25.
28. CHADWICK, cited in Ref. 25.
29. R. K. SMITH, R. L. HENKEL, and R. A. NOBLES, *Bull. Am. Phys. Soc.* 2, 196 (K4) (1957), revised values by HANSEN, McGUIRE, and SMITH (1968).
30. V. M. PANKRATOV, *Atomnaya Energiya* 14, 177 (1963), see also AE9, 399 (1960).
31. W. NYER, Report LAMS-938 (1950).
32. S. CIERJACKS, B. LEUGERS, K. KARI, B. BROTZ, D. ERBE, D. GROESCHEL, G. SCHMALZ, and F. VOSS, see 3rd paper this session (1976).
33. F. C. DIFILIPPO, R. B. PEREZ, G. De SAUSSURE, D. OLSEN, and R. INGLE, see 4th paper in this session (1976).
34. J. W. BEHRENS, Private Communication (1976).
35. G. W. CARLSON and J. W. BEHRENS, Report UCID-16981 (1975), see also 1st paper in this session (1976).
36. E. PFLETSCHINGER and F. KAEPPELER, *Nucl. Sci. Engineering* 40, 375 (1970).
37. P. H. WHITE and G. P. WARNER, *J. Nucl. Energy* 21, 671 (1967), see also 65 Salzburg, Vol. I, 219 (1965).

38. W. P. POENITZ, *Nucl. Sci. Engineering* 40, 383, (1970), and *NSE* 47, 228 (1972).
39. M. C. DAVIS, J. C. ROBERTSON, J. C. ENGBAHL, and G. F. KNOLL, *Proc. Am. Nucl. Soc.* 22, 663 (1975), see also 4th paper in next session (1976).
40. I. SZABO and J. P. MARQUETTE, see 3rd paper in next session. Earlier data are referenced therein (1976).
41. G. GWIN, R. W. INGLE, E. G. SILVER, H. WEAVER, *Proc. Am. Nucl. Soc.* 15, 481 (1972).
42. J. W. MEADOWS, see second paper in this session (1976).
43. B. I. FURSOV, V. KUPRIJANOV, and G. SMIRENKIN, *Proc. of Conf. on Neutron Physics*, Kiev 1975.

---

\* Work performed under the auspices of the U.S. Energy Research and Development Administration.

TABLE I

Energy Scales - Location of Structure in U8/U5 (in MeV)

Label E/MeV	A .9	B 1.5	C 2.1	D 3.0	E 6.5	F 11.5	G 13.0	H 17.0
Nordborg					6.75			
Coates*	.92	1.51	2.19	3.08	6.80	11.4	14.0	19.3
Cierjacks*		1.47			6.85	12.1	12.8	17.8
Difilippo*			2.12	2.97	6.65	11.2	13.1	17.2
Meadows		1.48			6.42			
Lamphere	.94	1.50	2.10					
Fursov		1.53	2.17	3.00	6.85			
Cancé					6.6			
Behrens*	.90	1.47	2.08	2.88	6.38	11.3	12.8	17.1
Ponkratov								17.2
Smith					6.8			17.0

TABLE II

Time-Zero Shifts Required in TOF-Measurements (in nsec)

Assumed Correct Scale	Assumed Incorrect Scale			
	Behrens	Coates	Cierjacks	Difilippo
Behrens	-	+10	+24	+12
Coates	-30	-	-25	-12
Cierjacks	-14	+5	-	-13
Difilippo	-11	+4	+19	-
Parameters				
Flight Path/m	34.26	11.8	~57	~40
Channel width nsec/m	6	3.6		2
Uncertainty nsec	2(5)			2
Pulse Width		1	<1	3
Adjustment	-4	+8	+16	+8

TABLE III

## U-238/U-235 Normalization Factors

Data	Ref.	2 - 20 MeV	2 - 3 MeV	14 - 15 MeV
Poenitz	10	$1.010 \pm .019$	$1.010 \pm .019$	
Meadows	6	$1.010 \pm .014$	$0.998 \pm .013$	
Behrens	11	$1.005 \pm .012$	$1.006 \pm .010$	$0.994 \pm .016$
Cance	12	$0.960 \pm .030$	$0.951 \pm .029$	$0.967 \pm .031$
Stein	13	$0.970 \pm .025$	$0.973 \pm .025$	
Lamphere	8	$1.040 \pm .100$	$1.040 \pm .100$	
White	14	$1.002 \pm .020$	$1.006 \pm .020$	$1.004 \pm .020$
Fursov	7	$0.977 \pm .025$	$1.005 \pm .025$	
Nordborg	15	$0.977 \pm .027$		
Allen	16	$0.850 \pm .100$	$0.850 \pm .100$	
Kuks	17	$0.972 \pm .052$	$0.972 \pm .052$	
Uttley	18	$0.958 \pm .041$		$0.958 \pm .041$
Netter	19	$0.976 \pm .100$	$0.953 \pm .100$	
Smirenkin	20	$1.042 \pm .100$	$1.042 \pm .100$	
Moat	21	$0.982 \pm .045$		$0.982 \pm .045$
Jarvis	22	$0.984 \pm .015$	$0.984 \pm .015$	
Iyer	23	$0.999 \pm .101$		$0.999 \pm .101$
Berenzin	24	$0.852 \pm .065$		$0.852 \pm .065$
Hall	25	$0.945 \pm .100$		
Bretcher	26	$0.896 \pm .100$		
Z-Group	27	$0.859 \pm .100$		
Chadwick	28	$0.714 \pm .100$		
Smith	29	$1.013 \pm .071$	$0.960 \pm .084$	$1.055 \pm .068$
Ponkratov	30	$0.926 \pm .100$		$0.937 \pm .100$
Nyer	31	$0.967 \pm .050$		$0.967 \pm .050$
Weighted Average		$0.993 \pm 0.005$	$0.997 \pm 0.004$	$0.989 \pm 0.009$

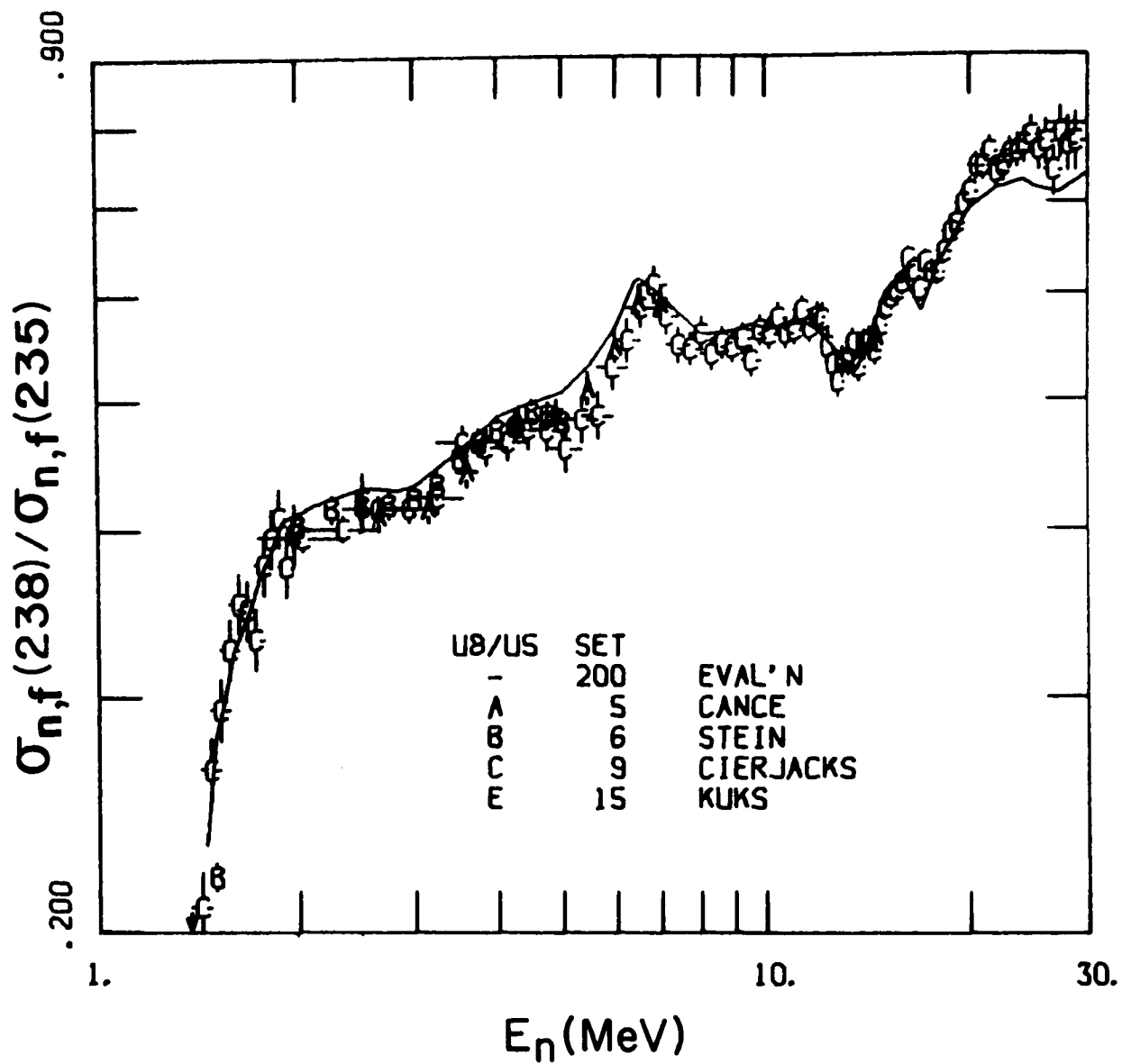


Figure 1. The evaluation result for U-238(n,f)/U-235(n,f) compared with those data which appear to contradict the result in a consistent way.

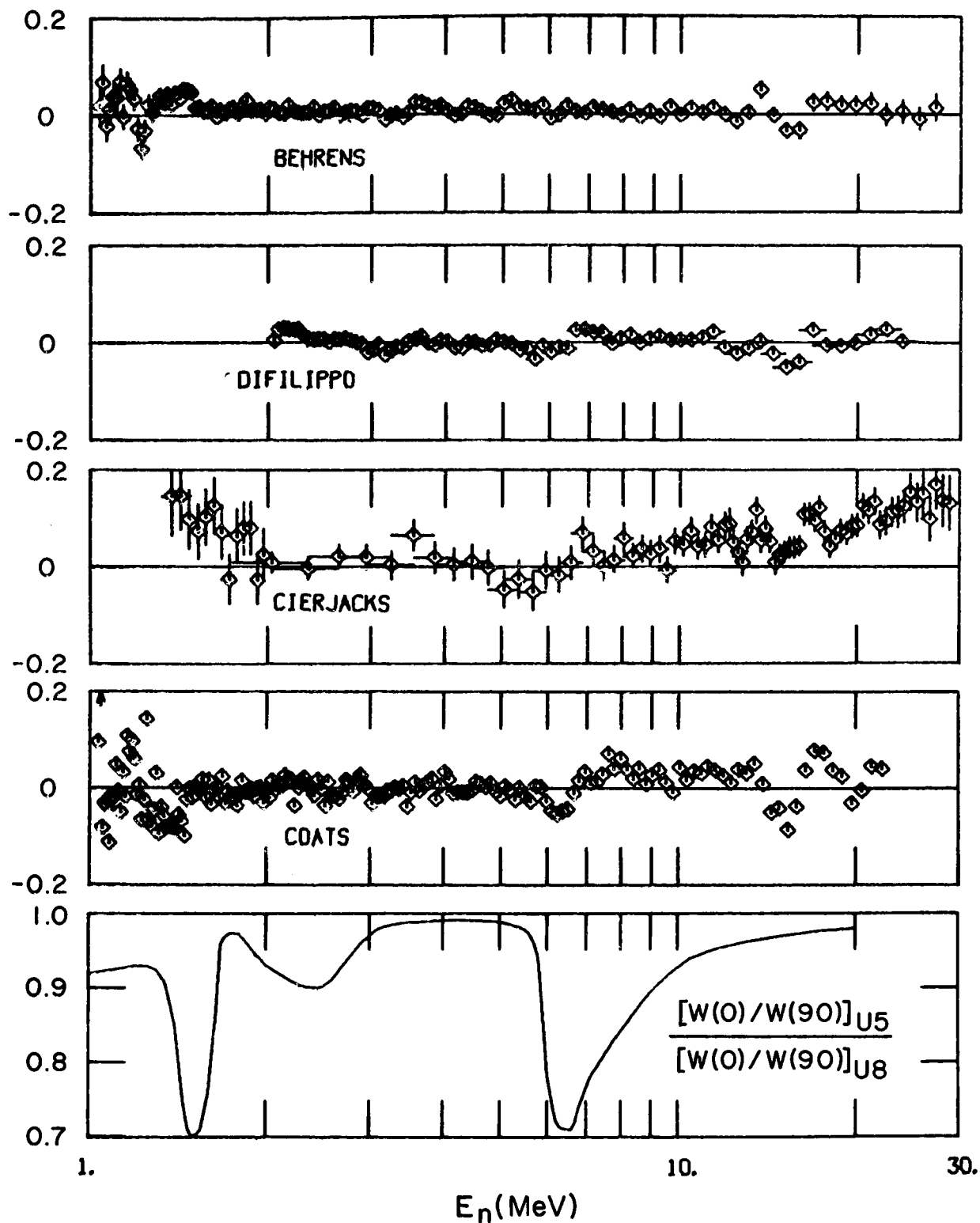


Figure 2. The differences between the evaluation result for U-238/U-235 and the time-of-flight data. The lowest sub-figure shows the angular distribution ratio which should show correlations with the data.

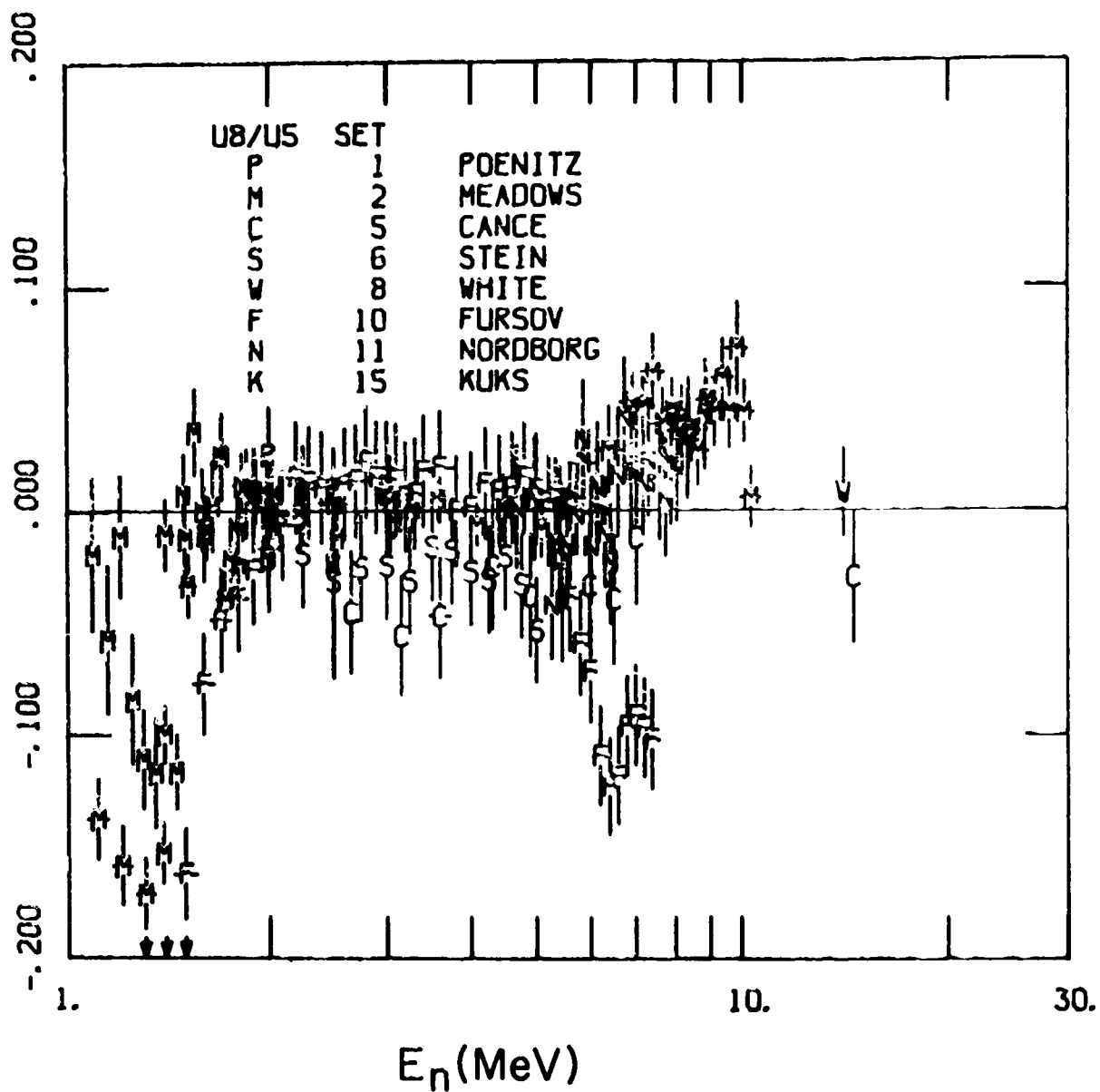


Figure 3. The differences between the evaluation result for U-238/U-235 and the monoenergetic measurements. In contrast to Fig. 2 these data sets were not normalized at one energy (see text).

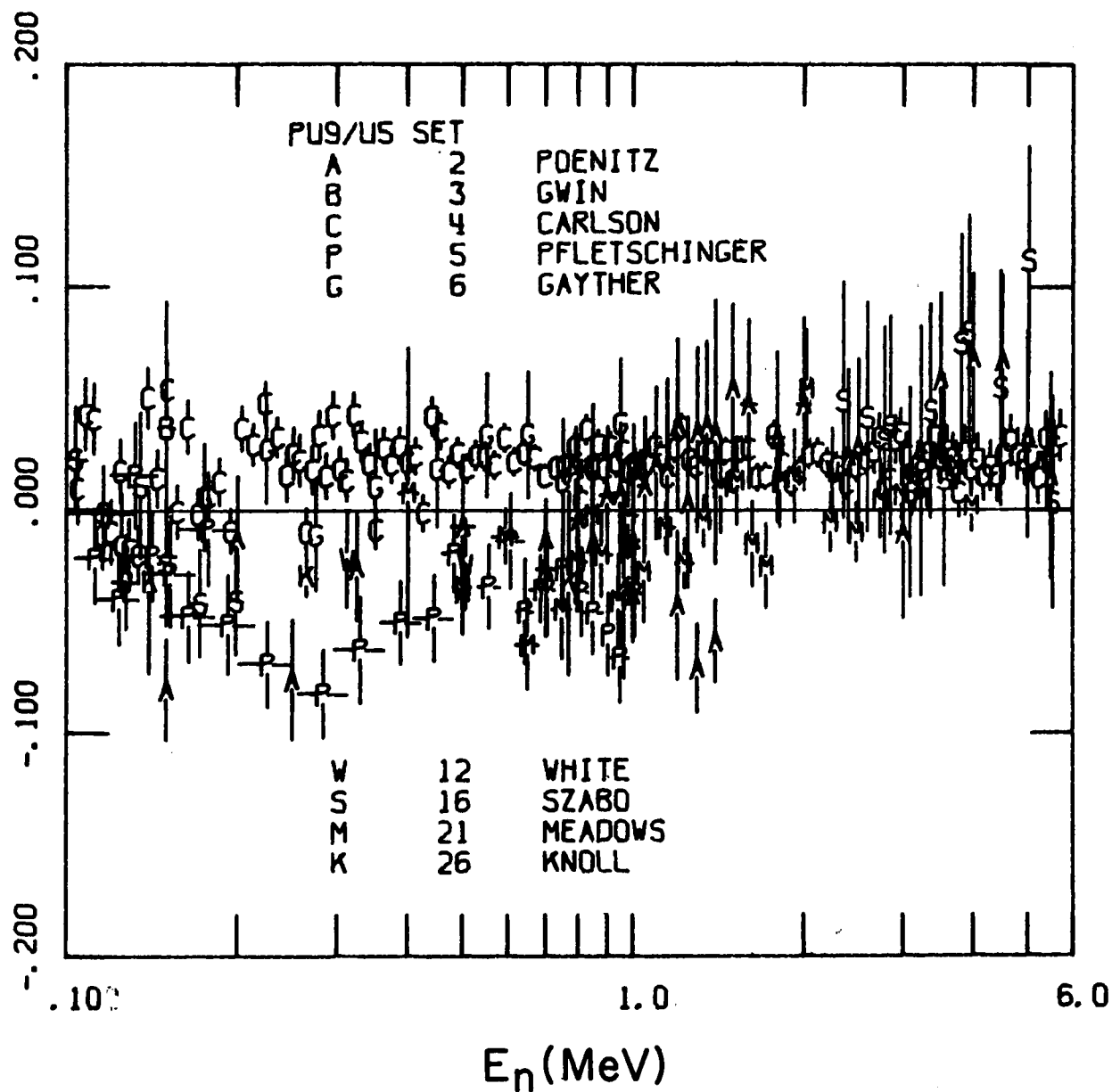


Figure 4. The differences between the evaluation result for Pu-239/U-235 and some newer data sets.

## DISCUSSIONS

J. Behrens You mentioned the structure around 300 keV. In a survey I did some time ago I found some structure at the same energy in data by Soleilhac.

W. Poenitz The data by Soleilhac shows structure everywhere. In addition his ratio drops off below 300 keV and vanishes into nowhere. I would not consider his structure at 300 keV as a strong confirmation so close to where something unrealistically happens.

H. Derrien The measurements by Soleilhac were part of an  $\alpha$ -measurement and he feels that this ratio is not the primary result of his measurements.

A. Smith You showed as a result of your evaluation of U-238/U-235 the differences of several sets compared with this result. Two sets should show an increased difference to the high side if one goes to higher energies, the other two were pretty flat. Were the high sets those obtained with gas scintillation counters and the flat ones those from ion chambers.

W. Poenitz Yes. Coates and Cierjacks use gas scintillation counters and Difilippo and Behrens use ion chambers. I should provide an additional piece of information. I observed in my gas scintillation counter measurements of Pu-239/U-235 that one may get high ratios at higher energies as a result of setting the threshold in the U-235 chamber somewhat lower, and may thus be picking up some noise.

S. Cierjacks That would not be an explanation in our case. We used identical counters for both.

W. Poenitz I did not try to explain your data.

G. Grenier The normalization of our data at 14 MeV have a different and independent normalization than the 2-7 MeV ratios.

W. Poenitz That would be indeed helpful. The shape of your 2-7 MeV values agrees well with the evaluated shape but not if one includes the 14 MeV point. One could then explain the differences with a different normalization of the 2-7 MeV data because the 14 MeV point is right on the curve.

S. Cierjacks This question concerns the normalization at 2.5 MeV in contrast to 14 MeV as a normalization point. One had the impression that the 14 MeV normalization would be a good thing and the values agreed quite well with 0.53. I observed there is quite some structure at 14 MeV. Do you think this could influence the normalization at 14 MeV.

W. Poenitz The U8/U5 ratio drops above 12 MeV, reaches a minimum around 13 MeV and then rises continuously until 16 MeV. The 14 MeV data points are in this rising range. This could contribute to the spread, but, most of the absolute 14 MeV measurements were carried out with a monoenergetic T(d,n) source which has no energy definition problems in this range.

S. Cierjacks They might have problems in the energy determination.

W. Poenitz No, I said no. You cannot go wrong with the T(d,n) energy. Not in this case. In other energy ranges maybe. But not here.

S. Cierjacks There might be a resolution problem.

W. Poenitz You would need a much more detailed fine-structure to get into problems. Such structure is unknown. The other problem you mentioned concerns the 0.53 ratio value. This was a value derived from evaluated 14 MeV data for U-235 and U-238. However, what one really should do, is to restrict the data used for the ratio normalization to direct ratio measurements or measurements with identical flux determinations. The evaluation of the normalization which I presented here contains only such consistent experimental data.



## *Session II*

### **Absolute Fast Neutron Fission Cross Sections**



# THE FISSION CROSS SECTION OF $^{235}\text{U}$ FROM 1 TO 6 MeV\*

D. M. Barton, B. C. Diven, G. E. Hansen, G. A. Jarvis,  
P. G. Koontz and R. K. Smith

Los Alamos Scientific Laboratory, University of California  
Los Alamos, New Mexico 87545

The ratio of the neutron-induced fission cross section of  $^{235}\text{U}$  to the neutron-proton scattering cross section was measured in the neutron energy region from 1 to 6 MeV. The neutron source was the T(p,n) reaction produced by a pulsed Van de Graaff proton beam on a thin tritium gas target. The use of monoenergetic neutrons allowed time-of-flight methods to be used to study carefully backgrounds and source characteristics. While this procedure results in much slower data acquisition than the use of a white neutron source, the added information improves our confidence in the data and eliminates errors in correction for room-return neutrons.

The detector systems and calibration procedure were designed to avoid independent measurements of an absolute neutron flux and absolute fission rate and to measure as directly as possible the ratio of the n-p scattering to fission cross sections. The fission deposit and proton radiator were back to back with solid state detectors used to count fission fragments and protons. The fission detector was located 0.6 mm from the  $^{235}\text{U}$  and counted fragments from 90% of the fissions, so that the anisotropy correction was small. Only protons recoiling near  $0^\circ$  to the neutron beam were accepted, the collimating aperture subtending one fourth of one percent of  $4\pi$  steradians from the proton radiator. Because the neutron beam was monoenergetic and only zero degree protons were accepted, the proton detector saw nearly monoenergetic protons that were detected with 100% efficiency. The six main observables that enter into the determination of the ratio of the hydrogen to fission cross sections are the proton and fission counting rates, the masses of hydrogen and  $^{235}\text{U}$  in the samples, and fractions of protons and fission fragments that are detected. The accuracy of the counting rates is determined largely by statistics and the masses of hydrogen and  $^{235}\text{U}$  are measurable to an accuracy better than 1%. The fraction of protons detected is determined by the counting geometry which can be measured accurately, but the fraction of fissions detected in nearly  $2\pi$  geometry cannot be calculated accurately. A calibration experiment was devised which allowed accurate

---

\* Work performed under the auspices of the United States Energy Research and Development Administration.

determination of the necessary quantities. The ratio of fission to hydrogen cross sections is determined from the fission and proton counting rates  $C_f$  and  $C_p$  by

$$\frac{\sigma_f}{\sigma_p} = \frac{C_f N_h \Omega_p}{C_p N_u \epsilon_f}$$

where  $\sigma_p$  is the cross section for  $0^\circ$  proton scattering in barns/ $4\pi$  steradians,  $N_h$  and  $N_u$  the number of hydrogen and  $^{235}\text{U}$  atoms,  $\Omega_p$  the effective fraction of  $4\pi$  steradians subtended at the proton radiator by the proton collimator, and  $\epsilon_f$  is the fraction of fission events detected. This fraction  $\epsilon_f$  is determined not only by geometrical factors, but also by energy losses of fragments in the uranium layer and the detector dead layer, whereas the corresponding fraction  $\Omega_p$  for the proton counter is purely geometrical. Of the six quantities that determine the cross section ratio, we determine directly the count rates and the number of hydrogen atoms in each radiator used. The separate calibration experiment determined the ratio  $\Omega_p/N_u\epsilon_f$ .

A thin  $^{235}\text{U}$  deposit whose mass is accurately known was substituted for the proton radiator and the counting system was placed in an isotropic thermal neutron flux. Now the "proton" counter detected fission fragments from the thin standard  $^{235}\text{U}$  and since only fragments normal to the foil were accepted, no fragments directed toward the proton counter lost enough energy to be missed in the counting system and the fraction detected was  $\Omega_p$ . As before, the fraction of fissions detected by the fission counter is  $\epsilon_f$  and the ratio of counts in the two detectors is

$$R = \frac{2N_s \Omega_p}{N_u \epsilon_f}$$

where  $N_s$  is the number of atoms in the standard. From this ratio we obtain  $\Omega_p/N_u\epsilon_f$  without the necessity of measuring any of the three quantities separately. By this means we avoid the measurement of both detector solid angles and the calculation of fission fragment losses in the uranium deposit and the fission detector.

Because the experimental procedure and corrections to the data are presented in detail in a paper in Nuclear Science and Engineering (1976) they are not repeated here. The results are shown in Table I.

Table I. Results of the Present Measurements

$E_n$ (MeV)	$\sigma_f(^{235}\text{U})/\sigma_a(\text{H})$	% Uncert.		$\sigma_a(\text{H})$	$\sigma_f(^{235}\text{U})$	% Uncert.	
		Stat.	Syst.			Stat.	Syst.
1.0	0.2884	0.9	0.8	4.261	1.229	0.9	1.1
1.1	0.3091	1.0	0.8	4.051	1.252	1.0	1.1
1.2	0.3219	0.8	0.8	3.668	1.245	0.8	1.1
1.3	0.3349	0.9	0.8	3.706	1.241	0.9	1.1
1.4	0.3438	1.7	0.8	3.561	1.224	1.7	1.1
1.5	0.3673	0.9	0.7	3.429	1.260	0.9	1.0
1.6	0.3722	0.9	0.7	3.309	1.232	0.9	1.0
1.7	0.4017	1.3	0.7	3.190	1.285	1.3	1.0
1.8	0.4089	1.2	0.7	3.097	1.267	1.2	1.0
1.9	0.4214	1.3	0.7	3.003	1.266	1.3	1.0
2.0	0.4327	0.5	0.7	2.915	1.262	0.5	1.0
2.2	0.4583	1.0	0.7	2.759	1.265	1.0	1.0
2.4	0.4746	1.7	0.7	2.622	1.245	1.7	1.0
2.5	0.4852	1.7	0.7	2.560	1.242	1.7	1.0
2.6	0.4839	0.8	0.7	2.501	1.210	0.8	1.0
2.7	0.4972	0.9	0.7	2.445	1.216	0.9	1.0
2.8	0.5023	1.0	0.7	2.392	1.201	1.0	1.0
2.9	0.5063	1.1	0.7	2.341	1.185	1.1	1.0
3.0	0.5238	0.3	0.7	2.293	1.201	0.3	1.0
3.2	0.5475	1.5	0.7	2.203	1.206	1.5	1.0
3.4	0.5544	1.5	0.7	2.120	1.175	1.5	1.0
3.5	0.5618	0.8	0.7	2.081	1.169	0.8	1.0
3.6	0.5745	1.5	0.7	2.043	1.173	1.5	1.0
3.7	0.5713	1.3	0.7	2.007	1.147	1.3	1.0
3.8	0.5858	1.6	0.7	1.973	1.156	1.6	1.0
4.0	0.5919	0.7	0.7	1.907	1.129	0.7	1.0
4.2	0.6153	1.7	0.8	1.845	1.135	1.7	1.1
4.4	0.6207	1.6	0.8	1.788	1.110	1.6	1.1
4.6	0.6289	1.6	0.8	1.734	1.090	1.6	1.1
4.8	0.6537	1.6	0.8	1.683	1.100	1.6	1.1
5.0	0.6614	1.2	0.8	1.635	1.081	1.2	1.1
5.1	0.6684	1.0	0.9	1.612	1.077	1.0	1.2
5.2	0.6812	1.2	0.9	1.589	1.082	1.2	1.2
5.3	0.6869	1.1	0.9	1.568	1.077	1.1	1.2
5.4	0.6847	0.7	0.9	1.547	1.059	0.7	1.2
5.5	0.6919	1.2	0.9	1.526	1.055	1.2	1.2
5.6	0.6910	1.0	0.9	1.506	1.041	1.0	1.2
5.7	0.7135	1.2	0.9	1.486	1.060	1.2	1.2
5.8	0.7394	2.3	0.9	1.467	1.084	2.3	1.2
5.9	0.7688	1.7	0.9	1.448	1.113	1.7	1.2
6.0	0.7950	2.1	0.9	1.430	1.137	2.1	1.2

## DISCUSSIONS

*Additional Remarks by B. Diven Concerning the Suggested Energy-Shift Between the LASL and LLL Data*

Sometimes people like to suggest also a discrepancy in energy scale between the LASL and LLL data. This discrepancy would be based on one point. At any rate, let us normalize the Livermore data between 5.0 and 5.5 MeV to the LASL data. This makes of course the difference look somewhat worse as Fig. 1 shows. Now there is one point which differs by as much as 2.5 standard deviations. I think this is a futile game to play. The energy scale is probably right within the uncertainty of about 10 keV and what we see are only statistical fluctuations. As a matter of fact, if we make a  $\chi^2$ -test over an energy region here, we find that we have much too good a fit. With this kind of game which is, I think, misleading you can shift the energy scale (see Fig. 2) and make all statistical errors disappear. This is of course ridiculous.

C. Bowman Do your foils have both the same composition?

B. Diven Yes they were all made from the same batch of material. There were 13 foils of different thicknesses, and the same diameter. Most were destroyed for analysis after they all had been  $\alpha$ -counted and fission counted.

C. Bowman Do you know what the chemical composition was?

B. Diven These were evaporated as  $\text{UO}_2$  and converted by heat to  $\text{U}_3\text{O}_8$ .

W. Poenitz You brought up the problem of the energy shift in the LASL data. It was suggested by L. Stewart that the possible effect on the cross section could be up to 6%. I also noted that in M. Bhat's contribution to this meeting the energy shift between the LASL and the LLL data is again considered. In order to help to clarify the problem I will try to play advocatus diaboli and argue the existence of an energy shift which you suggested does not exist. Let us look at the Fig. 3. The cross section changes very little with energy in the 2-5.5 MeV range compared with the fast rise due to second chance fission above 6 MeV. All the available data

shown in Fig. 3 were normalized in the 2-5.5 MeV range to match the average of the LASL data. This is of course a much larger range than the one you choose for normalization. The figure appears to indicate indeed an energy shift in the order of 150 keV. You will note that the figure does not show error bars on the points but indicates only the typical statistical error of the LASL and LLL measurements which is about 1%. The reason why I did not include the error bars is that most of them are not relevant to this consideration. This consideration is in contrast to your suggestion that "one can shift in normalization and in energy and make even the statistical errors disappear which would be ridiculous". As a matter of fact, if one normalizes over the many points in the 2-5.5 MeV range, one reduces the statistical error of the normalization tremendously and all that remains to be considered is: What is the probability that the three (or five) points around 6 MeV are systematically on the high side based on their statistical error. This probability is small. Other data are not very conclusive, but it appears that the Smith, Henkel, Nobels data and the new data from KFK support the LLL energy scale.

The other important point, which was suggested by L. Stewart is that if the energy shift of 150 keV applies to the total energy range, the required change in the reference cross section  $H(n,n)$ , would cause a 6% change in the LASL data around 1 MeV. Though I do not believe such drastic energy error for a monoenergetic source, it would have the advantage of resolving the present discrepancy in the shape of the LASL data with most other measurements between 1 and 2 MeV.

M. Bhat I think one can see that there is definitely an energy shift. Fig. 4 shows that if one shifts by 100 keV, one gets agreement between the LASL and the Czirr data. Unfortunately the LASL data do not go to higher energies and the conclusion must be based on a few points.

B. Diven That is essentially the same figure I showed where I shifted by 100 keV to show one can get ridiculously good agreement. But again, I do not believe there is any such shift. I think the disagreement between the two is statistical.

R. Peelle The paper shows the systematic uncertainties to be between 0.7 to 1.2%. Do these include everything, the mass, the reference cross section,

etc.?

B. Diven Yes, they do include everything the experimenters could think of. They do not include anything the experimenters could have guessed might go wrong.

R. Peelle Is it determined by the hydrogen cross section?

B. Diven The uncertainty in the angular distribution of the hydrogen cross section is a fairly large contributor at high energies.

H. Kuesters (Chairman) Just one remark here. What is quoted here as an uncertainty is on an average up to 4 MeV, about 2%. What strikes me a bit is the point which just was discussed; quoting a systematic error of 1 percent and seeing at the same time discrepancies of 3-4% with data of others. This might be the point you made that the experimenter did not include anything that might explain the 4% discrepancy.

# ENERGY BIN WIDTHS AND STATISTICAL ERRORS

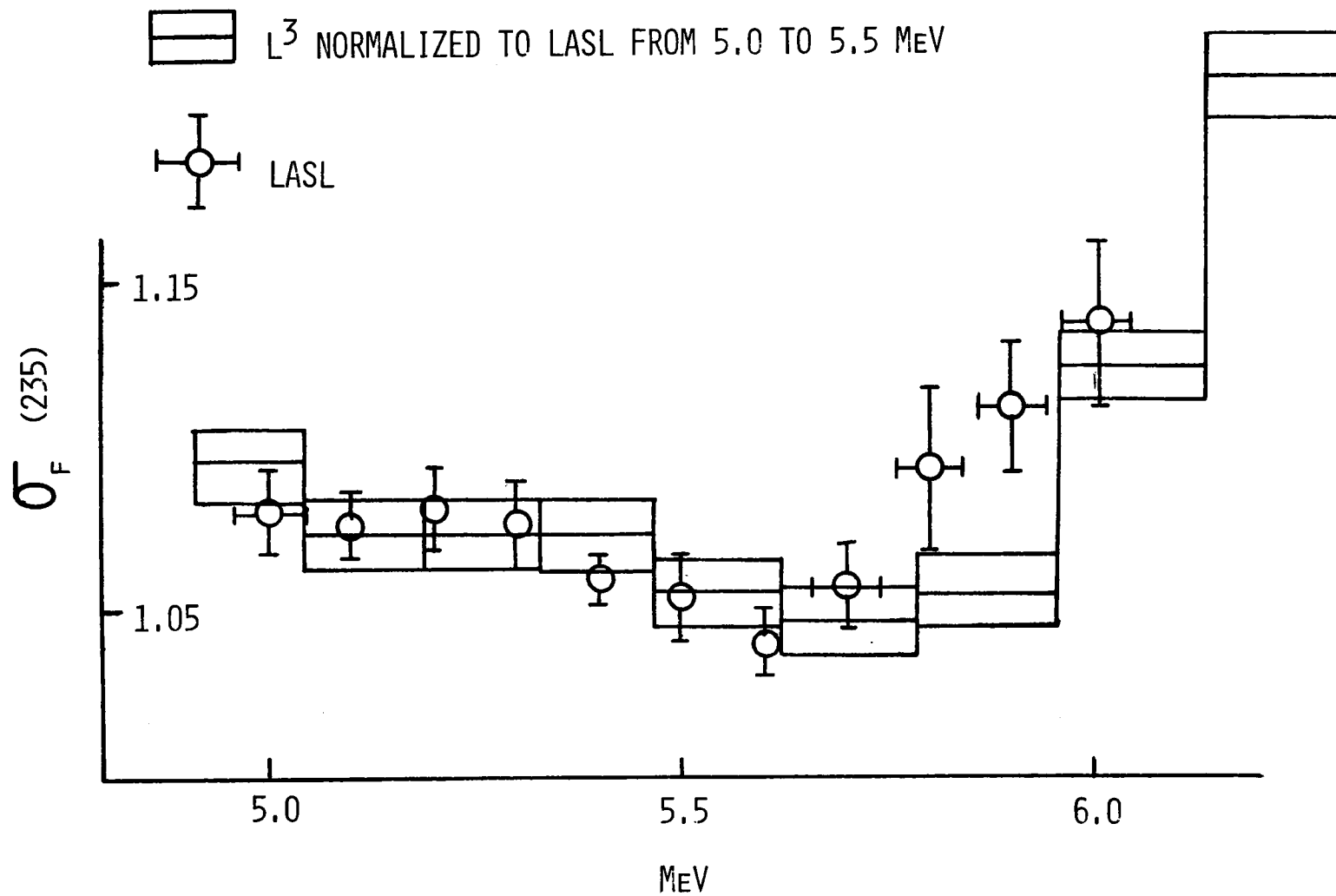


Fig. 1 See additional remarks by B. Diven

# ENERGY BIN WIDTHS AND STATISTICAL ERRORS

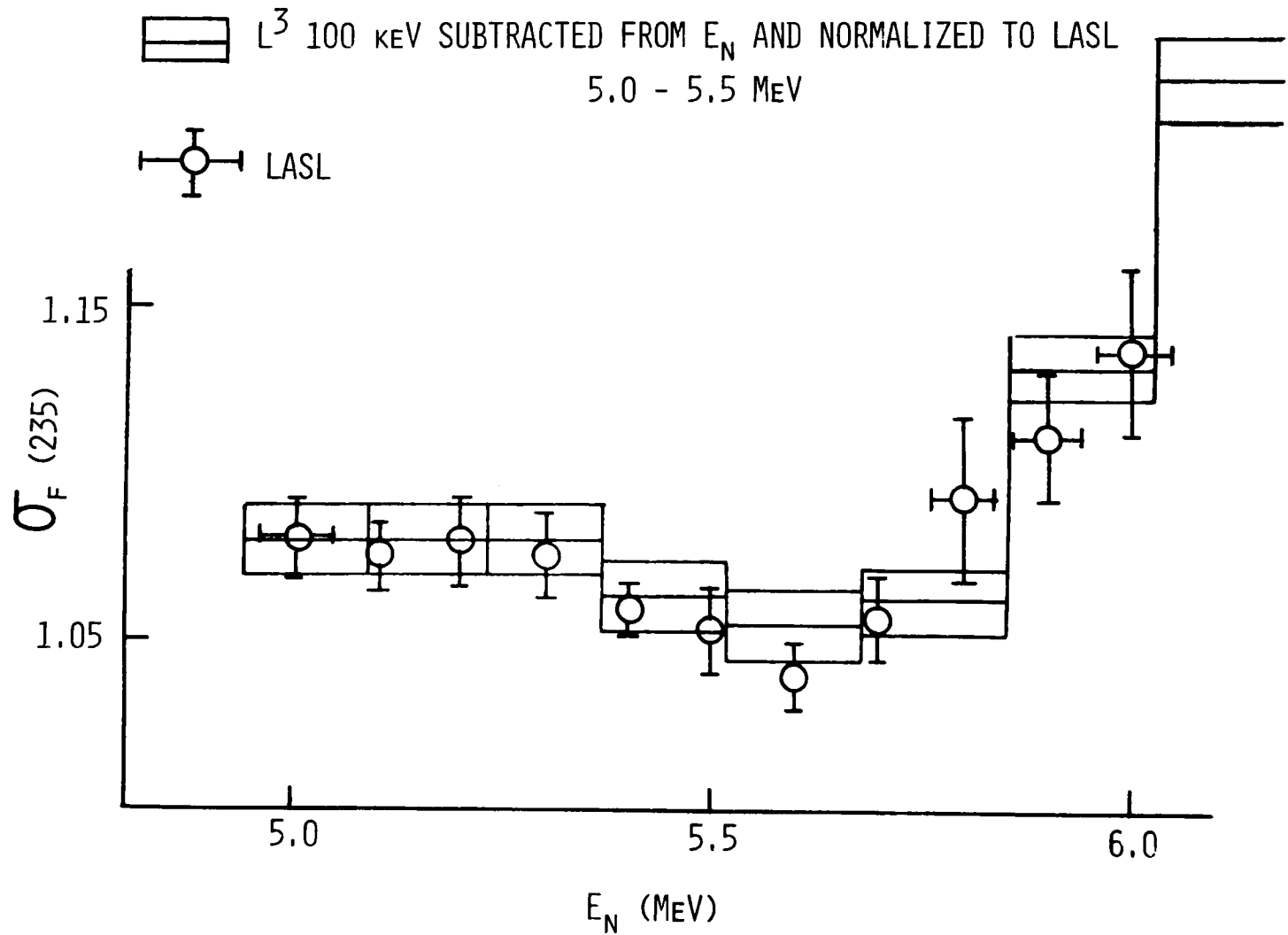


Fig. 2 See additional remarks by B. Diven

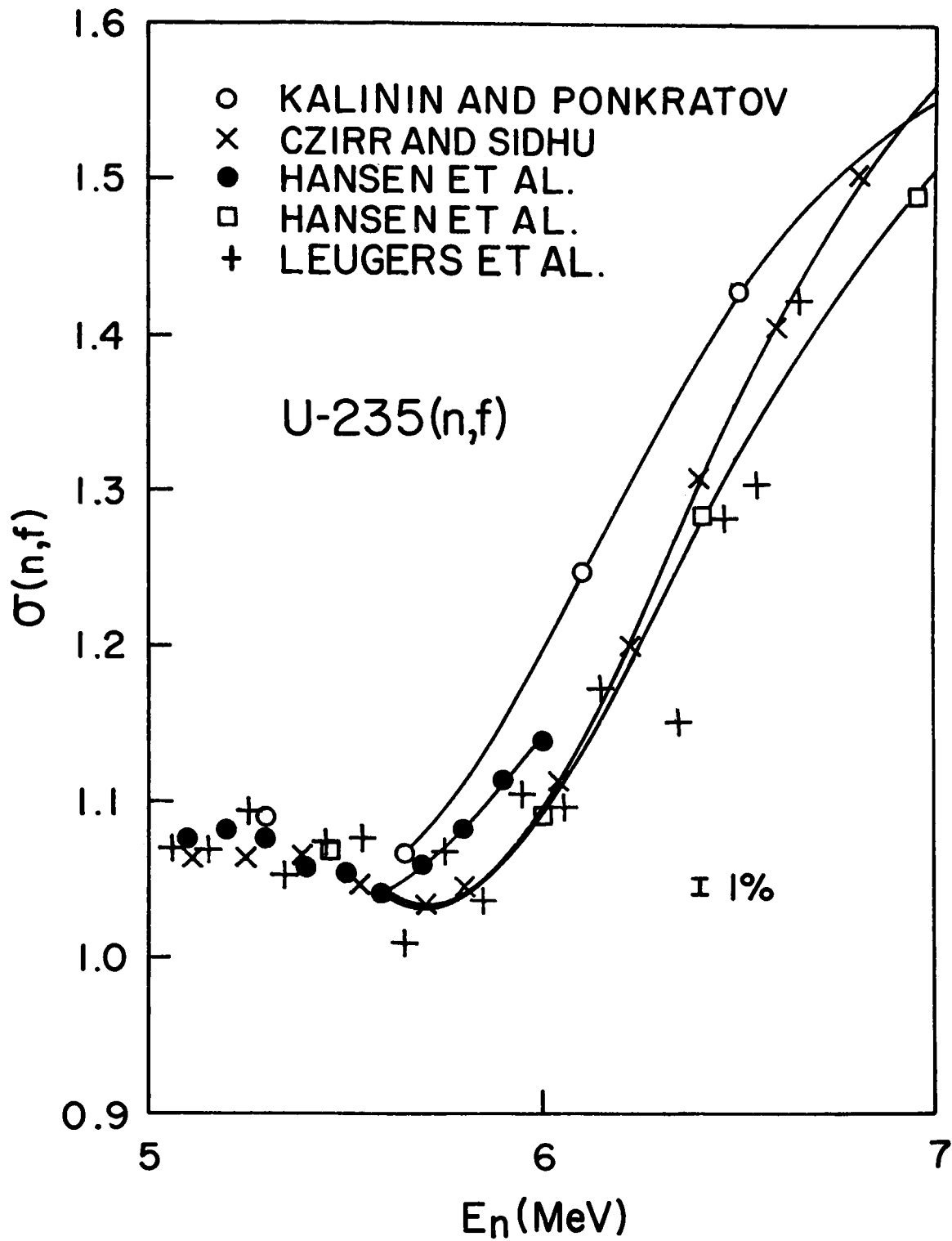


Fig. 3 See discussion by W. Poenitz

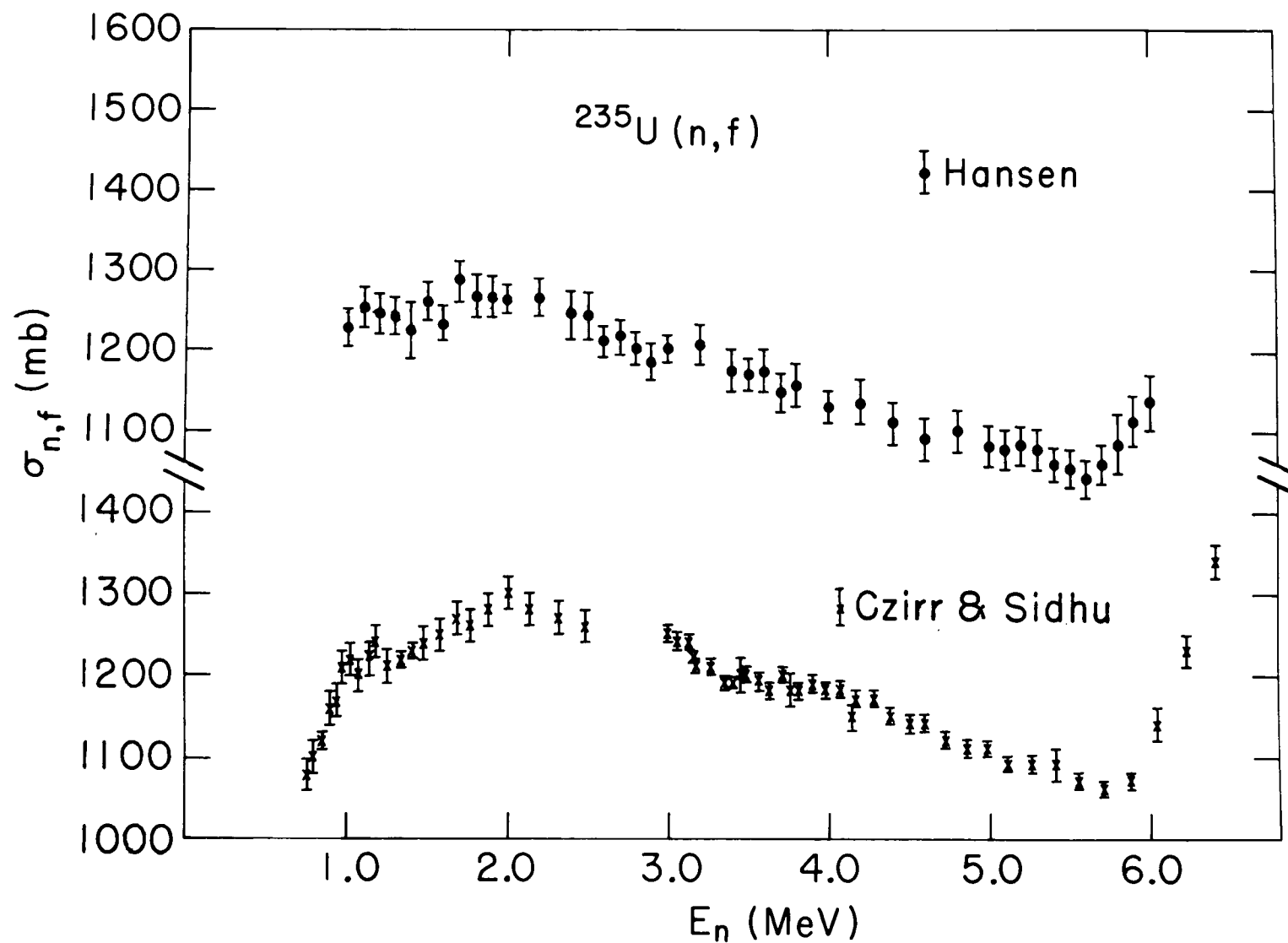


Fig. 4 See discussion by M. Bhat

THE  $^{235}\text{U}$  NEUTRON FISSION CROSS SECTION  
MEASUREMENT AT THE NBS LINAC

O. A. Wasson

National Bureau of Standards  
Washington, DC 20234, U.S.A.

ABSTRACT

The  $^{235}\text{U}$  neutron fission cross section was measured relative to neutron-proton scattering from 5 to 800 keV neutron energy. The experiment was performed on the 200 m flight path at the NBS electron linac using a hydrogen gas proportional counter as a neutron flux monitor. This relative measurement was normalized by means of a second experiment on the 23 m flight path. This experiment, which used a 0.5 mm  $^6\text{Li}$  glass for a flux monitor, covered the energy region from 6 eV to 30 keV, and, normalized to an integrated cross section of 238.4 eV b in the 7.8 to 11.0 eV region, yields an average cross section of  $2.48 \pm 0.05$  b for the 10 to 20 keV interval. The resultant cross section in the 200-800 keV interval is approximately 5% less than the ENDF/B-IV evaluation.

INTRODUCTION

This report contains the first results of a program at the National Bureau of Standards to improve the accuracy of the  $^{235}\text{U}(n,f)$  cross section in the kilovolt and megavolt energy region. This measurement, which covered the neutron energy interval from 5 keV to 800 keV, used a hydrogen proportional counter for a neutron flux monitor. The experiment, which was performed on the 200 m flight path of the NBS electron linac, yielded only a relative cross section. No attempt was made to make the measurement absolute by assessment of sample masses or detailed geometric dimensions. The same experimental arrangement was also used to measure the  $^6\text{Li}(n,\alpha)$  and  $^{10}\text{B}(n,\alpha\gamma)$  cross sections. The comparison of the three measurements provided us with confidence in the accuracy of the flux monitoring technique.

The relative cross section measurement was normalized by means of a second experiment utilizing the 23 m flight path. This measurement used a 0.5 mm  $^6\text{Li}$  glass scintillator for a flux monitor and covered the energy interval from 6 eV to 30 keV. Normalization was made to the integrated fission cross section from 7.8 to 11.0 eV.

## THE MEASUREMENT WITH THE HYDROGEN FLUX MONITOR

The  $^{235}\text{U}(n,f)$  cross section measurement using the hydrogen flux monitor was performed on the 200 m flight path. The linac operated with a 20 nsec pulse width, 100 MeV beam energy, 720 pps, and 4 kW of beam power on the water cooled neutron producing target. A one inch thick piece of polyethylene was employed as a moderator for the target. A fission chamber containing 10 surfaces each coated with approximately  $0.1 \text{ mg/cm}^2$  of  $^{235}\text{U}$  was placed at 69 m along the flight path with the plane of the plates normal to the beam direction. The neutron beam was collimated to a rectangular 10 cm by 10 cm beam size which was less than the active area of the fission chamber. The hydrogen counter was placed at the end of the 200 m beam line behind a 2.5 cm diameter collimator. The collimation was arranged so that both the fission chamber and the hydrogen counter could view the entire neutron source throughout the experiments. This guaranteed that both detectors would receive the same neutron flux shape. The output at both the hydrogen counter and fission chamber were sorted on-line simultaneously in both time-of-flight and pulse height and stored in the  $10^6$  words of a disk storage unit.

The geometry of the hydrogen counter is shown in Fig. 1. The counter is 5 cm in diameter and 60 cm long. The entrance window is composed of aluminum oxide ceramic. The high voltage connector was moved 15 cm downstream from the exit end of the counter to reduce backscattering. The counter gas consisted of hydrogen gas at atmospheric pressure with an admixture of 1.6% methane gas for quenching. This amount of methane assures that the neutron scattering from carbon is less than 0.5% of that from hydrogen for neutron energies less than 1 MeV. Subsequent measurements indicate that 0.1% methane would be adequate for quenching at this pressure.

The long length of the counter was chosen in order to minimize the end effect, which is the distortion in the detector gain caused by non-uniformities in the electric field near the end of the central electrode. The long length also reduces the effect of neutrons scattered from the exit window into the active volume of the gas to less than 0.5%. The neutron beam was collimated to a diameter of 2.5 cm in order to prevent the direct beam from striking the stainless steel cylindrical walls. This collimation provides a minimum path length of 1 cm in the gas for all recoil protons. Thus no recoil protons can collide with the cylindrical walls for neutron energies less than 100 keV. This restriction of the incident beam to the central 2.5 cm of the counter also reduces the timing spread of the counter from  $1.4 \text{ } \mu\text{sec}$  to  $0.6 \text{ } \mu\text{sec}$ . The corresponding timing spread for the fission chamber was 25 nsec. Careful measurements indicate that the relative zero timing uncertainty for the two counters was  $\pm 100 \text{ nsec}$ .

It was desired to keep the electronics as simple as possible. Thus the hydrogen counter was operated in an unusual manner in order to cover the 800:1 dynamic range of the experiment with only one amplifier setting. All events were recorded, although recoil proton events with energies greater than 25 keV all produced the same overload pulse amplitude. This required the use of leading edge timing and the resultant correction for the amplitude dependent timing shift. A typical hydrogen counter pulse height spectrum is shown in Fig. 2 for 19 keV incident neutrons. The fraction of the spectrum for several intervals is given. Approximately 1% of the events occur in a

high energy tail due to variations in gas multiplication while approximately 5% occur below the electronic threshold of approximately 1.1 keV.

The accuracy of the flux measurement is limited by the accuracy with which the number of events which occur below the electronic bias can be determined. The technique for doing this used the recoil proton ionization calibration determined by neutron time-of-flight for the neutron energy region from 1.5 to 15 keV. The ionization versus proton energy calibration was linear through this region and allowed the effective proton energy of the threshold to be determined from the extrapolation of this line to zero ionization. The validity of this technique does not depend on the shape of the ionization versus proton energy below the threshold. I have checked this technique by observing the change in the  $^{235}\text{U}$  cross section as both the bias channel and the energy calibration is varied during data analysis and conclude that the uncertainty in the threshold energy is  $\pm 0.05$  keV. Thus the accuracy of the method depends on neutron energy. It is  $\pm 1.3\%$  at 5 keV and improves with increasing energy.

Backgrounds were measured throughout the energy range by the resonance filter technique and were found to be largely ambient, that is independent of the linac operation, for both detectors. The ambient background is large at low energies (30% at 5 keV for the flux monitor) and, along with the bias calibration, forms the dominant flux uncertainty in this region ( $\pm 2\%$  at 5 keV).

The determination of the neutron flux incident on the fission chamber at 69 m requires that the flux measurement at 200 m be corrected for neutron attenuation in the intervening materials. These include the aluminum in the fission chamber, the beam pipe windows, 3.4 meters of air, and the aluminum oxide entrance window of the hydrogen counter. This correction reaches a maximum of 25% at the 35 keV aluminum resonance with a corresponding uncertainty of  $\pm 2.5\%$  in the cross section. The correction and its associated error in the cross section are much lower at other energies.

The response of the fission chamber, as shown in Fig. 3, was found to be constant throughout the neutron energy region of interest. The background was again largely ambient, but was much less (3% at 5 keV) than the flux monitor. The multiple scattering contribution to the fission chamber yield was calculated to be  $(0.18 \pm 0.02)\%$  per barn of the aluminum cross section by Czirr [1].

The various systematic errors in the relative cross section are plotted in Fig. 4 along with the total rms error. The systematic error is dominated by the flux monitor and reaches a maximum of  $\pm 2.5\%$  in the aluminum resonances and in the high energy region and is typically  $\pm 1\%$  elsewhere.

A total of two separate measurements of the  $^{235}\text{U}$  fission cross section were made over an eight month period. The thickness of the boron overlap filter and the electronic threshold was varied, but the gross shape of the cross sections agreed within statistical error. The final result is presented as a weighted sum of the two experiments and will be presented after the normalization measurement is described. It is emphasized that the shape of the cross section as measured with the hydrogen flux monitor is independent of the normalization experiment.

# THE MEASUREMENT WITH THE $^6\text{Li}$ FLUX MONITOR

The shape of the  $^{235}\text{U}$  cross section in the 5 to 800 keV interval was normalized by a set of measurements carried out on the 23 m flight tube. The experimental layout is shown in Fig. 5. A  $5 \times 5 \times 0.05$  cm plate of  $^6\text{Li}$  glass scintillator with the plane of the glass normal to the neutron beam was used as a flux monitor. A thin aluminum cylindrical can surrounded the glass to serve as a light reflector for the single photomultiplier tube which was positioned out of the neutron beam. The fission chamber was about 1 m downstream from the flux monitor. The beam was collimated to a 10 cm by 10 cm square size by a 1 m thick concrete wall. The thermal neutron background was reduced by Cd shielding near both detectors. This same  $^6\text{Li}$  glass detector was also used to measure the  $^6\text{Li}(n,\alpha)$  cross section relative to hydrogen scattering on the 200 m flight path.

Two measurements were made using a 20 nsec linac pulse width. The first extended from 2 eV to 5 keV using a  $^{238}\text{U}$  filter for background measurements at 6.7, 20.9, and 36.8 eV and a cadmium overlap filter. The linac pulse rate was 240 per second and the flight time channel widths were 1.024  $\mu\text{sec}$ . A second measurement covered the energy interval from 800 eV to 100 keV using B, Cd, Al, and NaCl as filters for background and overlap. The linac pulse rate was 600 per second and the flight time channel widths were 64 nsec. The backgrounds were typically 3% in both detectors. The zero timing of both detectors was determined from the  $\gamma$ -ray flash measurements during the linac beam pulse and compared by means of the common structure in the neutron flux. The response of the fission chamber was the same as that observed in Fig. 3 while that of the  $^6\text{Li}$  glass is shown in Fig. 6. Both spectra were constant throughout the neutron energy range of the experiment.

The data were analyzed in the following manner: The background, as determined from a linear extrapolation between the absorption dips, was subtracted from both detector yields. The  $^6\text{Li}$  yield was corrected for self-protection and multiple scattering in both the glass and the Al reflector. The fission chamber yield was corrected for transmission losses between the centers of the two detectors. The ratio of the fission chamber yield to  $^6\text{Li}$  yield for the same neutron energy interval was calculated for each fission time-of-flight channel. The ratio was multiplied by the  $^6\text{Li}(n,\alpha)$  cross section obtained by the Los Alamos R-Matrix code [2] to produce the  $^{235}\text{U}$  relative cross section. This relative cross section was integrated over selected energy intervals and normalized in the low energy region. This normalization constant was applicable to both measurements since the detectors were not moved.

The integral of the  $^{235}\text{U}$  fission cross section from 7.8 to 11.0 eV was normalized to a value of 238.4 barn eV. This is the value obtained from the measurement of Deruytter and Wagemans [3] after renormalization to a thermal cross section of 583.5 b. This normalization then yields an average cross section of  $2.48 \pm 0.05$  barns for the 10 to 20 keV energy interval. The error includes the rms statistical and systematic error in the NBS measurement, but not the error in the reference standard. This value is used to normalize the relative measurement made with the hydrogen flux monitor.

## EXPERIMENTAL RESULTS

The results of the measurement with the  $^6\text{Li}$  flux monitor are listed in Table I. The average cross section for the given energy interval is listed along with the statistical error (standard deviation). The systematic error due to background uncertainty of  $\pm 1\%$  and the normalization error are not listed. The average cross section for various energy intervals measured with the hydrogen flux monitor are listed in Table II. Both the standard deviation in the cross section due to statistics and the root mean square systematic errors are listed. The normalization error is not included in the systematic error.

A comparison of the two experiments in the region of overlap (6-30 keV) shows that the cross section from the hydrogen monitor is 5.3% greater than the cross section from the  $^6\text{Li}$  monitor for the interval from 6 to 10 keV while the agreement is within 1% for the 10-30 keV region. This difference in the 6-10 keV region still remains after several months of reanalysis. Because of the excellent results obtained for the  $^6\text{Li}(n, \alpha)$  and  $^{10}\text{B}(n, \alpha\gamma)$  measurements in the region below 10 keV from the hydrogen flux monitor and the more thorough testing of the hydrogen monitor, I am using the results from the hydrogen monitor as the correct  $^{235}\text{U}$  cross section for the 6-10 keV interval.

The results of the measurement with the  $^6\text{Li}$  flux monitor are compared with the results of Gwin et al [4], Czirr and Sidhu [5], and Wagemans and Deruytter [6] in Fig. 7. Due to the holes in the neutron flux of the present measurement, comparisons for the entire neutron energy interval from 7 eV to 30 keV are not possible. Only those values which are averaged over the same energy region are shown. All data sets have been renormalized to a thermal cross section of 583.54 b. Shown is the ratio of each result to the present experiment. The error bars include the statistical error of the present experiment as well as the error of the other experiment when given. The horizontal line indicates the NBS measurement. The results of the present experiment, Gwin et al, and Czirr and Sidhu appear to agree quite well (within  $\pm 4\%$ ) over nearly the entire energy region. The results of Wagemans and Deruytter are consistently 6-8% higher in the region above 1 keV and are even larger than the NBS results with the hydrogen monitor.

In Fig. 8 the hydrogen based data is shown as a histogram while the smooth curve is drawn through the data of Poenitz [7]. The NBS results are approximately 3% lower throughout the region from 40 - 800 keV although the agreement in shape is much better.

In order to compare the present results with other data sets in more detail, I shall show the ratios in the following figures. In Fig. 9 the ratio of the ENDF/B-IV evaluation [8] to the NBS hydrogen based data is shown. In order to more clearly show the systematic differences, I have only included the NBS statistical error. The NBS cross section is approximately 5% lower above 100 keV and is in rough agreement below 40 keV.

The ratio of the data of Gayther et al [9] to the NBS hydrogen based data is shown in Fig. 10. The two sets have been normalized to each other in the 10 to 20 keV interval. Again only the statistical error from the NBS data is shown. The two measurements appear to agree in detail except in the 40-80 keV region where the difference is as large as 4%.

The results of Gwin et al [4] are shown in Fig. 11. This data was re-normalized to a thermal cross section of 583.5 b and corrected for the  $^{10}\text{B}(n,\alpha)$  cross section given by the recent Los Alamos R-Matrix fit [2]. The NBS data is approximately 5% larger below 10 keV and 5% smaller in the 40-80 keV region. However, the average cross sections agree within 1% throughout the 100 to 200 keV region.

It thus appears that the general shapes of the four data sets agree within  $\pm 2\%$  throughout the region from 10 keV to 800 keV, if the local deviations (from 40-80 keV and from 5-10 keV) are ignored. In order to further clarify the situation and to see if the differences in absolute value of the data sets is the result of different normalization procedures, it is worthwhile to examine ratios between cross sections.

### $^{235}\text{U}$ TO $^6\text{Li}$ CROSS SECTION RATIOS

Three recent measurements of the  $^{235}\text{U}(n,f)$  to  $^6\text{Li}(n,\alpha)$  cross section ratios are now available. Czirr and Sidhu [5] have carried out measurements using an electron linac and  $^6\text{Li}$  glass. Poenitz [10] has carried out preliminary measurements using the Van de Graaff accelerator and a back-to-back ionization chamber with absolute mass determination. Both experiments were normalized at thermal energies. Lamaze at NBS [11] has measured the  $^6\text{Li}(n,\alpha)$  cross section relative to the hydrogen flux monitor on the 200 m flight path with  $^6\text{Li}$  glass. This result is combined with the  $^{235}\text{U}$  measurement in the same facility to provide the NBS ratio. Here the cross sections are normalized in the kilovolt region for Li and the 7.8 to 11.0 eV region for  $^{235}\text{U}$ . Since the ratio varies by a factor of 10, the relative ratios of the different experiments will be plotted in order to emphasize the differences. The NBS ratios are compared with the early ratios of Czirr and Sidhu in Fig. 12 and to those of Poenitz in Fig. 13. The total listed statistical errors are included. The ratios have not been corrected for different thermal normalizations which can change the absolute values by less than 0.8%.

In Fig. 13, where the NBS ratio is divided by the Poenitz ratio, there is an oscillation in the 200-350 keV region which is probably due to an energy calibration difference near the 240 keV Li resonance. Except for the local variation, the shape difference is less than 4% from 60 to 600 keV. In Fig. 12 the NBS ratios are divided by the ratios of Czirr and Sidhu. Except for a 4-8% drop in the 20-80 keV region, the shape difference throughout the region from 6 keV to 600 keV is less than 3%. I conclude that, except for local variations, the three measurements agree in shape to within 4%.

It is interesting, however, to note that the absolute value of the NBS ratio is approximately 5% larger than the other two measurements in spite of the fact that all three measurements are normalized, either directly or indirectly, to thermal cross sections which differ by less than 0.8%. This would also imply that the  $^{235}\text{U}$  cross sections as measured by Poenitz and by Czirr and Sidhu would be lower than the NBS value by approximately 4-5%.

#### SUMMARY

The shape of the  $^{235}\text{U}$  neutron fission cross section was measured relative to n-p scattering for the interval from 5 keV to 800 keV with a typical uncertainty of  $\pm 2\%$ . A separate experiment using a  $^6\text{Li}$  glass flux monitor provided a normalization of  $2.48 \pm 0.05$  b for the 10 to 20 keV interval which was based on a fission integral of 238.4 eV b for the 7.8 to 11.0 eV region. This lithium-based data agreed within  $\pm 2\%$  with the results of Gwin et al throughout most of the energy region from 6 eV to 30 keV. This normalization produces a hydrogen-based cross section in the 200-800 keV interval which is approximately 5% less than the ENDF/B-IV evaluation. A comparison of the hydrogen based data with a few data sets shows general agreement with the shape of Gayther throughout the 5 keV to 800 keV region and that of Poenitz from 40 keV to 800 keV. However, there are differences in normalizations which are not resolved by the recent measurements of the  $^{235}\text{U}(n,f)$  to  $^6\text{Li}(n,\alpha)$  ratios.

It should be emphasized that the relative cross section measurement with the hydrogen counter is a separate experiment independent of the normalization results from the lithium flux monitor. Thus different normalizations will not change the validity of the hydrogen based results. The relatively minor disagreement between the two measurements in the 6-10 keV region is of some concern. However, because of the greater effort spent on the hydrogen counter measurements and the excellent results obtained in the  $^6\text{Li}(n,\alpha)$  and  $^{10}\text{B}(n,\alpha\gamma)$  experiments with the same monitor, the author recommends the results listed in Table II for the cross section for this energy region.

This represents the first contribution by the Neutron Standards Section to the measurement of the  $^{235}\text{U}(n,f)$  standard cross section. It is planned to reduce the errors and expand the energy range in future experiments.

#### ACKNOWLEDGMENTS

The author acknowledges the many discussions with Drs. R. Gwin and J. B. Czirr during the course of the experiments. The advice and insights of Dr. C. D. Bowman is appreciated. The stimulating discussion and assistance of my colleagues, Drs. A. D. Carlson, G. P. Lamaze, and R. A. Schrack, made this initial voyage on the sea of neutron standards a memorable event.

## REFERENCES

1. J. B. CZIRR, Lawrence Livermore Laboratory, Private Communication (1976).
2. G. R. HALE, Private Communication to G. Lamaze (1976).
3. A. J. DERUYTTER and C. WAGEMANS, "Measurement and Normalization of the Relative  $^{235}\text{U}$  Fission Cross Section in the Low Resonance Region," *J. Nucl. Energy*, 25, 263 (1971).
4. R. GWIN et al, "Measurement of the Neutron Capture and Fission Cross Sections of  $^{239}\text{Pu}$  and  $^{235}\text{U}$ , 0.02 eV to 200 keV, the Neutron Capture Cross Sections of  $^{197}\text{Au}$ , 10 to 50 keV, and Neutron Fission Cross Sections of  $^{233}\text{U}$ , 5 to 200 keV," *Nucl. Sci. Eng.*, 59, 79 (1976).
5. J. B. CZIRR and G. S. SIDHU, "A Measurement of the Fission Cross Section of  $^{235}\text{U}$  from 100 eV to 680 keV," UCRL Report 77377, Lawrence Livermore Laboratory (Oct. 1975).
6. C. WAGEMANS and A. J. DERUYTTER, "The Neutron Induced Fission Cross Section of  $^{235}\text{U}$  in the Energy Region from 0.008 eV to 30 keV," *Ann. Nucl. Energy*, (submitted for publication 1976).
7. W. P. POENITZ, "Relative and Absolute Measurements of the Fast-Neutron Fission Cross Section of Uranium-235," *Nucl. Sci. Eng.*, 53, 370 (1974).
8. ENDF/B-IV, distributed by National Neutron Cross Section Center at Brookhaven National Laboratory (1975).
9. D. B. GAYTHER, D. A. BOYCE, and J. B. BRISLAND, "Measurement of the U-235 Fission Cross Section in the Energy Range 1 bev to 1 MeV," *Proc. Panel on Neutron Standard Reference Data*, 201 (1972).
10. W. P. POENITZ, Private Communication of Preliminary Data (Jan. 30, 1976).
11. G. P. LAMAZE, National Bureau of Standards, Private Communication (1976).

TABLE I

The average  $^{235}\text{U}(n,f)$  cross sections measured at the 23 m flight path with the  $^6\text{Li}$  glass flux monitor. The data is normalized to an integral cross section of 238.4 eV barn in the 7.8 to 11.0 eV interval. There is a  $\pm 1\%$  systematic error, excluding the normalization error.

E(lower),eV	E(upper),eV	$\sigma$ , barns	statistical error $\pm \Delta \sigma$ , b
7.8	11.0	74.5	0.6
7.4	10.0	85.2	0.7
10.68	13.7	47.5	0.5
13.7	17.6	31.2	0.4
22.6	29.0	43.1	0.5
10.0	15.0	43.5	0.4
15.0	20.5	58.6	0.5
22.0	33.0	34.2	0.3
41.0	50.0	34.8	0.4
70.0	100.0	26.2	0.3
100	200	20.3	0.2
200	300	19.9	0.2
400	500	13.1	0.2
500	600	14.3	0.2
600	800	10.9	0.2
800	1000	7.20	0.10
1,keV	2,keV	6.86	0.06
4	5	3.95	0.07
6	7	3.13	0.06
7	8	2.98	0.06
8	9	2.81	0.06
9	10	3.00	0.06
10	20	2.48	0.02
20	30	2.097	0.02

TABLE II

The average  $^{235}\text{U}(\text{n},\text{f})$  cross sections measured with the hydrogen flux monitor. The data is normalized to a value of 2.48 b in the 10 to 20 keV region. The listed systematic errors do not include a contribution from the normalization error.

---

E (lower),keV	E(upper), keV	$\sigma, \text{b}$	$\Delta\sigma, \text{b}^a$	$\Delta\sigma, \text{b}^b$
5	6	3.96	.04	.09
6	7	3.27	.04	.07
7	8	3.23	.04	.06
8	9	2.94	.04	.05
9	10	3.14	.04	.05
10	20	2.48	.01	.04
20	30	2.11	.02	.03
30	40	1.94	.02	.04
40	50	1.78	.02	.02
50	60	1.75	.02	.02
60	70	1.70	.02	.02
70	80	1.62	.02	.02
80	90	1.58	.02	.02
90	100	1.58	.02	.02
100	150	1.44	.01	.02
150	200	1.37	.01	.02
200	300	1.23	.01	.02
300	400	1.17	.01	.02
400	500	1.14	.01	.02
500	600	1.11	.01	.02
600	700	1.10	.01	.02
700	800	1.08	.01	.02

---

<sup>a</sup>Statistical standard deviation.

<sup>b</sup>Systematic root mean square.

## GAS COUNTER GEOMETRY

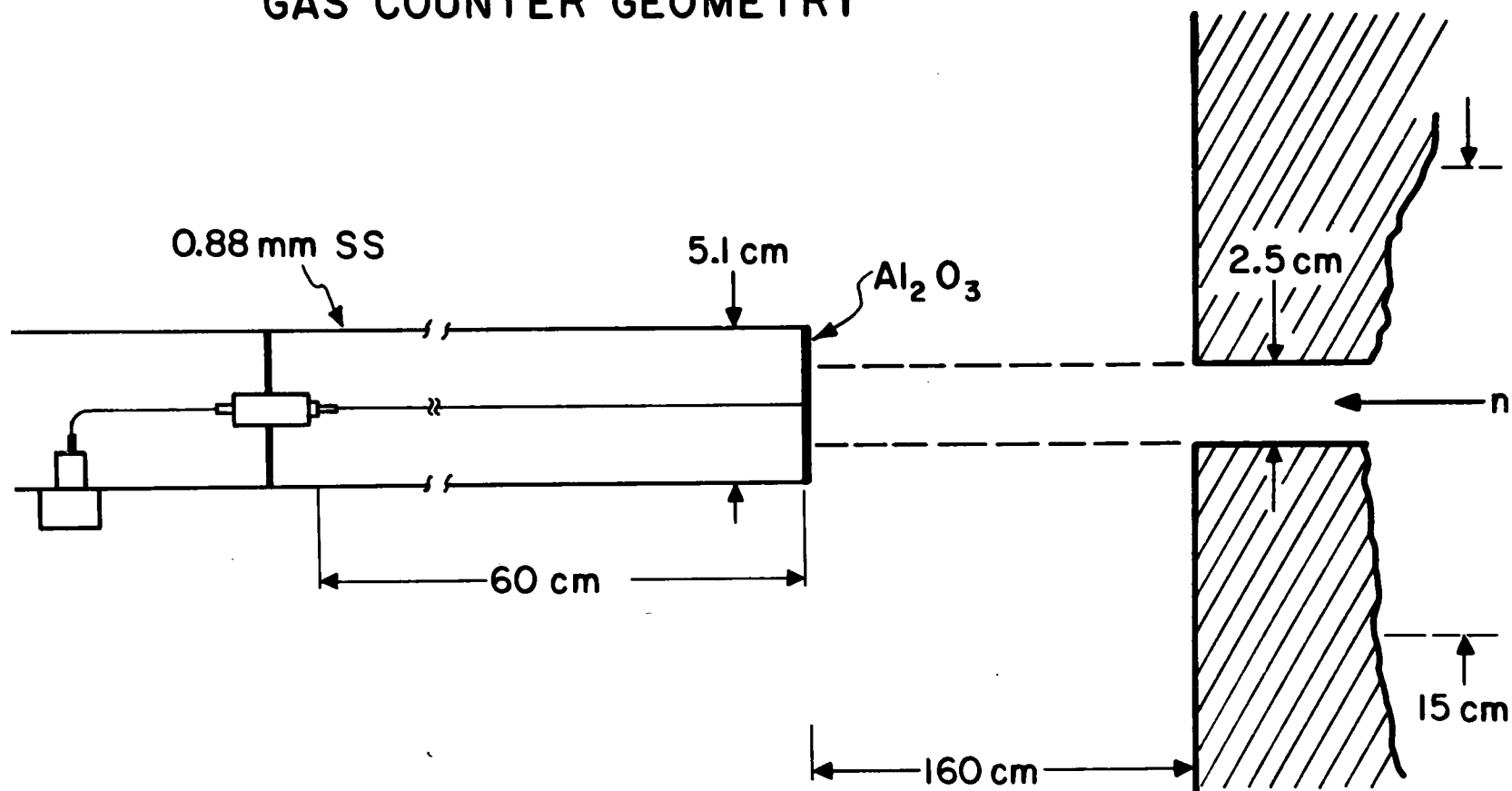


Fig. 1. Experimental geometry for hydrogen counter.

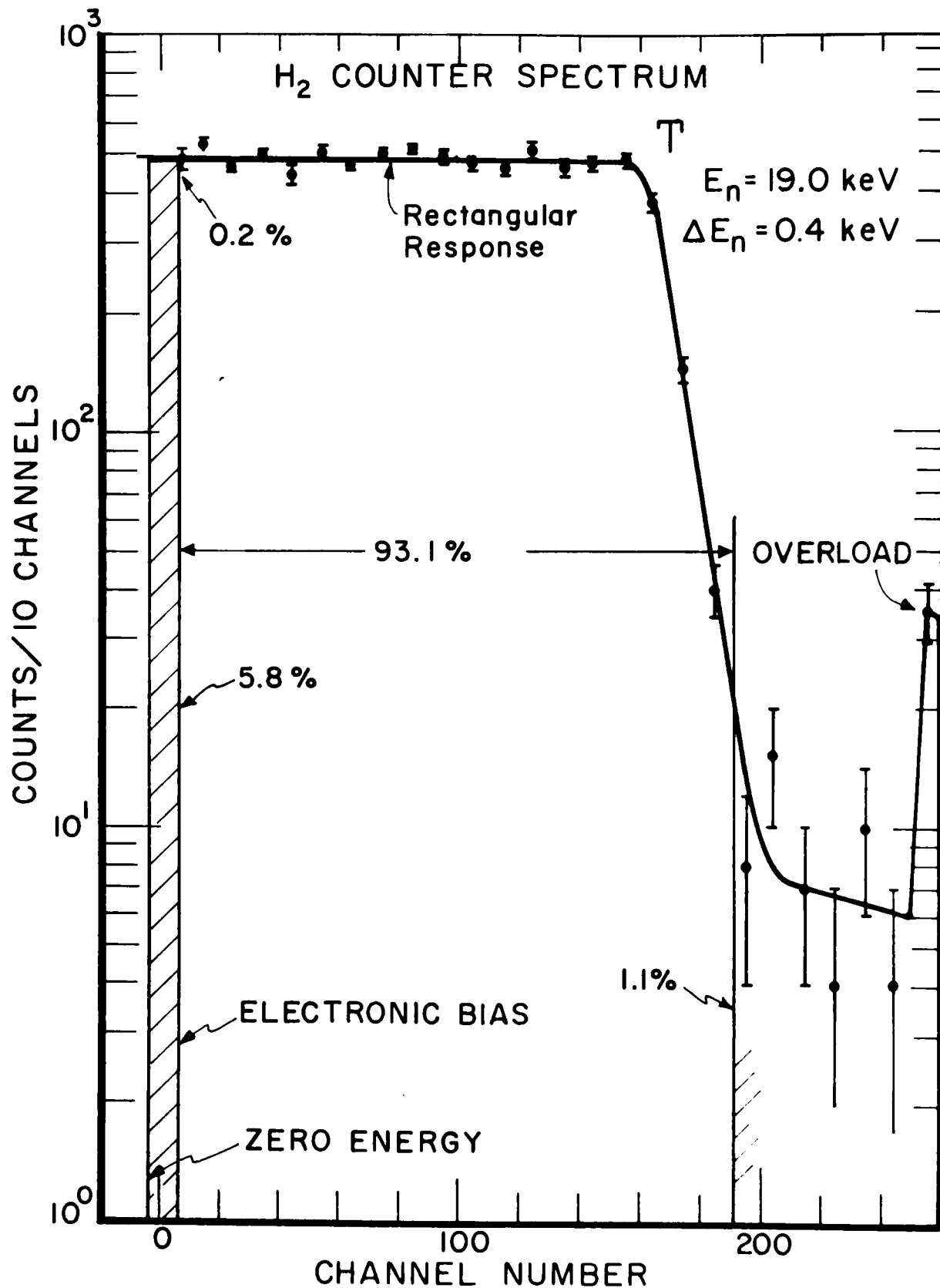


Fig. 2. Hydrogen counter pulse height spectrum for 19 keV neutrons.

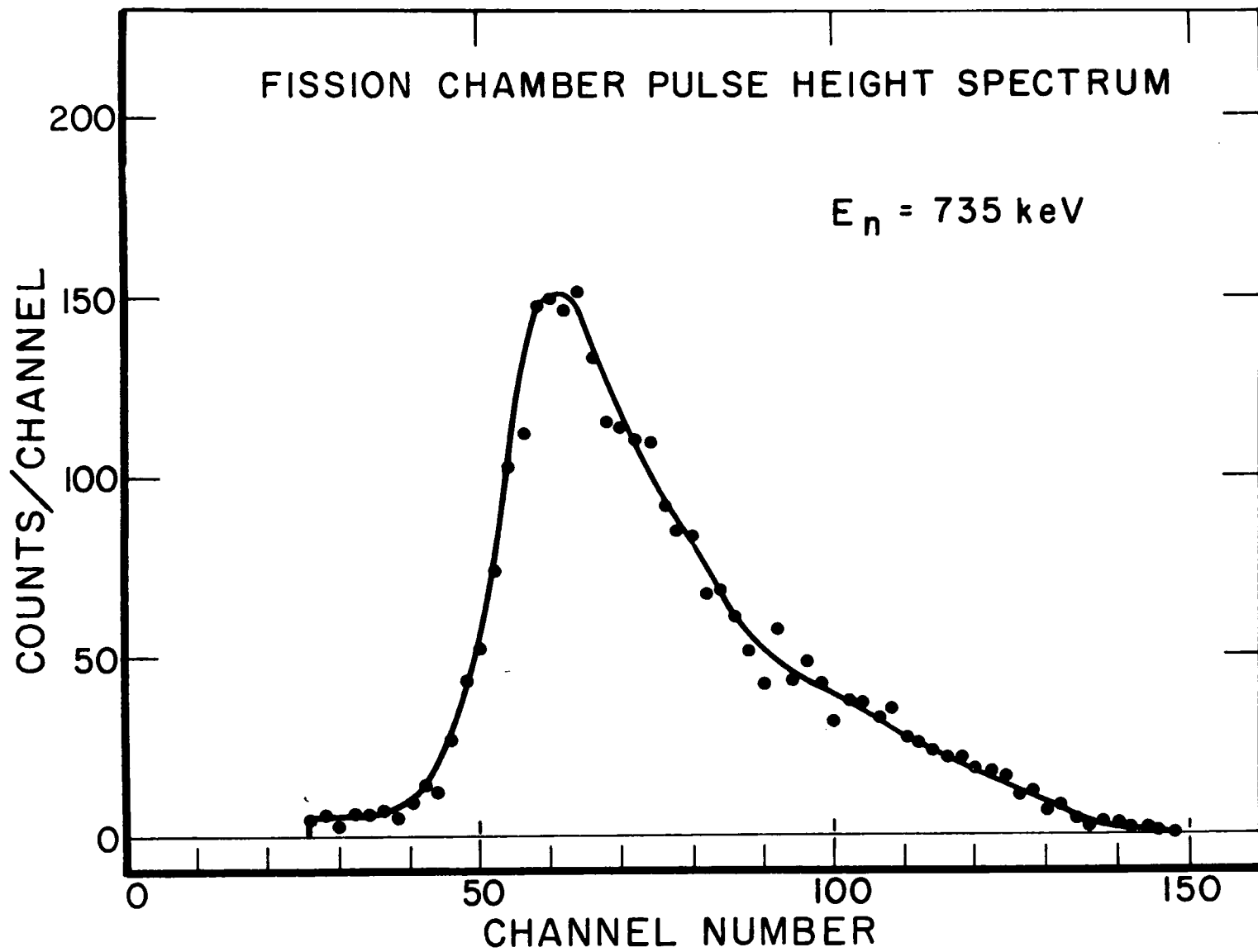


Fig. 3. Fission chamber pulse height spectrum.

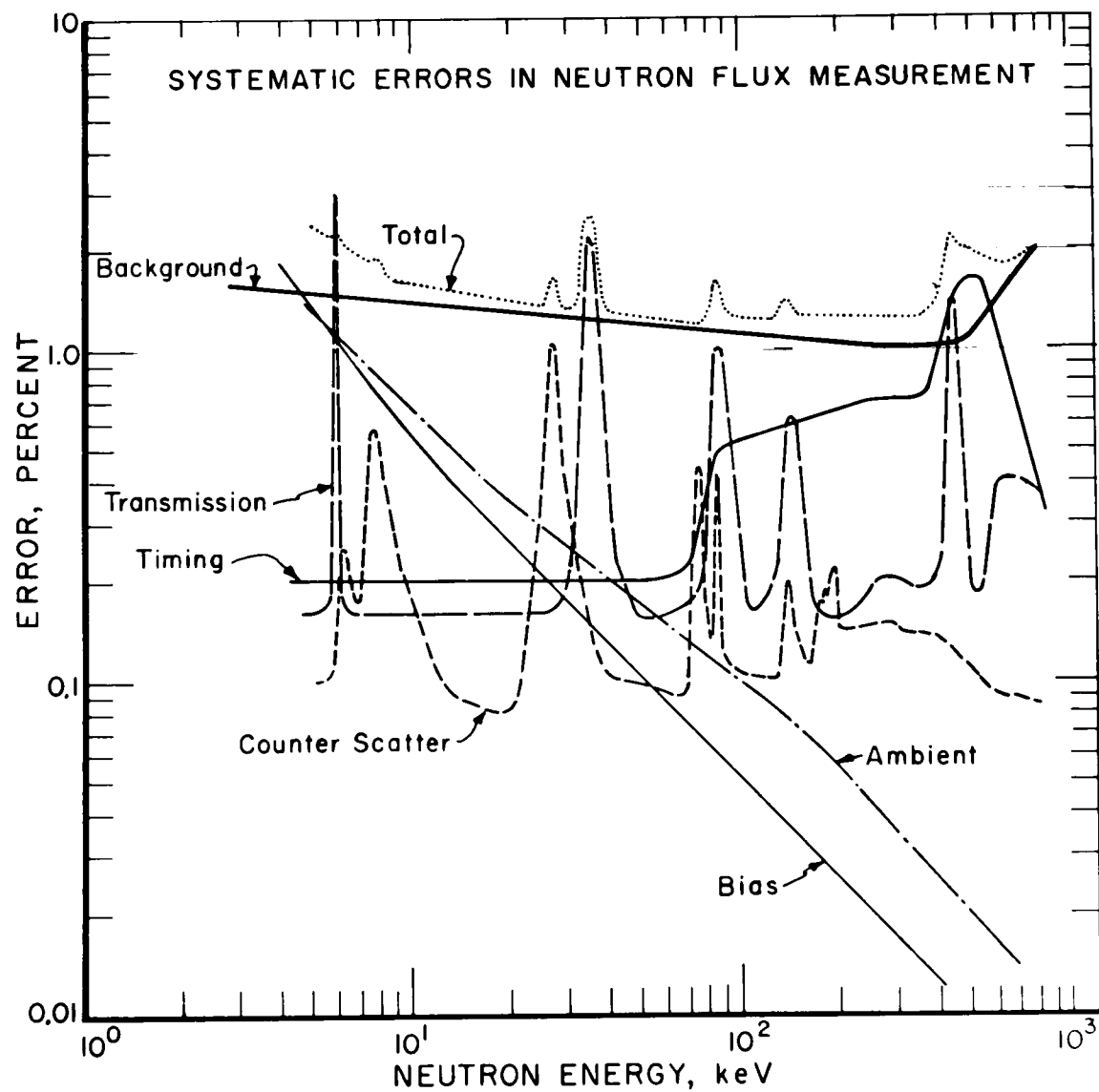


Fig. 4. Systematic errors for the  $^{235}\text{U}$  cross section.

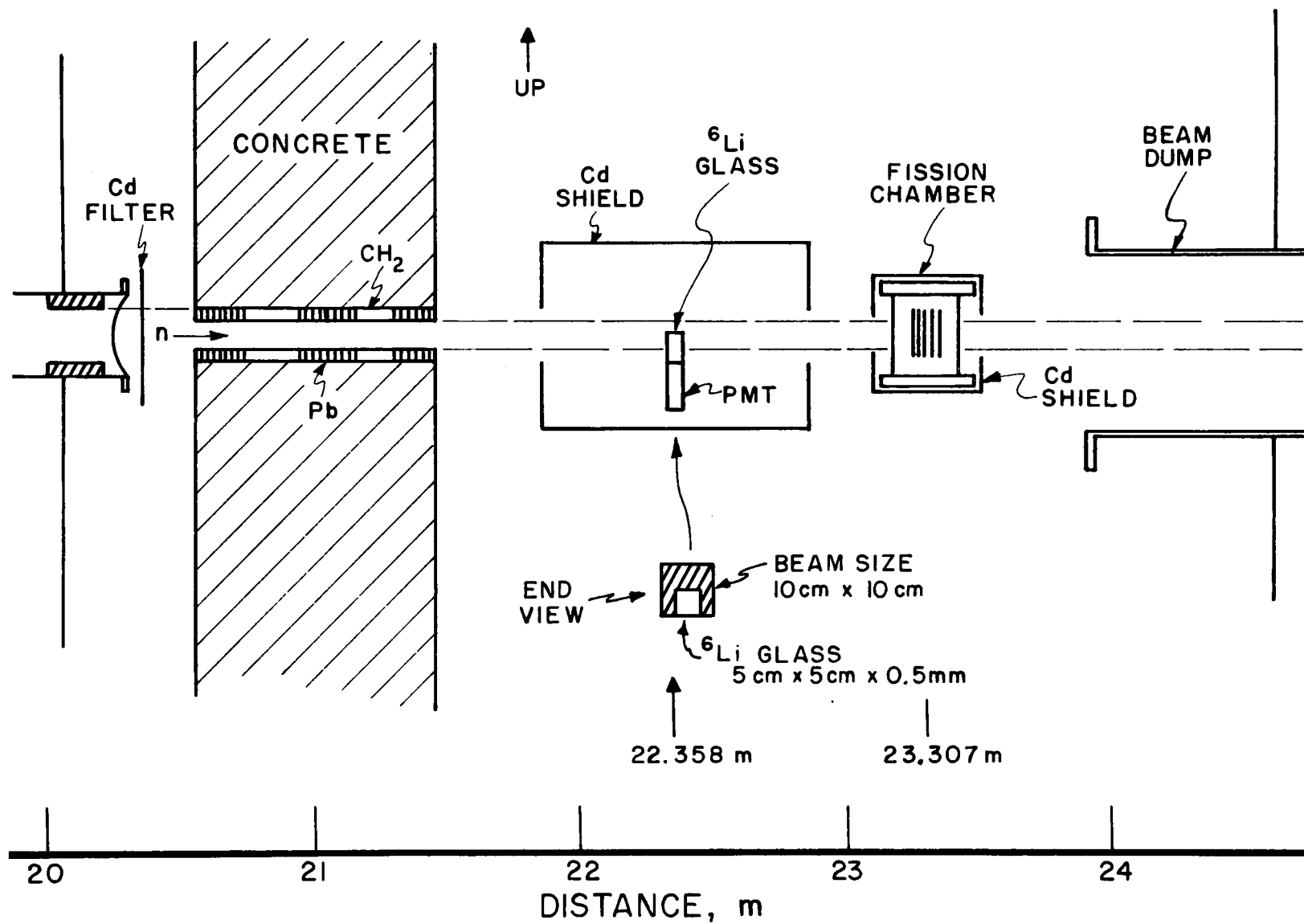


Fig. 5. Experimental geometry for the 23 m station.

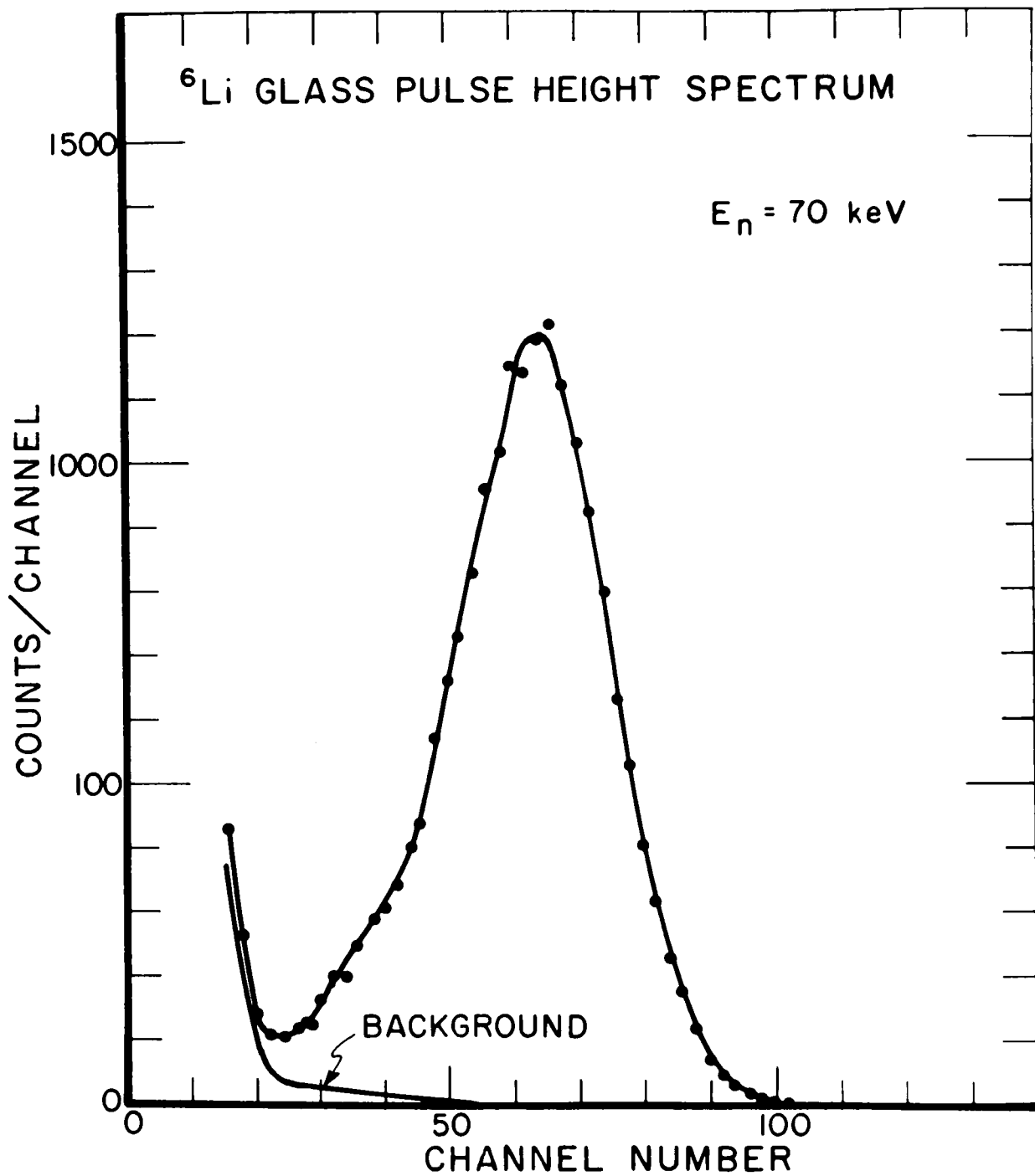


Fig. 6.  $^6\text{Li}$  glass pulse height spectrum.

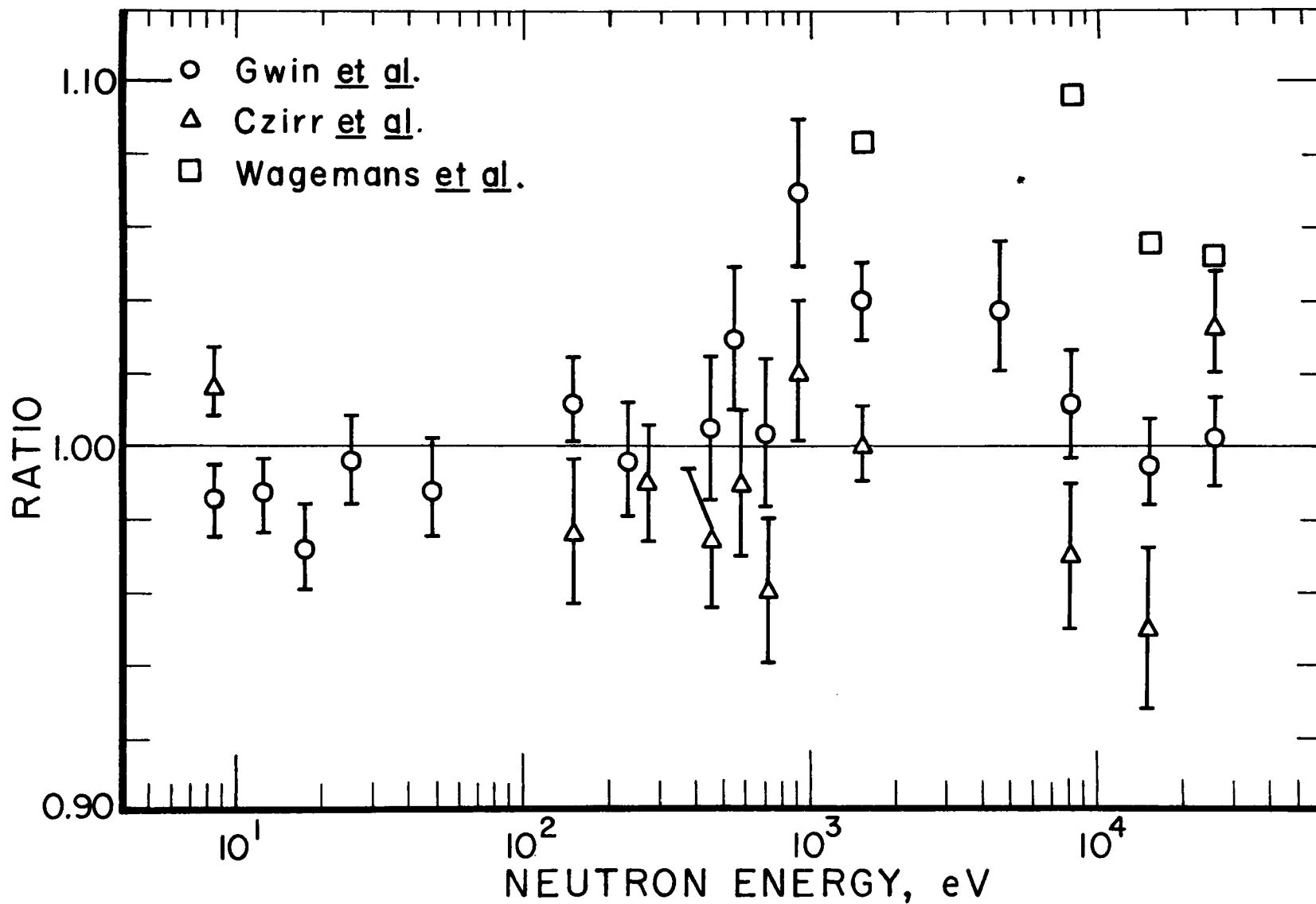


Fig. 7.  $^{235}\text{U}$  fission cross section measurements for three experimenters divided by the NBS cross section measured with the Li glass monitor.

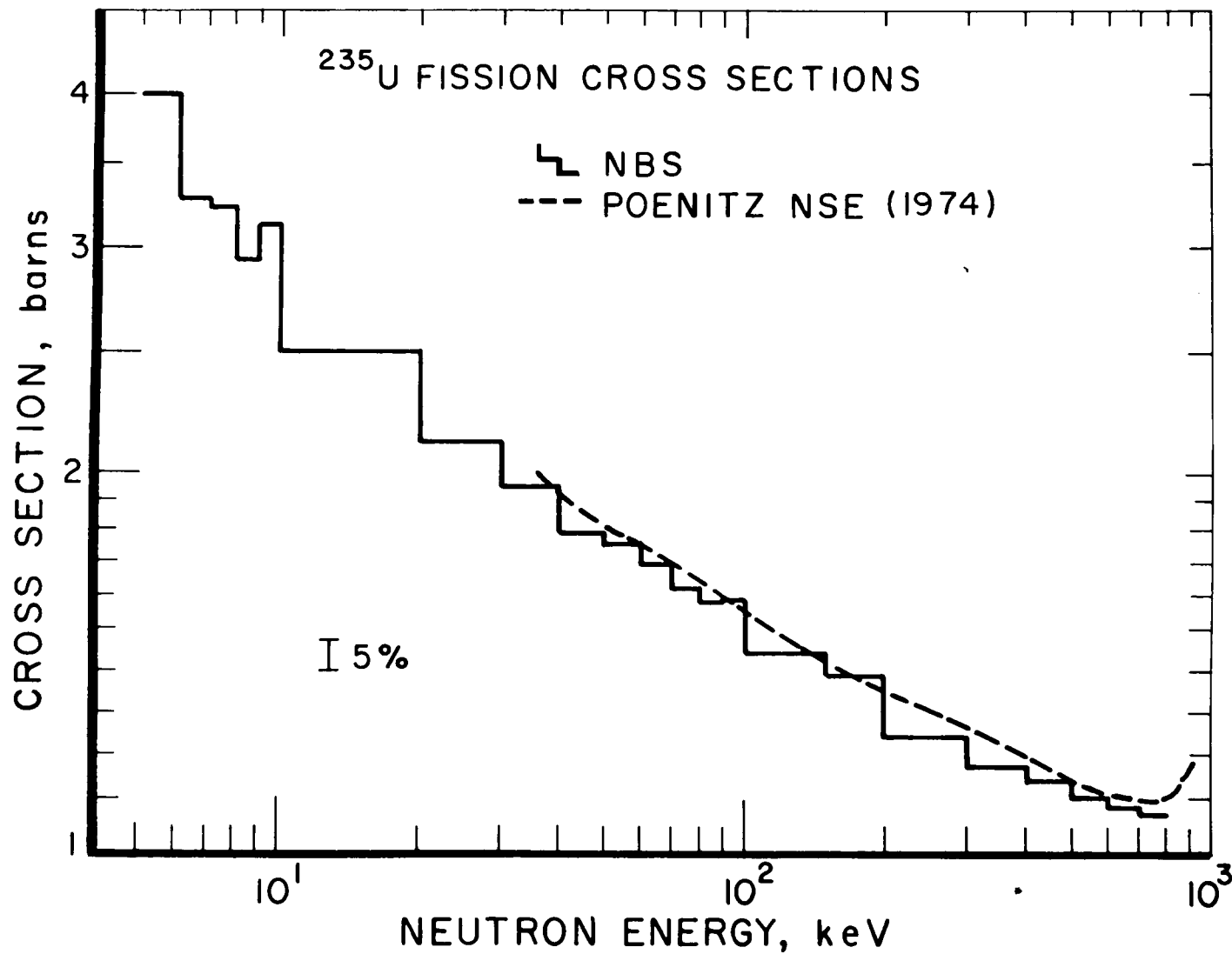


Fig. 8. The  $^{235}\text{U}$  fission cross section results. The NBS hydrogen based data are shown by the histogram while the results of Poenitz are shown by the smooth curve.

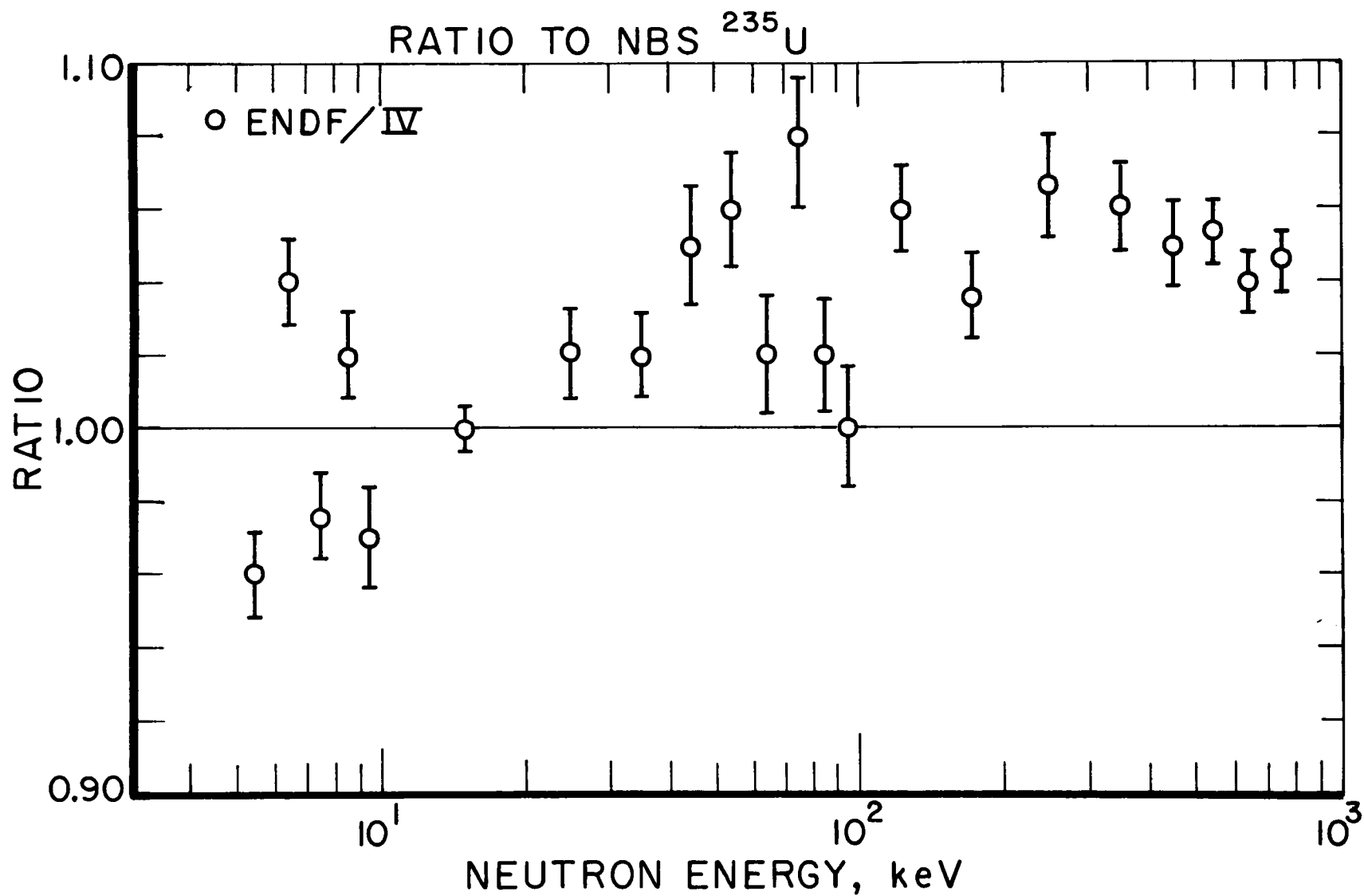


Fig. 9. The  $^{235}\text{U}$  data from the ENDF/BIV evaluation divided by the NBS hydrogen based cross section.

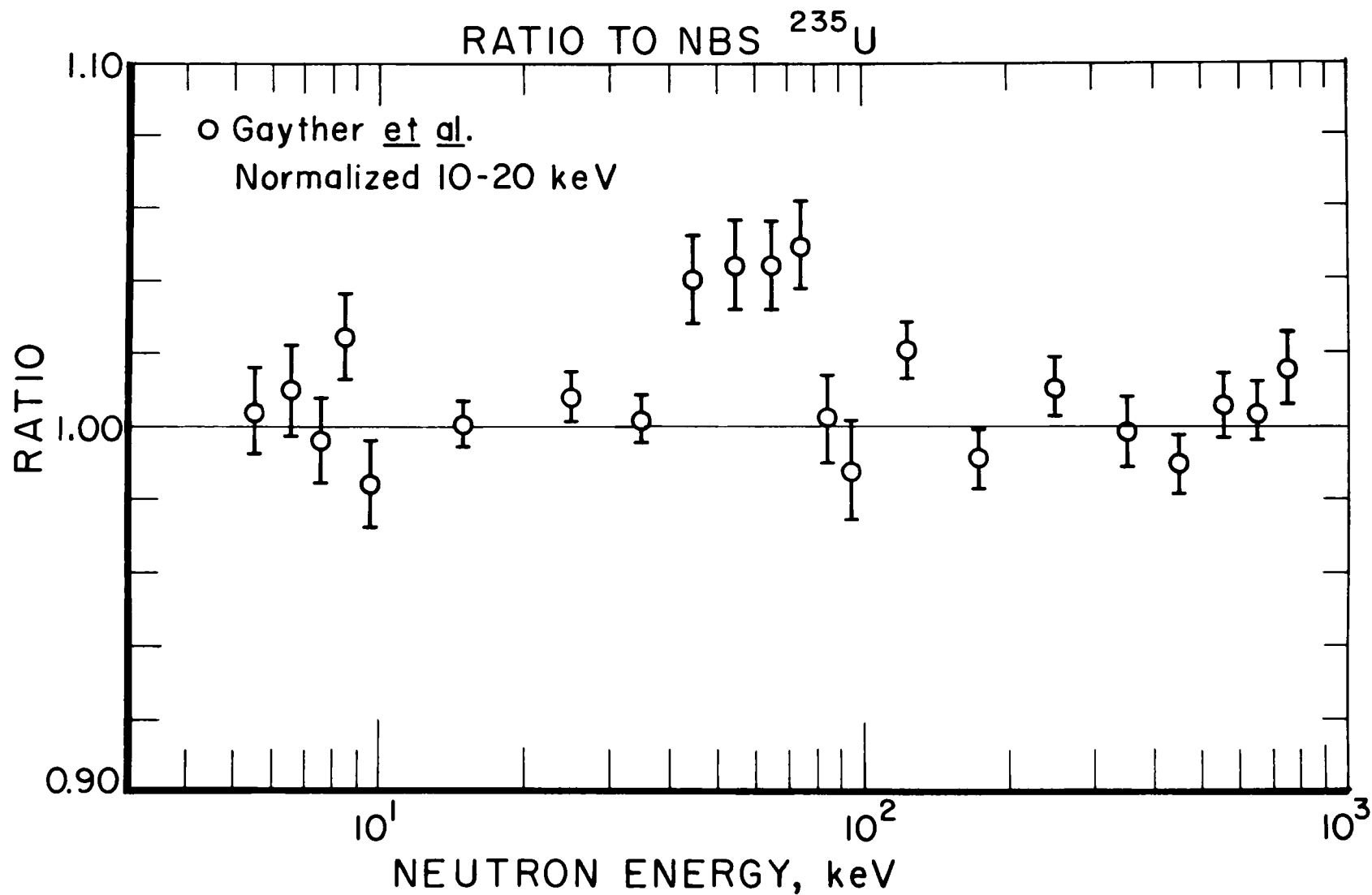


Fig.10. The cross section of Gayther et al. divided by the NBS cross section. The ratio was normalized in the 10 to 20 keV region.

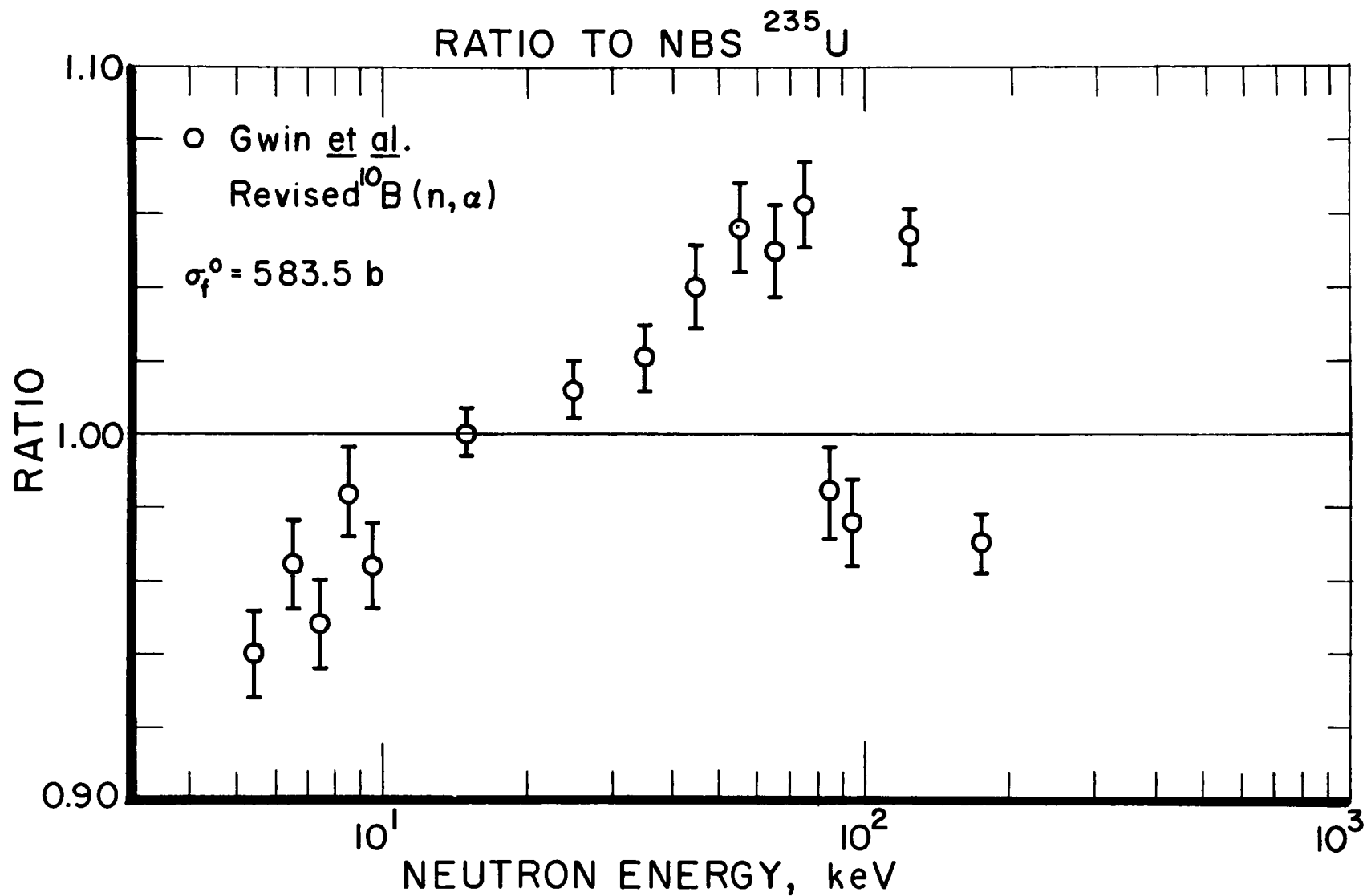


Fig.11. The cross section of Gwin et al. divided by the NBS cross section. The Gwin data was renormalized to a thermal cross section of 583.5 b and modified by the recent  $^{10}\text{B}(n, \alpha)$  cross section.

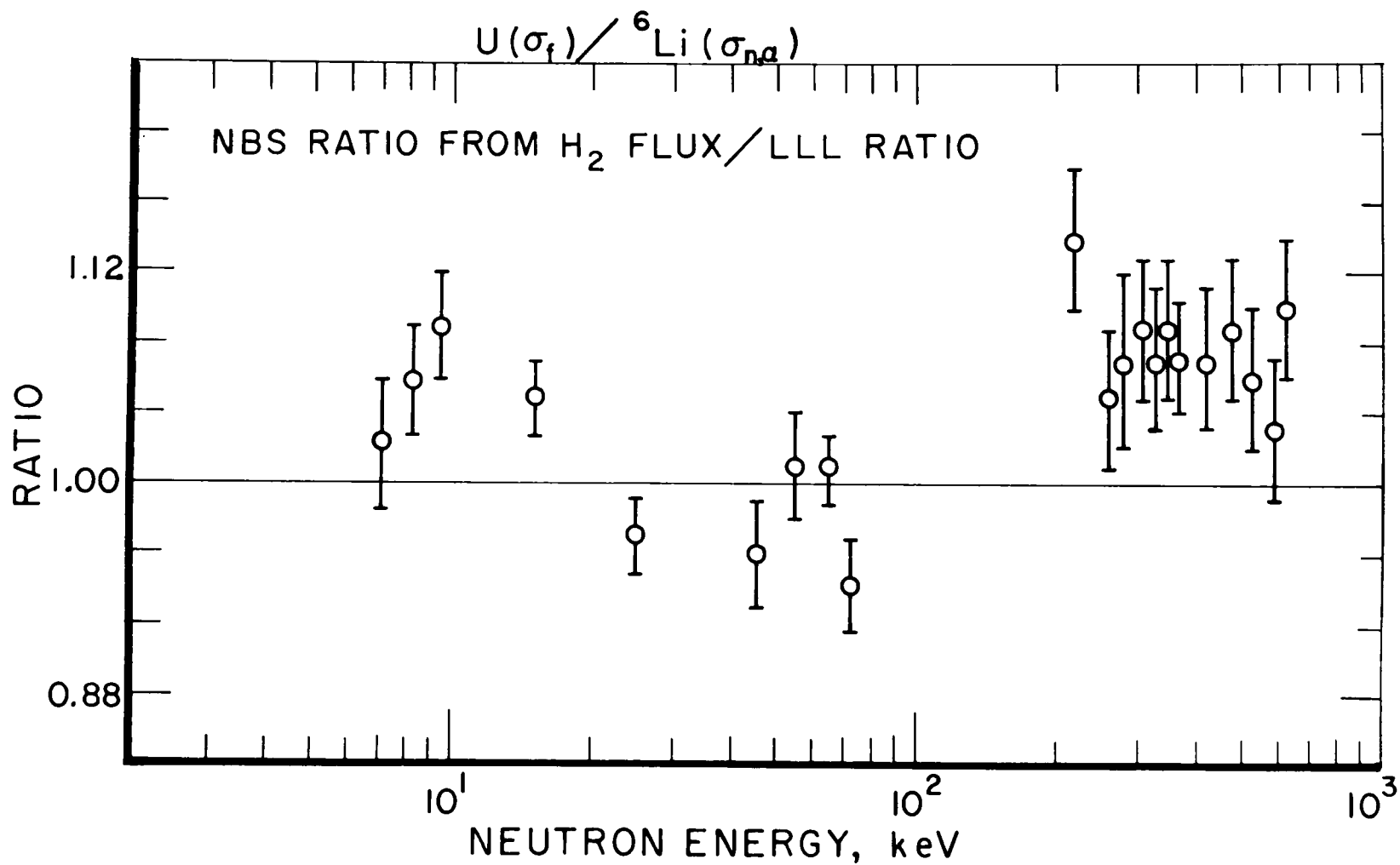


Fig.12. NBS measurement of the  ${}^{235}\text{U}(\text{n},\text{f})$  to  ${}^6\text{Li}(\text{n},\alpha)$  cross section ratio divided by that of Czirr and Sidhu.

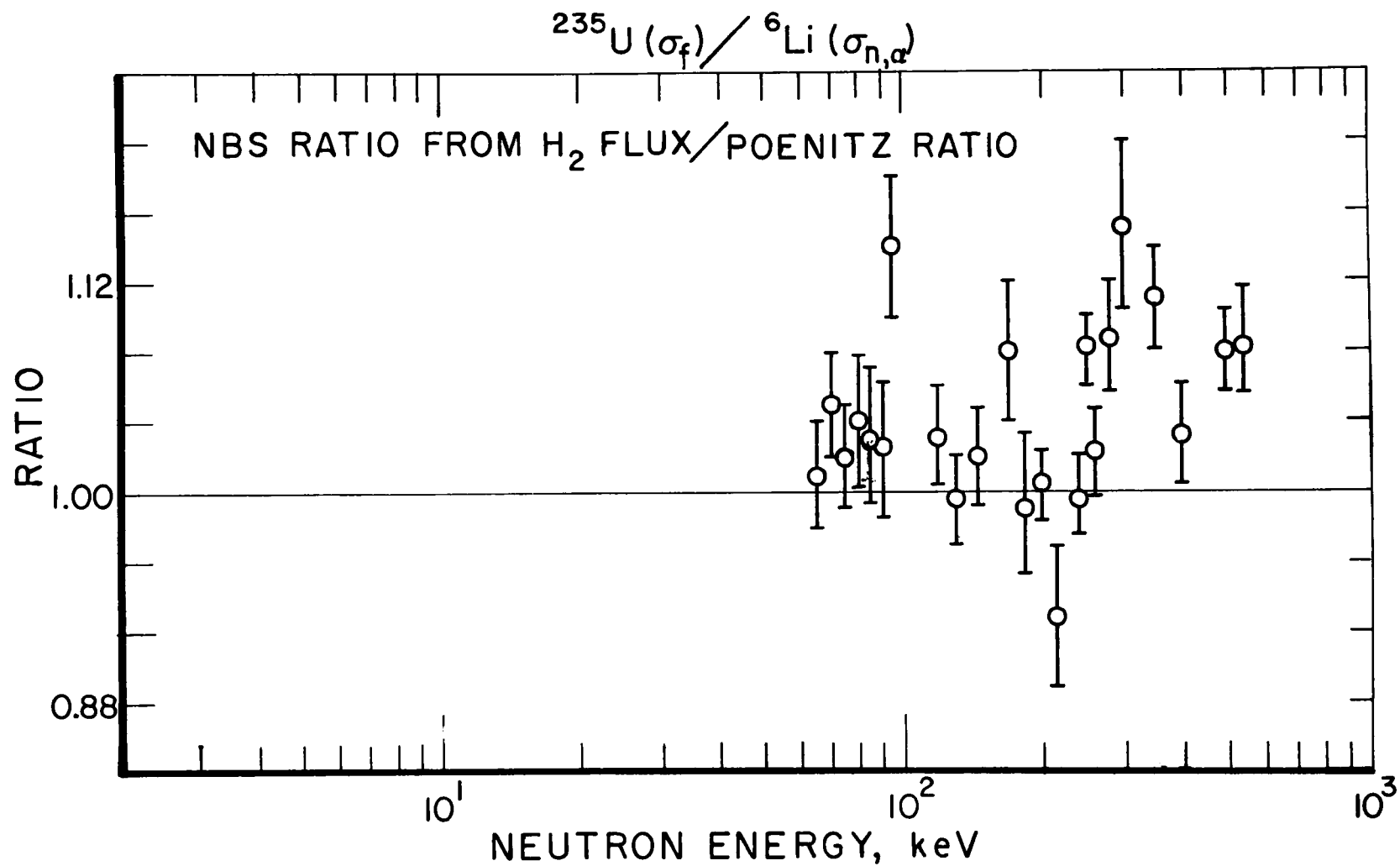


Fig.13. NBS measurement of  $^{235}\text{U}/^6\text{Li}$  divided by the preliminary ratio of Poenitz.

## DISCUSSIONS

W. Poenitz The U-235/Li-6 data from NBS have previously agreed with the data by Czirr and with our data. What caused the 5% change of the NBS data.

O. Wasson It depends upon what time you are referring to.

W. Poenitz I am referring to the memorandum by C. Bowman distributed at the CSEWG meeting at BNL this spring which showed a good agreement for the ratio and stated so. If there is now a 5% difference then there must have been a 5% change of your data.

O. Wasson The Li cross section has changed from the earlier time.

W. Poenitz That is the major problem. Somewhere in your measurements must be the overlap range which shows this discrepancy in the flux measurement between your two sets for U-235.

O. Wasson That was an entirely separate measurement, though some of the electronics and detectors were the same.

W. Poenitz The problem is that you measured the U-235/Li-6 ratio up to 30 keV and you normalized the U-235/H measurement between 10 and 20 keV to these values. If you used the NBS Li measurement as a reference for the U-235/Li-6 data then they should include the same systematic problem (below 10 keV) as the U-235/H because they used the same H-counter.

O. Wasson Oh yes, I guess I am confusing you here. There are two different Li-6 measurements which enter this problem.

W. Poenitz You did not include error bars in your Fig. 8 which compares your data for U-235 with my results which were published in NSE in 1974.

O. Wasson It was difficult to show an exact comparison because the energy region was different.

W. Poenitz Including the error bars would show that your data are everywhere within my error bars and your error bars are not that much different than mine. The exception is the 200-300 keV range where there is a disturbing discrepancy. In addition your figure was a little bit biased because

it does not show the other data which are available since my publication (e.g., data by Szabo, Kaeppler, U. Michigan). These other data would have shown a similar difference of 3% or more compared with your values.

O. Wasson This was not a complete comparison with other data. We selected some with which you are probably more familiar. This makes it a little bit easier to compare values.

W. Poenitz The 1% change of your U-235 data compared with the values you had at the BNL meeting--was that connected with the Li-glass correction which I suggested in a letter to G. Lamaze?

O. Wasson Yes, it probably resulted from an error of 0.7% associated with the Li-6 contents of the glass. Therefore, the self protection correction was changed.

H. Knitter I would like to make a comment on the measurements by Wagemans and Deruytter. They measured U-235(n,f) relative to B-10(n, $\alpha$ ) and Li-6(n, $\alpha$ ). They did not find agreement in the ratio between Li-6 and B-10. They preferred therefore to use the shape relative to B-10 only. They found excellent agreement with monoenergetic source values by Perkin, Szabo, and Knoll and Poenitz.

H. Derrien Did you compare your data with the De Saussure and the Perez data?

O. Wasson I did not.

H. Derrien The data by Perez agree very well with Wagemans.

W. Poenitz Perez is about 3% lower than Wagemans but they agree well within their uncertainties.

*At a later time the following statement was made:*

O. Wasson I like to make a correction to my previous talk. The change in the U-235/Li-6 ratio between C. Bowman's handout at BNL and the present values is entirely due to a change in the U-235 cross section and not to that of the Li-6. At that time we normalized in the 10-20 keV range to 2.385 b and subsequently to its present value of 2.48 b. That is a 4% difference and this is the cause of the change.

MEASUREMENT OF THE NEUTRON INDUCED FISSION CROSS SECTIONS  
OF URANIUM 235 AND PLUTONIUM 239  
IN THE MEV ENERGY RANGE

I. Szabo and J.P. Marquette

Centre d'Etudes Nucléaires de Cadarache  
Boîte Postale No.1  
13115 SAINT-PAUL-LEZ-DURANCE, FRANCE

presented by H. Derrien  
OECD NEA Neutron Data Compilation Centre  
91190 GIF-SUR-YVETTE, FRANCE

ABSTRACT

The fission cross sections of U-235 and Pu-239 were measured for incident neutron energies between 2.3 and 5.5 MeV. The neutron flux was measured by means of a calibrated directional counter and the fission events were detected in thin-walled ionization chambers. Time-of-flight technique was used in order to determine both the scattered neutrons and parasitic sources of neutrons.

For incident neutron energies lower than 2.5 MeV, a good agreement is observed with results from other measurements. For higher energies, the results of the present measurement when compared with the most recent data, are about 6 percent lower. However, they agree well with results from older sources.

Final, revised values of all of our previous measurements are also reported. The definitive set of data covers the energy range from 0.01 to 5.5 MeV.

INTRODUCTION

A few years ago, we measured the neutron induced cross sections of U-235, Pu-239 and Pu-241 at energies lower than a few MeV, i.e., in the main range of interest for fast reactor physicists. Besides its importance in the neutronics of nuclear reactors, the U-235 fission cross section has a broad scope of applications as a cross section standard. It is now well admitted that it can provide a good reference in the whole energy range from thermal to 15 MeV or even higher, except in a few regions where structures are observed.

This paper describes the new measurement of U-235 and Pu-239 fission cross sections which we made for incident neutron energies between 2.3 and 5.5 MeV. It reports also the revised and final values of all our previous measurements. The complete set of data which we obtained over the last few years covers the energy range from 0.01 to 5.5 MeV.

## EXPERIMENTAL SET-UP AND PROCEDURE

Features of the fissile samples that we used are summarised in Table I, extracted from reference /3/. In the present measurement, the foil from P.H. White was used in U-235 measurements and the B.C.M.N. foil for Pu-239 (foils denoted U 1 and Pu39 respectively in Table I).

For neutron energies lower than 3.8 MeV, the  $T(p,n)^3\text{He}$  reaction was used and the basic techniques were identical to the ones described in our previous papers (/2/ and /3/). For higher energies we had to use the  $D(d,n)^3\text{He}$  reaction to produce neutrons. With the latter reaction the procedure was somewhat complicated by the existence of secondary spurious neutron sources. A secondary  $D(d,n)^3\text{He}$  reaction could take place in occluded deuterium targets built up after a few minutes bombardment by the beam. In order to avoid deuterium absorption in materials located along the beam tube, no small slit or diaphragm was used to collimate the beam. The focalisation on the target was done by a special device located at 60 cm. from the solid deuterated target. This system consists of six pins which were regularly spaced in such a way as to divide the circular section of the beam tube into six equal sectors. The electric charges collected on each pin were measured and inter-compared. The beam focalisation was realised when these six measured intensities were as small as possible and nearly equal. The pin heads delimited a circular aperture and replaced advantageously a classical diaphragm since the quantity of material which would eventually be bombarded by the beam was much smaller.

Another source of spurious neutrons was due to the  $^{12}\text{C}(d,n)^{13}\text{N}$  reaction. Carbon from the vacuum pump oil formed a thin deposit on the target itself and  $^{12}\text{C}(d,n)^{13}\text{N}$  reaction took place, generating another group of neutrons of lower energy. As the neutron flux was measured by means of the directional counter which cannot distinguish between the two groups, a correction had to be made by weighing both the fission cross sections and the detector efficiencies with the flux ratio of the two groups. We measured this ratio by time-of-flight technique, using a calibrated NE 213 proton recoil scintillator. This detector was placed along the U-235 fission chamber axis, at 4.60 m. behind it. At this distance the two peaks, corresponding respectively to the  $D(d,n)^3\text{He}$  neutrons and to the  $^{12}\text{C}(d,n)^{13}\text{N}$  neutrons, could be well separated in the time-of-flight spectra.

The measured ratio varied from 0.02 to 0.40 as the neutron energy increased from 4 to 7 MeV. Furthermore this ratio depended on the age of the target used and on the emplacement of the beam spot on the target surface. So, it was necessary to measure simultaneously this ratio at every run and to control the reproductiveness of the different runs. At neutron energies higher than 6 MeV, the proportion of spurious neutrons became so important that the measurements were less accurate and less meaningful. For this reason, we limited our measurements below 5.5 MeV.

As pointed out above, the neutron flux was measured in the same way as in our previous measurements. The directional counter used was calibrated up to 2.2 MeV by two independent methods, one using a  $SO_4Mn$  bath and the other  $^3He$  associated particle counting in  $T(p,n)^3He$  reaction. Between 2 and 5 MeV, a relative curve was obtained using the symmetry property of the  $D(d,n)^3He$  reaction. This relative curve was then normalised to absolute values around 2.0 - 2.3 MeV and interpolated up to the absolute value we recently obtained at 14.8 MeV. As a consequence, the accuracy is about 3.0% above 2.5 MeV instead of 2.5% at lower energies.

#### NEW RESULTS

The present measurement concerned originally and essentially the U-235 fission cross section. However, as our experimental arrangement allowed simultaneous measurements in two fission chambers, we measured the Pu-239 fission cross section in the same run. Due to the alpha pile-up effect, this latter ionisation chamber was more difficult to handle; during this experiment, a rather high threshold was needed on the amplitude spectra and we made only relative measurements.

The new absolute values we obtained for the U-235 fission cross section are given in Table II and plotted in Figure 2. The absolute values of the Pu-239 fission cross section, as summarised in Table 2 and plotted in Figure 3, resulted from a normalization to two previous sets of absolute measurements in the energy range 2.0 - 3.3 MeV :

- the first set corresponds to results published in /3/;
- the second consists of two measurements at 2.85 and 3.23 MeV which we made in 1974 (not yet published - values given in Table II).

The accuracy of the fission cross section in the present measurement is about 4 percent, i.e., less than in measurements we made in the lower energy range, mainly because of the parasitic effects connected with the use of the  $D(d,n)^3He$  reaction and, to a lesser extent, owing to the greater error in flux measurement.

#### REVISED AND FINAL RESULTS

The results which are already published consist of three sets of values given in references /1/, /2/, and /3/. As explained in reference /3/, the measurements of /1/ and /2/ had to be renormalised. Since the modification was due to the determination of the atom contents in the foils, the published values were simply multiplied by a constant :

- 1.02 for U-235 fission cross section values of /2/ and, as a consequence, 0.98 for the corresponding fission cross section ratios of Pu-239 relative to U-235;

- 0.99 for Pu-241 fission cross section of reference /1/.

These modifications were effectively done three years ago and are recalled here for reasons of clarity.

We now turn to the last modification which has to be made for the results obtained in the incident neutron energy range above 800 keV. This modification is energy dependent, since it is mainly due to a change in the efficiency of the directional counter.

As we used an unique device to measure the neutron flux in the whole energy range, all our measurements depend on the calibration of the directional counter. Since the latest measurements published in 1973 /3/, further experiments have been performed in order to calibrate more accurately the directional counter, particularly in the MeV region. Especially, the associated particle method has been developed up to 2.2 MeV using  $T(p,n)^3\text{He}$  reaction; an absolute value has also been obtained at 14.8 MeV by means of the associated particle method applied to  $T(d,n)^4\text{He}$ . The compilation of all the measurements performed during the last ten years, using various independent methods, has led to an average efficiency curve which is slightly different from that used in our previous publication. Below about 0.8 MeV there is no change since the definitive calibration agrees with the previous one. Above 0.8 MeV, as shown in Figure 4, the results are somewhat higher than those obtained in 1970 using the  $\text{SO}_4\text{Mn}$  bath technique : so the new average curve is about 1 to 2% higher than the one used in references /1/ and /3/. Consequently, the cross section values given in references /1/ and /3/ have to be increased by the same amount in the incident neutron energy range above 0.8 MeV.

The final values of references /1/, /2/, and /3/ are given in Tables III, IV and V, respectively.

## DISCUSSION

### U-235 fission cross section

The revised values and the new measurement results are plotted altogether in Figure 2 and compared with some other measurements and evaluations.

Below 2.5 MeV, a good agreement is observed between the most recent results of Sidhu and Czirr /5/, those of Poenitz /6/, the earlier values of P.H. White /7/ and our own. The values of Hansen et al. /8/ and those of Diven /9/ are slightly higher.

Above 2.5 MeV, two groups of values appear clearly and show a discrepancy of 5 to 8 percent. In the higher-valued group we find the results of Poenitz /6/ and Hansen et al. /8/ as well as the relative measurement of Sidhu and Czirr /5/ which was normalised around 3.5 MeV to the absolute value of Poenitz. The lower-valued group includes the earlier values of Smith, Hansen and McGuire /10/, those of P.H. White /7/ and our present results. Therefore, a significant degree of disagreement continues to exist in the

3 - 6 MeV range. The situation would be worse if the relative measurement of Sidhu and Czirr were normalised to the well-established value of 2.15 barn at 14 MeV. However, the measurement which was recently made at Bruyères-le-Châtel by Grenier et al. /11/ tends to support a lower value at 14 MeV and thus supports the normalisation of the Sidhu and Czirr results around 3.5 MeV.

Compared with evaluations, our present measurement agrees quite well with the selected values of Davey /12/, but is about 3% lower than the more recent evaluation of Sowerby /13/ which is situated between the two above-mentioned groups of results, in the 3 - 6 MeV energy range.

There is obviously a need for further measurements in order to fulfill the high accuracy required for the use of the U-235 fission cross section as a standard in this energy range.

### Pu-239 fission cross section

Compared with U-235 there are less fission cross section measurements for Pu-239. Our present results are plotted in Figure 3 along with some evaluations /13/ and /14/. As in the case of U-235, the fission cross sections we obtained are somewhat lower than the evaluated values mainly deduced from ratio measurements.

### ACKNOWLEDGEMENTS

We would like to thank Dr H. Derrien for his useful discussions and comments, Miss L. Truran for her help in preparing the manuscript and Messrs Lequeue and Cloué for the operation of the Van de Graaff accelerator.

### REFERENCES

1. I. SZABO, C. FILLIPPI, J.L. HUET, J.L. LEROY and J.P. MARQUETTE. Proc. Conf. on Neutron Standards and Flux Normalization, AEC Symposium, Series 23 - p. 257, A.N.L. October 21-23, 1970.
2. I. SZABO, C. FILLIPPI, J.L. HUET, J.L. LEROY and J.P. MARQUETTE, Proc. Conf. on Neutron Cross Sections and Technology - Vol. II, p. 573. Knoxville, March 15-17, 1971.
3. I. SZABO, J.L. LEROY and J.P. MARQUETTE, 2ème Conférence Nationale Soviétique sur la Physique des Neutrons, Kiev, 1973.
4. I. SZABO, J.L. LEROY and J.P. MARQUETTE, Neutron Standard Reference Data, Proceedings of a Panel, Vienna, 20-24 November, 1972. IAEA, 1974.
5. G.S. SIDHU and J.B. CZIRR, URCL 76508 (1975) and Proc. Conf. on Nuclear Cross Sections and Technology, Washington D.C., March 3-7, 1975.
6. W.P. POENITZ, Nucl. Sci. and Eng. 53,370-392, 1974.

7. P. H. WHITE, J. Nucl. Energy, A/B, p.325, 1965.
8. G. HANSEN et al., Neutron Standard Reference Data, Proceedings of a Panel, Vienna, 20-24 November, 1972. I.A.E.A., 1974 (reported by B. C. DIVEN), p.227.
9. B. C. DIVEN, Phys. Rev., 105, 4, 1350-1353, 1957.
10. G. HANSEN, S. McGUIRE and R. K. SMITH (revised values).
11. G. GRENIER et al., The present meeting.
12. W. G. DAVEY, Nucl. Sc. Eng., 32, 34, 1968.
13. M. G. SOWERBY et al., Ann. of Nucl. Sc. Eng., Vol. 1, 718, p.409, 1974.
14. P. RIBON and G. LECOQ, CEA N 1484, 1971.

TABLE I

Characteristics of the different samples

Deposit	Isotopic composition % in atoms				Thick- ness mg/cm <sup>2</sup>	Nature of the backing	Fabrication procedure	Origin	Calibrations					
									Laboratory of origin				Cadarache	
	234	235	236	238					LG	2π	P	D	LG	2π
U1	1.196	93.013	0.179	5.612	0.5	0.13 mm Pt	painted U308	P.H. White	x	x	x	x	x	x
U2	0.169	99.502	0.025	0.303	0.5	0.3 mm Pt	electrospray. U308	BCMN	x			x	x	x
U3	1.1653	97.663	0.1491	0.5229	0.5	0.6 mm quartz	evaporation UF <sub>4</sub>	BCMN	x			x	x	x
Pu39	38	39	40	41	42	0.17	0.3 mm Pt	electrospray.	BCMN	x			x	x
	<0.01	99.27	0.71	0.02	<0.01									
Pu41	<0.01	0.868	2.968	94.658	1.497	0.13	0.3 mm Pt	electrolysis	CEA				x	x

Abbreviations

LG : Low geometry

P : Weighing

D : Destructive analysis made on similar deposits.

TABLE II

1975 - 1976 Measurements

$E_n$ MeV	U-235	Pu-239
	$\sigma_f$ barn	$\sigma_f$ barn
2.350 $\pm$ 0.032	1.256 $\pm$ 0.040	1.960 $\pm$ 0.069
2.590 $\pm$ 0.031	1.219 $\pm$ 0.040	1.88 $\pm$ 0.066
2.780 $\pm$ 0.030	1.206 $\pm$ 0.040	1.85 $\pm$ 0.065
2.850 $\pm$ 0.030	1.203 $\pm$ 0.036	1.86 $\pm$ 0.065
3.090 $\pm$ 0.029	1.167 $\pm$ 0.035	1.76 $\pm$ 0.062
3.230 $\pm$ 0.028	1.156 $\pm$ 0.034	1.77 $\pm$ 0.085
3.360 $\pm$ 0.020	1.130 $\pm$ 0.033	1.77 $\pm$ 0.065
3.550 $\pm$ 0.025	1.137 $\pm$ 0.035	1.73 $\pm$ 0.063
3.800 $\pm$ 0.024	1.100 $\pm$ 0.035	1.78 $\pm$ 0.065
3.920 $\pm$ 0.101	1.088 $\pm$ 0.038	1.77 $\pm$ 0.070
4.470 $\pm$ 0.083	1.100 $\pm$ 0.040	1.76 $\pm$ 0.070
5.015 $\pm$ 0.037	1.000 $\pm$ 0.036	1.70 $\pm$ 0.070
5.530 $\pm$ 0.024	1.030 $\pm$ 0.036	1.60 $\pm$ 0.065

TABLE III

Definitive results for reference 1 (Argonne 1970) :

U-235 and Pu-239 : no modification;  
 Pu-241 : 1% decrease after re-evaluation  
 of the number of atoms  
 (destructive analysis of  
 the deposit).

U-235		Pu-239		Pu-241	
$E_n$ keV	$\sigma_f$ barn	$E_n$ keV	$\sigma_f$ barn	$E_n$ keV	$\sigma_f$ barn
17.5 $\pm$ 3.5	2.150 $\pm$ 0.090	35 $\pm$ 4	1.530 $\pm$ 0.070	35 $\pm$ 4	2.64 $\pm$ 0.13
27 $\pm$ 3.5	2.10 $\pm$ 0.080	49 $\pm$ 5	1.495 $\pm$ 0.060	50 $\pm$ 5	2.39 $\pm$ 0.12
42 $\pm$ 5	1.80 $\pm$ 0.060	57 $\pm$ 8	1.505 $\pm$ 0.050	88 $\pm$ 4	2.06 $\pm$ 0.11
68 $\pm$ 5	1.765 $\pm$ 0.045	73 $\pm$ 7	1.540 $\pm$ 0.055	130 $\pm$ 20	2.02 $\pm$ 0.11
72.5 $\pm$ 6.5	1.740 $\pm$ 0.055	77.5 $\pm$ 8	1.530 $\pm$ 0.055	177 $\pm$ 10	1.91 $\pm$ 0.09
95 $\pm$ 5	1.540 $\pm$ 0.055	102 $\pm$ 8	1.565 $\pm$ 0.055	218 $\pm$ 8	1.71 $\pm$ 0.08
110 $\pm$ 10	1.530 $\pm$ 0.050	109 $\pm$ 8	1.500 $\pm$ 0.050	239 $\pm$ 7	1.72 $\pm$ 0.08
120 $\pm$ 8	1.570 $\pm$ 0.055	135 $\pm$ 5	1.470 $\pm$ 0.050	300 $\pm$ 12	1.59 $\pm$ 0.07
125 $\pm$ 7	1.500 $\pm$ 0.050	152 $\pm$ 10	1.440 $\pm$ 0.040	344 $\pm$ 10	1.56 $\pm$ 0.07
145 $\pm$ 9	1.500 $\pm$ 0.055	154 $\pm$ 7	1.475 $\pm$ 0.040	463 $\pm$ 12	1.44 $\pm$ 0.07
150 $\pm$ 6	1.450 $\pm$ 0.045	165 $\pm$ 13	1.420 $\pm$ 0.040	476 $\pm$ 10	1.50 $\pm$ 0.07
152 $\pm$ 10	1.440 $\pm$ 0.040	197 $\pm$ 16	1.420 $\pm$ 0.040	604 $\pm$ 30	1.42 $\pm$ 0.06
154 $\pm$ 14	1.440 $\pm$ 0.035	226 $\pm$ 12	1.400 $\pm$ 0.055	687 $\pm$ 29	1.41 $\pm$ 0.06
156 $\pm$ 12	1.450 $\pm$ 0.045	251 $\pm$ 10	1.480 $\pm$ 0.040	808 $\pm$ 29	1.49 $\pm$ 0.07
195 $\pm$ 11	1.365 $\pm$ 0.055	331 $\pm$ 12	1.545 $\pm$ 0.035	970 $\pm$ 25	1.52 $\pm$ 0.07
215 $\pm$ 10	1.325 $\pm$ 0.045	377 $\pm$ 9	1.530 $\pm$ 0.035		
227 $\pm$ 16	1.295 $\pm$ 0.035	453 $\pm$ 13	1.570 $\pm$ 0.040		
251 $\pm$ 11	1.285 $\pm$ 0.035	506 $\pm$ 16	1.590 $\pm$ 0.040		
257 $\pm$ 15	1.275 $\pm$ 0.055	665 $\pm$ 22	1.595 $\pm$ 0.04		
272 $\pm$ 15	1.275 $\pm$ 0.045	810 $\pm$ 35	1.700 $\pm$ 0.04		
286 $\pm$ 15	1.270 $\pm$ 0.035	972 $\pm$ 40	1.720 $\pm$ 0.04		
313 $\pm$ 15	1.285 $\pm$ 0.045				
320 $\pm$ 8	1.190 $\pm$ 0.045				
331 $\pm$ 15	1.210 $\pm$ 0.045				
369 $\pm$ 15	1.215 $\pm$ 0.045				
407 $\pm$ 15	1.205 $\pm$ 0.035				
506 $\pm$ 17	1.160 $\pm$ 0.030				
540 $\pm$ 10	1.160 $\pm$ 0.045				
665 $\pm$ 22	1.140 $\pm$ 0.035				
810 $\pm$ 35	1.135 $\pm$ 0.035				
1010 $\pm$ 40	1.205 $\pm$ 0.035				

TABLE IV

Definitive results for reference 2 (Knoxville 1971) :

Fission Pu-239 : no modification;  
 Fission U-235 : 2% increase after re-evaluation  
 of the number of atoms of  
 the deposit;  
 Ratio Pu-239/U-235 : 2% decrease.

$E_n$	$\sigma_f(\text{U-235})$	$\sigma_f(\text{Pu-239})$	$\sigma_f(\text{Pu-239})/\sigma_f(\text{U-235})$
11.5 $\pm$ 3	2.76 $\pm$ 0.09	1.778 $\pm$ 0.058	0.646 $\pm$ 0.022
15.0 $\pm$ 3	2.50 $\pm$ 0.07	1.75 $\pm$ 0.052	0.704 $\pm$ 0.021
22.5 $\pm$ 2.5	2.20 $\pm$ 0.06	1.71 $\pm$ 0.06	0.773 $\pm$ 0.030
33.0 $\pm$ 5	2.02 $\pm$ 0.06	1.59 $\pm$ 0.04	0.789 $\pm$ 0.020
46.0 $\pm$ 5	1.85 $\pm$ 0.05	1.59 $\pm$ 0.04	0.858 $\pm$ 0.024
58.0 $\pm$ 3	1.83 $\pm$ 0.05	1.55 $\pm$ 0.04	0.850 $\pm$ 0.023
78.0 $\pm$ 2.5	1.70 $\pm$ 0.05	1.55 $\pm$ 0.05	0.911 $\pm$ 0.027
83.5 $\pm$ 11	1.65 $\pm$ 0.05	1.53 $\pm$ 0.04	0.926 $\pm$ 0.024
93.0 $\pm$ 4	1.55 $\pm$ 0.04	1.58 $\pm$ 0.04	1.015 $\pm$ 0.026
103.5 $\pm$ 5.5	1.53 $\pm$ 0.04	1.54 $\pm$ 0.04	1.005 $\pm$ 0.024
116 $\pm$ 15	1.52 $\pm$ 0.04	1.59 $\pm$ 0.04	0.997 $\pm$ 0.022
135 $\pm$ 5	1.42 $\pm$ 0.04	1.46 $\pm$ 0.05	1.034 $\pm$ 0.034
150 $\pm$ 5	1.46 $\pm$ 0.04	1.49 $\pm$ 0.04	1.017 $\pm$ 0.030
172 $\pm$ 5.5	1.46 $\pm$ 0.04	1.48 $\pm$ 0.04	1.017 $\pm$ 0.026
199 $\pm$ 5.5	1.42 $\pm$ 0.040	1.49 $\pm$ 0.04	1.041 $\pm$ 0.027

TABLE V

Definitive results for reference 3 (Kiev 1973) :

1-2% modification above 0.8 MeV neutron  
energy (adjustment of neutron flux measurement).

U-235

$E_n$ keV	$\sigma_f$ barns	$E_n$ keV	$\sigma_f$ barns
$17 \pm 3$	$2.420 \pm 0.080$	$1020 \pm 25$	$1.187 \pm 0.035$
	$2.370 \pm 0.080$ *	$1080 \pm 25$	$1.187 \pm 0.035$
$19 \pm 3$	$2.480 \pm 0.090$	$1280 \pm 24$	$1.207 \pm 0.035$
$38 \pm 3$	$1.975 \pm 0.060$	$1405 \pm 23$	$1.229 \pm 0.035$
	$1.984 \pm 0.065$ *	$1485 \pm 22$	$1.255 \pm 0.030$
$40 \pm 3$	$2.047 \pm 0.070$	$1580 \pm 22$	$1.252 \pm 0.035$
$51 \pm 3$	$1.849 \pm 0.050$	$1680 \pm 21$	$1.272 \pm 0.035$
	$1.863 \pm 0.055$ *	$1800 \pm 20$	$1.306 \pm 0.035$
$55 \pm 3$	$1.822 \pm 0.050$	$1915 \pm 20$	$1.353 \pm 0.035$
$71 \pm 3$	$1.710 \pm 0.045$	$2000 \pm 19$	$1.315 \pm 0.030$
	$1.680 \pm 0.045$ *	$2040 \pm 19$	$1.330 \pm 0.035$
$75 \pm 3$	$1.707 \pm 0.050$	$2100 \pm 18$	$1.318 \pm 0.035$
$88 \pm 4$	$1.556 \pm 0.040$	$2180 \pm 18$	$1.294 \pm 0.035$
$124 \pm 4$	$1.580 \pm 0.040$	$2190 \pm 17$	$1.303 \pm 0.030$
	$1.540 \pm 0.040$ *	$2280 \pm 17$	$1.304 \pm 0.030$
$730 \pm 30$	$1.140 \pm 0.030$	$2300 \pm 17$	$1.293 \pm 0.030$
$880 \pm 26$	$1.140 \pm 0.035$	$2380 \pm 16$	$1.275 \pm 0.032$
$920 \pm 26$	$1.188 \pm 0.035$	$2610 \pm 16$	$1.270 \pm 0.030$

\* : two separate measurements at the same energy.

TABLE V (Cont/d)

Definitive results for reference 3 (Kiev 1973) :

1-2% modification above 0.8 MeV neutron  
energy (adjustment of neutron flux measurement).

## Pu-239

$E_n$ keV	$\sigma_f$ barns	$E_n$ keV	$\sigma_f$ barns
$805 \pm 27$	$1.564 \pm 0.045$	$1800 \pm 20$	$1.979 \pm 0.050$
$880 \pm 26$	$1.660 \pm 0.050$	$2000 \pm 19$	$1.967 \pm 0.060$
$920 \pm 26$	$1.706 \pm 0.050$	$2040 \pm 19$	$2.034 \pm 0.055$
$1190 \pm 25$	$1.856 \pm 0.050$	$2100 \pm 18$	$2.040 \pm 0.055$
$1280 \pm 24$	$1.823 \pm 0.045$	$2180 \pm 18$	$1.979 \pm 0.055$
$1405 \pm 23$	$1.876 \pm 0.047$	$2190 \pm 17$	$1.986 \pm 0.055$
$1465 \pm 23$	$1.969 \pm 0.050$	$2230 \pm 17$	$2.025 \pm 0.055$
$1485 \pm 22$	$1.900 \pm 0.048$	$2300 \pm 17$	$1.960 \pm 0.050$
$1580 \pm 22$	$1.906 \pm 0.050$	$2380 \pm 16$	$1.897 \pm 0.060$
$1680 \pm 21$	$1.973 \pm 0.055$	$2610 \pm 16$	$1.916 \pm 0.050$

## Pu-241

$E_n$ keV	$\sigma_f$ barns	$E_n$ keV	$\sigma_f$ barns
$1180 \pm 25$	$1.620 \pm 0.045$	$2010 \pm 19$	$1.700 \pm 0.050$
$1470 \pm 22$	$1.707 \pm 0.050$	$2240 \pm 17$	$1.613 \pm 0.050$
$1700 \pm 21$	$1.739 \pm 0.050$	$2630 \pm 16$	$1.569 \pm 0.055$

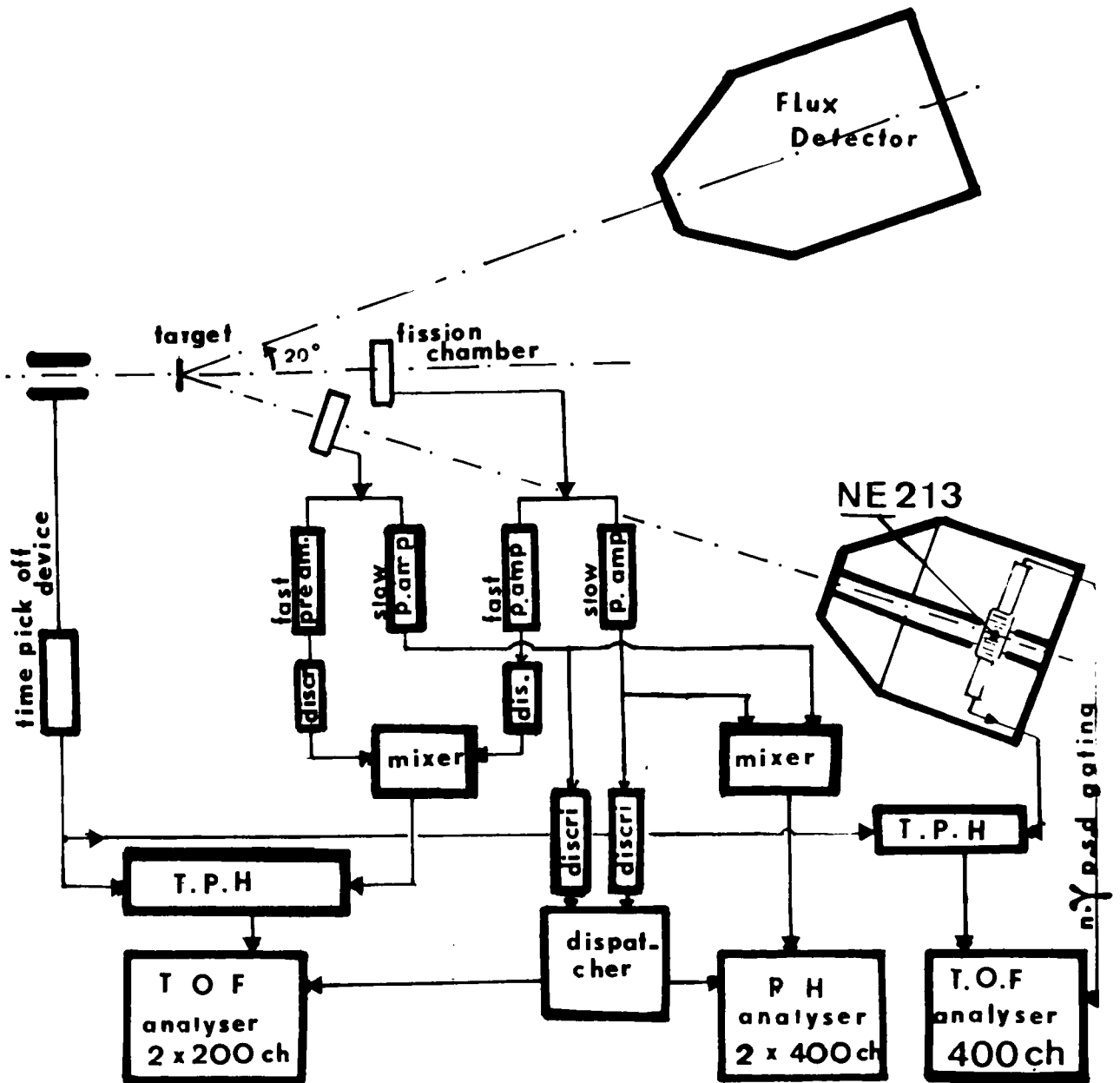


FIG 1 EXPERIMENTAL ARRANGEMENT

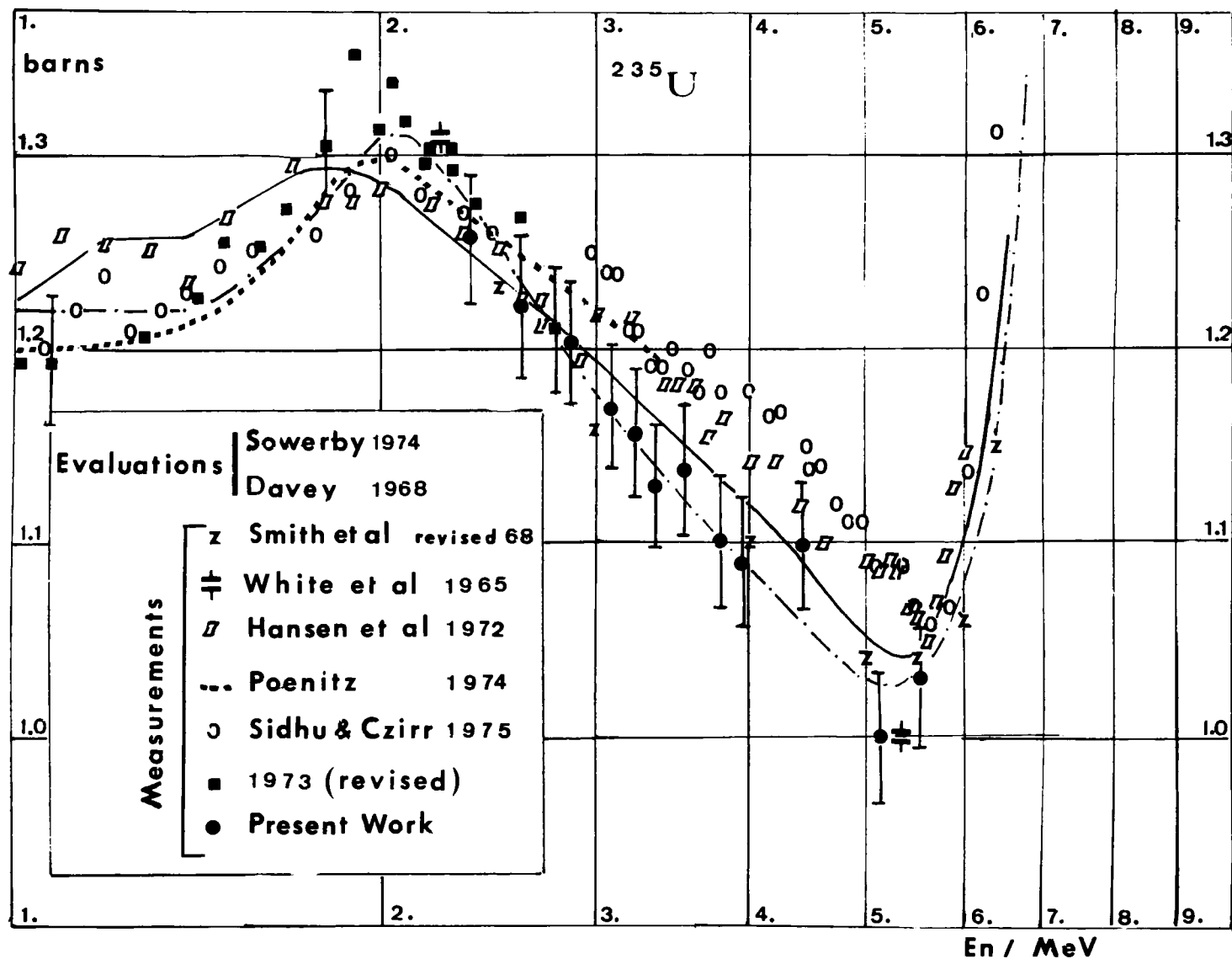


Figure 2. Present results for  $^{235}\text{U}$ , and comparison with other data.

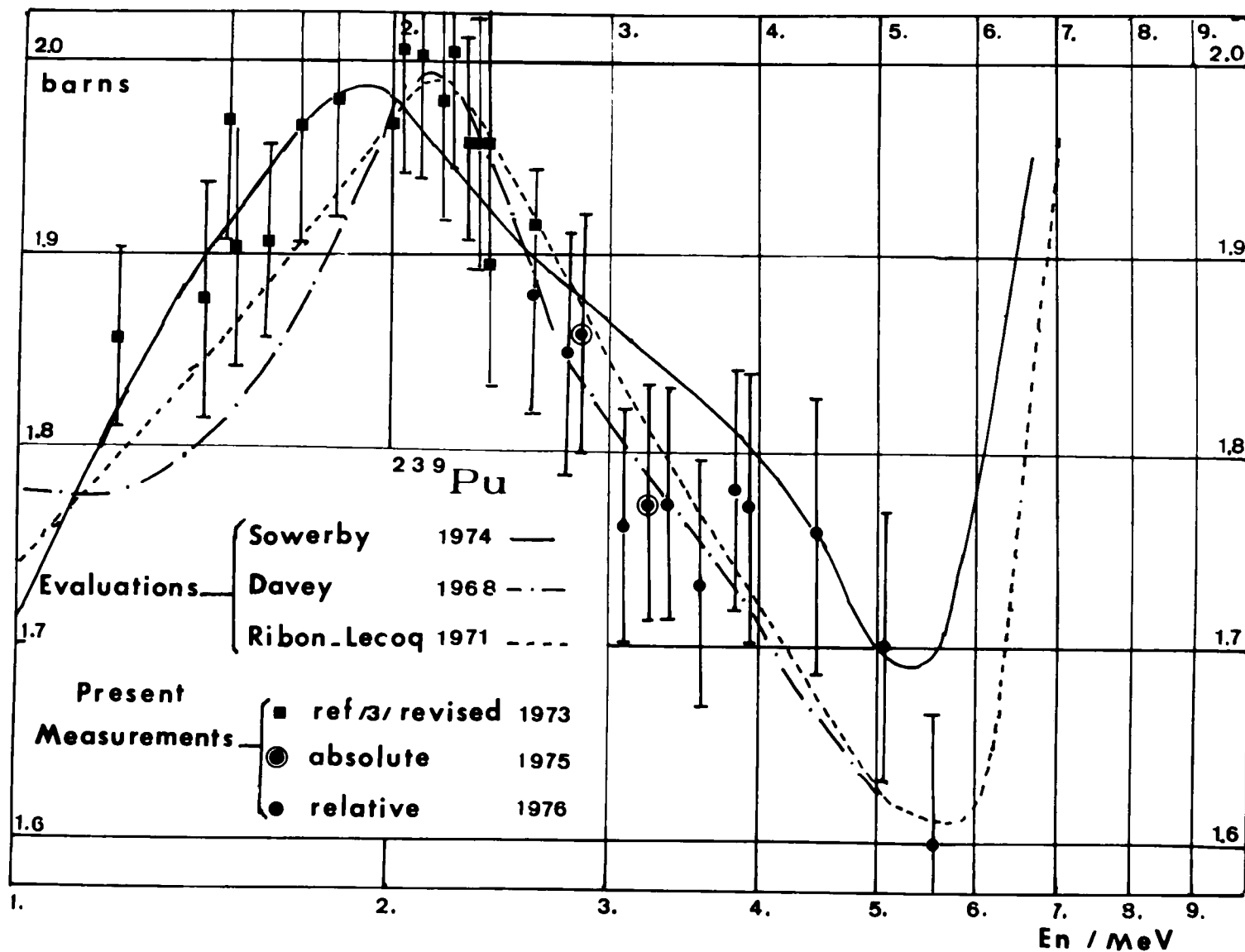
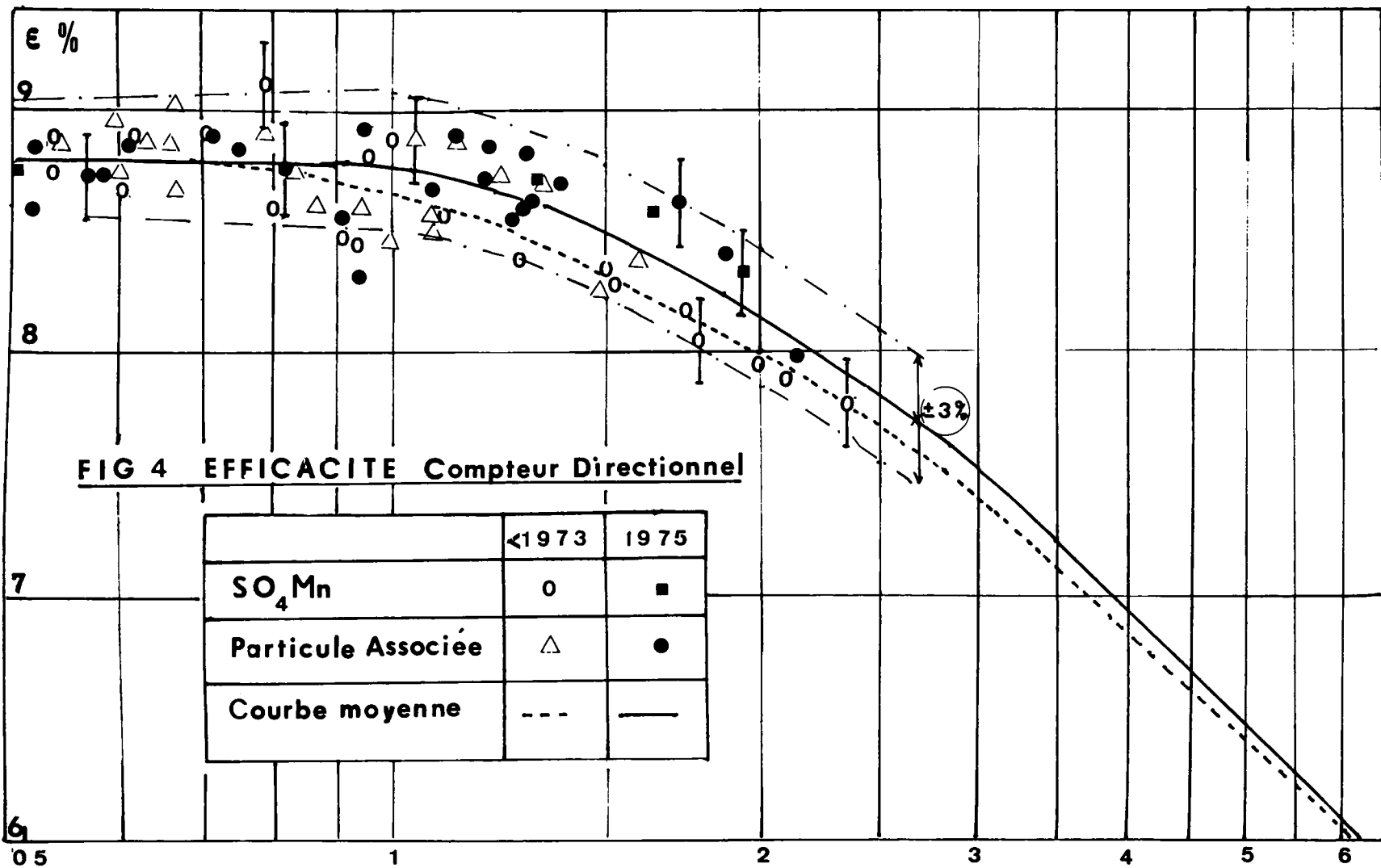


Figure 3. Present Results for  $^{239}\text{Pu}$ , and comparison with other Data.



## DISCUSSIONS

L. Stewart I only want to make a comment. I believe the Hansen data have been lowered by 1% since the Vienna meeting. Those you show may be the old data.

A. Smith I looked at this experiment briefly. The measurement depends on the ratio of the fission counter rate to that of a flat detector at an equal angle with respect to the  $D(d,n)$  reaction. Do you have an idea on how sensitive the result is to the exact angle?

H. Derrien No, I do not.

A. Smith The  $D(d,n)$  reaction has a drastic angular dependence. There may be a problem.

R. Peelle Does the paper indicate what the systematic errors are? Was it the same fission chamber as used before?

H. Derrien You will find information on the systematic errors in the previous papers ('73 Kiev, '71 Knoxville).

# ABSOLUTE MEASUREMENTS OF $^{235}\text{U}$ AND $^{239}\text{Pu}$ FISSION CROSS SECTIONS WITH PHOTONEUTRON SOURCES\*

M. C. Davis, G. F. Knoll, and J. C. Robertson

The University of Michigan  
Ann Arbor, Michigan 48109

## ABSTRACT

The fission cross sections of  $^{235}\text{U}$  and  $^{239}\text{Pu}$  for Na-Be, La-Be, Na-D, and Ga-D photoneutrons have been measured absolutely (i.e., without significant dependence on other cross section data). The neutron flux at the targets was calculated from the experimental geometry and by using a manganese bath to compare the photoneutron source yield with the standard source NBS-11. Fission counts were accumulated with the source positioned symmetrically between two identical foils and detectors in an experiment package suspended in a low-albedo laboratory. Fission fragments passing through limited solid angle apertures were recorded on polyester track-etch films. The masses of the foil deposits were determined by microbalance weighings and confirmed by thermal fission and alpha counting. After making a correction for the calculated energy distribution of the source neutrons, values of 1.471, 1.271, 1.161, and 1.210 barns were obtained for the  $^{235}\text{U}$  fission cross section at neutron energies of 140, 265, 770, and 964 keV, respectively. Corresponding values of 1.465, 1.490, 1.678, and 1.644 barns were derived for  $^{239}\text{Pu}$ . Present uncertainties are about 2.0% for the  $^{235}\text{U}$  values and 2.5% for the  $^{239}\text{Pu}$  results.

## INTRODUCTION

In the establishment of an accurate  $^{235}\text{U}$  fission cross section standard, it is highly desirable that independent methods of absolute neutron flux determination be employed. There are only a few absolute measurements of the  $^{239}\text{Pu}$  fission cross section in the 100 keV to 1 MeV energy region and there is clear need for further data. Noteworthy aspects of these measurements include using the manganese bath method as the basis for absolute flux determination, and applying track-etch techniques for fission fragment counting through limited solid-angle apertures.

---

\*Work supported by Division of Research, USERDA.

## EXPERIMENTAL METHOD

In the present work, four photoneutron sources emitting nearly-monoenergetic neutrons were employed to measure the  $^{235}\text{U}$  and  $^{239}\text{Pu}$  fission cross section at 140, 265, 770, and 964 keV. Details of the  $^{235}\text{U}$  measurement at 964 keV have been previously described [1]. The Ga-Be, Na-D, and La-Be neutron sources made use of interchangeable spherical cores of compacted  $\text{Ga}_2\text{O}_3$ , NaF, or  $\text{La}_2\text{O}_3$  powder sealed in thin aluminum shells. Hemispherical shells of deuterated polyethylene or beryllium surrounded the core. Fig. 1 shows the NaF core, the deuterated polyethylene shells, and mold used in forming the shells. The fourth neutron source consists of a compressed NaF core surrounded by a permanent spherical shell of beryllium. With the exception of the pre-assembled Na-Be source, the inner core is separately irradiated to prevent radiation damage to the outer shells in a reactor neutron flux of  $10^{12}$  n/cm<sup>2</sup>-sec.

TABLE I

Source Characteristics

Source	Inner Core Diameter (cm)	Outer Shell Diameter (cm)	Half-life (hrs)	Median Energy (keV)	Initial Neutron Activity (n/sec)
Na-Be	3.01	3.60	15.00	964	$5 \times 10^7$
La-Be	2.38	3.61	40.23	770	$2 \times 10^6$
Na-D	2.38	3.65	15.00	265	$2 \times 10^7$
Ga-D	2.38	3.65	13.95	140	$6 \times 10^6$

Uniform activation during the irradiation is assured by continuously rotating the source at the reactor mid-plane to a saturated activity. The source is then remotely transferred to the adjacent hot cave where the photoneutron target shells are added (not necessary for the pre-assembled Na-Be source). The assembled source is transferred to a low-albedo laboratory.

The fission rate measurement and the manganese bath source comparisons were carried out in a thick-walled concrete cell with a mean inside diameter of 4.2 m. All the interior surfaces of the cell are lined with a 5 cm layer of anhydrous borax to reduce the return of moderated neutrons into the experimental area. The manganese bath was drained during the fission rate measurement in order that the full advantage of the borax lining be realized.

At the center of the low-albedo cell, the photoneutron source was positioned symmetrically between two track-etch fission detectors as shown for a plutonium measurement in Fig. 2. The source and detectors were supported by a light-weight tubular framework which was enclosed in a cadmium-lined drum 60 cm in diameter. The uranium measurements at 140, 265, and 964 keV were in a helium environment whereas the 770 keV measurement was conducted in vacuum. All plutonium measurements were in vacuum using a smaller tubular framework inside a 23 cm diameter brass containment cylinder.

The total fission rate with the dual limited solid angle detectors is insensitive to the positioning of the neutron source, so that an accurate

measurement of the location of the highly radioactive photoneutron source was not necessary. Each detector supported one of two nearly identical target foils of  $1 \text{ mg/cm}^2$  thick deposits on 20 mil platinum. The timing of the track accumulation period was defined by placement of the photoneutron source in the detector package source well for the measurements in vacuum, and by electrically actuated shutters that interposed between the fissionable deposit and the track-etch film for the helium environment. Two runs were made for each measurement varying the dual foil spacing from 10 cm to 18 cm to permit evaluation of the background due to room-return neutrons.

The polyester track-etch films were etched in KOH to develop the tracks to an average diameter of about  $14 \text{ }\mu\text{m}$ . The tracks were counted manually on a projection microscope. A measurement of the track diameter distribution was carried out prior to counting each sample as a basis for distinguishing the larger fission tracks from the smaller alpha and background pits. Track counting of all close spacing runs were repeated with a reproducibility within 0.5%.

Following the fission rate measurements, the neutron source was transferred to a continuously sampled manganese bath. Measurements of the standard NBS-II before and after each run served to absolutely calibrate the bath. A computer code was developed to unfold the time dependence of the photoneutron exponential decay,  $^{56}\text{Mn}$  activation, and the mixing delays in the bath-detector system.

The masses of the deposits were determined by the supplier, Isotope Target Laboratory at Oak Ridge National Laboratory, by means of microbalance weighings. The relative isotopic content was determined by mass spectrographic analysis also performed by ORNL. Confirming mass assays by alpha and thermal fission counting were conducted at the National Bureau of Standards.

#### CORRECTIONS AND RESIDUAL UNCERTAINTIES

The largest single uncertainty in the experiment was approximately 1% error associated with track counting statistics, reproducibility, and discrimination between fission fragments tracks and alpha pits. The next largest source of error was the uncertainty in detector efficiency arising from uncertainties in the angular distribution of fission fragment emission. Table II summarizes our anisotropy evaluation based on the available data for the empirical fitting function  $W(\theta) = 1 + A \cos^2\theta$ . The column headed " $\Delta A$ " lists estimated uncertainties in the anisotropy factor, and the " $\Delta\sigma_f$ " column shows the corresponding uncertainties in the cross section which result. Independent measurements of the anisotropy factor at each of the source energies are currently underway, using facilities at the Argonne National Laboratory, and may eventually modify some of the cross section values reported here.

The neutron yield of NBS-II was taken as the average of the results of four independent calibrations by NBS, BIPM, NPL, and ANL. An uncertainty of  $\pm 0.5\%$  in the average was estimated based on intercomparison of the independent calibrations.

TABLE II

## Fission Fragment Emission Anisotropy Evaluation

Neutron Energy (keV)	$^{235}\text{U}$			$^{239}\text{Pu}$		
	<u>A</u>	<u><math>\Delta A</math></u>	<u><math>\Delta\sigma_f</math></u>	<u>A</u>	<u><math>\Delta A</math></u>	<u><math>\Delta\sigma_f</math></u>
140	.007	<u>+0.007</u>	<u>+2.262%</u>	.080	<u>+0.015</u>	<u>+7.709%</u>
265	.030	<u>+0.010</u>	<u>+4.458%</u>	.109	<u>+0.015</u>	<u>+6.686%</u>
770	.111	<u>+0.015</u>	<u>+5.517%</u>	.117	<u>+0.015</u>	<u>+4.467%</u>
964	.117	<u>+0.015</u>	<u>+6.643%</u>	.116	<u>+0.015</u>	<u>+6.681%</u>

The deposit masses are uncertain to an estimated  $\pm 0.5\%$  for  $^{235}\text{U}$  and  $\pm 1.4\%$  for  $^{239}\text{Pu}$ . For the uranium deposits, this uncertainty allows for an order of magnitude less accuracy in the weighings claimed by ORNL due to possible contamination during the deposition and firing operation and any stoichiometric imperfections. In addition, thermal fission counting at the National Bureau of Standards confirmed the original assay to within a 1.0% measurement uncertainty. A gold-overlay of the plutonium deposits since the original assay at ORNL necessitated a second mass determination by alpha counting performed at NBS relative to a standard plutonium foil. A resulting uncertainty of 1.4% is dominated by the uncertainty in the standard foil.

Neutron calibration by the manganese bath technique requires corrections for parasitic capture in elements other than  $^{56}\text{Mn}$ . Other corrections and residual errors investigated include absorption in the source dry well and in the source itself, photoactivation of the bath due to the natural deuterium content, neutron streaming and penetration, mixing delay in the bath-detector system, and bath counting statistics. Total estimated error from these corrections in the source yield ratio to NBS-II never exceed .3%.

Scattering from the deposit backing and immediate surrounding mass were calculated by Monte Carlo methods. These corrections are as much as 3.5 ( $\pm 0.5\%$ ) in increased flux at the deposit surface for Ga-D neutrons to as little as 2.0 ( $\pm 0.3\%$ ) for Na-Be neutrons. An additional 1 ( $\pm 0.3\%$ ) scattering contribution arises in the plutonium measurements from the containment vessel. Geometrical uncertainties in the source-detector spacing and deposit-aperture spacing contribute  $\pm 0.5\%$  uncertainty.

An adjustment to reduce the measured value to a point energy was calculated using the ENDF/B-IV fission cross section shape and Monte Carlo generated neutron energy spectra shown for the four photoneutron sources in Fig. 3. Since the fission cross section shape is slowly varying over the photoneutron energy range for both  $^{235}\text{U}$  and  $^{239}\text{Pu}$ , this correction is for most cases less than 1 ( $\pm 0.3\%$ ). The exceptions are the lower energy points, 140 and 265 keV, for  $^{235}\text{U}$  where a steeper negative slope (see Fig. 4) in the fission cross section results in a correction as large as 3%.

## RESULTS AND CONCLUSION

Fission cross section values and the  $^{239}\text{Pu}/^{235}\text{U}$  ratios are listed in Table III.

TABLE III

Fission Cross Section Values from Photoneutron Sources

<u>Neutron Energy (keV)</u>	<u>Cross Section (barns)</u>		<u><math>^{239}\text{Pu}/^{235}\text{U}</math></u>
	<u><math>^{235}\text{U}</math></u>	<u><math>^{239}\text{Pu}</math></u>	
140	1.471 $\pm$ .030	1.465 $\pm$ .040	0.996 $\pm$ .025
265	1.271 $\pm$ .025	1.490 $\pm$ .040	1.172 $\pm$ .030
770	1.161 $\pm$ .025	1.678 $\pm$ .045	1.445 $\pm$ .035
964	1.210 $\pm$ .025	1.644 $\pm$ .040	1.359 $\pm$ .035

Work remains in progress on a more accurate evaluation of the room-return background and in measurement of fission fragment anisotropy values. A recalibration of NBS-II will be carried out at the National Bureau of Standards in the near future.

## ACKNOWLEDGMENT

The measurement on  $^{235}\text{U}$  at 964 keV was principally carried out by D. M. Gilliam (see reference 1) and results are included here for completeness. Others who helped during various stages of the experimental work include W. P. Stephany, J. C. Engdahl, and D. J. Grady.

## REFERENCE

1. D. M. Gilliam and G. F. Knoll, Ann. Nucl. Energy, 2, 637 (1975).

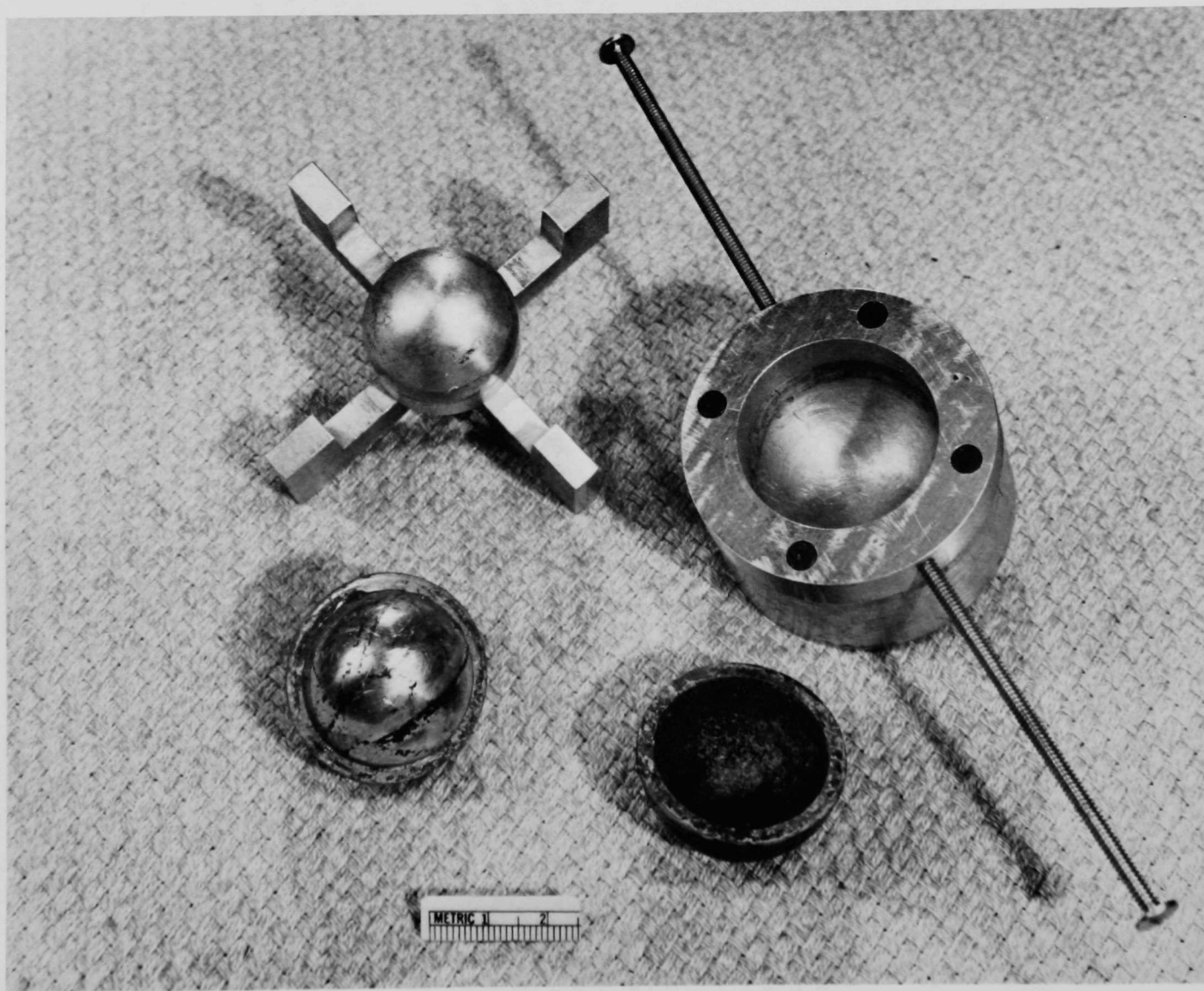


Figure 1. NaF Core, the Deuterated Polyethylene Shells, and Mold Used in Forming the Shells.

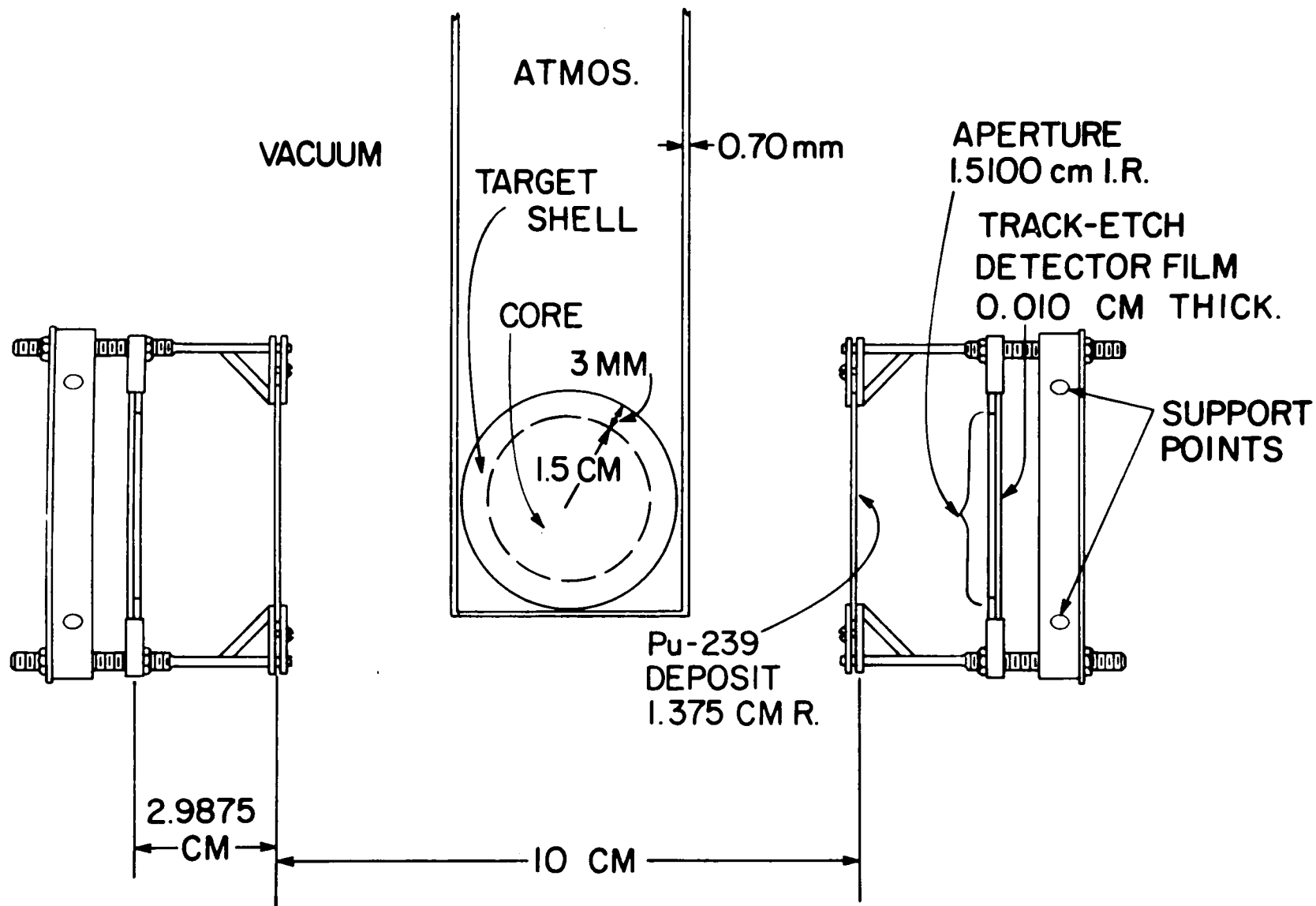


Figure 2. Arrangement for the Photoneutron Measurements.

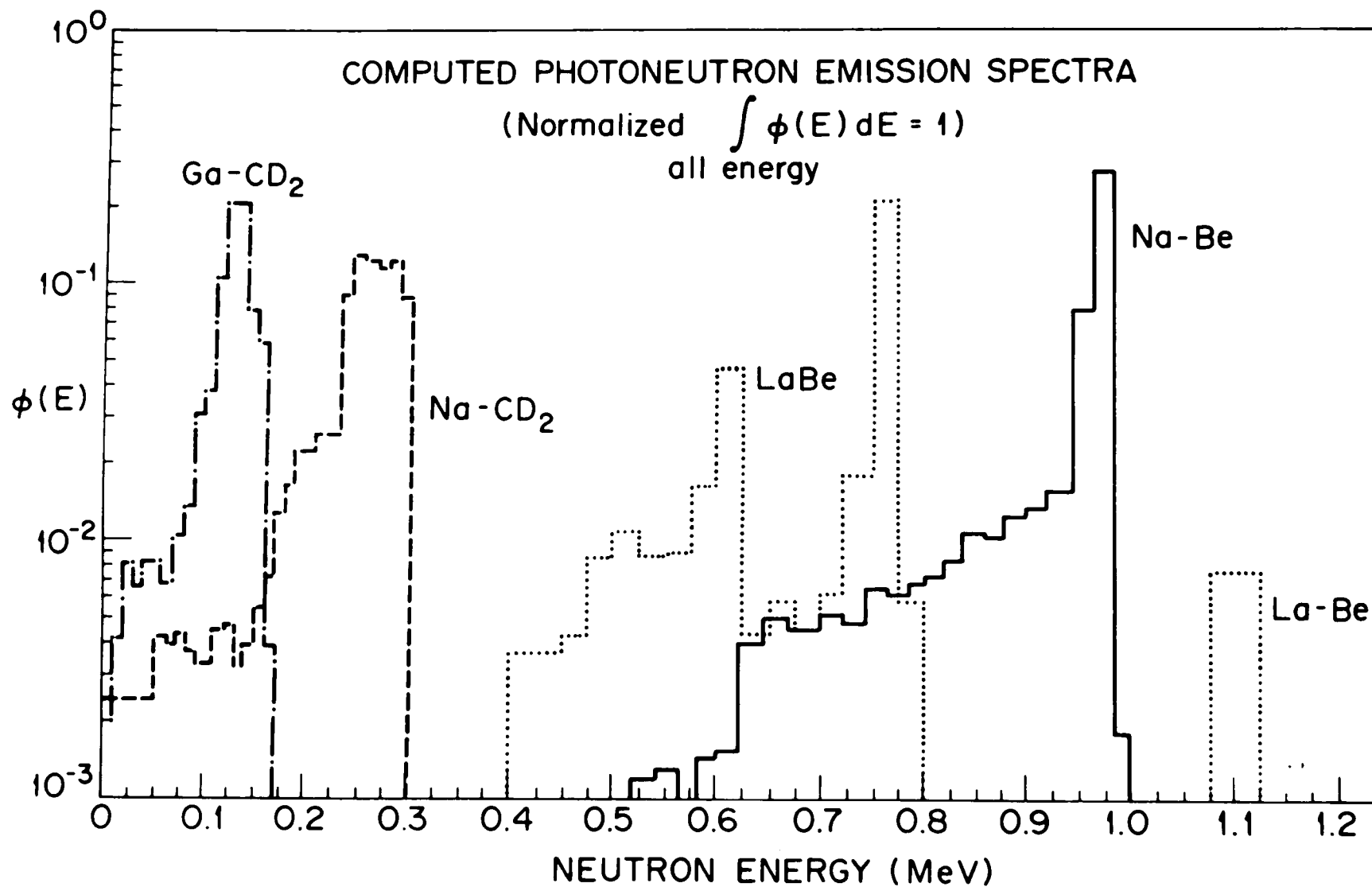


Figure 3. Computed Photoneutron Energy Emission Spectra.

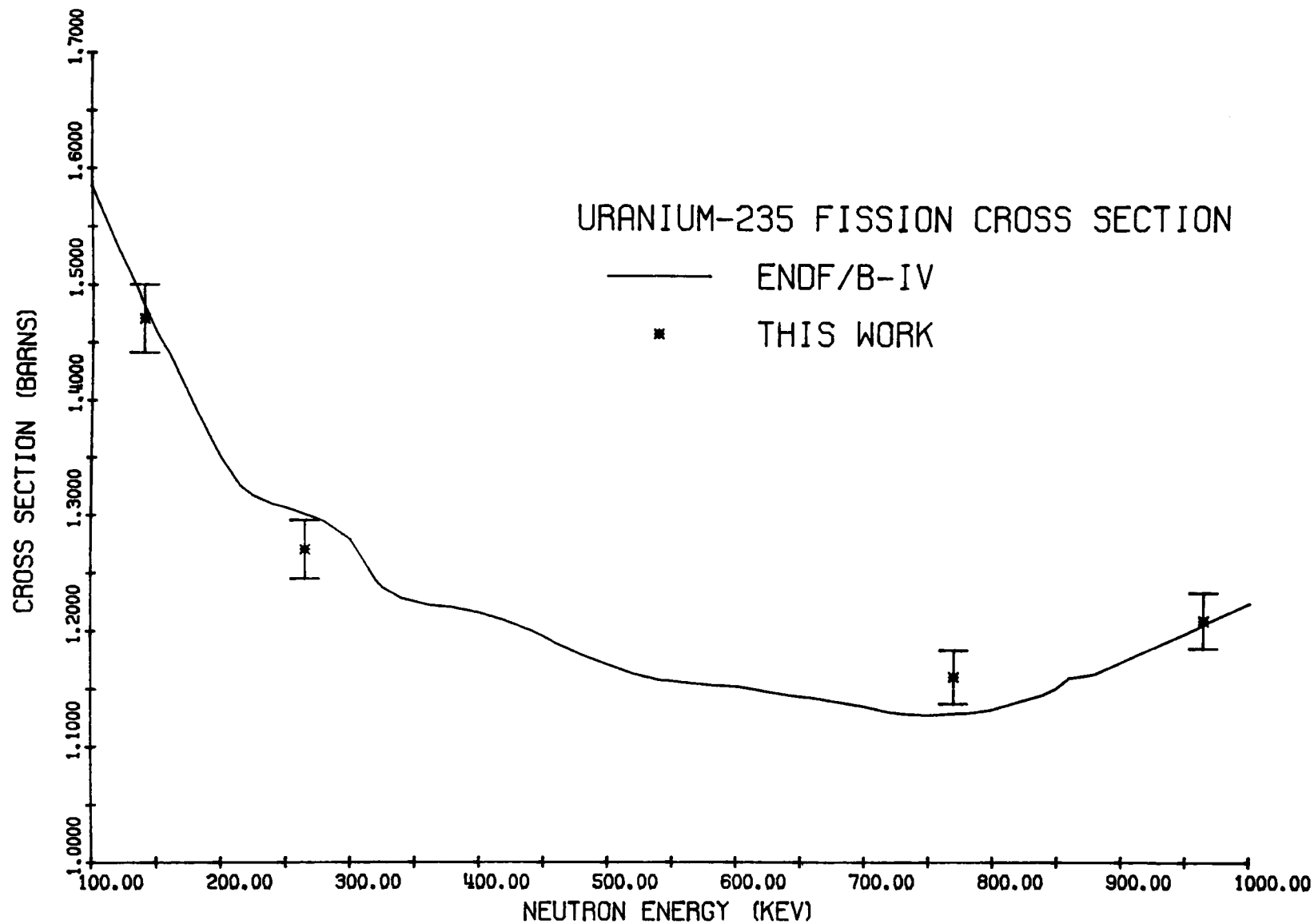


Figure 4.  $^{235}\text{U}$  Fission Cross Section Results.

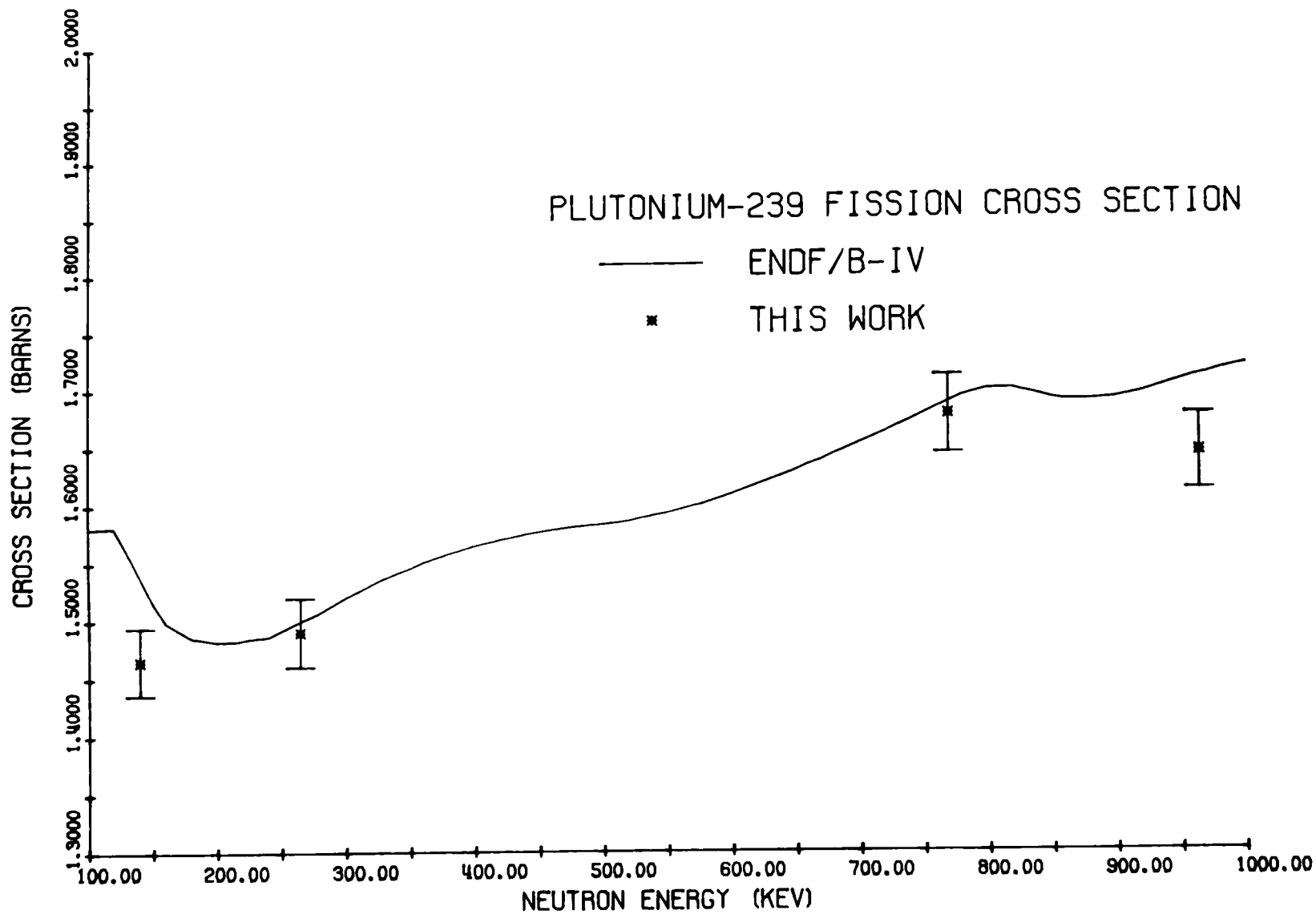


Figure 5.  $^{239}\text{Pu}$  Fission Cross Section Results.

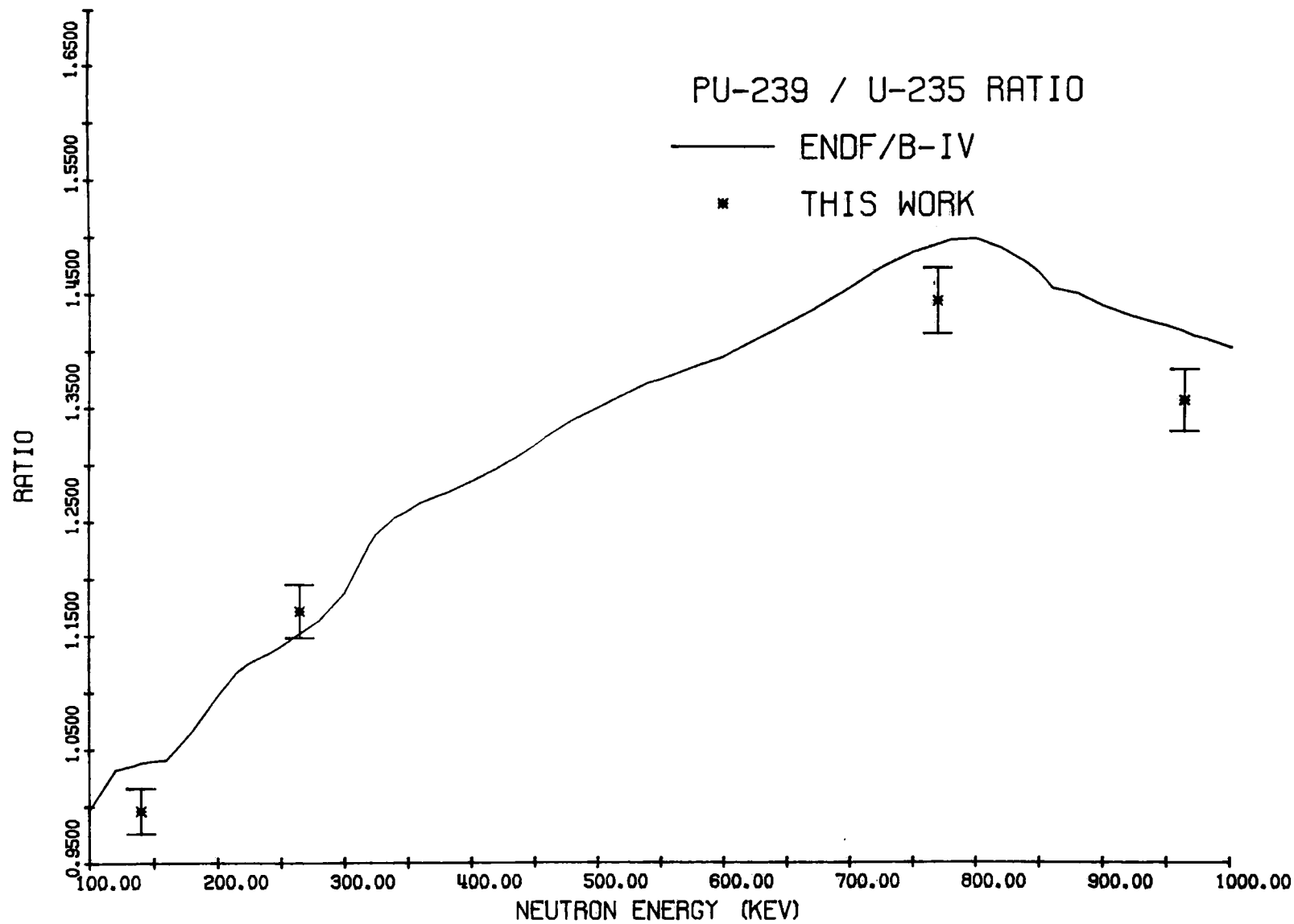


Figure 6.  $^{239}\text{Pu}/^{235}\text{U}$  Cross Section Ratios.

## DISCUSSIONS

C. Bowman By using two foils you reduce the error in the source distance determination, but there is also an error associated with the position of the source on the plain perpendicular to the sample-sample-line.

G. Knoll Yes. But both have zero slope. Both are in effect second order uncertainties. The uncertainty is much less severe in the plain parallel to the foils, than it is along the sample-sample-line.

J. Behrens On the uranium foils, you converted the  $\text{UO}_2$  at 800 degrees. On what were the 800 degrees based?

G. Knoll As far as I am concerned it was an arbitrary choice. I think it came originally from Geel.

J. Behrens The reason why I bring this up is that in a recent experiment I did, the same question came up and someone convinced me one should not go beyond 600 degrees. Then one starts to convert  $\text{U}_3\text{O}_8$  back to something less in oxygen.

G. Knoll I think there is documentation of the stoichiometry at this temperature.

S. Whetstone Do you depend on the NBS II Standard? How good is it?

G. Knoll We are completely dependent on NBS II Standard. There have been four independent calibrations of NBS II. All results are within  $\pm 0.5\%$ .

A. Smith Did you check your technique by measuring  $\bar{\nu}$  of Cf.

G. Knoll Yes, we did. I did not want to talk about this today, the value is preliminary and is embarrassingly close to the IAEA value.

PART.II      ABSOLUTE MEASUREMENT OF 14.6 MeV NEUTRON FISSION  
CROSS SECTIONS OF  $^{235}\text{U}$  AND  $^{238}\text{U}$

M. CANCE, G. GRENIER

*Service de Physique Nucléaire  
Centre d'Etudes de Bruyères-le-Châtel  
B.P. n° 61, 92120 Montrouge, France*

ABSTRACT

Absolute measurements of 14.6 MeV fission cross sections of  $^{235}\text{U}$  and  $^{238}\text{U}$  have been made with a double  $4\pi$  ionization chamber. The associated particle method was used.

The final values of  $\sigma_{\text{nf}}(^{235}\text{U})$ ,  $\sigma_{\text{nf}}(^{238}\text{U})$  and  $\sigma_{\text{nf}}(^{238}\text{U})/\sigma_{\text{nf}}(^{235}\text{U})$  are given with 1.9, 2.2 and 3 % uncertainty respectively.

INTRODUCTION

The value of the neutron fission cross section near 14 MeV is particularly important because measurements of cross section shapes are frequently normalized in this region. Furthermore, CZIRR and SIDHU [1] have obtained a value 7 % lower than that of ENDF/BIV evaluation for the  $^{235}\text{U}$  fission cross section near 14 MeV.

A first absolute measurement of 14.6 MeV neutron fission cross section of  $^{235}\text{U}$ , presented at the A.N.S. Conference at San Francisco [2], was in good agreement with this low value.

We have made a new measurement with other deposits permitting a better determination of the number of atoms per  $\text{cm}^2$ .

EXPERIMENTAL TECHNIQUE

The experimental arrangement is shown in Fig. 1.

1°) Fission detector

The fissions were detected in a double  $4\pi$  ionization chamber containing a deposit of  $^{235}\text{U}$  and one of  $^{238}\text{U}$  on vynes foils.

The chamber was cylindrical with a 6.6 cm diameter and a height of 10 cm; the inox cylinder wall was 0.08 cm thick and 0.05 cm for the front side.

## 2°) Neutron source

The 14.6 MeV neutrons were produced by the  $T(d,n)^4\text{He}$  reaction with a 550 keV Van de Graaff accelerator. The deuterons energy was 210 keV and the alpha detection angle was  $125^\circ$ .

## 3°) Samples

### Samples used for the first measurement

These samples were fabricated by the B.C.M.N. of EURATOM in Geel, Belgium. The deposits were 60 mm in diameter, about  $100 \mu\text{g}/\text{cm}^2$  of  $\text{UF}_4$  evaporated on  $85 \mu\text{g}/\text{cm}^2$  vynes foils, metalized by  $20 \mu\text{g}/\text{cm}^2$  Al. Table I gives the areal densities of deposits and isotopic compositions of the fissionable materials used.

TABLE I

Isotopic Compositions and Areal Densities  
of Deposits (1<sup>st</sup> Measurement)

Isotopic composition (at %)					Areal Density ( $\mu\text{g}/\text{cm}^2$ )
Sample	$^{234}\text{U}$	$^{235}\text{U}$	$^{236}\text{U}$	$^{238}\text{U}$	
$^{235}\text{U}$	1.6653	97.663	0.1491	0.5229	110.2
$^{238}\text{U}$	0.00016	0.01755	< 0.00001	99.9823	79.9

### Samples used for the second measurement.

These samples were fabricated at the Bruyères-le-Châtel Center. The deposits were 60 mm in diameter, about  $100 \mu\text{g}/\text{cm}^2$  of uranium acetate electrosprayed on  $20 \mu\text{g}/\text{cm}^2$  vynes foils, metalized by  $20 \mu\text{g}/\text{cm}^2$  Al. Table II gives the areal densities of deposits and isotopic compositions of the fissionable materials used.

## 4°) Experimental method and data acquisition

The absolute measurement was done with the associated particle technique; the alpha particles were detected by a solid state diode.

The time of flight method was used to determine the background due to the alpha activity of the deposit and to fissions induced by low energy neutrons. An accurate background correction was obtained using a biparametric acquisition of pulse height and time pulses.

TABLE II

Isotopic Compositions and Areal Densities  
of Deposits (2<sup>nd</sup> measurement)

	Isotopic Composition (at %)				Areal density ( $\mu\text{g}/\text{cm}^2$ )
Sample	$^{234}\text{U}$	$^{235}\text{U}$	$^{236}\text{U}$	$^{238}\text{U}$	
$^{235}\text{U}$	1.46	98.25	0.09	0.20	103.5
$^{238}\text{U}$	1.92	0.03		98.05	75.8

The associated particle method is based essentially on a good determination of the number of atoms per  $\text{cm}^2$  of the uranium deposit.

If the solid angle of the cone of neutrons associated with the detected  $\alpha$  particle is safely smaller than the solid angle subtended by the uranium deposit, no geometric factors enter into the calculation of fission cross section. Only fissions in coincidence with these  $\alpha$  particles are analyzed.

#### 5°) Determination of Number of Atoms Per $\text{cm}^2$

##### First Measurement

Our first measurement of the fission cross section of  $^{235}\text{U}$  was based on a number of atoms per  $\text{cm}^2$  ( $n_{\text{at}}$ ) obtained from low geometry  $\alpha$  counting made by B.C.M.N. at Geel. The same total alpha activity was obtained in our laboratory with this procedure. However other measurements made with different diaphragms placed between the deposit and the detector have shown an inhomogeneity of the deposit. These new measurements have given a number of atoms per  $\text{cm}^2$  for the area S, determined by the cone of neutrons associated on the deposit, 2.4 % smaller than the original  $n_{\text{at}}$ , with an uncertainty of 2.5 %.

The fission cross section of  $^{238}\text{U}$  was based on a number of atoms per  $\text{cm}^2$  obtained from  $4\pi$   $\alpha$  counting made by B.C.M.N. at Geel and in good agreement with our measurement. The very low  $\alpha$  activity of the sample does not permit us to measure the homogeneity of deposit, and the  $\sigma_{\text{nf}}(^{238}\text{U})$  obtained is not a significant value.

##### Second Measurement

The area of deposits were determined with good precision. Homogeneity measurements have been made from  $^{234}\text{U}$  alpha counting. A small difference between the average number of atoms per  $\text{cm}^2$  for the S area and the average  $n_{\text{at}}$  for the whole deposit has been found ; 0.1 % and 0.2 % for  $^{238}\text{U}$  and  $^{235}\text{U}$  deposits respectively.

The half lives of isotopes recommended by VANINBROUKX [3] were used.

### CORRECTIONS AND UNCERTAINTIES

For both measurements the following corrections have been made :

#### 1°) Fission Detector Efficiency

The fraction of fragments, which leave the deposit with energies below the electronic bias was obtained by extrapolation to zero pulse height. A 20 % uncertainty was allowed for that correction.

The fraction of fragments absorbed in the sample was calculated with a Monte Carlo technique.

The path length of the fission fragments in composite systems was obtained from an empirical stopping power relation [4]. A 20 % uncertainty was also assumed for this correction.

#### 2°) Neutron Attenuation in Target Backing and in Front Side of the Fission Chamber

The error on that attenuation was assumed to be 20 %.

#### 3°) Fissions Due to Other Isotopes of Uranium

These fissions were calculated and a 10 % uncertainty was assumed for this correction.

The effect upon the cross section caused by those corrections and the other uncertainties are listed in Table III and IV respectively for the first and the second measurement.

The total uncertainties are the root - mean - square of all the errors.

### RESULTS AND DISCUSSION

The final values of  $\sigma_{nf}(^{235}\text{U})$ ,  $\sigma_{nf}(^{238}\text{U})$  and  $\sigma_{nf}(^{238}\text{U})/\sigma_{nf}(^{235}\text{U})$  are given with 1.9, 2.2 and 3 % uncertainty respectively. Our results are compared to data from other experiments and to the values of ENDF/B IV in Table V.

Our first value of  $\sigma_{nf}(^{235}\text{U})$  though obtained with a large uncertainty is in very good agreement with our second value.

Our final values obtained from the second measurement agree very well with the recent data of CZIRR and SIDHU [1], BEHRENS et al. [5] and ALKAZOV [6] and confirm lower values than that of ENDF/B IV for  $\sigma_{nf}(^{235}\text{U})$  and  $\sigma_{nf}(^{238}\text{U})$ .

TABLE III

Uncertainties for the first measurement

EFFECT	Uncertainty, %	
	$^{235}\text{U}$	$^{238}\text{U}$
Statistical	1	1.7
Extrapolation to zero pulse height	0.23	0.5
Lost of fissions	0.18	0.14
Number of atoms per $\text{cm}^3$	2.5	Undetermined
Neutron attenuation in target backing	0.36	0.36
Neutron attenuation in front side of fission chamber	0.3	0.3
Fissions in other isotopes	0.15	Négligible
Total uncertainty of result	2.75	Undetermined

TABLE IV

Uncertainties for the second measurement

EFFECT	Uncertainty, %	
	$^{235}\text{U}$	$^{238}\text{U}$
Statistical	0.9	1.5
Extrapolation to zero pulse height	0.6	0.7
Lost of fissions	0.19	0.17
Number of atoms per $\text{cm}^2$	1.4	1.35
Neutron attenuation in target backing	0.36	0.36
Neutron attenuation in front side of fission chamber	0.3	0.3
Fission in other isotopes	0.2	0.4
Total uncertainty of result	1.85	2.23
Total uncertainty of ratio	2.82	

TABLE V

Comparison of various results

Fission cross section (barns) $E_n = 14.60 \pm 0.13 \text{ MeV}$	CZIRR and SIDHU [1]	BEHREMS et al. [5]	ALKAZOV [6]	ENDF/ B IV	Present Results (1st)	Present Results (2nd)
$^{235}\text{U}$	2.075 $\pm 0.04$			2.214	2.068 $\pm 0.058$	2.063 $\pm 0.039$
$^{238}\text{U}$			1.17 $\pm 0.01$	1.22		1.149 $\pm 0.025$
$^{238}\text{U}/^{235}\text{U}$		0.563 $\pm 0.009$		0.55		0.557 $\pm 0.017$

## REFERENCES

1. J.B. CZIRR and G.S. SIDHU "Fission Cross Section of Uranium 235 from 3 to 20 MeV" *Nucl. Sci. Eng.*, 57, 18 (1975).
2. M. CANCE and G. GRENIER "Absolute Measurement of the 14.6 MeV neutron fission Cross Section of  $^{235}\text{U}$  and  $^{238}\text{U}$ " A.N.S. Conference, San-Francisco (1975).
3. R. VANINBROUKX "The half lives of some long lived actinides. A Compilation" EUR 5194e C.B.M.N. (1974).
4. R. MÜLLER and F. GONNENWEIN "Slowing Down of Fission Fragments in Various Absorbers", *Nucl. Instrum. Methods*, 91, 357 (1971).
5. J.W. BEHRENS, G.W. CARLSON and R.W. BAUER, " $^{238}\text{U} : ^{235}\text{U}$  Fission Cross Section Ratio" UCRL 76219, Lawrence Livermore Laboratory (1975).
6. I.D. ALKAZOV, National Conf. on Neutron Phys., Kiev (1973).

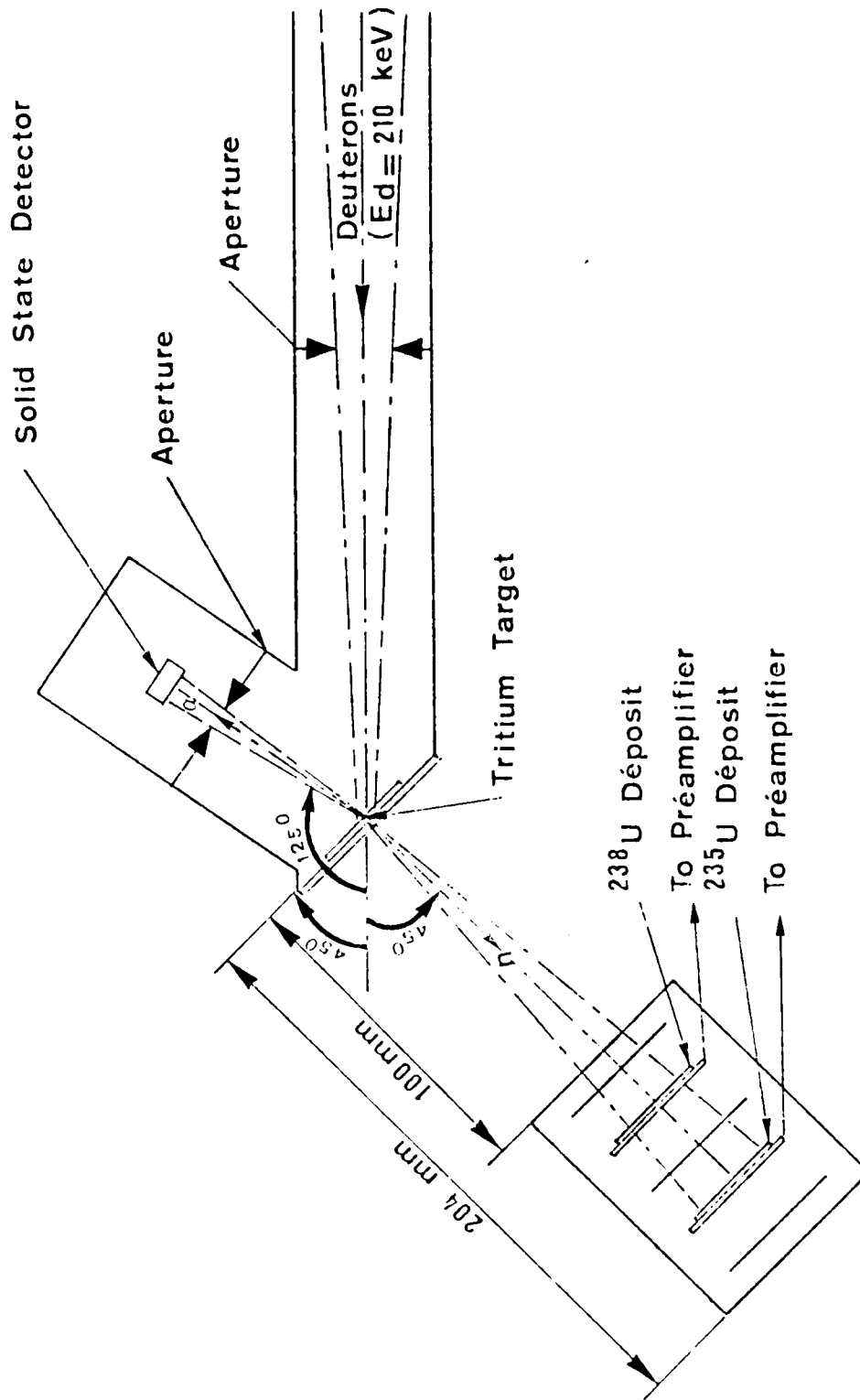


Figure 1. Experimental arrangement.

## DISCUSSIONS

R. Peelle Was the target much thinner than the deuteron range? Or did they stop in the target?

G. Grenier They stopped.

R. Peelle So the size of the fission plates was enough to take into account the change in angular distribution caused by the deuteron when it goes all the way from 200 keV to zero, because this changes the opening angle.

G. Grenier We first made a measurement of the neutron cone with a small scintillator and determined the axis.

R. Peelle You have mapped the neutrons as a function of position?

G. Grenier Yes.

R. Peelle Second question. Did you check the importance of the scattering of the  $\alpha$ -particles in the tritium source. The  $\alpha$ -particles can change direction due to scattering in the absorbing target material.

G. Grenier No, we did not.

L. Stewart I was more concerned that you have to know the solid angles of these detectors and you have not any error related to this.

R. Peelle Let me answer. The method is based on the assumption that all the neutrons go through the sample and it does not matter where they go through if the sample is uniform.

L. Stewart As long as the sample is uniform and the  $\alpha$ -detector has 100% efficiency.

R. Peelle All  $\alpha$ 's were detected.

# THE $^{235}\text{U}$ AND $^{238}\text{U}$ NEUTRON INDUCED FISSION CROSS SECTIONS RELATIVE TO THE $\text{H}(\text{n},\text{p})$ CROSS SECTION

B. Leugers, S. Cierjacks, P. Brotz, D. Erbe, D. Gröschel  
G. Schmalz, F. Voß

Institut für Angewandte Kernphysik  
Kernforschungszentrum Karlsruhe, F. R. Germany

## ABSTRACT

The fission cross sections of  $^{235}\text{U}$  and  $^{238}\text{U}$  have been measured with the fast neutron time-of-flight facility at the Karlsruhe Isochronous Cyclotron in the range from 1-20 MeV. Fission events were detected with gas scintillation counters requiring coincidences from both fission fragments. The fast neutron flux was measured with a telescope-like proton recoil detector. The transmission flux detector allowed a simultaneous measurement of the neutrons at the fission foil position. The fission cross sections have counting uncertainties of less than  $\sim 3\%$  for most of the  $^{235}\text{U}$ -data points and of less than  $\sim 4\%$  for most of the  $^{238}\text{U}$ -data points.

## INTRODUCTION

The knowledge of the fission cross section of  $^{238}\text{U}$  and  $^{235}\text{U}$  is essential for fast reactor technology. The cross section of  $^{238}\text{U}$  is of considerable importance with respect to its use as the major breeding material in a fast reactor. In addition its interest is due to the use of  $^{238}\text{U}(\text{n},\text{f})$  as a threshold reaction in neutron spectra measurements. The cross section of  $^{235}\text{U}$  is of major importance mainly because of its use as a standard reference cross section. The accuracy requested presently by the users of such data is of the order of 1-2 %. However major discrepancies exist between several groups of data, which are still as large as 5 %.

In this contribution we describe a new experiment for a determination of the fission cross sections of  $^{238}\text{U}$  and  $^{235}\text{U}$ . The experiment aimed to obtain additional information on the fission cross section in the whole energy range from 1-20 MeV. Such measurements seemed desirable, particularly since relatively few measurements covered the entire energy region of interest for applied purposes.

## EXPERIMENTAL

Only a brief description of the experimental method will be given here, since it has been described in detail in another contribution of the meeting<sup>1)</sup>.

For the measurement of the fission yields and the incident neutron energies standard time-of-flight techniques were employed. The fission detectors with fission foils of  $^{235}\text{U}$  and  $^{238}\text{U}$  were placed alternately in the same neutron beam at the 57 m flight path of the fast neutron time-of-flight facility at the isochronous cyclotron and irradiated simultaneously. The nominal overall resolution in the measurements was 0.08 ns/m. But, in the low energy range some channel grouping was employed to improve the counting statistics. A special collimation system provided a neutron beam of 7 cm diameter at the fission detector position.

### Fission Detectors

Fission events were detected by measurement of both fission fragments in gas scintillation counters. A detector arrangement of nine gas scintillation counters in series described previously was employed<sup>2)</sup>. Measurements were made on four  $^{238}\text{U}$  and four  $^{235}\text{U}$  samples of 7 cm diameter containing  $\sim 400 \mu\text{gr}/\text{cm}^2$  uranium. The uranium was in oxide form and was deposited on  $170 \mu\text{gr}/\text{cm}^2$  vycor foils metallized by  $20 \mu\text{gr}/\text{cm}^2$  aluminum. Sample preparation was made at the CBNM Euratom Laboratory in Geel. The foils divided optically two neighbouring chambers from each other in a plane perpendicular to the neutron beam. Each scintillator cell was viewed through a quartz window by one Valvo 56 DUVP photomultiplier. The scintillator was continuously flushed with a mixture of 85 % argon and 15 % nitrogen. Fission events were separated from  $\alpha$ -background and electronic noise by pulse height discrimination and by coincidences between the photomultipliers on each side of a fission foil.

### Flux Measurement

The incident neutron spectrum at the 57 m detector position was measured with a special telescope-like proton recoil device described elsewhere<sup>3)</sup>. The device, which was designed for fast neutron flux measurements between 1-30 MeV obtained with the Karlsruhe isochronous cyclotron, involves solid radiators and gas scintillation transmission counters. Neutron flux measurements over the entire region was accomplished with two different counter systems, one for the range from 1-6 MeV, another for the range between 5-30 MeV with a small energy range of overlap. In the range from 1-6 MeV where no spurious background from other neutron induced charged particle reactions is obtained, the protons from a thin radiator foil are detected in a single gas scintillation chamber viewed by three photomultipliers. For observation of a recoil proton a threefold coincidence within 15 nsec is required. Above the energy range of  $\sim 5$  MeV high energy protons are identified by coincidences in three scintillation chambers, which are arranged in series along the neutron beam axis, and by determination of their specific energy losses.

The arrangement of the flux counters in the neutron beam is shown in Fig. 1. Both counters are placed beyond the end-collimator as shown here.

The flux counters were set at a distance of  $\sim 1.5$  m apart from the fission detectors and fission foils were simultaneously irradiated in the same neutron beam. The diameter of the cylindrical chambers of the flux counters is chosen sufficiently large compared to the diameter of the traversing neutron beam, so that all massive parts are well shielded from neutrons and  $\gamma$ -rays coming from the cyclotron source. Thus, the neutron beam traverses only the thin entrance and exit windows of the chambers, the two radiator foils and the scintillator gas. This results in a high transmission of the flux counter of better than  $\sim 99.9$  % introducing only a negligible distortion of the original neutron spectrum. With the overall efficiencies of the flux counters, which range from  $1-4 \times 10^{-4}$  in the whole energy region between 1-30 MeV, an accuracy for the determination of the neutron flux of about 3-4 % was obtained between 1-30 MeV. Below 1 MeV the accuracy decreased to 8 % due to the rapid decrease of the efficiency for proton detection of the low energy system.

## DATA ANALYSIS

### Corrections

Corrections were applied for a number of effects which were small in general due to the conditions chosen for the experiment. As sources for corrections the following effects have been considered:

Background: The time-independent background was determined from the time-interval between the prompt  $\gamma$ -peak and the begin of the fast neutron spectrum. This background was low, typically smaller than 1 % and did not exceed 5 % even for  $^{238}\text{U}$  at the lowest measured energy of 1.2 MeV. Time-dependent background was investigated by a comparison of resonance transmission shapes of carbon. Such searches indicated that the time-dependent background was negligible in our experiments, although the possibility of a 2 % contribution from such background could not be excluded.

Energy dependent detectors efficiency: The energy dependence of the efficiency due to the incident neutron momentum was calculated with a computer program employing mainly the treatment of Rossi and Staub<sup>4</sup>). In this program the absorption of fission fragments in the foil and the backing is calculated from the thicknesses of the various layers of the samples, the ranges and the energy losses of fission products in the corresponding materials<sup>5</sup>). It turned out from these calculations that the total efficiencies in our experiment changed from 78.9 % at 1 MeV to 77.1 % at 20 MeV incident neutron energy.

Electronic threshold and dead time corrections: The electronic threshold correction was determined by extrapolating the pulse height distributions at both sides of the foil to the zero value. The result showed that at maximum in 20 % of the cases one of the two fission fragments was absorbed in the sample. The main error sources of the corresponding correction are thickness uncertainties of the aluminum and vycor layers. This can be kept small, if the energy loss of  $\alpha$  particles passing through the backing is measured accurately during the final mass determination. Since the experiment was performed at low overall counting rates of  $\sim 1$  kHz, dead time correction due to electronic losses

were small. These were typically of the order of 1 %.

Sample mass and isotopic composition: The actual areal densities and the isotopic composition of the fission foils used in the measurements are shown in Table II of ref. 1. It can be seen, that highly enriched  $^{238}\text{U}$  was used, requiring no correction. The main impurity in  $^{235}\text{U}$  is 5.8 % of  $^{238}\text{U}$ . Thus the contribution of fission events from this isotope was not negligible and required a correction. This was done with the help of the counting rates from the pure  $^{238}\text{U}$  sample which was irradiated in the same neutron beam.

Flux detector threshold: The largest contribution to the systematic uncertainty is coming from the neutron flux measurement. This contribution includes uncertainties in the relative efficiencies for proton detection in both fission counters (typically 2 %, max. 5 % at 1.2 MeV), in the  $\text{H}(n,n)$  cross section (2 %) and in the actual flux measurement itself (1-2 %).

### Total Errors

In addition to the standard deviation errors of the measurements which are included in the lists of our data we must assign a total systematic error to our measurement. The latter is generally energy dependent. Combining all systematic errors from spectrum and fission measurements described above, the following resulting systematic error was estimated: 4 % for energies between 3-14 MeV, 5 % between 2-3 MeV, 5-8 % between 1-2 MeV and between 14-20 MeV.

## RESULTS

In the discussion of our results it is definitely not intended to try an extensive comparison with measurements from other laboratories. A detailed comparison is part of the task of the Experts Meeting to which we contribute. It is understood that the production of comparative graphs is part of the service which is provided by the organizers.

### $^{235}\text{U}$ Fission Cross Section

The results of the measurements are shown in Fig. 2. The numerical values are listed in Table I. The measured relative cross sections were normalized at 14 MeV to give a cross section of 2.136 b. At energies below 2 MeV the data represent 50 keV energy averages of the original time-of-flight data. Between 2-12 MeV the data were averaged over 100 keV while above that energy a grouping of five time channels was made. The errors given in third column of the table and by the bars in the figure are statistical errors. In these values the effects of background subtractions and isotopic corrections were already included.

The fission cross section of  $^{235}\text{U}$  is compared in Fig. 2. With some other recent measurements made over a remarkable overlapping energy range<sup>6,7)</sup>. The relative shape of the present cross section agrees within better than 5 % with the results from Barton et al.<sup>6)</sup> and with the recent Livermore measurements<sup>6)</sup> throughout the complete range of overlap.

## $^{238}\text{U}$ Fission Cross Section

The  $^{238}\text{U}$  fission cross section is shown in Fig. 3. A listing of the Karlsruhe results is given in Table II. Energy averages of the data and channel grouping was made in the same way as for  $^{235}\text{U}$ . The relative shape of the present cross section was normalized to 1.207 b and 14 MeV.

In Fig. 3 our results are compared with some high energy results<sup>8-10</sup>) prior to 1967. The agreement of our data with the data LASL data is satisfactory over the whole range from threshold to 20 Mev. The present results agree within  $\pm 3\%$  also with those of Pankratov et al..

### ACKNOWLEDGEMENT

The authors are indebted to Prof. Schatz for his interest in the continuation of this work. They wish also to thank Drs. Lauer and Verdingh for the preparation of the samples and the preliminary mass determination. The help of the cyclotron group headed by Dr. H. Schweickert and Mr. F. Schulz is greatly acknowledged.

### REFERENCES

1. S. CIERJACKS, B. LEUGERS, K. KARI, B. BROTZ, D. ERBE, D. GRÖSCHEL, G. SCHMALZ, F. VOSS, "Measurements of Neutron Induced Fission Cross Section at the Isochronous Cyclotron, this proceedings.
2. S. CIERJACKS, D. KOPSCH, J. NEBE, G. SCHMALZ, F. VOSS, *Proc. 3rd Conf. on Neutron Cross Sections and Technology*, Knoxville, Tenn. March 1971, p. 280, CONF-710301.
3. I. SCHOUKY, S. CIERJACKS, P. BROTZ, D. GRÖSCHEL, B. LEUGERS, *Proc. Conf. on Nucl. Cross Sections and Technology*, Washington D.C., March 1975, p. 277-280.
4. B.B. ROSSI, H.H. STAUB, *Ionization Chambers and Counters*, Mc Graw-Hill, New York (1949) 227.
5. L.C. NORTHCLIFF, R.F. SCHILLING, *Nuclear Data Tables A7* (1970) 235.
6. BARTON et al., Los Alamos Scientific Laboratory, USNDC-9, 1973 (unpublished).
7. J.B. CZIRR et al, *Nucl. Sci. Eng.* 57 (1975) 18.
8. P.H. WHITE, *J. Nucl. Energ.* 21 (1967) 671.
9. V.M. PANKRATOV, *Sov. J. At. Energy*, 14 (1963) 167.
10. G. HANSEN, Report WASH 1074, 1967.

TABLE I  
Fission Cross Section of  $^{235}\text{U}$

$E_n$ (MeV)	$\sigma_f^{235}\text{U(b)}$	Stat. Unc. (%)	$E_n$ (MeV)	$\sigma_f^{235}\text{U(b)}$	Stat. Unc. (%)	$E_n$ (MeV)	$\sigma_f^{235}\text{U(b)}$	Stat. Unc. (%)
20.075	1.947	1.1	10.140	1.746	2.1	5.541	1.078	2.9
19.641	1.947	1.1	10.046	1.700	2.1	5.442	1.073	3.0
19.221	2.026	1.0	9.954	1.726	2.1	5.344	1.050	3.0
18.814	2.079	1.0	9.833	1.718	1.9	5.250	1.096	2.8
18.420	2.119	1.0	9.743	1.717	2.2	5.146	1.078	2.9
18.039	2.158	1.0	9.655	1.738	2.2	5.046	1.078	2.9
17.670	2.167	1.0	9.539	1.741	1.9	4.949	1.142	2.8
17.311	2.164	1.0	9.454	1.806	2.2	4.843	1.172	2.7
16.964	2.211	1.0	9.342	1.735	2.0	4.742	1.152	2.7
16.627	2.221	1.0	9.232	1.697	2.0	4.643	1.169	2.7
16.301	2.220	1.0	9.150	1.731	2.3	4.548	1.189	2.6
15.983	2.312	0.9	9.044	1.706	2.1	4.446	1.143	2.6
15.675	2.276	1.0	8.939	1.741	2.1	4.348	1.116	2.7
15.376	2.274	1.0	8.836	1.791	2.1	4.244	1.149	2.5
15.086	2.242	1.0	8.734	1.751	2.1	4.144	1.176	2.5
14.803	2.213	1.0	8.635	1.819	2.1	4.048	1.187	2.4
14.529	2.186	1.0	8.537	1.724	2.2	3.947	1.186	2.4
14.262	2.100	1.0	8.441	1.750	2.2	3.850	1.212	2.4
14.003	2.136	1.0	8.346	1.717	2.3	3.750	1.146	2.3
13.750	2.130	1.1	8.253	1.774	2.0	3.647	1.164	2.3
13.505	2.040	1.1	8.139	1.745	2.3	3.547	1.177	2.2
13.266	2.013	1.1	8.050	1.630	2.2	3.446	1.167	2.2
13.033	1.954	1.2	7.940	1.712	2.4	3.349	1.182	2.1
12.807	1.924	1.2	7.853	1.771	2.2	3.250	1.183	2.1
12.586	1.822	1.2	7.748	1.704	2.2	3.151	1.218	1.9
12.371	1.795	1.3	7.644	1.701	2.3	3.050	1.206	2.0
12.161	1.763	1.3	7.542	1.730	2.3	2.950	1.264	1.8
12.038	1.773	2.1	7.443	1.689	2.3	2.849	1.237	1.8
11.957	1.759	1.7	7.345	1.650	2.4	2.750	1.247	1.8
11.837	1.669	2.2	7.249	1.603	2.5	2.647	1.203	1.8
11.758	1.719	1.8	7.155	1.595	2.5	2.549	1.257	1.7
11.641	1.748	1.8	7.045	1.461	2.4	2.450	1.245	1.6
11.526	1.759	2.2	5.937	1.497	2.4	2.349	1.290	1.6
11.450	1.740	1.8	6.849	1.558	2.6	2.248	1.276	1.5
11.337	1.723	1.8	6.746	1.397	2.6	2.147	1.325	1.5
11.227	1.698	2.3	6.645	1.424	2.6	2.047	1.274	1.5
11.154	1.705	1.9	6.547	1.305	2.7	1.973	1.308	2.1
11.046	1.720	1.9	6.450	1.285	2.6	1.923	1.286	2.0
10.939	1.723	1.9	6.340	1.151	3.0	1.872	1.273	2.1
10.834	1.670	2.4	6.248	1.191	2.8	1.824	1.290	2.0
10.765	1.741	1.9	6.143	1.173	3.1	1.775	1.280	2.1
10.663	1.688	2.0	6.056	1.098	3.0	1.726	1.308	2.0
10.562	1.675	2.0	5.956	1.108	3.0	1.674	1.275	2.0
10.462	1.712	2.0	5.844	1.037	2.9	1.625	1.244	2.0
10.364	1.722	2.0	5.750	1.071	3.1	1.574	1.291	2.0
10.235	1.739	1.8	5.644	1.008	3.0	1.524	1.293	1.9

TABLE I (Contd.)

$E_n$ (MeV)	$\sigma_f^{235}\text{U}(\text{b})$	Stat. Uncertainty (%)
1.474	1.291	1.9
1.424	1.232	2.0
1.374	1.264	1.9
1.324	1.278	1.9
1.274	1.211	1.9
1.224	1.252	1.9

TABLE II

Fission Cross Section of  $^{238}\text{U}$ 

$E_n$ (MeV)	$\sigma_f^{238}\text{U}(\text{b})$	Stat. Unc. (%)	$E_n$ (MeV)	$\sigma_f^{238}\text{U}$	Stat. Unc. (%)	$E_n$ (MeV)	$\sigma_f^{238}\text{U}$	Stat. Unc. (%)
20.075	1.424	1.3	10.140	0.968	2.8	5.541	0.528	4.2
19.641	1.397	1.3	10.046	0.983	2.8	5.442	0.557	4.1
19.221	1.404	1.3	9.954	0.976	2.8	5.344	0.533	4.3
18.814	1.419	1.2	9.833	0.995	2.4	5.250	0.514	4.1
18.420	1.400	1.2	9.743	1.017	2.8	5.146	0.525	4.1
18.039	1.377	1.2	9.655	0.948	2.9	5.046	0.500	4.3
17.670	1.381	1.2	9.539	0.949	2.6	4.949	0.534	4.1
17.311	1.404	1.2	9.454	1.006	2.9	4.843	0.570	3.8
16.964	1.369	1.2	9.342	0.967	2.6	4.742	0.543	3.9
16.627	1.421	1.2	9.232	0.991	2.6	4.643	0.592	3.8
16.301	1.449	1.2	9.150	0.987	3.1	4.548	0.561	3.7
15.983	1.449	1.2	9.044	0.955	2.7	4.446	0.564	3.7
15.675	1.404	1.2	8.939	1.012	2.7	4.348	0.560	3.7
15.376	1.390	1.2	8.836	0.974	2.8	4.244	0.568	3.6
15.086	1.344	1.3	8.734	0.961	2.9	4.144	0.558	3.6
14.803	1.290	1.3	8.635	1.049	2.8	4.048	0.557	3.5
14.529	1.219	1.3	8.537	0.986	2.9	3.947	0.561	3.5
14.262	1.192	1.4	8.441	1.002	2.9	4.850	0.536	3.5
14.003	1.207	1.4	8.346	0.961	3.0	3.750	0.575	3.2
13.750	1.156	1.4	8.253	0.955	2.8	3.647	0.566	3.3
13.505	1.153	1.5	8.139	0.966	3.1	3.547	0.542	3.2
13.266	1.103	1.5	8.050	0.972	2.8	3.446	0.567	3.1
13.033	1.070	1.6	7.940	0.981	3.2	3.349	0.511	3.2
12.807	1.018	1.6	7.853	1.009	2.9	3.250	0.507	3.2
12.586	0.994	1.7	7.748	0.970	3.0	3.151	0.538	2.9
12.371	1.008	1.7	7.644	0.918	3.1	3.050	0.519	3.0
12.161	1.037	1.7	7.542	0.968	3.1	2.950	0.540	2.8
12.038	1.053	2.7	7.443	0.964	3.1	2.849	0.527	2.8
11.957	1.031	2.2	7.345	0.926	3.2	2.750	0.529	2.7
11.837	0.998	2.8	7.249	0.930	3.2	2.647	0.534	2.6
11.758	1.013	2.3	7.155	0.918	3.3	2.549	0.516	2.6
11.641	1.009	2.3	7.045	0.908	3.1	2.450	0.519	2.5
11.526	1.005	2.9	6.937	0.951	3.0	2.349	0.508	2.5
11.450	1.012	2.4	6.849	0.910	3.5	2.248	0.542	2.4
11.337	1.049	2.3	6.746	0.916	3.2	2.147	0.534	2.4
11.227	1.031	2.9	6.645	0.842	3.4	2.047	0.531	2.3
11.154	1.010	2.4	6.547	0.826	3.4	1.973	0.535	3.3
11.046	0.998	2.5	6.450	0.751	3.4	1.923	0.497	3.3
10.939	0.971	2.5	6.340	0.718	3.8	1.872	0.535	3.2
10.834	1.016	3.0	6.248	0.646	3.8	1.824	0.523	3.2
10.765	0.976	2.6	6.143	0.639	4.1	1.775	0.495	3.3
10.663	0.958	2.6	6.056	0.672	3.8	1.726	0.446	3.4
10.562	0.977	2.6	5.956	0.560	4.2	1.674	0.457	3.3
10.462	1.056	2.5	5.844	0.532	4.1	1.625	0.451	3.3
10.364	0.982	2.7	5.750	0.531	4.4	1.574	0.433	3.4
10.235	1.021	2.3	5.644	0.520	4.2	1.524	0.390	3.5

TABLE II (Contd.)

$E_n$ (MeV)	$\sigma_f^{238}\text{U}(\text{b})$	Stat. Uncert. (%)
1.474	0.352	3.7
1.424	0.265	4.3
1.374	0.171	5.2
1.324	0.104	6.6
1.274	0.087	7.2
1.224	0.053	9.1

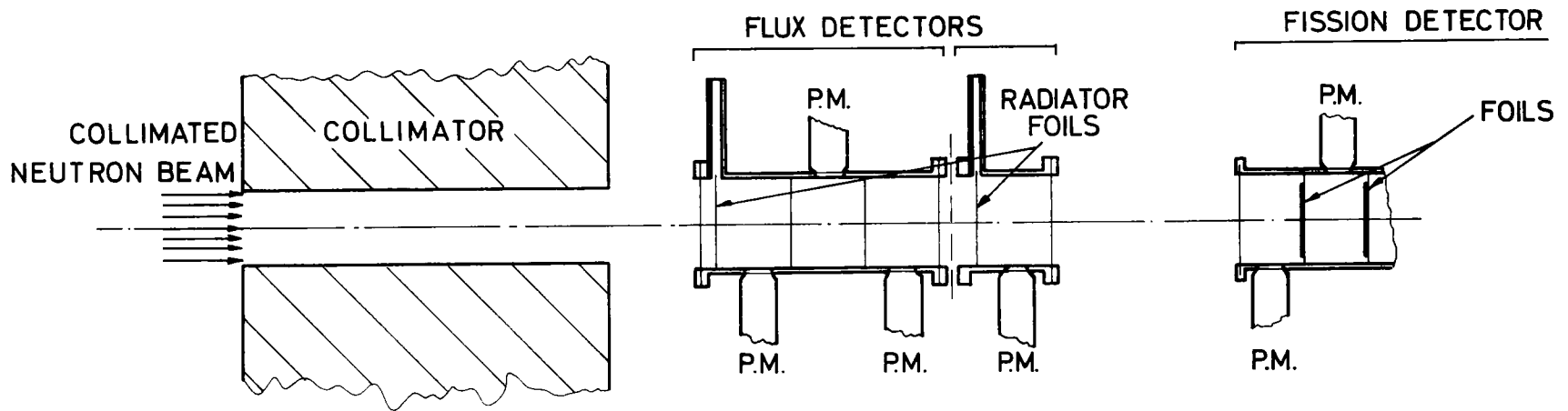
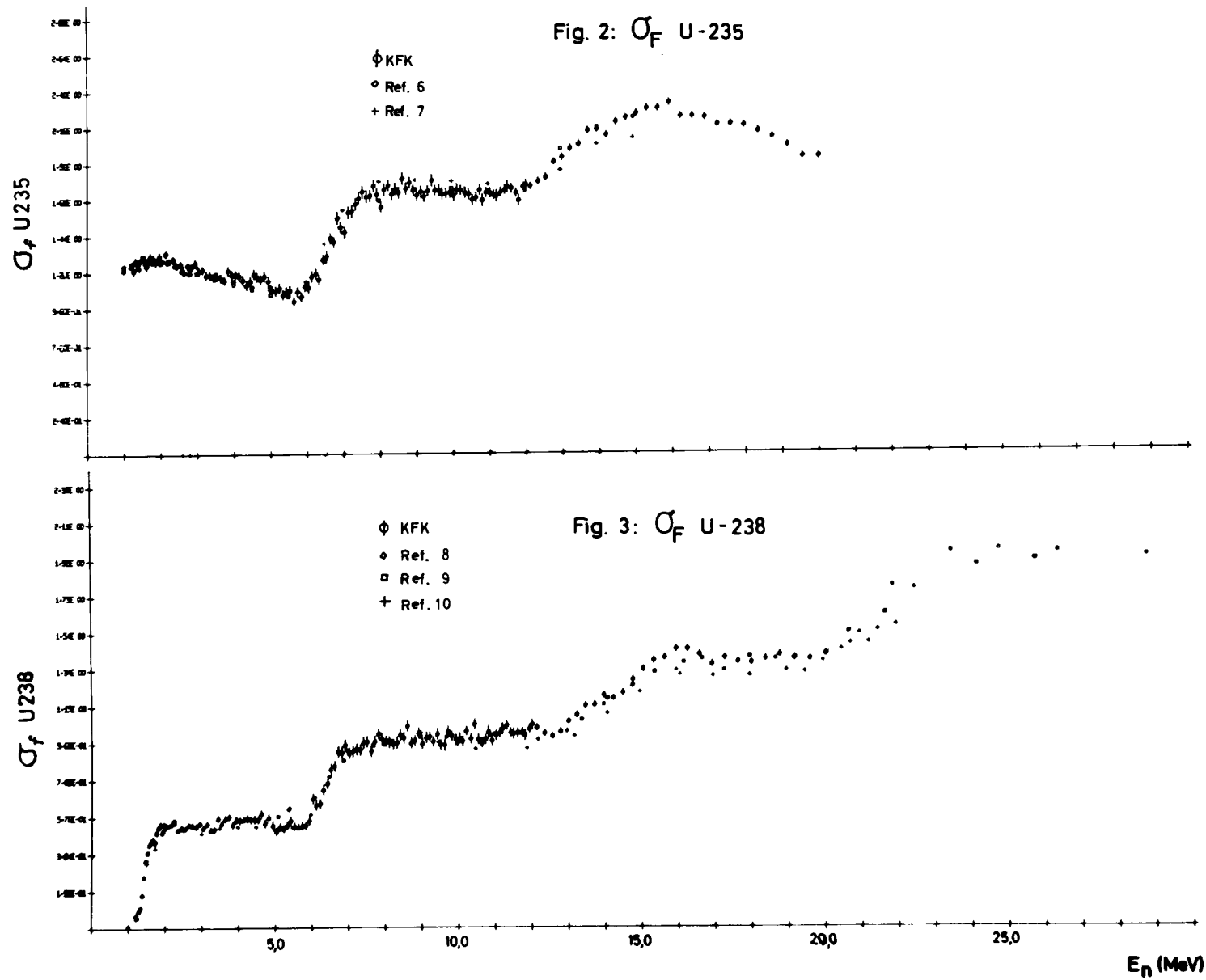


FIG.1: SCHEMATICAL DRAWING OF THE GEOMETRICAL ARRANGEMENT OF THE NEUTRON FLUX DETECTORS



## DISCUSSIONS

W. Poenitz I would like to have a point clarified. We formed from your data on U-235 and U-238 relative to hydrogen the ratio  $U-238/U-235$  and this agrees at some energies with your quoted ratio values. We concluded that the ratio data were not another independent experiment, but derived from the measurements relative to H. However, at some energies averages were formed.

S. Cierjacks That is correct. There is only one new normalization for Pu-239 which was obtained at the 11 m flight path with quite good statistics.

## CLARIFICATION

The data reported for the ratio of  $U-238/U-235$  and the absolute values for U-238 and for U-235 (basing on the Hydrogen reference cross section) are both from a single measurement. However, the normalization of the data is somewhat different for the ratio than it is for the individual cross sections. Also some channels were averaged for the ratio data but not for the individual cross sections.

(Note added by the Editors after discussion with S. Cierjacks after the meeting).

# THE STATUS OF U-235 FISSION AS A CROSS SECTION STANDARD †

G. W. Carlson and J. B. Czirr

Lawrence Livermore Laboratory  
University of California  
Livermore, California 94550

## ABSTRACT

The present paper is a review of the current status of U-235 fission cross section data from thermal to 20 MeV neutron energies. The accuracy achieved is compared with the 1% accuracy required of a reaction-cross-section standard throughout this range. The energy ranges from thermal to 10 keV, 10 keV to 0.8 MeV and 0.8 to 20 MeV are considered separately because of the different experimental techniques required in each. The goal of normalizing all fission cross sections to the thermal value and the current degree of success is discussed.

## I INTRODUCTION

The fission cross section of  $^{235}\text{U}$  affords an ideal standard cross section above approximately 30 keV--it is large enough at high energies that essentially transparent detectors can be constructed (for use in a transmission mode), detectors are easily built and stable, and the Q value is so large that the pulse height is independent of neutron energy.

I will outline the current status of  $\sigma_f$  in three energy regions: a) thermal to 10 keV, b) 10 keV to 0.8 MeV, c) 0.8 MeV to 20 MeV. This choice divides the 9 decades into the 3 regions where different flux measurement techniques are currently needed.

The emphasis on the cross section below 30 keV is based upon the on-going attempt to normalize the high energy region to the accurately known thermal value. This program, if successful would afford a valuable check on the absolute measurements made above 20 keV, with the potential for improved accuracy.

II  $\sigma_f$  FROM THERMAL TO 10 keVA. Status

- 1) Flux measured with the  ${}^6\text{Li}$  (n, $\alpha$ ) reaction using glass scintillators.
- 2) Total error  $\leq 1.5\%$  from 7 eV to 10 keV (in wide energy bins).
- 3) Not limited by  ${}^6\text{Li}$  cross section errors.
- 4) Self shielding less than 1%.

In Table I, we list the results from several measurements made at the Livermore 100-MeV Linac. The cross sections from thermal to 1 keV represent the weighted average of four data sets obtained with three different fission chambers, two different flight paths (and neutron targets) and with the flux monitor in front of and also behind the fission chamber. The common feature of all measurements was the 1/2 mm thick Li glass scintillator used as a flux monitor. The error listed is the calculated statistical error on the weighted mean and the column labeled Scale Factor is the square root of the observed chi-squared per degree of freedom. When the scale factor is significantly larger than 1.0, it indicates the possibility of systematic differences between the four data sets and should be multiplied into the calculated error. (This product is not to be used, of course, if the scale factor is less than 1.0.)

In each case, the data were normalized in the region from 0.02 to 0.10 eV to a thermal value of 585.4 b, using the cross section shape of Leonard. [1].

B. Confirmation

Most measurements in this energy range have been normalized to the lowest energy region attained in the experiment. This approach sometimes suffers from large self-shielding corrections, from reduced flux available at the lower energies, etc. Instead of choosing the lowest energy available, we will normalize the various data sets in an intermediate energy region where the corrections are more manageable. Table II lists several cross section ratios relative to the thermally normalized Livermore data. In each case, the average cross section from 300 eV to 1 keV has been set equal to 10.78 b. (The Deruytter data were normalized to 585.4 b at thermal since the highest energy obtained was 20.5 eV.) The renormalization constant (k) necessary to achieve this is listed at the bottom of each column.

It is encouraging to note that the average value of  $\sigma_i/\sigma_L$  seldom deviates by more than 1% from unity in the region above 200 eV. We may use this last column as an indication of the accuracy with which the shape of  $\sigma_f$  is known in the region from 200 eV to 70 keV. All of the data listed were obtained with a  ${}^{10}\text{B}$  flux monitor except the LASL (Lemley) and Livermore

sets, which used  ${}^6\text{Li}$ . In Table II, the energy dependence of the various  $\sigma_i$  has not been adjusted for more recent evaluated cross sections of B or Li, but was accepted as published. Of course, any error in the energy dependence of these standard cross sections is reflected in the uncertainty of  $\sigma_f$  but would not appear in  $\sigma_i/\sigma_L$  if the ratio of  $\sigma_B$  to  $\sigma_{Li}$  is approximately correct.

Below 200 eV the picture changes entirely. We notice both a downward trend in all  $\sigma_i/\sigma_L$  and an increased dispersion in the values. It is these two effects which are pinpointed by normalizing in the 300- to 1000-eV region. We may then separate the problems into two areas: 1) What is the energy dependence of the cross section relative to the above normalization region? 2) What is the average cross section in the 300- to 1000-eV region relative to a thermal normalization?

I believe that the results listed in Table I present a convincing case for the lower-than-traditional cross section of 10.78 b in the 300- to 1000-eV region and that we know the absolute cross section below 10 keV to a total uncertainty of approximately  $\pm 1\%$ .

### III $\sigma_f$ FROM 10 keV TO 0.8 MeV

Because of larger uncertainties in the  ${}^{10}\text{B}$  and  ${}^6\text{Li}$  cross sections throughout this energy region, the lower-energy techniques are not applicable at present. One published [7] and two unpublished [8] [9] measurements of  $\sigma_f(235)/\sigma_{n\alpha}({}^6\text{Li})$  over this energy range seem to agree satisfactorily, but these results cannot be applied to the U-235 problem because of uncertainties in  $\sigma_{n\alpha}$  ( $\pm 3\%$  at 50 keV, and larger at higher energies).

Preliminary data from NBS cover the energy range from 5 to 600 keV with a coterminous measurement of  $\sigma_f(235)$  relative to a hydrogen-recoil proportional counter. [10] Such measurements should considerably reduce the error in  $\sigma_f$  in this energy region by extending the advantages of thermal normalization above 10 keV.

Prior to the publication and acceptance of the above work or an improved  $\sigma_{n\alpha}({}^6\text{Li})$  measurement, the absolute monoenergetic results as summarized in the forthcoming ENDF/B-V files represent the closest approach to the 1% accuracy required of a standard cross section.

### IV $\sigma_f$ FROM 0.8 TO 20 MeV

#### A. Status

- 1) Shape measurement relative to n,p scattering cross section.

- 2) Total error in shape  $\pm 1\%$  from 0.8 to 7 MeV  
 $\pm 2\%$  at 14 MeV  
 $\pm 10\%$  at 20 MeV
- 3) Normalization uncertainty  $\pm 2\%$ .

Because of the breakdown in the thermal normalization technique, described in section III, the available shape measurements above 0.8 MeV must rely on absolute monoenergetic measurements for accurate normalization. When used in combination, the two methods (shape plus absolute) yield an uncertainty of 2-3% below 15 MeV. The proposed ENDF/B-V evaluated cross section follows closely the single white-source (relative) measurement [11], from 0.8 to 14 MeV, when the latter is normalized to 1198 mb over the 3-4 MeV range. From 14 to 20 MeV, version V represents a compromise between the data of Reference 11 and earlier, higher results. The uncertainty at these higher energies is increased to encompass the discrepant measurements and invalidates U-235 as a standard above approximately 15 MeV.

#### B. Confirmation

Most of the monoenergetic data from 0.8 to 15 MeV lie within  $\pm 5\%$  of the accepted curve (ENDF/B-V), with approximately equal occurrence of positive and negative deviations. Since the spread is considerably larger than the errors quoted in Reference 11, it is proposed that the published errors be accepted (or rejected) on their own merit.

### V FUTURE IMPROVEMENTS

At least four areas of improvement are apparent from the above summary.

- 1) Better flux measurement techniques in the 10 keV to 1 MeV region.
- 2) Better statistical precision from a white-source measurement above 7 MeV.
- 3) Confirmation of the average cross section in the 300- to 1000-eV region relative to a precise thermal normalization (preferably in a single white-source run).
- 4) A precise measurement of the fission cross section in the 1-20 MeV region as a function of the angle of the fission foils relative to the incident neutron beam.

Finally, I will list the ultimate accuracy predicted for several regions covering the full range of energy.

$E_{\min}$	$E_{\max}$	Systematic error limit	
		Accepted	Conjectured
Thermal	100 eV	$\pm 0.5 \%$	$\pm 0.3 \%$
0.1	10 keV	0.6 %	0.4 %
10	150 keV	3 %	0.6 %
150	1000 keV	$\sim 10 \%$	0.6 %
1	7 MeV	0.7 %	0.7 %
7	14 MeV	1 %	1 %

The "systematic error limit" assumes negligible statistical error and applies to the cross section shape only. The "accepted" limit refers to a published result, while the "conjectured" limit is the predicted limit based on firm constraints.

## REFERENCES

1. B. R. LEONARD, private communication
2. R. GWIN, E. G. SILVER, R. W. INGLE, and H. WEAVER, "Measurement of the Neutron Capture and Fission Cross Sections of  $^{239}\text{Pu}$  and  $^{235}\text{U}$ , 0.02 eV to 200 keV, etc." Nucl. Sci. Eng., **59**, 79 (1976).
3. R. B. PEREZ, G. DE SAUSSURE, E. G. SILVER, R. W. INGLE, and H. WEAVER, "Measurement of the Fission Cross Section of Uranium-235 for Incident Neutrons with Energies between 2 and 100 keV." Nucl. Sci. Eng., **55**, 203 (1974).
4. J. BLONS, G. DEBRIL, J. FERMANDJIAN, and A. MICHAUDON, "Measure et Analyse des Sections Efficaces de Fission de l'Uranium-235 et du Plutonium-241." Proc. Second International Conference on Nuclear Data for Reactors, Volume 1, p. 469, International Atomic Energy Agency, Vienna, 1970.
5. J. R. LEMLEY, G. A. KEYWORTH, and B. C. DIVEN, "High Resolution Fission Cross Section of Uranium-235 from 20 eV to 100 keV." Nucl. Sci. Eng., **43**, 281 (1971).
6. A. J. DERUYTTER and C. WAGEMANS, "Measurement and Normalization of the Relative  $^{235}\text{U}$  Fission Cross Section in the Low Resonance Region." Journal of Nuclear Energy, **25**, 263 (1971).
7. J. B. CZIRR and G. S. SIDHU, "A Measurement of the Fission Cross Section of  $^{235}\text{U}$  from 100 eV to 680 keV," UCRL-77377, Lawrence Livermore Laboratory (1975). Accepted for publication in Nucl. Sci. Eng.
8. W. P. POENITZ, private communication.
9. C. D. BOWMAN, private communication.
10. O. A. WASSON, private communication.
11. J. B. CZIRR and G. S. SIDHU, "Fission Cross Section of Uranium-235 from 3 to 20 MeV," Nucl. Sci. Eng., **57**, 18 (1975), and Fission Cross Section of Uranium-235 from 0.8 to 4 MeV," Nucl. Sci. Eng., **58**, 371 (1975).

<sup>†</sup>Work performed under the auspices of the U.S. Energy Research and Development Administration. W-7405-Eng-48

TABLE I

Weighted Average  $^{235}\sigma_f$  (Livermore Data)

<u>E<sub>min</sub></u>	<u>E<sub>max</sub></u>	<u><math>\sigma_f</math> (LOW)</u>	<u><math>\sigma_f</math> (HIGH)</u>	<u><math>\epsilon_{\text{LOW}}^a</math></u>	<u>Scale Factor</u>
0.0254 eV		585.4 b			
7.4	10	87.67		$\pm 0.53\%$	0.75
7.8	11	76.48		0.50	1.0
10	15	43.65		0.50	3.1
15	20.5	60.32		0.71	1.1
20.5	33	36.68		0.54	0.41
33	41	62.83		0.77	1.5
41	60	49.31		0.55	1.3
60	100	24.02		0.63	0.55
100	200	20.25	20.23 b	0.55	1.0
200	300	19.95	19.30	0.69	1.1
300	400	12.25	12.51	1.0	0.77
400	500	12.73	12.88	1.1	0.96
500	600	14.46	14.21	1.1	0.65
600	800	10.55	10.52	1.0	1.8
800	1000	7.41	7.40	1.3	0.83
300	1000	10.78 <sup>c</sup>	10.78		
1	2 KeV		6.871		
4	5		4.010		
7	8		2.984		
8	9		2.754		
9	10		2.821		
10	20		2.340		
20	30		2.016		
40	50		1.732		
50	60		1.710		
60	70		1.706		

- a)  $\epsilon_{\text{LOW}}$  is the calculated statistical error of  $\sigma_f$  (LOW). The common systematic error applicable to the low energy data arises primarily from the thermal normalization and equals  $\pm 0.3\%$ .
- c) The observed standard deviation of the four data sets is  $\pm 0.4\%$  for the 300- to 1000- eV region.

TABLE II

 $^{235}\text{U}$  Cross Section Comparison

$E_{\min}$	$E_{\max}$	$\sigma_i/\sigma_L^a$					$\left\langle \frac{\sigma_i}{\sigma_L} \right\rangle^b$
		GWIN [2]	PEREZ [3]	BLONS [4]	LEMLEY [5]	DERUYTTER [6]	
0.0254	eV	.967				1.00	
7.4	10	.925				.984	
7.8	11	--				.988	
10	15	.949				1.002	
15	20.5	.911				.972	
20.5	33	.931	.890		.892		.904
33	41	.934	.896		.959		.930
41	60	.935	.913	~.92	.980		.937
60	100	.954	.942	.960	.973		.957
100	200	.984	.959	.963	1.005		.978
200	300	.994	.999	.981	1.014		.997
300	400	.991	.983	.988	1.00		.987
400	500	.988	.996	.991	1.00		.992
500	600	1.004	1.010	.994	1.00		1.001
600	800	1.010	1.009	1.009	1.00		1.009
800	1000	1.000	.994	1.011	1.00		1.002
1	2keV	1.001	1.009	1.009	.953		.993
4	5	.989	1.003	1.025	.971		.997
7	8	.994	.996	.996	--		.995
8	9	1.016	1.062	1.009	--		1.029
9	10	1.037	1.016	1.015	--		1.023
10	20	1.021	.995	.982	.970		.992
20	30	1.017	.995	.973	1.012		.999
40	50	1.021	1.038	--	1.013		1.024
50	60	1.035	1.027	--	1.006		1.023
60	70	1.003	1.006	--	.975		.995
$k^c$		0.9720	0.9214	0.9311	0.9714	1.0067	--

a)  $\sigma_i$  is the  $^{235}\text{U}$  fission cross section published by the listed author, after renormalization.  $\sigma_L$  is the  $^{235}\text{U}$  fission cross section measured at Livermore.

b)  $\left\langle \frac{\sigma_i}{\sigma_L} \right\rangle$  is the unweighted average of the ratio.

c)  $k$  is the renormalization constant needed to yield a  $\bar{\sigma}_i$  of 10.78 b when averaged from 300 to 1000 eV.

## DISCUSSIONS

H. Derrien It appears that you have a discrepancy only with your data in the resonance region.

J. Czirr There is a discrepancy with our data and there is a lot of jumping around between different sets of data. This should not be a difficult region. The background is small, you can well define the energy, but the self-shielding problems begin to hurt.

J. Browne How large is the self-shielding correction?

J. Czirr Our correction is about 0.1%.

R. Peelle Does the paper by Wagemans cover this energy range and would it not go in the opposite direction?

J. Czirr I did not show this here because the paper is not published. Yes, that would be in violent disagreement with the whole thing.

C. Bowman What happens to the values at low energies if you normalize in the 300-1000 eV range?

J. Czirr At 9 eV the value would be 1.915 and thus it would be 6% higher. One cannot explain this with the B-10. There appears to be a shape difference throughout the whole range.

C. Bowman What about Poenitz, can his data be treated the same way?

J. Czirr I don't know--they cannot.

W. Poenitz I certainly have no data at this .3 - 1. keV energy range.

W. Poenitz There are several other sets which could be considered in this comparison (Michaudon, etc.). Why did you leave them out?

J. Czirr We considered only newer data. The only two which I would have liked to include are the data from NBS and Wagemans. NBS would be in pretty good shape, and Wagemans would be in terrible shape in this comparison.

B. Leonard When you talk about Gwin's self-shielding problem one should look at his publication. I think the self-shielding in U-235 was negligible.

J. Czirr The samples were 1.7 mg each, I think this is a little bit misleading in the way it is stated. It was a very thick target. The correction was 20%.

B. Leonard The flux monitor was quite thick, but if you accept the error, the maximum effect on the shape is only a 1%. If you normalize at thermal, as I did, it is even smaller than that.

J. Czirr I must admit that I am floundering to explain the differences. I have not gone deep enough into the matter. All I am saying is that self-shielding gets worse if you go to lower energies. A thick chamber is something to think about.

H. Knitter Wagemans compares his result in a table with other data. It appears to me that it was not a shape difference but a constant difference with two or three sets, but he agrees well with others.

J. Czirr I know what you mean. To me it is very confusing if the normalization is not done as I have shown here.

L. Stewart In the range up to 7 MeV I would be a little bit careful after the data by Szabo has been presented. There is a difference in shape of 5-9% in the whole range above 1 MeV. So, 0.7% is very small.

J. Czirr I would like to make sure that you understand what I am saying. The 0.7% is in shape without statistics.

L. Stewart Let me correct that. We can take your relative shape and actually draw a completely different curve through it. If you have a sharp rise in the cross section as at 7 MeV, putting such a small error in it is asking for problems.

J. Czirr It should be pointed out which systematic errors are listed.

L. Stewart I would draw a different curve through the data than you do.

J. Czirr I did not draw a curve. I gave a histogram.

L. Stewart Well then on the histogram, the Szabo values are drastically lower at 5 MeV.

C. Bowman If you take your U-235 data relative to Li-6 and use the ENDF-V Li-6 cross section, where do you come out for U-235?

J. Czirr The U-235 is low, some 5% compared with ENDF-IV. The most reasonable U-235 shape I get is by using the ENDF-IV Li-6 cross section.

W. Poenitz It is an interesting point that you have a completely different shape than the Wasson data around 280 keV. Did you notice that?

J. Czirr No. It must be an artifact because we have the same U-235/Li-6 ratio. It must be due to which of the Li-6 cross sections I chose to use.

W. Poenitz It is a very local problem, it will be shown in the plots at the Working Sessions.

J. Czirr I see, no I did not notice it.

H. Kuesters We have seen something like a 6% discrepancy in these fission cross sections. I would like to remind you that a 10% uncertainty of Pu-239 is reflected in more than 1% in  $k_{\text{eff}}$  for the fast reactors. I think there is a definite need to bring down this uncertainty. I wonder whether the Working Sessions will be able to bring down the uncertainties. I do not quite see whether present techniques can improve the uncertainties or whether new techniques have to be invented. I would like to have comments on this.

W. Poenitz First of all: "10% in cross section (U-235(n,f)) should bring 1% change in  $k_{\text{eff}}$ "--I think the figure is much larger--a 10% change in U-235 would bring a 5% in  $k_{\text{eff}}$ .

H. Kuesters Yes, in certain important regions, if you integrate it is less. The one shown this morning was a 0.5% in  $k_{\text{eff}}$  for 1% in  $\sigma_f$ .

W. Poenitz Yes, it was ZPR-6. Now to comment on your question: you see the 6% difference in U-235, however, this is the difference between the extreme results. After all, all measurements in the last 5 years lie in a  $\pm 3\%$  band. This is true with few exceptions at less important local regions. All these measurements are really not claiming anything better than a 2-3% uncertainty. The problem is much more to now come down from the 2-3% range to a 1% uncertainty level, but the required effort for this may go up exponentially.

H. Kuesters O.K. That is one thing, to reduce this 3% to 1%. I think first one should clear up the difference between the high set and the low

set.

M. Bhat If you plot 5% bands they appear to include all experimental results.

W. Poenitz I have a plot of my data and all data published since then (1974). All values appear to be in that  $\pm 3\%$  band with the exception of the data by Wasson between 250 and 300 keV and the data by Kaeppler around 700-800 keV. I do not think that any experimenter can quarrel about a difference as long as the error bars overlap. In other words, you can draw a line which is covered by all experimental error bars. Some data (e.g., Szabo, Kaeppler) are on the high side, others (e.g., Wasson) are on the low side. Even if future measurements of lesser uncertainties would come out on the low side, this would be only a 3% difference from the center of the present  $\pm 3\%$  band.

L. Stewart Szabo is now on the low side.

W. Poenitz Only his data at higher energies are low, everywhere below 2 MeV his data are on the high side.

M. Bhat The difficulty is that these are systematic errors.

W. Poenitz But these are systematic errors which are accounted for. Nobody can say he is better than what he quotes for the error.

L. Stewart Unfortunately, I have found that the errors which are assigned are more related to the experimenter than with the experiment. Some assign small errors, some assign large errors. They always do it that way.

W. Poenitz The evaluator may assess the correctness of the quoted uncertainty.

# STRUCTURE LIMITATION ON ACCURACY OF $^{235}\text{U}$ FISSION CROSS SECTION MEASUREMENTS

C. D. Bowman, G. P. Lamaze, K. C. Duvall, and R. A. Schrack

National Bureau of Standards  
Washington, D.C. 20234, U.S.A.

## ABSTRACT

High resolution measurements of the  $^{235}\text{U}$  fission cross section carried out at LLL in 1970 have been averaged using Gaussian averaging functions with a FWHM = 1%, 2.5%, 5%, and 10%. Deviations from the 10% average are calculated and the results expressed in a table which permits an estimate of uncertainties introduced by the cross section fine structure for monoenergetic measurements of known resolution.

The width and spacing of nuclear levels in the neutron-induced fission cross section of  $^{235}\text{U}$  suggests that the higher keV fission cross section might be almost the smoothest reaction which can be measured. However, high resolution measurements [1] at LLL demonstrate the existence of fine structure at the  $\pm 3\%$  level even above 200 keV. The LLL experiment, therefore, has been useful as a guide in interpreting existing measurements, in planning future measurements and in evaluating the usefulness of  $^{235}\text{U}$  as a standard.

The intent of this note is to try to establish a more quantitative basis for estimating the interplay of fine structure and resolution in keV  $^{235}\text{U}$  fission experiments. To accomplish this the LLL data in the 20 to 300 keV range have been averaged with a Gaussian resolution function with FWHM,  $\alpha$ , of 1%, 2.5%, 5%, and 10%. A weighted average was obtained using the expression:

$$\bar{\sigma}_f(E_1) = \frac{1}{\sqrt{2\pi}\sigma_1} \sum_k \sigma_f(E_k) e^{-(E_k - E_1)^2 / 2\sigma_1^2} \quad (1)$$

where:

$\bar{\sigma}_f(E_1)$  - the average fission cross section at energy  $E_1$

$\sigma_f(E_k)$  - the fine resolution cross section at energy  $E_k$

$\sigma_1 = \alpha E_1 / 2.35$

$\alpha = 0.01, .025, 0.05, 0.10.$

The average is carried out over the interval from  $E_i - \alpha E_i$  up to  $E_i + \alpha E_i$ . Appropriate values of  $k$  were determined to calculate the weighted average over the energy span desired for each data point.

The Gaussian weighting function has the advantage that it produces a "running average" of the data that approximates what would be seen by an experiment with lower resolution. Running averages that have flat weighting between the limits of the average introduce derivative effects in the running average obtained. These derivative effects caused by the sharp edge of the running sum produce structure in the running average that is comparable in width to the structure in the unaveraged data but displaced and reduced in amplitude. Such effects are quite bothersome to the eye and can be a source of minor confusion in interpretation even when the averaging interval  $\Delta E/E$  is .10.

As the averaging interval for the Gaussian function is increased the smoothness of the curves increase to a point where it ceases to change. In the 100 to 300 keV range this appeared to occur between  $\alpha = 0.10$  and 0.20. In the interest of reducing end effect data losses as much as possible, the 10% average was taken as a reference curve and all other curves compared to it. The difference between the  $\alpha = 0.01, 0.025, 0.05$  curves and the  $\alpha = 0.10$  curve is shown in the figure as the difference cross sections plotted against energy. The display is a little confusing, but the three curves can be fairly easily separated by the significant dependence of structure on  $\alpha$ .

To place these differences on a quantitative basis we have calculated the fractional mean deviation  $\delta$  from the data shown in Fig. 1 using the expression

$$\delta = \sum_i |\Delta\sigma_{\alpha i}|/n \quad (2)$$

where  $\Delta\sigma_{\alpha i}$  is the difference between the average for a given  $\alpha$  and the average for  $\alpha = 0.1$ ,  $i$  is the index on the averaged cross section point, and the range of  $i$  is throughout the  $n$  data points in the set. This averaging technique was used rather than the standard deviation in the difference since the authors felt that the squaring process in evaluating the average standard deviation weighted too highly the larger differences.

The results of this process are shown in Table I where  $\delta$  is given for energy intervals and for three values of  $\alpha$ . The quantity  $\delta$  for the unaveraged structure is given also in the first column. This table then permits one to estimate the uncertainty in a measurement associated with the interplay between his experimental resolution and the fine structure. For example, if an experimenter uses a resolution of 2.5% in the energy range from 50-100 keV, he derives a 2% uncertainty to be combined with the other uncertainties of his experiment.

The data of Table I are shown also in Fig. 2 where percent mean deviation is plotted against neutron energy.

It appears that the data of Table I and Fig. 2 can be fitted approximately with the empirical relationship  $\delta = aE^{-0.75}$  where  $\delta$  is the fractional mean deviation expressed in percent,  $E$  is in keV and  $a$  is 100, 60, and 33 for  $\alpha = 0.01$ , .025, and 0.05, respectively. With 10 keV resolution at 1 MeV the observed structure is expected to be at the 0.5% level.

Below 200 keV the fine structure data can be fitted with a curve of the same slope as the averaged data. This infers that an averaging phenomenon in the fission experiment appears to be operating with an effective resolution of 0.4%.

This is not related to the resolution of the experiment since the experimental resolution was much better than 0.4% except at the highest energies. The experimental resolution  $\Delta E/E$  also is not a constant but has the form

$$\Delta E \propto 0.002 \frac{E}{100}^{3/2}$$

with  $E$  in keV.

This apparent natural resolution can be interpreted as an upper limit to the rate at which the fission cross section can change. Assuming the nucleus somehow is performing a Gaussian average over its fine structure with a resolution  $\Delta E/E = .004$  one can derive a maximum slope. This is done by finding the maximum slope of a cross section given in the Gaussian form

$$\sigma = \sigma_0 e^{-(E-E_0)^2/2\sigma_1^2} \quad (3)$$

where  $\sigma_1$  is the standard deviation and is related to the FWHM by the expression  $\text{FWHM} = 2.35\sigma_1$ . The result of the calculation for a FWHM,  $\Delta E = .004E$ :

$$\frac{d\sigma}{dE} \leq \frac{350\sigma}{E}. \quad (4)$$

Such a limit is also related to the maximum rate of change of the logarithm derivative at the nuclear surface and therefore to fundamental properties of the nucleus. However, a thorough study of this subject is beyond the scope of this paper. We only point out that similar high resolution measurements are now possible across a wide mass range so that systematic studies of this type of limit are now possible.

#### ACKNOWLEDGMENTS

The authors gratefully acknowledge the encouragement of A. D. Carlson and M. Bhat to provide an alternative emphasis to the earlier analysis of the LLL experiment.

## REFERENCES

1. C. D. BOWMAN, G. S. SIDHU, M. L. STELTS, and J. C. BROWNE, *Proc. of the Third Conference on Neutron Cross Sections and Technology*, Univ. of Tennessee, Knoxville, Tennessee, p. 584 (1971).

TABLE I

Fractional Mean Deviation of  $^{235}\text{U}(\text{n},\text{f})$  Cross Section

E(keV)	Fine	1%	2.5%	5%
22-50	.1349	.0581	.0386	.0214
50-100	.0817	.0333	.0203	.0116
100-200	.0501	.0219	.0130	.0069
200-330	.0293	.0144	.0091	.0061

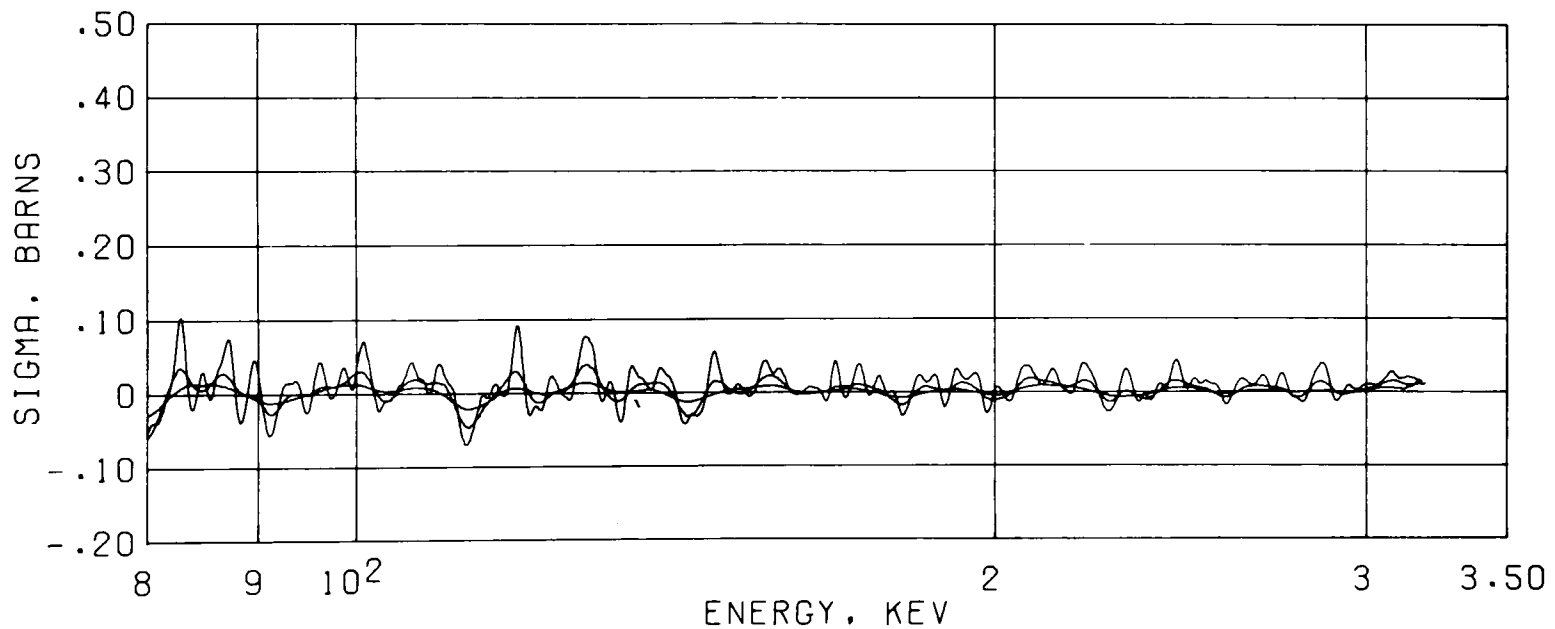
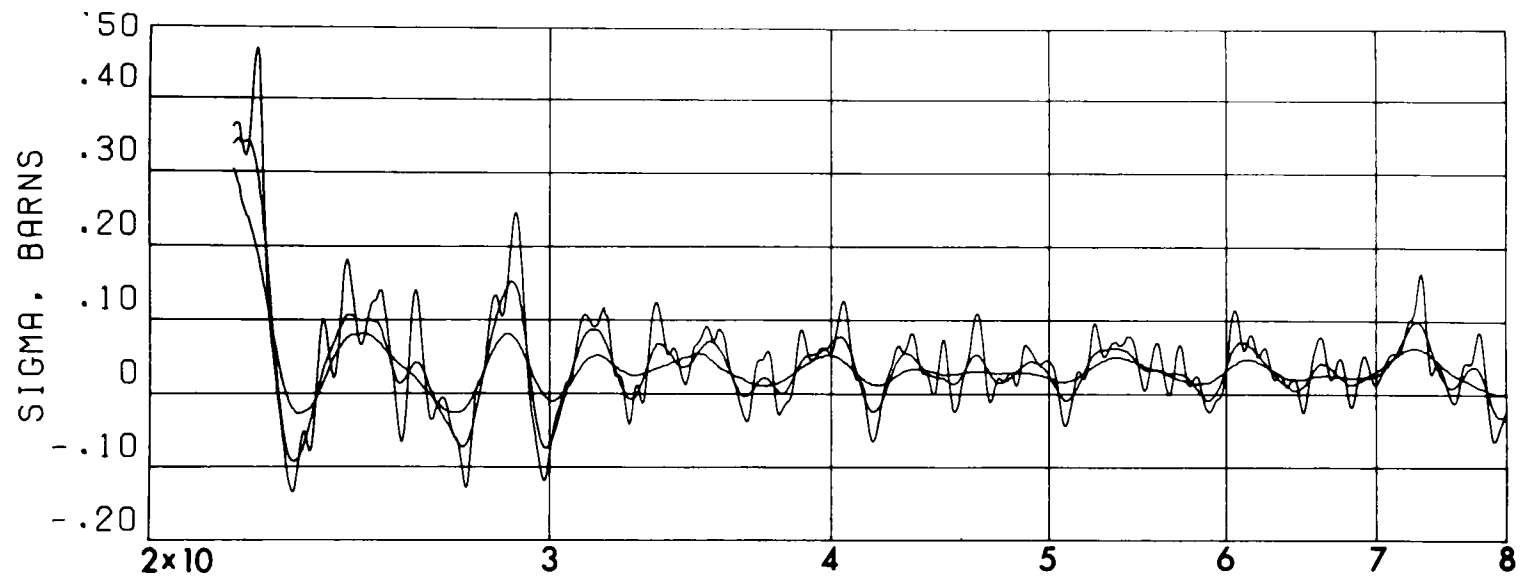


Figure 1. The difference between the  $\alpha = 0.01, 0.025, 0.05$  curves and the  $\alpha = 0.10$  curve is shown as the difference cross section against neutron energy.

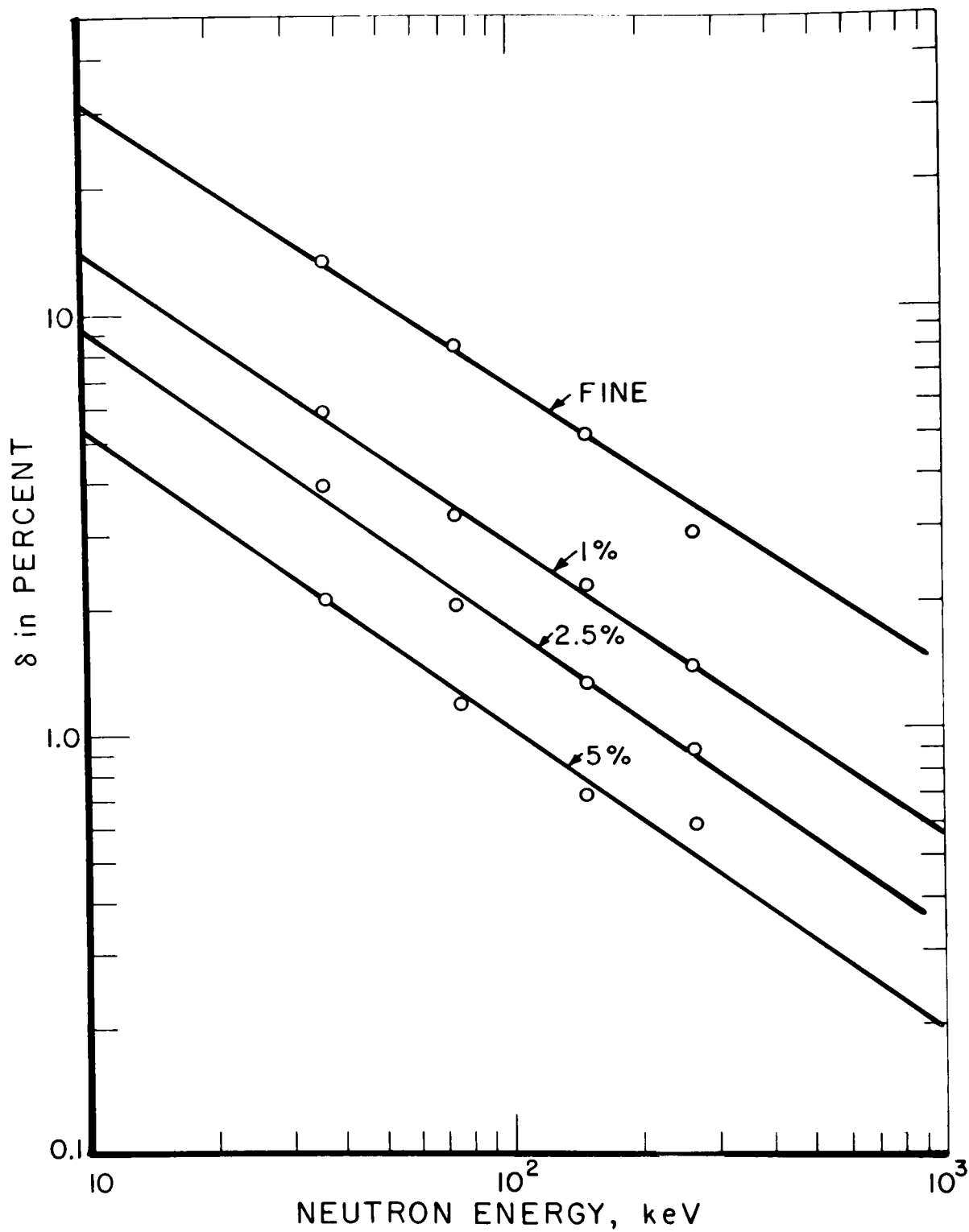


Fig. 2 - The data of Table 1 are shown on a log-log scale fitted with parallel solid lines of the form  $\delta = aE^{-0.75}$ .

## DISCUSSIONS

M. Moore I should repeat for the benefit of the others what I told you earlier. One ought to worry whether this is not the intrinsic resolution of the experiment. The effect I am talking about is moderator hold-up time which really does go like  $\Delta E/E$ .

C. Bowman I checked that after we discussed it. There is no way that this would be it. The flight path was 250m, the detector thickness was 1/2 cm and the source itself was 5 cm in size.

R. Peelle My first question is a version of M. Moore's question. At the lowest energy, like 10 keV, the time dispersion of the neutron moderator is----. How does this figure out?

C. Bowman It is much less than a tenth of a percent at the low energies. The resolution does not have this kind of energy dependence. This is done with a  $\Delta E/E$  which is constant.

R. Peelle The other question. You determined uncertainty associated with a narrow energy interval. I guess this is uncertainty in the sense that if you take a nearby energy interval you get a different answer. The curves you show indicate the extent that you can expect to get a different result, but it is not the uncertainty in the sense that if you measure the same interval over again, that you get the same answer. So it is only the uncertainty for mis-aligning the energy if you do the experiment.

C. Bowman Yes that is the exact point. And then there is the point that if you compare sets of data with a spacing between points much greater than the resolution, there is much more scatter of the points from the structure. It may be difficult to interpret the data if you don't know the scatter comes from the structure.



*Session III*

**Special Topics**



# COMMON NORMALIZATION OF SEVERAL $^{235}\text{U}$ FISSION DATA SETS IN THE THERMAL AND RESONANCE REGION

B. R. Leonard, Jr.

Battelle-Northwest  
Richland, Washington 99352 U.S.A.

## ABSTRACT

An evaluation of the cross sections of  $^{235}\text{U}$  below 1 eV was recently completed at Battelle-Northwest (BNW). In this evaluation, energy-dependent data of all of the partial cross sections, their ratios and total were simultaneously fitted by a non-linear least-squares fitting code, SIGLEARN, to a modified Adler-Adler multilevel resonance fission and multilevel Breit-Wigner scattering formalism. The data of eight relative fission cross section measurements were compared to the evaluated shape using SIGLEARN to establish best-estimate normalization values at 2200 m/s and their uncertainties on a consistent basis. The indicated uncertainties of these shape-fitted normalizations due to uncertainties in: the evaluated shape, deviations from the evaluated shape, data precisions, energy region used in the normalization, internal data discrepancies and other unknown factors were less than one percent for six of the experiments. The most significant problem appeared in the thermal normalization of the data of Deruytter and Wagemans where the possible normalization values differed by over two percent. Values of the integral fission cross section from 7.8- to 11-eV were then calculated by a consistent method for each data set renormalized to  $\sigma_f^0 = 583.54$  b, the value proposed for version V of ENDF/B. The resultant values of the fission integrals were then evaluated by a working group to obtain a best-estimate value to which fission data sets, which do not go down below 1 eV, could be normalized. The value obtained was 241.24 b·eV but an uncertainty of nearly three percent is required to reasonably cover the spread of the values.

## INTRODUCTION

Until this year (1976), there had not been an experiment which measured the differential  $^{235}\text{U}$  fission cross section through the thermal energy region which extended to energies of tens of keV or higher and could, thus, be used to normalize high-energy data to the relatively well known thermal

value. In the past, normalizations of data which extended down to a few eV had frequently been normalized to the data of Shore and Sailor [1]. These relative data had themselves been normalized above 0.1 eV to the relative data of Leonard, et al [2] which extended to lower energies but had to be normalized to some chosen thermal value. Thus, three separate normalizations of varying and mostly unspecified uncertainty were required. More recently, Deruytter and Wagemans [3] made relative measurements from 0.02 eV to 20 eV. An integral fission cross section value from 7.8- to 11-eV was obtained by an integral normalization of the data from 0.0206- to 0.06239-eV to the absolute fission integral obtained by Deruytter, et al [4].

Differential relative fission data which extend through the thermal region have recently been reported up to 200 keV by Gwin, et al [5] and up to 75 keV by Czirr and Sidhu [6]. These data are equivalent to those of Deruytter and Wagemans and can be used, in principle, to improve the value and confidence of the fission integral in the resonance region.

The present author and his colleagues at Battelle-Northwest have recently completed an evaluation of all of the partial cross sections of  $^{235}\text{U}$  below 1 eV by simultaneous least-squares (LSQ) fitting [7]. The methodology of this evaluation has been used to normalize the relative fission data to the evaluated shape by the method of LSQ. Since the evaluated shape extends to 1 eV, thermal normalizations can be obtained on a common basis not only for the data sets in the thermal region but also for those that extend down to a few tenths of an eV. The results of these normalizations have then been extended to study the normalizations in the resonance region.

#### BASIS FOR THE THERMAL LSQ NORMALIZATIONS

The details of the  $^{235}\text{U}$  evaluation are given in a recently published report [7] and the methodology employed will only be summarized here. The basis for the fit is a modification of Adler-Adler multilevel fission resonance formalism [8] where fission,  $f$ , and capture,  $c$ , are described by

$$\sigma_f \sqrt{E} = \frac{\pi \hbar^2}{2M_n} \left\{ \sum_{k=1}^N \frac{g_k \Gamma_k^0 \Gamma_{fk} + F_k (E-E_k)}{(E-E_k)^2 + (\Gamma_k/2)^2} + C_{f1} \right\} \quad (1)$$

$$\sigma_c \sqrt{E} = \frac{\pi \hbar^2}{2M_n} \left\{ \sum_{k=1}^N \frac{g_k \Gamma_k^0 \Gamma_{ck}}{(E-E_k)^2 + (\Gamma_k/2)^2} + C_{c1} \right\} \quad (2)$$

$$\Gamma_k = \Gamma_{fk} + \Gamma_{ck} + \Gamma_k^0 \sqrt{E} . \quad (3)$$

The constraint of requiring the resonance energies,  $E_k$ , to be the same in both the fission and capture channels allows the scattering cross section to be described in the usual multilevel Breit-Wigner resonance formalism.

These resonance theories were programmed into the general non-linear LSQ fitting program LEARN [9]. The resulting computer program, SIGLEARN, has been documented in detail by Kottwitz [10].

Four resonances were used in the fit to the  $^{235}\text{U}$  data. The parameters of the 1.135 eV resonance were held fixed except for the fission interference term. The remaining resonances whose parameters were adjusted iteratively in LSQ fits were the visible resonance near 0.287 eV and two negative-energy resonances at -0.916 eV and -0.0638 eV. The LSQ fit was significantly improved when two negative-energy resonances were allowed, rather than one.

All of the experimental data were entered in the fits as relative data with individual normalization constants which adjusted in the LSQ fit. The absolute values were constrained by 2200 m/s values with errors obtained from evaluations of the separate reaction channels except for the potential scattering radius and nubar which were fixed input for each LSQ fit.

The final LSQ fit resulted from fitting simultaneously selected energy-dependent data for total, fission, capture, eta, scattering and alpha. The data of Gwin, et al.[5] cast as absorption cross section were also added and fitted simultaneously in other fits.

#### NORMALIZATIONS IN THE THERMAL RANGE

Each of the fission data sets was compared to the final evaluated fission shape in LSQ fits where only the normalization constants were adjusted. The fitted normalization constant then gives the best-fit 2200 m/s value based on the evaluated shape. The program also calculates a sophisticated one standard deviation error estimate of the goodness of the fit to the shape. This error is estimated on the basis of the fit of the average data over its entire energy range to the shape with which it is compared. It does not include the precision of the fit due to the randomness of the data. This component is estimated from the value of chi-squared per degree of freedom ( $\chi^2/\text{DF}$ ). In the tabulations of this paper, the error estimates on the normalization values have been increased by the square root of  $\chi^2/\text{DF}$  when the value of  $\chi^2/\text{DF}$  exceeded 1.3 and the  $\chi^2/\text{DF}$  values are also tabulated. The resultant error is assigned to the 2200 m/s value but is determined by the fit over the entire energy range of the data set. It does not include any component due to the error estimate on the final fitted fission shape. That error estimate was  $\pm 1.7$  b and did not depend significantly on the fitted absolute fission value in a given LSQ fit.

In determining the best thermal normalization and its error a number of factors need to be considered. One of these is the energy range of the data used in the fit. The fitted cross section shape is determined much more precisely in the thermal range because of the quality of the differential data used to derive the shape. Another factor is in the representation of the data, i.e., the density of data values per energy interval used in condensing time-of-flight data. Generally, this factor was found to be of little significance in this study. These factors and others will be discussed in the normalizations of the individual data sets.

Data of Bowman, et al.[11]

These data were taken in 1966 in two separate runs with different resolutions. The low-energy data are shown on Fig. 1 and the high-energy data on Fig. 2. In all cases the solid curve is the comparison evaluated shape. In these and the plots of all the figures of this paper the theoretical shape has been renormalized to best fit the data. The normalization values and errors are given in Table I. The low-energy data are seen to be in excellent agreement with the fitted shape except for a small systematic departure to higher values at the lowest energies. This systematic departure is undoubtedly the reason why the LSQ fitted value is lower than that assigned by the authors. If these data were deleted the normalization of  $\sigma_f$  value would be somewhat lower. This data set was included in the final LSQ fit of the evaluated shape.

The higher-energy run shown on Fig. 2 is also seen to be in excellent agreement with the fitted shape except for a single datum at the resonance peak which causes the normalization value of  $\sigma_f$  to be slightly higher than it would be otherwise. The difference in the normalization of the high- and low-energy runs shown in Table I, 0.6%, is typical of hidden uncertainties on internormalizations determined in this study. This high-energy data set was also included as a separate set in the final LSQ evaluated fit. The normalization used for the resonance region was that of the high-energy run since these data were continuous to that region.

Data of Gwin, et al.[5]

The comparison of the entire data set below 1 eV is shown on Fig. 3 and for only the region below 0.1 eV on Fig. 4. Some small but systematic departures from the fitted shape are evident for the data above 0.1 eV although the shape at lower energies is in excellent agreement with the data. The average of the two normalization values shown in Table I is in excellent agreement with that assigned by the authors based on the data below 0.4 eV and that value has been used to normalize the resonance region data. The data shown on Fig. 3, however, above 0.3 eV lie systematically lower than the fitted curve implying that the values in the resonance region should be increased. This implication will be seen to be borne out by most of the data comparisons in the resonance region. These data were not used in the final LSQ evaluation fit because the correlated data for alpha obtained in the same experiment were used in that fit.

Data of Czirr and Sidhu [6]

The comparison of the data below 1 eV is shown on Fig. 5 and the data below 0.1 eV are shown on Fig. 6. The difference in normalization factors for these two data sets as shown on Table I is significant, 0.74 percent. The magnitude of this difference is effected by the fact that the 19 data point representation used for the data below 0.1 eV has been reduced to seven values for the data set extending to 1 eV. The 7 and 19 point representations used only below 0.1 eV do not, however, differ significantly in normalization. In view of the random nature evident in these data, it is not clear that the apparent systematic departure of the five highest energy data values evident on Fig. 5 is significant. The small difference between the author's normalization and that of the thermal data is due to the fact that

the authors' normalization was determined by us by fitting to a preliminary fit based on fitting only fission, capture, and eta data [12]. The normalization used for the resonance region was that of the thermal data alone based on the possibility that the fit to the entire data set may be overly influenced by a few data points. It is evident, however, that the uncertainty of the thermal normalization of these data must be the order of 1% due to the observed discrepancy. The Czirr and Sidhu data were not included in the final LSQ fit of the evaluation because, in part, they do not appear to contain as much information as some other data.

#### Data of Deruytter and Wagemans [3]

These data below 1 eV are shown compared with the evaluated shape on Fig. 7. A systematic departure in shape is obvious as all of the data above 0.21 eV lie below the curve. Investigation of these data revealed that a time-channel width change was apparently made at the energy at which the data appear to be discontinuous. This observation was confirmed by Deruytter [13] who could offer no explanation as to why this could have caused a shift in apparent normalization. He did, however, refer to the possibility of "small timing errors," presumably meaning errors in the determination of time zero. In view of this apparent discontinuity, these data were studied as two separate data sets. The data below 0.2 eV are compared with the evaluated shape on Fig. 8 after the two lowest-energy values, which showed a systematic departure on Fig. 7, had been removed. The normalization values for these data sets are given in Table II. The removal of the two lowest-energy values has only a minor effect on the normalization,  $<0.1\%$ , but reduces the value of  $\chi^2/DF$  by almost a factor of two. The shape-fitted normalization differs from that obtained in the integral normalization of Deruytter and Wagemans by 0.2-0.3% besides the  $\sim 0.3\%$  uncertainty due to the shape uncertainty. Again, normalization uncertainties of this indicated magnitude have frequently been neglected or underestimated.

The data above 0.21 eV are compared with the evaluated shape on Fig. 9 and the normalization value is given in Table II. The data shown on the figure indicate no obvious systematic departures in shape from the evaluated curve. The value of  $\chi^2/DF$  for these data is, however, about a factor of two larger than those of Bowman, et al, Gwin, et al, or Czirr and Sidhu for this energy region. The normalization factor for these data is some two percent different than obtained for the thermal data. It is not possible to assess the proper normalization of the resonance region data or its uncertainty without determining that the apparent discontinuity is real and, if so, its source since three further time channel width changes were made in the measurements up to 11 eV. The data set above 0.21 eV was included in the final LSQ evaluated fit.

#### Data of Shore and Sailor [1]

The data of Shore and Sailor are compared with the evaluated shape on Fig. 10. No obvious departures in shape are evident. These data appear to show more random departures than most of the later TOF data but they really do not as the  $\chi^2/DF$  value given in Table III is essentially equal to that of those data. The randomness is more apparent than real since these data have not been condensed to nearly the extent of the TOF data. The normalization of these data differs by  $\sim 0.5\%$  from that obtained by the authors by joining

to data in the thermal region. The normalization should be quite good since it is heavily weighted by the more precise and bulk of the data below 0.4 eV where the evaluated shape is most reliable. This data set was included in the final LSQ evaluated fit.

#### Data of Desaussure, et al.[14]

These data extend down only to 0.4 eV and are shown on Fig. 11 compared with the evaluated shape. The normalization value given on Table III is about 0.5% lower than that obtained by the authors who normalized to the Shore and Sailor data in this region. A more reliable normalization, and one closer to the authors' value, might have been obtained by deleting the data above ~0.9 eV in the comparison. These data lie systematically below the curve and the difference in fit may be due to the wings of the 1.135 eV resonance. The SIGLEARN theory does not include Doppler-broadening or resolution effects. This data set was not included in the final LSQ evaluation fit because, in part, the correlated capture data obtained in the same experiment were included.

#### Data of Michaudon, et al.[15]

These data begin at 0.38 eV and the 625 values to 1 eV given on CSISRS have been condensed to 13 data points in the comparison shown on Fig. 12. Possible small systematic departures are seen and, as the Desaussure data, a more reliable normalization might have been obtained if the data had been terminated at a lower energy. The normalization obtained for these data is, however, ~2% larger than that obtained by the authors as shown in Table III. The large value of  $\chi^2/DF$  is further evidence of real systematic departures from the evaluated shape. This data set was, however, included in the final LSQ evaluated fit.

#### Data of Wang, et al.[16]

The 321 data values given on CSISRS for this experiment have been condensed to the 28 point set compared with the evaluated shape as shown on Fig. 13. The data show significant departures below 0.3 eV and this is reflected in the very large value of  $\chi^2/DF$ , 26.5, given in Table III. The effect of the systematic departure here on the normalization value is compensated by a departure in the opposite direction at the high energy end.

### THE FISSION INTEGRAL FROM 7 TO 11 EV

The fission cross section data sets were all renormalized to the 2200 m/s value  $\sigma_f^0 = 583.54$  b which is the presently recommended value of the BNW evaluation [7]. The actual fitted values of  $\sigma_f^0$  used in the renormalization are reiterated for each data set in the 2nd column of Table IV. The fission integral values were also calculated on a common basis using subroutines of the SLAVE program [17]. These calculations were performed at Brookhaven National Laboratory by Mulki R. Bhat, the responsible evaluator of  $^{235}\text{U}$  data for version V of ENDF/B. Fission integrals were calculated for the two energy intervals 7.4 to 10-eV,  $I_1$ , and 7.8- to 11-eV,  $I_2$ . The purpose of calculating these two integrals was to be able to estimate a value of the more commonly used integral,  $I_2$ , for the data of Shore and Sailor [1] which

did not extend to 11 eV. The values of the ratio  $I_2:I_1$  for the first five data sets shown in Table IV are very consistent with a total spread less than 0.6 percent. The data of Michaudon, et al., [15] and of Wang, et al. [16], however, each give values of  $I_2:I_1$  two percent larger than this. This significant shape difference, coupled with observed systematic differences in the thermal region for these data sets, indicates that they should not be used in attempting to derive a best-estimate value for the value of  $I_2$ . Members of the Normalization and Standards Subcommittee of the Cross Section Evaluation Working Group working with Mulki Bhat arrived at a value of  $I_2$  of 241.24 b.eV from the values shown on Table IV. This value rests on the following additional assumptions:

1. The value of the Shore and Sailor data was not used on the bases that since it came from the extreme high-energy end of the experiment the data were not reliable to high-precision. The fact that the derived value of  $I_2$  is significantly lower than that of the first five sets shown on Table IV was taken as evidence of this.
2. The value of Bowman et al was downweighted by a factor of three based on the observation that it represents a significant extremum.
3. The larger  $I_2$  value of Deruytter and Wagemans data shown in Table IV corresponding to the normalization above 0.21 eV was used for this set. The choice assumes that the effect, if real, is connected only with the thermal region or the large widths of the time channels used at thermal. At higher energies, the bulk of the fission data were taken with narrow time-channels similar to that of the 0.21- to 1-eV region and systematic errors due to counting-loss corrections would be minimal.

For the recommended average value of  $I = 241.24$  b.eV it would be necessary to assign an uncertainty of  $\pm 2.8\%$  to allow the Gwin value at 50% probability, even if the lower value of  $\sigma_f^0$  shown in Table I were used for the normalization of these data. The most crucial assumption regarding the average value (and possibly its assigned error) is in the Deruytter and Wagemans data. A further disturbing result of the present study is the  $\sim 2.5\%$  discrepancy in the  $I_2$  values of Gwin, et al., and of Czirr and Sidhu. One certain result of the present study is that the  $\pm 0.8\%$  accuracy assigned to the value of  $I_2$  by Deruytter and Wagemans is much too small.

#### ACKNOWLEDGMENTS

The calculations of the fission integrals in the resonance region were done by M. R. Bhat, BNL.

The study of the thermal fission LSQ shape normalizations were done in collaboration with Jack K. Thompson, BNW and some of the earlier normalizations with David A. Kottwitz, BNW.

Major contributors to the evaluation of the relationship of the thermal normalizations to the resonance fission integrals besides Mulki Bhat included, C. D. Bowman and A. D. Carlson of NBS, J. B. Czirr of LLL, R. W. Peelle of ORNL, W. P. Poenitz of ANL, and J. R. Smith of INEL.

The author's work was supported by the Electric Power Research Institute.

## REFERENCES

1. F. J. Shore and V. L. Sailor, "Slow Neutron Resonances in  $^{235}\text{U}$ ," *Phys. Rev.* 112, 191 (1958).
2. B. R. Leonard, Jr., E. J. Seppi and W. J. Friesen, "Low Energy Fission Cross Section of  $^{235}\text{U}$ ," USAEC Report HW-33384 (1954).
3. A. J. Deruytter and C. Wagemans, "Measurement and Normalization of the Relative  $^{235}\text{U}$  Fission Cross Section in the Low Resonance Region," *J. Nucl. Energy*, 25, 263 (1971).
4. A. J. Deruytter, J. Spaepen and P. Pelfer, "The Accurate Fission Cross Section of  $^{235}\text{U}$  from 0.002 to 0.15 eV and its Reference Value at 2200 m/s," *J. Nucl. Energy*, 27, 645 (1973).
5. R. Gwin, E. G. Silver, R. W. Ingle and H. Weaver, "Measurements of the Neutron Capture and Fission Cross Sections of  $^{239}\text{Pu}$  and  $^{235}\text{U}$ , 0.02 eV to 200 keV, The Neutron Capture Cross Sections of  $^{197}\text{Au}$ , 10 to 50 keV, and Neutron Fission Cross Sections of  $^{233}\text{U}$ , 5 to 200 keV," *Nucl. Sci. Engr.*, 59, 79 (1976).
6. J. B. Czirr and G. S. Sidhu, "A Measurement of the Fission Cross Section of  $^{235}\text{U}$  from 100 eV to 680 keV," *Nucl. Sci. Engr.* (in publication) (1976).
7. B. R. Leonard, Jr., D. A. Kottwitz and J. K. Thompson, "Evaluation of the Neutron Cross Sections of  $^{235}\text{U}$  in the Thermal Energy Region," Electric Power Research Institute Final Report, EPRI-NP-167- Project 512 (1976).
8. D. B. Adler and F. T. Adler, "Cross Sections for Fissile Elements: A Simple Approach to the Multilevel Formalism," *Trans. Am. Nucl. Soc.*, 5, 53 (1962).
9. B. H. Duane, "Maximum Likelihood Nonlinear Correlated Fields (BNW Program LIKELY)," USAEC Report BNWL-390 (1967).
10. D. A. Kottwitz, "SIGLEARN: A Program for Simultaneous Least-Squares Fitting of Thermal Cross Sections and Related Ratios." Electric Power Research Institute Topical Report, EPRI-CCN-2 (1976).
11. C. D. Bowman, G. F. Auchampaugh, S. C. Fultz, M. S. Moore and F. B. Simpson, "The Epithermal Fission Cross Section of  $^{235}\text{U}$ ," *Conf. on Neutron Cross Section Techn.*, Report CONF-660303, 2, 1004 (1966).
12. B. R. Leonard, Jr. and D. A. Kottwitz, "Simultaneous Fits to Capture, Fission and Eta Data for  $^{235}\text{U}$  in the Thermal Region," *Trans. Am. Nucl. Soc.*, 21, 507 (1975).
13. A. J. Deruytter, Letter to B. R. Leonard, Jr. dated 14 Oct. 1975.

14. G. DeSaussure, L. W. Weston, R. Gwin, R. W. Ingle, J. H. Todd, ORNL; R. W. Hockenbury, R. R. Fullwood, RPI; and A. Lottin, Saclay, "Measurement of the Neutron Capture and Fission Cross Sections and of their Ratio Alpha for  $^{233}\text{U}$ ,  $^{235}\text{U}$  and  $^{239}\text{Pu}$ ," *Nuclear Data for Reactors, Paris II*, 233 (1966).
15. A. Michaudon, H. Derrien, P. Ribon and M. Sanche, "Proprieties Statistiques Des Niveaux De  $1' \text{U}^{236}$  Induits Dans  $1' \text{U}^{235}$  Par Les Neutrons Lents," *Nucl. Phys.*, 69, 545 (1965).
16. S. D. Wang, Y. C. Wang, E. Dermendzhiev and Yu. V. Ryabov, "The Interaction of Neutrons with  $\text{U}^{235}$ ," *Proc. 1965 Salzburg Conf.*, 1, 287 (1965).
17. O. Ozer, Editor, "Description of ENDF/B Processing Codes and Retrieval Subroutines," Report ENDF-110 (August 1971).

TABLE I

Values of 2200 m/s Fission Cross Sections of  $^{235}\text{U}$  Obtained from LSQ Fits to the Evaluated Shape of Leonard, et al.[7]

Author <sup>a</sup>	Value(b)		Energy Range (eV)	Data
	LSQ Fit	$\chi^2/\text{DF}$		
577.1	573.4 $\pm$ 1.9	4.0	0.01 - 0.26	Bowman, et al.(1966)[11]
	569.9 $\pm$ 2.0	1.2	0.28 - 0.9	
580.2	582.1 $\pm$ 2.0	0.2	0.015 - 0.095	Gwin, et al.(1976 [5]
	578.0 $\pm$ 1.8	1.7	0.011 - 0.91	
585.4	585.0 $\pm$ 2.6	3.4	0.02 - 0.10	Czirr & Sidhu (1976) [6]
	580.7 $\pm$ 2.2	1.5	0.025 - 0.85	

<sup>a</sup>Value quoted by author for data as given in listings.

TABLE II

Values of 2200 m/s Fission Cross Sections of  $^{235}\text{U}$  Obtained From LSQ Fits of the Data of Deruytter and Wagemans (1971)[3] to the Evaluated Shape of Leonard, et al.[7]

Author <sup>a</sup>	Value (b)		Energy Range (eV)	Comment
	LSQ Fit	$\chi^2/\text{DF}$		
580.2 $\pm$ 1.8	580.3 $\pm$ 1.9	5.8	0.02 - 0.92	Full Data Set
	582.0 $\pm$ 1.9	3.8	0.02 - 0.21	Data below time channel width change
	581.5 $\pm$ 1.8	2.1	0.02 - 0.21	Two lowest-energy data removed
	569.8 $\pm$ 2.3	3.0	0.21 - 0.92	Above time channel width change

<sup>a</sup>Normalization of data given in CSISRS 20131.002

TABLE III

Values of 2200 m/s Fission Cross Sections of  $^{235}\text{U}$  Obtained  
From LSQ Fits of Data Sets Which do not Extend to the  
Thermal Range to the Evaluated Shape of Leonard, et al.[7]

Author <sup>a</sup>	Value (b)	$\chi^2/\text{DF}$	Energy Range (eV)	Data
	LSQ Fit			
580.0	577.3 $\pm$ 1.8	1.4	0.1 - 0.9	Shore & Sailor (1958) [1]
577.1	574.1 $\pm$ 2.3	0.9	0.4 - 1.0	Desaussure, et al.(1966)[14]
580.2	591.4 $\pm$ 2.8	6.4	0.4 - 1.0	Michaudon, et al.(1965) [15]
?	537.1 $\pm$ 5.9	26.5	0.22- 1.0	Wang, et al.(1965) [16]

<sup>a</sup>Value quoted by author for data as given in listings.

TABLE IV

Integral Fission Cross-Section Values for  $^{235}\text{U}$  for  
Data Sets which have been Renormalized in the Thermal  
Energy Range to the Evaluated Shape of Leonard, et al.[7]

Data	LSQ Fit $\sigma_f^0(\text{b})$	$I_1^a = \int_{7.4}^{10} \sigma_f dE(\text{b}\cdot\text{eV})$	$I_2^a = \int_{7.8}^{11} \sigma_f dE(\text{b}\cdot\text{eV})$
Deruytter & Wagemans [3]	569.8 $\pm$ 2.3 580.3 $\pm$ 1.9	225.8 221.7	243.1 238.7
Czirr & Sidhu [6]	585.0 $\pm$ 2.6	224.3 <sup>d</sup>	240.6 <sup>d</sup>
Gwin, et al [5]	580.05 $\pm$ 2.0	218.8	235.9
Desaussure, et al [14]	574.1 $\pm$ 2.3	224.9	241.3
Bowman, et al [11]	569.9 $\pm$ 2.0	234.2	251.9
Shore & Sailor [1]	577.3 $\pm$ 1.8	215.6	(231.9) <sup>c</sup>
Michaudon, et al [15]	591.4 $\pm$ 2.8	(209.7) <sup>b</sup>	(229.7) <sup>b</sup>
Wang, et al [16]	537.1 $\pm$ 5.9	(215.6) <sup>b</sup>	(236.3) <sup>b</sup>

<sup>a</sup>All values are normalized to  $\sigma_f^0 = 583.54 \text{ b}$ .

<sup>b</sup>Overlapping runs in the eV range have been normalized by the authors.

<sup>c</sup>Based on an average value of 1.07533 for the ratio of  $I_2$  to  $I_1$ .

<sup>d</sup>Also renormalized to version V  $^6\text{Li} (n, \alpha)$

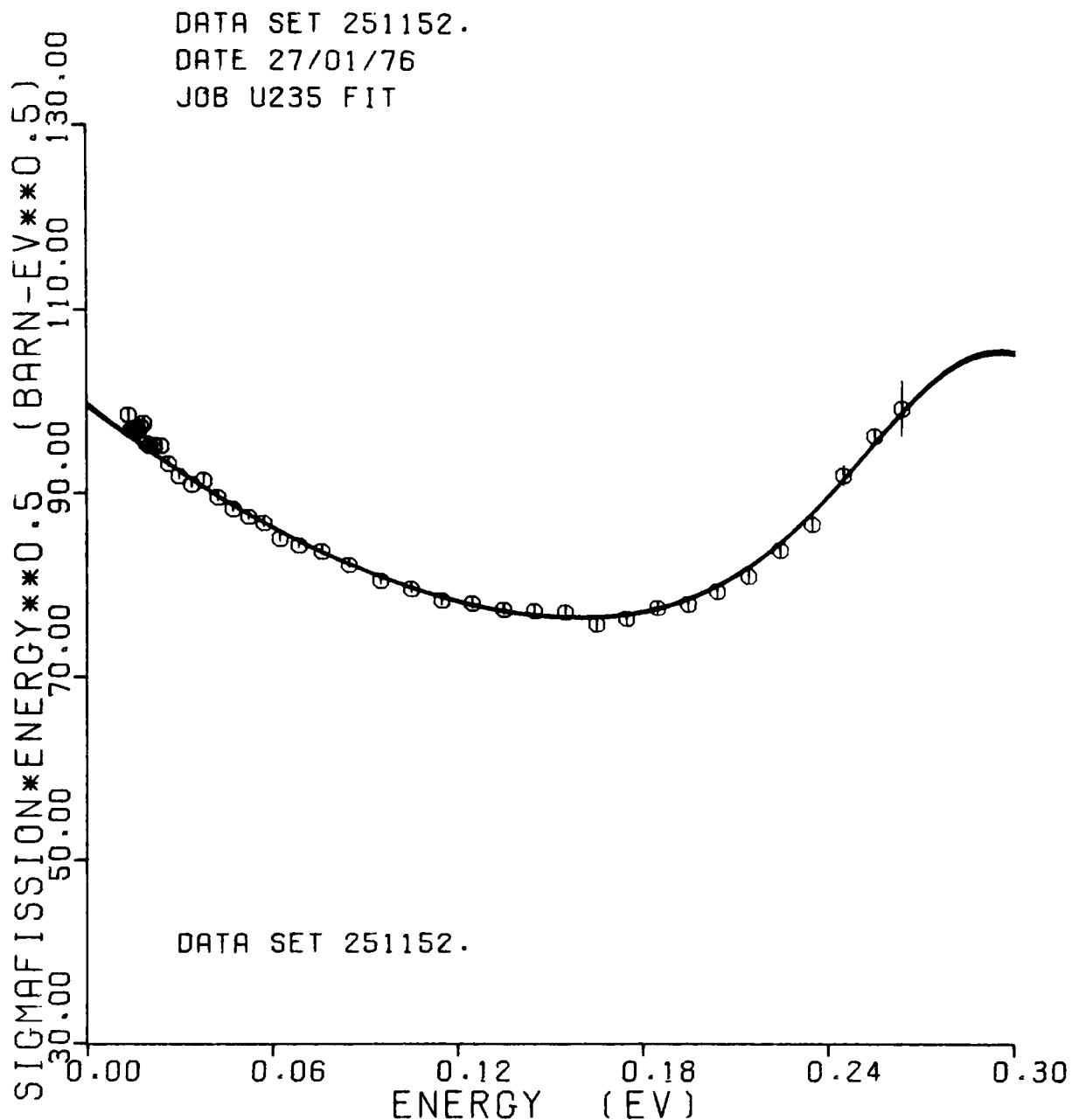


Fig. 1 The low-energy run data of Bowman, et al.[11] LSQ fitted to the evaluated shape. Note the small systematic shape discrepancy at the lowest energies.

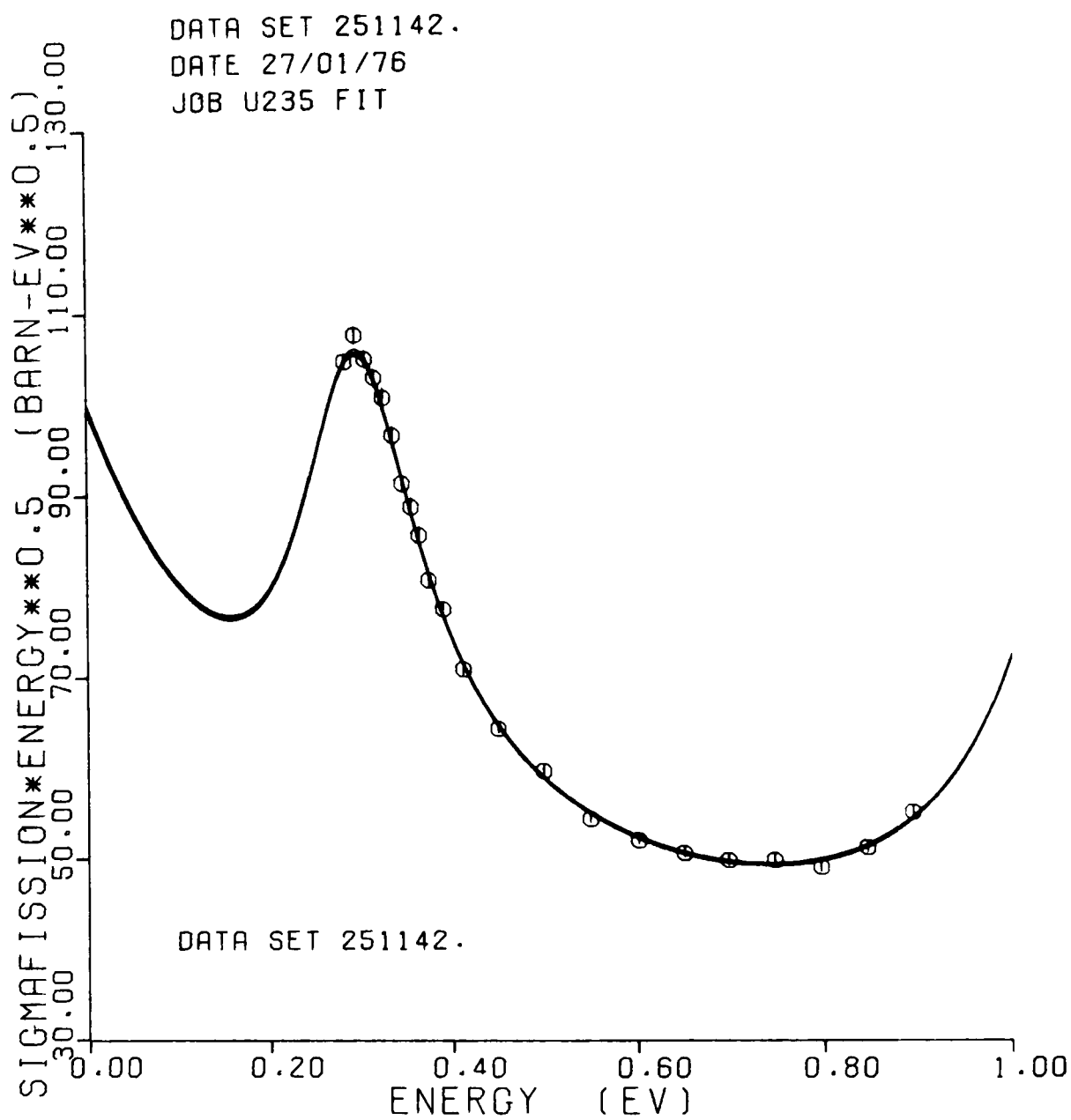


Fig. 2 The higher-energy run data of Bowman, et al.[11] LSQ fitted to the evaluated shape.

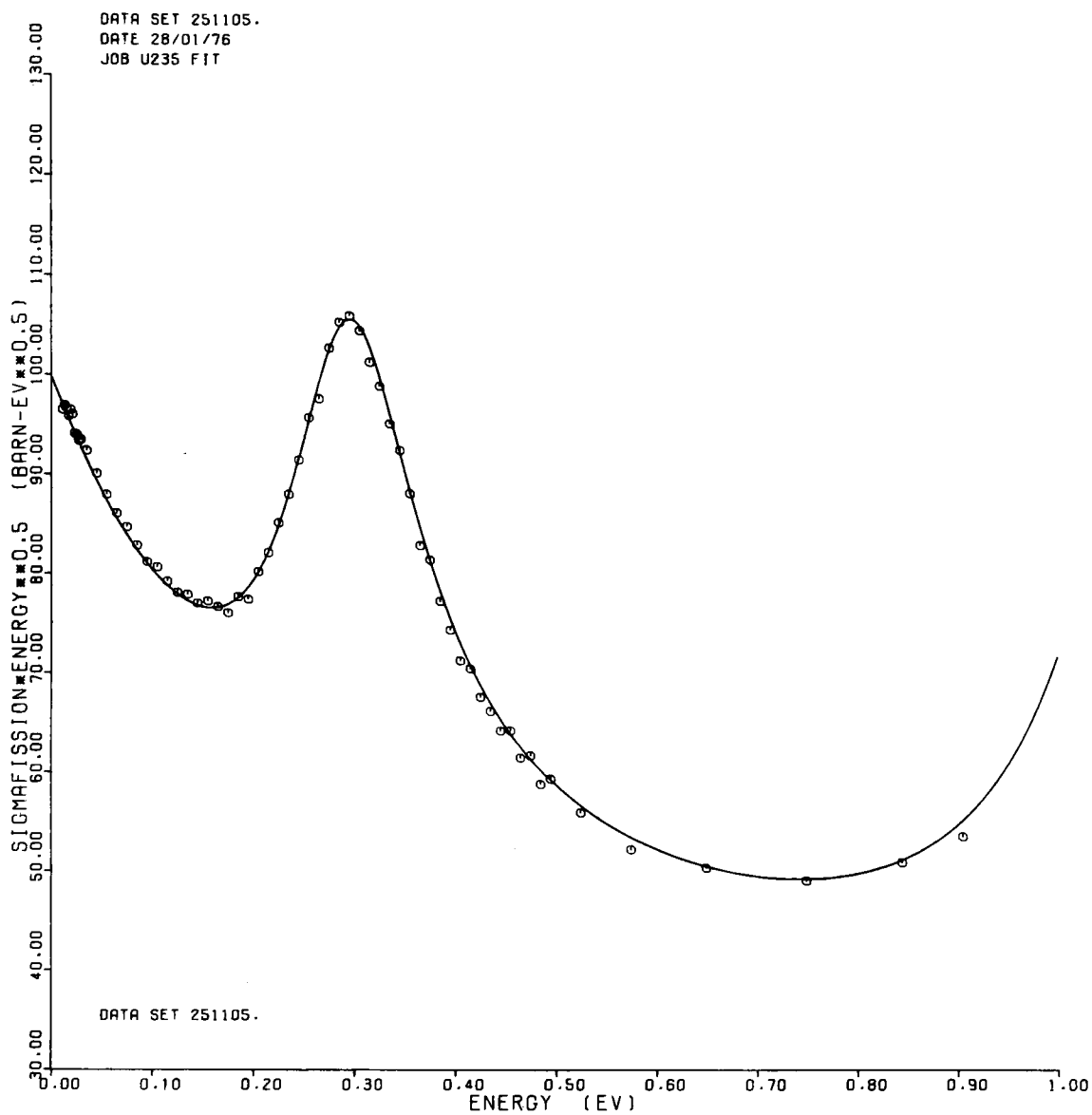


Fig. 3 The data of Gwin, et al.[5] LSQ fitted to the evaluated shape. Some small but systematic departures are observed.

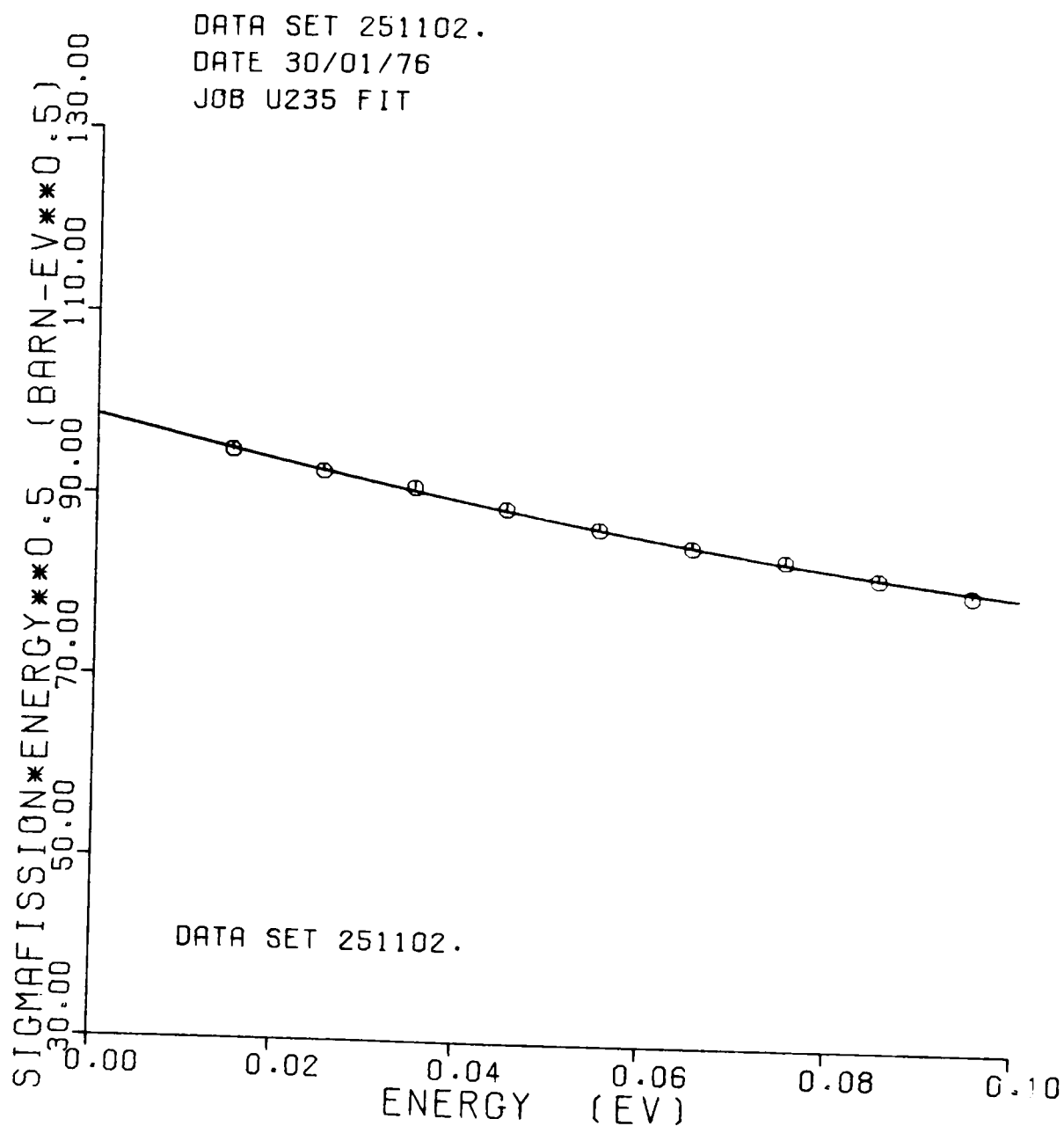


Fig. 4 The LSQ fit to the evaluated shape of the data of Gwin, et al. [5] when only the data below 0.1 eV are fitted. The value of  $\chi^2/DF$  for this fit is only 0.20.

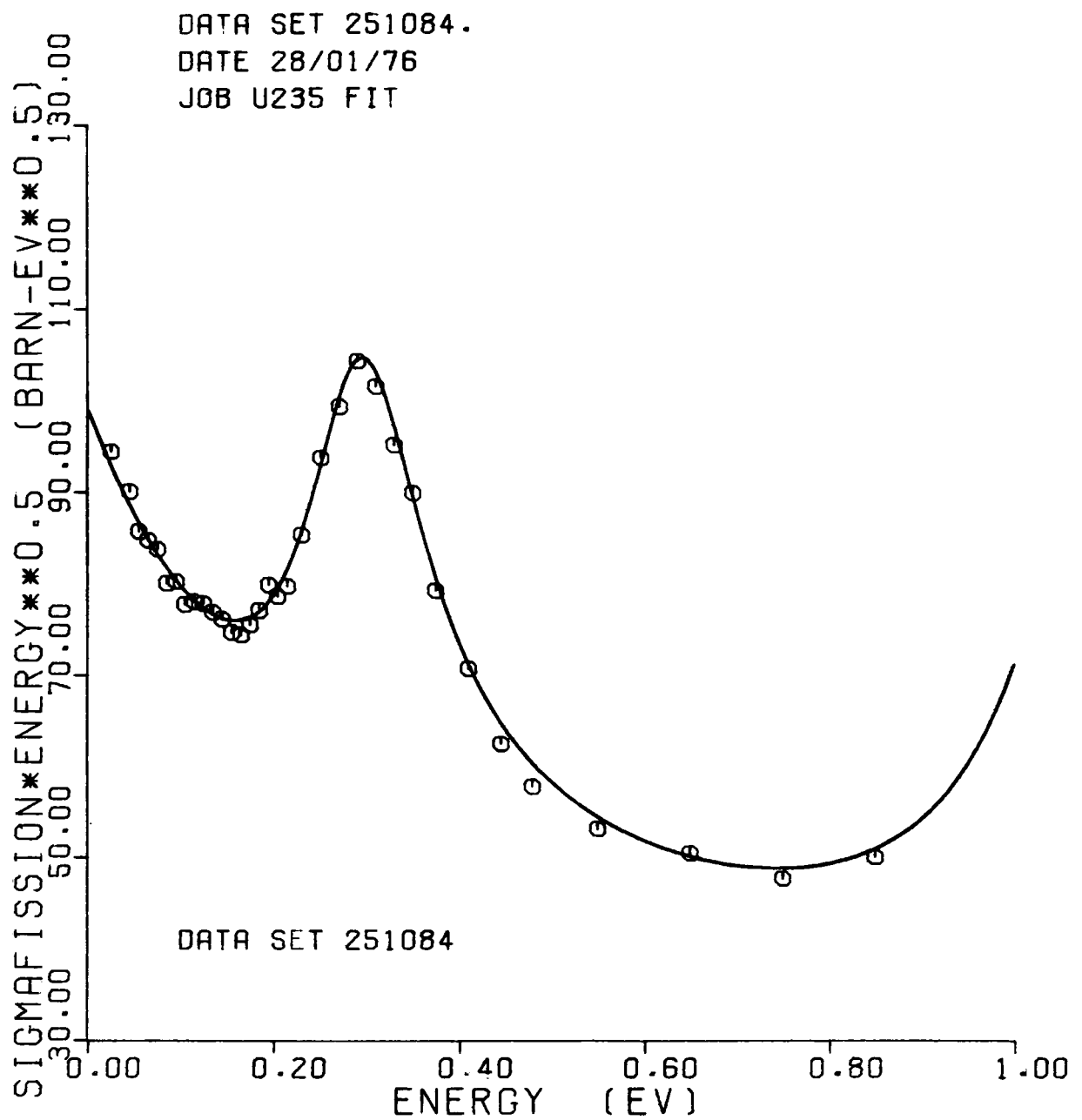


Fig. 5 The LSQ fit of the data of Czirr and Sidhu [6] to the evaluated shape.

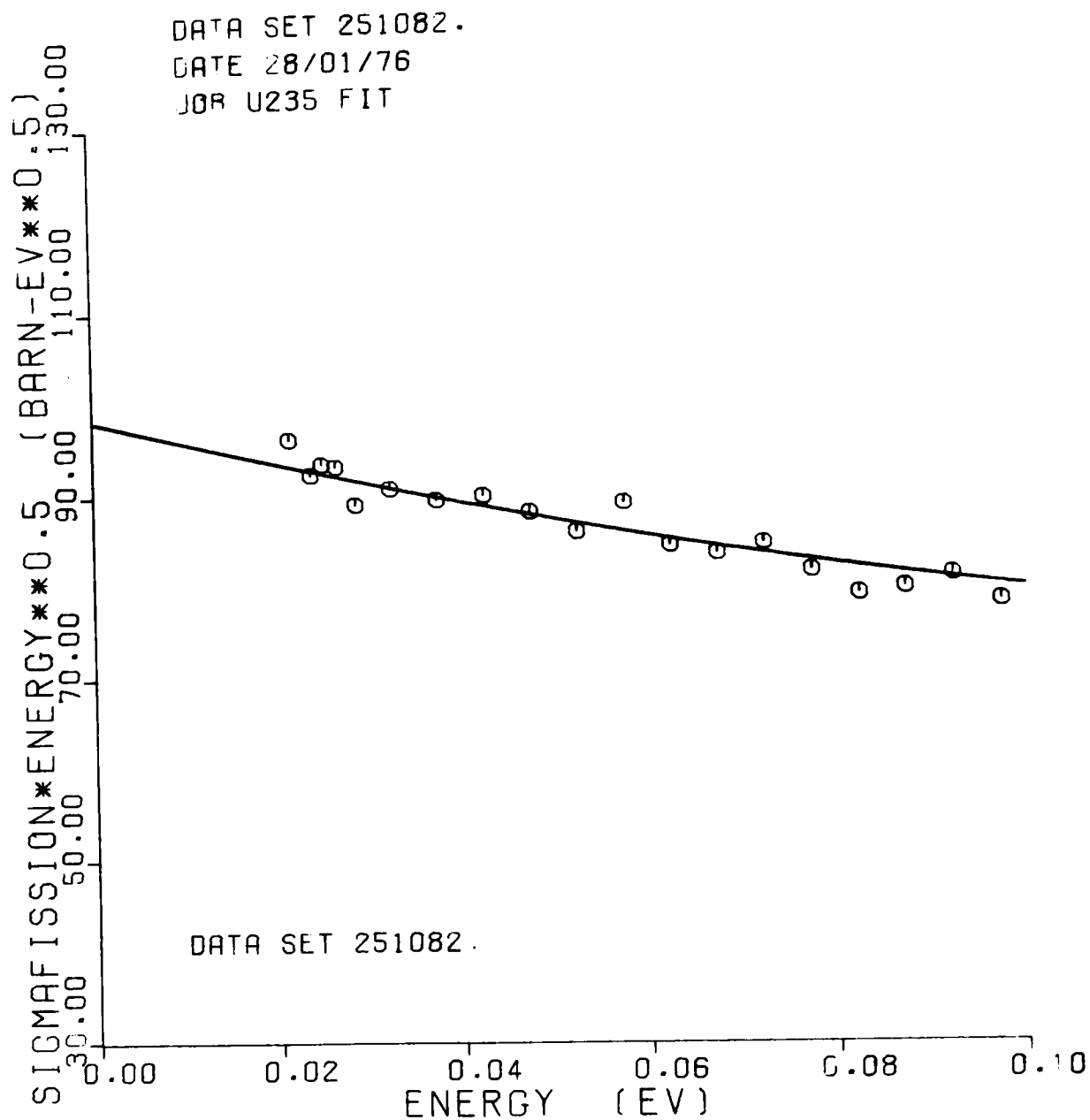


Fig. 6 The LSQ fit to the evaluated shape of the data of Czirr and Sidhu [6] when only the data below 0.1 eV are fitted. These data show a randomness much larger than their statistical precision.

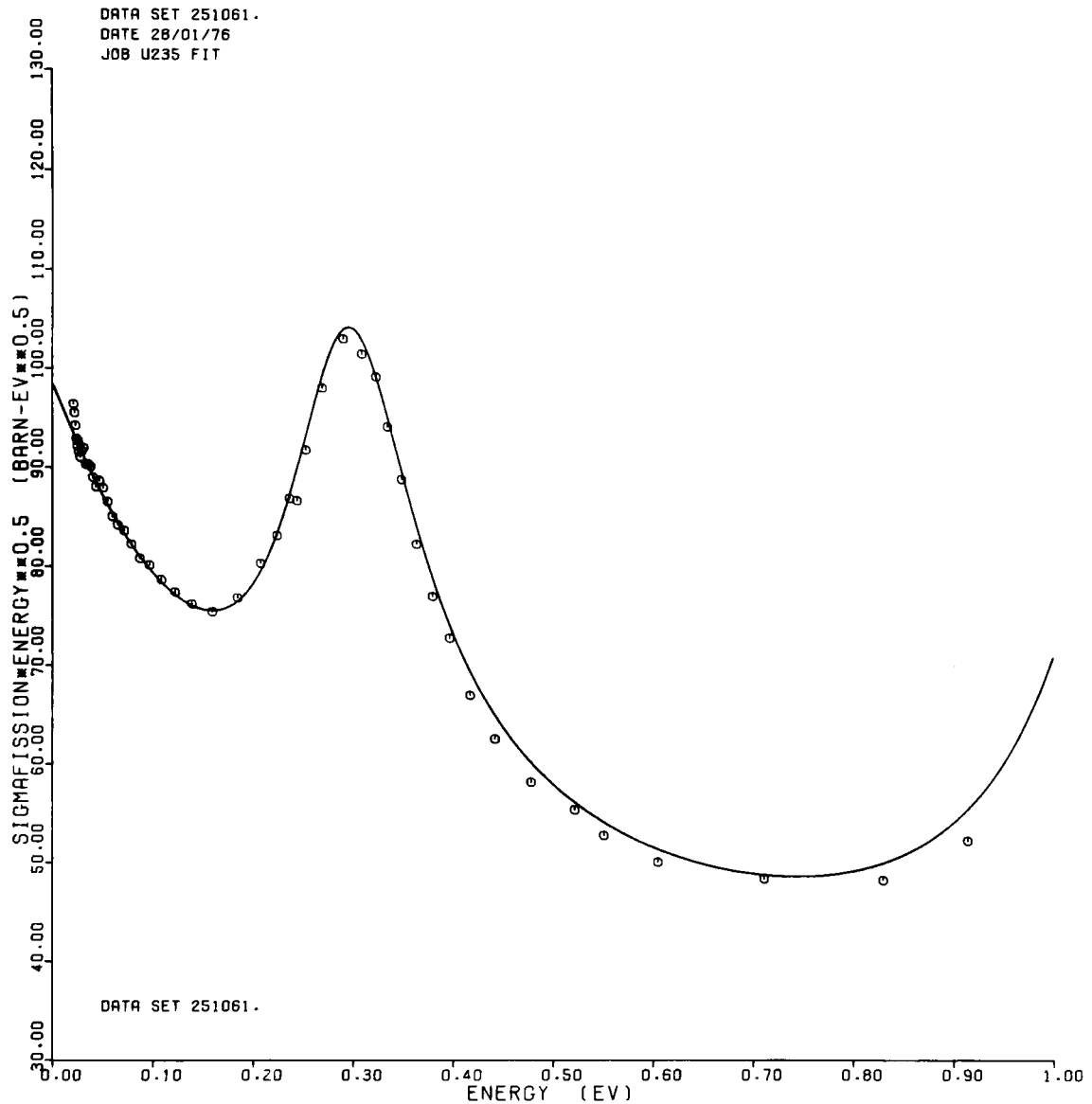


Fig. 7 The LSQ fit to the evaluated shape of the data of Deruytter and Wagemans [3]. The abrupt departure in shape at 0.21 eV occurs at the point at which the time-channel width was changed.

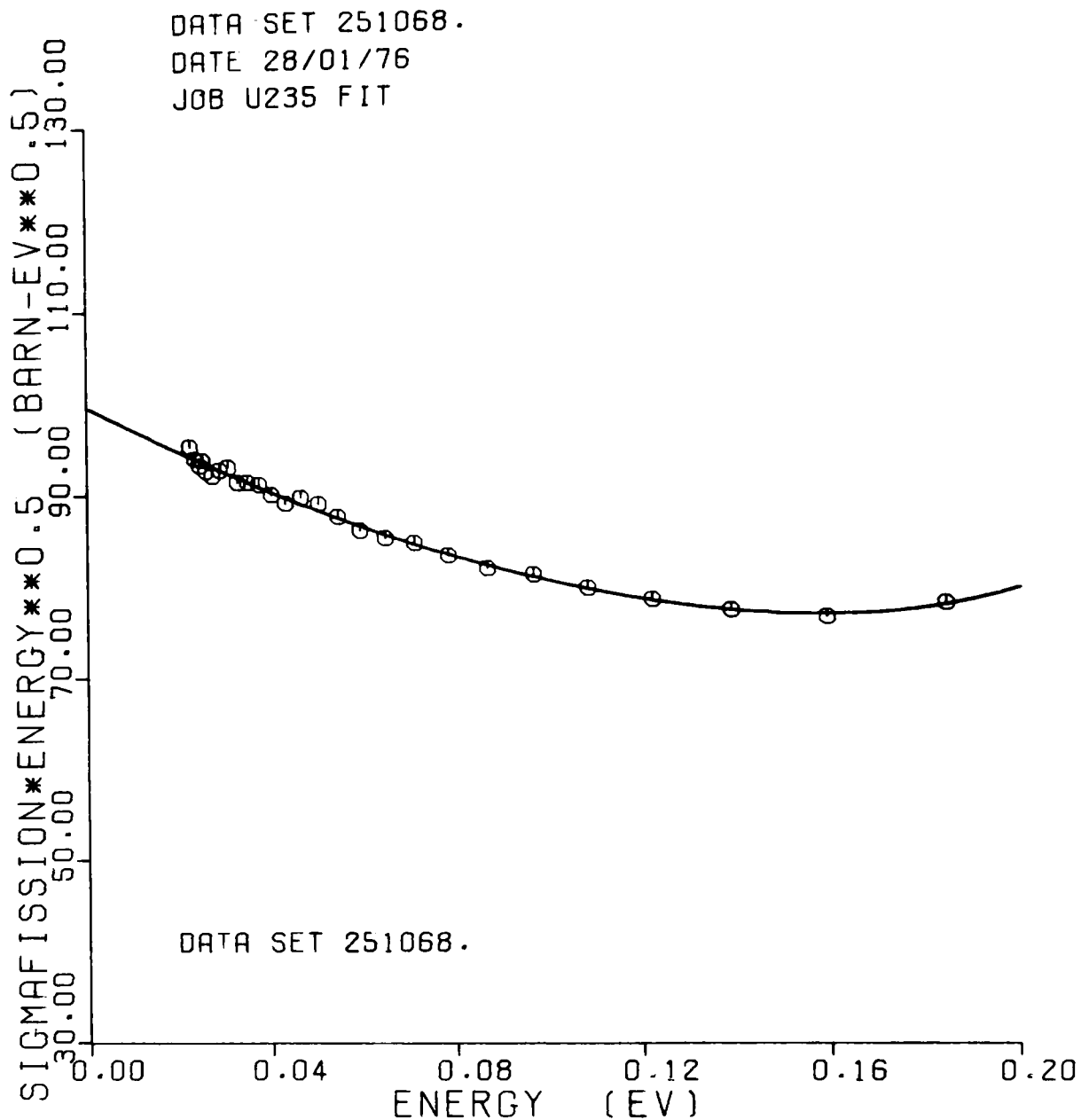


Fig. 8 The LSQ fit to the evaluated shape of the data of Deruytter and Wagemans [3] when only the data below 0.2 eV are fitted. In addition, some data at the lowest energies which are systematically higher than the fitted shape have been deleted.

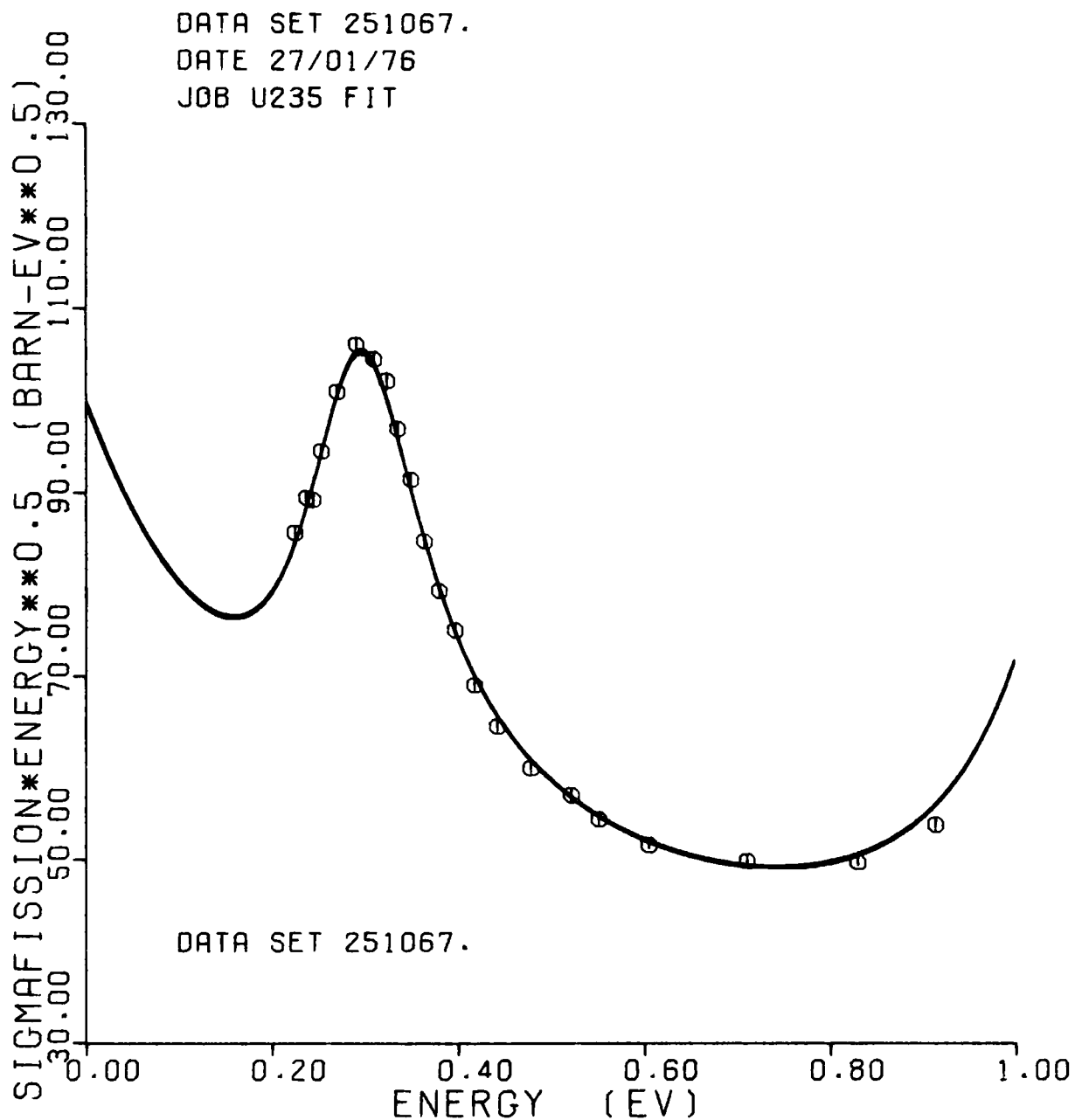


Fig. 9 The LSQ fit of the data of Deruytter and Wagemans [3] above 0.21 eV to the evaluated shape. No systematic departures in shape are obvious.

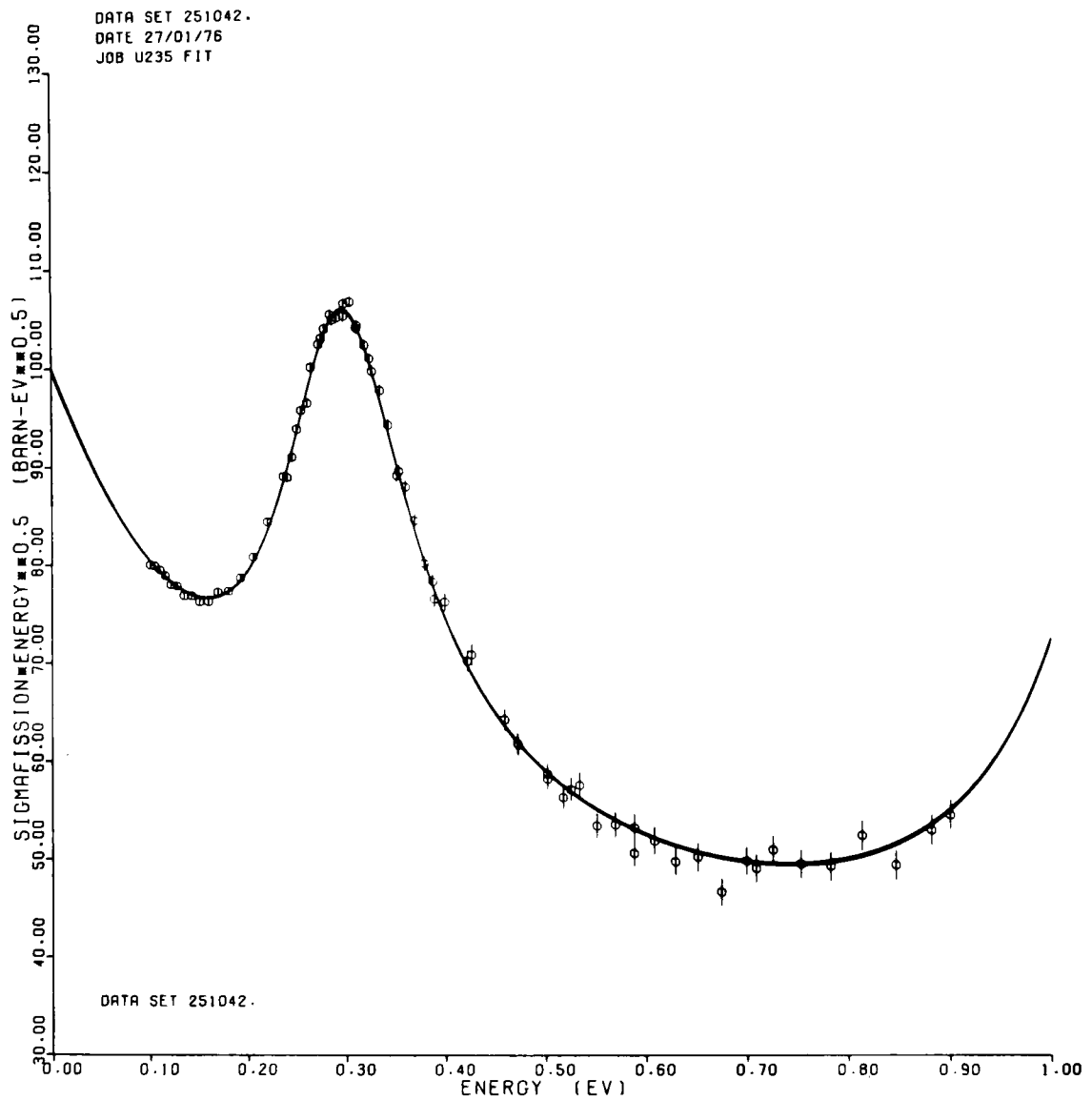


Fig. 10 The LSQ fit of the data of Shore and Sailor [1] to the evaluated shape.

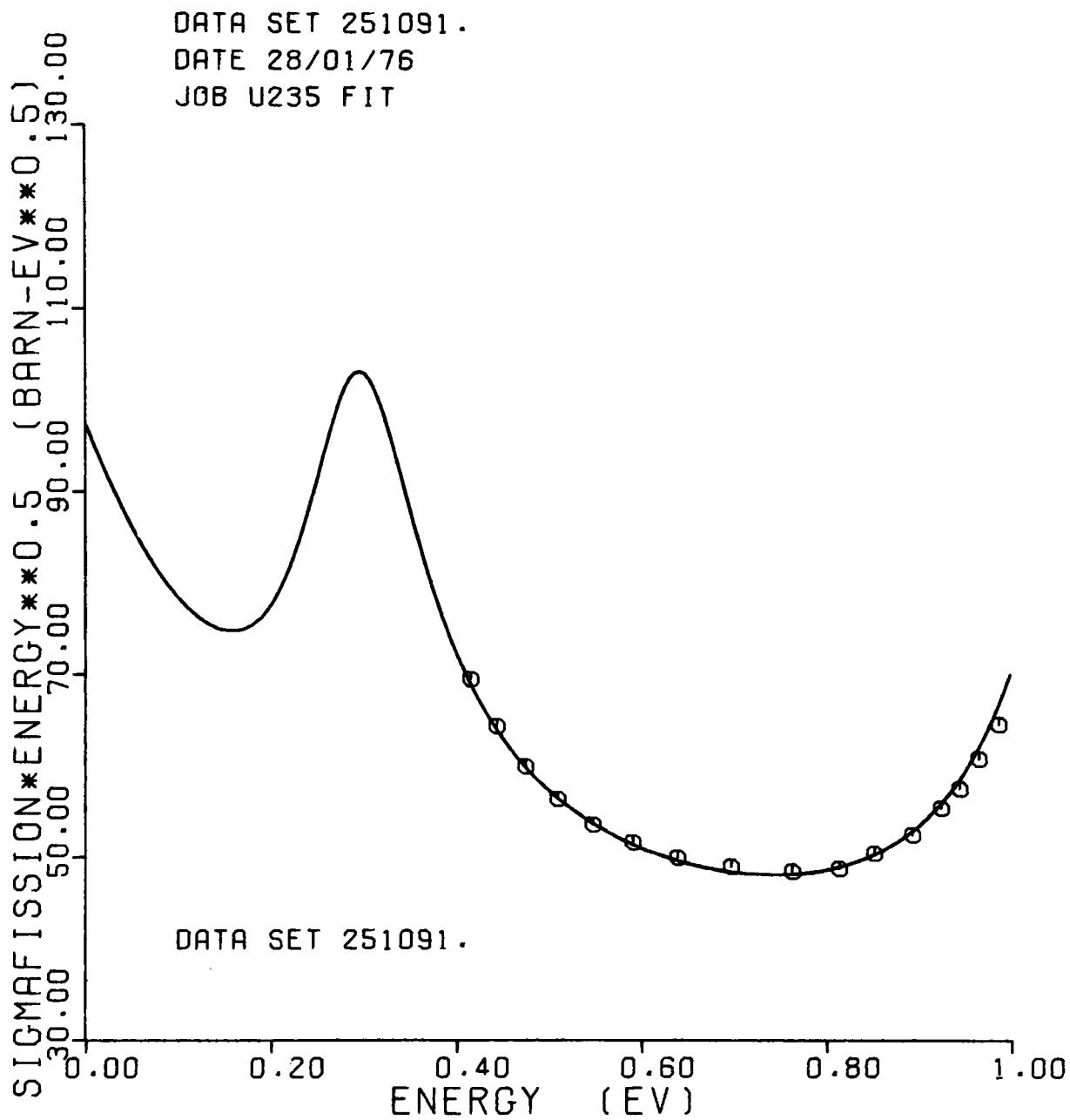


Fig. 11 The LSQ fit of the data of Desaussure, et al.[14] to the evaluated shape.

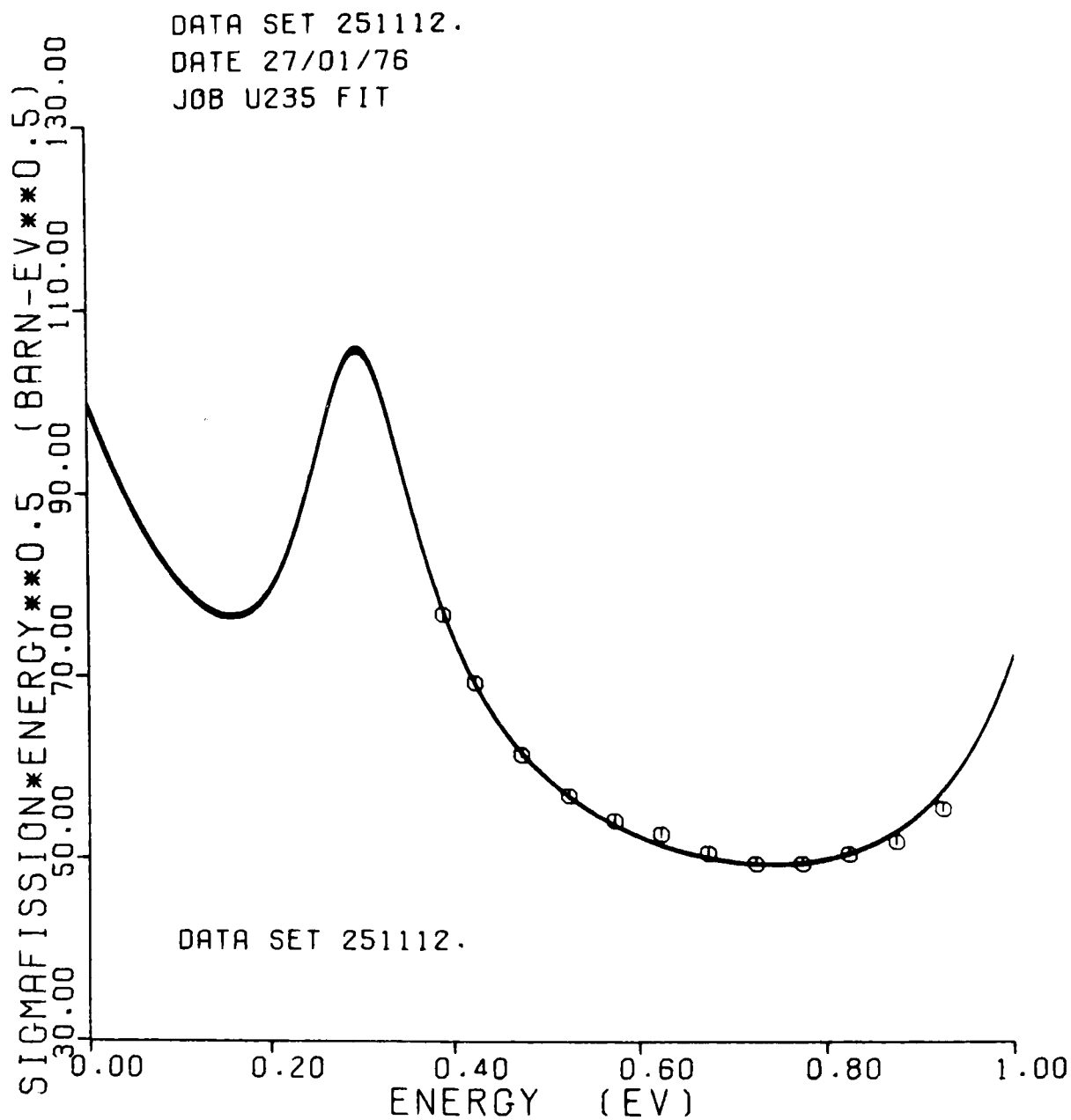


Fig. 12 The LSQ fit of the data of Michaudon, et al.[15] to the evaluated shape. Some systematic departures are apparent.

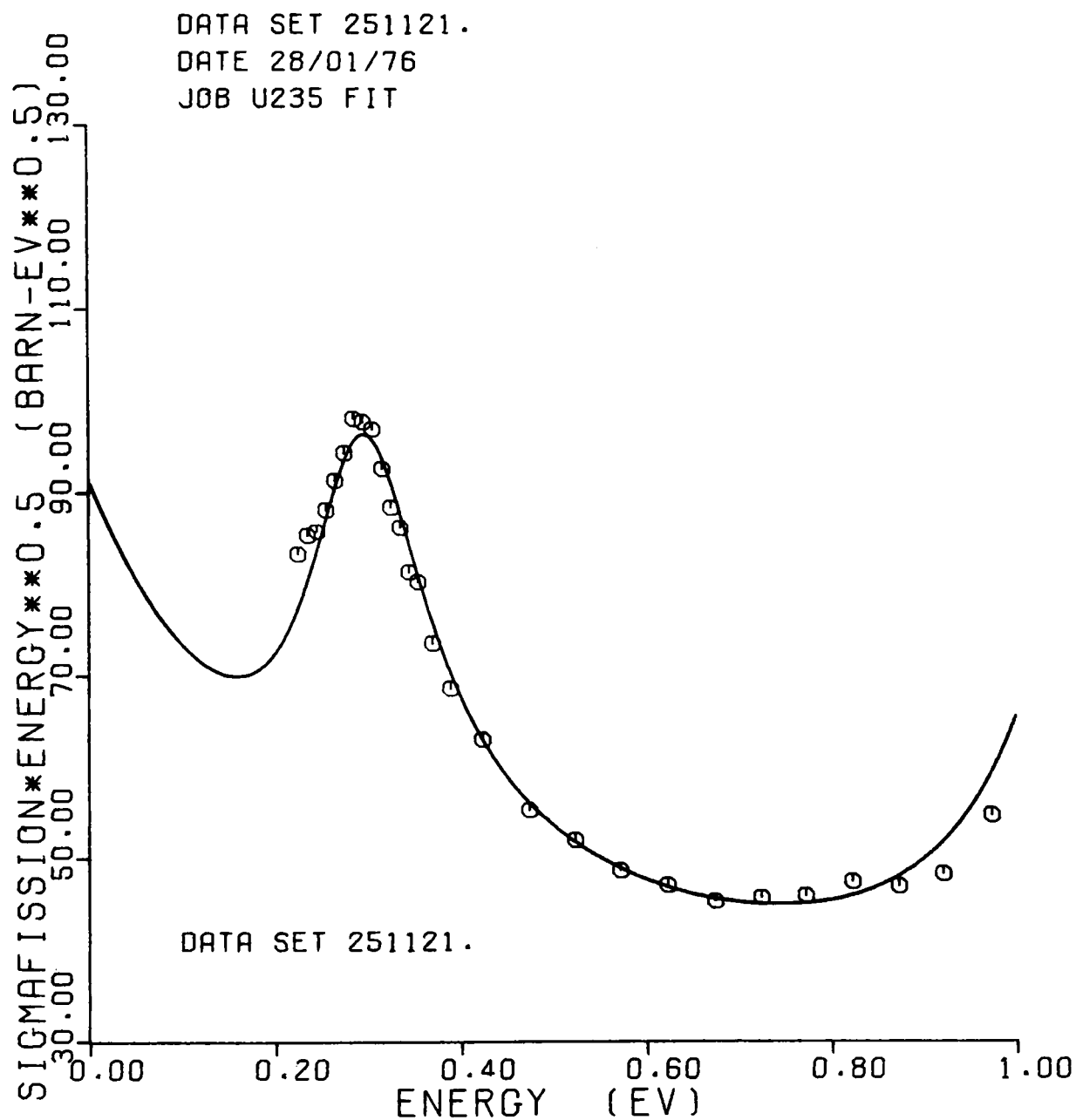


Fig. 13 The LSQ fit of the data of Wang, et al.[16] to the evaluated shape. Large departures are obvious at both high- and low-energies.

## DISCUSSIONS

A. Smith What kind of an error do you assign to that integral value from your evaluation?

B. Leonard I assigned an error of 2.8% based on the deviation of the Gwin data from the mean value and the assumption that there is at least a 50% chance that the Gwin-value is correct.

R. Peelle Say it again.

B. Leonard We calculated the mean value and looked at the dispersion. On the basis that there is a 50% probability that the Gwin-value is correct I assigned an uncertainty of 2.8%.

W. Poenitz This 2.8% would be the present limitation for the accuracy of low energy normalized cross section measurements.

B. Leonard Yes. The situation might be improved if one can establish what happened in the Deruytter and Wagemans experiment.

L. Stewart The data by Bowman appear to be those which were normalized differently in different energy intervals. Is that the set you considered? They were not absolute?

C. Bowman B. Leonard is referring to the set which M. Moore and I did at Livermore. We went down to thermal.

L. Stewart There were two sets.

EVALUATION OF THE  $^{235}\text{U}$  FISSION CROSS-SECTION  
FROM  
100 EV to 20 MEV

M. R. Bhat

Brookhaven National Laboratory  
Upton, L.I., N.Y. 11973

ABSTRACT

The evaluation of the  $^{235}\text{U}$  fission cross-section from 100 eV to 20 MeV for ENDF/B-V is described. The evaluated average cross-sections from 100 eV to 200 keV are given, and it is proposed to include structure in the cross-section in this energy region. Above 200 keV, the cross-section is given as a smooth curve, and is recommended as a standard. Preliminary error estimates in the cross-section are also given.

INTRODUCTION

This paper describes the evaluation of the  $^{235}\text{U}$  fission cross-section from 100 eV - 20 MeV for ENDF/B-V as carried out in conjunction with the Task Force [1] assembled by the Standards and Normalization Subcommittee of CSEWG. It should be considered as a status report of the work in progress. The results given should be considered preliminary until they are approved by CSEWG. The evaluation was done in two parts: from 100 eV - 200 keV where experimental data indicate structure in the cross-section and from 200 keV to 20 MeV where the cross-section may be represented by a smooth curve, and is recommended as one of the primary standards.

In order to obtain a consistent set of primary standards for ENDF/B-V, experimental data on (n,p),  $^6\text{Li}(n,\alpha)$  and  $^{10}\text{B}(n,\alpha)$  cross-sections were reviewed and assessed. It was decided to retain the ENDF/B-IV evaluation of the hydrogen scattering cross-section as a standard because of lack of any significant new data, and the feeling that this evaluation continues to be the best valid estimate of the cross-section. This evaluation is by L. Stewart, et.al. [2], and includes the analysis by Hopkins and Breit [3]. The  $^6\text{Li}(n,\alpha)$  and  $^{10}\text{B}(n,\alpha)$  cross-sections were evaluated by Hale and Dodder [4], and Hale and Arthur [5] respectively using R-matrix analysis and having as input experimental data on all the relevant reaction channels. Further details of these analyses will be published soon. In addition, the present  $^{235}\text{U}$  (n,f) evaluation is based on the results of the analysis in the thermal region by Leonard, et.al., [6]. This gives a fission cross-section of  $583.54 \pm 1.7$  b.,

at 0.0253 eV and the details of this evaluation will be presented by Leonard [7] at this meeting. In the following discussion, all experimental data have been renormalized to the thermal value of Leonard and the  ${}^6\text{Li}(n,\alpha)$  and  ${}^{10}\text{B}(n,\alpha)$  evaluations of Hale which have been accepted as ENDF/B-V standards.

### ${}^{235}\text{U}(n,f)$ CROSS-SECTION BETWEEN 100 EV - 200 KEV

The evaluation procedure adopted in this energy region is to normalize the low energy fission data to a common 2200 m/sec value of 583.54b and obtain an average value for the fission integral between 7.8 eV - 11.0 eV which has been suggested by Deruytter [8] as a possible region for cross-normalization of various data sets. The higher energy data could then be renormalized to this consensus value and compared with one another. Such a comparison would give one a second fission integral from 0.1-1.0 keV which could again be used for renormalizing the data at higher energy; and so on. The results of these calculations are as follows.

The Fission Integral from 7.8 - 11 eV  $\left(I_{7.8}^{11}\right)$

The data sets considered are by Deruytter and Wagemans [8], Czirr [9], Gwin [10], deSaussure [11] Bowman [12] and Shore, and Sailor [13]. The fission integrals from 7.4 - 10 eV  $\left(I_{7.4}^{10}\right)$ , and from 7.8 - 11 eV  $\left(I_{7.8}^{11}\right)$  obtained from these data sets are given in Table I. The second column gives the thermal cross-sections of the different data sets as obtained by the fit of Leonard [6], and have been used to renormalize the data. The third and fourth columns give the fission integrals as obtained from the CSISRS (Cross-Section Information Storage and Retrieval System at the National Neutron Cross-Section Center at Brookhaven) data and column six gives the fission integral from 7.8-11 eV normalized to the ENDF/B-V standards. The next column gives the errors assigned in obtaining a weighted average of 241.2 b. eV for this integral. The Shore and Sailor data extend only up to 10 eV; hence, the fission integral  $I_{7.8}^{11}$  was calculated using the mean value of the ratio  $I_{7.8}^{11}/I_{7.4}^{10}$ . However, the value thus obtained was rejected as being too low.

The Fission Integral from 0.1 - 1.0 keV  $\left(I_{0.1}^{1.0}\right)$

In order to obtain this integral, the data considered are those of Gwin [10], Czirr [9], deSaussure [11], Wasson [14] and Wagemans and Deruytter [15]. The low energy data of Wasson were measured relative to a 0.5mm  ${}^6\text{Li}$  glass scintillator and extend from a few eV to 70 keV, and were normalized to  $I_{7.8}^{11} = 238.4\text{b. eV}$ . These data were renormalized to a value of 241.2b. eV for this integral. These data do not cover the energy region from 300 - 400 eV due to filters in the beam. Hence, to obtain the fission integral the mean of  $I/I'$ , (See Table II) from the data of Gwin, Czirr, deSaussure, Blons [16] and Lemley [17] was used, and the  $I'$  as determined by Wasson. The data of Wagemans, et.al.[15] were measured with respect to  ${}^{10}\text{B}(n,\alpha)$  assumed to be a  $1/v$  cross-section, and the  $I_{7.8}^{11} = 240.0\text{ b. eV}$ . These data were renormalized to  $I_{7.8}^{11} = 241.2\text{ b. eV}$  and the ENDF/B-V  ${}^{10}\text{B}(n,\alpha)$  cross-section. The results thus obtained are shown in Table II. There is a spread of about 9% in the values

of the fission integral from 0.1 - 1.0 keV though the precision claimed by the individual experiments are much smaller. A mean (unweighted) of the five data sets listed in Table II is found to be  $1.1924\text{E}+04$  b. eV. The average cross-sections from 100 eV to 1 keV are shown in Fig. 1. The data of Blons [16] were normalized to this fission integral. Similarly, the data of Perez, et. al., [18, 19] at higher energies were normalized to the same integral. The average cross-sections thus obtained from 1 to 10 keV are shown in Fig. 2. An average of the fission integral of Gwin, Czirr, Perez, Blons and Wagemans between 10 - 50 keV ( $I_{10}^{50} = 8.339\text{E}+04$  b. eV) was used to normalize the high energy data of Wasson from 5 - 800 keV measured with respect to hydrogen. These data have been used in the present evaluation above 5 keV as suggested by Wasson though there are some data by the same author measured with respect to  $^6\text{Li}$  ( $n, \alpha$ ) up to 70 keV. The average fission integral between 10 - 50 keV was also used to normalize the Gayther [20] data. Lemley [17] data were not used in this evaluation as the raw data were not available to correct for the ( $n, \alpha$ ) angular distribution in the flux monitor using ENDF/B-V evaluation. It is estimated [21] that this correction amounts to about +3% at 100 keV, though it decreases at lower energies. Thus, from 10 - 100 keV a mean of the data of Gwin, Czirr, Wasson, Perez, Blons, Wagemans and Deruytter, and Gayther, was obtained as the representation of the fission cross-section. A comparison of the cross-sections as given by the different data sets in the same energy bins indicates quite a wide variation by as much as 12% in the 80 - 90 keV region. In the energy region from 100 - 200 keV, only the data of Gwin, Wasson and Gayther were used; they also show a spread of as much as 10% from 110 - 120 keV. These average values were compared with the Van de Graaff data of Szabo [22,23,24], Poenitz [25], White [26], and increased by 1% between 10 - 200 keV to improve their agreement with the measurements at isolated energies. The experimental data and the evaluated average cross-sections from about 10 keV to 100 keV are shown in Figs 3 and 4. Similarly the data from 100-200 keV and the final average cross-sections are shown in Figs 5 & 6. In these figures, the ENDF/B-IV evaluation is also shown for comparison. The average cross-sections from 100 eV to 200 keV are listed in Table III. In the energy region between 30 - 100 keV the ENDF/B-V averages are 2 - 4% lower than the corresponding version IV values; between 100 - 200 keV these differences vary from 1 - 5%.

### Structure in the Fission Cross Section

To determine the structure in the fission cross-section in this energy region, the data of Gwin, Perez, Blons, Lemley, Bowman [27] will be compared, shifted with respect to one another to correspond to a common energy scale and whatever structure that is common to them will be adopted in the evaluation. The structure will then be variously normalized as a function of neutron energy to agree with the evaluated average cross-sections given above.

### $^{235}\text{U}$ FISSION CROSS-SECTION BETWEEN 200 KEV-20 MEV

The energy region under consideration may be conveniently divided into roughly three parts: from 200 keV to 1 MeV, 1 MeV - 3 MeV, and 3 to 20 MeV. The data considered up to 1 MeV are shown in Figs 7 and 8. These are by Szabo [22,23,24], Poenitz [25], White [26], Knoll. et al.[28], Hansen, et al. [29], and Czirr [30]. In addition, the Wasson data measured with respect to hydrogen and the Czirr data using  $^6\text{Li}(n, \alpha)$  as the standard are also shown.

The Wasson data in this energy region were renormalized to the Leonard thermal value and further increased by 1% to allow for any uncertainty in the low energy normalization. This normalization and the low energy normalization of the same data described earlier agree within 0.5%. The experimental data indicate that there is a flat region in the cross-section between 300 - 400 keV, and the evaluated curve drawn is shown in Figs 7 and 8. In general, it lies lower than the Szabo data and higher than the Wasson and Czirr measurements, and passes through the Poenitz associated activity results between 550 - 650 keV. For comparison, the ENDF/B-IV evaluation is also shown in the same plots; the current evaluation lies lower than version IV by 1 - 6%. In this region the renormalized Gayther data (renormalization factor 0.9733) agrees quite well with Wasson data. Above 800 keV Gayther data agree with Czirr and Poenitz results. Above 700 keV, the evaluated curve follows the general trend of Czirr and Poenitz data, and passes through the Gilliam and Knoll data point at 964 keV, and close to the White data point at 1.0 MeV. The evaluated cross-section at the step at 0.97 MeV thus agrees with these data as well as the Hansen measurement. The  $^{239}\text{Pu}(n,f)/^{235}\text{U}(n,f)$  ratios of Carlson and Behrens [31] when used with the ENDF/B-IV  $^{239}\text{Pu}(n,f)$  cross-section give 1.205 b for the  $^{235}\text{U}(n,f)$  cross-section at 0.99 MeV in good agreement with other data.

Above 1.0 MeV (Fig. 9) the evaluated curve follows the Czirr data [32] up to 3.0 MeV. Between 1 - 1.3 MeV the Hansen data are higher than the evaluated curve by about 2 - 2.5%, while the Poenitz black detector and Szabo data are systematically lower. Above 1.6 MeV the evaluated curve passes close to the Poenitz black detector and the Szabo data, and lies higher than Hansen measurements. On comparing the Hansen and Czirr data there appears to be a strong possibility of an energy shift of one data set with respect to the other, such that  $E_{\text{Czirr}} - 100 \text{ keV} = E_{\text{Hansen}}$ . Unfortunately, the Hansen data end at 6.0 MeV just at the beginning of the rise in the cross-section so that this energy shift cannot be definitely confirmed. Further, such a shift would imply a decrease of the Hansen data by about 5% at 1.0 MeV and by about 1 - 1½% at 6.0 MeV due to the (n,p) cross-section used as a standard. The data shown in the plot have not been shifted in energy and perhaps this problem should be clarified by further work. Between 1 - 1.5 MeV the evaluated curve is lower than ENDF/B-IV by 1 - 3%; from 1.6 - 2.2 MeV it is higher than ENDF/B-IV by less than 1%, and from 2.2 - 3.2 MeV it is lower than ENDF/B-IV by about 1% or less.

The data from 0.6 - 6.6 MeV are shown in Fig. 10. The White datum at 5.4 MeV was increased by 1.5% to allow for the angular distribution of (n,p) scattering [33]. The evaluated curve above 3.0 MeV is drawn to lie between the Czirr and Hansen data points. The data above 6.0 MeV are shown in Fig. 11. In addition to Czirr, the data considered here are those of White and Cance and Grenier [34]. The evaluation follows the Czirr data up to about 13.5 MeV and is drawn to pass between the White and Cance data points, and to have the shape of the Czirr data. The difference between the White measurement at 14.1 MeV and the Czirr data should be noted and could be resolved by a few absolute measurements between 10 and 16 MeV. The present evaluation and ENDF/B-IV differ by a maximum of 1% between 3 - 6 MeV. From 6.0 MeV to 8.0 MeV the present evaluation rises faster than ENDF/B-IV; is less shallow in the dip at 11.0 MeV, and is lower than ENDF/B-IV from 12.5 to 19 MeV differing from it by as much as 4.4% at 15.5 MeV. The evaluated cross-sections from .2 - 20.0 MeV are given in Table IV.

## ERROR ESTIMATES

It is proposed to carry out a detailed analysis of the variance covariance estimates of the  $^{235}\text{U}$  fission cross-section with the help of the Data Covariance Subcommittee of CSEWG, and the experts at Oak Ridge National Laboratory, before the evaluated data files are finalized. This would take into account the effects of various thermal and low energy normalizations, as well as the influence of the uncertainties in the standard cross-sections. Therefore, the following are to be considered as a few tentative estimates of the errors in the evaluated cross-section.

Leonard [7] has suggested an uncertainty of about 3% in the fission integral  $I_{7.8}^{11} = 241.2\text{b. eV}$ . The fission integral from 0.1 - 1.0 keV as determined from various data sets shown in Table II, differ by as much as 9%, though the individual data sets claim a precision of 1.5 - 3%. The five values fall into three groups: the low Czirr value, the Gwin and Wasson data near the average, and the ORNL-RPI, and the Wagemans measurements at the upper end. From these data, it appears that the uncertainty in this fission integral is about 5%. The average cross-sections from the 1 - 10 keV given in 1 keV bins, differ by as much as 8 - 14% in a bin. From 10 keV - 700 keV, the evaluated curve when plotted with  $\pm 5\%$  and  $\pm 7\%$  bands about it are found to encompass almost all of the data shown in the plots, including the Van de Graaff data. The uncertainty in the cross-section between 1 - 700 keV thus appears to be 5 - 7%. The Czirr data, however, are found to lie systematically on the low side of the 7% band in parts of the energy range. From 700 keV to 6 MeV, the uncertainty in the evaluated cross-section is 3% as a  $\pm 3\%$  band about the evaluated curve includes almost all of the data points, except for a few; even for these, their error bars overlap the 3% band. From 6 to 13.5 MeV, the evaluations follows the Czirr data; in the 14 MeV region there are three absolute measurements by White, Cance and Grenier, and Alhazov, et al. [35], which are discrepant. The last two values differ by about 15%. At these energies, because of the fast rising cross-section, any uncertainties in the energy scales of different data sets become important. Some of these problems could be resolved by a number of absolute measurements in this region at well-defined energies. From the data available at present, any error estimates in this energy region less than 5 - 7% appear to be overly optimistic.

## ACKNOWLEDGMENTS

My grateful thanks are due to B.R. Leonard, Jr., (BNW), R.C. Block (RPI), C.D. Bowman (NBS), A.D. Carlson (NBS), J.B. Czirr (LLL), N.E. Holden (BNL), M.S. Moore (LASL), R.W. Peelle (ORNL), W.P. Poenitz (ANL), R. Sher (Stanford), J.R. Smith (INEL), L. Stewart (LASL), and O.A. Wasson (NBS), for their helpful advice, criticism, and participation in this work. This work was supported by U.S. Energy Research and Development Administration.

## REFERENCES

1. The Task Force members are: B.R. LEONARD, JR., (BNW), (Chairman); M.R. BHAT (BNL), R.C. BLOCK (RPI), C.D. BOWMAN (NBS), A.D. CARLSON (NBS),

- J.B. CZIRR (LLL), N.E. HOLDEN (BNL), M.S. MOORE (LASL), R.W. PEELLE (ORNL), W.P. POENITZ (ANL), R. SHER (Stanford), J.R. SMITH (INEL), L. STEWART (LASL), O.A. WASSON (NBS).
2. L. STEWART, R.J. LABAUVE and P.G. YOUNG, "Evaluated Nuclear Data for Hydrogen in the ENDF/B-II Format" USAEC Rep. LA-4574, Los Alamos Scientific Laboratory (1971).
  3. J.C. HOPKINS and G. BREIT, "The  $^1\text{H}(n,n)^1\text{H}$  Scattering Observables Required for High Precision Fast-Neutron Measurements", Nuclear Data A9, 137 (1971).
  4. G.M. HALE and D.C. DODDER, Los Alamos Scientific Laboratory, Private Communication (1976).
  5. G.M. HALE and E.D. ARTHUR, Los Alamos Scientific Laboratory, Private Communication (1976).
  6. B.R. LEONARD, JR., D.A. KOTTWITZ and J.K. THOMPSON, "Evaluation of the Neutron Cross Sections of  $^{235}\text{U}$  In the Thermal Energy Region", EPRI-512, Electric Power Research Institute (1976).
  7. B.R. LEONARD, JR., "Common Normalization of Several  $^{235}\text{U}$  Fission Data Sets in the Thermal and Resonance Region". Proceedings of This Conference.
  8. A.J. DERUYTER and C. WAGEMANS, "Measurement and Normalization of the Relative  $^{235}\text{U}$  Fission Cross-Section in the Low Resonance Region". J. Nucl. Energy, 25, 263 (1971).
  9. J.B. CZIRR and G.S. SIDHU, "A Measurement of the Fission Cross-Section of  $^{235}\text{U}$  from 100 eV to 75 keV", USERDA Rep. UCRL-77377 (Preprint), Lawrence Livermore Laboratory (1975), and Private Communication (1976).
  10. R. GWIN, et al., "Measurement of the Neutron Capture and Fission Cross Sections of  $^{239}\text{Pu}$  and  $^{235}\text{U}$ , 0.02 eV to 200 keV, the Neutron Capture Cross Sections of  $^{197}\text{Au}$ , 10 to 50 keV and Neutron Fission Cross Sections of  $^{233}\text{U}$ , 5 to 200 keV", Nucl. Sci. Eng. 59, 79 (1976).
  11. G. DE SAUSSURE, et al., "Simultaneous Measurements of the Neutron Fission and Capture Cross Sections for  $^{235}\text{U}$  for Incident Neutron Energies from 0.4 eV to 3 keV", USAEC. Rep. ORNL-TM-1804, Oak Ridge National Laboratory (1967).
  12. C.D. BOWMAN, et al., "The Epithermal Fission Cross Section of  $^{235}\text{U}$ " Conference on Neutron Cross Section Technology, March 22-24 (1966) 2, 1004, (1966). Conf.- 660303.
  13. F. SHORE and V. SAILOR, "Slow Neutron Resonances in  $^{235}\text{U}$ ", Phys. Rev., 112, 191 (1958).
  14. O.A. WASSON, National Bureau of Standards, Private Communication (1976).

15. C. WAGEMANS and A.J. DERUYTTER, "The Neutron Induced Fission Cross Section of  $^{235}\text{U}$  in the Energy Region from 0.008 eV to 30 keV", Ann., Nucl. Energy (Submitted for publication).
16. J. BLONS, "High Resolution Measurements of Neutron-Induced Fission Cross Sections for  $^{233}\text{U}$ ,  $^{235}\text{U}$ ,  $^{239}\text{Pu}$  and  $^{241}\text{Pu}$  Below 30 keV". Nucl., Sci. Eng. 51, 130 (1973).
17. J.R. LEMLEY, G.A. KEYWORTH and B.C. DIVEN, "High Resolution Fission Cross-Section of Uranium 235 from 20 eV to 100 keV". Nucl. Sci. Eng., 43, 281 (1971).
18. R.B. PEREZ, et al., "Simultaneous Measurements of the Neutron Fission and Capture Cross Sections for Uranium-235 for Neutron Energies from 8 eV to 10 keV", Nucl. Sci. Eng. 52, 46 (1973).
19. R.B. PEREZ, et al., "Measurement of the Fission Cross Section of Uranium-235 for Incident Neutron Energies Between 2 and 100 keV". Nucl. Sci. Eng. 55, 203 (1974).
20. D.B. GAYTHER, D.A. BOYCE and J.B. BRISLAND, "Measurement of the  $^{235}\text{U}$  Fission Cross-Section in the Energy Range 1 keV to 1 MeV". Proc. of a Panel on Neutron Standard Reference Data p. 201 (1974). I.A.E.A., Vienna.
21. M.S. MOORE, Los Alamos Scientific Laboratory, Private Communication (1976).
22. I. SZABO, et al., "New Absolute Measurement of the Neutron-Induced Fission Cross-Sections of  $^{235}\text{U}$ ,  $^{239}\text{Pu}$  and  $^{241}\text{Pu}$  from 17 keV to 1 MeV", Neutron Standard and Flux Normalization Proc. of a Symposium held at Argonne AEC. Symposium Series, 23, p. 257 (1970).
23. I. SZABO, et al., " $^{235}\text{U}$  Fission Cross-Section from 10 keV to 200 keV". Proc. of the Third Conference on Neutron Cross Sections and Technology, 2, 573 (1971) and Private Communication (1975).
24. I. SZABO, J.L. LEROY and J.P. MARQUETTE, "Mesure Absolue de la Section Efficace de Fission de  $^{235}\text{U}$ , de  $^{239}\text{Pu}$  et de  $^{241}\text{Pu}$  entre 10 keV et 2.6 MeV". Conf. on Neutron Physics, Kiev, 3, 27 (1973).
25. W.P. POENITZ, "Relative and Absolute Measurements of the Fast-Neutron Fission Cross Section of Uranium-235". Nucl. Sci. Eng. 53, 370 (1974).
26. P.H. WHITE, "Measurements of the  $^{235}\text{U}$  Neutron Fission Cross Section in the Energy Range 0.04 - 14 MeV". Nucl. Energy A/B19, 325 (1965).
27. C.D. BOWMAN, M.L. STELTS and R.J. BAGLAN, "The keV Fission Cross-Section of  $^{235}\text{U}$  Measured with High Resolution". Second IAEA. Conference on Nuclear Data for Reactors, Helsinki 2, 65 (1970).
28. G.F. KNOLL, The University of Michigan, Private Communication (1975).

29. D.M. BARTON, B.C. DIVEN, G.E. HANSEN, G.A. JARVIS, P.G. KOONTZ and R.K. SMITH, "Measurement of the  $^{235}\text{U}$  Fission Cross-Section over the Neutron Energy Range 1 to 6 MeV". Preprint Los Alamos Scientific Laboratory (1975).
30. J.B. CZIRR and G.S. SIDHU, "Fission Cross-Section of  $^{235}\text{U}$  from 0.8 to 4 MeV". USERDA, Rep. UCRL-76676 (1975).
31. G.W. CARLSON and J.W. BEHRENS, "Fission Cross-Section Ratio of  $^{239}\text{Pu}$  to  $^{235}\text{U}$  from 0.1 to 30 MeV". USERDA, Rep. UCID-16981, Lawrence Livermore Laboratory (1975).
32. J.B. CZIRR and G.S. SIDHU, "Fission Cross-Section of Uranium-235 from 3 to 20 MeV". Nucl. Sci. Eng. 57, 18 (1975).
33. L. STEWART, Los Alamos Scientific Laboratory, Private Communication (1975).
34. M. CANCE and G. GRENIER, "Absolute Measurement of the 14.6 MeV Neutron Fission Cross-Section of  $^{235}\text{U}$  and  $^{238}\text{U}$ ". Trans. Am. Nucl. Soc. 22, 664 (1975) and Private Communication to L. STEWART.
35. I.D. ALHAZOV, et al., Proceedings of the 3rd All-Union Conference on Neutron Physics, Kiev, June 1975.

TABLE I

Low Energy Fission Integrals for  $^{235}\text{U}$ 

Author & Data Set	Thermal <sup>a</sup> Fit	$I_{7.4}^{10}$ (1)	$I_{7.8}^{11}$ (2)	$\frac{(2)}{(1)}$	$I_{7.8}^{11}$ Relative to Version V Standards	Error
Deruytter & Wagemans AN/SN-20131/2	569.8 ± 2.3	220.47	237.35	1.07656	243.07	1%
Czirr Private Communication April 30'76	585.0 ± 2.6	225.86	242.27	1.07266	240.57	1%
Gwin AN/SN-10267/24	580.05 ± 2.0	217.49	234.62	1.07876	235.92	1.5%
ORNL-RPI AN/SN-10270/6	574.1 ± 2.3	221.24	237.40	1.07304	241.30	2%
Bowman AN/SN-52041/2	569.9 ± 2.0	228.72	246.02	1.07564	251.91	3%
Shore & Sailor AN/SN-51291/20	577.3 ± 1.8	213.31	---	$\left\langle \frac{(2)}{(1)} \right\rangle$ =1.07533	231.86	Reject

Weighted Mean

241.2 b. eV<sup>a</sup>B.R. Leonard, Jr., et al., Ref 6

TABLE II

Fission Integral of  $^{235}\text{U}$  from 0.1-1.0 keV

Author	I (b. eV) <sup>a</sup>	I' (b. eV) <sup>b</sup>	I/I'
Gwin	1.1799E+04	1.0515E+04	1.12211
Czirr	1.1403E+04	1.0162E+04	1.12212
ORNL-RPI	1.2399E+04	1.1063E+04	1.12076
Wasson	1.1815E+04	1.0534E+04	---
Wagemans	1.2204E+04	----	---
Mean Unweighted.	1.1924E+04		
Blons	1.2333E+04	1.0995E+04	1.12169
Lemley	1.1782E+04	1.0509E+04	1.12113
		Mean	1.12156

$$^a_I = \int_{.1 \text{ keV}}^{1 \text{ keV}} \sigma_f dE$$

$$^b_{I'} = \int_{.1 \text{ keV}}^{.3 \text{ keV}} \sigma_f dE + \int_{.4 \text{ keV}}^{1 \text{ keV}} \sigma_f dE$$

TABLE III

Average  $^{235}\text{U}$  Fission Cross-Section from 0.1-200 keV

Energy Bin Limits (keV)	$\langle \sigma_f \rangle$ (b)
0.1 - 0.2	20.54
0.2 - 0.3	20.16
0.3 - 1.0	11.22
1.0 - 2.0	7.167
2.0 - 3.0	5.344
3.0 - 4.0	4.763
4.0 - 5.0	4.187
5.0 - 6.0	3.909
6.0 - 7.0	3.287
7.0 - 8.0	3.165
8.0 - 9.0	2.935
9.0 - 10.0	3.025
10.0 - 20.0	2.482
20.0 - 30.0	2.127
30.0 - 40.0	1.977
40.0 - 50.0	1.827
50.0 - 60.0	1.803
60.0 - 70.0	1.752
70.0 - 80.0	1.695
80.0 - 90.0	1.558
90.0 - 100.0	1.572
100.0 - 110.0	1.568
110.0 - 120.0	1.527
120.0 - 130.0	1.525
130.0 - 140.0	1.426
140.0 - 150.0	1.415
150.0 - 160.0	1.413
160.0 - 170.0	1.386
170.0 - 180.0	1.360
180.0 - 190.0	1.359
190.0 - 200.0	1.282

TABLE IV

 $^{235}\text{U}$  Fission Cross-Section from 0.2-20.0 MeV

E (MeV)	$\sigma_f$ (b)	E (MeV)	$\sigma_f$ (b)	E (MeV)	$\sigma_f$ (b)
0.200	1.316	1.60	1.257	8.25	1.835
0.210	1.296	1.70	1.268	8.50	1.825
0.220	1.279	1.80	1.276	9.00	1.810
0.230	1.264	1.90	1.281	9.50	1.800
0.240	1.254	2.00	1.284	10.0	1.788
0.258	1.240	2.10	1.283	10.5	1.780
0.270	1.232	2.20	1.279	11.0	1.775
0.300	1.216	2.40	1.265	11.5	1.775
0.320	1.210	2.60	1.250	12.0	1.790
0.350	1.202	2.80	1.236	12.2	1.805
0.360	1.200	3.00	1.224	12.4	1.820
0.374	1.197	3.20	1.211	12.5	1.835
0.400	1.186	3.60	1.188	12.75	1.865
0.420	1.172	4.00	1.164	13.0	1.915
0.450	1.152	4.20	1.151	13.5	2.015
0.460	1.148	4.50	1.131	13.75	2.060
0.480	1.142	4.70	1.117	13.85	2.075
0.500	1.136	5.00	1.096	14.0	2.090
0.540	1.125	5.20	1.082	14.25	2.112
0.570	1.118	5.30	1.074	14.5	2.130
0.620	1.107	5.40	1.067	14.75	2.141
0.660	1.098	5.50	1.061	15.0	2.150
0.700	1.094	5.70	1.059	15.25	2.150
0.740	1.097	5.80	1.071	15.5	2.145
0.770	1.099	5.90	1.091	15.75	2.139
0.800	1.104	6.00	1.127	16.0	2.125
0.830	1.112	6.20	1.219	16.5	2.095
0.850	1.119	6.40	1.338	17.0	2.065
0.900	1.155	6.50	1.400	17.5	2.035
0.960	1.206	6.70	1.492	17.75	2.027
0.980	1.212	7.00	1.605	18.0	2.025
1.00	1.214	7.25	1.690	18.25	2.025
1.05	1.214	7.50	1.760	18.5	2.030
1.15	1.216	7.75	1.802	19.0	2.048
1.25	1.220	8.00	1.830	19.5	2.080
1.40	1.232	8.15	1.835	20.0	2.120

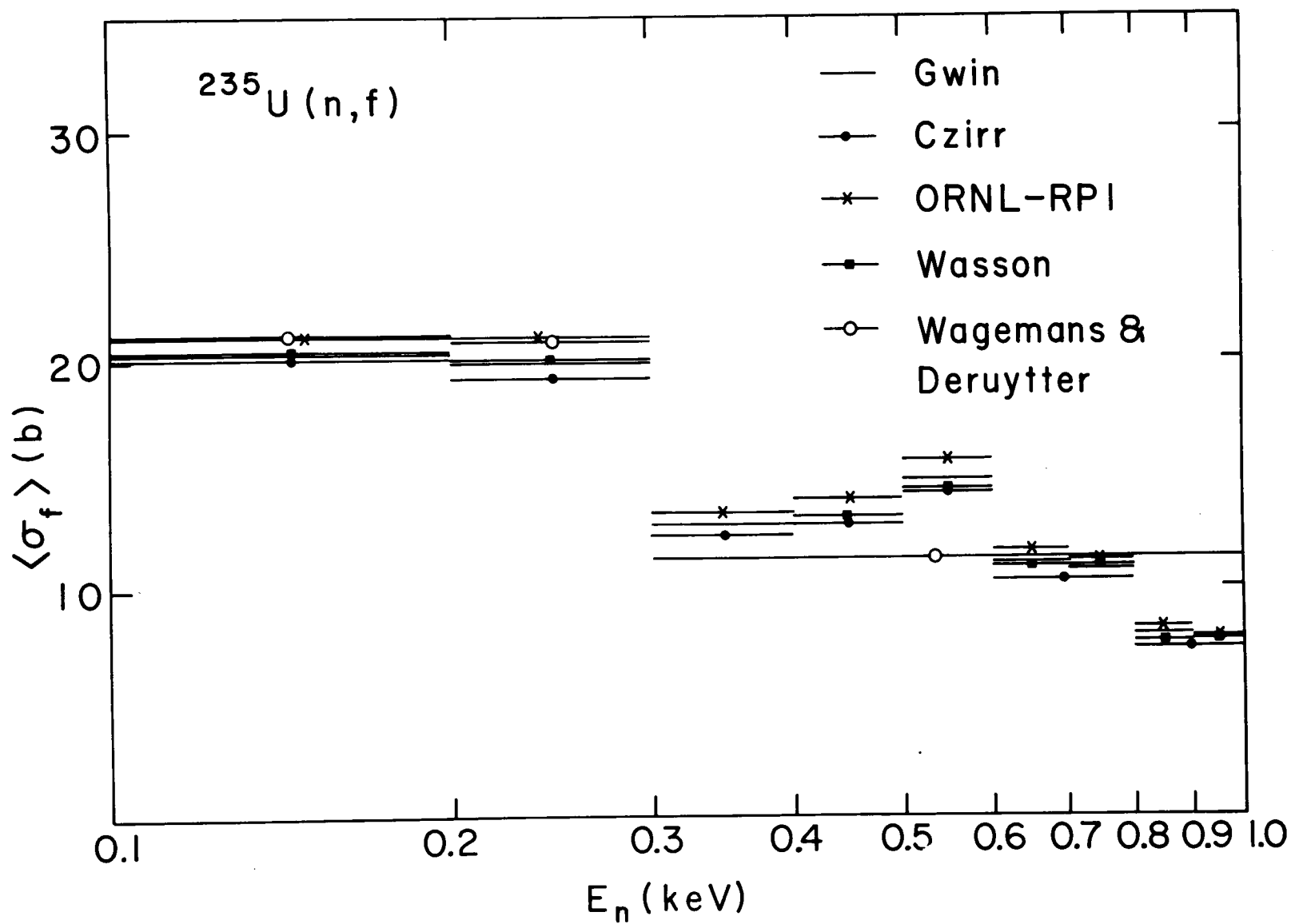


Fig. 1 Average  $^{235}\text{U}(n, f)$  Cross-Section 0.1 - 1.0 keV.

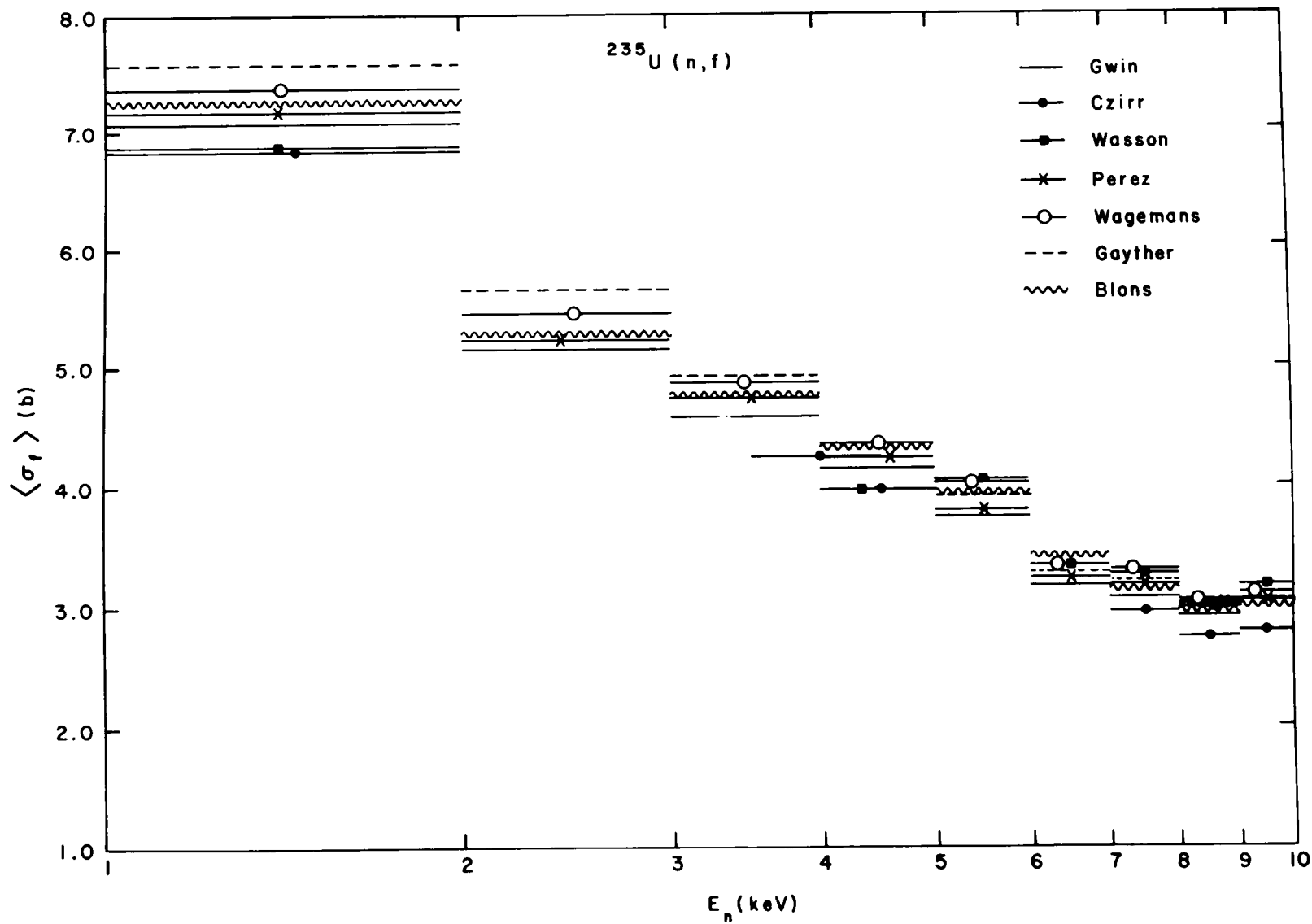


Fig. 2 Average  $^{235}\text{U}(n, f)$  Cross-Section 1.0 - 10.0 keV.

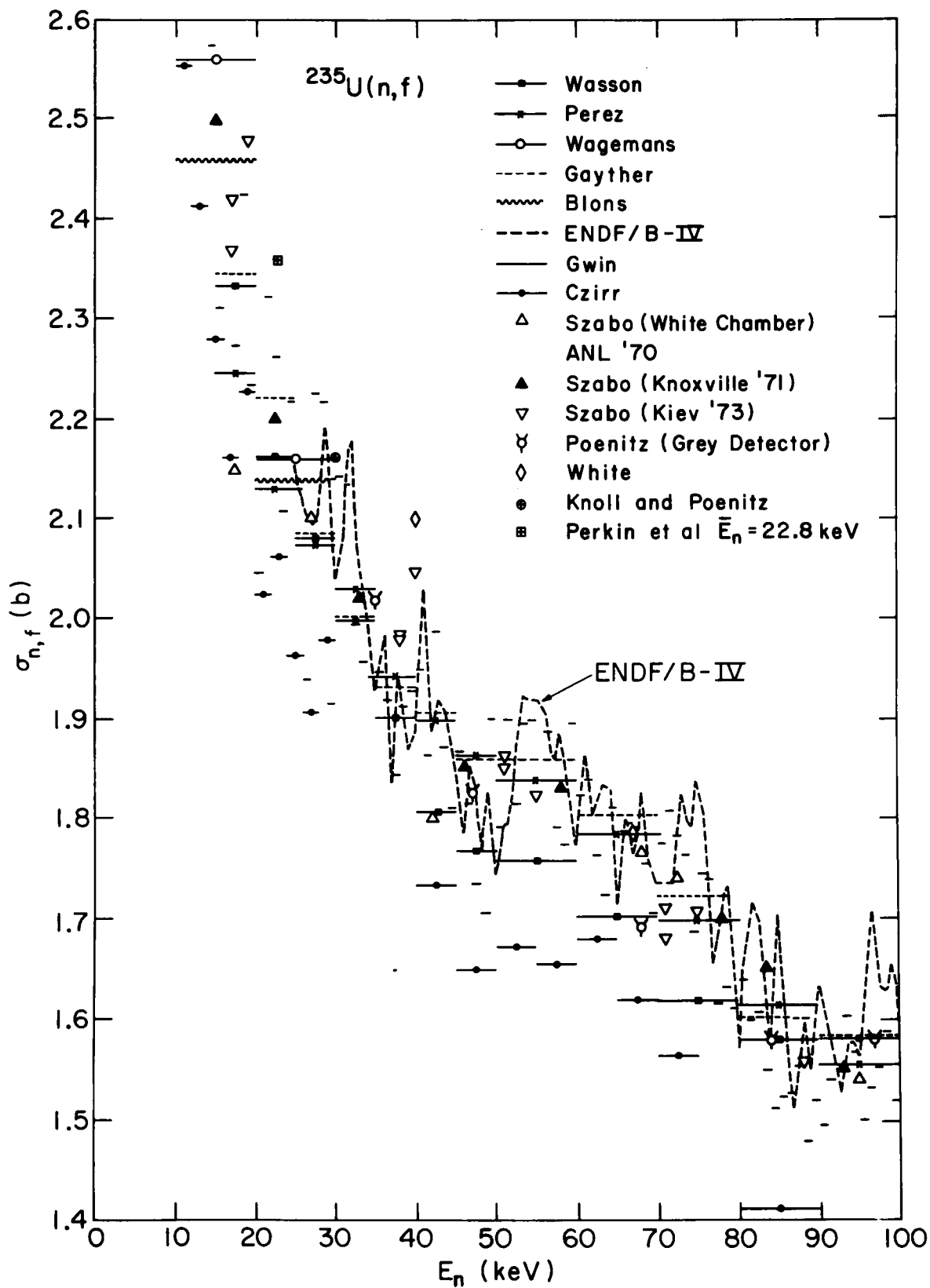


Fig. 3

 $^{235}\text{U}(n,f)$  Data up to 100 keV.

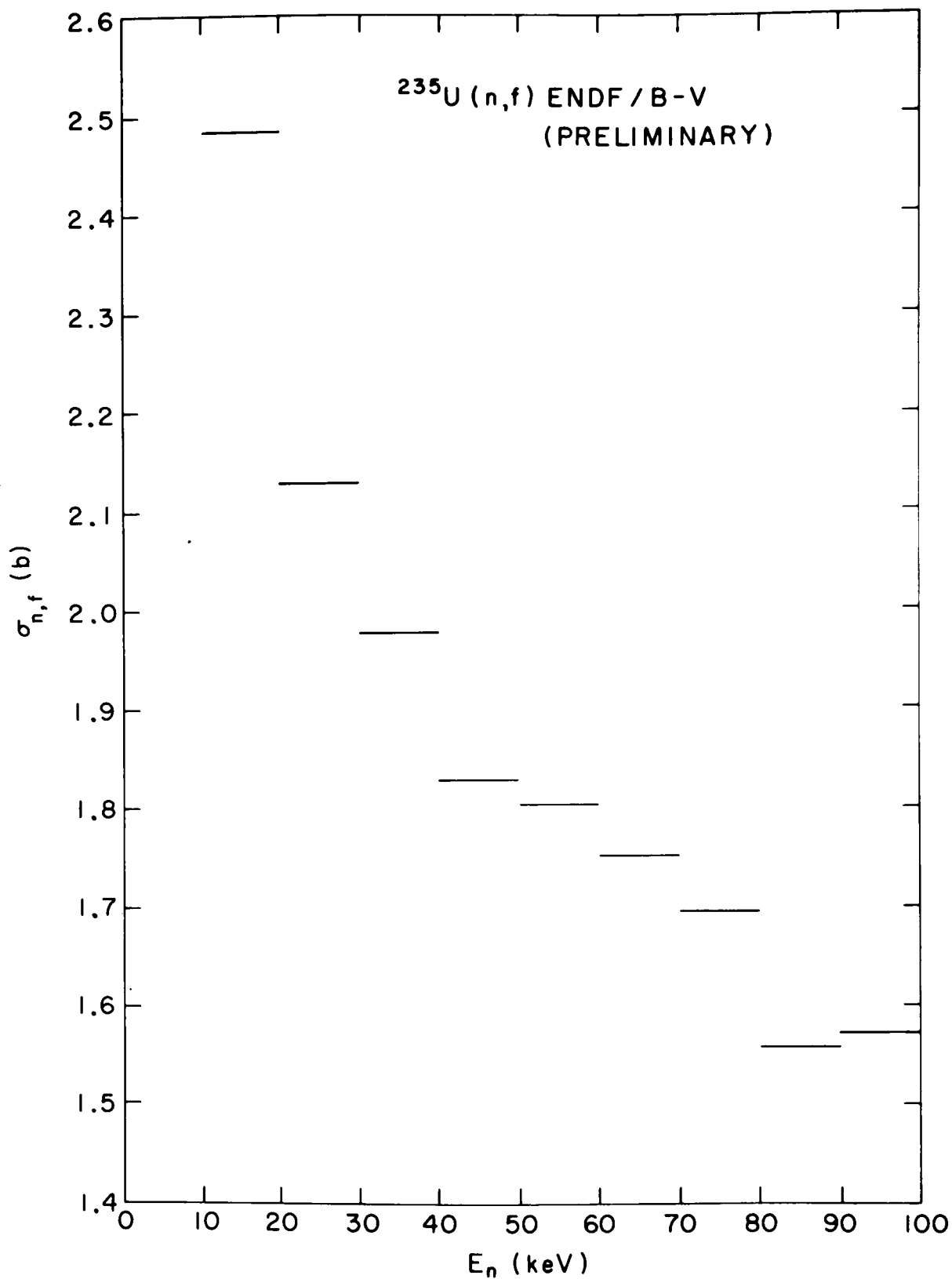


Fig. 4  $^{235}\text{U}(n,f)$  Evaluation up to 100 keV.

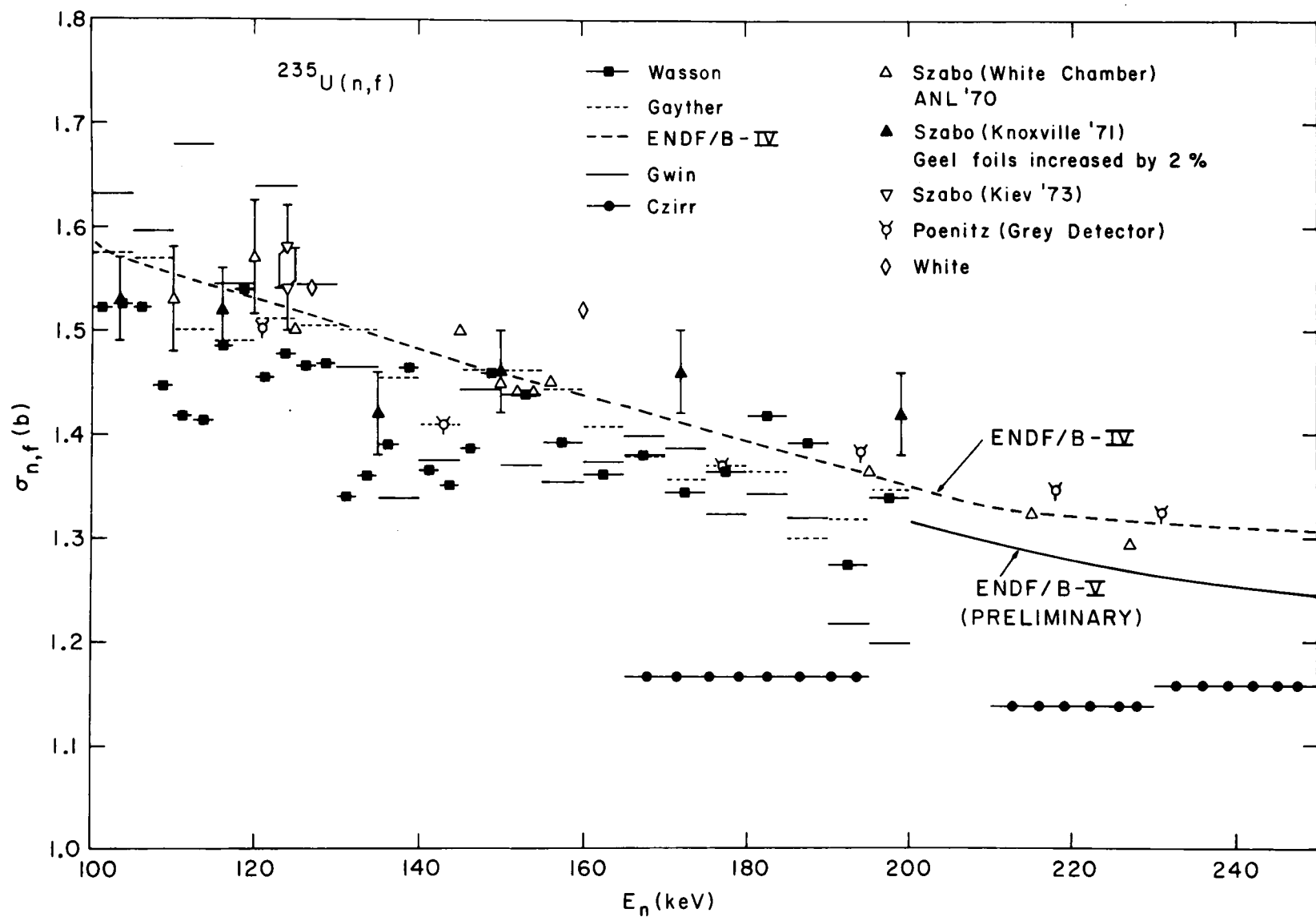


Fig. 5  $^{235}\text{U}(n,f)$  Data 100 - 200 keV.

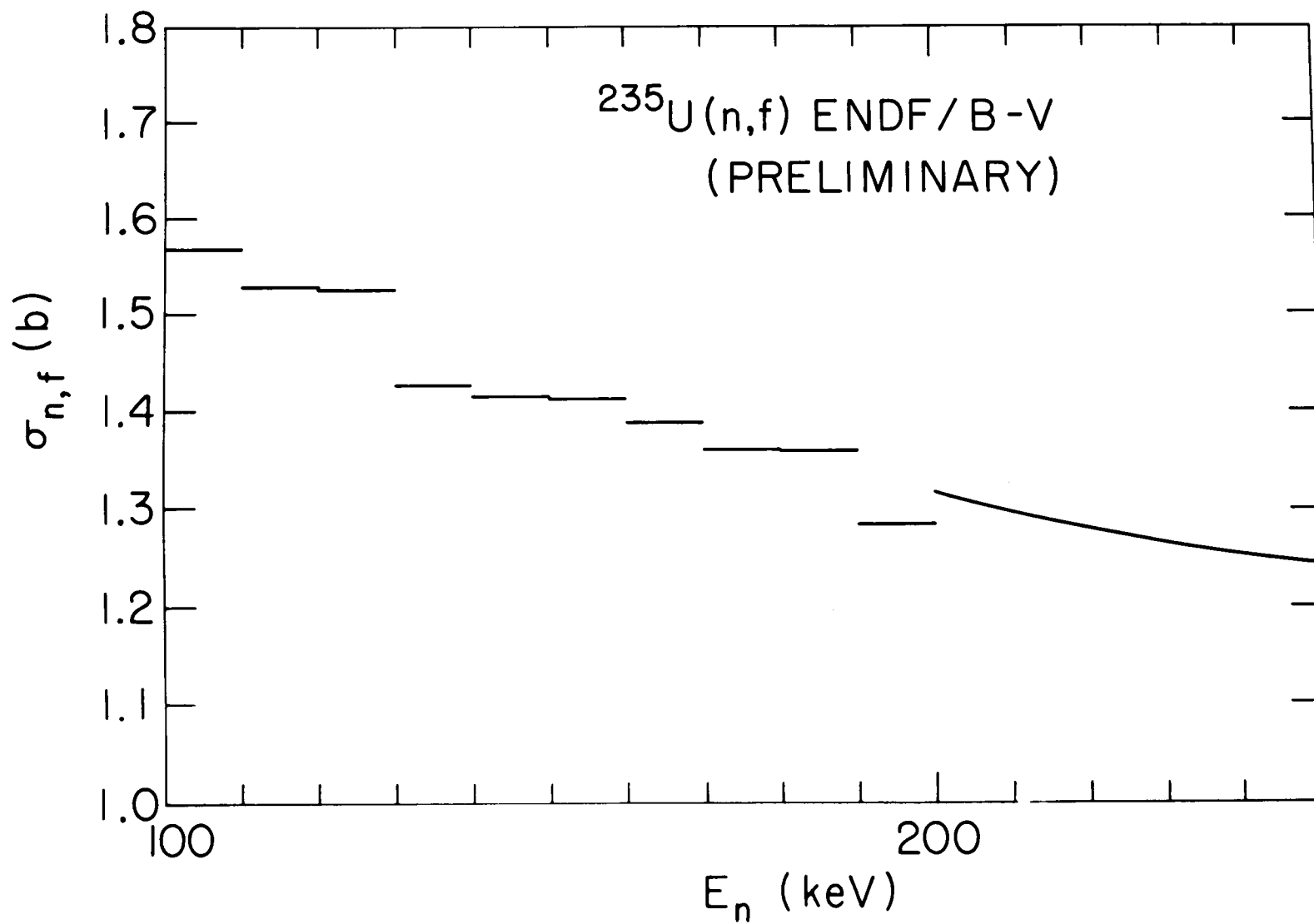


Fig. 6  $^{235}\text{U}(n,f)$  Evaluation 100 - 200 keV.

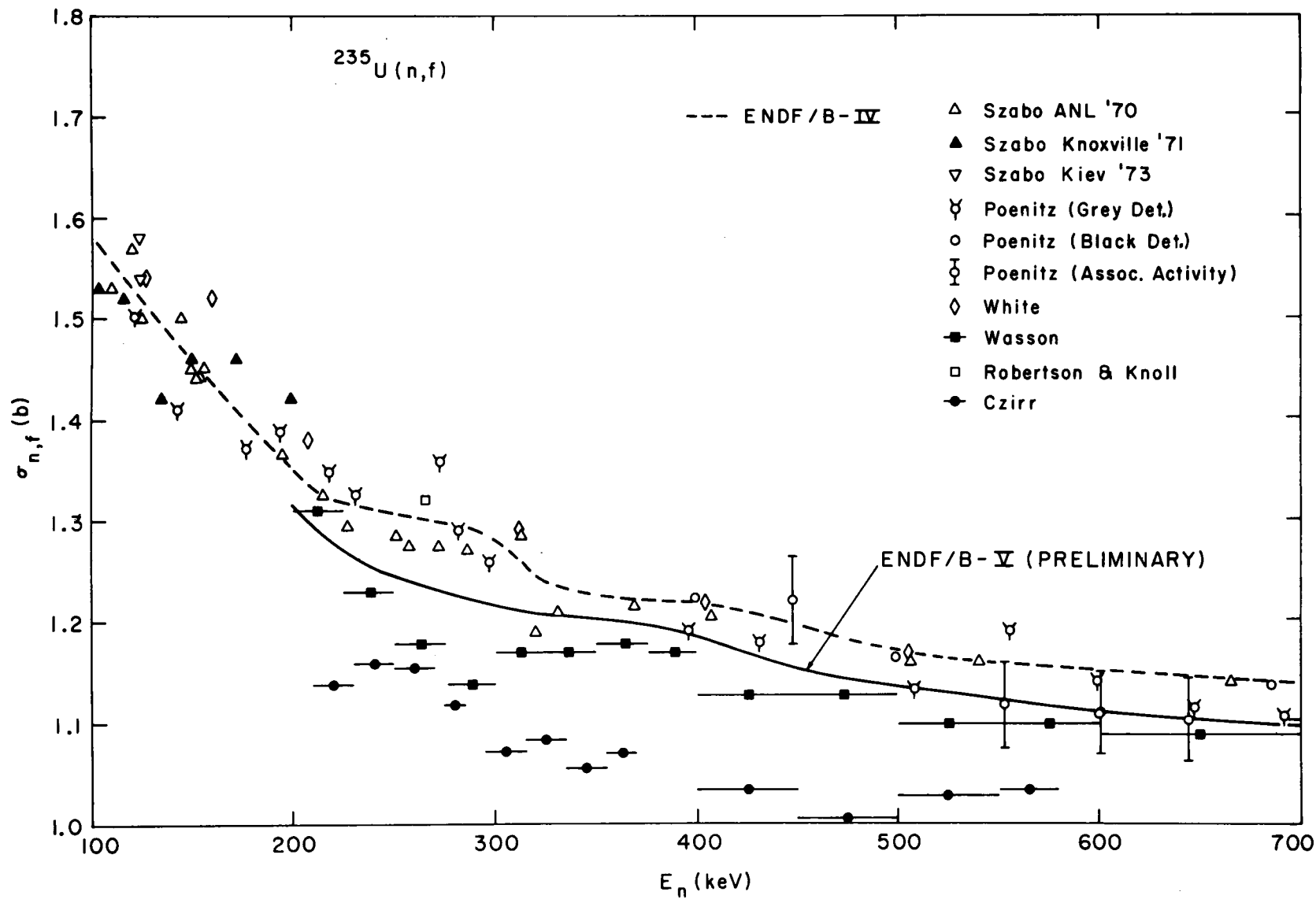


Fig. 7  $^{235}\text{U}(n,f)$  Data and Evaluation 100 - 700 keV.

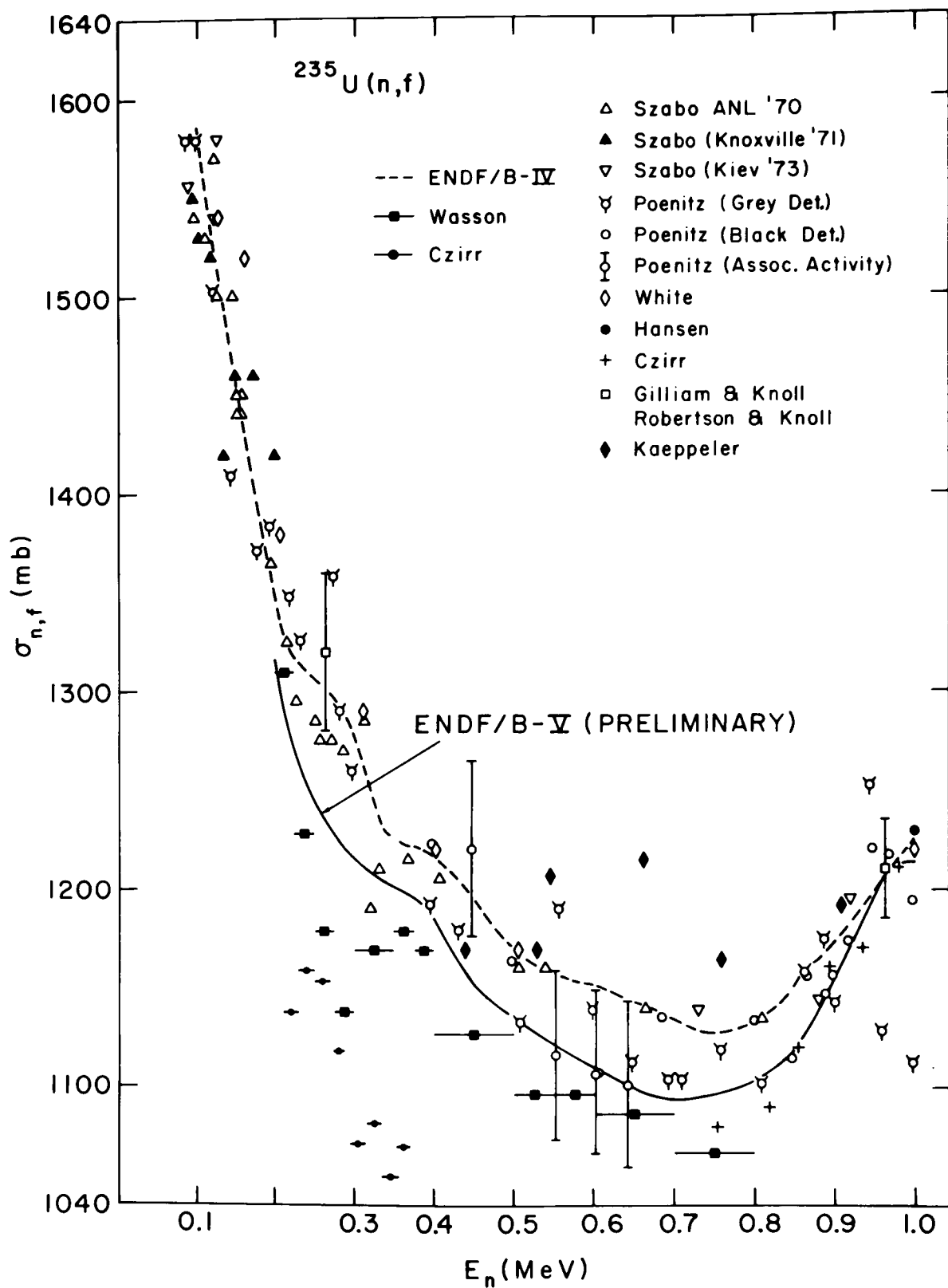


Fig. 8  $^{235}\text{U}(n,f)$  Data and Evaluation 0.1 - 1.0 MeV.

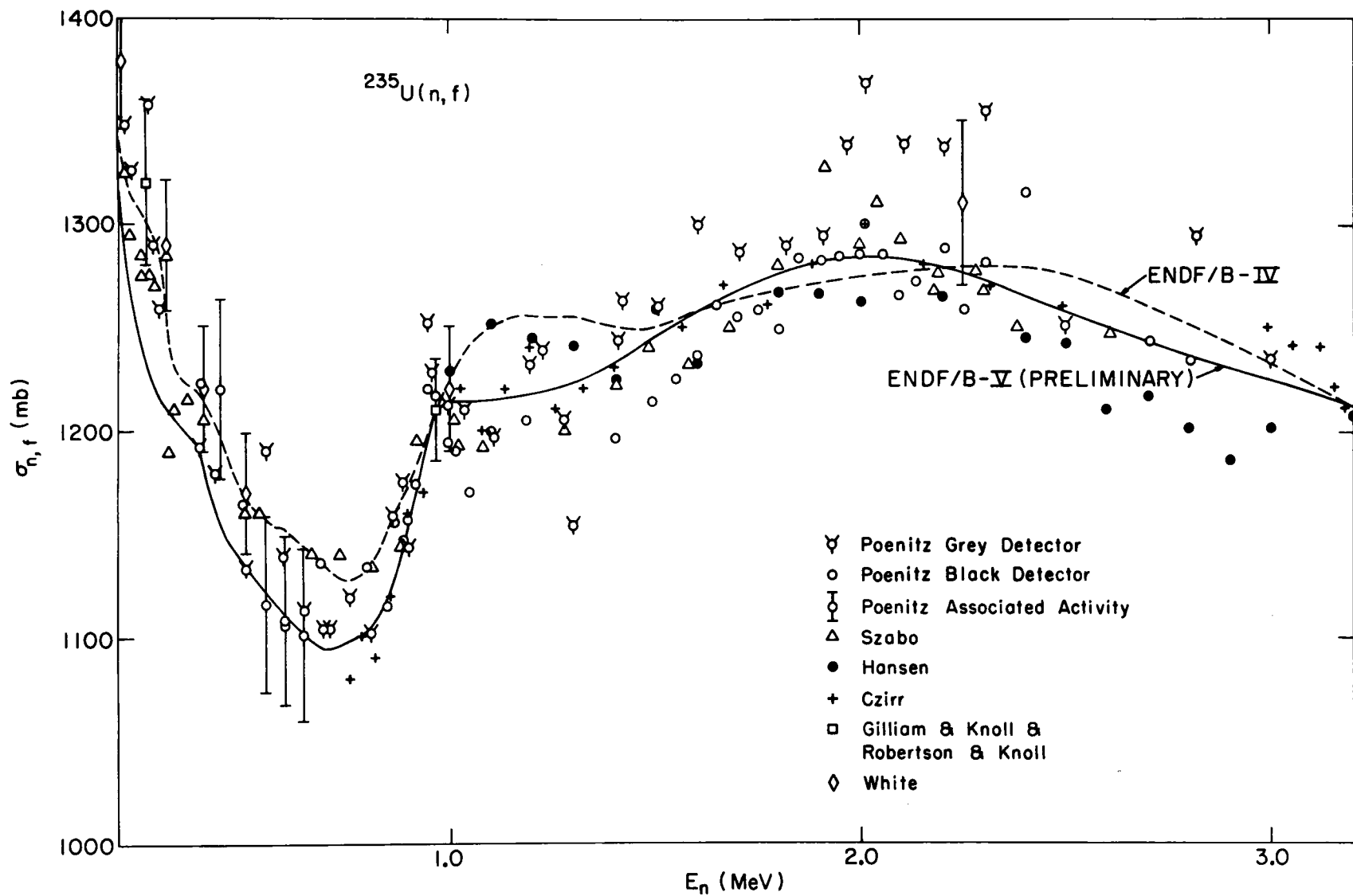


Fig. 9  $^{235}\text{U}(n, f)$  Data and Evaluation 0.2 - 3.2 MeV.

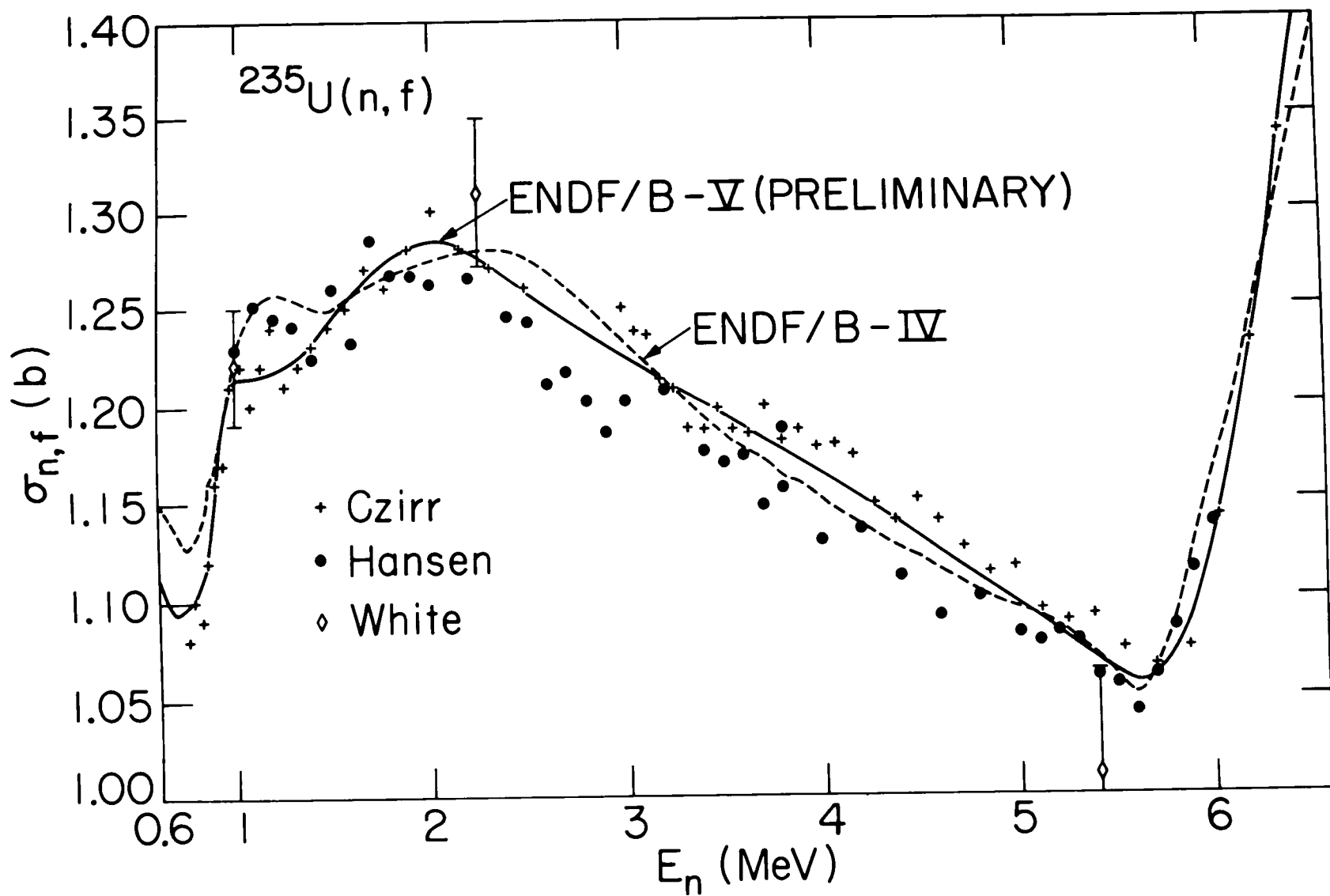


Fig. 10

$^{235}\text{U}(n, f)$  Data and Evaluation 0.6 - 6.6 MeV.

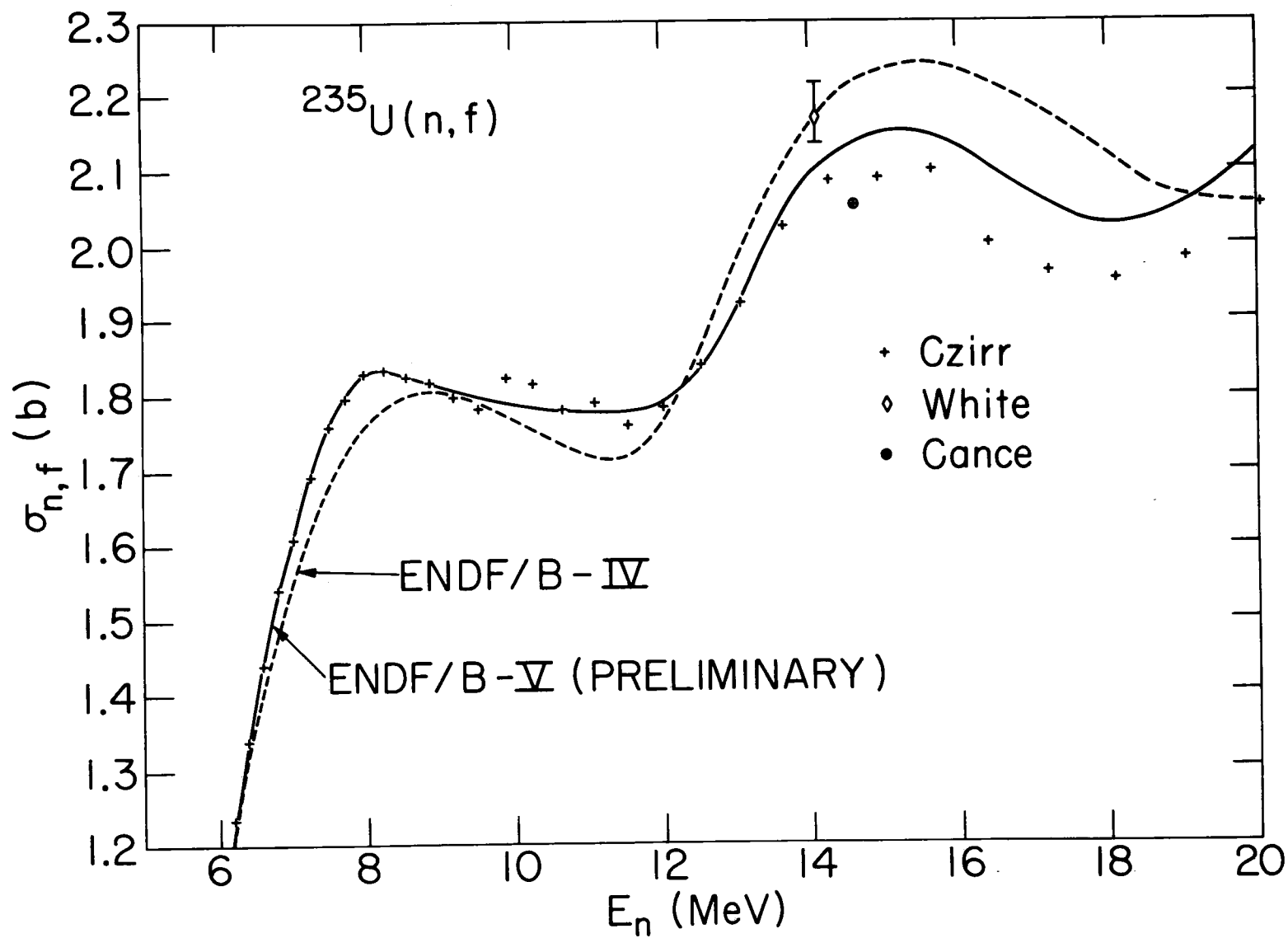


Fig. 11  $^{235}\text{U}(n,f)$  Data and Evaluation 5.0 - 20.0 MeV.

## DISCUSSIONS

A. Smith Are the input data for the evaluation all formally published, or are you using preliminary data?

M. Bhat We have been using preliminary data, for example, the Wasson data.

A. Smith How do you justify using preliminary data?

R. Peelle Let me answer. In this case the new data appeared not to increase the scatter of the data; they appeared to fall into the band of previous data. There was not the type of problem as in the past.

A. Smith Yes, there were a lot of problems from this procedure in the past. I think of some capture cross sections, for example.

L. Stewart I think, A. Wasson told us at the time or at least now, that this (data) was what it was going to finally be.

G. Wasson As far as I know now there won't be many changes.

W. Poenitz There is another point here. You had a "first-estimate" evaluation for ENDF-V distributed prior to the BNL meeting. At 250 keV your curve went through a point from the U. Michigan (Robertson) which was some 3% higher than what I had evaluated[1]. The evaluated ENDF-V now is some 4% lower than what I evaluated at this energy. The only data set which has been added since the "first approximation" is the preliminary NBS data. Which means that the U-235 evaluated cross section has been changed based on a preliminary data set by some 7%. Not only preliminary data are used, but they are used with much higher weight than others.

M. Bhat I guess your statement assumes that the first curve was suggested as the final thing, however, it was only a zero approximation. I agree that the cross section was brought down because of the NBS measurements.

W. Poenitz The other thing I wonder about is the spread of about 10% which you have among the low energy normalized data. If you look at the newer monoenergetic measurements (for example, those Szabo measured, or my data, or those from the U. Michigan) you find that the spread is usually

3%. Why then don't you use these data to normalize the shape data, instead of going over the low energy data which spread by 10%?

M. Bhat That is a good question. But I suppose there is some justification to go from thermal to get a consistent normalization.

R. Peelle As far as I had a part in this, I had the impression that the curve obtained from the low energy normalization and the higher energy data did not differ by more than the uncertainty of either one. This may have been fortuitous. You remember we used the shape by Gayther and normalized to the data above 200 keV, ignoring the white source measurements. Then we normalized Gayther to the data going down to thermal, and the change was two percent or so.

G. Knoll Let me comment on the Michigan data which by chance is in a range of some interest here, roughly from 100 to 1000 keV. Since the start in 1970 our purpose has been to provide normalization values and this was the sole purpose. The comment I want to make is that there seems to be tendency here to accept some of the points, for example, the 960 keV point, and to feel free to deviate from others. I think that is dangerous. They ought to be all accepted or bypassed on the one side or other. There are so many things common to these points that they are expected to be all correct, or all high or low.

M. Bhat But your sources are different.

G. Knoll They are different, but the calibration is the same, the samples are identical, etc.

H. Knitter I would like to show a figure from the work of Wagemans.\* What he finds is an extremely good agreement with other monoenergetic measurements.

C. Bowman I would like to hear more on what the Li-6 results were.

H. Knitter I have this report with me. I think there are discrepancies up to 3 to 4%, compared with B-10.

L. Stewart If I may remark, the data at Oak Ridge were taken with both, Li-6 and B-10, and they found no difference in this energy range.

R. Peelle I would not put emphasis on these ORNL findings.

L. Stewart In this energy range the deviation from  $1/v$  is essentially zero.

M. Bhat 3 or 8%.

H. Knitter One must be careful with the  $\text{Li-6}(n,\alpha)$  because it is not isotropic.

C. Bowman Was the Li-6 done with a foil or a glass?

H. Knitter With a foil and detected with a solid state detector.

[1] W. P. Poenitz, "Evaluation of U-235 (n,f) Data Available at and since the 1972 Vienna Panel", Memorandum to the participants of the CSEWG Normalization and Standards Subcommittee Working Session, Oct. 1975.

\* The figure which was shown is from the paper by C. Wagemans and A. J. Deruytter on "The Neutron Induced Fission Cross Section of U-235 in the Energy Region from 0.008 eV to 30 KeV", to be published in Ann. of Nucl. Energy (Fig. 6).

FISSION CROSS SECTIONS OF  $^{235}\text{U}$ ,  $^{238}\text{U}$ , AND  $^{239}\text{Pu}$   
 AVERAGED OVER THE  $^{252}\text{Cf}$  NEUTRON SPECTRUM

H. T. Heaton II, D. M. Gilliam, V. Spiegel,  
 C. Eisenhauer, and J. A. Grundl

National Bureau of Standards  
 Washington, D.C. 20234

ABSTRACT

A measurement was made in a  $^{252}\text{Cf}$  spontaneous fission neutron field to determine the absolute fission cross section of  $^{235}\text{U}$  ( $1205 \pm 27$  mb), and at the same time to determine the fission cross section ratio of  $^{238}\text{U}/^{235}\text{U}$  ( $0.2644 \pm 0.0035$ ) and  $^{239}\text{Pu}/^{235}\text{U}$  ( $1.500 \pm 0.024$ ). Two NBS double fission chambers were mounted 5 cm on either side of a singly encapsulated  $^{252}\text{Cf}$  source ( $4 \times 10^7$  n/sec,  $1.4 \text{ mm}^3$  emission volume) in compensated beam geometry. The Cf neutron source strength was calibrated in a Manganous Sulfate Bath relative to the NBS-I, the internationally compared Ra-Be photo-neutron source. Corrections were made for geometrical effects ( $1.0085 \pm 0.0064$ ), for undetected fission fragments (typically  $1.0222 \pm 0.0030$ ), for neutron elastic scattering (typically  $0.9587 \pm 0.0199$ ) and for inelastic scattering to subthreshold energy for  $^{238}\text{U}$  ( $0.986 \pm 0.007$ ). Integral results are compared with various differential data sets using an evaluated  $^{252}\text{Cf}$  fission spectrum.

INTRODUCTION

Useful information in nuclear data validation is provided by experiments with intense, small volume  $^{252}\text{Cf}$  spontaneous fission neutron sources used in point geometry configurations with light-weight fission chambers in "compensated beam geometry." Such integral measurements are simple to perform and the results depend primarily on the neutron source strength, fission deposit mass, and geometric measurements. Corrections due to neutron scattering, undetected fission fragments, and flux gradients are generally small.

This paper will review the measurement of the absolute  $^{235}\text{U}$  fission cross section and the  $^{238}\text{U}/^{235}\text{U}$  and  $^{239}\text{Pu}/^{235}\text{U}$  fission cross section ratios reported [1,2] at the Nuclear Cross Section and Technology Conference together with corrections made since that time.

In comparing the integral results with predictions of data differential in energy, the shape of the fission neutron spectrum is required. For elements such as  $^{235}\text{U}$  and  $^{239}\text{Pu}$ , which have a relatively flat cross section over fission neutron energies, a detailed knowledge of the fission spectrum is not necessary as a change in the average energy for a Maxwellian shape fission spectrum of 8% causes less than a 0.5% change in the spectrum averaged cross section. For threshold reaction such as the  $^{238}\text{U}$  fission cross section, a more detailed knowledge of the fission spectrum shape is required. The comparison of the integral results presented in this paper employs an evaluated  $^{252}\text{Cf}$  fission spectrum of Grundl and Eisenhauer [3,4]. The average cross section, obtained from the integral from 0.4 eV to 20 MeV of the fission spectrum times the differential cross section, includes errors due to uncertainties in the evaluated spectrum.

### INTEGRAL MEASUREMENTS

Figure 1 shows the physical arrangement used in making the integral fission cross section measurement. For primary measurements, two NBS double fission chambers are separated by about 10 cm by a rigid, lightweight support structure. The Cf source, whose details are shown in the bottom of the figure, is located midway between the chambers. In this compensated beam geometry, the sum of the fission rates recorded separately for each chamber depends on the square of the deposit separation, with second order corrections depending on the exact location of the source and on the mass difference of the deposits in each chamber.

The data for the absolute  $^{235}\text{U}$  fission cross section and the  $^{238}\text{U}/^{235}\text{U}$  and  $^{239}\text{Pu}/^{235}\text{U}$  ratio were taken simultaneously. The  $^{235}\text{U}$  deposit was always located in the "bottom" half of the double fission chamber. Mechanical measurements to the platinum foil backing were made with a depth micrometer fitted with an electrical contact to an average accuracy of  $\pm 56 \mu\text{m}$ . Measurements of the chamber separation were made using a theodolite (calibrated with a steel rule temporarily located under the chambers) to an accuracy of  $\pm 75 \mu\text{m}$  by observing a scribe mark on each chamber, and by measuring four points around the surface of the fission chamber head. To make the second order correction, the position of a dummy source was also recorded. The total error in the absolute measurement due to distance uncertainties is 0.6% at 10 cm deposit separation. For the ratio measurement, the absolute chamber separation is unimportant and only a gradient due to the finite thickness of the polished platinum backing (19.1 mm diameter and 0.13 mm thick) of the fissionable deposits (12.7 mm diameter oxides) is important. By rotating the chambers  $180^\circ$  about their stems and taking equal weighting of the data obtained in each orientation the gradient effect is automatically included, as are effects due to fission fragment momentum and effects of scattering in the platinum backing. A stringent test of the spatial measurement technique used in the absolute measurement can be made by comparing the mass ratios inferred from measurements in the thermal beam of the NBS reactor and from measurements with the Cf source. The former depends on a simple  $180^\circ$  rotation of the fission chamber while the latter depends on the source-to-deposit distance as well as the  $180^\circ$  chamber rotation. These two methods of determining the mass ratio agree within  $(0.15 \pm 0.4)\%$ .

The two largest uncertainties in the absolute  $^{235}\text{U}$  measurement are the determination of the Cf source strength (1.2%) and the determination of the fission deposit masses (1.3%). Both of these are currently being reviewed to determine what improvements can be made in their accuracy. Hence only a brief summary will be made.

The Cf source was calibrated in the NBS Manganous Sulfate Bath facility against the absolutely calibrated Ra-Be photoneutron source NBS-I as reported by Noyce [5]. The Cf source was calibrated several times during the experiment and had a nominal value of  $4 \times 10^9$  n/sec. The source strength for day to day runs was corrected for decay using a half-life of 2.638 years. The source consists of  $\text{Cf}_2\text{O}_2\text{SO}_4$  particles imbedded in a stainless steel and aluminum capsule in the form of a cylinder with the diameter equal to the height, 0.762 cm. An X-ray of the source showed the source emission volume to be about  $1.4 \text{ mm}^3$ . To further understand the errors involved in source strength measurements, the National Bureau of Standards (NBS) is currently involved in a source strength comparison program with Physikalisches Technische Bundesanstalt (PTB). This involves comparing neutron sources calibrated at each location by transfer methods using gold foils and the double fission chambers.

For each isotope, there is a "reference" deposit. Working deposits are normally compared relative to the reference using the double fission chamber at the thermal beam of the reactor. The determination of the reference mass has been previously described [6]. Unfortunately due to a reactor shutdown, the determination of the mass ratio of the working deposits to reference deposit using the fission chamber was not completed for the results reported at the Technology Conference, and these results depended on preliminary alpha counting data. The fission chamber comparison of the working deposit to the reference deposit have now been completed and the results are given in Table I. For  $^{235}\text{U}$  two sets of deposits were used: one of a nominal  $500 \mu\text{g}/\text{cm}^2$  which was used in conjunction with the  $^{238}\text{U}$  ratio data and the other of a nominal  $200 \mu\text{g}/\text{cm}^2$  used in conjunction with the  $^{239}\text{Pu}$  and  $^{238}\text{U}$  ratio data. The thermal beam determination of masses lead to a 0.54% change in the value of the  $500 \mu\text{g}$  deposits and virtually no change in the  $200 \mu\text{g}$  deposits. The corrections in the  $^{235}\text{U}$  and  $^{238}\text{U}$  results due to this mass redetermination are respectively 0.24% and 0.54%. The  $^{238}\text{U}$  deposits were natural uranium containing  $(0.720 \pm 0.005)\%$  of  $^{235}\text{U}$ . This allows a direct comparison of the  $^{235}\text{U}/^{238}\text{U}$  deposit mass ratios using the thermal neutron beam. The errors on the  $^{238}\text{U}$  masses given in Table I are the errors on this mass ratio obtained measuring the ratio of the  $^{235}\text{U}$  content of the  $^{238}\text{U}$  deposit relative to the  $^{235}\text{U}$  deposit used in the ratio measurement.

Table II summarizes the corrections and uncertainties for the absolute  $^{235}\text{U}$  measurement. Both corrections for the extrapolation to zero pulse height (ETZ) (to account for pulses below the lowest discriminator setting used in the normal triple scaler arrangement [6]) and absorption of the fissionable deposit depend linearly on mass of the deposit. For the two foil sets used in the  $^{235}\text{U}$  measurement, the ETZ correction was 0.9% and 1.7% and the absorption corrections were 1.3% and 3.2%. For the  $^{239}\text{Pu}$  and  $^{238}\text{U}$  data the ETZ corrections were 0.5% and 1.9% respectively. To reduce the room return background to 0.45%, the fission chambers and the Cf source were surrounded by a large cadmium cylinder (90 cm length by 69 cm diameter).

The background was measured by two methods. The first method makes use of the  $^{235}\text{U}$  data alone with deposit separations of 10 and 20 cm, and the second depends on the  $^{238}\text{U}/^{235}\text{U}$  ratio data at these two distances assuming no background in the  $^{238}\text{U}$  data. Since the results reported at the Technology Conference, [1] the source anisotropy has been measured directly, by observing fission rates as the source was rotated to selected positions about an axis at right angles to the capsule stem shown in Fig. 1, instead of relying only on calculations as was the case earlier. This caused the source capsule correction to be changed from our earlier value of  $0.9940 \pm 0.008$  to the current value of  $0.9922 \pm .003$ . The platinum-backing scattering correction was determined by observing the change in the  $^{235}\text{U}$  reaction rate for one, two, and three normal thicknesses of platinum. Corrections for scattering from the support material and the fission chambers are made only by calculations.

For the  $^{238}\text{U}/^{235}\text{U}$  and  $^{239}\text{Pu}/^{235}\text{U}$  data, the correction for fission in other isotopes was  $(0.65 \pm 0.3)\%$  for the  $^{240}\text{Pu}$  in the  $^{239}\text{Pu}$  deposit and  $(2.76 \pm 0.1)\%$  for the  $^{235}\text{U}$  in the  $^{238}\text{U}$  deposit. For  $^{238}\text{U}$ , the correction for neutrons inelastically scattered below the fission threshold was  $0.986 \pm 0.007$ .

### $^{252}\text{Cf}$ NEUTRON SPECTRUM

The Grundl and Eisenhauer [3,4] evaluation of the  $^{252}\text{Cf}$  and  $^{235}\text{U}$  neutron spectra began with fitting all of the available experimental data with a Maxwellian function to determine the best average energy parameter,  $E_{av} = 2.13$  for  $^{252}\text{Cf}$  and  $E_{av} = 1.97$  for  $^{235}\text{U}$ , over the energy interval 0.25 to 8 MeV. The total energy interval was divided into five energy intervals with approximately equal group fluxes plus two more to account for data below 0.25 MeV and above 8 MeV. For the Technology Conference [3] a weighted average deviation of the experimental data from the reference Maxwellian for each of the seven regions was calculated. For the Petten meeting [4] the deviations were refitted with four linear segments which are continuous across the energy boundaries. Since above 6 MeV the experimental data deviate fairly rapidly from a Maxwellian function, this region was fitted with an exponential segment which is continuous across the 6 MeV boundary. Table III lists the group fluxes for the  $^{252}\text{Cf}$  neutron spectrum for both the reference Maxwellian, with  $E_{av} = 2.13$ , and the segment-adjusted Maxwellian. It can be seen that the main difference occurs in the high energy region. The last column lists the percent uncertainty in the evaluated spectrum at the 67% and 95% confidence levels. Table IV lists the parameters used to adjust the reference Maxwellian.

### INTEGRAL-DIFFERENTIAL COMPARISON

Figures 2-4 show the type of comparison possible between the integral and differential data using the segment-adjusted Maxwellian. The lower portion contains two curves representing two cumulative responses from 0.4 eV to the neutron energy,  $E$ . The curve labeled F is the cumulative spectrum of the segment-adjusted Maxwellian. The curve labeled R is the cumulative response of the segment-adjusted Maxwellian times the differential cross section. The average cross section,  $\langle \sigma \rangle$ , is defined by the expression:

$$\langle \sigma \rangle = \int_{0.4 \text{ eV}}^{20 \text{ MeV}} \sigma(E) \phi(E) dE$$

The actual values used to generate these curves and the average cross section value were calculated with the computer code DETAN [7] using the SAND-II 620 group energy structure. The upper portion of Figs. 2-4 is the differential fission cross section for  $^{235}\text{U}$ ,  $^{238}\text{U}$  and  $^{239}\text{Pu}$  respectively taken from ENDF/B-IV. The dashed line is the average cross section value as calculated by Eq. (1). For the flux, arrows locate the median energy, and the energies of the 5th and 95th percentiles. Corresponding energies for each response are also indicated.

For both the  $^{235}\text{U}$  and  $^{239}\text{Pu}$  cross section the curves F and R have nearly the same value, implying that the differential cross section does not differ from its average by a large amount over an energy range where most of the neutrons from the Cf source occur. For  $^{235}\text{U}$ , Fig. 2, for energies from 0.26 to 5.5 MeV, corresponding to 90% of the Cf neutrons, the maximum deviation from the average value is 15%. For  $^{239}\text{Pu}$ , Fig. 3, for energies from 10 keV to 5.7 MeV, which covers 95% of the Cf neutrons, the difference from the average value is 17%. In fact, for energies which cover essentially the entire response of neutrons from Cf, 10 keV to 10 MeV, the deviation is 31%. For  $^{238}\text{U}$ , Fig. 4, with its threshold, the behavior is quite different.

Table V summarizes the energy at which the cumulative response is 0.05, 0.5, and 0.95. Since the energies are nearly the same for  $^{235}\text{U}$ ,  $^{239}\text{Pu}$  and the segment-adjusted Maxwellian, the integral data can be used over a broad range to normalize shape differential data instead of at a single point as is often done.

Specific comparisons of our integral results with various differential data are given in Tables VI and VII. Table VI compares the integral results with the evaluated ENDF/B-IV and for the  $^{235}\text{U}$  case, the average of Poenitz [8] of data since the Vienna meeting which omits the revised data of Adamov, Cauce, etc. The errors listed for the differential results are those due to the uncertainties in the evaluated Cf spectrum and are computed by Eq. (2).

$$e^2_{\frac{\sigma}{\phi}} = \frac{1}{\left[\sum_i \chi_i^2\right]^2} \sum_i \chi_i^2 \left(\sigma_i - \sigma\right)^2 \frac{e^2_{\phi_i}}{\phi_i^2} \quad (2)$$

where the group flux,  $\chi_i = \phi_i \Delta E_i$ , and its percent error are given in Table III.

Table VI compares the integral results with various differential ratio measurements, namely those of Behrens, et al. [9,10] and Coates [11]. To make the comparison, it is necessary to first convert the ratio data into an inferred cross section which is then averaged using the Cf spectrum as a

weighting function. The inferred cross section and their percentage differences from the inferred values listed in Table VII were obtained from Behrens [B], and Coates [C], ratios using the  $^{235}\text{U}$  cross section from ENDF/B-IV and Poenitz. It can be seen that the  $^{238}\text{U}$  results of Behrens agree better with the integral results than do the results of Coates. In fact for both  $^{238}\text{U}$  and  $^{239}\text{Pu}$  the data of Behrens et al. agree better with the integral results than the data from the ENDF/B-IV files.

A comparison of the ENDF/B-IV results given in Table VII shows a greater difference in the cross section ratios than in the individual cross sections and the differences are outside the experimental error in the integral results. Fabry's [12] cross section ratio measurements, which average over a  $^{235}\text{U}$  fission spectrum, also show this difference. The  $^{235}\text{U}$  fission spectrum is generated at the center of a one meter diameter spherical cavity within a graphite thermal column. Simple and variable geometrical arrangements were used and evaluated for neutron field purity. The fission rates were measured in three fission chambers of different size and design and the fissionable deposits were fabricated and calibrated in different locations. Table VIII gives the  $^{235}\text{U}/^{238}\text{U}$  ratio averaged over a  $^{235}\text{U}$  fission spectrum from Fabry who used fission chambers and deposits from: NBS; GfK, Karlsruhe; and Saclay. The difference between Fabry's integral results and the ENDF/B-IV data weighted by the evaluated  $^{235}\text{U}$  fission spectrum is 6.5% for  $^{235}\text{U}/^{238}\text{U}$  and 4.7% for  $^{239}\text{Pu}/^{235}\text{U}$ .

Table IX compares the  $^{235}\text{U}$  and  $^{239}\text{Pu}$  cross sections taken from ENDF/B-IV weighted by the reference Maxwellian fission spectra for  $^{252}\text{Cf}$  ( $E_{\text{av}} = 2.13$ ) and  $^{235}\text{U}$  ( $E_{\text{av}} = 1.97$ ). From the table it can be seen that the difference in the average cross section for the two fission spectra is less than 0.1% for the  $^{235}\text{U}$  cross section and 0.4% for the  $^{239}\text{Pu}$  cross section and that the  $^{239}\text{Pu}/^{235}\text{U}$  ratio should be 0.4% higher for the  $^{252}\text{Cf}$  spectrum. Experimentally the  $^{239}\text{Pu}/^{235}\text{U}$  ratio is  $1.500 \pm .024$  for the  $^{252}\text{Cf}$  spectrum and  $1.504 \pm .030$  for the  $^{235}\text{U}$  spectrum. The average of all the differential data for this ratio is 1.45 which is about 3.3% lower than the integral results.

Since the average cross section for  $^{235}\text{U}$  is insensitive to the difference between the  $^{252}\text{Cf}$  and  $^{235}\text{U}$  fission spectra, our value of the  $^{235}\text{U}$  cross section can be used to obtain cross section from Fabry's ratios. This procedure gives  $306 \pm 9$  mb for the  $^{238}\text{U}$  results. This can be compared with the value of  $313 \pm 3.4$  mb deduced from the Leachman and Schmitt [13] value of  $(0.756 \pm 0.008)/v$  and using a value of 2.419 for the total number of neutrons per  $^{235}\text{U}$  fission.

In an attempt to obtain more information than is available from a single value for the integral results, one often performs a multigroup analysis. Such an analysis must be done with care, including a careful error analysis, and all data must be examined to insure that contradictory conclusions are not reached. A multigroup analysis which tries to infer something about the  $^{235}\text{U}$  cross section below the threshold of the  $^{238}\text{U}(n,f)$  reaction,  $E_T$ , and the type of problems which occur is given below. From Table VII it can be seen that there is good agreement between the  $^{238}\text{U}$  cross section inferred from Behrens ratio data and the integral value. Hence make the following four assumptions and see what conclusions can be reached: (1) the integral

$^{238}\text{U}/^{235}\text{U}$  ratio correct, (2) Behrens  $^{238}\text{U}/^{235}\text{U}$  ratio measurement is correct, (3) the integral value of the  $^{235}\text{U}$  average cross section is correct, and (4) the evaluated Cf fission spectrum is correct. To obtain the inferred  $^{238}\text{U}$  cross section, a differential  $^{235}\text{U}$  cross section is needed to convert the ratio into a  $^{238}\text{U}$  cross section which can then be compared with the integral value according to Eq. 3.

$$\langle \sigma \rangle_I = \int_{E_T}^{20} R(E) \sigma(E) \phi(E) dE \quad (3)$$

where  $I$  denotes the integral measurement,  $R(E)$  the differential  $^{238}\text{U}/^{235}\text{U}$  measurement,  $\sigma(E)$  the differential  $^{235}\text{U}$  cross section,  $\phi(E)$  the Cf spectrum. From Table VII it can be seen that both the  $^{235}\text{U}$  from ENDF/B-IV and the average of Poenitz give the same value of the inferred  $^{238}\text{U}$  cross section which then agrees with the integral result. This implies that the  $^{235}\text{U}$  cross section above  $E_T$  is correct. This portion of the  $^{235}\text{U}$  cross section is denoted by  $\langle \sigma_{25} \rangle_+$  in Eq. 4. To infer information about the  $^{235}\text{U}$  cross section below  $E_T$ , one can do a two group analysis. The integral  $^{235}\text{U}$  cross section can be split into two regions above, (+), and below, (-), the  $^{238}\text{U}$  threshold. Assume that to bring the integral results into agreement with the calculated differential values, the  $^{235}\text{U}$  cross section can be renormalized. Eq. (1) can be rewritten as:

$$\langle \sigma_{25} \rangle_I = \chi_- \langle \sigma_{25} \rangle_- + \chi_+ \langle \sigma_{25} \rangle_+ \quad (4)$$

with

$$\chi_- \langle \sigma_{25} \rangle_- = \int_{E_T}^{E_T} \sigma(E) \phi(E) dE \quad (5)$$

Eq. (4) can be solved for  $\langle \sigma_{25} \rangle_-$  which, using the ENDF/B-IV  $^{235}\text{U}$  cross section and the other experimental results implies that this cross section should be lowered by 5.9% from  $E_T$  down to where the response from the Cf neutron is unimportant (about 6 keV). Carrying out the associated error analysis on Eq. (4), the uncertainty on  $\langle \sigma_{25} \rangle_-$  is  $\pm 4.1\%$ . Hence one can make either of the following statements about the ENDF/B-IV  $^{235}\text{U}$  cross section: from the two group analysis it should be lowered by  $(5.9 \pm 4.1)\%$  between 6 keV and  $E_T$ ; and from the one group analysis (Table VI) it should be lowered by  $(3.0 \pm 2.2)\%$  between 6 keV and 6 MeV. There is, however, more data which should be considered before any conclusions are reached. There is also good agreement between the  $^{239}\text{Pu}$  cross section inferred from the Behrens et al ratio measurement and the  $^{235}\text{U}$  cross section from the ENDF/B-IV with the integral value. In assumptions 1-4 replace  $^{238}\text{U}$  with  $^{239}\text{Pu}$ . Since Pu is not a threshold reaction, some further assumption is necessary if a two group analysis is to be done. To check the consistency of the previous result, assume that the  $^{235}\text{U}$  cross section is correct above  $E_T$ . Carrying out similar analysis for Pu with these assumptions leads to the result that the ENDF/B-IV  $^{235}\text{U}$  cross section should be increased by  $(0.5 \pm 4.3)\%$  below the  $^{238}\text{U}$  threshold. This result is in contradiction to the conclusions

reached by examining only the  $^{238}\text{U}$  case. The results of this type of analysis shows that there is no one cross section or region of cross section which can bring all of the differential and integral results into agreement to better than a few percent.

### CONCLUSIONS

Absolute  $^{235}\text{U}$  fission cross section measurements were made simultaneously with  $^{238}\text{U}/^{235}\text{U}$  and  $^{239}\text{Pu}/^{235}\text{U}$  ratio measurements for  $^{252}\text{Cf}$  neutrons using two NBS double fission chambers. The respective values are  $1205 \pm 27$  mb,  $0.2644 \pm 0.003$  and  $1.500 \pm 0.024$ . The results were compared with various differential data sets weighted by a segment adjusted reference Maxwellian Cf neutron spectrum. The uncertainties in the folded cross sections due to uncertainties in the fission spectrum were less than 0.2% for  $^{235}\text{U}$  and  $^{239}\text{Pu}$  and 0.9% for  $^{238}\text{U}$ . The following conclusions can be reached:

1. Integral data can be used to determine preference within various differential data.
2. Independent of the integral values, weighting the differential data by the Cf spectrum can be used to normalize differential data over a broad energy instead of at a single point (i.e., 14 MeV) or a narrow energy region (2 - 3 MeV) as is often done.
3. There is no one cross section or cross section region which will bring all of the data into agreement to better than a few percent.
4. The best overall agreement of the integral results favor a lower  $^{235}\text{U}$  cross section, such as the average of Poenitz [8] or the proposed ENDF/B-V and the cross sections inferred using this cross section and Behrens et al. ratio data.

### REFERENCES

1. H. T. HEATON II, J. A. GRUNDL, V. SPIEGEL, JR., D. M. GILLIAM and C. EISENHAUER, "Absolute  $^{235}\text{U}$  Fission Cross Section for  $^{252}\text{Cf}$  Spontaneous Fission Neutrons," in Nuclear Cross Sections and Technology, NBS Special Publication 425, Washington, D.C. (1975), p. 266.
2. D. M. GILLIAM, C. EISENHAUER, H. T. HEATON II, and J. A. GRUNDL, "Fission Cross Section Ratios in the  $^{252}\text{Cf}$  Neutron Spectrum ( $^{235}\text{U}$ :  $^{238}\text{U}$ :  $^{239}\text{Pu}$ :  $^{237}\text{Np}$ )," in Nuclear Cross Sections and Technology, NBS Special Publication 425, Washington, D.C. (1975), p. 270.
3. J. A. GRUNDL and C. M. EISENHAUER, "Fission Spectrum Neutrons for Cross Section Validation and Neutron Flux Transfer," in Nuclear Cross Sections and Technology, NBS Special Publication 425, Washington, D.C. (1975), p. 250.

4. J. A. GRUNDL and C. EISENHAUER, "Fission Rate Measurements for Materials Neutron Dosimetry in Reactor Environments," in Proc. of ASTM-EURATOM Symposium on Reactor Dosimetry, Petten (1975) in Press.
5. R. H. NOYCE, E. R. MOSBURG, JR., J. B. GARFINKEL, and R. S. CASWELL, "Absolute Calibration of the National Bureau of Standards Photoneutron Source III Absorption in Heavy Water Solution of Manganous Sulfate," Reactor Sci. Technol. (J. Nucl. Energy, Part A1B), 17, 313 (1963).
6. J. A. GRUNDL, D. M. GILLIAM, N. D. DUDEY and R. J. POPEK, "Measurements of Absolute Fission Rates," Nuclear Technology, 25, 237 (1975).
7. DETAN computer code available on request.
8. W. P. POENITZ, straight average of  $^{235}\text{U}$  data since the Vienna Meeting but does not include revised data of Caucé, Adamov, etc. Private communication (1975).
9. J. W. BEHRENS, G. W. CARLSON, and R. W. BAUER, "Neutron-Induced Fission Cross Sections of  $^{233}\text{U}$ ,  $^{234}\text{U}$ ,  $^{236}\text{U}$ , and  $^{238}\text{U}$  with respect to  $^{235}\text{U}$ ," in Nuclear Cross Sections and Technology, NBS Special Publication 425, Washington, D.C. (1975), p. 591.
10. J. W. BEHRENS, and G. W. CARLSON, "Measurements of Neutron Induced Fission Cross Section Involving Isotopes of Uranium and Plutonium. This conference.
11. M. S. COATES, D. B. GAYTHER, and N. J. PATTENDEN, "A Measurement of the  $^{238}\text{U}/^{235}\text{U}$  Fission Cross-Section Ratio," in Nuclear Cross Sections and Technology, NBS Special Publication 425, Washington, D.C. (1975), p. 568.
12. A. FABRY, J. A. GRUNDL, and C. EISENHAUER, "Fundamental Integral Cross Section Ratio Measurements in the Thermal-Neutron-Induced Uranium-235 Fission Neutron Spectrum in Nuclear Cross Sections and Technology, NBS Special Publication 425, Washington, D.C. (1975), p. 254.
13. R. B. LEACHMAN and H. W. SCHMITT, "The Cross Section for  $^{238}\text{U}$  Fission by Fission Neutrons," J. Nuclear Energy, 4 (1957), p. 38.

TABLE I

## Deposit Masses

Element	Mass ( $\mu\text{g}$ )
$^{235}\text{U}$	$248.3 \pm 3.0$
	$234.7 \pm 2.9$
	$620.7 \pm 8.7$
	$556.3 \pm 7.8$
$^{238}\text{U}^a$	$694.8 \pm 9.3$
	$546.8 \pm 7.3$
$^{239}\text{Pu}$	$104.0 \pm 1.4$
	$104.7 \pm 1.4$

<sup>a</sup>Error on the mass is the error in measuring the ratio of the  $^{235}\text{U}$  content in the  $^{238}\text{U}$  deposit relative to the  $^{235}\text{U}$  deposit used in the ratio measurement.

TABLE II

Error Components of  $^{235}\text{U}$  Fission Cross Section

	Correction	Percent Error <sup>(a)</sup>
Mass of Fission Deposit		1.3
Cf Source Strength		1.2
Fission in other isotopes	0.9987	0.1
<u>Geometrical</u>		
Deposit Separation		0.6
Finite Deposit Diameter	1.0075	0.1
Source not at midpoint	1.001	0.2
<u>Undetected Fission Fragments <sup>(b)</sup></u>		
Extrapolation to zero pulse height	1.0090	0.5
Absorption in deposit	1.0132	0.3
<u>Neutron Scattering</u>		
Total room return	0.9955	0.2
Source capsule	0.9922	0.3
Fission chamber	0.9888	0.4
Support structures	0.9945	0.5
Platinum deposit backing	0.9870	0.8
Total Error		2.25

(a) Percent error in  $^{235}\text{U}(n,f)$  due to uncertainty in listed component

(b) For light deposit

TABLE III

## Evaluated Cf Fission Spectrum

Energy Boundary	Reference <sup>(a)</sup> Maxwellian	Evaluated <sup>(b)</sup> Spectrum	Uncertainties (%)	
			$\pm 1\sigma$	$\pm 2\sigma$
0.0-0.25	0.050	0.047	13	26
0.25-0.8	0.179	0.184	1.1	3.3
0.8-1.5	0.222	0.220	1.8	3.6
1.5-2.3	0.193	0.194	1.0	3.1
2.3-3.7	0.199	0.200	2.0	3.0
3.7-8	0.147	0.146	2.1	4.8
8-12	0.0097	0.0087	8.5	17
12-20	(0.0007)	(0.00058)		

(a) The group-flux,  $\chi(E)$ , is proportional to  $\sqrt{E} \exp(-1.5E/E_{av}) \Delta E$

(b) Group-fluxes for the segment-adjusted Maxwellian

TABLE IV

## Segment Parameters For Adjusting the Reference Maxwellian

Energy Region	$F(E)^{(a)}$
0.0 - 0.25	$0.763 + 1.20E$
0.25 - 0.8	$1.098 - 0.14E$
0.8 - 1.5	$0.9668 + 0.024E$
1.5 - 6.0	$1.0037 - 0.0006E$
6.0 - 20	$1.0 \exp(-0.03(E-6))$

(a) The segment-adjusted Maxwellian is obtained from  $\chi(E)F(E)$ , with  $E$  in MeV

TABLE V

## Energy of Cumulative Response

Element	E at Response of		
	0.05	0.5	0.95
Seg. Adjusted Maxwellian	0.26	1.7	5.5
$^{235}\text{U}$	0.22	1.7	5.8
$^{238}\text{U}$	1.5	2.8	7.2
$^{239}\text{Pu}$	0.29	1.8	5.7

TABLE VI

Comparsion of Integral Results With Differential Results

Cross Section	Intergal	ENDF/B-IV		Poenitz <sup>235</sup> U Average <sup>(a)</sup>	
		Value	% Difference	Value	% Difference
<sup>235</sup> U	1.205 ± 0.027	1.241 ± 0.002	-3.0	1.228 ± 0.002	-1.9
<sup>238</sup> U	0.3186 ± 0.0080	0.3154 ± 0.003	1.0		
<sup>239</sup> Pu	1.808 ± 0.045	1.789 ± 0.002	1.0		
<sup>238</sup> U/ <sup>235</sup> U	0.2644 ± 0.003	0.2541 ± 0.002	3.9		
<sup>239</sup> Pu/ <sup>235</sup> U	1.500 ± 0.024	1.442 ± 0.002	3.9		

<sup>(a)</sup> See reference [8]

TABLE VII

Comparsion of Integral Results with Differential Ratio Results

Inferred Cross Section <sup>(a)</sup>	ENDF/B-IV		Poenitz <sup>235</sup> U average	
	Value	% Difference	Value	% Difference
<sup>238</sup> U <sup>B</sup>	0.3206	-0.6	0.3206	-0.6
<sup>238</sup> U <sup>C</sup>	0.3032	4.8	0.3034	4.8
<sup>239</sup> Pu <sup>B</sup>	1.809	-0.1	1.791	0.9

<sup>(a)</sup> B=Beherns et al.[9,10], C=Coates[11]

TABLE VIII

Integral Cross Section Ratios for Three  
Types of Fission Chambers (a)

Fission Chamber	$\bar{\sigma}_f(^{235}\text{U}, \chi_{235}) / \bar{\sigma}_f(^{238}\text{U}, \chi_{235})$
NBS	$3.94 \pm 0.08$
GfK	$3.93 \pm 0.09$
Saclay	$3.88 \pm 0.10$

(a) From reference [12]

TABLE IX

Comparison of ENDF/B-IV data Averaged With  
 $^{252}\text{Cf}$  and  $^{235}\text{U}$  Fission Spectra

Cross Section	Fission Spectrum	
	$^{252}\text{Cf}$	$^{235}\text{U}$
$^{235}\text{U}$	1244	1243
$^{239}\text{Pu}$	1790	1782

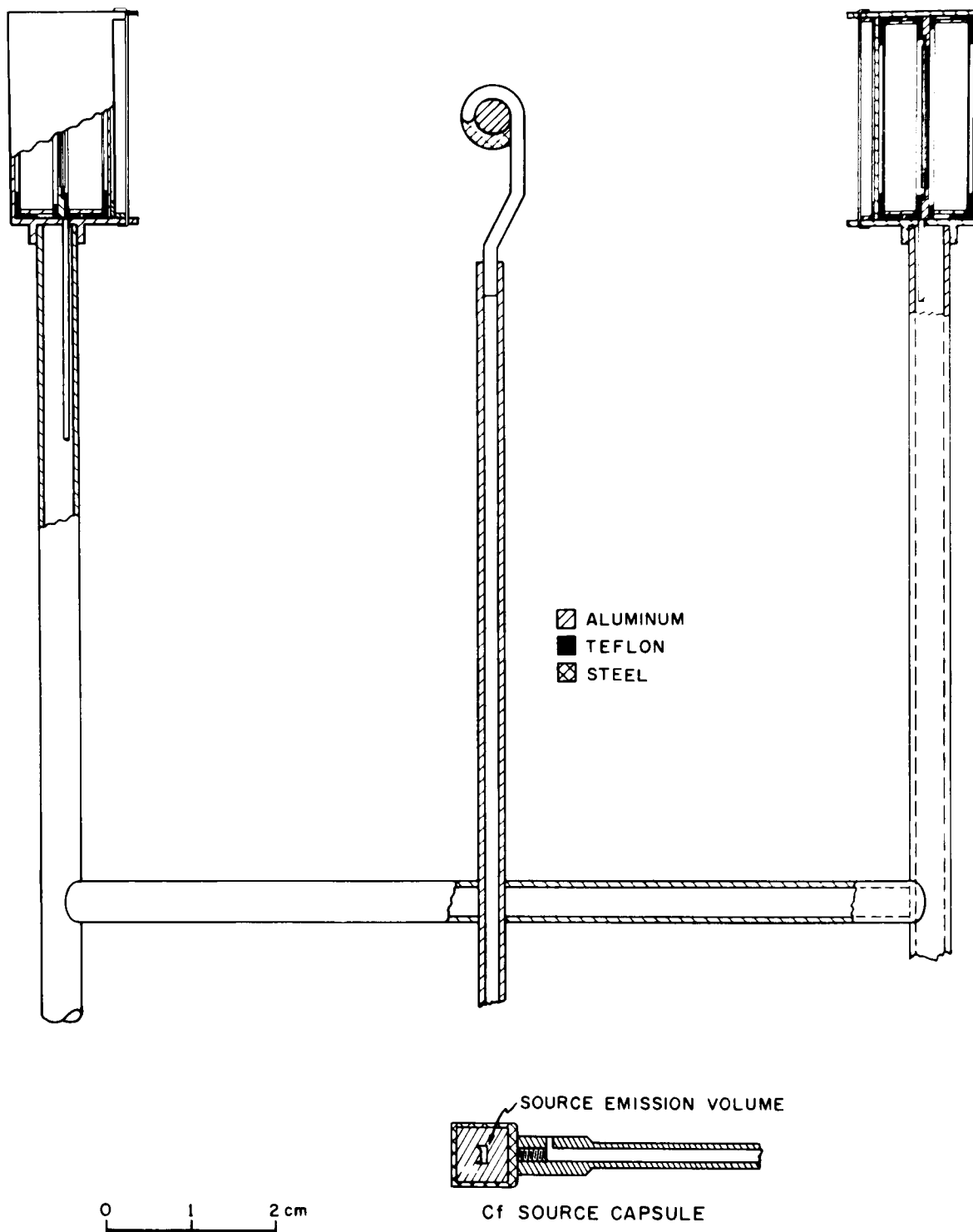


Figure 1. Physical arrangement for measuring Cf spectrum averaged fission cross sections. A Cf source capsule is located midway between a pair of NBS double fission chambers. Each chamber contains a pair of fissionable deposits. A schematic side view of the Cf source capsule with the emission column is shown at the bottom.

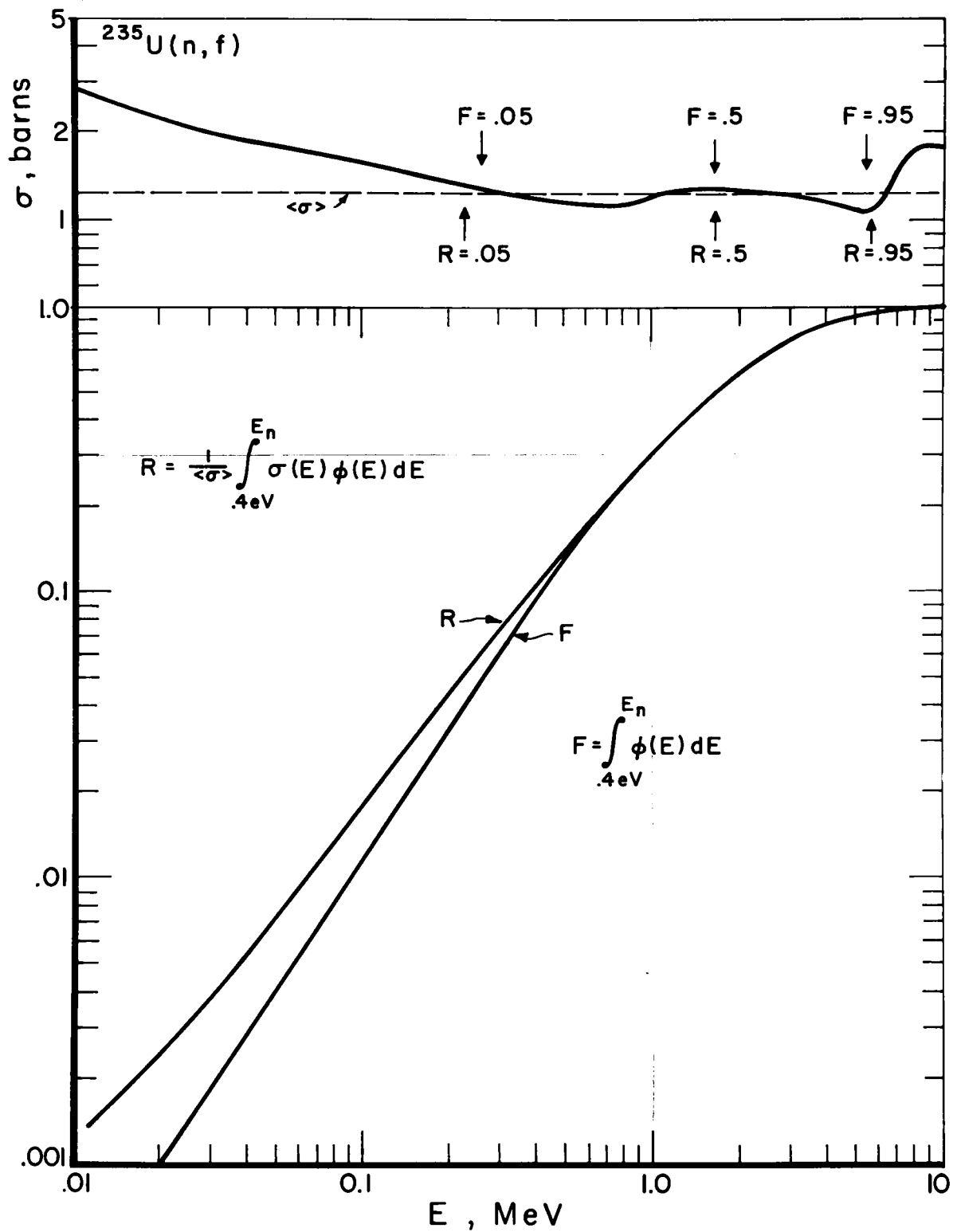


Figure 2. Comparison of  $^{235}\text{U}(n, f)$  differential cross section data with its computed average value using an evaluated segment adjusted Maxwellian fission spectrum.

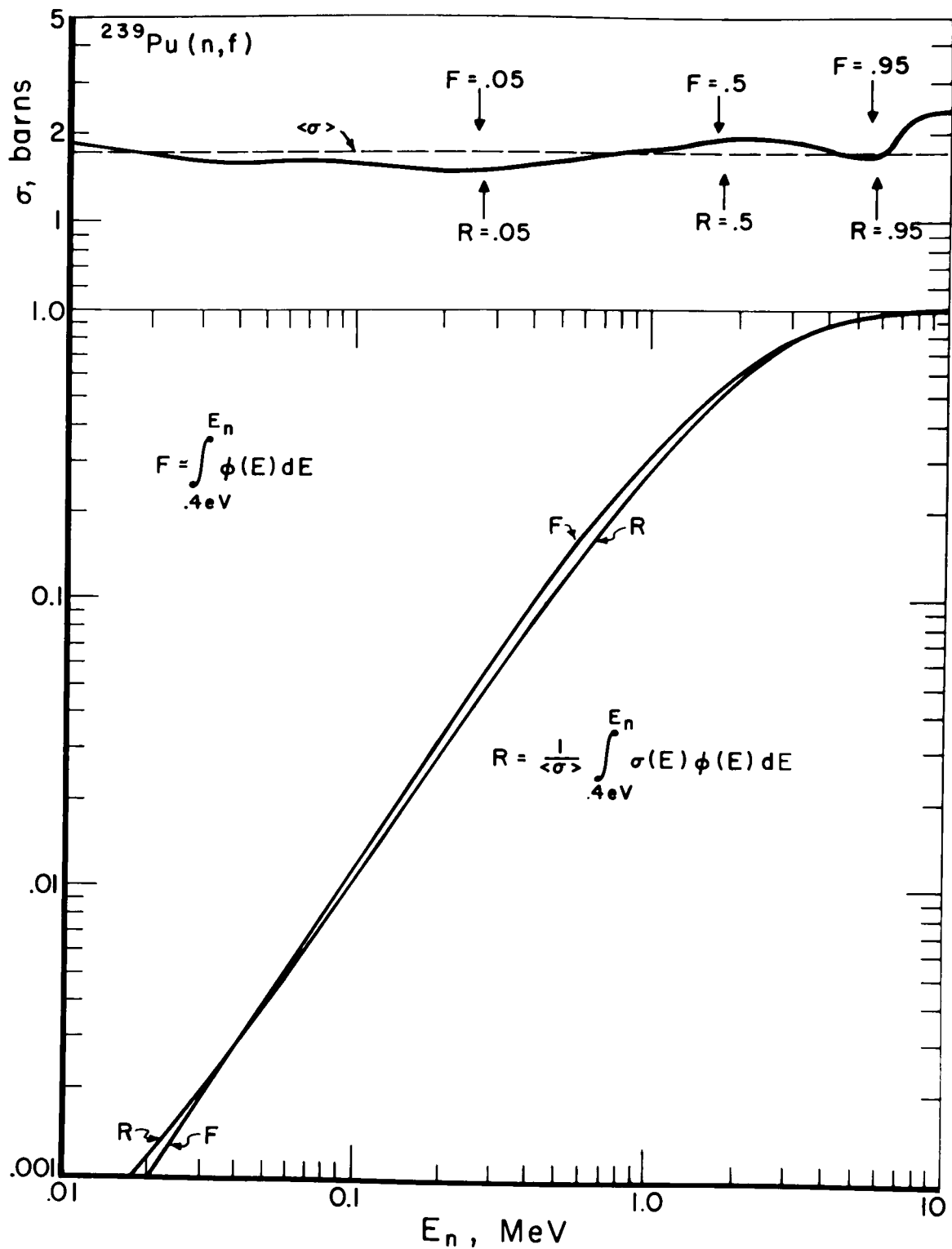


Figure 3. Comparison of  $^{239}\text{Pu}(n,f)$  differential cross section data with its computed average value using an evaluated segment adjusted Maxwellian fission spectrum.

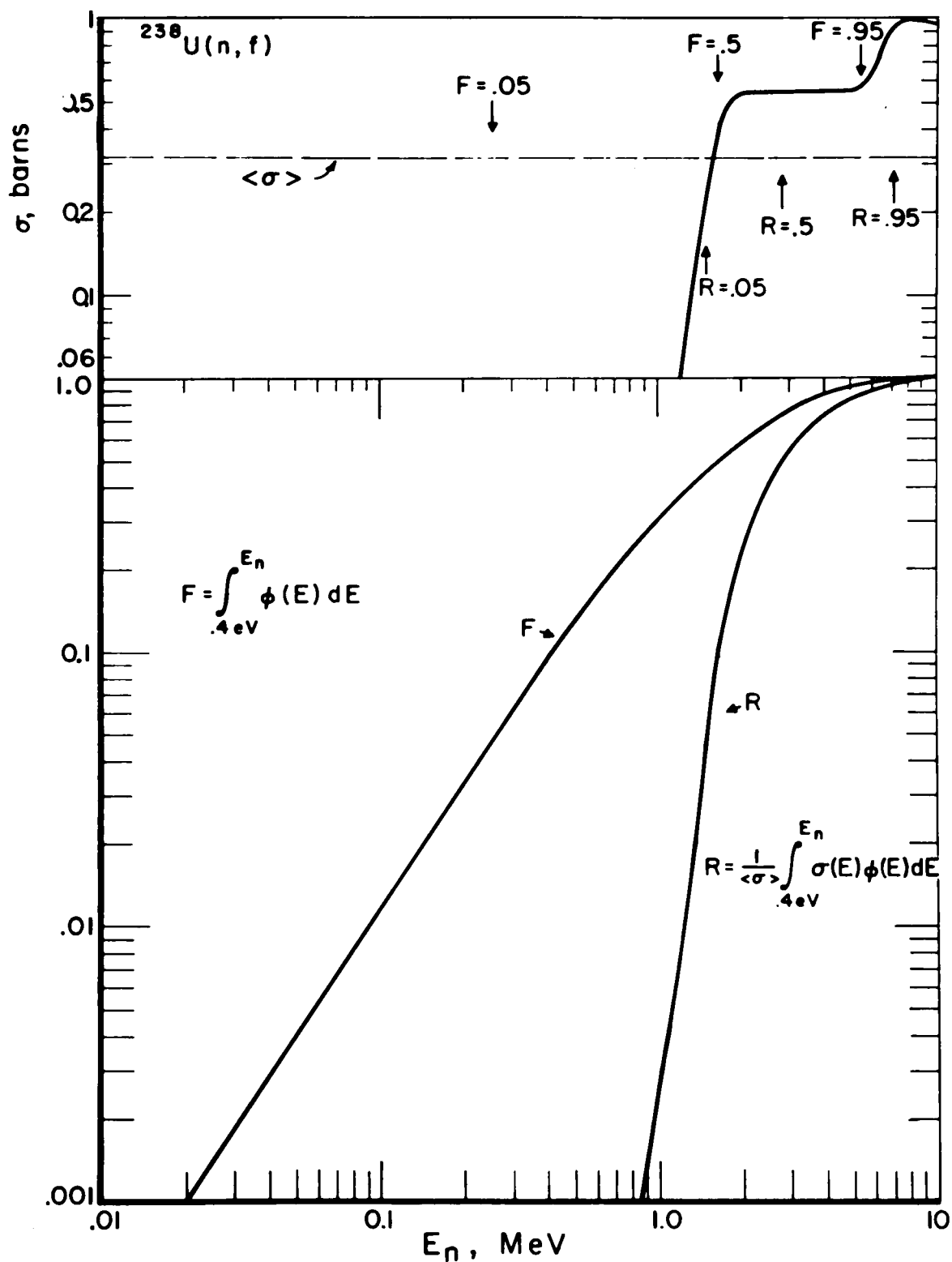


Figure 4. Comparison of  $^{238}\text{U}(n, f)$  differential cross section data with its computed average value using an evaluated segment adjusted Maxwellian fission spectrum.

*DISCUSSIONS*

A. Smith Did you check your numbers against what M. Bhat got for his proposed U-235?

H. Heaton Yes, we had to assume something below 200 keV, but the number we get is 1.288 which essentially agree with our results. That is why we were happy with the Bhat and the Poenitz curves because it gave a lower number than ENDF-IV.

G. Knoll I would like to comment that we have done essentially the same measurement. It is dangerous to quote preliminary numbers, but our value is within 1% of the NBS result.

UNRESOLVED RESONANCE PARAMETERS OBTAINED FROM  
POLARIZATION MEASUREMENTS ON  $^{235}\text{U}$

G. A. Keyworth, M. S. Moore and J. D. Moses

University of California, Los Alamos Scientific Laboratory\*  
Los Alamos, New Mexico 87545, U.S.A.

ABSTRACT

Recent measurements using polarized neutrons and a polarized  $^{235}\text{U}$  target are analyzed with the objective of providing guidance to evaluation efforts for ENDF/B-V. This study is particularly addressed to the unresolved resonance region and above, where fluctuations are observed in the partial cross sections. We find strong evidence to support the hypothesis that these fluctuations are associated with local enhancements due to the double-humped fission barrier. We discuss the applicability of these data in improving estimates for various average parameters (level density, fission width, radiative capture width, s- and p-wave strength functions) and arrive at a recommended procedure for evaluating the observed structure.

INTRODUCTION

The existence of pronounced structure in the neutron-induced fission and total cross sections of  $^{235}\text{U}$  below  $\sim 100$  keV is well established, and several analyses have been performed [1-4] which indicate that the structure in the fission cross section cannot be explained by the usual statistical model treatment of unresolved resonances. It has been suggested [1,3,4] that the fluctuations can be attributed to modulations or local enhancements due to states in the second well of the double-humped fission barrier. If this suggestion is correct, it would imply that the present treatment of unresolved resonance cross sections using evaluated data from ENDF/B is inadequate, and could lead to substantive differences in the calculation of self-shielding factors, reactivity coefficients, and the general treatment of cross sections for reactor design.

The only mechanism which is known to lead to intermediate structure in fission is enhancement of the fission widths by states of the second well of a double-humped fission barrier (Class II states). Cao [1] has pointed

---

\*Work performed under the auspices of the United States Energy Research and Development Administration.

out that the observed frequency of the fluctuations in ( $^{235}\text{U} + n$ ) is consistent with the systematics of sub-threshold fission for non-fissile targets and of second well parameters deduced from fission isomers. This mechanism requires that the fluctuations be produced by Class II states of definite spin. This has been experimentally verified by Keyworth et al.[5] for ( $^{237}\text{Np} + n$ ). Thus we expect that if the structure in ( $^{235}\text{U} + n$ ) arises from such a mechanism, the statistical tests which indicate non-statistical behavior in the fission cross section should show this spin dependence.

The technique of using polarized neutrons on a polarized target of  $^{235}\text{U}$ , as the definitive method of determining the spins of resonances in the compound nucleus  $^{236}\text{U}$  has been discussed by Keyworth et al.[6,7], who reported spin assignments to 60 eV. In 1974, a second series of runs was made by Keyworth et al. on the Oak Ridge Electron Linear Accelerator with increased polarization. A preliminary report of the results obtained was given at the 1974 Nuclear Cross Sections and Technology Conference [8]. These data extend from 1 eV to 50 keV, and contain high enough statistical accuracy to permit a more nearly complete analysis to be carried out over the entire resonance region, both resolved and unresolved. It should be pointed out that the polarized-neutron-polarized-target technique gives definitive results only for s-wave neutron resonances, which implies that the range of applicability roughly corresponds to the current ENDF/B definition of the resonance region for  $^{235}\text{U}$ : 0 - 25 keV.

#### SUMMARY OF THE EXPERIMENTAL MEASUREMENT AND DATA REDUCTIONS

A complete description of the polarization measurement is not necessary to the present discussion, but a brief summary is provided to show the unique properties of the results obtained. The neutron beam was polarized by transmission through  $\text{La}_2\text{Mg}_3(\text{NO}_3)_{12} \cdot 24\text{H}_2\text{O}$  in which the hydrogen in the water of hydration was polarized. The target was a polarized sample of  $^{235}\text{U}$ . The data consisted of time-of-flight spectra of fission events occurring in the sample with the neutron beam polarized parallel and anti-parallel to the target, and of the transmitted neutron beam under the same conditions.

For present purposes it is adequate to represent the spin 3<sup>-</sup> and spin 4<sup>-</sup> enhanced count rates by

$$N_3 = A_3\sigma_3\phi + A_4\sigma_4\phi, \quad (1a)$$

$$\text{and} \quad N_4 = B_3\sigma_3\phi + B_4\sigma_4\phi, \quad (1b)$$

where  $\sigma_3$  and  $\sigma_4$  are the spin-3 and spin-4 cross sections,  $\phi$  is the flux, and the constants  $A_3$ ,  $A_4$ ,  $B_3$ ,  $B_4$  are calculated from known neutron polarizations, the nuclear polarization, and the target spin. Equations (1a) and (1b) are solved for the quantities

$$\sigma_4\phi = (A_3N_4 - B_3N_3)/(A_3B_4 - B_3A_4) \quad (2a)$$

$$\text{and} \quad \sigma_3\phi = (B_4N_3 - A_4N_4)/(A_3B_4 - B_3A_4) \quad (2b)$$

These quantities are plotted for energy regions 8 - 20 eV (in the resolved range) and 200 - 260 eV (in the unresolved range), in Figs. 1 and 2. From such plots, it is easy to make spin assignments for essentially all the observed resonance structure and to extract average or effective  $J$  values for broad bins in the unresolved region. Here we define  $J_{\text{effective}} = 3 + \sigma_4/(\sigma_3 + \sigma_4)$ . It should also be noted that these data show clearly the existence of previously unresolved doublets of different spin -- for example, the weak spin-3 resonance at 9 eV.

#### SPIN DEPENDENCE OF STRUCTURE IN THE UNRESOLVED RESONANCE REGION

The question to be addressed is whether the large fluctuations in the fission cross section are spin dependent. In the summed counts ( $N_3 + N_4$ ), the fluctuations are clearly seen, as shown in Fig. 3 for the energy range 8 - 20 keV. However, visual inspection of the spin-separated data, shown in Fig. 4 over the same energy region, shows only slight evidence that any of this structure is associated with one spin or the other. The statistical accuracy of the data is low, and we might assume that it requires quantitative statistical tests on broad-bin averages to reveal any spin dependence. Following Migneco et al. [4], we first carried out a Wald-Wolfowitz runs-distribution test from 0.1 to 25 keV on  $J_{\text{eff}} - \langle J_{\text{eff}} \rangle$  with bins of 240 and 400 eV, and from 0.1 to 10 keV with bins of 85 eV. Migneco et al. reported that this test gave highly significant results when applied to  $\sigma_f$  for  $^{235}\text{U}$ , but the test applied to the polarization data gave results consistent with a random distribution of spin. We next calculated the serial correlation coefficients of  $J_{\text{eff}}$  with a bin size of 240 eV from 0.1 to 25 keV, followed by a Wald-Wolfowitz test on these coefficients; the same test was also used by Migneco et al. [4]. The results again showed no significant departure from a random distribution. Following James et al. [3], we tried the Levene-Wolfowitz runs-up-and-down test on  $J_{\text{eff}}$  with a bin width of 240 eV from 0.1 to 25 keV. Again, the results were completely consistent with the null hypothesis of a random distribution.

The next test, however, showed a much more interesting result. We calculated the correlation coefficient between the spin-3 data and the summed counts and between the spin-4 data and the summed counts, for broad-bin averages. The results, shown in Table I, indicate that the observed structure is attributable to spin 4. Apparently there is still enough statistical error associated with the broad-bin averages that it masked the effect when we used the usual tests for intermediate structure. The results shown in Table I, however, are definitive, showing that essentially all the fluctuating part of the  $^{235}\text{U}$  fission cross section has  $J = 4$ .

We conclude that the polarization data give strong support to the hypothesis that the fluctuations in the fission cross section of  $^{235}\text{U}$  are a second-well phenomenon. We note that the general procedure used in previous versions of ENDF/B for the unresolved resonance region should be modified in order to treat this phenomenon properly.

## AVERAGE PARAMETERS FOR THE UNRESOLVED RESONANCE REGION

The polarization data can also be used to provide better estimates of the average parameters for the unresolved region. The first of these is the level density. Fig. 5 shows the usual staircase distribution of spacings for spin-3 and spin-4 resonances below 360 eV. (Only the tips of the stairs are plotted.) Below 60 eV, we used the  $\Delta_3$  test of Dyson and Mehta [9] as a criterion for arriving at the recommended average spacing of 1.153 eV and 0.896 eV for spin 3 and spin 4, respectively, which would imply a total of 119 levels of both spins between 0 and 60 eV. If the spacing distribution follows the prediction of the Gaussian Orthogonal Ensemble (GOE), then the  $\Delta_3$  test as a missing-level indicator is a very powerful one. Jain and Blons [10] have questioned the applicability of the GOE for nuclides near  $A = 240$ . To check this for ( $^{235}\text{U} + n$ ), we have devised an independent missing level estimator, which is based on two assumptions: (1) the neutron width distribution is Porter-Thomas; and (2) the larger widths are accurately known. For the resonance region in ( $^{235}\text{U} + n$ ), a lower limit of  $\langle \Gamma n^\circ \rangle / 4$  seems appropriate. It can be easily shown that the Porter-Thomas distribution has the following properties:

$$\int_{1/4}^{\infty} f(x) dx = 0.617, \quad (3a)$$

$$\int_{1/4}^{\infty} \sqrt{\Gamma n^\circ} f(x) dx = 0.704 \langle \Gamma n^\circ \rangle^{1/2}, \quad (3b)$$

$$\text{and} \quad \int_{1/4}^{\infty} \Gamma n^\circ f(x) dx = 0.969 \langle \Gamma n^\circ \rangle, \quad (3c)$$

where  $x = \Gamma n^\circ / \langle \Gamma n^\circ \rangle$ , and  $f(x) = \frac{1}{\sqrt{2\pi x}} \exp(-x/2)$ .

If one forms the ratio:

$$\frac{\sum_{\langle \Gamma n^\circ \rangle / 4}^{\infty} g \Gamma n^\circ}{\langle \Gamma n^\circ \rangle / 4} / \left( \frac{\sum_{\langle \Gamma n^\circ \rangle / 4}^{\infty} \sqrt{g \Gamma n^\circ}}{\langle \Gamma n^\circ \rangle / 4} \right)^2,$$

it has the expectation value

$$\frac{0.969}{(0.704)^2} \cdot \frac{0.617}{n} = 1.206/n$$

where  $n$  is the number of levels having  $\Gamma n^\circ$  larger than  $\langle \Gamma n^\circ \rangle / 4$ . To use the missing-level estimator, one calculates the quantity  $n \Sigma g \Gamma n^\circ / (\Sigma \sqrt{g \Gamma n^\circ})^2$ , starting with the largest value of  $g \Gamma n^\circ$  in the interval and adding additional levels, one at a time, going from larger to smaller values in the ordered array of observed values of  $g \Gamma n^\circ$ . When this quantity equals 1.206, the total

number of levels in the interval is  $n/0.617$ . It should be noted that the estimator is independent of any assumptions of  $\langle g\Gamma_n^\circ \rangle$ ; in fact, an estimate of this quantity is derived along with the total number of levels. We tested the missing-level estimator by Monte-Carlo sampling from a Porter-Thomas distribution as shown in Fig. 6; the expected relative error varies as  $1/\sqrt{N}$ , where  $N$  is the total number of levels in the sample, or  $\sim 9\%$  for 120 levels.

To use the missing-level estimator for  $(^{235}\text{U} + n)$ , we first note that the s-wave neutron strength function,  $\langle \Gamma_n^\circ/D \rangle$ , as calculated from Mughabghab's recommended parameters [11], is independent of spin. The spin independence of the s-wave strength function and the almost perfect agreement of the staircase spacing distribution (Fig. 5) with the expected  $(2J + 1)$  slope below 60 eV suggests that we can use the quantity  $g\Gamma_n^\circ$  as a spin-independent variable in checking for missing levels. It may be useful to point out that the strength function is protected against missing levels so that the spin independence of the strength function is valid even if we miss more levels of one spin than of the other.

We used this estimator with three recommended sets of resonance parameters for  $^{235}\text{U}$ , those of Mughabghab [11], those of Smith and Young [12] for ENDF/B-III, and those of Reynolds [13] for ENDF/B-V; the estimator gives  $107 \pm 10$ ,  $117 \pm 10$ , and  $110 \pm 10$ , respectively, as the total number of levels of both spins between 0 and 60 eV. These results are consistent with the 119 predicted by using the spacings obtained with the  $\Delta_3$  test. We conclude that the GOE gives an accurate representation of the spacing distribution, and that the  $(2J + 1)$  variation of the level density seems to be confirmed for  $^{235}\text{U}$ ; we see no need for a spin cutoff factor, at least for spins  $\leq 4$ . The number of levels which are missed in the usual type of measurement (in which the spins are not separated) seems to be substantially lower than the statistical analysis of Garrison [14] would indicate. We see no evidence for a large number of missing levels as suggested, for example, by Felvinci et al [15].

The average fission widths for the two spin states are different -- the three sets of recommended parameters [11-13] suggest that  $\langle \Gamma_f \rangle_{3-}$  is about twice as large as  $\langle \Gamma_f \rangle_{4-}$ . The resolved resonance parameters of Smith and Young [12] and of Reynolds [13] are based on multilevel analysis of total and all measured partial cross sections, and should be a more accurate representation than those of Mughabghab [11]. The results of the two multilevel fits do not agree, however. Using the Smith and Young parameters, we get  $\langle \Gamma_f \rangle_{3-} = 0.179$  eV,  $\langle \Gamma_f \rangle_{4-} = 0.090$  eV; using the Reynolds parameters we get  $\langle \Gamma_f \rangle_{3-} = 0.220$  eV,  $\langle \Gamma_f \rangle_{4-} = 0.098$  eV. The discrepancy can be attributed to the assumed value for the radiation width: Smith and Young obtain  $\langle \Gamma_\gamma \rangle = 0.0355$  eV; Reynolds uses 0.042 eV. The ratios  $\langle \Gamma_f \rangle / \langle \Gamma_\gamma \rangle$  agree; we obtain  $\langle \Gamma_f \rangle_{3-} / \langle \Gamma_\gamma \rangle = 5.18$  and  $\langle \Gamma_f \rangle_{4-} / \langle \Gamma_\gamma \rangle = 2.45$  for the energy range 0 - 60 eV, using the average of both multilevel analyses [12,13]. We prefer the narrower set of widths from Smith and Young [12] for two reasons. First, we expect that narrower widths will give better agreement with the resonance self-shielding experiments of Bramblett and Czirr [16-18], and secondly, we find that an average capture width of 0.042 eV appears to be less consistent with nuclear systematics than is 0.0355 eV. We can calculate the energy dependence of the average radiation width [19], which can be normalized at the neutron binding energy (less the pairing correction) to data for non-fissile targets in the

lower actinides. The pairing correction we obtain from a plot of the reduced level spacings  $D(2J + 1)$ , which also shows a systematic excitation energy dependence, as may be seen in Fig. 7 [20].

The results of this exercise are shown in Fig. 8; they suggest a value of  $\langle \Gamma_\gamma \rangle = 0.037$  eV for  $^{235}\text{U}$ , although the scatter of data points does not preclude any value in the range of 0.035 to 0.040. We see little reason to change the value of  $\langle \Gamma_\gamma \rangle = 0.035$  eV recommended by Pitterle et al. [21] for ENDF/B-III.

Using the Smith and Young average radiation width of 0.0355 eV gives  $\langle \Gamma_f \rangle_3 = 0.184$  eV and  $\langle \Gamma_f \rangle_4 = 0.087$  eV for the resolved resonance region. It is instructive to see what the Bohr-Wheeler estimate would be. Using a single-humped barrier, the estimate is

$$\left\langle \frac{\Gamma_f}{D} \right\rangle = \frac{n}{2\pi} \quad (4)$$

where  $n$  is the number of open fission channels. If the barrier has more than one hump, and if the compound nucleus assumption is valid for states in the second well, then the reaction rate follows the expression given by Eyring [22] for sequential processes:

$$k' = \left( \sum_i k_i^{-1} \right)^{-1} \quad (5)$$

where  $k'$  is the overall rate constant and  $k_i$  is the rate constant for each barrier. This leads to the now familiar expression

$$P_{AB} = \frac{P_A P_B}{P_A + P_B} \quad (6)$$

for a two-humped barrier, where  $P_{AB}$  is the total penetrability, and  $P_A$  and  $P_B$  are the penetrabilities for each of the two barriers.

For excitations near the top of the barrier, the configuration in the second well may well be represented as an independent compound nucleus with various decay modes, such that Eqs. 5 and 6 are valid. For fully open channels, we see that the Bohr-Wheeler estimate is modified to read

$$\langle \Gamma_f \rangle = \frac{nD}{4\pi} \quad (4')$$

If we calculate this quantity, using the recommended spacings for spin 3 and spin 4, we find  $\langle \Gamma_f \rangle_3 = 0.092$  eV and  $\langle \Gamma_f \rangle_4 = 0.071$  eV for each open channel. We can thus infer that, for spin 3, the observed fission width is consistent with two fully open channels, or more than two, if they are only partially open. The observed fission width  $\langle \Gamma_f \rangle_4$  corresponds to no more than one fully open channel. This is reasonably consistent with the distribution of widths for the resolved resonances: Keyworth et al [8] reported  $\nu = 2.04 \pm 0.65$  and  $1.27 \pm 0.33$  for spin-3 and spin-4 fission widths, respectively, based on a fit to the chi-squared distribution with  $\nu$  degrees of freedom, using the method of maximum likelihood. The Bohr-Wheeler estimate is in surprisingly good agreement with our recommended values of  $\langle \Gamma_f \rangle_3 = 0.184$  eV and  $\langle \Gamma_f \rangle_4 = 0.087$  eV; we calculate  $\langle \Gamma_f \rangle_3 = 2.04 * 0.092 = 0.188$  eV, and  $\langle \Gamma_f \rangle_4 = 1.27 * 0.071 = 0.090$  eV (with errors of 30%).

The data of Pattenden and Postma [23] can be used to give additional information on the fission channel quantum numbers. Pattenden and Postma measured angular distributions of fission fragments with aligned target nuclei of  $^{235}\text{U}$ , reporting their results in terms of  $A_2$ , the coefficient of the  $P_2$  term in the Legendre expansion of the angular distribution. The coefficient  $A_2$  is a function of both  $J$  and  $K$ , the projection of  $J$  on the nuclear symmetry axis.

We find that  $A_2$  is significantly correlated with  $J_{\text{eff}}$  (at the significance level of  $10^{-8}$  as defined in Table I.) A plot of  $A_2$  versus  $J_{\text{eff}}$  is shown in Fig. 9. We use a linear least-squares fit to these data, shown by the solid line in Fig. 9, to infer the average value of  $A_2$  for pure spin-3 resonances ( $J_{\text{eff}} = 3.0$ ) and for pure spin-4 resonances ( $J_{\text{eff}} = 4.0$ ), obtaining  $\langle A_2 \rangle_3 = -1.22$ ,  $\langle A_2 \rangle_4 = -2.01$ . For  $J = 4$ , we assume that the lowest two channels,  $K = 1$  and  $K = 2$ , are open. Knowing the characteristic  $A_2$  for each  $J, K$  (shown as the bars on the right hand side of Fig. 9) enables us to calculate the contributions from each channel; we find  $\langle \Gamma_f \rangle_{J,K=4,1} = 0.071$  eV,  $\langle \Gamma_f \rangle_{J,K=4,2} = 0.016$  eV if the total width is 0.087 eV. We infer that the  $J,K = 4,1$  channel is fully open, the  $J,K = 4,2$  channel is only partially open. For  $J = 3$ , we have an apparent inconsistency. We expect three possible channels, for  $K = 0,1,2$ , and we expect that if the  $J,K = 4,1$  channel is fully open, the  $J,K = 3,1$  channel (which presumably lies at lower excitation) will also be fully open, with an average fission width of 0.092 eV. With these assumptions, we can solve for  $\langle \Gamma_f \rangle_{J,K=3,0}$  and  $\langle \Gamma_f \rangle_{J,K=3,2}$ , finding  $\langle \Gamma_f \rangle_{3,0} = 0.019$  eV,  $\langle \Gamma_f \rangle_{3,2} = 0.073$  eV for a total width of 0.184 eV. Within the error on the least squares fit, we could use  $\langle \Gamma_f \rangle_{3,1} = \langle \Gamma_f \rangle_{3,2} = 0.092$  eV and  $\langle \Gamma_f \rangle_{3,0} = 0$ .

These results are not new; essentially they confirm those of the earlier polarization measurements of Keyworth et al [7], who arrived at the same conclusion. But they are not what had been expected. For many years, the assumption was made that the channels open in order of ascending  $K$ , following the sequence of octupole vibrational band heads observed near the ground state of even-even nuclides. Why the  $J,K = 3,0$  channel seems to be forbidden remains an unanswered question.

THE VARIATION OF  $\langle\alpha\rangle$ 

The most important result of the present study, that the structure in the fission cross section of  $^{235}\text{U}$  can be attributed to the double-humped barrier, and, in particular, to the  $J = 4^-$  spin state for s-wave neutron-induced fission, leads to a new understanding of the variation of the capture-to-fission ratio, and to the necessity of a revised treatment of the capture cross section and  $\langle\alpha\rangle$ . While earlier work [1-4] had strongly suggested that the double-humped barrier might be of importance in causing fluctuations in  $\sigma_f$  for  $^{235}\text{U}$ , there was no prescription for treating this effect in an evaluation. For ENDF/B, the approved procedure for treating the fluctuations in the unresolved resonance region and for File 3 (the "smooth" cross sections) is as follows: one looks at the fluctuations in the capture and fission cross sections and holding  $\langle\Gamma_\gamma\rangle$  fixed one solves for a pointwise variable  $\langle\Gamma_f\rangle$  and  $\langle\Gamma_n\rangle$  for one or both spin states which describes the fluctuations, in broad-bin averages, to the desired degree of accuracy. The difficulty, at least with previous versions of ENDF/B, is that  $\langle\alpha\rangle$  above 3 keV was given with too coarse a bin structure ( $\sim 1$  keV) to describe the intermediate structure; the result was that the capture and fission cross sections tended to show the same structure, and their ratio,  $\langle\alpha\rangle$ , was more or less featureless.

The present results suggest a completely different treatment. If the structure in fission is due to enhancement of the  $4^-$  resonances related to the double-humped barrier, the capture and fission cross section structure will show a strong negative correlation, and  $\langle\alpha\rangle$  will reflect this in showing pronounced fluctuations; it is hardly necessary to add that we should expect a considerable difference in the calculated self-shielding factors and Doppler coefficients.

The purpose of the present section is to show that evidence exists to support the anticorrelation of the fission and capture cross sections of  $^{235}\text{U}$ , and, in particular, to show that it is the  $J, K = 4, 2$  component which reflects the intermediate structure in  $^{235}\text{U}$  fission. We begin by showing, in Fig. 10, the fission and capture cross sections (multiplied by  $\sqrt{E}$  for greater clarity) from 0.1 to 1 keV as reported by Gwin et al. [24]. The correlation coefficient is strong (-0.494) but hardly conclusive, since there are only nine data points. We also calculated the correlation coefficient between  $\langle\alpha\rangle$  from ENDF/B-IV and  $J_{\text{eff}}$  from 80 eV to 1 keV, finding much the same result: the correlation is strong (-0.511) but not conclusive, because there are too few data points below 1 keV, and the bin structure above 1 keV is too coarse to show the effect.

Next we note, as shown in Fig. 11, the data reported by Pattenden and Postma on the variation of  $A_2$  below 2 keV. The data have very large uncertainties at the highest energies, but they seem to suggest a trend, a lowering of  $-A_2$  with increasing energy. If we calculate the expected variation of  $A_2$  using the double-hump barrier parameters of Back et al. [25] for the compound nucleus  $^{236}\text{U}$ , we find that there is no way we can get a variation much larger than 1% in 2 keV, except by assuming second-well enhancement.

If we make the assumption that any variation in  $A_2$  is due to the spin-4 component,  $A_2$  for spin 3 remaining fixed at -1.22, then we can solve for  $\langle A_2 \rangle_4$  as a function of energy. This is shown in Fig. 12 over the energy region 0.1 - 1.5 keV; plotted in the same figure is  $\langle \alpha \rangle$  reported by Gwin and  $\langle \alpha \rangle$  given in ENDF/B-IV. The positive correlation is obvious:  $\langle \alpha \rangle$  is low when the J,K = 4,2 channel is large (low values of  $-A_2$ ); again the correlation is not conclusive because there are too few data points. No one piece of evidence is conclusive, yet they all point in the same direction: the fluctuations in  $\sigma_f$  are due to second-well enhancement of the J,K = 4,2 channel, which is reflected in  $\langle \alpha \rangle$ .

#### RECOMMENDATIONS FOR ENDF/B-V

To use the present results in the evaluation of the unresolved resonance region requires a change in the approved procedure, and, unfortunately, in the processing codes which use ENDF/B. The problem is that width-fluctuation corrections are not properly made if the two spin-4 fission channels have different widths. A change in procedure is not possible for ENDF/B-V because of deadlines which the evaluators must meet, but we shall outline what we consider to be deficiencies of the present treatment for consideration in the future. The present format allows a pointwise variable (in energy) average neutron width with one or two degrees of freedom, to account for structure in the total and elastic scattering cross sections, a fixed  $\langle \Gamma_\gamma \rangle$  with an infinite number of degrees of freedom, and a pointwise variable average fission width with an integral number of degrees of freedom for each spin state, to account for structure in  $\langle \sigma_f \rangle$  and  $\langle \alpha \rangle$ . To generate the average fission, capture, and elastic scattering cross sections from relatively coarse binned data which reflect the structure, one uses the code UR [26], which performs the integrals over the appropriate chi-squared distributions to obtain width-fluctuation corrections, and then uses an iterative procedure to extract the appropriate average widths which fit the binned data. The most time-consuming part of the code is the width-fluctuation calculation. If one performed this calculation from first principles; it would involve a multiple integral over a Porter-Thomas distribution for each of the partial widths which may exist. The code UR contains an expression by Dresner [27], which uses the superposition theorem for chi-squared distributions to reduce the multiple integral to a single integral, with the restriction that the number of degrees of freedom be integral. We had hoped, by a suitable definition of a non-integral number of degrees of freedom to describe the case  $\langle \Gamma_f \rangle_{J,K=4,1} \neq \langle \Gamma_f \rangle_{J,K=4,2}$ , that the Dresner expression could still be used, but unfortunately it does not give the right answer for the width fluctuation correction integrals unless  $\langle \Gamma_f \rangle_{4,1} = \langle \Gamma_f \rangle_{4,2}$  or unless one of the two partial widths is zero. We find that the width-fluctuation integrals given by the Dresner expression differ from the correct integrals by as much as 5% for  $\nu_{eff}$  non-integral. Perhaps there is a definition of  $\nu_{eff}$  which would allow general use of the Dresner formula, but we have not found it.

We recommend that, after ENDF/B-V, use of the Dresner expression be discontinued, both in UR and in the processing codes which use ENDF/B, in favor of a somewhat more complicated but presumably more accurate representation by Shaker and Lukyanov [29], which treats the case that the reaction channels can be divided into a small number of groups with a different average

width for each of the groups. Alternatively, one might consider an approach similar to the quick and simple one we devised for testing the Dresner formula: we actually carried out the triple integration, replacing each integral by a weighted sum over 20 levels judiciously chosen from the appropriate chi-squared distribution. We found that we could calculate width-fluctuation corrections in agreement with the Dresner formula (where it is applicable) to less than 1% in all cases we tried, and generally the agreement extended to the fourth decimal place. Furthermore, most of the computer time was spent in evaluating the Dresner formula. Additional time savings might be achieved by selecting the twenty widths from a non-integral chi-squared function, in which case one reduces the triple sum to a double sum.

If the problem of calculating width-fluctuation corrections for a non-integral number of fission channels were solved, then the s-wave parameterization given in Table II could be used as a starting point for the extraction of energy dependent widths in the unresolved region.

Table II also contains recommended p-wave parameters. To obtain these, we chose p-wave strength functions consistent with an extrapolation of the  $p^{1/2}$  and  $p^{3/2}$  optical model parameters of Lagrange [30] to  $^{238}\text{U}$ , a constant radiation width, equal to that for s-waves, and fission widths which give a reasonable representation of  $\langle\alpha\rangle$  above the unresolved resonance region. The results of a calculation based on this parameterization are shown in Fig. 13. Again, it should be pointed out that these are initial guesses only, and are open to modification as required by the detailed fitting of the structure. It is interesting to note that the recommendations made by Pitterle et al. [21] for ENDF/B-III are remarkably close to those shown in Table II, especially considering that essentially none of the data we have used were available to them at that time. It also might be noted that we deliberately refrained from studying Pitterle's report until the present study was completed.

For ENDF/B-V, we are still restricted to integral values of the number of fission degrees of freedom because of the widespread use of the Dresner formula in treating width-fluctuation corrections. We recommend that both  $\langle\Gamma_f\rangle_{J\pi,K=4^-,1}$  and  $\langle\Gamma_f\rangle_{J\pi,K=4^-,2}$  be varied together, with  $\nu = 2$ . This should be a much better representation than earlier versions which varied  $\langle\Gamma_f\rangle$  for both spins, and, while it is not strictly accurate, may be a reasonable compromise.

## ACKNOWLEDGMENTS

The authors would like to thank Dr. Mulki R. Bhat of the National Neutron Cross Section Center of Brookhaven National Laboratory, who has overall responsibility for the evaluation of  $^{235}\text{U}$  for ENDF/B-V, for several helpful suggestions, and for a critical reading of the manuscript.

## REFERENCES

1. M. G. CAO, E. MIGNECO and J. P. THEOBOLD, *Phys. Letters*, 27B, 409 (1968).
2. R. B. PEREZ, G. de SAUSSURE, E. G. SILVER, R. W. INGLE and H. WEAVER, *Nuc. Sci. Eng.*, 55, 203 (1974).
3. G. D. JAMES, G. de SAUSSURE AND R. B. PEREZ, *Trans. Am. Nuc. Soc.*, 17, 495 (1973); see also UKNDC (74) P63, 38 (1974).
4. E. MIGNECO, P. BONSIGNORE, G. LANZANO, J. A. WARTENA and H. WEIGMANN, *Nuclear Cross Sections and Technology*, NBS Special Publication 425, 607 (1975).
5. G. A. KEYWORTH, J. R. LEMLEY, C. E. OLSEN, F. T. SEIBEL, J. W. T. DABBS and N. W. HILL, *Phys. Rev.*, C8, 2362 (1973).
6. G. A. KEYWORTH, J. R. LEMLEY, C. E. OLSEN, F. T. SEIBEL, J. W. T. DABBS and N. W. HILL, *Physics and Chemistry of Fission 1973*, I, 97, IAEA, Vienna (1974).
7. G. A. KEYWORTH, C. E. OLSEN, F. T. SEIBEL, J. W. T. DABBS and N. W. HILL, *Phys. Rev. Letters*, 31, 1077 (1973).
8. G. A. KEYWORTH, C. E. OLSEN, J. D. MOSES, J. W. T. DABBS and N. W. HILL, *Nuclear Cross Sections and Technology*, NBS Special Publication 425, 576 (1975).
9. F. J. DYSON and M. L. MEHTA, *J. Math. Phys.*, 4, 703 (1963).
10. A. P. JAIN and J. BLONS, *Nuc. Phys.*, A242, 45 (1975).
11. S. MUGHABGHAB and D. I. GARBER, BNL 325, Third Ed., Vol. I (1973).
12. J. R. SMITH and R. C. YOUNG, ANCR-1044 (1971).
13. J. T. REYNOLDS, KAPL-M-7396 (1975), and Private Communication.
14. J. D. GARRISON, *Phys. Rev. Letters*, 29, 1185 (1972).
15. J. FELVINCI, E. MELKONIAN and W. W. HAVENS, JR., *Nuclear Cross Sections and Technology*, NBS Special Publication 425, 580 (1975).
16. R. L. BRAMBLETT and J. B. CZIRR, *Nuc. Sci. Eng.*, 35, 350 (1969).

17. D. R. KOENIG and L. L. CARTER, *Trans. Am. Nuc. Soc.*, 17, 491 (1973).
18. D. E. CULLEN and E. F. PLECHATY, *Trans. Am. Nuc. Soc.*, 17, 490 (1973).
19. M. S. MOORE, *Nuclear Cross Sections and Technology*, NBS Special Publication 425, 129 (1975).
20. M. S. MOORE and O. D. SIMPSON, *Neutron Cross Section Technology*, CONF-660303, 840 (1966).
21. T. A. PITTERLE, N. C. PAIK and C. DURSTON, WARD-4210T4-1 (1971).
22. H. EYRING, *Rev. Mod. Phys.*, 34, 616 (1962).
23. N. J. PATTENDEN and H. POSTMA, *Nuc. Phys.*, A167, 225 (1971).
24. R. GWIN, E. G. SILVER, R. W. INGLE and H. WEAVER, *Nuc. Sci. Eng.*, 59, 79 (1976).
25. B. B. BACK, O. HANSEN, H. C. BRITT and J. D. GARRETT, *Phys. Rev.*, C9, 1924 (1974).
26. E. M. PENNINGTON, Private Communication to M. Bhat, March (1973).
27. L. DRESNER, ORNL-2659 (1959).
28. L. WILETS, *Physics Rev. Letters*, 9, 430 (1962).
29. M. O. SHAKER and A. A. LUKYANOV, *Physics Letters*, 19, 197 (1965).
30. CH. LAGRANGE, in "Critique of Nuclear Models and Their Validity in the Evaluation of Nuclear Data," EANDC Topical Discussion, Tokyo, March (1974).

TABLE I

Correlation coefficients and significance levels for the correlation of spin-3 and spin-4 data with structure in  $^{235}\text{U}$   $\sigma_f$ , from 8 - 25 keV. In this table, the significance level is the probability that the observed correlation or larger would occur with a randomly selected sample.

Energy Range (keV)	Bin Width (keV)	$\rho(N_3, \Sigma)$	Significance of $\rho(N_3, \Sigma)$	$\rho(N_4, \Sigma)$	Significance of $\rho(N_4, \Sigma)$
8.0 - 10.4	0.12	-0.01617	~0.50	0.7048	0.0003
10.4 - 12.8	0.12	0.2148	0.18	0.6148	0.002
12.8 - 15.2	0.12	0.0889	0.35	0.3815	0.05
15.2 - 20.0	0.24	0.1996	0.20	0.7111	0.0002
20.0 - 24.8	0.24	0.2336	0.16	0.7443	0.0001
24.8 - 34.4	0.48	0.2864	0.11	0.8194	<0.00001

TABLE II

Unresolved Resonance Parameters for  $^{235}\text{U}$ 

$S_0$	$= \langle \Gamma_n^0/D \rangle \sim 1.0 \times 10^{-4}$ and variable, depending on structure in $\langle \sigma_T \rangle$ .
$S_{1,1/2}$	$= \langle \Gamma_n^1/D \rangle_{1/2} = 1.26 \times 10^{-4}$
$S_{1,3/2}$	$= \langle \Gamma_n^1/D \rangle_{3/2} = 1.76 \times 10^{-4}$
$r_0$	$= 9.5663 \text{ fm}$ (unchanged from ENDF/B-IV)
$D_{J=2}$	$= 1.6135 \text{ eV}$
$D_{J=3}$	$= 1.1525 \text{ eV}$
$D_{J=4}$	$= 0.8958 \text{ eV}$
$D_{J=5}$	$= 0.7334 \text{ eV}$
$\langle \Gamma_f \rangle_{3^-}$	$= 0.184 \text{ eV}, \nu = 2$
$\langle \Gamma_f \rangle_{J^\pi, K = 4^-, 1}$	$= 0.071 \text{ eV}, \nu = 1$
$\langle \Gamma_f \rangle_{J^\pi, K = 4^-, 2}$	$\sim 0.04 \text{ eV}$ and variable, depending on structure in $\langle \sigma_f \rangle$ and $\langle \alpha \rangle$ , $\nu = 1$
$\langle \Gamma_Y \rangle$	$= 0.035 \text{ eV}^*$ , $\nu = \infty$ (unchanged from ENDF/B-IV)
$\langle \Gamma_f \rangle_{2^+}$	$= 0.513 \text{ eV}, \nu = 4$
$\langle \Gamma_f \rangle_{3^+}$	$= 0.276 \text{ eV}, \nu = 3$
$\langle \Gamma_f \rangle_{4^+}$	$= 0.285 \text{ eV}, \nu = 4$
$\langle \Gamma_f \rangle_{5^+}$	$= 0.173 \text{ eV}, \nu = 3$

\*Calculations shown in Fig. 13 used  $\langle \Gamma_Y \rangle = 0.037 \text{ eV}$ .

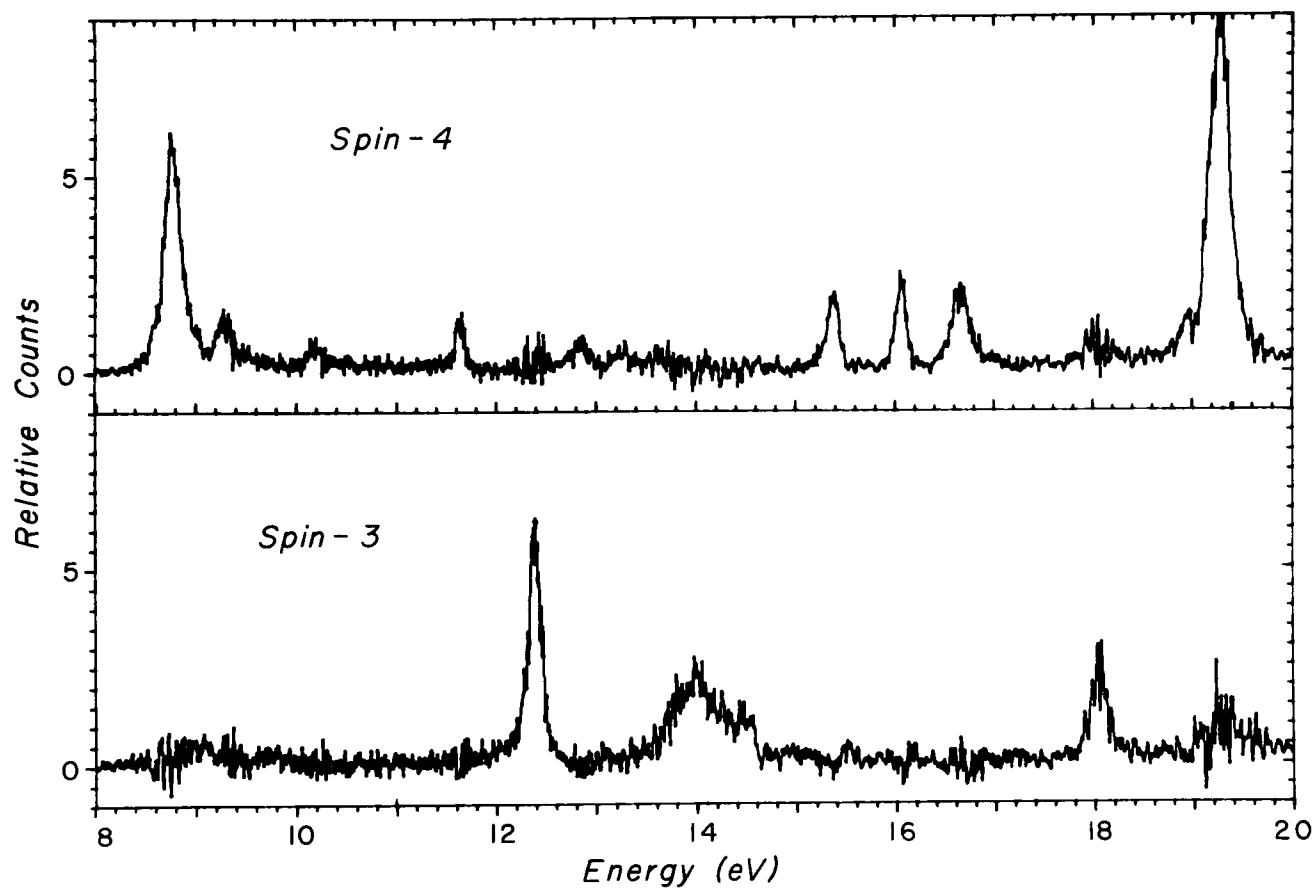


Figure 1. Spin-separated resonance structure in the fission of ( $^{235}\text{U} + n$ ) versus neutron energy in the energy range from 8 to 20 eV.

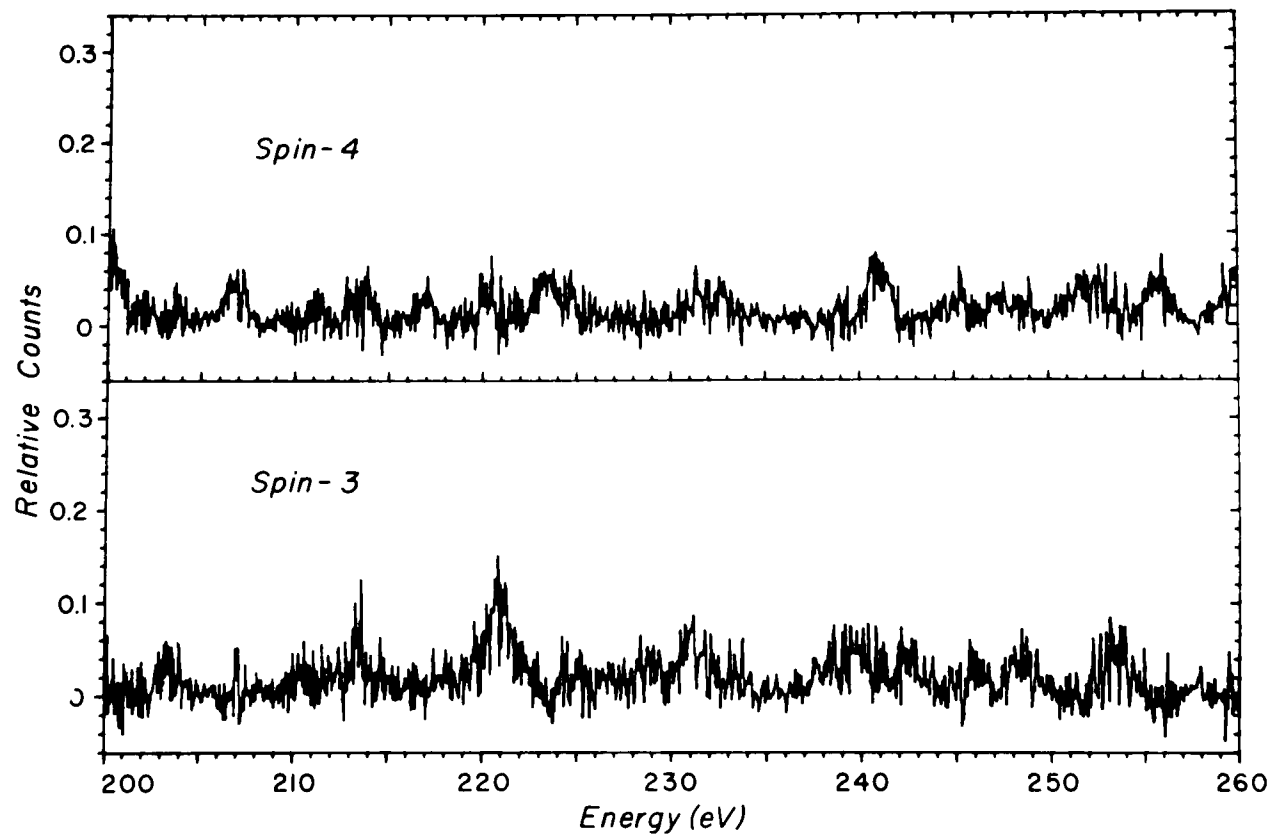


Figure 2. Spin-separated resonance structure in the fission of  $(^{235}\text{U} + n)$  versus neutron energy in the energy range from 200 to 260 eV.

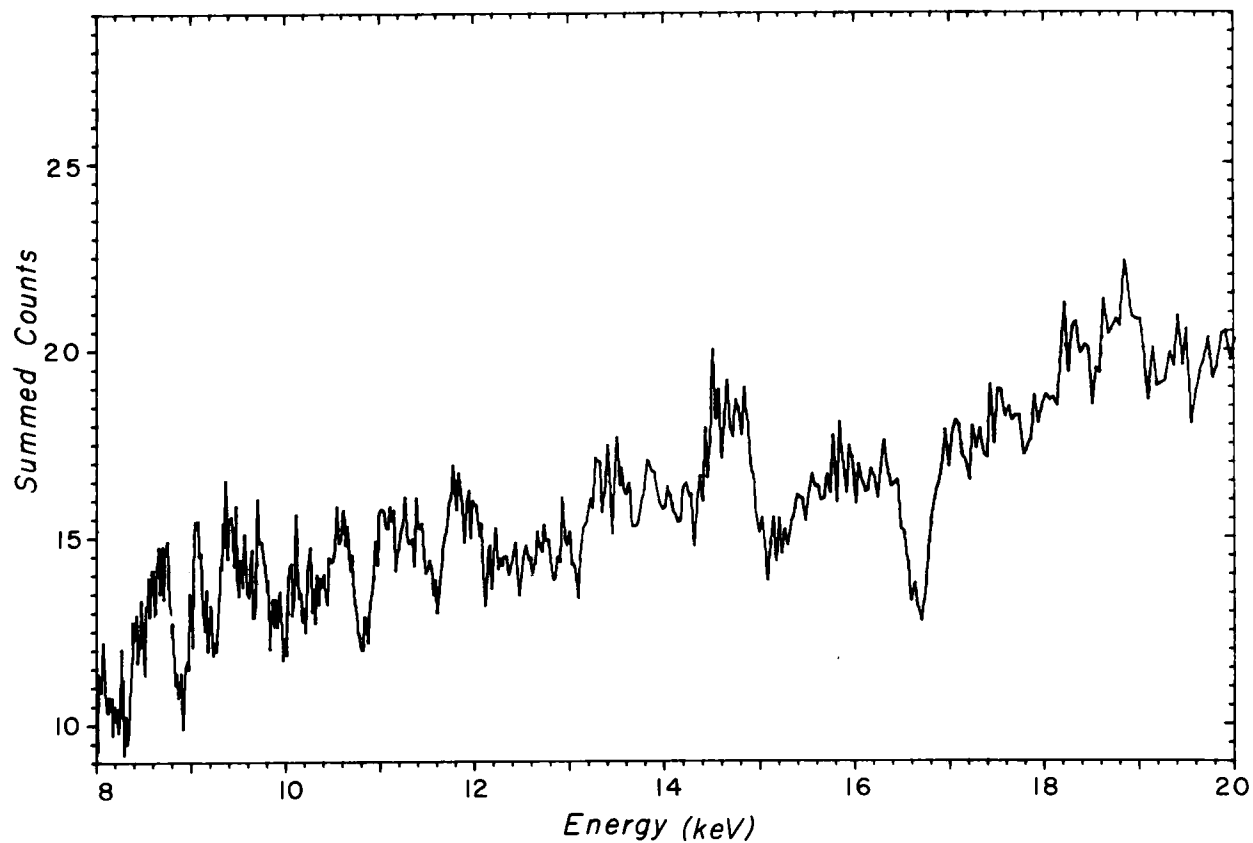


Figure 3. Summed counts (spin-3 enhanced plus spin-4 enhanced count rates) observed in the fission of ( $^{235}\text{U} + \text{n}$ ) versus neutron energy in the energy range from 8 to 20 eV. The structure corresponds to the well known fluctuations previously observed [1-4].

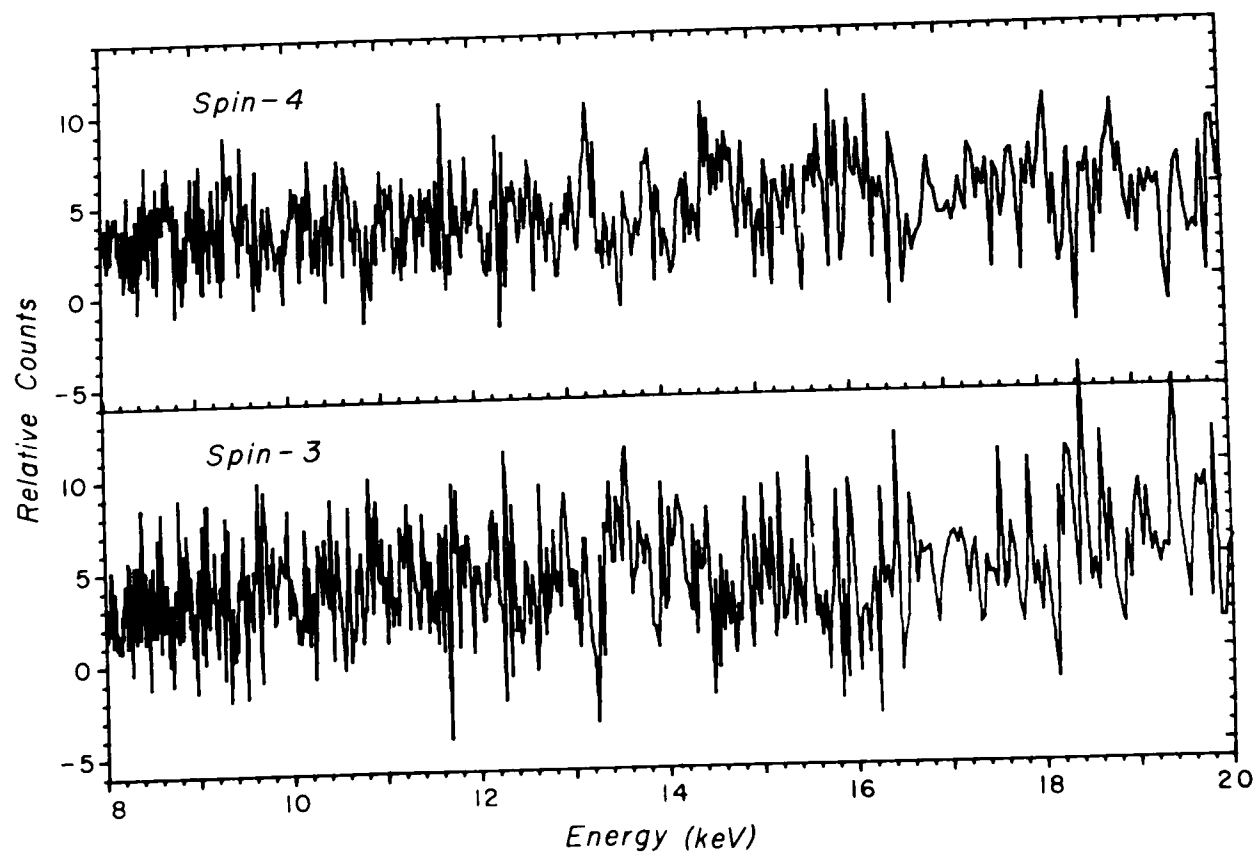


Figure 4. Spin-separated count rates in the fission of ( $^{235}\text{U} + \text{n}$ ) versus neutron energy in the energy range from 8 to 20 keV. Except for the cluster between 14 and 15 keV, which is clearly spin 4, it is not obvious that either of these curves correlates with that shown in Fig. 3.

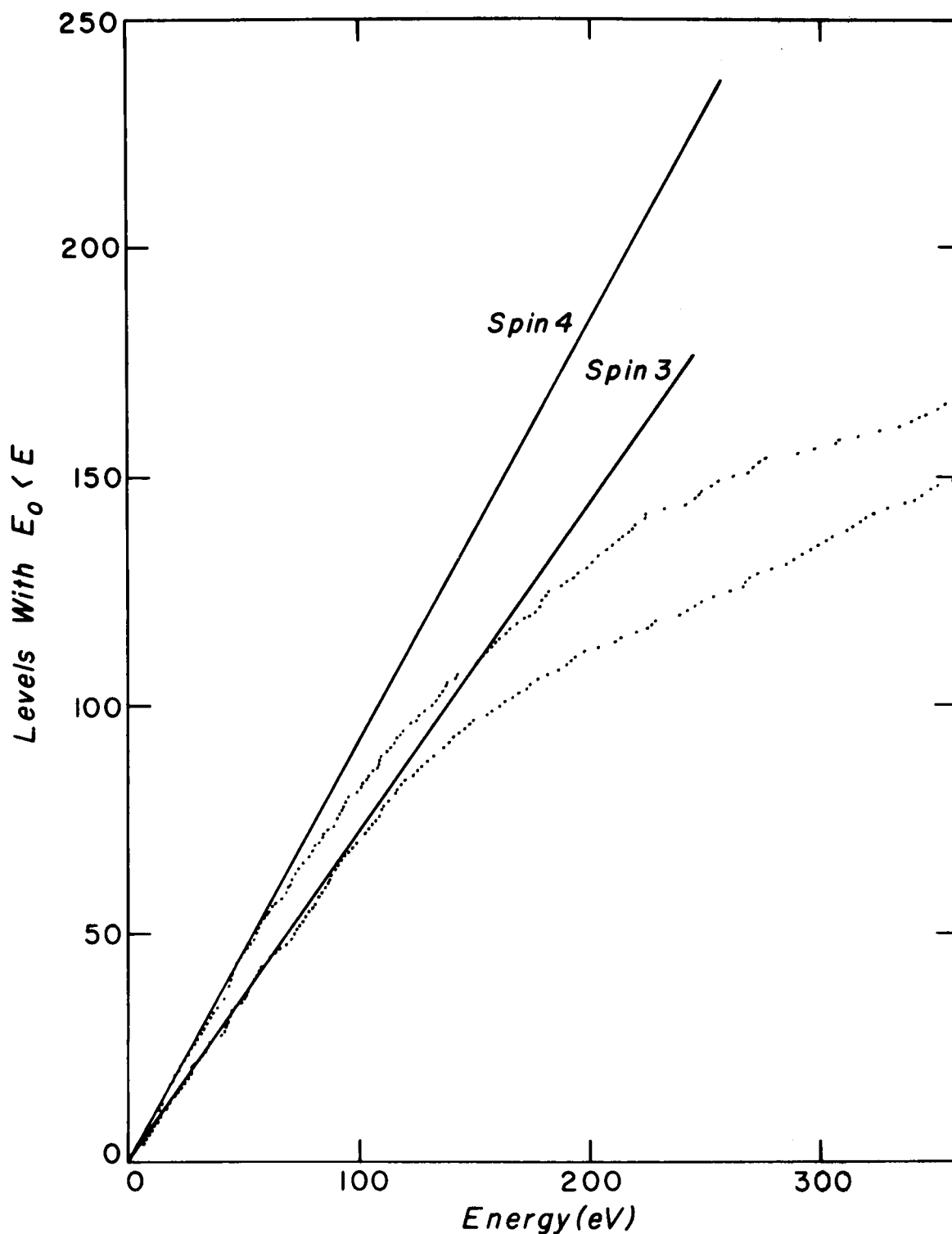


Figure 5. Observed resonance spacing distribution in  $(^{235}\text{U} + n)$  below 360 eV. Data points give the number of levels having a resonance energy less than the energy shown on the abscissa, and correspond to the tips of the stairs in the usual staircase plot. The solid lines represent a fit to the data points below 60 eV, and show the expected  $(2J + 1)$  slope.

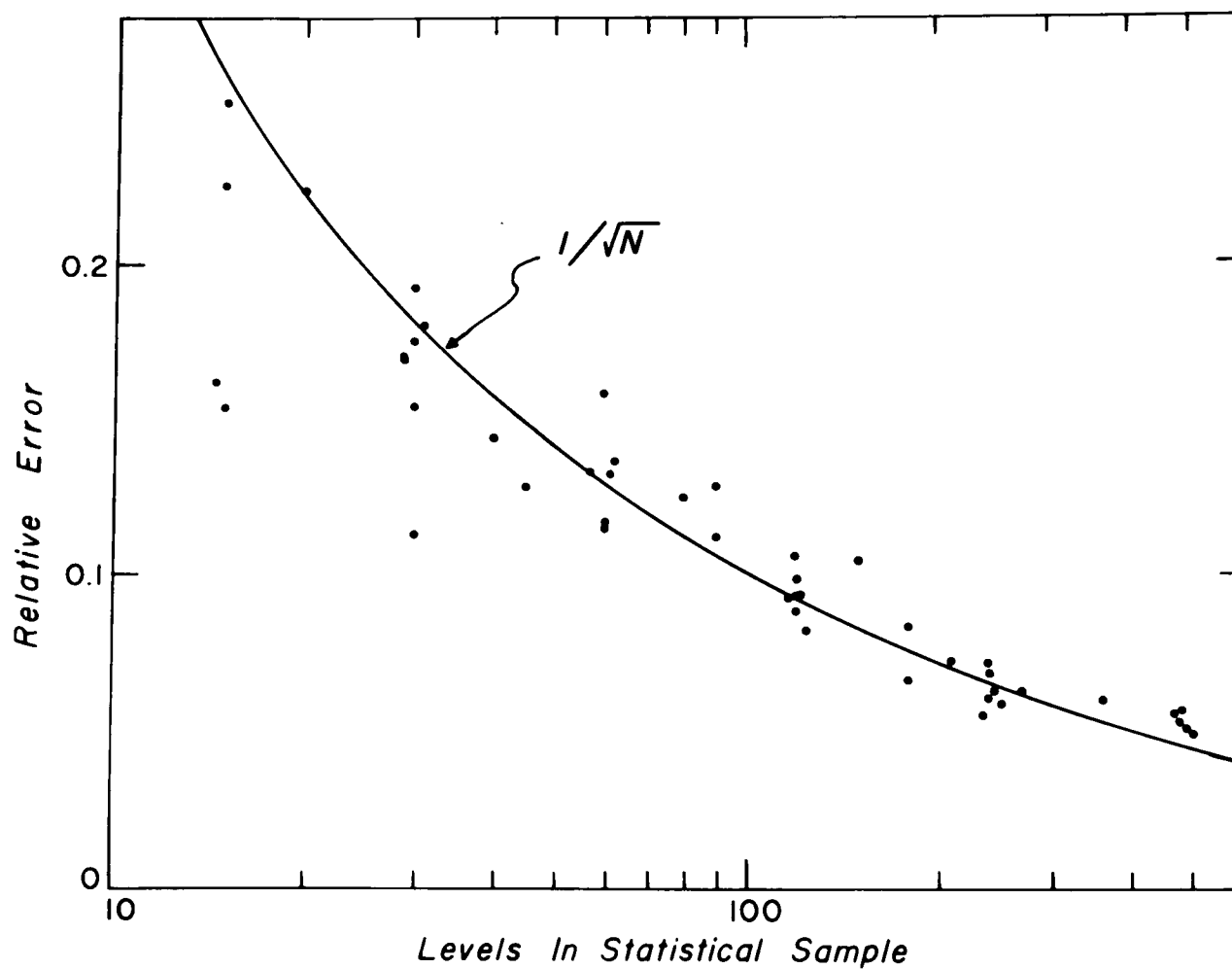


Figure 6. Distribution of relative error in a random sampling of levels from a Porter-Thomas distribution for the missing-level estimator described in the text, versus the number of levels in the statistical sample. The solid line shows the curve  $\Delta N/N = 1/\sqrt{N}$ , where  $N$  is the number of levels in the sample.

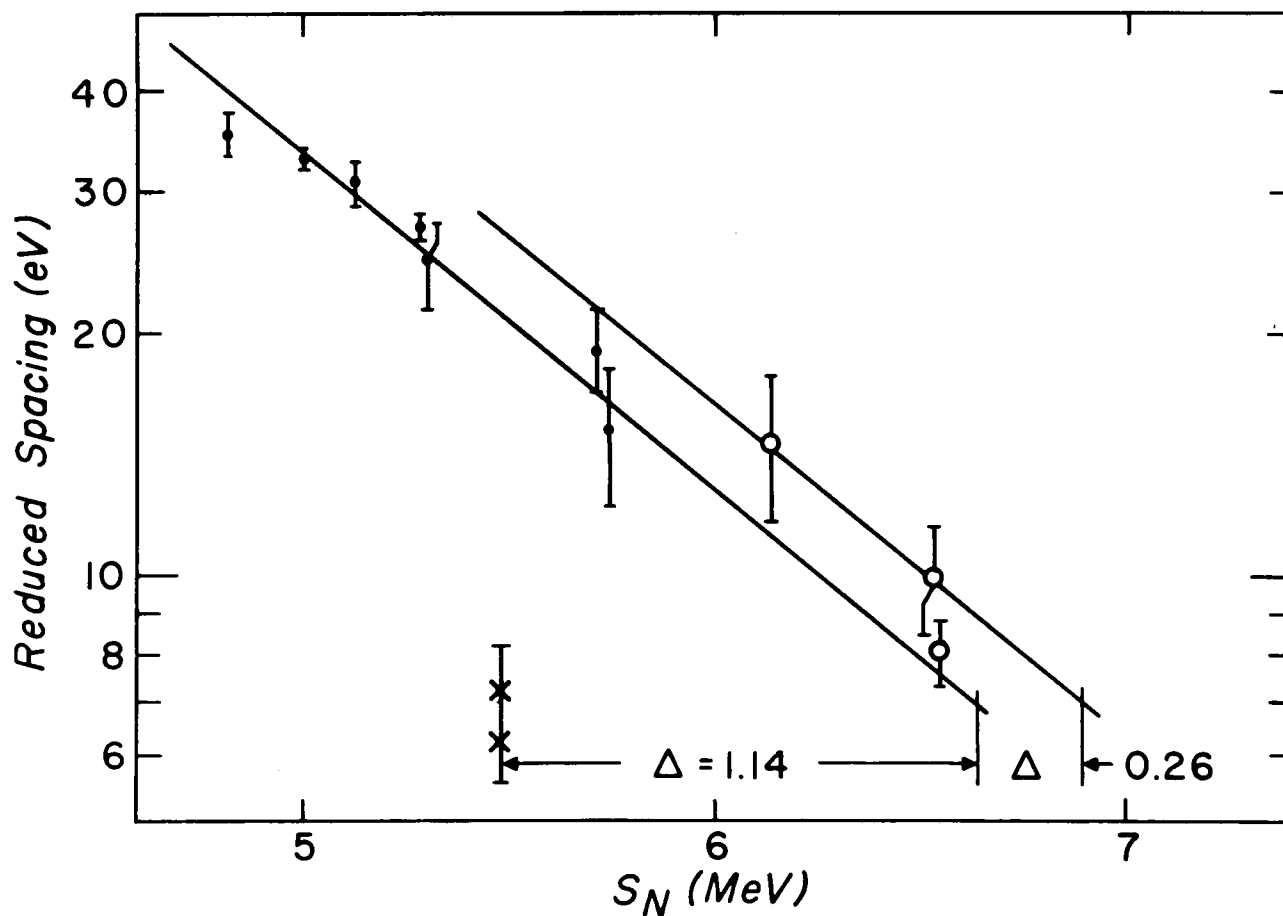


Figure 7. Reduced level spacing  $D(2J + 1)$  for several actinide nuclides for which  $D$  is reasonably well determined, versus the neutron separation energy of the compound system. Open circles represent even-even, solid circles even-odd, and x's odd-odd compound nuclei. The deltas represent the energy shift which is necessary to make the points follow the same curve.

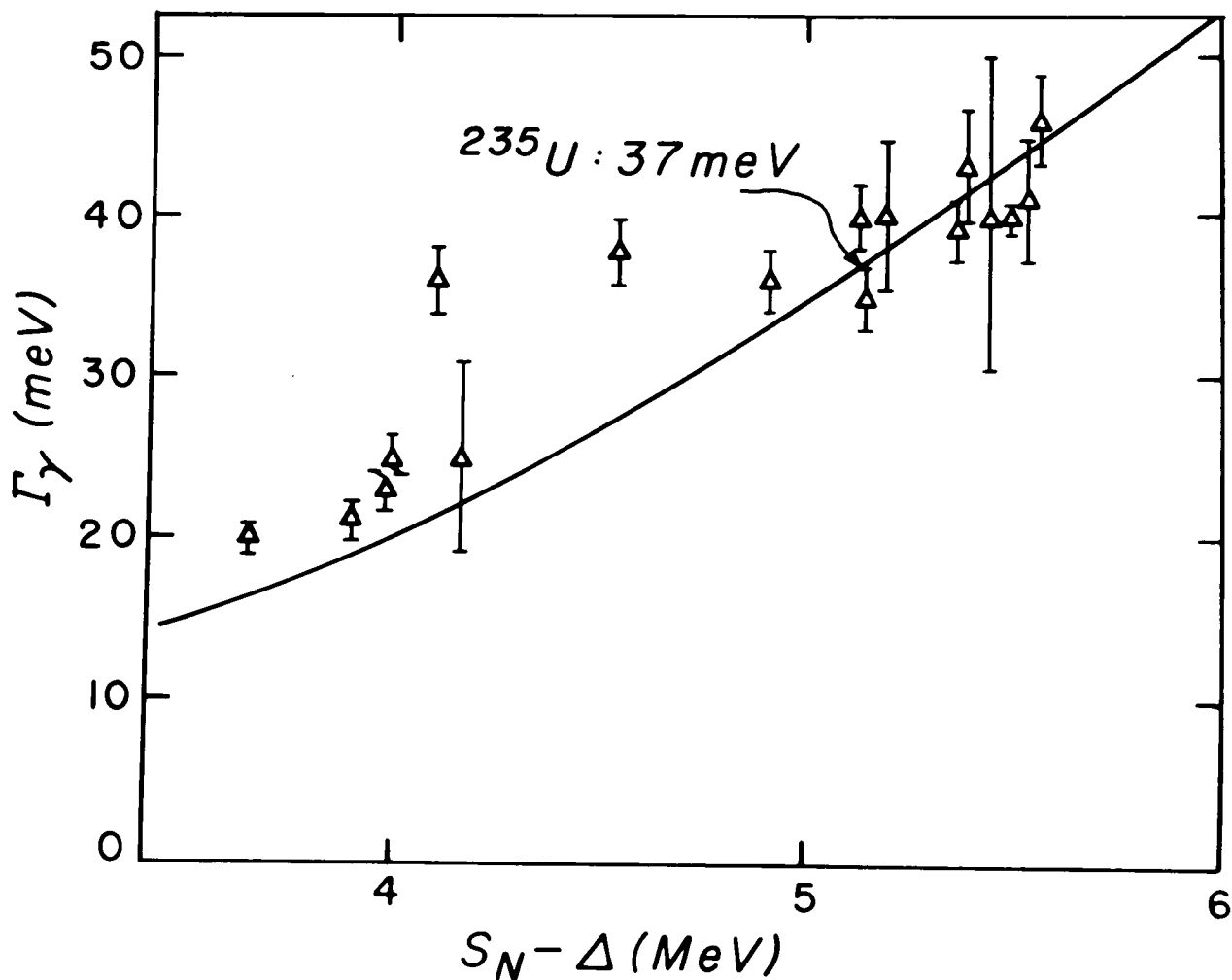


Figure 8. The variation of the radiative capture width for selected resonances of isotopes of Th, Pa, U, Np, Pu, and Am, versus the neutron separation energy of the compound system less the correction term determined from Fig. 7. The solid line shows the results of a model calculation of the radiative capture width versus excitation energy, normalized to these data.

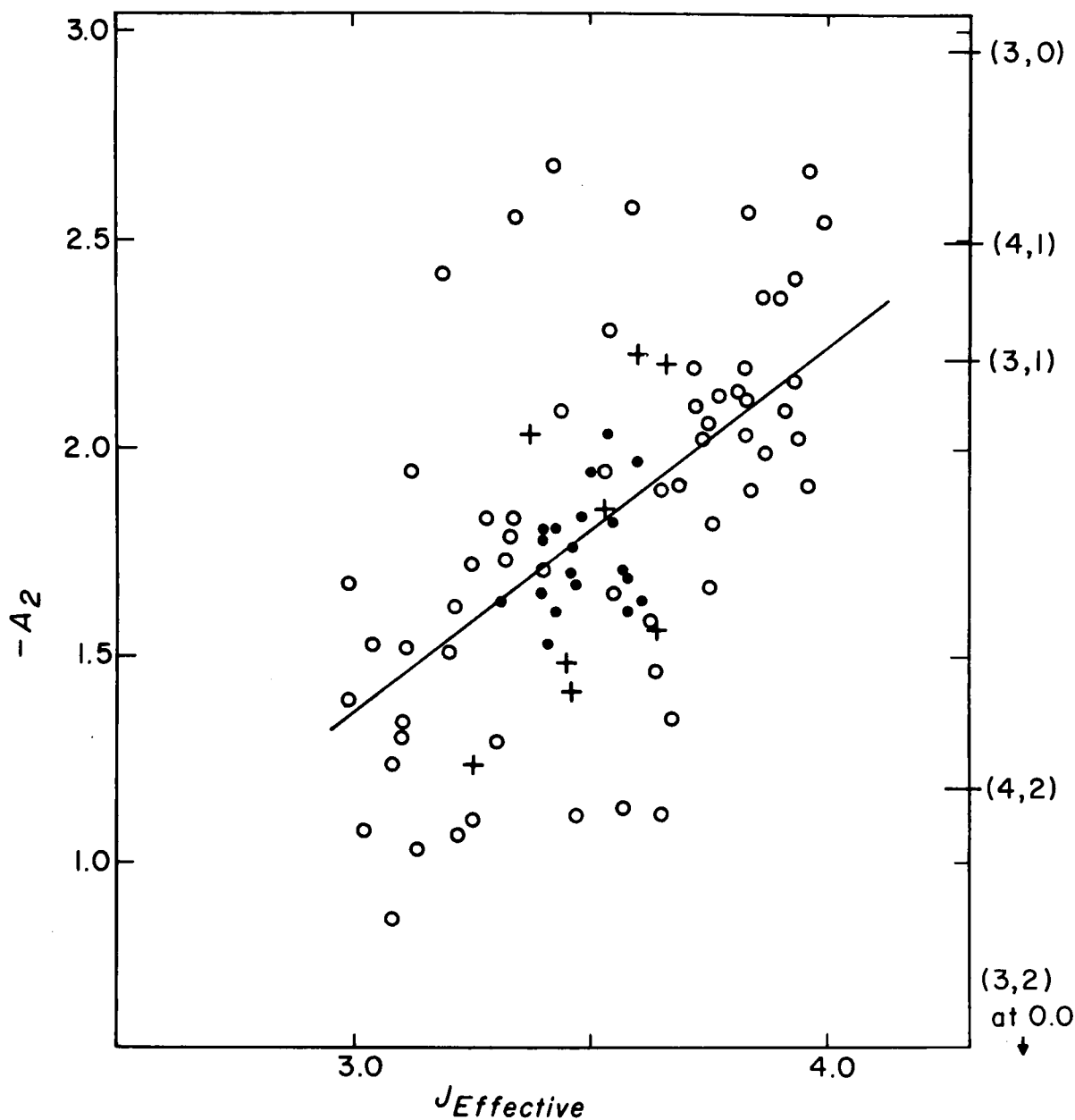


Figure 9. The variation of  $A_2$  from Pattenden and Postma versus  $J_{\text{effective}} = 3 + \sigma_4/(\sigma_3 + \sigma_4)$ . The straight line shows a linear least-squares fit to these data. The open circles show  $A_2$  data for resonance structure, the closed circles data for the unresolved region below 2 keV, and the plus signs data for the between-resonance background regions reported by Pattenden and Postma.

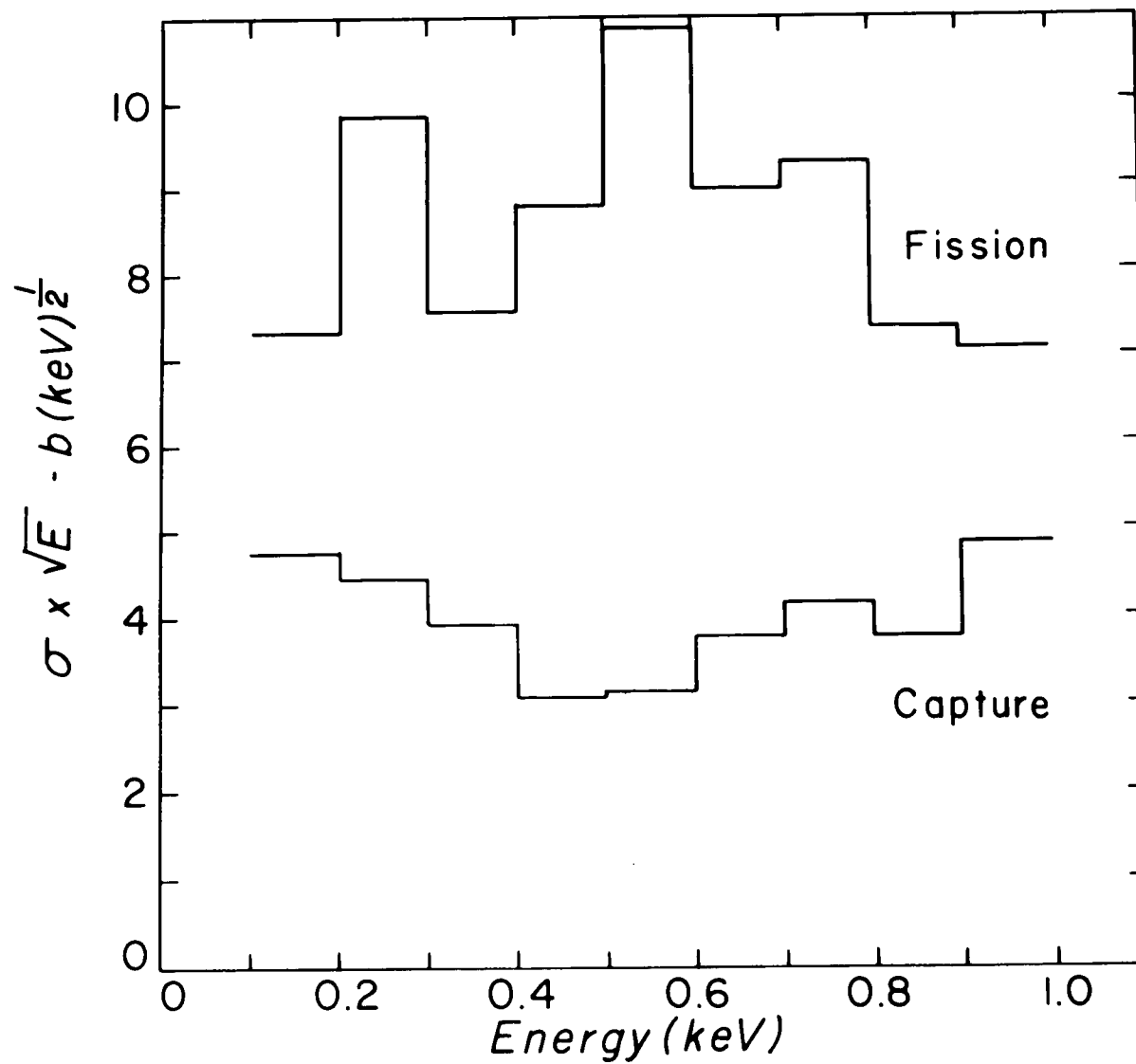


Figure 10. Fission and capture cross sections of  $^{235}\text{U}$  between 0.1 and 1 keV, multiplied by the square root of the neutron energy.

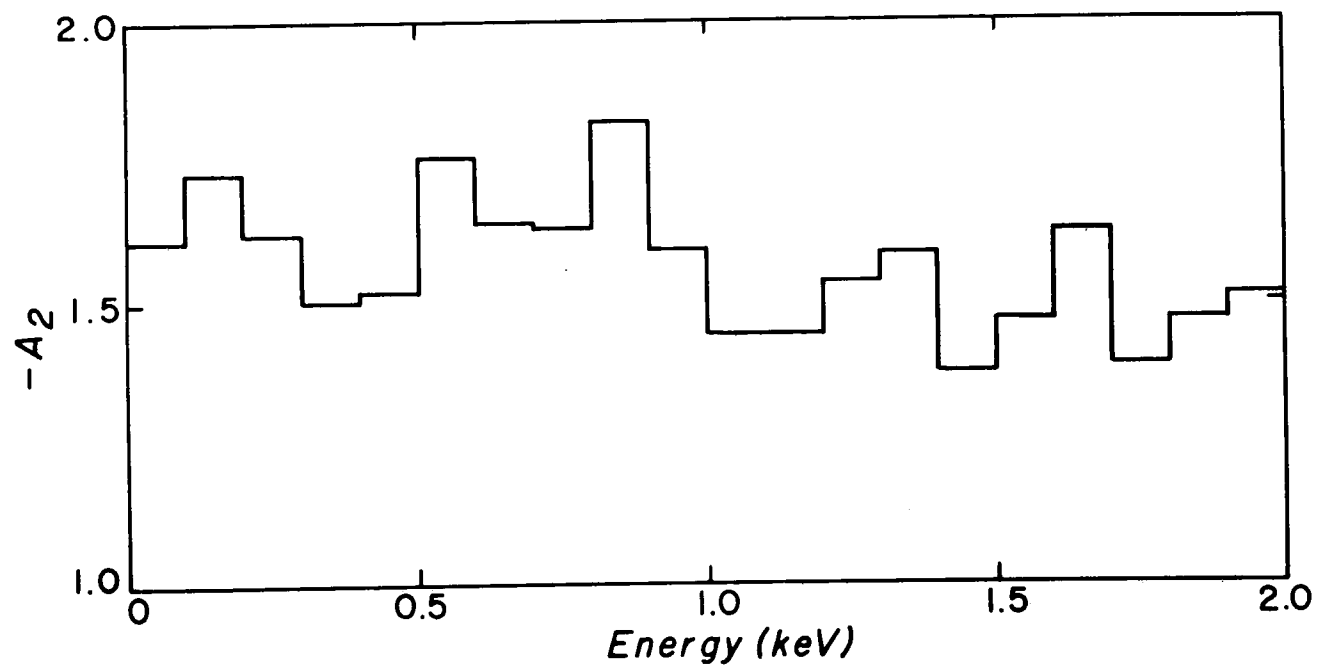


Figure 11. The variation of  $A_2$ , from Pattenden and Postma, versus neutron energy below 2 keV.

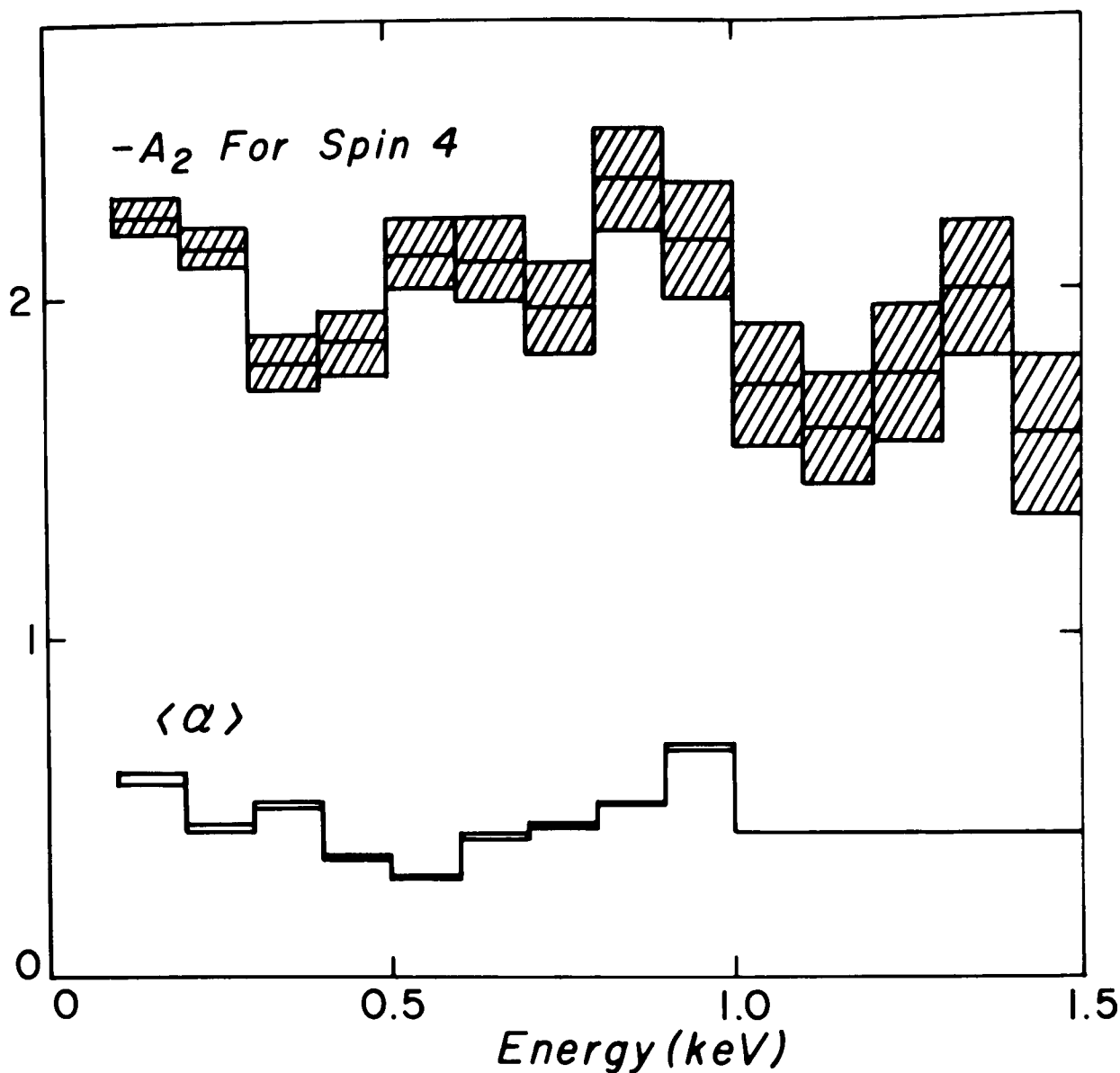


Figure 12. The variation of  $A_2$  from Pattenden and Postma, versus neutron energy below 1.5 keV, calculated under the assumption that the variation is entirely attributable to the spin-4 component. Plotted as the lower curve in this figure is  $\langle \alpha \rangle$ , the capture-to-fission ratio.

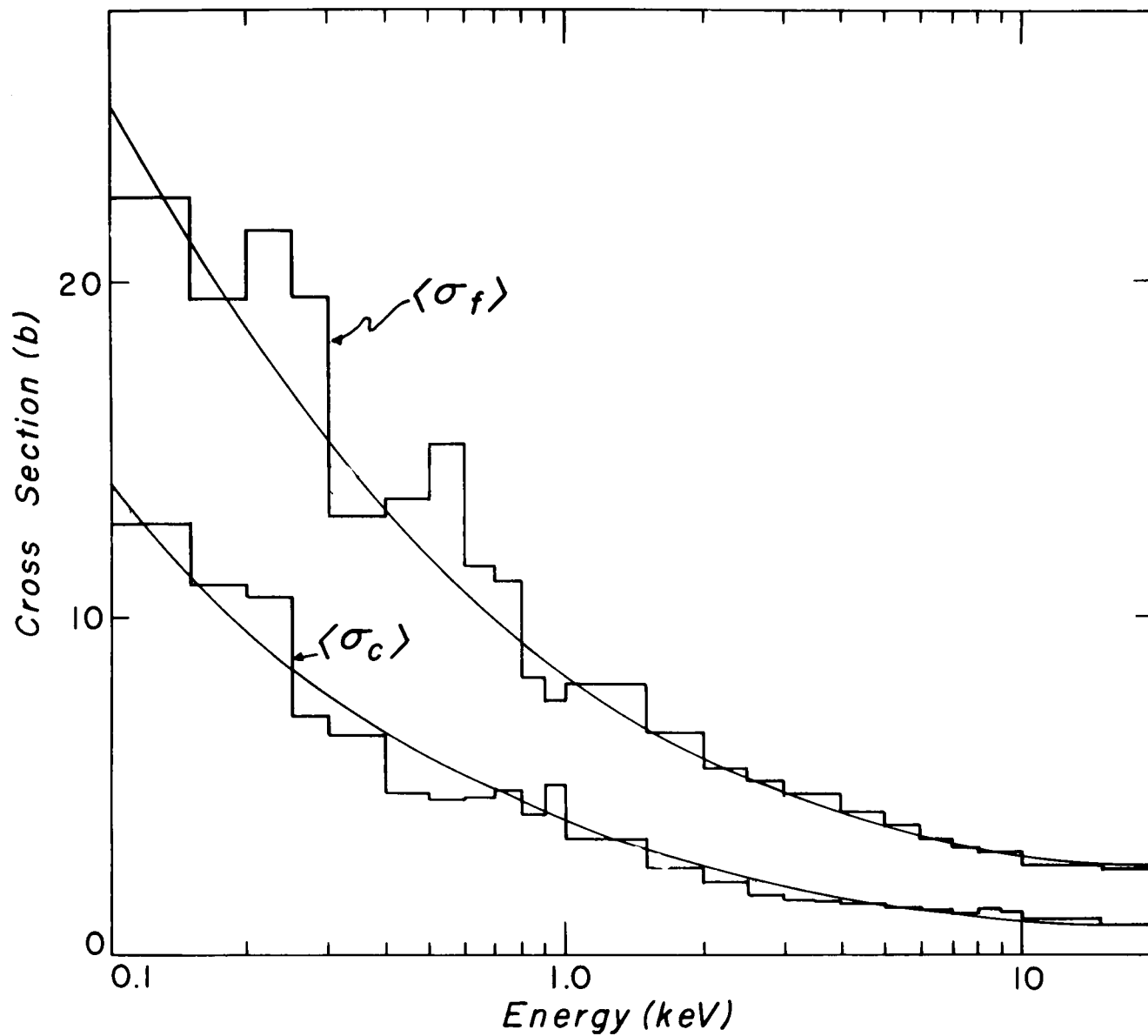


Figure 13. The fission and capture cross sections of  $^{235}\text{U}$  below 25 keV. The histograms reflect the cross section structure reported in ENDF/B-IV; the smooth curves are calculated from parameters in Table II.

## DISCUSSIONS

F. Kaeppler I would like to make a comment. We measured  $\alpha$  in the keV range and find large fluctuations between 20 and 30 keV, much larger than in the fission cross section. The peak-to-valley ratios are 20 to 30%.

M. Moore Where do I get the data?

F. Kaeppler I will present these data at the Lowell Conference.

M. Moore That is just what we need.

C. Bowman The fission cross section fluctuates already by 20 to 30%.

F. Kaeppler Maybe I remember the wrong number. It is definitely more than the fluctuation in the fission cross section.

O. Wasson What is the uncertainty in those  $\gamma$ -values,  $-2.04 \pm$  ?

M. Moore 0.5, that is why I said it is much better than we have any right to expect.

C. Bowman Could you show again the slide with the  $J=4$  cross section in the 8-20 keV range? (Fig. 4)

M. Moore I know the effect you want to point out. If you get a high point in  $J=3$  you expect to get a corresponding low point in  $J=4$ , and you do. These are only the statistical fluctuations and you expect that sort of thing. The statistics are very poor and that is why our Wolfowitz runs-distribution and Levene-Wolfowitz runs-up-and-down tests and serial correlation coefficients followed by a runs-test did not show anything. These things are really fluctuating very wildly.

C. Bowman If you add these two curves together .....

M. Moore You don't get unity.

C. Bowman What do you get? What you are supposed to get for the fission cross section? One that shows a lot less structure?

M. Moore That's right.

C. Bowman You said that if the fission cross section is up, the capture is down. Isn't that obvious from compound nucleus decay, because there is the formation cross section and then there is a total width and .....

M. Moore Yes, but what we are saying is that this is occurring in a definite channel, namely where the fission width is already very small so that the variations which are quite large for the fission width in that channel introduce wild fluctuations.

SIMULATION OF THE STRUCTURE IN  $^{235}\text{U}$  CROSS SECTIONS

G.D. James

UKAEA, Atomic Energy Research Establishment, Harwell, England

## ABSTRACT

The significant structure which has been shown to exist in the neutron induced fission and capture cross sections of  $^{235}\text{U}$  over the energy range 10 keV to 40 keV has been accurately reproduced by a simulation process which enables the energy dependence of the average fission width to be deduced.

## INTRODUCTION

It has been established by several experimenters [1-4] that the fission cross section of  $^{235}\text{U}$  exhibits large fluctuations in the unresolved resonance region. It has also been shown [5] by statistical analyses of simulated  $^{235}\text{U}$  fission and capture cross sections that the observed fluctuations cannot arise from statistical fluctuation of the resonance parameters about energy independent mean values. Furthermore, it was shown [5] that the observed fluctuations could be explained by assuming that the average fission width,  $\Gamma_f$ , is modulated by the presence of levels in the second fission potential barrier minimum according to the equation

$$\Gamma_f' = \Gamma_f + \sum_{\mu} \frac{A^2 \lambda_{\mu} \Gamma_{\mu}}{(E - E_{\mu})^2 + \Gamma_{\mu}^2/4}, \quad (1)$$

Here  $\Gamma_f$  is an energy independent component which belongs to the Class I levels,  $\Gamma_{\mu}$  and  $E_{\mu}$  are the fission widths and level energies for the class II levels and  $A \lambda_{\mu}$  is the coupling between the two potential wells. The work described in reference [5] has been extended by the use of a powerful correlation test due to Wald and Wolfowitz [6] and also by further simulation work to establish values for the four free parameters, in eq(1), which reproduce accurately four statistical quantities derived by applying the Wald and Wolfowitz correlation test and runs test to both the  $^{235}\text{U}$  fission cross section and capture cross section over the energy range 10 keV to 40 keV. This brief report gives a preview of the work which will be published, jointly with G. de Saussure and R. Perez, in a forthcoming paper. A description of the statistical tests applied, the simulation performed and the results obtained in extending the work of reference [5] is given in the next section. In section 3 the results are discussed and summarised and two further investigations which remain to be done are noted.

## STRUCTURE TESTS AND SIMULATION

The quantities simulated and tested for energy dependent structure are average values of the fission and capture cross section of  $^{235}\text{U}$  over 100 eV intervals from 10 keV to 40 keV. In the more recent simulation, quantities FM and GM are generated which, except for an  $E^{-2}$  term, are proportional to 100 eV average values of the fission and capture cross section respectively. They are functions of the spin weighting factors  $g_3$  and  $g_4$ , the neutron widths  $\Gamma_{n3}$  and  $\Gamma_{n4}$ , the fission widths  $\Gamma_{f3}$  and  $\Gamma_{f4}$ , the capture widths  $\Gamma_{\gamma 3}$  and  $\Gamma_{\gamma 4}$  and the level spacings  $D_3$  and  $D_4$  for the spin  $J=3$  and  $J=4$  sequences of resonances and are given by the equations

$$\text{FM} = \sum_{\lambda_3} \frac{g_3 \Gamma_{n3} \Gamma_{f3}}{\Gamma_{n3} + \Gamma_{f3} + \Gamma_{\gamma 3}} + \sum_{\lambda_4} \frac{g_4 \Gamma_{n4} \Gamma_{\gamma 4}}{\Gamma_{n4} + \Gamma_{f4} + \Gamma_{\gamma 4}}$$

$$\text{GM} = \sum_{\lambda_3} \frac{g_3 \Gamma_{n3} \Gamma_{\gamma 3}}{\Gamma_{n3} + \Gamma_{f3} + \Gamma_{\gamma 3}} + \sum_{\lambda_4} \frac{g_4 \Gamma_{n4} \Gamma_{\gamma 4}}{\Gamma_{n4} + \Gamma_{f4} + \Gamma_{\gamma 4}}$$

Here,  $\lambda_3$  and  $\lambda_4$  are respectively the number of  $J=3$  and  $J=4$  levels within a 100 eV interval as determined by selecting levels from a Wigner distribution with level spacing  $D_3$  and  $D_4$ . The following average parameters, taken from Table VI of Milton and Fraser's review paper [7] have been used in the analysis:  $D_3 = 1.26$  eV,  $\Gamma_{f3} = 0.061$  eV,  $\Gamma_{\gamma 3} = 0.046$  eV,  $D_4 = 0.98$  eV,  $\Gamma_{f4} = 0.030$  eV and  $\Gamma_{\gamma 4} = 0.046$  eV. A spin independent strength function of  $10^{-4}$  is assumed, to give  $\Gamma_{n3} = 10^{-4} D_3$  and  $\Gamma_{n4} = 10^{-4} D_4$  at 1 eV. In the analysis carried out so far it is assumed that the average value of  $\Gamma_{f4}$  is energy independent but that  $\Gamma_{f3}$  is given by  $\Gamma_{\lambda f}$  of eq.(1) in such a way that  $\Gamma_{f3} = 0.061$  eV on average over the 30 keV energy range used in the simulation. Individual values of neutron and fission widths are obtained by selecting random values from a Porter-Thomas distribution with the average values given above.

The effectiveness of three statistical tests in detecting the kind of structure likely to be present in the  $^{235}\text{U}$  fission and capture cross sections has been investigated. The tests are the correlation test  $R$  of Wald and Wolfowitz [6], the runs test  $U$  of Wald and Wolfowitz [8] and the runs up-and-down test of  $R(n)$  for runs of length  $n$  of Levene and Wolfowitz [9]. It has been suggested [10] that the use of this last test can be useful when the number of events in the sample is low. It is beyond the scope of this paper to describe these tests and the determination of their significance levels in detail. Comparisons between simulated and actual data are made by means of a factor  $F$  which represents the difference between the observed and expectation values of e.g.  $R$  or  $U$  in units of the standard deviations  $\sigma(R)$  and  $\sigma(U)$ . Thus for the correlation test  $F = (R - E(R))/\sigma(R)$  whereas for the runs test, because of its discrete nature,  $F = (|U - E(U)|/\sqrt{-1/2})/\sigma(U)$ . Values of  $F$  for the Levene and Wolfowitz test are derived from tabulations.

In order to examine these tests, two mock  $^{235}\text{U}$  fission cross section data were obtained, one with intense fission width modulation and one without modulation. These were mixed in ten varying proportions and tested for structure using the three tests listed above. The results obtained, together with the results obtained from  $^{235}\text{U}$  fission cross section [4], are shown in fig. 1. Values of  $F$  for  $R$  and  $U$  increase monotonically with increasing fraction of modulated data finally reaching deviations of about 14 and 11 standard deviations respectively for the maximum modulation. The corresponding values for the  $^{235}\text{U}$  fission cross section are  $F(R) = 8.94$  and  $F(U) = 6.48$ . The lower curves in fig. 1 refer to the runs up-and-down test of run length one,  $R(1)$ , and of run length of maximum significance,  $R_{\max}(n)$ . Neither of these statistics proves useful in detecting the structure under investigation. The  $F$  value for  $R(1)$  remains almost constant at 1.7 SD and is almost independent of the fraction of modulated data. As a function of the fraction of modulated data the  $F$  value for  $R_{\max}(n)$  starts at 1.6 SD and increases to 3.2 SD only to decrease again as the fraction of modulated data increases to 100%. Furthermore, simulated values of  $R(1)$  do not reach the value 3.38 observed for  $^{235}\text{U}$  fission cross section data.

Thus the Levene and Wolfowitz test was abandoned and we restrict our attention to the two Wald and Wolfowitz tests. From fig. 1 it will be seen that the correlation test indicates that the  $^{235}\text{U}$  fission cross section data correspond to a fraction of modulated data of 0.48 whereas the runs test indicates a fraction of 0.61. It is interesting to discover whether these two fractions differ significantly from one another and whether, by changing the four free parameters in eq.(1), mock fission and capture cross sections can be generated for which the four  $F$  values obtained by applying the  $R$  and  $U$  tests to each of these cross sections correspond within statistical accuracy with the values obtained for  $^{235}\text{U}$  viz:  $F(R) = 8.94$  and  $F(U) = 6.48$  for fission and  $F(R) = 3.75$  and  $F(U) = 3.95$  for capture. This analysis has been carried out using the simulated quantities  $FM$  and  $GM$  given in eq.(2). To date, the average fission width modulation given by eq.(1) has been applied only to the  $J=3$  levels and the  $E_1^2$  energy dependence of  $\Gamma_{n3}$  and  $\Gamma_{n4}$  has been omitted. The results obtained over a limited range of unmodulated component of  $3^-$  fission width (the  $\Gamma_{lf}$  of eq.(1)) are shown in fig. 2. The simulated data are illustrated by vertical bars which extend over 2SD in the mean of 10 results and represent the errors which correspond to changing the set of random numbers used in the simulation. These errors were estimated by carrying out each simulation for ten different sets of random numbers. However, not all the vertical bars in fig. (2) were obtained from an actual simulation; in fact, ten simulations were carried out only at  $\Gamma_{lf} = 0.0$  eV, 0.005 eV and 0.01 eV. The circles in fig. 2 represent  $F$  values for  $^{235}\text{U}$  data. They have been plotted at a value of  $\Gamma_{lf} = 0.009$  eV to minimize the discrepancy between the circles and the simulated data. It is found that  $\Gamma_{lf}$  and  $A^2\lambda_{\mu}$  in eq.(1) are linearly related in the process of making  $\Gamma_{lf} = 0.060$  and the positioning of the  $^{235}\text{U}$  data at  $\Gamma_{lf} = 0.009$  corresponds to the following average modulation parameters:

$$\langle A^2\lambda_{\mu} \rangle = 18.7 \pm 7.1 \text{ eV}, \quad \langle \Gamma_{\mu} \rangle = 1000 \pm 380 \text{ eV}, \quad \langle D_{\mu} \rangle = 2000 \pm 800 \text{ eV}.$$

The errors quoted here are derived from the Porter-Thomas and Wigner distributions of these parameters for the 14 levels used, on average, in the analysis. Table I lists the simulated and experimental values of  $F$  obtained

at  $\Gamma_f = 0.009$  eV and their difference in units of SD in an individual reading. Fig. 3 shows an example of GM and FM and the 100 eV average modulated fission width ( $\Gamma_f$  of eq.(1)) obtained in one of the simulations.

### CONCLUSION

The results presented in this paper show that of the three distribution free statistical tests examined, only the two due to Wald and Wolfowitz are suitable for detecting the kind of structure encountered in the  $^{235}\text{U}$  fission cross section. These two tests show conclusively at a high significance level the presence of structure in the fission and capture cross sections of  $^{235}\text{U}$  averaged over 100 eV intervals in the energy range 10 keV to 40 keV. The correlation test is more powerful than the runs test and gives a significance level for the structure in the  $^{235}\text{U}$  fission cross section equal to that corresponding to 8.94 SD for a normal distribution. It has been possible to simulate the statistical results derived from the fission and capture cross sections of  $^{235}\text{U}$  by modulating the  $\bar{\Gamma}$  average fission width according to eq.(1) with modulation parameters which are given in the text. These results would enable the  $^{235}\text{U}$  cross sections to be simulated more accurately in reactor calculations, for instance. However, the derived class II level spacing of 2000 eV can be translated, using a level density formula [11], into a difference in height between the first and second fission potential barrier minimum of 4.12 MeV. This is not in agreement with the currently accepted difference of about 3 MeV (see reference [11] fig. 94). which corresponds to a class II level spacing of about 200 eV. An investigation will be carried out to see if a solution as acceptable as the present one is possible with a much reduced class II level spacing. The effect of modulating the J=4 resonances rather than the J=3 resonances will also be examined.

### REFERENCES

1. B.H. PATRICK, et al., J. Nucl. Energy, 24, 269 (1970).
2. J.R. LEMLEY, et al., Nucl. Sci. Eng., 43, 281 (1971).
3. C.D. BOWMAN, et al., Proc. Second Conf. on Nuclear Data for Reactors, IAEA, Vienna (1970) II. p.65.
4. G. de SAUSSURE et al. Trans. Am. Nucl. Soc., 14, 370 (1971).
5. G.D. JAMES, G. de SAUSSURE and R. PEREZ. Trans. Am. Nucl. Soc. 17, 495 (1973).
6. A. WALD and J. WOLFOWITZ, Annals Math. Stat. 14, 378 (1943).
7. J.D. MILTON and J.S. FRASER, Annual Rev. Nucl. Sci. 16 (1966).
8. A. WALD and J. WOLFOWITZ, Annals Math. Stat. 2, 147 (1940).
9. H. LEVENE and J. WOLFOWITZ, Annals Math. Stat. 15, 58 (1944).
10. Y. BAUDINET-ROBINET and C. MAHAUX, Phys. Lett. 42B, 392 (1972).

11. A. MICHAUDON, Nuclear Fission. Advances in Nuclear Physics (Eds. M. Barranger and E. Vogt) Plenum Press, New York, 1973 p.173.

TABLE I

Simulated and experimental F values for  $^{235}\text{U}$

	Simulated F	Experimental F	Difference/SD
$\sigma_F$ Correlation	9.35 $\pm$ 1.54	8.94	0.27
$\sigma_F$ Runs	5.95 $\pm$ 1.67	6.48	0.32
$\sigma_C$ Correlation	4.85 $\pm$ 2.01	3.75	0.55
$\sigma_C$ Runs	3.45 $\pm$ 2.06	3.27	0.09
Average $\Gamma_{f3}$	0.060 $\pm$ 0.021 eV	0.060 eV	0.0

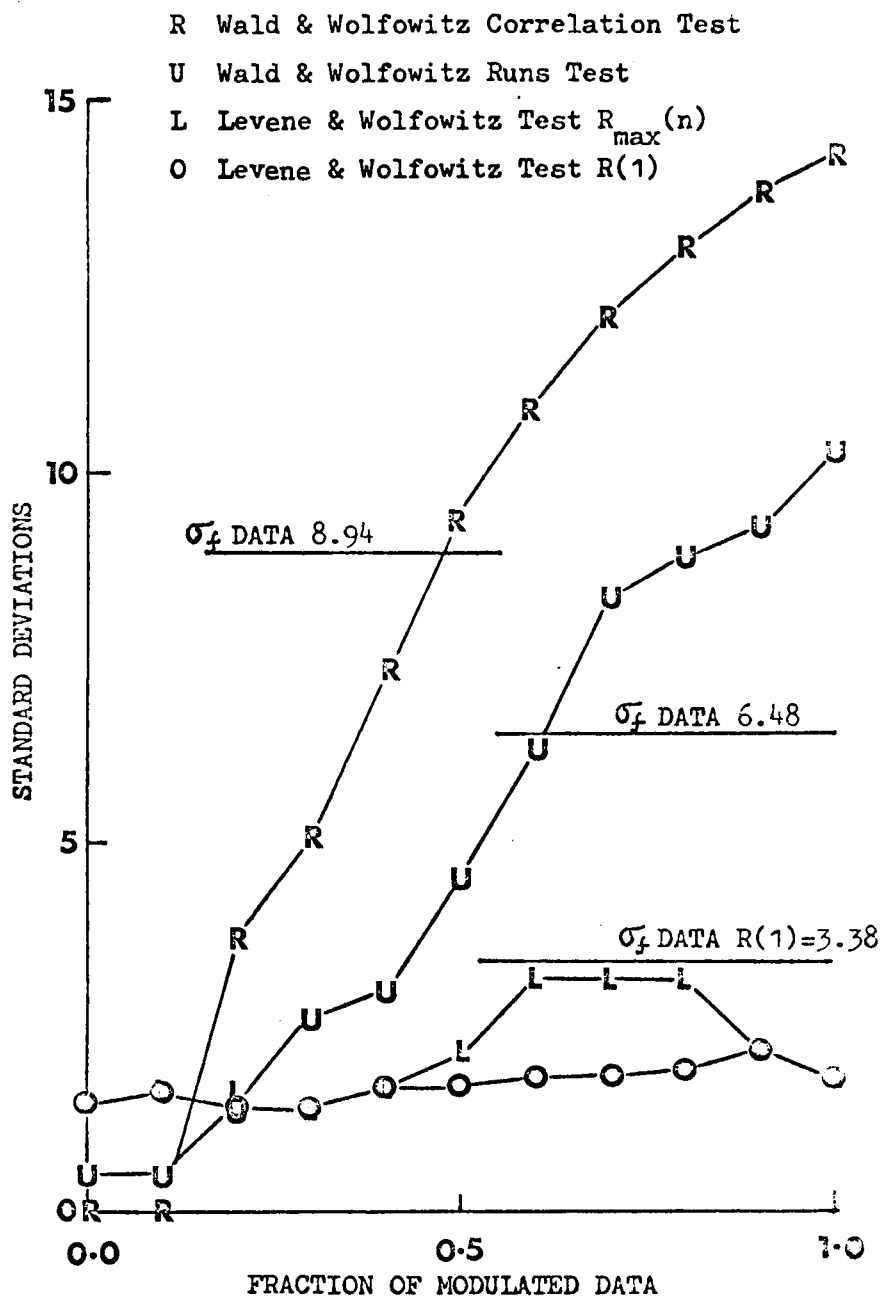


Figure 1. Results of three statistical tests on simulated fission cross section data obtained by mixing a data set with a constant average fission width with a data set in which the fission widths are strongly modulated by class II levels. Both tests due to Wald and Wolfowitz show a monotonic increase with increasing modulation of  $\Gamma_f$  up to 14.2 SD and 10.2 SD respectively. Both these tests indicate that the measured  $^{235}\text{U}$  fission cross section is similar to the simulated data at 50% of the maximum fission width modulation. The runs up-and-down test of Levene and Wolfowitz gives an unreliable indication of the degree of modulation in this instance.  $R(1)$  is completely independent of the fraction of modulated data.

## Structure statistics for U-235 compared with simulated data

- Data for U-235 from  $\sigma_f$  and  $\sigma_c$
- | Simulated results. Range of two S.D.

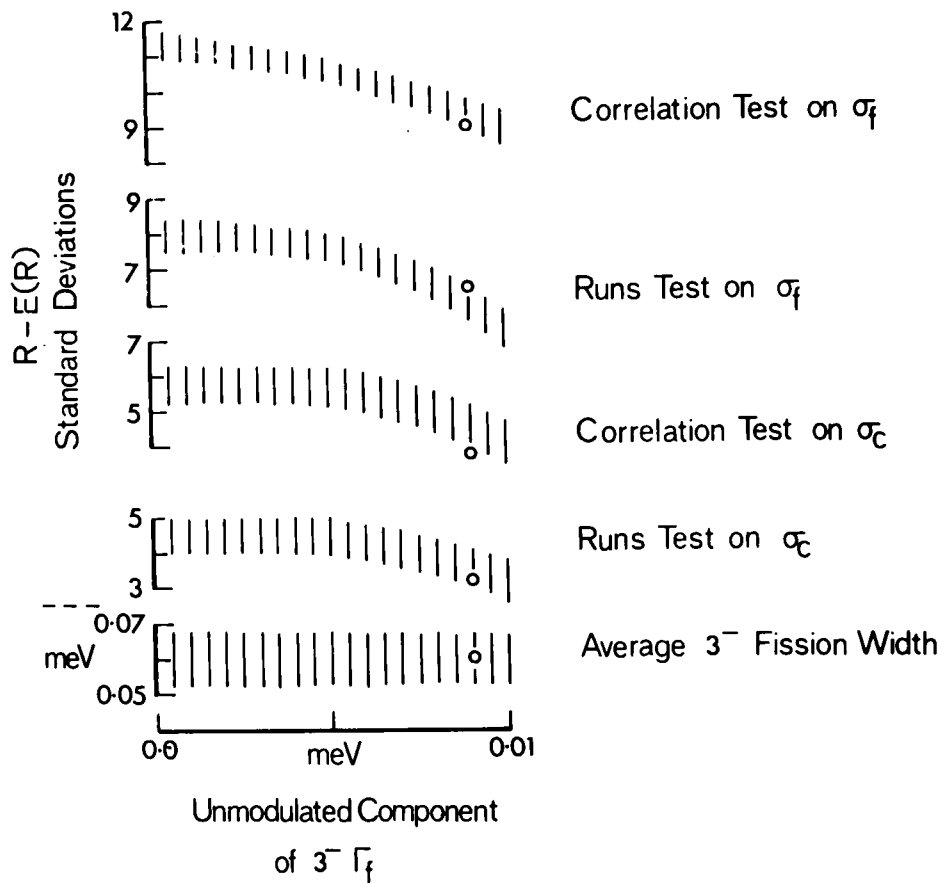


Figure 2. Structure statistics for U-235 compared with simulated data. Results obtained by applying the correlation test and the runs test to 100 eV average values of the  $^{235}\text{U}$  fission and capture cross are shown by the open circles and compared with simulated results, derived from the functions FM and GM, which are shown by vertical bars representing a range of 2SD. The abscissa shows the  $\Gamma\lambda f$  of eq.(1).

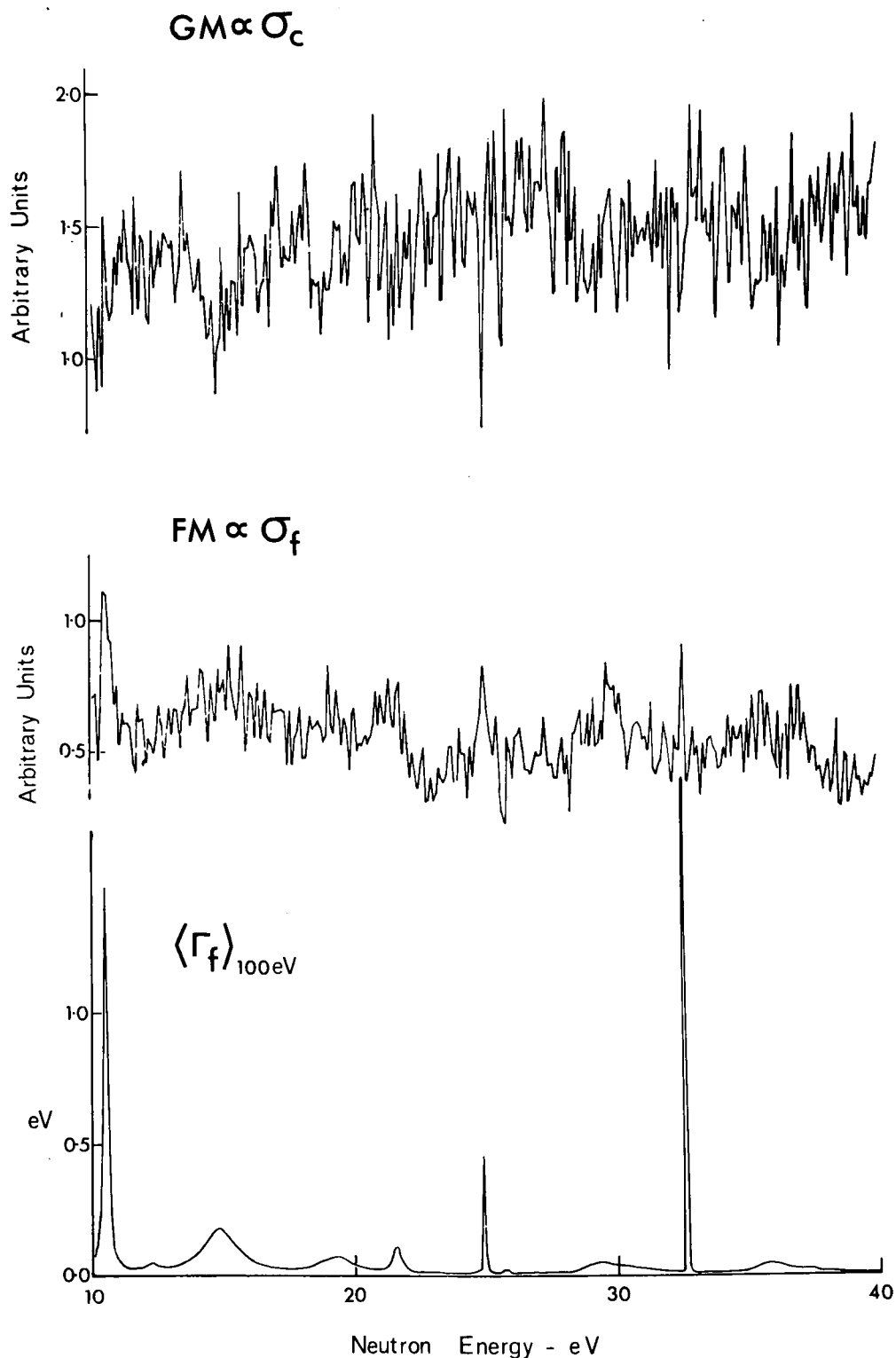


Figure 3. A particular example of the simulated functions FM and GM which, ignoring an  $E^{-1/2}$  energy dependence, are proportional to the  $^{235}\text{U}$  fission and capture cross section when averaged over 100 eV intervals. The average modulated fission width defined by eq.(1) is also shown.

*DISCUSSIONS*

C. Bowman How high in energy did you feel you would be able to predict structure in U-235?

G. James Once you know what the crude cause is, I do not see why you should not do it up to any energy you like. Whether you still can see anything is another question.

# THE ENERGY GAP AT THE SADDLE POINT DEFORMATION OF $^{236}\text{U}$

F. Käppeler and F. Dickmann  
Kernforschungszentrum Karlsruhe,  
75 Karlsruhe, Postfach 3640,  
West Germany

## ABSTRACT

A steep increase in the fission cross section of  $^{235}\text{U}$  at .95 MeV neutron energy was interpreted as due to the onset of quasi particle excitations in  $^{236}\text{U}$ . Together with the result of a recent evaluation of the  $^{236}\text{U}$  fission barrier an improved value of the energy gap at the saddle point deformation  $2\Delta_{\text{gs}} = 1.79 \pm 0.2$  MeV was determined. This value is discussed with respect to current assumptions on the deformation dependence of the pairing force parameter  $G$ .

## INTRODUCTION

Experimental information on the deformation dependence of single particle parameters or the pairing force matrix element  $G$  is of particular interest for the description of nuclear fission because quantitative calculations still suffer from systematic uncertainties due to assumptions or extrapolations of these quantities.

## DETERMINATION OF THE PAIRING GAP

As the energy gap  $2\Delta$  is closely related to the pairing force parameter  $G$  [Ref. 1] a comparison of the energy gap in the ground state and the saddle point yields information about the variation of  $G$  with increasing nuclear deformation. Fig. 1 shows a typical fission barrier with the respective energy gap for the ground state and saddle point deformations. For the ground state deformation the magnitude of the energy gap is equal to the energy of the first two quasi particle excitations as is indicated in Fig. 1. In  $^{236}\text{U}$  these states have been observed by Katori et al. [2] in a recent (d,p)-measurement with excellent energy resolution. From their result the experimental value for the energy gap is

$$2\Delta_{\text{gs}} = 0.970 \pm 0.002 \text{ MeV.}$$

This value is in good agreement with the energy gap given by Gilbert and Cameron [3], which however has an uncertainty of about 200 keV. Compared to

this experimental result the energy gap calculated from mass differences of adjacent nuclei is found to be 0.3 MeV larger when corrections for differences in the surface, coulomb and symmetry energies are applied [4,5]. Furthermore we shall refer to the value of Katori et al. because the pairing gap at the saddle point will also be determined from the energy of the first two quasi particle excitations.

As is obvious from Fig. 1 the pairing gap at the saddle point is the difference of the two quasi particle energy  $E^*$  relative to the ground state and the energy of the fission barrier  $E_B$ ,  $2\Delta_s = E^* - E_B$ . Experimental values for the fission barrier of the even compound nuclei were derived by Back et al. [6] from the fission probability in charged particle induced fission. These authors report an inner barrier  $E_A = 5.70 \pm 0.2$  MeV and an outer barrier  $E_B = 5.68 \pm 0.2$  MeV.

An experimental determination of  $E^*$  can be expected from the observation of those quantities which are affected by the increase of intrinsic excitations caused by the population of two quasi particle states. This concerns mainly the fission cross sections and the fragment angular distributions.

A value of  $E^* = 7.4 \pm 0.2$  MeV was found by Britt et al. [7] from the analysis of the fragment angular anisotropy in the  $^{235}\text{U}$  (d,pf) reaction. From this value together with the new barrier parameters Britt and Huizenga [8] estimated the energy gap at the saddle of  $^{236}\text{U}$  to be  $2\Delta_s = 1.70 \pm 0.4$  MeV. This value is much smaller than the older result in Ref. [7] which was  $2\Delta_s = 2.10$  MeV. It should be noted that according to Ref. [2] two quasi particle excitations with appreciable spin ( $K = 4^-$ ) show up only 80 keV above the lowest two quasi particle excitations with  $K = 1^-$ . The small K-value of the lowest two quasi particle excitations make it difficult to observe their appearance via the angular anisotropy.

It was pointed out earlier by Britt et al. [9] that the onset of quasi-particle states should also be observed in neutron fission cross sections. An increase in  $\sigma_f$  due to these new fission channels is expected at a neutron energy  $E_n = E^* - B_n$ , where  $B_n$  denotes the neutron binding energy. Up to 1972 the fission cross section data for  $^{235}\text{U}$  around 1 MeV have not been sufficient in resolution to allow an evaluation of  $E^*$ . Recently, three new measurements were reported [10,11,12] which all show a distinct increase of  $\sigma_f$  at 1 MeV. Fig. 2 shows the results of Ref. [11]. In neutron energy the resolution is about 23 keV. The error bars of Fig. 2 include only uncertainties due to counting statistics and energy dependent corrections since here our main interest is the shape of the cross section curve and not its absolute value. The step-like increase of about 15 % at a neutron energy of  $E_n = 945 \pm 25$  keV can be interpreted as the onset of quasiparticle states for two reasons. First, the width of the increase is much smaller than can be expected for a collective fission channel. From the fission barrier parameters the width of the increase in  $\sigma_f$  due to the opening of collective channels is expected to be several hundred keV while the structure of Fig. 2 is only 50 to 100 keV broad. The second argument for the above interpretation is the behaviour of the fragment angular anisotropy A, as a function of neutron energy. Values of A from Ref. [13,14,15] are also shown in Fig. 2. Although the experimental uncertainties of these data are considerably larger than for the cross section values, the correlation between both quantities is obvious. For small values of the quantum number K (due to collective states) the anis-

otropy rises with neutron energy because of the increasing angular momentum transfer. The decrease beyond 945 keV is caused by the larger K values of the quasi particle states which are then available.

The neutron binding energy  $B_n$  is taken from Matussek et al. [16] who found  $B_n = 6545 \text{ keV} \pm 1 \text{ keV}$ . Thus the onset of two quasiparticle states in  $^{236}\text{U}$  due to the break-up of a neutron pair can be calculated. One finds  $E^* = E_n + B_n = 7.490 \pm 0.025 \text{ MeV}$ . Together with the fission barrier value of Ref. [6] the energy gap in  $^{236}\text{U}$  results,

$$2\Delta_s = 1.79 \pm 0.2 \text{ MeV},$$

in good agreement with Ref. [8]. It should be mentioned that Poenitz [12] measured the fission cross section to higher energies and found a less pronounced structure in the range of excitation energies from 8.0 - 8.5 MeV. A corresponding decrease in the angular anisotropy A was reported in Ref. [7] and tentatively interpreted as the break-up of a proton pair.

## DISCUSSION

As the present value for the neutron gap  $2\Delta_s$  is less uncertain than previous results, it might be of interest to compare it to theoretical values for different assumptions about the deformation dependence of the pairing force parameter G. This comparison is based on the work of Pauli and Ledergerber [17] and of Brack et al. [18]. Starting from the ground state values  $\Delta_{gs}$  and  $G_{gs}$  the respective quantities at the saddle point configuration were determined assuming  $G = \text{const}$  as well as G proportional to the surface S of the nucleus. In order to avoid systematic uncertainties the ratios  $\Delta_s/\Delta_{gs}$  are used for the comparison. Both, theoretical and experimental values are listed in Table I. The increase of  $\Delta$  for  $G = \text{const}$ . is caused by the higher level density near the fermi surface at the saddle point deformation. The comparison with the experimental ratio shows immediately that the calculated result for  $G = \text{const}$ . lies outside the error limits of the experimental values. On the other hand  $G \sim S$  leads to a theoretical value of  $\Delta_s$  which is smaller than the experimental one. A similar behaviour - but not as well established - shows up for the above mentioned proton gap. For this case the calculation yields  $\Delta_s/\Delta_{gs} = 1.37$  while the experimental estimate is  $1.87 \pm 0.6$ .

The strength of the residual interaction also influences the collective inertia and thus the dynamics of the fission process. Theoretical calculations [19] using the cranking model for the mass-tensor can reproduce spontaneous fission half lives only if the pairing force is assumed to increase with deformation.

In summary, it seems well established that the energy gap  $\Delta$  shows a pronounced increase with deformation. For a consistent theoretical explanation one therefore has to assume that the pairing force parameter G is also deformation dependent. However, the experimental value for  $\Delta_s$  is not accurate enough to allow a conclusion as to whether the surface pairing hypothesis  $G \sim S$  holds. It might be that G depends even stronger on the nuclear deformation. An alternative possibility to obtain a larger pairing gap  $\Delta$  with increasing deformation is offered by the quadrupole pairing model [20].

## REFERENCES

1. A. BOHR, B.R. MOTTELSON and R.A. PINES, *Phys. Rev.* 110 (1958) 936.
2. K. KATORI, A.M. FRIEDMAN and J.R. ERSKINE, *Phys. Rev.* C8 (1973) 2336.
3. A. GILBERT and A.G.W. CAMERON, *Can. J. Phys.* 43 (1965) 1446.
4. P.E. NEMIROWSKY and Yu. V. ADAMCHUK, *Nucl. Phys.* 39 (1962) 551.
5. A.H. WAPSTRA and N.B. GOVE, *Nuclear Data Tables* 9 (1971) 267.
6. B.B. BACK, O. HANSEN, H.C. BRITT, and J.D. GARRETT, *Phys. Rev.* C9 (1974) 1924.
7. H.C. BRITT, F.A. RICKEY and W.S. HALL, *Phys. Rev.* 175 (1968) 1525.
8. H.C. BRITT, and J.R. HUIZENGA, *Phys. Rev.* C9 (1974) 435.
9. H.C. BRITT, W.R. GIBBS, J.J. GRIFFIN and R.H. STOKES, *Phys. Rev.* 139 B (1965) 354.
10. D.B. GAYTHER, D.A. BOYCE and J.B. BRISLAND, *Neutron Standard Reference Data*, IAEA, Vienna, (1974) p. 201.
11. F. KÄPPELER, *Neutron Standard Reference Data*, IAEA, Vienna, (1974), p.213.
12. W.P. POENITZ, *Neutron Standard Reference Data*, IAEA, Vienna (1974), p.189.
13. V.G. NESTEROV, G.N. SMIRENKIN and I.I. BONDARENKO, *Sov. J. At. Energy* 11 (1962) 900.
14. R.B. LEACHMAN and L. BLUMBERG, *Phys. Rev.* 137 B (1965) 814.
15. J.E. SIMMONS and R.L. HENKEL, *Phys. Rev.* 120 (1960) 198.
16. P. MATUSSEK, W. MICHAELIS, C. WEITKAMP and H. WODA, *Proc. IAEA Symp. on Progress in Safeguard Techniques* (IAEA, Vienna, 1970), Vol. II, p.113.
17. H.C. PAULI, and T. LEDERGERBER, *Nucl. Phys.* A 175 (1971) 545; also private communication.
18. M. BRACK, J. DAMGAARD, A.S. JENSEN, H.C. PAULI, V.M. STRUTINSKY and C.Y. WONG, *Rev. Mod. Phys.* 44 (1972) 320.
19. T. LEDERGERBER and H.C. PAULI, *Nucl. Phys.* A 207 (1973) 1.
20. D.R. BES and R. BROGLIA, *Phys. Rev.* C3 (1971) 2349;  
D.R. BES, R. BROGLIA and B. NILSSON, *Phys. Lett.* 40B (1972) 338.

TABLE I

Ground state and saddle point values of the pairing force parameter  $G$  and the gap parameter  $\Delta$  for  $^{236}\text{U}$

	$B_s^a$	Calculated Values				Experimental Values
		G=const.		$G \sim S$		$\Delta$ (MeV)
		G(MeV)	$\Delta$ (MeV)	G(MeV)	$\Delta$ (MeV)	
Ground State	1.013	.122	.52	.124	.55	.485 $\pm$ .001
Saddle Point	1.105	.122	.64	.136	.913	.895 $\pm$ .1
Ratios	1.095	1.00	1.23	1.095	1.66	1.84 $\pm$ .2

$$B_s^a = \frac{\text{surface } S}{\text{spherical surface } S_0}$$

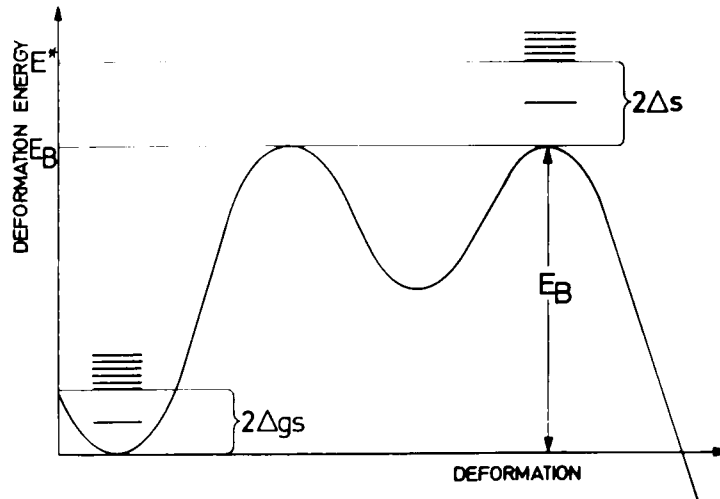


Fig. 1 Schematic view of the two-humped fission barrier indicating the energy gaps for the ground state and saddle point deformation.

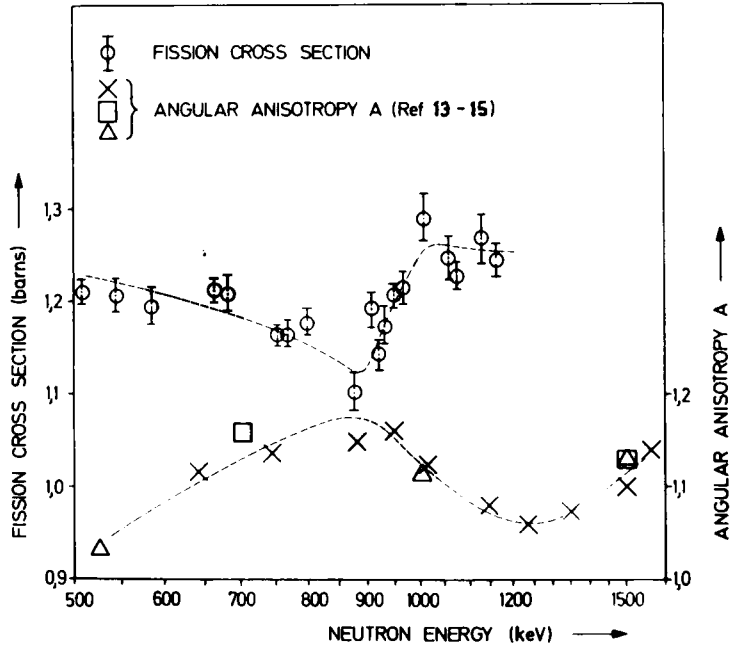


Fig. 2 Correlation between the fission cross section and the fragment angular anisotropy  $A = d\sigma_f(0^\circ)/d\sigma_f(90^\circ)$  for  $^{236}\text{U}$ .

## DISCUSSIONS

A. Smith It looks to me that the anisotropic you showed is smaller than G. Knoll reported.

G. Knoll I did not catch the numbers.

A. Smith You are running something like 1.2.

F. Kaeppeler The anisotropic had the scale on the right side--you may have picked the values from the fission cross section.

W. Poenitz How about other nuclei like U-233 or Pu-239?

F. Kaeppeler We looked only at U-235. It appears at least in Pu-239 that there is no structure at these energies.

# WHAT HAPPENS TO THE FISSION PROCESS ABOVE THE 2ND- AND 3RD-CHANCE FISSION THRESHOLDS?

Leona Stewart

Los Alamos Scientific Laboratory, University of California  
Los Alamos, New Mexico 87545

Robert J. Howerton

Lawrence Livermore Laboratory  
Livermore, California 94550

## ABSTRACT

Although the multiple fission process is important at high neutron energies, most of the evaluations available today do not include these individual fission cross sections or their associated fission spectra. The representations used in the Los Alamos and Livermore libraries are described and calculations compared with 14-MeV integral experiments available on  $^{235}\text{U}$ ,  $^{238}\text{U}$ , and  $^{239}\text{Pu}$ . Further work is needed to clearly delineate the specific problems in order to propose unique solutions.

## INTRODUCTION

For several decades, experimentalists have reported a significant increase in the total fission cross section for all fissionable nuclides above the 2nd- and 3rd-chance fission thresholds. As late as the 1970's, however, most evaluators have consistently ignored the individual fission channels ( $n, n'f$  and  $n, 2nf$ ) in their analyses of the energy-dependent cross sections and the spectra of the neutrons associated with the fission process. For example, explicit representations of the  $n, n'f$  and  $n, 2nf$  cross sections are omitted in all of the ENDF/B-IV evaluations except for  $^{235}\text{U}$ ,  $^{238}\text{U}$ ,  $^{239}\text{Pu}$ , and  $^{240}\text{Pu}$ .† The evaluations of Howerton included in the LLL-ENDL files [1] represent these processes implicitly by presenting a total fission cross section with pre-processed tabular energy distributions derived from consideration of the individual fission channels. While the LASL and LLL evaluations differ in form of presentation, both laboratories take into account the 2nd-, 3rd-, and 4th-chance fission processes. On the other hand, the evaluations of Konshin [2] and Sowerby et al. [3] deal only with the total fission cross sections and thereby ignore the multiple-chance fission processes.

It is thus appropriate at this time to bring the needs of the evaluators and users to the attention of the experimentalists and theorists involved in the study of the fission process. Because little is known about 2nd- and 3rd-chance fission, except that the competing channels exist, the evaluator must make estimates in order to present hopefully reasonable spectral information of the fission neutrons. The first known attempts to represent these processes were made and published by Howerton [4] and, in fact, the representations used today are not changed very much from this original attempt.

### THE MULTIPLE FISSION PROCESS

In much of the discussion which follows,  $^{238}\text{U}$  has been chosen as an example. Our conclusions, however, apply to all of the fissionable nuclides.

Figure 1 is a schematic showing the reaction channels available when neutrons are incident on  $^{238}\text{U}$ . Although the diagram is simplistic, it is not intended to limit the interactions to compound nuclear processes. For example, the  $(n, n'\gamma)$  channel includes both pre-equilibrium and compound nuclear reactions. Note that first-chance fission defines the fissioning of the aggregate nucleus  $^{239}\text{U}$ ; second-chance,  $^{238}\text{U}$ ; third-chance,  $^{237}\text{U}$ , etc.

Figure 2 shows the fission cross sections for  $^{238}\text{U}$  for each individual fission channel. While this representation is taken from ENDF/B-IV, the ENDL library is quite similar in all of the aspects discussed here. Note that first-chance fission is assumed to be constant upon the onset of second-chance fission. This is in contradiction to the evaluation of Tuttle [5] who reduced the first-chance fission cross section to approximately zero immediately upon the onset of second-chance fission.

In most of the evaluations used today, the emission of charged-particles is assumed to be zero due to the high Coulomb barrier and the reportedly low charged-particle yields for the few experiments available. With this assumption, the only channels available to the system below the  $(n, 2n)$  and  $(n, n'f)$  threshold (6.07 MeV for  $^{238}\text{U}$ ), are the elastic,  $(n, \gamma)$ ,  $(n, n'\gamma)$  and  $(n, f)$ . At 11.51 MeV, the  $(n, 3n)$  and  $(n, 2nf)$  channels open and lend to the confusion of separating the competition into individual channels.

Although the total fission cross section  $(\sigma_{n, F})^{\dagger\dagger}$  may be well determined, the spectra of the neutrons associated with the fission process are not, especially in the MeV range. The problem is often related to the method used in the determination of the spectra; for example, most measurements are made of the total neutron emission cross section, that is

$$\sigma_{\text{emis}} = \sigma_{n,n} + \sigma_{n,n'} + 2\sigma_{n,2n} + 3\sigma_{n,3n} + \bar{\nu}\sigma_F + \dots, \quad (1)$$

and usually restricted to data taking at one angle, only. Unfolding the measurements in order to obtain the fission spectra is subject to large errors due to the many assumptions which must be introduced. Following a suggestion of Batchelor et al. [6], Howerton and Doyas [7,8] investigated fission temperatures in 1969 and 1971. The main thrust of the Batchelor et al. suggestion was that the value of  $\bar{\nu}$  used in the well-known Terrell relationship [9] should be appropriate only to that fraction of the neutrons which comes from the direct fission process. The practical consequence of this suggestion is that assumptions must be made in the separation of the direct, 2nd-, and 3rd-chance fission processes above the  $n,n'$ ;  $n,2n$ ; and  $n,3n$  thresholds. After attributing these fractions, a quantity  $\bar{\nu}_f(E)$  can be deduced that is more appropriate for application in the Terrell relationship.

It is readily apparent from Eq. (1) that few of the cross sections are well known at energies near 14 MeV. Almost nothing is known about the angular or energy distributions of the emitted neutrons, with the possible exception of the elastic (plus some inelastic) cross section. Even though we know that the angular distributions of the fission fragments are often very anisotropic and we include the fact that the neutrons emitted at the scission point are emitted from the moving fragments, all of the evaluations in use today contain the assumption that the fission neutrons are emitted isotropically in the laboratory reference frame. Therefore, both the evaluated spectrum and angle of emission of the fission neutrons are often incorrect.

The final sine qua non of the fission process that must be supplied by the evaluator is  $\bar{\nu}(E)$ . For several of the most important fissionable isotopes, this quantity has been determined by experiment [10]. In 1964 Schuster and Howerton [11] addressed the problem for uranium with a plausibility argument for the derivation of an empirical relationship between  $\bar{\nu}$  and  $E_n$ . In 1971, Howerton [12] extended the previous work to provide a method for predicting  $\bar{\nu}(E)$  for thorium, uranium, and plutonium isotopes in cases where this quantity has not been determined by measurement. Essentially the same assumptions about the energy dependence of the multiple-chance fission processes were made by Vasil'ev et al. [13] who also introduced the plausibility of nonlinear variation of  $\bar{\nu}(E)$  above the 2nd-chance fission threshold. These authors, however, provided no quantitative estimates of  $\bar{\nu}(E)$ .

Although not the subject of this paper, it should be noted that the  $(n,n')$ ,  $(n,2n)$ , and  $(n,3n)$  cross sections are rarely well determined experimentally at high neutron energies and the spectra have not been measured at all. Minimal information can be obtained from the observation of the total emission spectra,

at least for the contribution of the pre-equilibrium processes since these stand out above the various fission channels at the high-energy end. The only recent detailed experiments are those of Kammerdeiner [14], who measured the spectra at several angles for 14-MeV neutrons incident on  $^{235}\text{U}$ ,  $^{238}\text{U}$ , and  $^{239}\text{Pu}$ .

The main purpose of this paper is to call attention to the fact that the evaluator must supply much more information on fission than a measure of the total fission cross section. For the fissile and fertile materials, measurements of the other cross sections are also very important, especially at the higher energies.

In most of the evaluations in use today, the fission process is treated in one of the following ways:

1. Only the total fission cross section is represented; the fission neutron energy distribution is assumed to be Maxwellian in shape with the average energy increasing with incident neutron energy.
2. The total fission cross section is separated into its various parts; the choice made in ENDF/B-IV is shown in Fig. 2. Then, the neutron (or neutrons) which precedes scission is assumed to be emitted with a spectrum far softer than allowed for the scission neutrons. For example, at 14 MeV for  $^{238}\text{U}$ , the two neutrons which come off before scission would have energies between zero and 2.49 MeV (the total energy available to the pre-scission neutrons). Therefore, it is apparent that the treatment of the competition of the first- and second-chance fission process should be an important part of each evaluation.

#### COMPARISON WITH SOME 14-MeV INTEGRAL EXPERIMENTS

Two different types of integral experiments have been carried out, one at LASL by Ragan et al. [15] which was made on  $^{235}\text{U}$  with a multiplication of approximately 10-11, and one at LLL by Wong et al. [16] on  $^{235}\text{U}$ ,  $^{238}\text{U}$ , and  $^{239}\text{Pu}$  which are more differential in nature with a multiplication of approximately 0.9 for  $^{238}\text{U}$  and 1.4 for  $^{235}\text{U}$  and  $^{239}\text{Pu}$ . In both experiments, spherical shells of the target surround a 14-MeV neutron source and the neutron spectra emerging from the sphere are recorded at one or more angles with respect to the incident neutron direction.

Figures 3a and 3b compare the spectrum of the neutrons as measured by Ragan et al. [15] and with the calculation using the ENDF/B-IV data file (MAT-1262) and the ENDL evaluation by Hower-ton [1]. Note that the energy scale in Figs. 3a and 3b is changed near 4 MeV in order to show all of the data on the same graph.

While ENDF/B-IV shows fairly good agreement with experiment except for the energy bins between 6 and 10 MeV, the differences between the ENDF and ENDL evaluations are much larger than one would expect from a perusal of the data in the files, themselves. These differences are better illustrated in Fig. 4, which shows the ratio of the calculated to experimental measurements (C/E) for both the ENDF and ENDL evaluations.

Figure 5 shows the comparable experiment performed on  $^{235}\text{U}$  at LLL. To complete the analysis on the available data, the LLL experiments on  $^{238}\text{U}$  and  $^{239}\text{Pu}$  have been compared with calculations in Figs. 6 and 7. Table I gives tabular values of the integrals of the calculated and experimental spectra in three energy domains of the emitted neutrons.

### SUMMARY AND CONCLUSIONS

In summary, this paper points out various problem areas in the evaluation of the cross sections and parameters associated with the fissionable nuclides. In addition, the comparison of the ENDF and ENDL libraries with experiment may even suggest errors in the files or in the calculational procedures presently employed. While all of the calculations shown were made using Monte Carlo techniques and thereby suffer somewhat from statistical accuracy, they did include all of the geometrical factors of the experiments. Further work will be undertaken to elucidate these problem areas.

At the same time, however, experimental information above 8-10 MeV is urgently required. For example, a measurement of the fission spectrum at several angles using fragment coincidence techniques would be very useful, especially if carried out at several incident neutron energies. (A need for (n,2n) and (n,3n) experiments using coincidence and anti-coincidence techniques is also apparent as are determinations of the direct and/or pre-equilibrium components of the (n,n' $\gamma$ ) reaction.) At several energies below 9 MeV, the shape of the fission spectrum should be measured at several angles; again a fragment coincidence experiment is required. Similar experiments should be repeated in the 14-MeV range.

Finally, theorists could lend great insight into determining how to treat the fission process, especially in the region above the second- and third-chance fission thresholds. Most of the calculations available today are limited to the study of only a few of the many available channels, while others which are more complete studies of the cross sections do not treat the spectral distributions of any of the emitted neutrons. In addition to the fission cross sections for the individual channels,  $\bar{\nu}(E)$ , and the energy and angular distributions of the neutrons are impor-

tant input for the evaluator who must provide these data for neutronics calculations.

#### REFERENCES

1. R. J. Howerton et al., "The LLL Evaluated Nuclear Data Library (ENDL): Evaluation Techniques, Reaction Index, and Descriptions of Individual Evaluations," UCRL 50400, Vol. 15, Part A, Lawrence Livermore Laboratory (1975).
2. V. A. Konshin and M. N. Nikolaev, "Evaluations of the  $^{235}\text{U}$  Fission Cross Sections," INDC(CCP)-26/U (September 1972).
3. M. G. Sowerby, B. H. Patrick, and D. S. Mather, Annals of Nuclear Science and Engineering, 1, 409 (1974).
4. R. J. Howerton, "Semi-Empirical Neutron Cross Sections 0.5-15 MeV," UCRL 5351, University of California Lawrence Radiation Laboratory (1958).
5. R. J. Tuttle, Nucl. Sci. and Eng. 56, 37 (1975).
6. R. Batchelor, W. B. Gilboy, and J. H. Towle, Nucl. Phys. 65, 236 (1965).
7. R. J. Doyas and R. J. Howerton, "Incident Energy Dependence of Fission Spectra," UCRL 50755, Lawrence Livermore Laboratory (1969).
8. R. J. Howerton and R. J. Doyas, Nucl. Sci. and Eng. 46, 414 (1971).
9. J. Terrell, Phys. Rev. 113, 527 (1959).
10. F. Manero and V. A. Konshin, Atomic Energy Review 10, 637 (1972).
11. S. H. Schuster and R. J. Howerton, Journal of Nucl. Energy, Parts A/B 18, 125 (1964).
12. R. J. Howerton, Nucl. Sci. and Eng. 46, 42 (1971).
13. Yu. A. Vasil'ev et al., J. Exptl. Theoret. Phys. 38, 671 (1960).
14. J. L. Kammerdeiner, "Neutron Spectra Emitted by  $\text{Pu}^{239}$ ,  $\text{U}^{238}$ ,  $\text{U}^{235}$ , Pb, Nb, Ni, Al, and C, Irradiated by 14 MeV Neutrons," UCRL 51232, Lawrence Livermore Laboratory (1972).

15. C. E. Ragan et al., "Neutron Spectrum from an Oralloid Sphere," LA-5949-MS, Los Alamos Scientific Laboratory (1975).
16. C. Wong et al., "Livermore Pulsed Sphere Program: Program Summary Through July 1971," Lawrence Livermore Laboratory (1972).

#### FOOTNOTES

- †. Those evaluations currently in ENDF were provided by LASL.
- ††. Where  $\sigma_{nF}$  is the sum of all the partials.

TABLE I

Comparison of Total Integrals, the Integrals Under the Elastic Peak, and Integrals Between the Elastic Peak and ~2.0 MeV<sup>a</sup>

Nuclide	Evaluated Library	$\int_0^{401} N(t)dt$			$\int_0^{161} N(t)dt$			$\int_{161}^{401} N(t)dt$		
		Exp.	Calc.	$\frac{\text{Calc}-\text{Exp}}{\text{Exp}}$	Exp.	Calc.	$\frac{\text{Calc}-\text{Exp}}{\text{Exp}}$	Exp.	Calc.	$\frac{\text{Calc}-\text{Exp}}{\text{Exp}}$
<sup>235</sup> U	ENDF/B-IV	1.436	1.345	- 6%	.644	.697	+ 8%	.792	.648	-18%
	ENDL	1.436	1.330	- 7%	.644	.672	+ 4%	.792	.658	-17%
<sup>238</sup> U	ENDF/B-IV	.907	.869	- 4%	.643	.655	+ 2%	.264	.214	-19%
	ENDL	.907	.892	- 2%	.643	.642	-0.2%	.264	.250	- 5%
<sup>239</sup> Pu	ENDF/B-IV	1.421	1.381	- 3%	.648	.704	+ 9%	.773	.677	-12%
	ENDL	1.421	1.372	- 3%	.648	.736	+14%	.773	.636	-18%

<sup>a</sup>The limits on the integrals represent the time bins of the experiment.

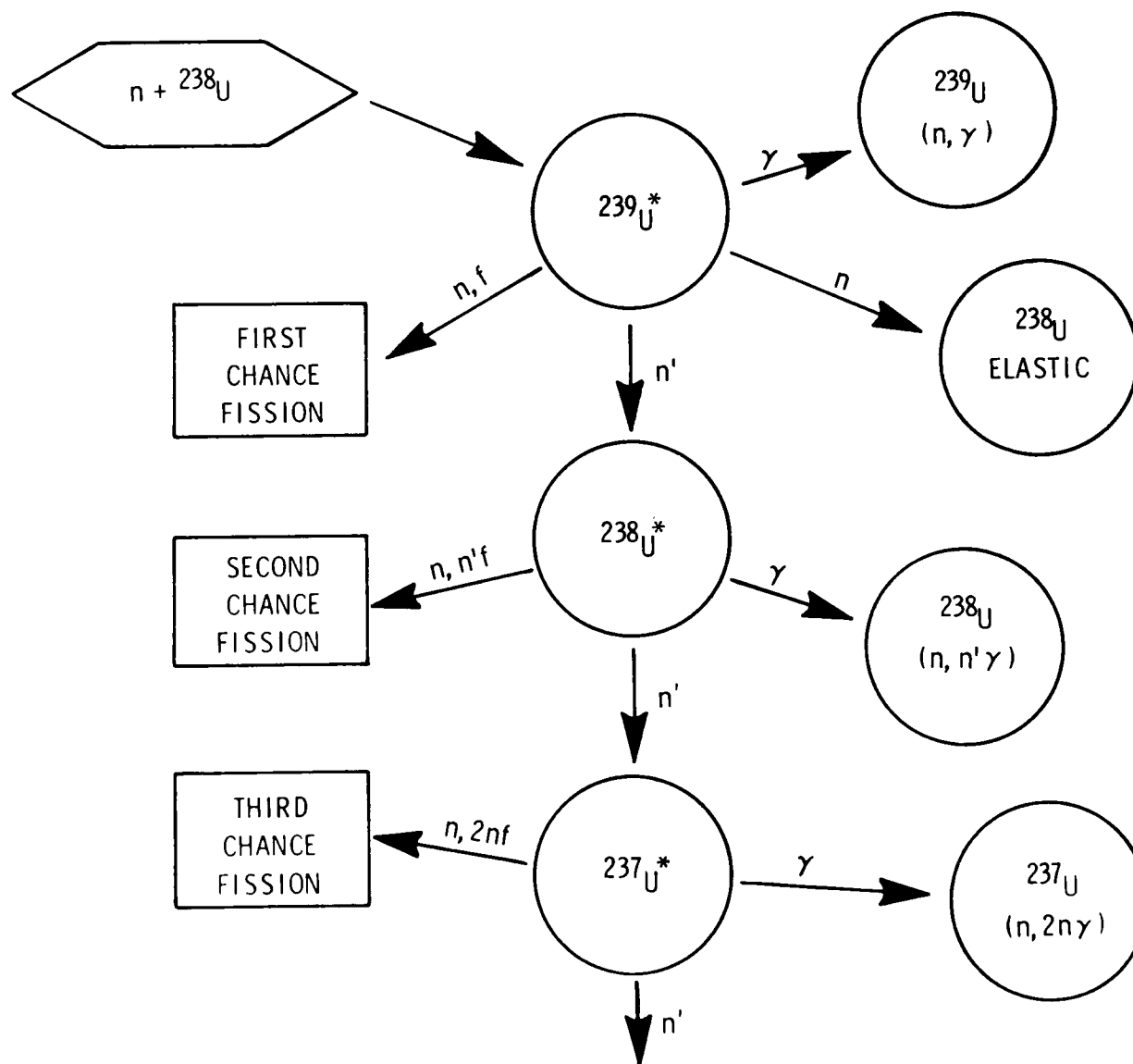


Fig. 1. Schematic showing the reactions considered for neutrons incident on  $^{238}\text{U}$ .

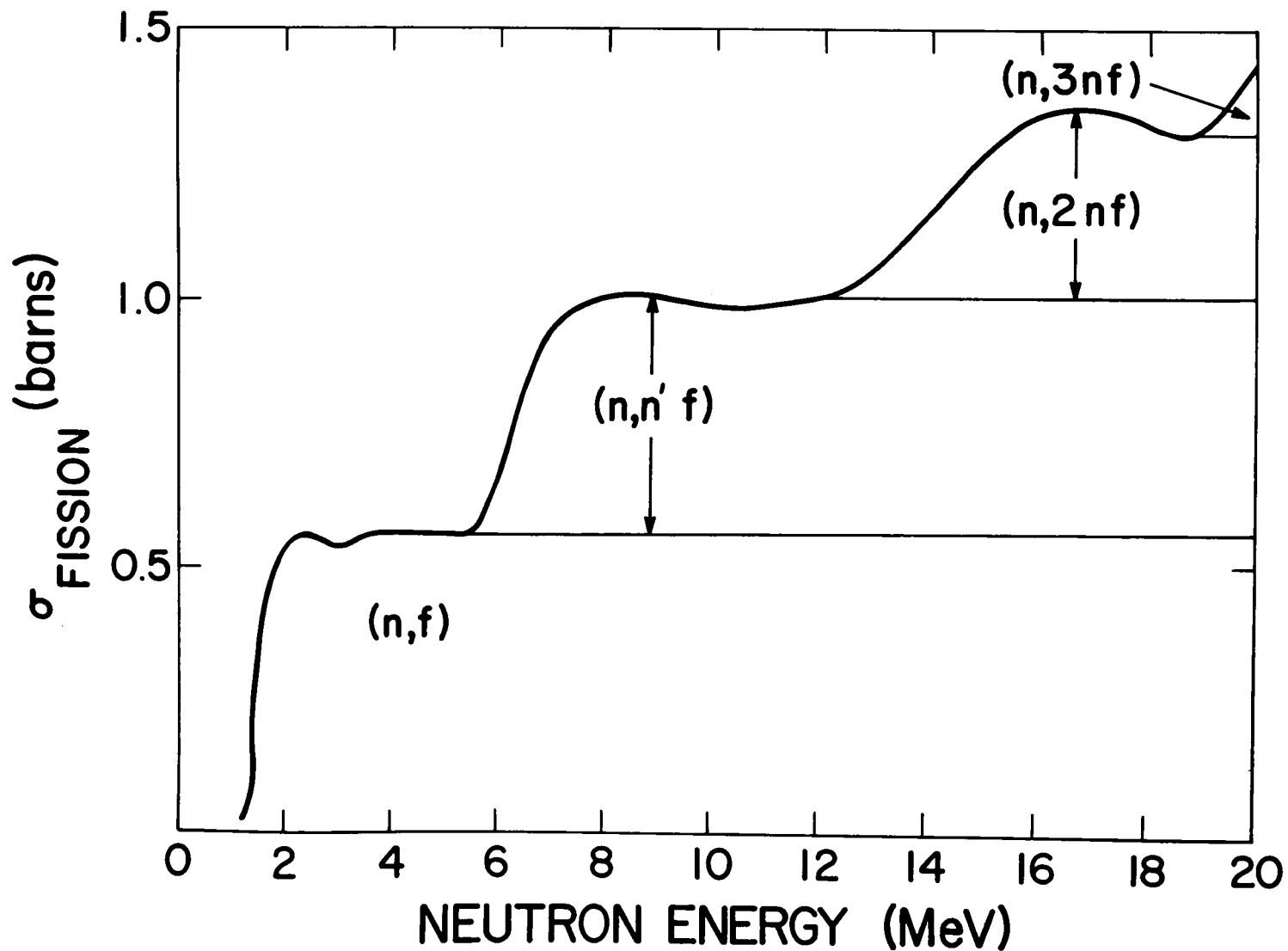


Fig. 2. The Evaluated fission cross sections for  $^{238}\text{U}$  taken from ENDF/B-IV. The top curve represents the total fission cross section.

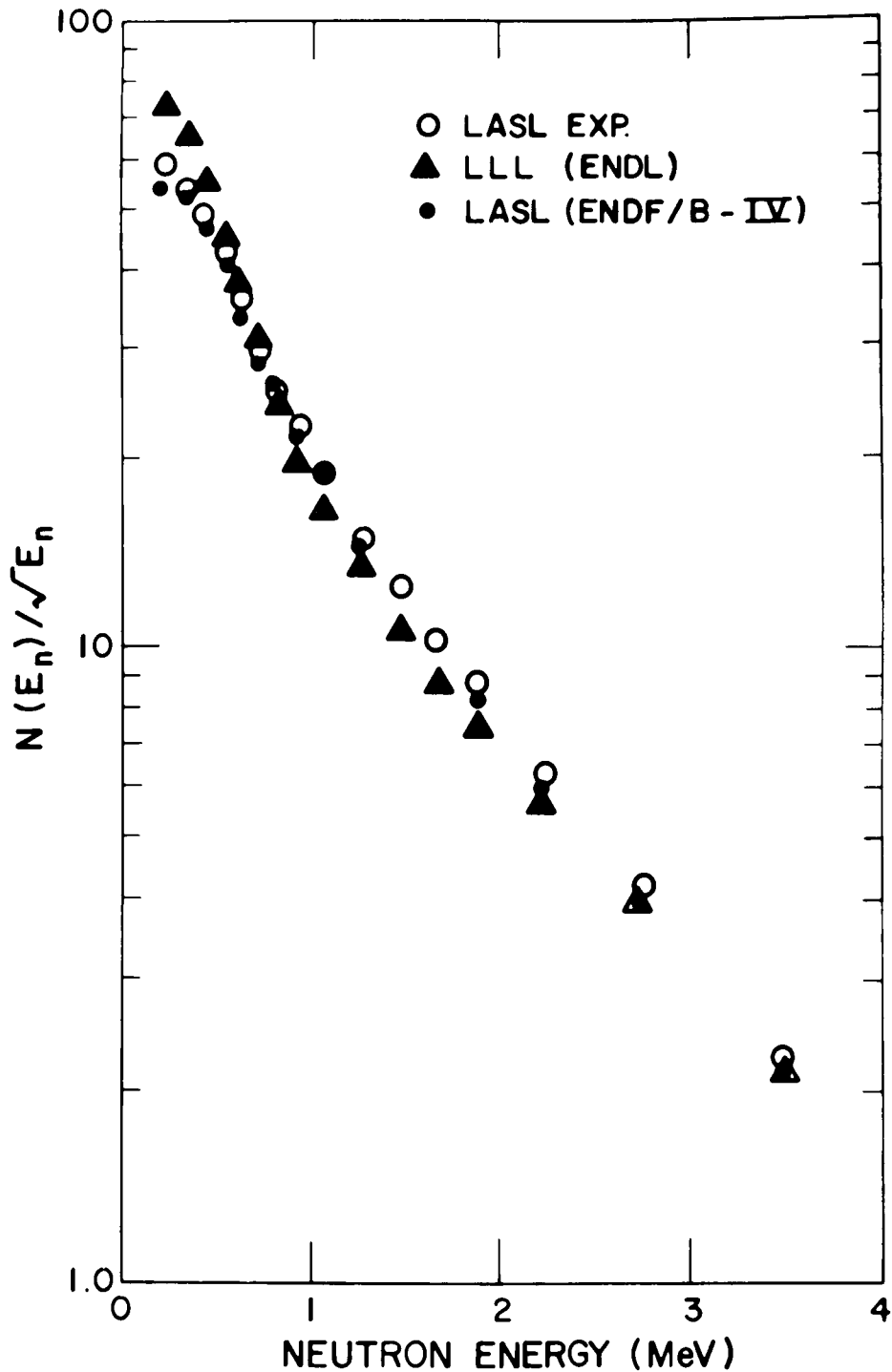


Figure 3a. Spectrum of the neutrons from 14-MeV neutrons incident on an or alloy sphere. The experimental points, taken from the experiment of Ragan et al. [15], are compared with calculations using the ENDF/B-IV evaluated library and using the ENDL library. Note that the largest discrepancies between calculation and experiment occur in the energy bins where the flux is down by two to three orders of magnitude.

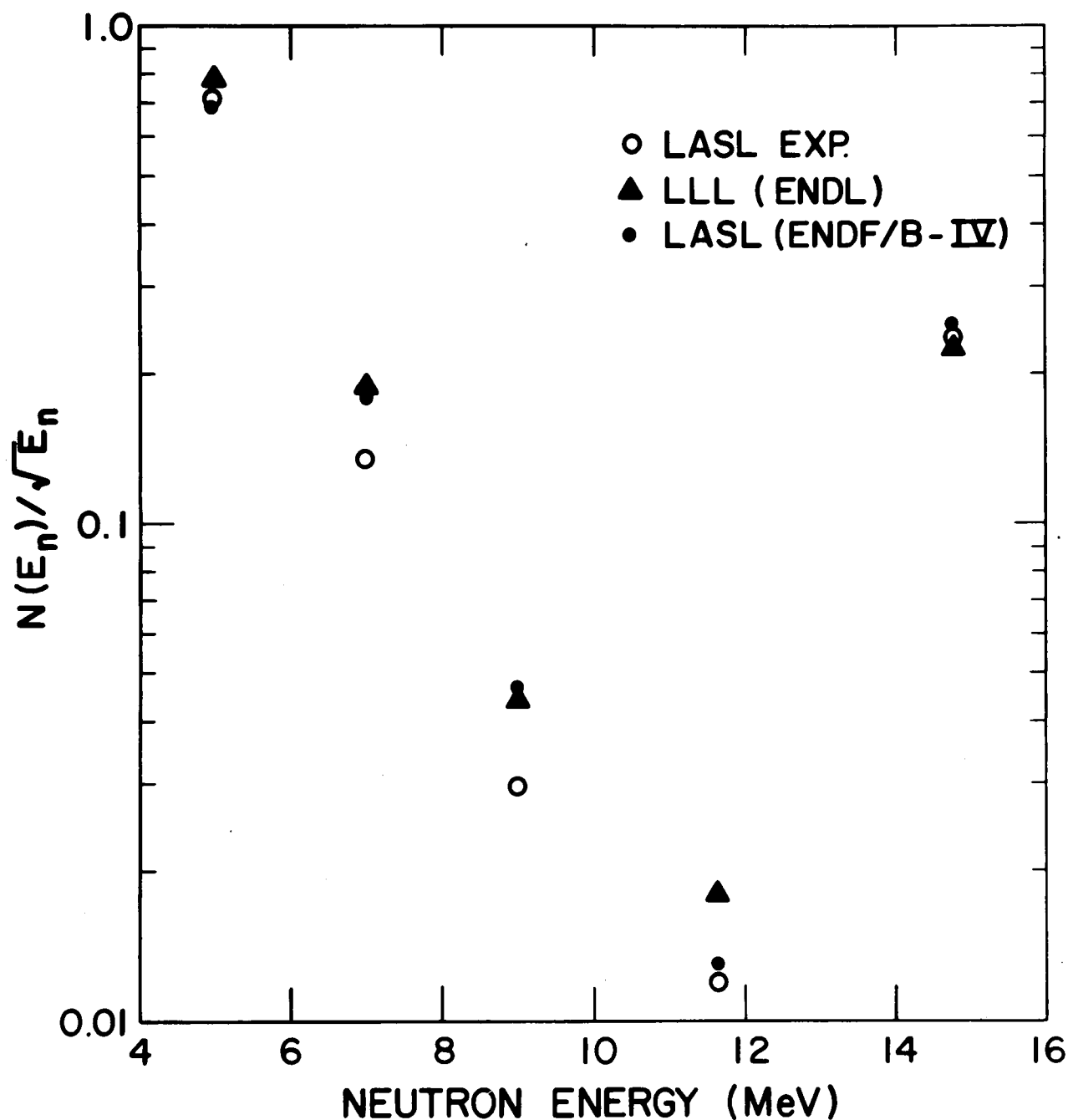


Figure 3b. Spectrum of the neutrons from 14MeV neutrons incident on an oralloy sphere. The experimental points, taken from the experiment of Ragan et al. [15], are compared with calculations using the ENDF/B-IV evaluated library and using the ENDL library. Note that the largest discrepancies between calculation and experiment occur in the energy bins where the flux is down by two to three orders of magnitude.

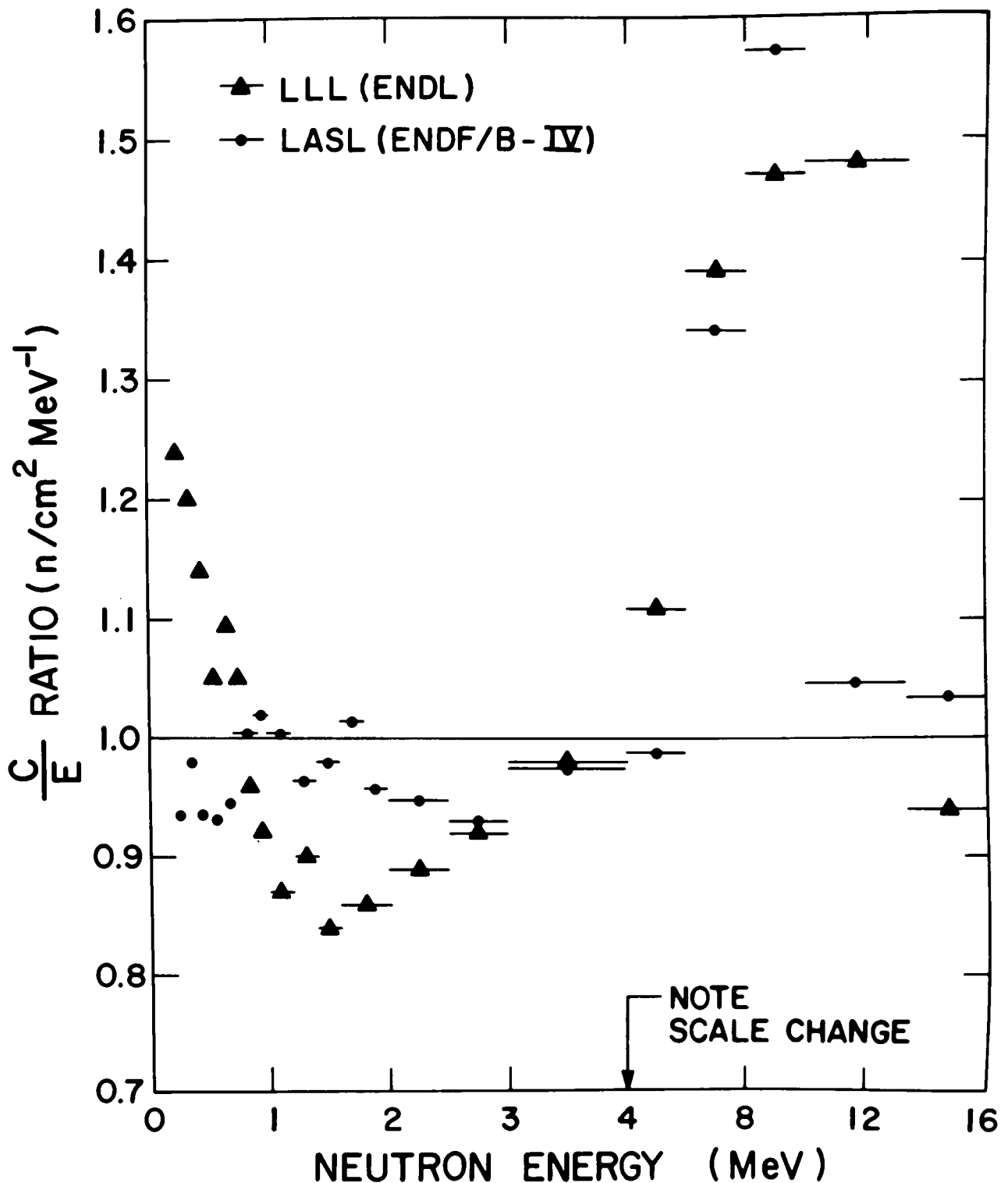


Fig. 4. The same results shown in Figs. 3a and 3b are plotted as calculated/experimental ratios for each of the neutron energy bins. The differences below 2.5 MeV in the calculations using the two evaluated libraries are not well understood.

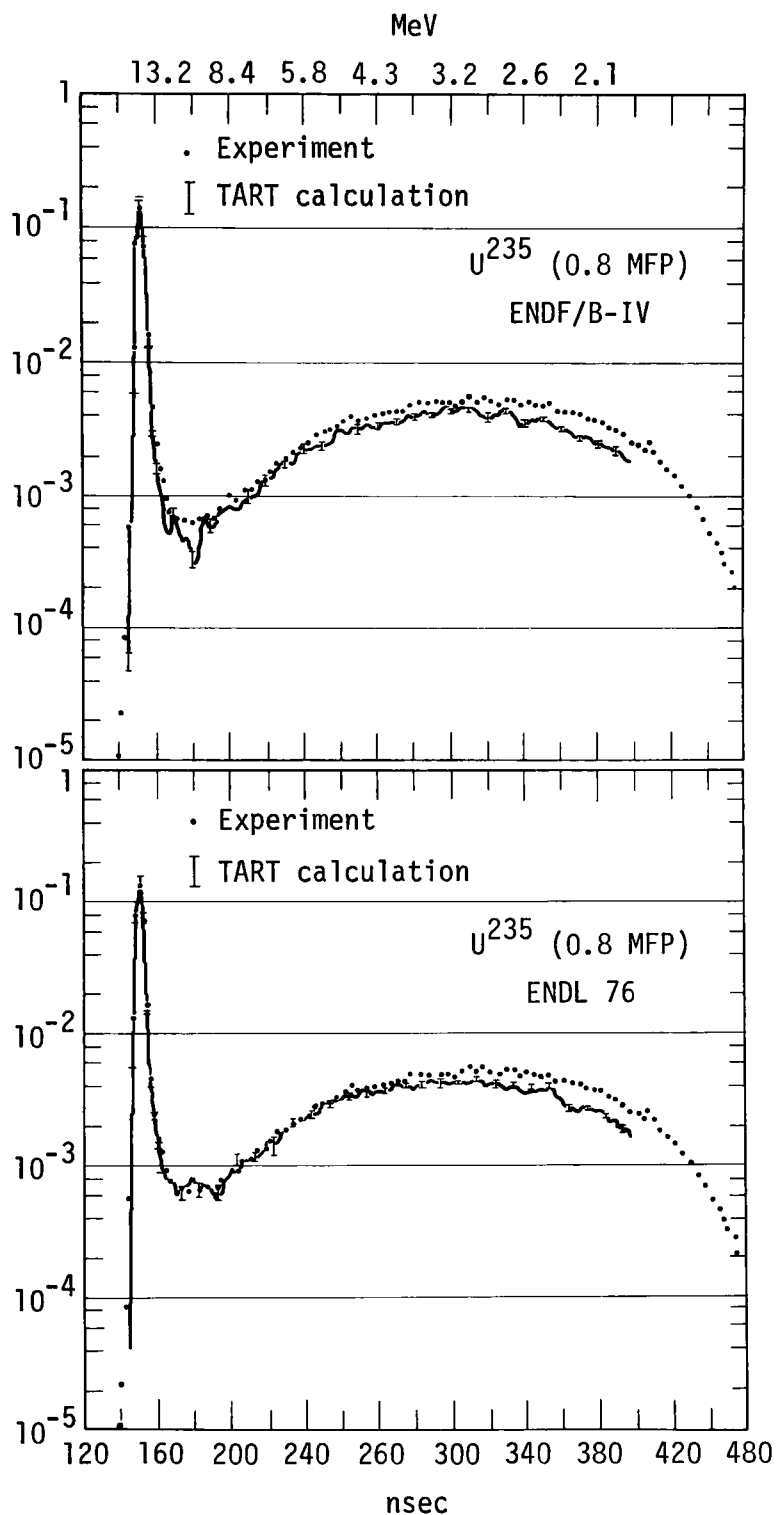


Fig. 5. Comparison of calculated and experimental neutron spectra from a 0.8 mean-free-path hollow sphere of  $^{235}\text{U}$  with a nominal 14-MeV neutron source at the center. The TART 175 group Monte Carlo neutronics code was used.

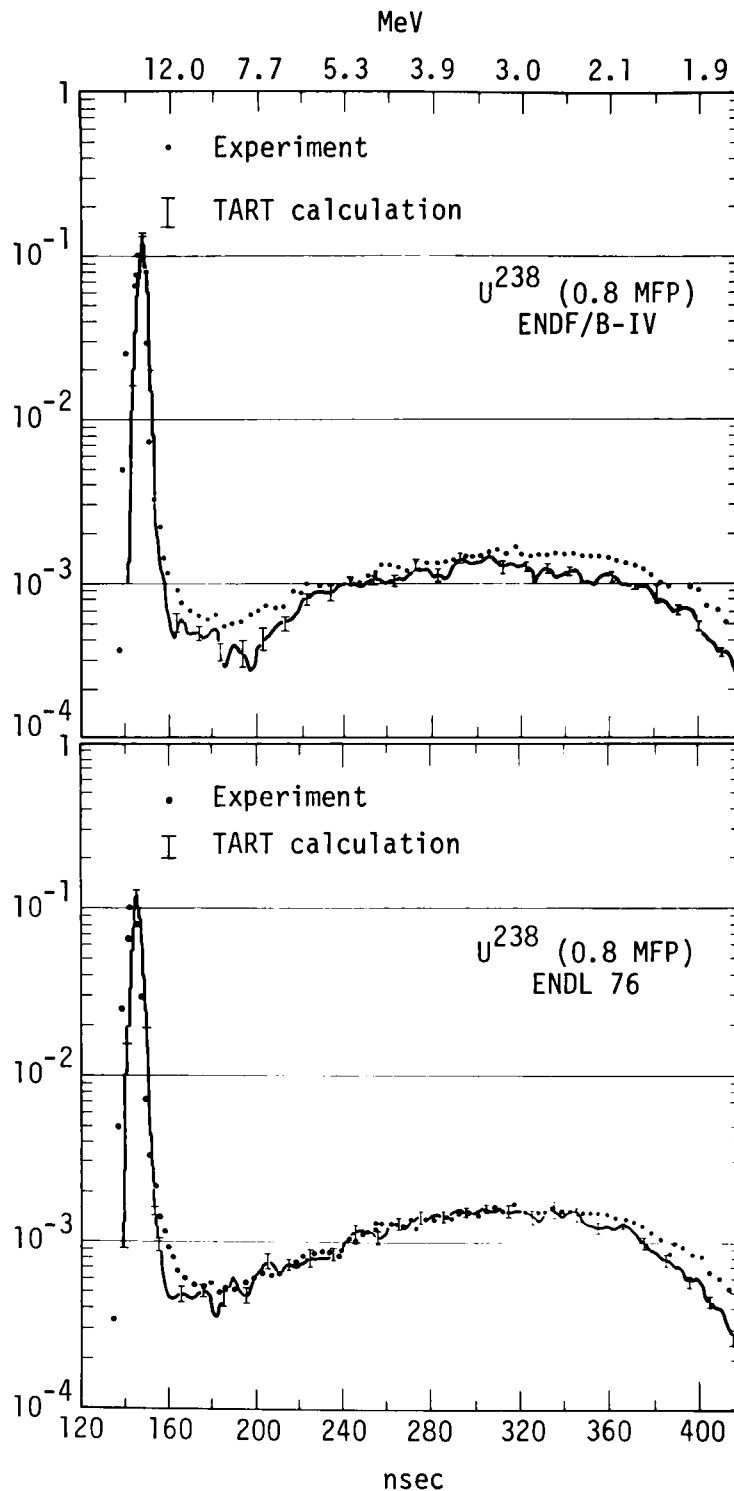


Fig. 6. Comparison of calculated and experimental neutron spectra from a 0.8 mean-free-path hollow sphere of  $^{238}\text{U}$  with a nominal 14-MeV neutron source at the center. The TART 175 group Monte Carlo neutronics code was used.

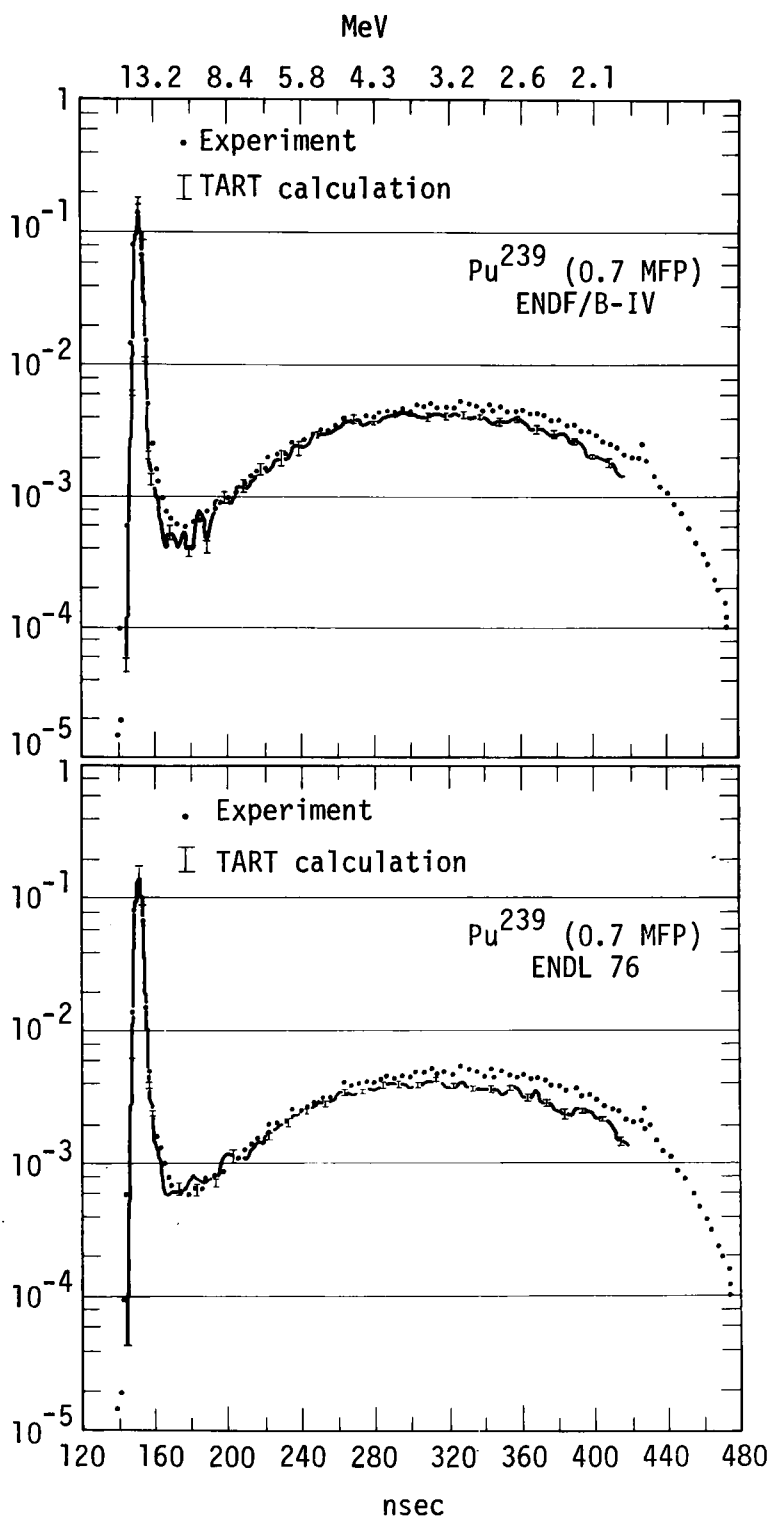


Fig. 7. Comparison of calculated and experimental neutron spectra from a 0.7 mean-free-path hollow sphere of  $^{239}\text{Pu}$  with a nominal 14-MeV neutron source at the center. The TART 175 group Monte Carlo neutronics code was used.

*DISCUSSIONS*

B. Leonard I remember I read some ten years ago a paper on second chance fission. The argument in that paper was that the fission cross section for second chance fission decreased slowly with energy rather than staying constant. I don't remember the basis for that but it might be worth looking into this.

L. Stewart I am familiar with some of this and also with the fact that the odd nuclei look different than the even ones. It is very difficult to draw some of the curves, say for U-235 or Pu-239 because they have a tendency to decline just before the second chance fission threshold.

# A IONIZATION CHAMBER WITH FAST TIMING PROPERTIES AND GOOD ENERGY RESOLUTION FOR FISSION FRAGMENT DETECTION

C. Budtz-Jørgensen and H. -H. Knitter

Commission of the European Community,  
Central Bureau for Nuclear Measurements  
B-2440 Geel, Belgium

## ABSTRACT

A twin ionization chamber for fission fragment detection is described. The chamber allows to extract both, fast timing- and energy proportional signals. A time resolution of 1.62 ns FWHM was obtained between two fission fragments detected in the two halves of the chamber. For  $^{241}\text{Am}$   $\alpha$ -particles the chamber gave an energy resolution of 1.3. %. As counting gas methane NTP was used.

## INTRODUCTION

For detection of fission fragments in experiments to measure neutron induced fission cross sections one has certain demands concerning the characteristics of a detector. If one wants to use it together with a pulsed accelerator, the detector should have timing properties which are comparable with those of the accelerator, that means in the order of 1 ns. The detector should show no effects due to radiation damage in the presence of highly  $\alpha$ -active fissionable deposits. The detector should allow to make a discrimination between  $\alpha$ -particles and fission products. In the cases where high accuracy is demanded in the determination of a cross section, the detector should give also an energy proportional signal. This seems necessary, in order to control the corrections to be made for the finite fission foil thickness.

## DESCRIPTION AND PROPERTIES OF THE CHAMBER

The wanted characteristics are fulfilled to a large extent by a double grided ionization chamber as shown in Fig. 1. The detector consists of a grounded cathode which supports the fissile or spontaneously fissioning material deposited on a thin foil, two timing grids on each side at a distance of 2 to 3 mm, two Frisch grids at a distance such that the fission products are stopped before they reach it and two anode plates at a few millimeters distance from the Frisch grids. The grids consist of parallel Inox wires 0.1mm

in diameter. The distances between the wires are 4 mm and 1 mm for the timing- and Frisch grid respectively.

Methane NTP was used as counting gas. Risetimes of 20 ns and 250 ns, were observed at the timing grid and the collector plate respectively. In order to check the timing resolution of this chamber, the two signals from the timing grids were fed into a time to pulse height converter. The recorded time spectrum is plotted in Fig. 2. It shows that the time resolution is 1.62 ns FWHM and that 99 % of the counts are contained within a time range of 4.4 ns. This is a timing resolution as good as one obtains with a parallel plate ionization chamber using same electronics.

The energy proportional signals are obtained from the anode plates. The energy resolution of the chamber was checked with  $\alpha$ -particles from  $^{241}\text{Am}$ . An energy resolution of 1.3 % was obtained. In Fig. 3 the energy spectra of fission fragments of  $^{252}\text{Cf}$  are shown. The lower section shows a straight forward pulse height spectrum and at the low energy side the  $\alpha$ -particles are observed. The upper section shows a pure fission fragment spectrum which was obtained by gating the analyser by coincident events at the timing grids.

## FISSION CHAMBER

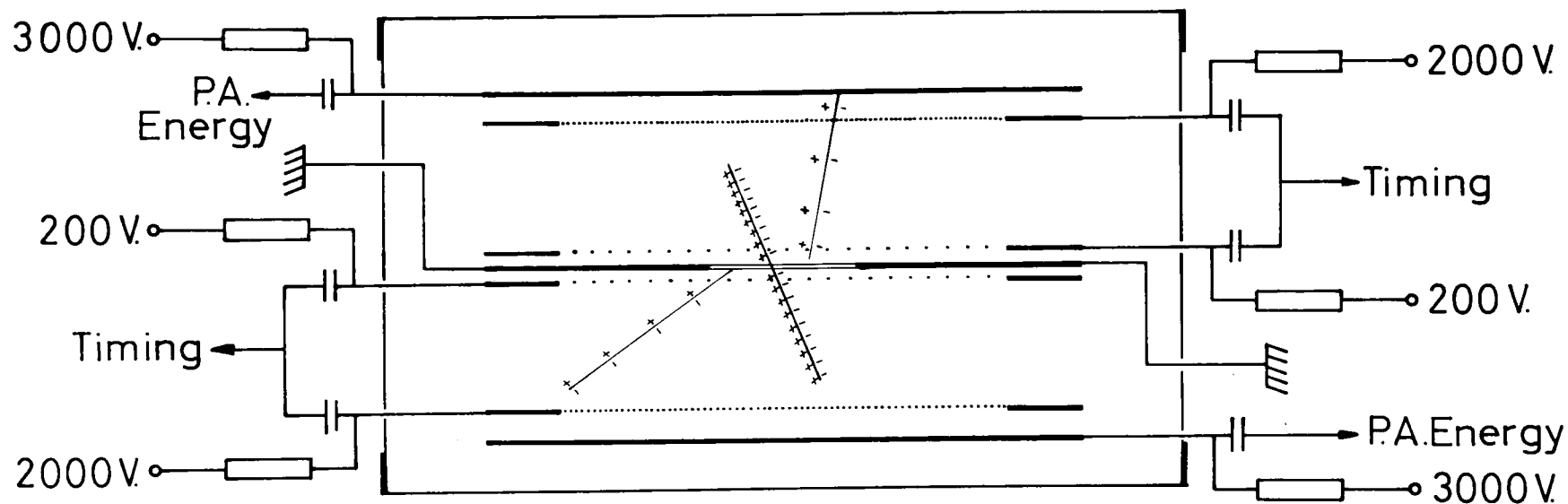


Figure 1. Schematic drawing of the fission chamber indicating the position of the timing- and Frisch grids as well as collector plates. The supplied tensions and the signal outputs are shown.

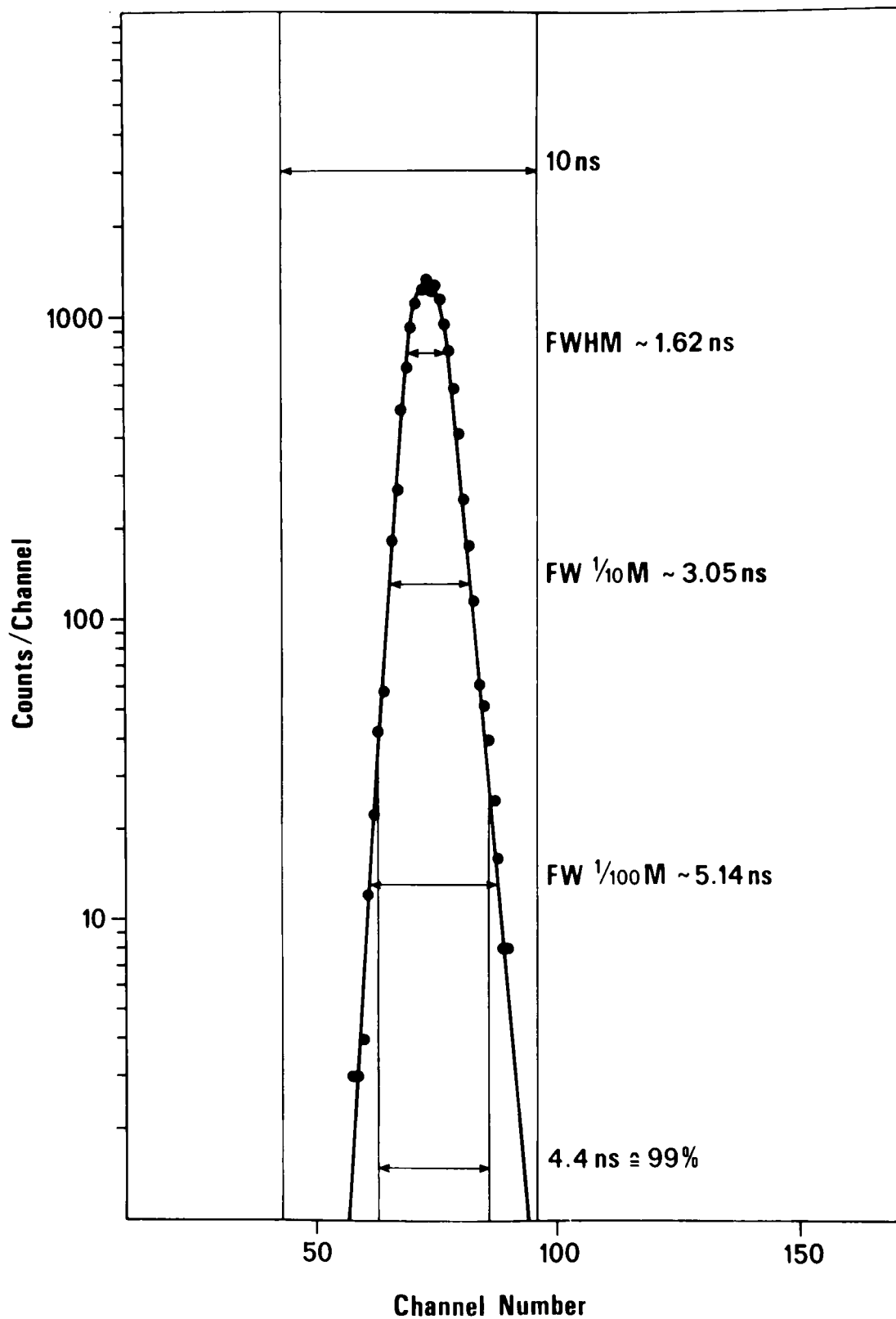


Figure 2. The time resolution curve for coincident fission fragments obtained from the fast signals of the timing outputs is shown.

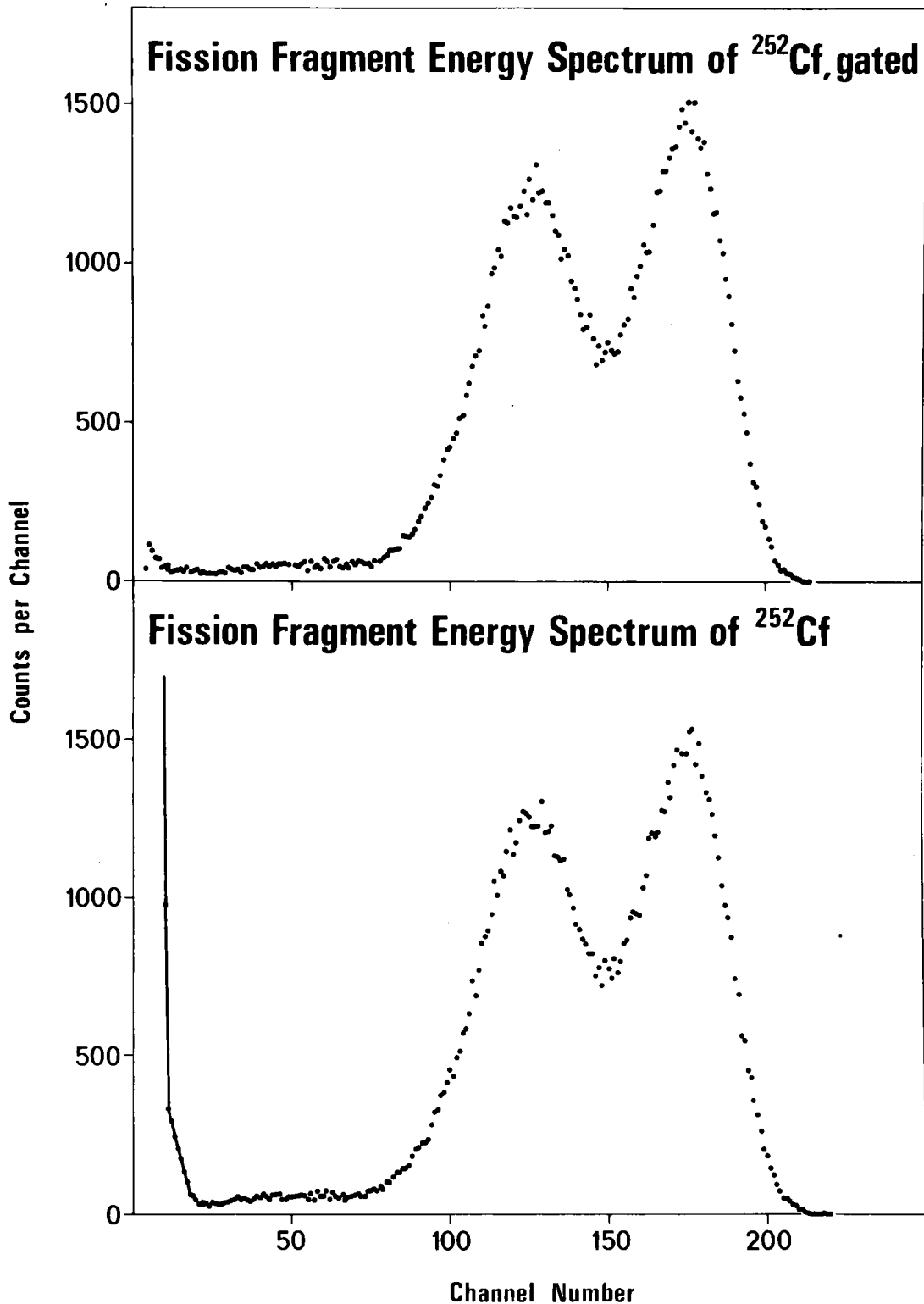


Figure 3. The lower section of the figure shows the pulse height distribution from a  $^{252}\text{Cf}$ -source obtained from one of the collector plates. The upper section shows the same spectrum but gated with the fast coincidences.

## DISCUSSIONS

W. Poenitz How do you measure the timing? With coincidence with the fission  $\gamma$ -rays?

H. Knitter We have used also this technique. However, the figure you have seen here was the coincidence between the two halves of the fission chamber. We have done it also with a  $\gamma$ -ray detector.

J. Browne Why does the first technique you mentioned not work with  $\alpha$  pile-up--even though you have good time resolution?

H. Knitter If you have half-lives of  $< 10^5$  years you have trouble. The rise time of the timing-signals is 20 nsec and of the energy proportional signals it is about 200 nsec.

J. Behrens A comment. Many studies of fragment distributions or of the efficiencies use the low energy side of the pulse-height spectra, as you showed to determine lost pulses. Studies of this type are in many cases motivated by trying to determine absolute cross sections by determining efficiency, masses, etc. I would like to point out that the technique we use for our ratios tries to avoid these difficult techniques. Close examination of our paper will show that the threshold method bypasses this completely. I think this is very important.

H. Knitter In ratio measurements this is not severe. If you make ratio measurements these corrections are similar and contribute little to the uncertainty.

## REQUIREMENTS ON EXPERIMENT REPORTING TO MEET EVALUATION NEEDS\*

Robert W. Peelle

Oak Ridge National Laboratory  
Oak Ridge, Tennessee 37830, U.S.A.

## ABSTRACT

To define the requirements placed by the evaluation of nuclear cross sections upon the reporting of experimental results, a model of part of the evaluation process is presented. The model is a straightforward application of nondiagonal weighted least-squares estimation to average cross sections in the energy regions where the shape of the cross section is not given by theory. To combine in a logical way the existing evaluated information with one or more new sets of experimental results, the estimated covariance matrix of each experimenter's results needs to be known on an appropriate mesh. The likelihood that each experimenter may underestimate the uncertainties in his results does not remove the need for him to record for users the estimated magnitudes and correlation patterns of these uncertainties.

## INTRODUCTION

When neutron cross section experimental data are combined, a relative weight must be placed on each datum or set to conserve the available information. Furthermore, the evaluator must characterize the uncertainties in his evaluated result, for instance to make possible the estimation of uncertainties in reactor physics parameters computed from the evaluated data base. [1] The processes of input weighting and output uncertainty estimation should be closely tied together.

Experimenters have generally included some estimated uncertainty information, particularly in reporting rather precise work, to give the reader/user an idea of data quality. Sometimes a breakdown of the components of the uncertainty is given so that the reader can understand the sources of the uncertainties and incidentally sense the degree of correlation among the reported results. Rarely have experimenters revealed the full extent of their own understanding about uncertainties. This shortcut has been taken because all analysis is hard work, because no likely use of such information was apparent, because editors have not always treated detailed information kindly, and

---

\* Research sponsored by the Energy Research and Development Administration under contract with the Union Carbide Corporation.

because so often some unrecognized uncertainties have dominated the differences between the results of various experiments.

To discover what are the logical requirements upon experimenters, part of the nuclear data evaluator's role is replaced here by a mathematical model of the data combination portion of the evaluation process. While few evaluations have so far been performed using any model similar to that given, [2, 3] a human evaluator exercising best judgment has no divine powers and so requires the same information as would the model evaluator. If the difficulty in mentally processing the required information should become too complex, a computer program could carry out any desired portion of the data combination process.

The "model evaluator" discussed here is not concerned with regions of neutron cross sections where data may be precisely fit through proper choice of the parameters of theoretical formulae, though in that case the requirements on experiment reporting are not much different from the result indicated below. Instead, our evaluator will deal with the region of "smooth" cross sections; more exactly the model will be concerned only with the (infinitely dilute) average cross sections within each of a discrete number of energy groups. These group cross sections  $\sigma_i$  are the basic variables of concern to the "evaluator;" the output values of these variables are to be determined from measurements of differential cross sections, ratios of these cross sections, and possibly a variety of integral quantities.

After noting the formal requirements for input to the evaluator, we suggest the simplifications possible in favorable cases, deal briefly with the problem of inconsistent data, and give an elementary example.

None of the material here is new, but the ideas have not been applied much to differential nuclear data. The author believes that the significance of the ideas has not been fully appreciated because nuclear data in the past have relatively infrequently been of sufficient quality, because the applicability to this case of the least-squares or equivalent approaches has not always been recognized, and because in the past the resulting covariance matrices would not have been used.

#### A MODEL EVALUATION PROCESS

An evaluator desires "best" values of  $\sigma_i$  [ $i=1, \dots, I$ ], infinitely dilute group average cross sections on a suitable mesh, and finds himself with an overdetermined set of equations linking these variables with observed quantities  $\xi_m$  [ $m=1, \dots, M$ ];  $I < M$ . Unlike the typical curve-fitting problem these equations have a variety of forms, expressing whatever the relationship is between the group-average cross sections and the values one would expect to observe in the experiments performed. (Both depend on the underlying differential cross sections.) Paragraphs below explain how a variety of observations can be accommodated by casting the equations in terms of small differences. The  $\xi_i$  already contain any necessary updated corrections to reported results.

Our model evaluator combines the data in the least-squares sense to obtain best values of the  $\sigma_i$  and the output covariance matrix elements  $\text{Cov}(\sigma_i, \sigma_j) = \langle \delta\sigma_i \delta\sigma_j \rangle$ . The term in angle brackets denotes the expectation value of a product of small-error variates  $\delta\sigma_i$ . This expectation value is the average over the ensemble of hypothetical evaluations obtained from equivalent input data bases which could have been obtained in the experiments performed. The index (i) ranges over energy groups, reaction types, and materials.

To proceed, the general form of the least-squares equations must be recalled; in the next paragraph the variables will be identified with the evaluation problem. If an overdetermined set of M approximation equations of the form  $\sum_i A_{mi} s_i \approx y_m$ , or  $\underline{A} \underline{s} \approx \underline{y}$ , link the variables  $s_i$  to the observations  $y_m$ , and if the covariance matrix of the observation vector  $\underline{y}$  is  $\underline{V} = \text{Cov}(\underline{y})$ , minimization of the quadratic form  $\chi^2 = (\underline{y} - \underline{A} \underline{s})^t \underline{V}^{-1} (\underline{y} - \underline{A} \underline{s})$  leads to the matrix normal equations and their solution

$$\underline{s} = \underline{C} \underline{A}^t \underline{V}^{-1} \underline{y}, \quad (1)$$

where

$$\underline{C} = (\underline{A}^t \underline{V}^{-1} \underline{A})^{-1} = \text{Cov}(\underline{s}) . \quad (2)$$

The output covariance  $\underline{C}$  is propagated from the input variance matrix  $\underline{V}$ , and so shares whatever validity the input variance matrix has. This validity can be tested because the quantity  $\chi^2$  should be distributed as a chi-square distribution with M - I degrees of freedom. Chi-square can be computed from the solution using the equation

$$\chi^2 = \underline{y}^t \underline{V}^{-1} \underline{y} - \underline{s}^t (\underline{A}^t \underline{V}^{-1} \underline{A}) \underline{s} . \quad (3)$$

The choice of  $\underline{V}^{-1}$  as the (generally nondiagonal) weighting matrix yields the minimum-variance result for the parameter vector  $\underline{s}$ . [4] In the equations, underlined lower case symbols are vectors, upper case underlined symbols denote matrices, and  $(^t)$  indicates a transpose.

There is always a prior evaluated cross section set of fairly good group values  $\hat{\sigma}_i$  which need to be refined. Banking on these, our present model evaluator employs variables corresponding to the (presumably small) relative differences between the new results and the prior evaluation, as follows:

$$\begin{aligned} s_i &\equiv (\sigma_i - \hat{\sigma}_i) / \hat{\sigma}_i \\ y_m &\equiv (\xi_m - \hat{\xi}_m) / \hat{\xi}_m \\ A_{mi} &\equiv \left. \partial y_m / \partial s_i \right|_{\underline{s}=0} . \end{aligned} \quad (4)$$

In this relative-difference language  $\underline{V}$  is the relative covariance matrix of the original variables. The  $\hat{\xi}_m$  are the values of the observed quantities which would be estimated assuming the  $\hat{\sigma}_i$ .

One sees that at least one general evaluation procedure exists which promises to give optimal values of the needed average cross sections as well as the needed covariance quantities if there is available the covariance matrix of the input experimental quantities and if the equations can be solved.

### CAN MECHANICAL EVALUATION BE PRACTICAL?

The familiar formulation above appears intimidating for application to nuclear data, for it appears there are formidable numerical tasks after one completes the normal job of updating input information and the new one of specifying the input covariance matrix elements. We are not accustomed to nondiagonal input data weighting with its promise of inversion of a very large  $M \times M$  matrix as well as the  $I \times I$  matrix needed to obtain the solution.

There are several reasons why the task may not be so forbidding, reasons to believe such systems will be employed to the extent they are not being used already.

a) The set of  $\sigma_i$  considered in one solution may be confined to those linked by the equations and by strong correlations among the relevant observed quantities. Even for the variables which must be considered together, there will usually be large blocks of zeros in the covariance matrix  $V$ .

b) Where the observed quantities are themselves cross sections, the corresponding portion of the  $A$  matrix consists of a unit matrix as large as the number of groups covered by the experiment. In important cases like this the simplicity of the  $A$  matrix, i. e. of the relations between the observed quantities and the group cross sections, will allow the equations to be rewritten with smaller dimension.

c) By this method cross section ratio measurements as well as direct measurements of the same quantities are handled in a natural and correct manner. For example, if an observed quantity  $\xi_m \approx \sigma_1/\sigma_2$ ,

$$y_m = \Delta \xi_m / \hat{\xi}_m \approx \frac{\partial \xi_m}{\partial \sigma_1} \frac{\Delta \sigma_1}{\hat{\xi}_m} + \frac{\partial \xi_m}{\partial \sigma_2} \frac{\Delta \sigma_2}{\hat{\xi}_m} = s_1 - s_2 ,$$

based on a first-order Taylor's expansion of  $\Delta \xi_m = \xi_m - \hat{\xi}_m$  in the variables  $\Delta \sigma_i = \sigma_i - \hat{\sigma}_i$ , and if the ratio measurements are available for several groups the corresponding portion of the  $A$  matrix is a pair of unit matrices of opposite sign.

d) All the data sets which cover the same range of cross sections need not be entered at once. One set of "observations" can be the combination of all the sets previously considered. If the reference cross section vector  $\underline{\sigma}$  is updated each time the equations include another set of input data, the portion of the  $y$  vector corresponding to the current partial evaluation is null and the equations are simplified. [5]

e) The equations are the same as those used for evaluation including the results of integral experiments, in which case the corresponding portion of the  $A$  matrix would contain the appropriate sensitivity coefficients. [6]

f) An evaluation performed as indicated above naturally generates the covariance matrix of the evaluated results. Otherwise this covariance matrix must be obtained separately, probably using a less rigorous procedure which itself entails considerable data manipulation. [7]

Thoughtful objections can be raised to any proposal for broad use of such an evaluation system; the primary objection is that such a method would only quantify input discrepancies already known to be important, and that in the face of such discrepancies neither the procedure nor the output covariance matrices can be valid. Indeed, one expects that inconsistent data would often provide a dominant difficulty, but the careful assessment of data uncertainties required to obtain the input covariance matrix will sometimes reward the evaluator by revealing that some of the experiments merely disagree within their uncertainties. Actual use of experimenters' covariance matrices would lead to more careful uncertainty analyses and eventual subsequent reduction of systematic errors. If the  $\chi^2$  test of Eq. (3) does indicate inconsistent data but the evaluator believes the input variance estimations give the correct relative weight to the various experiments, the "shape" of the output covariance matrix can be adopted while the magnitudes of the elements of  $\underline{C}$  are scaled up by the factor  $\chi^2/(M - I)$ .

Of course, the model evaluator cannot deal with any structure finer than the energy mesh used, so a separate within-group shape must be adopted for these fine details. Where the evaluation employs "point" cross sections measured with relatively broad energy resolution, the shape details should be used to help derive appropriate  $y_i$  values to represent these input data.

Table I shows a very small example of application of the evaluation model to partly correlated measurements of two cross sections and of their ratio. Evidently the same approach would work as well for any overdetermined combination of such measurements and ratios. With this method it is not necessary, as in some other methods [8], to define extra variables to handle the known correlations among input data.

#### RESPONSE NEEDED FROM EXPERIMENTERS

Increasing utilization of evaluation techniques such as given above seems assured because of coherence with methods of fitting which are used when theory is known to apply, because of the relative ease of adding new differential or integral information to a previously evaluated data base, and because of the current need to find good ways to obtain valid uncertainty matrices for evaluated data.

Experimenters should cooperate with this trend by making as clear as possible just what is the estimated covariance matrix of the results presented. One way to present this information would be to give the matrix itself on an appropriate grid! Another way, closer to past practice, would be to indicate the known correlation patterns as well as uncertainty magnitudes associated with each recognized uncertainty component. The first method could fail to convey the understanding required if the energy mesh is to be altered, while the second may not always be sufficiently explicit. A combination of the two approaches seems most desirable. The definiteness of such reporting will aid evaluators even when they employ mental rather than mathematical data processing techniques.

If experimenters do not provide such information, they may have to be satisfied with even rougher and perhaps unfair assignments of covariance matrix components by evaluators, assignments which may differ from the experimenter's preference not out of technical disagreement but out of the

evaluator's impossibility to understand the effects of complex equipment and analysis procedures on the correlations among experimental values. Evaluations will be more valid if the experimenters themselves offer for consideration the needed uncertainty matrix information.

#### ACKNOWLEDGMENTS

This paper was motivated and influenced by discussions with many scientists; in particular with F. G. Perey, C. R. Weisbin, and W. P. Poenitz.

#### REFERENCES

1. E. M. OBLOW, "Survey of Shielding Sensitivity Analysis Development and Applications Program at ORNL," ORNL-TM-5176, Oak Ridge National Laboratory (1976), also to be published in *Proc. Specialists' Meeting on Sensitivity Studies and Shielding Benchmarks*, Paris, France, October 1975, sponsored by the Organization for Economic Cooperation and Development and the International Atomic Energy Agency. E. M. OBLOW, "Reactor Cross-Section Sensitivity Studies Using Transport Theory," ORNL-TM-4437, Oak Ridge National Laboratory (1974). C. R. WEISBIN, E. M. OBLOW, J. CHING, J. E. WHITE, R. Q. WRIGHT and J. DRISCHLER, "Cross Section and Method Uncertainties: The Application of Sensitivity Analysis to Study Their Relationship in Calculational Benchmark Problems," in *Proc. Conf. Nuclear Cross Sections and Technology*, NBS Special Publication 425 (1975), p. 831. C. R. WEISBIN, E. M. OBLOW, F. R. MYNATT, and G. FLANAGAN, "The FORSS Sensitivity Analysis Code System," *Trans. Am. Nucl. Soc.* 22, 792 (1975). Papers subsequent to the last reference will detail a practical realization of performance parameter uncertainty analysis based on (ENDF) cross section uncertainty files.
2. W. P. POENITZ, Argonne National Laboratory, private communication to participants in a CSEWG Normalization and Standards Subcommittee (October 7, 1975). Also, W. P. POENITZ, "Interpretation and Intercomparison of Standard Cross Sections," in *Proc. Symp. on Neutron Standards and Flux Normalization*, CONF-701002, Argonne National Laboratory (1970). The methods discussed by Poenitz are somewhat different than those described in the current paper, but are similarly motivated. See also M. K. SOWERBY and B. H. PATRICK, "A Simultaneous Evaluation of the Fission Cross Sections of  $^{235}\text{U}$ ,  $^{239}\text{Pu}$ , and  $^{238}\text{U}$  and the Capture Cross Section of  $^{238}\text{U}$  in the Energy Range 100 eV to 20 MeV, *Proc. Conf. on Nuclear Data for Reactors*, International Atomic Energy Agency, Vienna (1970), p. vol. I, p. 703.
3. C. Y. FU and F. G. PEREY, Oak Ridge National Laboratory, private communication (May 1976). These authors are applying essentially the model of this paper to the restricted case of the total neutron cross section for carbon below 2 MeV. Nondiagonal weighting matrices are employed and each data set is successively combined with the information previously considered. See footnote 5 below.

4. H. SCHEFFE, *The Analysis of Variance*, John Wiley and Sons, New York (1959). Chapters 1 and 2, especially sections 1.4, 1.5, and 2.1. More precisely, any estimable function  $f = \underline{a}^t \underline{s}$  of the solution, Eq. (1), has minimum variance if the input weight matrix  $\underline{V}^{-1}$  is used. The function  $f$  is estimable if  $\underline{a}^t$  is any linear combination of the rows of  $\underline{A}$ .
5. Assume an existing data base  $\underline{\sigma}_0$  with covariance  $\underline{C}_0$ , and a new set of observations  $\underline{\xi}_1$  with covariance  $\underline{V}_1$ ,  $\underline{\xi}_1$  uncorrelated with  $\underline{\sigma}_0$ . Let  $\hat{\underline{\sigma}}_1 = \underline{\sigma}_0$ , and write Eq. (1) for the data combination as

$$\underline{s}_1 = \underline{C}_1 \begin{pmatrix} \underline{A}_0 \\ \underline{A}_1 \end{pmatrix}^t \begin{pmatrix} \underline{C}_0 & 0 \\ 0 & \underline{V}_1 \end{pmatrix}^{-1} \begin{pmatrix} 0 \\ \underline{y}_1 \end{pmatrix} = \underline{C}_1 \underline{A}_1^t \underline{V}_1^{-1} \underline{y}_1 ,$$

where

$$\underline{C}_1^{-1} = \begin{pmatrix} \underline{A}_0 \\ \underline{A}_1 \end{pmatrix}^t \begin{pmatrix} \underline{C}_0 & 0 \\ 0 & \underline{V}_1 \end{pmatrix}^{-1} \begin{pmatrix} \underline{A}_0 \\ \underline{A}_1 \end{pmatrix} = \underline{C}_0^{-1} + \underline{A}_1^t \underline{V}_1^{-1} \underline{A}_1 ,$$

since as defined  $\underline{A}_0 = \underline{1}$ . The formulae can be expanded for any number of new data sets uncorrelated with each other, or used iteratively. Equivalent but simpler formulae have been derived from Bayes' theorem by F. G. Perey, private communication (1975). If the data set  $\underline{\xi}_1$  are direct cross section measurements the equations are further simplified because  $\underline{A}_1$  is a unit matrix augmented with zero columns if not all energy groups are covered.

6. The equations of footnote 5 apply if  $\underline{\xi}_1$  and  $\underline{V}_1$  contain the results of integral experiments,  $\underline{\sigma}_0$  and  $\underline{C}_0$  contain the information from differential experiments, and  $\underline{A}_1$  consists of the relevant sensitivity coefficients, if integral and differential observations are uncorrelated.

See D. R. HARRIS, W. A. REUPKE, and W. B. WILSON, "Consistency Among Differential Nuclear Data and Integral Observations: The ALVIN Code for Data Adjustment, for Sensitivity Calculations, and for Identification of Inconsistent Data," LA-5987, Los Alamos Scientific Laboratory (1975). Harris *et al.* cover the whole framework of equations discussed in the present report, but in the context of adjustment of data using integral information rather than in the context of evaluation of differential data. See also A. Gandini, "Nuclear Data and Integral Measurements Correlation for Fast Reactors. Part 1: Statistical Formulation," CNEN-RT/FI(73)5, Laboratorio Fisica e Calcolo Reattori (1973).

7. F. C. DIFILIPPO, "SUR, A Program to Generate Error Covariance Files," ORNL-TM-5223, Oak Ridge National Laboratory (1976).
8. H. D. LEMMEL "The Third IAEA Evaluation of the 2200 m/s and 20°C Maxwellian Neutron Data for U-233, U-235, Pu-239, and Pu-241," *Proc. Conf. Nuclear Cross Sections and Technology*, NBS Special Publication 425

(1975) p. 286. See also D. McPHERSON and J. H. JOHNSON, "LSF: An Interpreter for a Class of Least Square Fitting Problems," Atomic Energy of Canada, Limited, Chalk River Nuclear Laboratories (1972), AECL-3415.

TABLE I  
A Sample Data Combination

<u>Observations</u>	<u>Prior Estimates</u>
$\xi_1 (\approx \sigma_1) = 5.7 \pm 0.1$	$\hat{\sigma}_1 = 5.6$
$\xi_2 (\approx \sigma_2) = 6.8 \pm 0.2$	$\hat{\sigma}_2 = 6.9$
Correlation coefficient $\rho(\xi_1, \xi_2) = 0.40$	$(\hat{\sigma}_1 / \hat{\sigma}_2 = 0.8116)$
$\xi_3 (\approx \sigma_1 / \sigma_2) = 0.77 \pm 0.02$	

Transformed Input Information

$$\underline{y} = \begin{pmatrix} 1.79 \\ -1.45 \\ -5.13 \end{pmatrix} \times 10^{-2}; \quad \underline{A} = \begin{pmatrix} 1 & 0 \\ 0 & 1 \\ 1 & -1 \end{pmatrix}; \quad \underline{V} = \begin{pmatrix} 3.19 & 2.07 & 0 \\ 2.07 & 8.40 & 0 \\ 0 & 0 & 6.07 \end{pmatrix} \times 10^{-4}$$

Intermediate Quantities and Results

$$\underline{V}^{-1} = \begin{pmatrix} 0.373 & -.092 & 0 \\ -.092 & 0.142 & 0 \\ 0 & 0 & 0.165 \end{pmatrix} \times 10^4 \quad \underline{A}^t \underline{V}^{-1} \underline{A} = \begin{pmatrix} 0.538 & -.257 \\ -.257 & 0.306 \end{pmatrix} \times 10^4$$

$$\underline{\text{Cov}}(\underline{s}) = \underline{C} = [\underline{A}^t \underline{V}^{-1} \underline{A}]^{-1} = \begin{pmatrix} 3.10 & 2.59 \\ 2.59 & 5.44 \end{pmatrix} \times 10^{-4} \quad \underline{A}^t \underline{V}^{-1} \underline{y} = \begin{pmatrix} -.044 \\ 0.474 \end{pmatrix} \times 10^2$$

$$\underline{s}_1 = (1.09 \pm 1.76) \times 10^{-2} \quad \sigma_1^a = 5.66 \pm 0.10^b$$

$$\underline{s}_2 = (2.47 \pm 2.33) \times 10^{-2} \quad \sigma_2 = 7.07 \pm 0.16$$

$$\text{Correlation coefficient } \rho(\sigma_1, \sigma_2) = 0.63 \quad \sigma_1 / \sigma_2 = 0.801 \pm 0.015$$

$$\chi_1^2 = 5.2^b$$

<sup>a</sup>Since nonlinear estimation is involved, an additional iteration should in principle be carried out using the output  $\underline{\sigma}$  given here as the new  $\underline{\sigma}$ . In this example the second iteration gave the same result for  $\underline{\sigma}$  to the precision quoted above.

<sup>b</sup>There is an ~2% probability that so large a value of  $\chi^2$  would be found if the input  $\underline{V}$  is correct. If the relative uncertainties are accepted, the scatter of the data would justify a decision to multiply the quoted output uncertainties by  $\sqrt{5.2} = 2.3$ .

*DISCUSSIONS*

J. Behrens I recognize the complexity of the covariance matrix and I also remember some comments made at BNL where it was said that at least the standards should include the covariance matrix information. My question is, would it be appropriate to include the covariance for the ratios, say in ENDF-V, or is that too much work.

R. Peelle If evaluations would use a method as described in this paper or something similar, the covariance matrix for the absolute input data and your ratio data, which would be input data, would be required. At the output would appear the covariance matrix of the output data which then would appear in ENDF.

J. Behrens It would be a enormous task to analyze all the data in this way.

R. Peelle It always will be a mammoth task to do the job right.

L. Stewart You probably said it but we find it quite useful to have the statistical error quoted separate from the correlated error.

*Summary Session*

Summaries of the Working Groups on  
Fission Cross Section Ratios and on  
Absolute Fission Cross Sections



*Report of the Working Group Session on Cross Section Ratios*

by

C. D. Bowman

Someone said at afternoon lunch, "If one can't measure ratios right, he ought to be fired." Thus, we at the Bureau, working under Civil Service regulations, are not permitted to measure ratios--only absolute cross sections which everyone knows is difficult.

The extreme action recommended by the above comment conveys the fact that the ratio eliminates some very important measurement problems that one has if one gets involved with absolute measurements. Of course the most important is the necessity of measuring flux, and often the absolute mass of the sample involved. If one gets rid of these problems, one is left with energy scales, mass-ratios, anisotropy of fission fragments, mass distributions, backgrounds, and detector efficiencies. In comparing ratio experiments, one is able to detect the effects of these factors on experiments much more readily than is possible by comparison of absolute measurement.

We spent most of our time looking carefully for the effects of these problems in ratio measurements. For several reasons we concentrated almost all of our attention on the U-238 vs U-235 ratio. First, there was more data available on that than on anything else. Those who measured another ratio seemed to have also measured this ratio. Systematic effects which are detected in the U-238/U-235 ratio are likely to exist in the other ratios measured in the same experiment. The U-238/U-235 ratio also is much more sensitive to energy shifts than the other ratios considered at this meeting. We reviewed all the experiments which were presented here usually in the presence of the experimenter. Ample time was available to question the experimenter, and also to give the experimenter an opportunity to restate things he said during Session I of the meeting. We tried to examine all the experiments which had been so carefully assembled and plotted for us. I can't say we did justice to all of them because of lack of time. But there

was certainly nothing lacking on the part of the Argonne staff, there was not a single thing that we wanted which we could not get at in half a minute, and that was very, very helpful.

We looked at each experiment in terms of the type of detectors used, effect of anisotropy on the detector, the means of determining mass, other factors related to normalization, the energy scales which were used and how they were derived, anisotropy of the neutron source, background and its influence on the experiment, influence of the energy resolution, and a re-assessment of the experimenter's estimate of the accuracy.

Let me go on and try to mention the results from looking at the U-238/U-235 ratio and of course I want the members of the Working Group to call attention to any I might omit. I think the most remarkable thing that we felt came out of this work is that a large number of experiments can be brought into what some would consider excellent agreement in the energy region from threshold to 10 MeV after energy scale changes and after adjustments for possible mass changes.

Let me first say something about white source energy scales. You heard some about this on Monday and you remember at that time there was a large discrepancy between other scales and the Coates measurement at Harwell. For that reason James did a measurement with the same detector primarily to check the energy scale and he arrived at a result which agrees very well with the Livermore energy scale. At this point Coates took a second look at his energy scale determination. He had first determined an energy scale by measuring the flight path. In addition he had obtained an energy calibration with the carbon resonances which gave a different scale. He chose the latter resonance energy scale which is higher than James's scale and the LLL measurements. After James's measurement he checked the accuracy with which he had done the resonance calibration and concluded that the accuracy was actually much less than he thought. Using the original path length scale which was consistent with the resonance energy scale within the uncertainty of the measurement he derived an energy scale in good agreement with James's. If one renormalizes his data higher by a couple of percent, then one obtains a cross section in excellent agreement with the James and the LLL cross section.

Two other measurements were available from white sources; the Cierjacks

measurement, and the Difilippo measurement. If you now compare these five measurements from Cierjacks, James, Coates, LLL and Difilippo, it appears that there is no energy shift and in this region from zero to 10 MeV. Where they overlap the agreement is quite good and, I think, one would expect an evaluation to yield a number at least as good as 2 percent.

We looked next at the Van de Graaff data and took quite some time to consider the ratios measured at Argonne. There is an apparent energy shift of Meadow's measurements relative to the bulk of the white source measurements as described above. By shifting Meadow's data down by 20 keV, it appears the agreement with the white source measurements is very good. The observation was made by someone who looked at this carefully--I think it was James who has been studying energy scales--that in virtually every case, Van de Graaff measurements tend to come out high in nuclear data measurements of this kind including the narrow carbon resonances. The exceptions are Davis and Barschall, and Johnson who measure the same energy scale as white sources measurers. Meadows felt it would be very important to do that measurement at Argonne and see what the result yielded.

The recommendation of the group was that Van de Graaff measurers should check the resonance at 2.07 MeV in carbon to assure that they have a proper energy scale. (See footnote on p.443. Note added by the Editors).

I have already stated that we can achieve an evaluated ratio of better than 2% in the range up to 10 MeV. If you add other Van de Graaff measurements and adjust them up or down in mass as uncertainties permit, one achieves, with maybe one or two exceptions, very good agreement with the curve you get from the white sources. That also adds to my confidence that an evaluation could now achieve better than  $\pm 2\%$  accuracy.

Above 10 MeV the data becomes more sparse and there appear to be discrepancies in the white source data. There are two cyclotron measurements and two linac measurements extending to 20 MeV or higher. There is a divergence between cyclotron and linac measurements above 12 MeV. The cyclotron measurements increase more rapidly and, by the time one reaches 20 MeV, the difference is about 10% or larger. This is very surprising and disturbing in view of the agreement at lower energies. One possible source of the difference is that cyclotrons both used gas scintillators and the linacs both used ion chambers. One recommendation of the group was to have some

kind of detector exchange start between these different facilities to assess this problem in this energy range. This energy range is increasing in importance owing to fusion program needs.

Only an hour of our time remained when we moved on to consider the very important Pu-239/U-235 ratio. There were several factors in the Pu-239/U-235 ratio which were significantly different from U-238/U-235. First, one has much higher  $\alpha$ -activity in Pu-239 which might have effects not present in the other ratio. The energy scale which is very important in the other ratio is not so important here since the energy dependence for both cross sections is similar. It appears that the U-238/U-235 ratio can provide guidance on appropriate energy shifts for the Pu-239/U-235 ratio. We were able to do a little bit of this apparently with positive results. Also anisotropy, which is a major concern in U-238, is much less a concern in this ratio because it is small and tends to behave the same way with energy for both Pu-239 and U-235. The final point is that there often is a significant contamination of Pu-240 requiring correction. Those were the four things we felt were significantly different from the other ratio.

In view of the fact that there is significantly less possibility for energy scale and anisotropy problems, one expects the Pu-239/U-235 results to agree better than U-238/U-235 which does not appear to be the case. There are differences--some of which will be corrected by energy scale transformations but the biggest problem appears to be in mass normalization. Most of these experiments claim mass determination to 1%, maybe a bit poorer. Yet there are many examples of discrepancies at the 4% level and the systematics of the effect appear to indicate mass determination problems. No guidance was available as to whose mass might be most accurate.

Moving on to the U-233/U-235 ratio, the situation appears to be similar only that the data are even more sparse. There is a mass problem and there are also differences in shape which are not correlated with energy shifts. Above 14 MeV there is hardly any data at all except for the LLL ratio measurements.

For Pu-239/U-235 and U-233/U-235, it appears that there is a significant problem with mass determination and the typical error may be 3-5%. A large part of this might be related to uncertainties in the efficiency of the detector although it was not possible to consider this carefully. The

group also felt that there is an insufficiency of measurements of these ratios. It was a great help to have the mass of information on U-238/U-235 out of which an accurate ratio probably can now be derived and, where problems still exist, the required measurements can be clearly stated.

When we look at these last two ratios, we see something like a 4% difference where we have eliminated the flux problem. One might infer from that how accurately one can get the Pu-239 cross section when one derives it from the ratios and the absolute U-235 cross section.

Finally, there are several recommendations mentioned earlier which I summarize below:

#### Recommendations:

1. Measurers in the MeV range should include a check on the energy of the 2.07 MeV carbon resonance to confirm the accuracy of MeV energy scales.
2. If differences for the U-238/U-235 ratio in the energy range above 10 MeV are not cleared up by a restudy of existing data, a detector exchange should be initiated to resolve any possible problem between gas scintillators and ionization chambers.
3. Most measurers generally measure more than one ratio. The energy scale differences encountered at threshold in the U-238/U-235 ratio, should be used to transform the scales of other ratio measurements by the same authors which should result in more consistent data sets for evaluation.
4. Special care must be given in determining the Pu-239 mass or the Pu-239/U-235 mass ratio in future experiments since the present data show significantly larger normalization differences than expected on the basis of the authors' stated mass uncertainties. The situation appears to be more difficult than the U-238/U-235 mass ratio.
5. Care should be taken in evaluating the influence of the higher alpha activity of Pu-239 and U-233 on the efficiency of the fission chamber.
6. More measurements must be made on the Pu-239/U-235 and U-233/U-235, particularly at high energies, to obtain evaluated ratios to an accuracy of  $\pm 2\%$  or better with a high level of confidence.

## DISCUSSIONS

R. Peelle Let me return to the energy scale problem. Do you want to also say that the white source measurers should also measure resonances? Why does it refer only to Van de Graaff measurers?

C. Bowman Well, white source measurers usually do the measurement anyway and, with a little care, have demonstrated the capability to get the correct energy scale. Perhaps we should change our recommendation. I am sure the group would be willing to include the white source measurers in the recommendation.

B. Diven That 20 keV shift is at threshold? What is the reference point?

C. Bowman We refer to the shift in the energy of the U-238 fission threshold. There is one other point which I would like to mention. If there is an energy shift in the white source experiments, then the energy shift would get much worse at higher energies. However, if you compare the Van de Graaff and white source data at higher energies, this does not appear to be the case. This is additional evidence that the Van de Graaff energy scales are in error rather than the white sources.

J. Behrens I would like to comment on the normalization problem. In our measurements we do not necessarily make mass determinations. We have two independent ways of normalizing to make our ratios absolute. We get very good agreement, we have a thermal normalization and the threshold technique which appears to agree for Pu-239/U-235 with 0.3%.\* If you realize mass determination implies experiments other than those recently completed at Livermore, the statement is correct.

---

\*The uncertainty for this comparison was 2.4%.

Comparisons for other ratios are given in Table III of the paper by J. W. Behrens and G. W. Carlson, the first paper of Session I. (Note added by the Editors)

C. Bowman Let me respond to this if I can and maybe defend some of the other experiments. I think that the Livermore group has done a very careful job to get that part of the experiment in order, but if you ask the other experimenters a similar question they might have used different techniques to get the proper mass, isotopic dilution, destroying foils, all the whole spectrum of techniques. If we have to rely on what the experimenters tell us, it may be difficult to make an evaluation. Everybody tried hard.

G. Carlson I think you are a bit pessimistic about the dispersion between experiments on the Pu-239/U-235. I seem to see a better agreement than the 3 or 5%. I agree the U-233/U-235 is much more uncertain but in the Pu-239/U-235 there is a whole set of values you can look at which appears in a band of 2%. I would say the agreement is more in a 2% range.

C. Bowman Maybe this is an important point that I misrepresented and I would like to ask the group to respond.

J. Meadows The 2% may be too optimistic. If you look at the data, there are a whole set of experiments which should have a normalization in the one or two percent range. There are too many which fall out of that range for comfort.

W. Poenitz I think it is a pity that there are really too few data available over an extended energy range. But if one compares in the restricted range which is overlapped with many independent data sets and with the LLL data, then I get the impression that it was not only a normalization problem, but that it was a shape problem. If one normalizes above 1 MeV, the data for Pu-239/U-235 starts to diverge below 1 MeV and converge around 100 keV the Livermore data being in conflict with all other data but that of Gaytner who measured the shape over this range.

C. Bowman We had that one measurement which we did not have the time to discuss but which bears on this problem. Tom, (Heaton) would you like to report on your measurement?

T. Heaton We measured the average over the Cf-spectrum. We think that the accuracy of our mass scale is 1.2%. We do find a result which is about 3% higher than the whole of the differential results.

A. Smith Did you mention anything about the structure in Pu-239/U-235 around 300 keV?

C. Bowman Yes, we looked at this. Again I have to speak for the group. I think there was the feeling that there was not a good reason to feel that the structure was false.

A. Smith Did you reach any conclusion as to what the cause is? Is it in Pu-239 or U-235?

C. Bowman We just noted that there is a much larger peak in the ratio at 800 keV, and if there is any at 300 it is less significant.

A. Smith If it is in U-235 why do you not see it in U-233/U-235? There is only very slight indication there.

C. Bowman Nobody said where it was.

J. Behrens I would like to point out that we noticed it in U-233/U-235. There is also a peak around 6 MeV. Of course we are not suggesting that there is a resonance at 6 MeV. One reason is changing shape.

A. Smith That is an interesting peak for another reason too.

W. Poenitz The reason for this peak at 6 MeV is that there is a shift in the second chance fission threshold between U-233 and U-235. The ratio U-233/U-235 rises with second chance fission in U-233 and drops sharply with the onset of second chance fission in U-235 at higher energies.

L. Stewart But the problem is that the shift is in opposite direction than what you would expect.

A. Smith The other question is why does the Livermore peak occur at the same energy as observed by Meadows, and still you suggest an energy shift in U-238/U-235.

J. Behrens The shift in U-238/U-235 is 20 keV below 1 MeV, at 6 MeV you would not see that.

A. Smith Let's return to the question, what the cause for the structure in Pu-239/U-235 is. Is it in Pu-239 or U-235?

C. Bowman I think the point Behrens and Carlson made is that if you have a range where U-235 and Pu-239 have different slopes you end up with something

like peaks which are not present in either one. This is a statistical thing.

L. Stewart But it is also in U-235, that is what A. Smith wants to suggest.

A. Smith I am trying to relate it to what also appears to be in U-235.

C. Bowman The dip you say is in U-235. We heard of proposed aluminum resonances. There is nothing in anybody's experiments which would relate to that.

R. Peelle If I understood your report about the Pu-239/U-235 ratio correctly, the data base is in a disastrous condition. Maybe I over-reacted.

C. Bowman It appears to be a fairly serious level of disagreement.

*Appendix to the Report by the Working Group on Ratios*

WORKING GROUP CONCLUSIONS ON KEV AND MEV FISSION RATIOS

The Working Group reviewed a number of experiments, usually in the presence of at least one of the experimenters who participated in the measurement. Generally speaking there was enough time for the group to ask any questions it chose of the experimenters. Comments derived by consensus of the group are summarized below for each experiment. We begin with the U-238 to U-235 ratio, referring to each experiment by means of at least one of the names of the authors of the papers. The data by Behrens and Carlson was arbitrarily chosen as a reference in order to facilitate the comparison of different data.

Behrens and Carlson

There appears to be no significant problems with the detector. Anisotropy and momentum effects seem to be a matter of concern to the experimenters and were apparently handled satisfactorily by using sufficiently thin foils and applying the corrections as appropriate. Questions on zero-time determination, clock calibration, flight path length were answered to the satisfaction of the group. No problems could be uncovered which might indicate problems with the energy scale. The resolution appeared to be sufficiently good to delineate the existing structure in the cross section sufficiently. The authors designed the experiment apparently very carefully to eliminate background problems. This was important because the background was not measured above 440 keV. However, at 440 keV the authors found a background less than 0.1%. The authors estimated an accuracy of  $\pm 5\%$  across the full energy range which the Working Group felt inclined to accept if statistical errors and normalization or mass measurement problems were excluded.

### Meadows

The group concluded that as long as fission foil thickness was less than  $0.5 \text{ g/cm}^2$  and foils were either rotated  $180^\circ$  in the beam or the chamber built in such a way that as many foils face one way as the other that there should be no anisotropy problem. The experimental geometry and technique appeared to assure no problem in this regard. Considerable discussion centered around the energy scale which the author claimed to be accurate to  $\sim 3 \text{ keV}$  at  $1.5 \text{ MeV}$ . It was clear that excellent agreement could be obtained with the Behrens-Carlson experiment with a reduction in the neutron energy of the Meadows experiment by  $20 \text{ keV}$ . The group recommended that the energy of the  $2.08 \text{ MeV}$  resonance in carbon be measured to assure that there is no problem with energy scale.\*

### Conde

No problems in this experiment could be found in the detector system. The normalization involved thermal neutrons and mixtures of U-235 and U-238, the U-238 being  $\text{UO}_2$  and the U-235 being uranium fluoride. The energy scale was calibrated using 5 or 6 different reactions. No reason to doubt the validity of the experiments was uncovered.

### Evans

This measurement was undertaken primarily to resolve the discrepancy between the energy scales of Behrens and Carlson and of Coates. It covered the energy range from  $1.2$  to  $2 \text{ MeV}$ . No effort was made to measure the backgrounds and the curve was not absolute. The author recommended that the data not be included in evaluation except for the contribution it makes in determination of the proper energy scale. A more complete and more reliable measurement of the ratio will begin soon. The error on the energy scale is claimed to be  $2$  or  $3 \text{ keV}$  at  $1.5 \text{ MeV}$ . In view of

---

\* Measurements of the C-resonance at  $2.077 \text{ MeV}$  by J. Meadow after the meeting resulted in differences of no more than  $3 \text{ keV}$  which agrees with the experimental uncertainty (Note added by the Editors).

the absence of opportunity to measure background and a number of other attributes of the experiment, the author was unwilling to estimate the accuracy of the results. However, the energy scale agreed well with that of Behrens and Carlson.

### Coates

Coates had two possible energy scales--one determined by flight path length measurement and the other determined by analysis of carbon resonance position. His original data were published with the carbon resonance energy scale. Upon completion of the James experiment, Coates returned to the resonance calibration method and after some study found it to be significantly less accurate than it had first appeared. The uncertainty estimated was found to overlap the energy calibration determined by flight path length measurement. The flight path length measurement brings the Coates data into reasonable agreement with the Behrens and Carlson data and the James data. Owing to neutron-induced reactions in the foil it was necessary to use a high bias which might have made the experiment more sensitive to fission fragment angular anisotropy. However, no corrections for this effect were applied. Measurement of background were made using total cross section measurements of samples of different thickness. The result showed that any backgrounds present were below the 2.5% level. After shifting the data to bring the energy scales into alignment with the Livermore data, excellent agreement with the Livermore data could be obtained by shifting the normalization of the data up by 2%.

### Grenier

The author estimated a 9% background correction which could be corrected with 10% uncertainty so that background uncertainty should have been less than 1%. The mass determination was done to an accuracy of 2.4%. However, the data would have to be increased by 4% to bring them into agreement with the Behrens and Carlson result.

Difilippo

Rather thick foils were used in this relative measurement so that there might be possible angular anisotropy problems which have not been corrected for. The flight path was not measured but known resonances were used for energy calibration. There appeared to be no resolution effect of significance in the experiment; no background was measured. The author estimated a 1.5% systematic uncertainty. The data agree quite well with Behrens and Carlson after the normalization is adjusted.

Lamphere

This is a Van de Graaff measurement. The energy scale appears to be higher as appears generally to be the case of positive ion accelerators as compared to white neutron sources. The fission chamber contained a large amount of material and there was a significant problem with the mass which has been known for a number of years. Fairly good agreement with Behrens and Carlson can be obtained if the cross-section is shifted in energy and the mass renormalized to the Behrens-Carlson experiment. Lamphere was not present to defend his experiment.

Fursov

This is another Van de Graaff experiment which also shows an energy scale shift to high energy compared with the white source techniques. Above threshold between 2 and 5 MeV the cross section agreed fairly well, and this has improved somewhat with the energy shift. However, above 5 MeV serious problems appear which discourage the use of the data above that energy.

Poenitz

This was a single point measurement at 2.5 MeV where the cross section is relatively flat and neutron energy determination is not an issue. A gas scintillator was used apparently in such a way as not to encounter problems in angular distribution arising from overly thick foils. The mass determination according to the author is good to about 1% and the value

for the cross section ratio appears to be supported by the recent Behrens and Carlson measurement.

### Cierjacks

A gas scintillator detector was used in this experiment which involved a coincidence technique. The sample thickness was  $0.4 \text{ mg per cm}^2$  of  $\text{UO}_2$  which is near but below the thickness where significant angular anisotropy effects might be important. The experiment was carried out with a 50 meter flight path which was the longest of any of the white source experiments. There is a decided shape difference above 10 MeV when one normalizes at 2.5 MeV where the cross section is flat. Below 10 MeV the results appear to be in very good agreement with the Behrens-Carlson measurement. A comparison of the data by Behrens-Carlson with the Coates experiment shows the same kind of differences above 10 MeV. Both the Cierjacks and Coates experiments were carried out using cyclotronbased white sources and also using scintillator fission detectors. The group felt that if the planned measurements of Coates continued to be inconsistent with linac ion chamber measurements that a detector exchange program should be established to resolve the uncertainties in the region above 10 MeV.

### Other Experiments

The following comments are made with regard to experimenters for which time was not available to give as much attention as those described above.

The White measurements were viewed by the group to be useful with no energy shift or renormalization necessary.

It appears that the data of Stein must be renormalized.

The data of Smith if renormalized upward could be brought into good agreement in the energy region below 10 MeV.

### The Ratio of Pu-239 to U-235

The group felt that there were certain factors relating to this ratio which affected the attainable accuracy in a significantly different way from that for the U-238 to U-235 ratio. The increased alpha activity of the Pu-239 usually results in the use of thinner foils and poorer statistics or in a higher bias and a resulting lower efficiency to eliminate alpha pile-up pulses. On the positive side the energy dependence is much weaker than that for the U-238 to U-235 ratio and therefore the energy scale should be a less significant factor. However, since the U-238 to U-235 ratio is so sensitive to the energy shift, an energy dependence found there and correction for such dependence probably can be carried over to the Pu-239 to U-235 ratio. In general this appears to be helpful in bringing different measurements into agreement. Anisotropy seems to be less of a problem since the energy dependence of anisotropy for the two isotopes are similar.

### Meadows

The Meadows data claim a .8% uncertainty in the mass ratio measurement as compared to a 1.3% value for the Carlson-Behrens data. The detector efficiency in Meadows' experiment was thought to be 98%. Thermal neutrons were used in the mass determination. There appeared to be a significant disagreement in normalization between the results of Carlson and Behrens and Meadows. The statistical accuracy for the Meadows experiment was somewhat less than desirable. According to Meadows it is practical to improve this experiment using longer running time.

### Pletschinger

The experimenter apparently undertook a very careful measurement which he claims to be accurate to 1%. The detector efficiency was somewhat less than 90%. A correction for Pu-240 content of 3.5% was applied. The estimated accuracy is expected to be around the amount of 2%.

Carlson-Behrens

The data were normalized by the threshold technique and by extending the measurement down to thermal energies. The estimated uncertainty in the mass is 1.7%. The detector efficiency for Pu-239 was 90%. All statistically significant structure in the ratio is reproducible.

Soleilhac

The group was advised by its European members that these data need not be considered in an evaluation since an accurate fission ratio was not the primary objective of this experiment.

Poenitz

Measured from 120 keV to 1.4 MeV using a gas scintillator. The group uncovered no uncertainties in the experiment which appeared to undermine its validity.

Cierjacks

The data were taken with a 12 meter flight path which is sufficiently short to possibly have some impact on the energy scale, although this could not be demonstrated at the time of the group discussion. The data swing high above 10 MeV as do the U-238 to U-235 ratio compared to other white sources. In addition, there appeared to be a shape difference of about 4% over the energy range from 0.8 to 8 MeV.\*

General Comments

Several general comments about the Pu-239 to U-235 ratio seemed appropriate. First, there appeared to be significantly fewer high quality measurements of this ratio. Second, the absolute accuracy obtainable for this ratio appeared to be significantly poorer than the accuracies obtained for the U-238 to U-235 ratio even though the masses apparently

---

\* Data considered at the working group session were corrected since then and included in these proceedings (Note added by the Editors).

were obtained to roughly the same accuracy. No reason for this difference seems apparent, but one possible problem might be in accurately determining the detector efficiencies when the efficiency is in the neighborhood of 90% or somewhat lower. Future efforts on Pu-239 should be especially careful in determining the detector efficiency as well as the Pu mass.

#### The Ratio of U-233 to U-235

Generally speaking the data on this ratio were even more sparse than those on Pu-239. The most recent measurements of Behrens and Carlson and of Meadows disagree. The Livermore measurement has two normalizations as obtained by the threshold technique and as obtained by extension down to thermal energies. These two normalizations disagree with the Meadows experiment by 5% and 2% respectively. The data become particularly sparse in the region of 14 MeV and above. As time was short for the Committee's work and few recent high quality experiments had been performed, this ratio received only a small amount of attention from the working group. At least two more highly quality energy dependent measurements are required before an accurate ratio of cross sections can be established for this isotope in the higher MeV range.

## *Report of the Working Group on Absolute Fission Measurements*

by

R. W. Peelle

### Introduction

As a result of the importance of the problem area a great wealth of direct fission cross section data has been generated within the last two decades. Yet, even for U-235 fission, some of the recent measurements by experienced experts differ one from the other by several percent. The spread originates in the great difficulty of the measurements. Values presented for the first time at this meeting should contribute to the eventual clarification of which fission cross section values should be taken as most nearly correct.

For the considerations in this report we include as "direct" measurements both the true absolute measurements and the measurements which have been performed relative to various cross section standards such as n-p scattering and, below 100 keV, the Li-6(n,alpha) and B-10(n,alpha) reaction cross sections. The committee chose to limit its attention to the energy region above 20 keV except to the extent that values obtained at lower energies determine the normalization at energies greater than 20 keV.

Several general experimental problems were discussed, and then subcommittees were formed to deal with the U-235(n,f) cross section in the various energy regions and with direct fission measurements on the other nuclides of concern.

The remainder of this committee report is organized according to the topics considered.

### Experimental Problems

For a gas scintillation fission chamber of simple design, A. B. Smith noted that his test experimental data revealed effects of a very serious (x2)

nature which may be interpreted as inefficiency for certain fragment angles, an inefficiency not apparent through inspection of the pulse-height spectrum observed. Seemingly, the effect must be connected with some light collection phenomenon. Other workers have not seen this strong effect using their own counter geometries and relying on their own experimental checks. It is recommended that experimenters be watchful for this effect until it is fully understood and can be protected against.

The anisotropy of fission fragments relative to the beam direction has been used to make corrections to much of the fission chamber data presented at this meeting. For many measurements these corrections are small; however, others utilize detectors sensitive for only a portion of the space angle. Since there is some doubt about values of the anisotropy to use even for the major nuclides whose fission cross sections are most important, it is recommended that new measurements or evaluations be performed to assure that these fission chamber efficiency corrections can be correctly performed.

Auxiliary quantities such as the decay half-life of Pu-239 continue to be of crucial importance to fission cross section data analysis. It is recommended that work on these secondary quantities be continued until the uncertainties associated with these values no longer impact on overall cross section uncertainties.

#### Use of Preliminary Data in Evaluations

The use of preliminary data, which was discussed after the presentation of the paper by M. Bhat, was again considered. It was recommended that evaluators should avoid or restrict the use of preliminary experimental results.

#### Need for Clean Physics Criticals

The usefulness of clean "physics" integral experiments, specifically fast critical assemblies, was discussed. The need was emphasized to make the results of such experiments more accessible to cross section specialists.

#### Value of Direct Fission Measurements on Nuclides Other Than U-235

The question was discussed whether one should measure directly the fission cross sections of greatest interest - Pu-239(n,f) for instance - ,

or rely almost completely on a combination of fission ratio measurements with values of the  $U-235(n,f)$  standard cross section. Opinions varied, but there existed nearly a consensus that whenever experimental techniques can be applied with equivalent accuracy to  $Pu-239$  and  $U-235$  fission samples, the direct measurements on  $Pu-239$  should be included to provide reduced uncertainties for values of the most crucial fission cross sections.

#### Status of Absolute Measurements on $Pu-239$

(Chairmen: G. Knoll and F. Kaeppler)

Data by Allen and Ferguson, by Szabo, and from the Univ. of Michigan were compared between 140 and 3200 keV with a curve derived from the ratio measurements of Carlson and Behrens and the proposed ENDF-V evaluation of the  $U-235(n,f)$  cross section. The validity of any conclusion from such consideration is somewhat confused by the nonindependence of ENDF-V from some of the absolute measurements (the  $U-235$  data by Szabo and from the Univ. of Michigan were considered in the evaluation of  $U-235$  ENDF-V) and restricted by the somewhat arbitrary selection of the ratio (for example, the ratio derived from the Univ. of Michigan data is in conflict with the ratio by Carlson and Behrens).

The main discrepancy appears to be in the 200-700 keV range where the Allen and Ferguson data lie some 10% above the other data. The difference probably reflects a problem in the flux measurement since a similar discrepancy exists for their  $U-235$  data. Without the Allen and Ferguson data, a reasonable confirmation of the shape derived from the data by Carlson and Behrens and ENDF-V (although ENDF-IV might also be satisfactory) was obtained. However, a shift in the normalization of the Carlson and Behrens data (or ENDF-V) over the entire range to lower the resulting curve for  $Pu-239$  by 0.05 b appears desirable.

#### Summary on Low-Energy Normalization of the $U-235(n,f)$ Cross Sections

(Chairmen: B. R. Leonard and O. A. Wasson)

The thermal cross section, of 583.5b derived by B. Leonard, with an uncertainty of 0.5% for the absolute value is recommended for the use in

the normalization of data going to thermal energies.

The integral from 7.8 to 11.0 eV is convenient for the normalization of shape data and often used. The spread of values is 3.5% which suggests a 1.7% uncertainty. It is recommended to use a value of 241.2 b.eV with a 2.4% standard deviation.

The 0.3-1.0 keV range is of interest because shape differences above this energy are less ( $\pm 2\%$  in 5 data sets from 300 eV to 30 keV) than at lower energies. By contrast, there is a 5% absolute difference between the data sets of Gwin and Czirr after normalization to the same thermal value. The uncertainty for normalization in this 0.3 to 1.0 keV interval, relative to thermal energy, is 3.5%.

The average value obtained by M. Bhat based on low-energy normalizations is 3.6% below the Univ. of Michigan value at 140 keV or roughly in consensus with the center of a  $\pm 3\%$  band of data which is based on normalization at higher energies. The data by Wasson, normalized at 7.8 - 11 eV, agree with Gwin's results within  $\pm 2\%$  near 140 keV.

#### Summary on the 0.2 to 8 MeV Range for U-235

(Chairmen: B. C. Diven and M. Bhat)

Between 1 and 8 MeV there is no major controversy regarding the evaluated curve with a  $\pm 3\%$  uncertainty. In this region the energy scales of the different experiments were questioned but may be consistent with one another.

Below 1 MeV the data sets are consistent with an evaluation known to 3% except from 0.25 to 0.4 MeV, where the scatter of data suggests  $\pm 5\%$  uncertainty and causes some problems in deciding on a best evaluated curve. The  $\pm 5\%$  uncertainty reflects differences in apparent structure among the various experimental results which should and will be investigated.

Because of the larger differences in part of the region below 1 MeV which is of crucial importance for fast reactor design, new measurements should be made in this range to reduce the uncertainties to at least the 2 to 3% range. Data should be obtained using both white and mono-energetic neutron sources, since both types of sources are well suited

to this energy region.

### Summary on the Above 8 MeV Range for U-235

(Chairmen: J. B. Czirr and S. Cierjacks)

Some information on the uncertainty of the relative shape above 8 MeV can be obtained from ratios at selected energies obtained in four relative and three absolute measurements. The values are given in Table I and were derived from numbers picked from the graphs. It should be noted in considering the  $\langle\delta\rangle$ 's that there are two groups of data on either side of the mean for all the ratios listed. It is possible that the differences are correlated with either the flux measurement or the fission measurement techniques (or both). One observation is that the ratio of cross sections at 14.0 to 5.4 MeV as measured by White is not reproduced by any of the four relative measurements. A broader conclusion is that the data show good internal consistency over the broad span represented by the  $\sigma(14)/\sigma(3.5)$  ratio.

Above 15 MeV the various sets diverge badly in shape and only a gross ( $\sim \pm 10\%$ ) estimate of the cross section can be obtainable.

### Summary of the Energy Range above 10 keV

The Table II gives a summary offered by W. Poenitz of observations and recommendations for the U-235 cross section above 10 keV. Fig. 1 shows a  $\pm 3\%$  band around a reasonable 'guess' curve for U-235 which seems to cover most of the more recent experimental data.

### Conclusions

Though impressive and meticulous efforts have allowed the present level of cross section accuracy to be achieved, at every stage it is possible to see how systematic efforts can be further reduced or more accurately corrected for. In some cases improved counter design can help future work. If an uncertainty less than 2% in the evaluated U-235(n,f) cross section is to be approached even greater care will be required to avoid small spurious errors. To reach this goal, more careful documentation will be needed of correction methods for systematic effects. This documentation will also be required for the evaluation of cross section correlations between the various energy regions.

Since discovery of systematic errors usually depends upon comparison of results from competing methods, it is important that absolute cross section work at isolated energies (for example 14 MeV) continue to be pressed where opportunities present themselves.

Finally, one should be pleased with the data in hand but work diligently to make further improvements.

Table I. Cross Section Ratios for U-235 at Higher Energies

(R = $\sigma(E_1)/\sigma(E_2)$ )					
Data	$\frac{E_1}{E_2}$	$\frac{\text{Max } (\sim 7 \text{ MeV})}{\text{Min } (\sim 5 \text{ MeV})}$	$\frac{14.1}{3.5}$	$\frac{14.1}{5.4}$	$\frac{14.1}{7}$ $\frac{16.1}{10.0}$
<hr/>					
Leugers		1.66	1.79	2.00	1.21 1.34
Czirr		1.71	1.72	1.92	1.113 1.14
Pankratov		1.61	1.77	1.97	1.22 1.27
Smith		1.65	1.72	1.87	1.13 1.27
White		-	-	2.17	- -
Cance/Hansen		-	1.74	-	- -
Cance/Poenitz		-	1.69	-	- -
<hr/>					
Averages					
All Data					
R		1.658	1.738	1.986	1.173 1.255
< $\delta$ >		1.7%	1.6%	4.0%	3.6% 4.6%
Shape Data					
R		1.656	1.750	1.936	1.172 1.240
< $\delta$ >		1.7%	1.9%	2.4%	3.6% 8.1%
<hr/>					

Table II. Summary of U-235 Cross Section Status above 10 keV

Observations		Solutions	Recommendations	
Status	Problems, Discrepancies		Specific	General
Agreement within a $\pm 3\%$ band. On the high side of this band:	1. Shape disagreement between Hansen and most others in 1-2 MeV range.	1. Majority shape accepted.	1. None needed.	Higher precision and lesser uncertainty of individual measurements by improving
	2. Shape disagreement between Wasson and most others in .25-.30 MeV range.	2. Suggested correlation with Al-cross section. Solution: None.	2. Simple shape measurement desired.	
Szabo, <1 MeV Kuks Abramov (Cf) Wagemans "Reactors"	3. Shape disagreement between Szabo and most others in 2 - 6 MeV range.	3. Suggested D(d,n) angular distribution. Solution: None.	3. Planned NBS-Carlson, ANL-Poenitz measurements will help.	corrections to achieve a sub 2% level.
Hansen, < 2 MeV Perez	4. Energy shift between Hansen and others at 6 MeV would imply a 3.8% uncertainty per 100 KeV above 6 MeV and up to 6% around 1 MeV.	4. Suggested that statistics not sufficient to prove a trend. Solution: None.	4. Planned NBS-Carlson, ANL-Poenitz measurements will help.	Better documentation of experiments.
In the middle: Gayther, norm. to U. Michigan Poenitz, Cierjacks, <6 MeV Czirr, <10 MeV norm. to Cance,	5. Shape and absolute value-disagreement between Kaeppler and most others in .5 - .8 MeV range.	5. None.		
On the low side: Szabo >2.5 MeV Hansen >2.5 MeV Wasson Heaton (Cf) Czirr (rel. Li) Gwin	6. Poorer situation above 14 MeV.	6. None.	6. NBS-measurements may help.	Use of independent at selected energies to discover systematic errors.

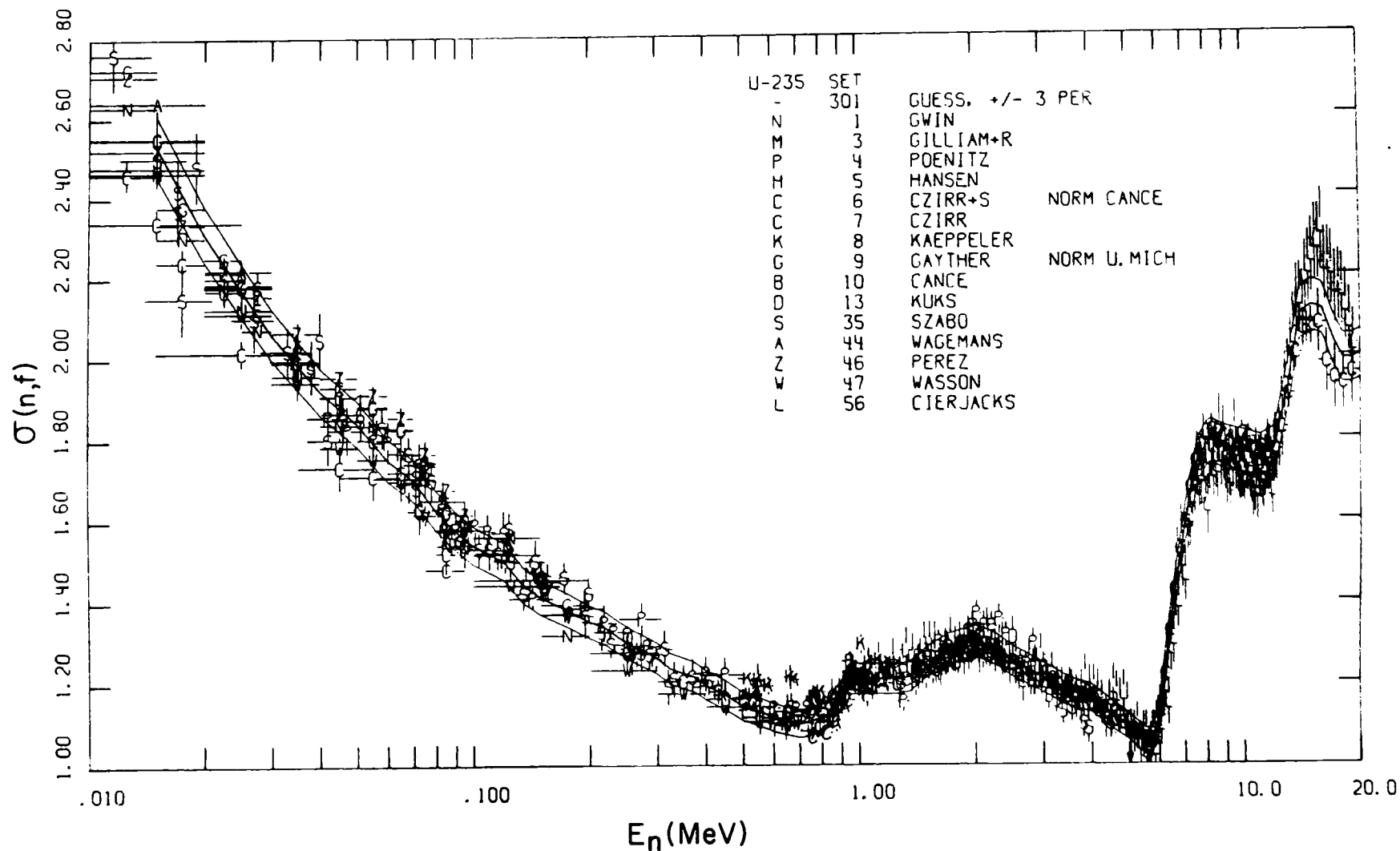


Figure 1 A reasonable but arbitrary guessed curve for U-235 and a  $\pm 3\%$  band. Only newer data are shown. See discussions on the preceeding pages.

## DISCUSSIONS

L. Stewart You might want to mention that the  $\pm 3\%$  U-235 uncertainty is based in some cases on a 7% difference between results obtained with different techniques.

R. Peelle Yes there is a case where we showed a mean absolute difference of  $\pm 3.5\%$ , but it really two groups 7% apart.

J. Czirr I would like to sharpen up this 3%. What do you suggest is the probability that the actual value is found in that  $\pm 3\%$  band.

R. Peelle I would like to refer this question to the subcommittee-chairman.

B. Diven You may get different answers if you ask different people. I would say that there is less than a 32% chance (this would be the chance for one standard distribution) that the true value is outside this  $\pm 3\%$  range. Poenitz may not agree.

W. Poenitz I agree with the exception of certain limited ranges. You can construct certain consistent data sets which agree much better than the  $\pm 3\%$ . For example, if you consider the shape measured by Czirr, you get only a 1% difference for the normalization of this shape if you use the 14 MeV value of Cance instead of the 3.5 MeV value from my measurements. On the other hand, one can find arguments for the higher or lower side of the band. It probably is more a square-distribution.

R. Peelle If I can summarize this, the standard distribution with 3% being one standard deviation is probably too pessimistic. Does the figure show all the data? (See Fig. 1).

W. Poenitz No, these are only the more recent data.

R. Peelle So, if we add some older data which we might not know how to reject, a bigger scatter might result.

W. Poenitz No, not an increased scatter, you will get a systematic effect. The older data will be systematically higher, you get the scatter only to one side, as high as the sky.

J. Czirr I wonder, should we not give the users some information that the 3% is not a standard deviation. We should carefully state what we mean by this.

R. Peelle What the figure shows is the consistency of the modern data.

L. Stewart We have seen that problem before. What is the chance that a new measurement is within that band?

W. Poenitz The implications of the question are not quite justified. The measurements within the last five years are really within that band.

L. Stewart The data by Wasson and by Czirr are outside. They are much lower.

W. Poenitz No, averaging over fluctuations they are in the band, they are on the low side of the band. This, of course, excludes the Czirr data above 100 keV where the Li cross section is the major uncertainty.

C. Bowman I would like to comment on your recommendation to measure directly absolute cross sections (for example Pu-239) instead of measuring ratios and the absolute U-235 cross section. In measuring ratios you eliminate the flux which I claim is the major source of problems. If anybody wants to spend more time on measuring absolute cross sections, I strongly urge him to measure U-235. Get that cross section better and better. I expect that a measurement of Pu-239 is going to be a new data set which will be compared with others, etc. We will do all over again what we did for U-235. That has little meaning. I think that direct measurements on something other than U-235 may only be more confusing.

W. Poenitz I completely agree that direct measurements of Pu-239 will only be confusing. The problem is that most people who would measure Pu-239, measure U-235 anyway and then the evaluator has the trouble with non-independent data sets. However, I feel, the restriction should be only for the same type of reaction (fission in this case). If you consider capture, you have a com-

pletely different situation. It is a different type of reaction and you might avoid many problems present in absolute fission cross section measurements. As a matter of fact, it was from absolute capture measurements that the lower U-235 fission data were first predicted.

C. Bowman I did not want to imply with my comment that one should stay away from absolute measurements of other types of reaction cross sections.

R. Peelle I should emphasize that we did not mean to recommend that the absolute measurements for U-235 should not be made. For many cross sections the ratio measurement is clearly preferable.

G. Knoll As a supporter of the statement in the summary, I would like to repeat the reason for it: Which way to choose to go depends very much on the experimental technique. In our case, it is clearly preferable to measure the absolute U-235 and the absolute Pu-239. It would be more difficult to measure the ratio. We would get larger uncertainties. I also think if you can make as easily the direct measurement as you can make the ratio measurement, then you should make the direct measurement. This is for obvious error propagation reasons. If you have say 50 factors which contribute to the absolute value, you have to tag on another 30 factors which contribute to the ratio measurement, though these 30 factors do not include the flux.

W. Poenitz Some of the 30 factors are identical with some of the 50 factors. They cancel out again.

C. Bowman You ignore that there is a long history of measurements for U-235 which we might not repeat for another isotope. But I agree, if you can measure the cross section easier absolutely than the reatio because of some specific arrangement, you should do it. But if it is equally easy, I think you should not spend the time for the absolute measurement, but measure the ratio.

L. Stewart There is of course the problem that many people measure only relative ratios, one can normalize them as one chooses. The main reason why I would like to see some measurements on Pu-239 is that there is so much

structure in both, the U-235 and the ratio. Sometimes they are opposite to one another. Even if you know U-235 to  $\pm 3\%$ , it is difficult to get Pu-239 to 6%. It is so important that it would be good to have some direct measurements.

B. Leonard I would like to mention a problem which exists in the normalization of data in the thermal energy range. One must be very careful to have a spatially uniform response of both, your fission detector and your flux monitor. It has been demonstrated repeatedly that you can get many percent differences in shape if you do not have a uniform response because you can have spatial variations of the flux with energy.

R. Peelle I guess I would like to add one more point to the controversy of whether one should make direct Pu-239 measurement where feasible. With feasible I mean where a technique has not much more uncertainty if applied to Pu-239 instead of U-235. I align myself as strongly as I can with the subcommittee report. It seems that the error propagation suggests the most direct measurement possible. By this I do not suggest we ignore the available measurements for U-235 and the ratios. One should use these as well as one can. The few data we have for Pu-239 probably do not scatter much more than data for U-235. And as we learned a while ago, the ratios are not in as good a shape as we wish, which does not suggest that the flux measurements are in as bad a shape as suggested.

L. Stewart I think it is a problem that many of the recent absolute cross sections are relative and we had to choose the normalization. That is why I would like to see some more points to pin it down. This does not mean that I suggest one should not continue to do the ratio measurement, I think that is the way to go.

C. Bowman There is a final limitation in the resources. You cannot have it all, the absolute measurements and the ratios.

C. Bowman I have another question about these low energy cross sections, how they agree, I think you said something like 3%.....

R. Peelle 2.5% from 7 to 11 eV and 3.5% from .3 to 1 keV and then you are home free.

C. Bowman Did the subcommittee come up with a possible suggestion on how the problem can be resolved.

B. Leonard No, we do not know why different measurements which go from thermal to this 7.8 to 11 eV range should differ by more than 1%. The difference is almost 3.5% in this integral value. A problem may be to combine high resolution and low resolution data in a range where you have many resonances.

R. Peelle In the region we are concerned with, it would not be difficult to look at the data themselves. I am sure that the same energy regions have been used. Deruytter and Wagemans said they ought to be able to get the 7.8 to 11 eV range with 1%.

B. Leonard The Czirr and the Wagemans data differ around 1 keV nearly 10%, and still they start with essentially the same thermal values. If you normalize both sets at 1 keV, then they agree at higher energies.

J. Czirr With respect to the problem B. Leonard mentioned with matching different energy regions; I think with modern techniques that should not be a problem, one ought to be able to do that.

C. Bowman Let me ask in regard to the light-water reactors. Is it important in view of the light-water reactors that these cross sections are known much better, or is there no problem around 1 eV.

B. Leonard No, the only data where there is a problem to get the thermal normalization to 1 eV is in the original data by Wagemans and Deruytter which show a discontinuity. The other differences in this range - as shown in my paper - are in the order of 0.5%.

J. Czirr The cross sections which you need to calculate a thermal reactor - you think they are still sufficiently known?

B. Leonard The U-235 evaluation did not consider the ability to calculate

thermal reactors. As a matter of fact, it make it slightly worse.

B. Peelle With this I would like to return the chair to the chairman of the meeting.

## CONCLUDING REMARKS

A. Smith I would like to conclude the meeting with some remarks that are the result of my observations during the past three days. It appears that one of the two most important aspects of the meeting is the wealth of new data presented. The other is the problem areas which were so well highlighted. The latter may, in themselves, imply a problem as the discussions and summaries of the working groups may give the impression that there are an overwhelming number of problems and discrepancies. This is, in fact, deceptive as it is the proper nature of meetings such as this to give emphasis to problem areas while ignoring massive regions of really very good agreement. Many of the outstanding problems appear to me to be of a relatively minor and local nature. As a consequence, they can be resolved with minimal effort. This is, I think, a very significant advance from the situation of only a few years ago. An example is the structure in the U-235 cross section in the 250 to 300 keV region which is the principle source of the approximately 5% discrepancy in this local area. Relatively simple experiments should quickly resolve the issue. Another example is the energy-scale problem. I am glad to see that previous--and nearly fantastic--discrepancies--have largely vanished and the differences have been reduced to a relatively minor 20 keV problem. The resolution of even this small discrepancy appears simple, as verification measurements using resonances such as that at 2.08 MeV in carbon to accuracies of several keV should present no particular problem using a number of techniques.

I would like to have seen the positive achievements of the past few years more emphasized than they were. It seems to me there have been tremendous improvements in the basic-reference U-235 cross section which may now be generally known to 3% or better over very much of the fast energy range. Similarly the situation for the U-238/U-235 relative ratio seems to be generally good excepting the very high energies. Absolute ratio data which are with one exception from monoenergetic neutron source measurements determine the normalization of U-238/U-235 with a high level of confidence. I am pleased to note that nothing has appeared that would be a catastrophe for such applications as the fast reactor program though

obviously some detailed discrepancies and ultimate accuracies remain matters of concern.

I feel there are two goals for the future. First is the resolution of some of the outstanding local discrepancies; e.g., the U-235 structure near 280 keV. The second is the more difficult and general objective of realizing accuracies of 2% or better on an absolute scale. The latter will be a far more tedious and difficult task. Hopefully, this meeting will stimulate work toward both of these objectives.

In closing, I wish to thank all the attendees for their excellent contributions to the meeting and to express my appreciation for the able direction provided by the session chairmen. I am convinced that these small specialists meetings are the most productive way of attacking specialized problem areas and I feel it has been so in this instance. May I wish you all a pleasant journey.

## SUBJECT INDEX

- Anisotropy, 112, 140, 153, 154,  
224, 397.
- Background, 92, 113.
- Counters, 170, 415, 450.
- Cross Sections of  
U-235, 173, 183, 208, 225, 237,  
246, 258, 450, 452.  
Pu-239, 208, 225, 452.  
U-238, 237, 246.
- Dectector Efficiency, 71, 92, 112,  
153.
- Energy Scales, 71, 92, 127, 149,  
153, 154, 169, 176, 438.
- Evaluations of  
U-235, 258, 287, 307.  
U-238/U-235, 154.  
Pu-239/U-235, 154.
- Neutron Source Standard, 236.
- Normalization, 70, 153, 170, 206,  
257, 267, 331, 420, 438, 450.  
at low energies, 281, 307, 452.
- $\bar{\nu}$  of Cf, 236.
- Ratios of  
U-238/U-235, 47, 73, 94, 114, 128,  
141, 149, 153, 433, 438.  
U-233/U-235, 47, 73, 433, 438.  
U-234/U-235, 47, 73.  
U-236/U-235, 47, 73  
Pu-239/U-235, 47, 73, 94, 153, 433, 438.  
Pu-240/U-235, 47, 73  
Pu-241/U-235, 47, 73.  
Pu-242/U-235, 47, 73.  
Pu-244/U-235, 47.  
U-235/Li-6, 183, 206, 267.
- Reactor Sensitivity, 31, 268, 398.
- Resonance Parameters, 353, 382.
- Samples, 176, 236.
- 2nd chance fission, 398, 414.
- Shape at 280 keV, 168, 206, 268, 330, 440.
- Structure, 170, 270, 353, 382.
- Theory, 3, 353, 382, 390.
- Uncertainty of,  
U-235, 269, 306, 331, 352.

## AUTHOR INDEX

- Barton, D. M., 173.  
 Behrens, J. W., 47, 70, 92, 112, 153, 168, 236, 420, 430, 438.  
 Bhat, M., 117, 269, 307, 330.  
 Bohn, E. M., 31.  
 Bowman, C., 93, 140, 176, 236, 226, 270, 277, 306, 331, 380, 390, 433, 438, 460.  
 Brotz, B., 94, 246.  
 Browne, J.C., 266.  
 Budtz-Jorgensen, C., 415.  
 Cance, M., 141, 237.  
 Carlson, A. D., 93.  
 Carlson, G. W., 47, 70, 93, 112, 258, 439.  
 Cierjacks, S., 70, 92, 94 112, 140, 168, 246, 257.  
 Conde, H., 92, 128, 140.  
 Czirr, J. B., 258, 266, 459.  
 Davis, M. C., 225.  
 Derrien, H., 168, 206, 208, 224, 266.  
 de Saussure, G., 114.  
 Dickmann, F., 391.  
 Difilippo, F. C., 114.  
 Diven, B. C., 173, 176, 438, 459.  
 Duvall, K. C., 270.  
 Eisenhauer, C., 333.  
 Erbe, D., 94, 246.  
 Evans, P. A. R., 149.  
 Gilliam, D. M., 333  
 Grenier, G., 141, 148, 168, 237, 245.  
 Groeschel, D., 94, 246.  
 Grundl, J. A., 333.  
 Guenther, P., 153  
 Hansen, G. E., 173  
 Heaton II, H. T., 333, 352, 439.  
 Howerton, R. J., 398  
 Huxtable, G. B., 149.  
 Ingle, R., 114.  
 James, G. D., 149, 153, 382, 390.  
 Jarvis, G. A., 173  
 Kaeppeler, F., 380, 391, 397.  
 Kari, K., 94.  
 Keyworth, G. A., 353.  
 Knitter, H., 140, 206, 267, 331, 415, 420.  
 Knoll, G. F., 71, 225, 236, 331, 352, 397, 380, 461.  
 Koontz, P. G., 173.  
 Kuesters, H., 178, 268.  
 Lamaze, G. P., 270.  
 Leonard, Jr., B. R., 266, 281, 306, 414, 462.  
 Leugers, B., 94, 246.  
 Marquette, J. P., 208  
 McKnight, R. D., 31.  
 Meadows, Jr., J. W., 73, 92, 439.  
 Moore, M. S., 71, 112, 127, 277, 353, 380.

- Mosel, U., 3.  
 Moses, J. D., 353.  
 Nordborg, C., 128.  
 Olsen, D., 114.  
 Peelle, R. W., 71, 92, 127, 177, 224,  
     245, 266, 277, 306,  
     330, 421, 430, 438,  
     450, 459.  
 Perez, R. B., 114.  
 Poenitz, W. P., 70, 93, 127, 140, 153,  
     154, 168, 176, 206,  
     257, 268, 330, 397,  
     420, 439, 459.  
 Robertson, J. C., 225.  
 Schmalz, G., 94, 246.  
 Schrack, R. A., 270.  
 Smith, A. B., II, 93, 140, 148, 168,  
     224, 236, 306, 330,  
     352, 397, 439, 464.  
 Smith, R. K., 173.  
 Spiegel, V., 333.  
 Stewart, L., 140, 153, 224, 245, 267,  
     306, 330, 398, 414, 430,  
     439, 459.  
 Stroemberg, L. G., 128.  
 Szabo, I., 208.  
 Till, C. E., I  
 Voss, F., 94, 246.  
 Wasson, A. O., 183, 206, 330.  
 Whetstone, S. L., 236.

## PARTICIPANTS

J. W. Behrens  
Lawrence Livermore Laboratory  
P. O. Box 808, L-24  
Livermore, Calif. 94550  
U.S.A.

M. R. Bhat  
National Neutron Cross Section  
Center  
Brookhaven National Laboratory  
Upton, Long Island, N.Y. 11973  
U.S.A.

E. M. Bohn  
Argonne National Laboratory  
9700 S. Cass Avenue  
Argonne, Ill. 60439  
U.S.A.

C. D. Bowman  
Center for Radiation Research  
National Bureau of Standards  
Washington, D. C. 20234  
U.S.A.

J. C. Browne  
Lawrence Livermore Laboratory  
P. O. Box 808, L-221  
Livermore, Calif. 94550  
U.S.A.

A. D. Carlson  
Center for Radiation Research  
National Bureau of Standards  
Washington, D. C. 20234  
U.S.A.

G. W. Carlson  
Lawrence Livermore Laboratory  
P. O. Box 808, L-24  
Livermore, Calif. 94550  
U.S.A.

S. Cierjacks  
Institut fuer Angewandte  
Kernphysik  
Kernforschungszentrum Karlsruhe  
Postfach 3640  
D-7500 Karlsruhe  
Germany

H. Condé  
The Research Institute of the  
Swedish National Defence  
FOA-4 S-104 50  
Stockholm 80  
Sweden

J. B. Czirr  
Lawrence Livermore Laboratory  
P. O. 808, L-221  
Livermore, Calif. 94550  
U.S.A.

M. C. Davis  
2266 GGBL  
University of Michigan  
Ann Arbor, Mich. 48105  
U.S.A.

H. Derrien  
Nuclear Energy Agency, OECD  
Neutron Data Compilation Center  
B.P. #9  
91190 - Gif-Sur-Yvette  
France

B. C. Diven  
Los Alamos Scientific Laboratory  
P. O. Box 1663  
Los Alamos, New Mexico 87545

G. Grenier  
Service de Physique Nucleaire  
Centre D'Etudes de Bruyeres-le-Chatel  
B.P. No. 61  
92120 Montrouge  
France

H. T. Heaton, II  
Center for Radiation Research  
National Bureau of Standards  
Washington, D. C. 20234  
U.S.A.

R. J. Howerton  
Lawrence Livermore Laboratory  
P. O. Box 808, L-71  
Livermore, Calif. 94550  
U.S.A.

G. D. James  
Nuclear Physics Division  
AERE Harwell, Oxfordshire  
OX11 0RA  
U.K.

F. Kaeppler  
Institut fuer Angewandte  
Kernphysik  
Kernforschungszentrum Karlsruhe  
Postfach 3640  
D-7500 Karlsruhe  
Germany

H. H. Knitter  
Commission Des Communautes Europeennes  
Directorat-General  
Centre Commun De Recherche  
Bureau Central De Mesures Nucleaires  
Steenweg Naar Retie  
B-2440 Geel  
Belgium

G. F. Knoll  
2266 GGBL  
University of Michigan  
Ann Arbor, Mich. 48105  
U.S.A.

H. Kuesters  
Institut fuer Neutronenphysik und  
Reaktortechnik  
Kernforschungszentrum Karlsruhe  
Postfach 3640  
D-7500 Karlsruhe  
Germany

E. Kujawski  
Fast Breeder Reactor Department  
General Electric Company  
310 De Guigne Drive  
Sunnyvale, Calif. 94086  
U.S.A.

B. R. Leonard, Jr.  
Battelle Northwest  
Pacific Northwest Laboratory  
Battelle Boulevard  
Richland, Washington 99352  
U.S.A.

J. W. Meadows, Jr.  
Argonne National Laboratory  
9700 S. Cass Avenue  
Argonne, Ill. 60439  
U.S.A.

M. S. Moore  
Los Alamos Scientific Laboratory  
P. O. Box 1663  
Los Alamos, New Mexico 87545  
U.S.A.

U. Mosel  
Justus Liebig-Universitaet  
Fachbereich Physik  
Institut fuer Theoretische Physik  
63 Giessen  
Heinrich-Buff-Ring 15  
Germany

C. Nordborg  
Tandem Accelerator Laboratory  
Box 533  
S-751 21 Uppsala  
Sweden

R. W. Peelle  
Oak Ridge National Laboratory  
Bldg. 6010 - P. O. Box X  
Oak Ridge, Tenn. 37830  
U.S.A.

W. P. Poenitz  
Argonne National Laboratory  
9700 S. Cass Avenue  
Argonne, Ill. 60439  
U.S.A.

L. Stewart  
Los Alamos Scientific Laboratory  
P. O. Box 1663  
Los Alamos, New Mexico 87545  
U.S.A.

A. B. Smith  
Argonne National Laboratory  
9700 S. Cass Avenue  
Argonne, Ill. 60439  
U.S.A.

S. Tanaka  
Japan Atomic Energy Research  
Institute  
Tokie Research Establishment  
Tokie-Mura, Nara-Gun,  
Ibaraki-Ken  
Japan

O. A. Wasson  
Center for Radiation Research  
National Bureau of Standards  
Washington, D. C. 20234  
U.S.A.

S. L. Whetstone  
Nuclear Science  
Division of Physical Research  
U.S. Energy Research  
and Development Administration  
Washington, D. C. 20545  
U.S.A.

ARGONNE NATIONAL LAB WEST



3 4444 00023008 6